Vol. 43, No. 2 / 2014

e: ISSN 2068 – 2239
p: ISSN 2068 – 4215

INMATEH – AGRICULTURAL ENGINEERING

MAY - AUGUST

Editorial

The National Institute of Research-Development for Machines and Installations designed to Agriculture and Food Industry - INMA Bucharest has the oldest and most prestigious research activity in the field of agricultural machinery and mechanizing technologies in Romania.

Short History

- In 1927, the first research **Center for Agricultural Machinery** in Agricultural Research Institute of Romania - ICAR (Establishing Law was published in O.D. no. 97/05.05.1927) was established;
- In 1930, was founded **The Testing Department of Agricultural Machinery and Tools** by transforming Agricultural Research Centre of ICAR - that founded the science of methodologies and experimental techniques in the field (Decision no. 2000/1930 of ICAR Manager - GHEORGHE IONESCU ŞIŞEŞTI);
- In 1952, was established the Research Institute for Mechanization and Electrification of Agriculture - ICMA Băneasa, by transforming the Department of Agricultural Machines and Tools Testing;
- In 1979, the Research Institute of Scientific and Technological Engineering for Agricultural Machinery and Tools – ICSITMUA was founded - subordinated to Ministry of Machine Building Industry - MICM, by unifying ICMA subordinated to MAA with ICPMA subordinated to MICM;
- In 1996 the National Institute of Research-Development for Machines and Installations designed to Agriculture and Food Industry – INMA was founded – according to G.D. no.1308/25.11.1996, by reorganizing ICSITMUA, G.D no. 1308/1996 coordinated by the Ministry of Education and Research G.D. no. 823/2004;
- In 2008 INMA has been accredited to carry out research and developing activities financed from public funds under G.D. no. 551/2007, Decision of the National Authority for Scientific Research - ANCS no. 9634/2008.

As a result of widening the spectrum of communication, dissemination and implementation of scientific research results, in 2000 was founded the institute magazine, issued under the name of SCIENTIFIC PAPERS **(INMATEH)**, ISSN 1583 – 1019.

Starting with volume 30, no. 1/2010, the magazine changed its name to **INMATEH - Agricultural Engineering**, appearing both in print format (ISSN 2068 - 4215), and online (ISSN online: 2068 - 2239). The magazine is bilingual, being published in Romanian and English, with a rhythm of three issues / year: January-April, May-August, September-December and is recognized by CNCSIS – with B^+ category. Published articles are from the field of AGRICULTURAL ENGINEERING: technologies and technical equipment for agriculture and food industry, ecological agriculture, renewable energy, machinery testing, environment, transport in agriculture etc. and are evaluated by specialists inside the country and abroad, in mentioned domains.

Technical level and performance processes, technology and machinery for agriculture and food industry increasing, according to national requirements and European and international regulations , as well as exploitation of renewable resources in terms of efficiency, life, health and environment protection represent referential elements for the magazine „**INMATEH - Agricultural Engineering**".

We are thankful to all readers, publishers and assessors.

Editor in chief,
Ph.D. Eng. Pîrnă Ion

Managing Editorial Board - INMA Bucharest

In the present, *INMATEH - Agricultural Engineering* journal is indexed in the next international databases:
ULRICHSWeb: Global Serials Directory**, CABI, SCIPIO, ELSEVIER /SciVerse SCOPUS**, **Index COPERNICUS International EBSCO Publishing, Elektronische Zeitschriftenbibliothek**

INMATEH - Agricultural Engineering
vol. **43**, no. **2** / **2014**
NATIONAL INSTITUTE OF RESEARCH-DEVELOPMENT FOR MACHINES AND INSTALLATIONS DESIGNED TO AGRICULTURE AND FOOD INDUSTRY - INMA Bucharest
6 Ion Ionescu de la Brad Blvd., sector 1, Bucharest
Three issues per year,
e ISSN: 2068 – 2239
p ISSN: 2068 – 4215
Edited by: INMA Bucharest

CUPRINS / *CONTENTS*

COMPARATIVE STUDY OF STRUCTURAL ANALYSIS APPLIED TO AGRICULTURAL MACHINES BODIES AND ACCOMPLISHED WITH SOLID WORKS AND AUTODESK INVENTOR PROGRAMS
/
STUDIU COMPARATIV DE ANALIZA STRUCTURALA APLICATA LA ORGANE DE MASINI AGRICOLE SI REALIZAT CU PROGRAMELE SOLIDWORKS SI AUTODESK INVENTOR

Eng. Sfîru R., Ph.D. Eng. Constantin N., Eng. Ludig M., Math. Cârdei P., Ph.D. Eng. Muraru V.
INMA Bucharest / Romania
Tel: 021.269.32.76; E-mail: raluca_sfiru@yahoo.com

Abstract: *This study comprises two structural analyses applications, having as subject the same structure, very common for agricultural machinery designed to tillage,namely a beam, [5], [7]. The two applications are made in well known CAD[1] programs, each including its own structural analysis module: SolidWorks and Autodesk Inventor. The study aims to demonstrate the easiness with which the analysis is performed in either of the two programs, but especially, the way in which the results of the two analyses converge. The converged results are able to show, that the use of one or other of the programs is irrelevant, of course, in terms of the analysis modules, that both programs have. In this study it compares the performances in terms of linear static analysis (check the resistance) and the modal analysis (analysis in frequencies or calculating of a number of structure natural frequencies). It can be said that, the results obtained without doing an additional study of convergence and stability on meshing are satisfactory, possibly good enough in the case of the maximum equivalent stress in the structure.*

Keywords: *structural analysis, agricultural machinery, comparative solutions*

INTRODUCTION

The geometric model is a tridimensional one made in CAD SolidWorks program and it was exported in Autodesk Inventor for analysis, for training. The beam thickness is set to 10 mm, the outer diameter of small holes situated at the top of the plate is 5 mm and the large hole has a diameter of 10 mm. Those three holes situated at the top of the shank forms a catching system of the beam on the portant structure of soil working machine. One of the holes with smaller diameter is pierced on the half of the beam thickness (5 mm), namely from the back of the beam.

The general calculus of resistance is mainly aimed to determine the equivalent stress field (structure is built entirely of metal) in the structure. It is noted, the extreme values and their locations, for possible consolidation, or in case of small requests in relation to the resistance capacity of the material, the shape optimization for weight reduction [1], [2], [3].

It is also important the determination, within the same resistance classic calculation of the relative displacement field (vector field with three components by the three axes). The resultant relative displacement is called strain in engineering language (not to be confused with specific strain, tensorial field calculated in linear theory as the gradient of the relative displacement).

Rezumat: *Acest studiu cuprinde doua aplicatii de analiza structurala, avand ca subiect aceeasi structura des intalnita la masinile agricole destinate lucrarilor solului, o bârsa, [5], [7]. Cele doua aplicatii sunt efectuate in programe CAD [1] foarte cunoscute, fiecare incluzand modulul sau de analiza structurala: SolidWorks si Autodesk Inventor. Studiul urmareste sa demonstreze usurinta cu care analiza se efectueaza in oricare dintre cele doua programe, dar, mai ales, masura in care rezultatele celor doua analize converg. Rezultatele convergente sunt in masura sa arate ca utilizarea unuia sau altuia dintre programe este indiferenta, binenteles in ceea ce priveste modulele de analiza pe care le poseda ambele programe. In acest studiu performantele se compara in termenii analizei statice liniare (verificarea la rezistenta) si analizei modale (analiza in frecvente sau calculul unui numar de frecvente proprii ale structurii). Se poate afirma ca rezultatele obtinute, fara a face un studiu suplimentar de convergenta si stabilitate pe discretizare, sunt satisfacatoare, eventual suficient de bune in cazul tensiunii echivalente maxime in structura.*

Cuvinte cheie*: analiza structurala, masini agricole, solutii comparative*

INTRODUCERE

Modelul geometric este unul tridimensional, a fost creat în programul CAD SolidWorks si a fost exportat in Autodesk Inventor pentru analiza in scopul instruirii. Grosimea barsei are valoarea 10 mm, diametrul exterior al gaurilor mici de la partea superioara a placii este de 5 mm, iar gaura mare are diametrul de 10 mm. Cele trei găuri de la partea superioară formează un sistem de prindere al barsei la structura portanta a masinii de lucrat solul. Una dintre gaurile de diametru mai mic este strapunsa pe jumatate din grosimea barsei (5 mm), anume cea din partea dorsala a barsei.

Calculul general de rezistentă are ca obiectiv principal determinarea campului de tensiune echivalenta (structura este construita integral din metal) in structura. Se urmaresc valorile extreme si locatiile acestora, pentru eventuala lor consolidare, sau in cazul unei solicitari mici in raport cu capacitatea de rezistenta a materialului, optimizarea de forma pentru reducerea masei [1], [2], [3].

De asemenea este importanta determinarea, in cadrul aceluiasi calcul clasic de rezistenta, a campului de deplasare relativa (camp vectorial cu trei componente dupa cele trei axe de coordonate). Deplasarea relativa rezultanta se numeste in limbaj ingineresc deformatie (a nu se confunda cu deformatia specifica, camp tensorial calculat in teoria liniara ca gradientul deplasarii relative).

[1] Computer Aided Design

MATERIALS AND METHODS

Structural model

The structural model of a working body, ensemble or subassembly has five main components:

- geometry of the structure;
- bearing or border conditions or conditions related to the external environment;
- loading or tasks;
- material or materials used to build the structure;
- meshing.

This was made on the basis of hypothetical conditions.

For this study, the structural model defined above by meshing of its main components is the same for both computer programs used. The beam structure geometry is represented in Fig.1, where, also appear the main geometric characteristics of the structure. The images are taken from both programs by means of which the problem was addressed.

MATERIALE SI METODE

Modelul structural

Modelul structural al unui organ de lucru, ansamblu sau subansamblu, are cinci componente principale:

- geometria structurii;
- rezemarea sau conditiile la frontiera sau conditiile de legatura cu mediul exterior;
- incarcarea sau sarcinile;
- materialul sau materialele din care este construita structura;
- discretizarea.

Acesta a fost realizat pe baza unor conditii ipotetice.

Pentru acest studiu, modelul structural definit mai sus prin discretizarea componentelor sale principale este acelasi pentru ambele programe de calcul folosite. Geometria structurii – barsa – este reprezentata in fig.1, unde apar si principalele caracteristici geometrice ale structurii. Imaginile sunt preluate din ambele programe cu ajutorul carora s-a abordat problema.

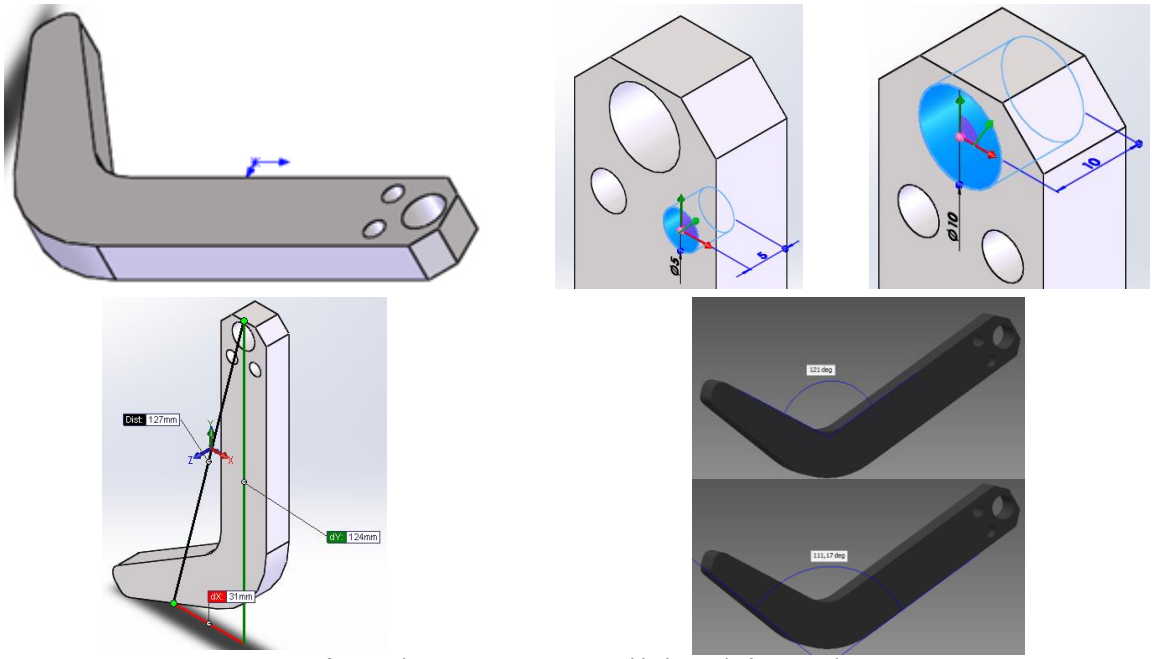

Fig. 1 - The structure geometry with the main features /

The material characteristics from which the beam is built can be extracted from the analysis report of any of programs and are given in Table 1.

Carcteristicile materialului din care este construita barsa se pot extrage din raportul de analiza al oricaruia dintre programe si sunt date in tabelul 1.

Table 1

The material properties used (carbon steel)

The reference model	Properties	
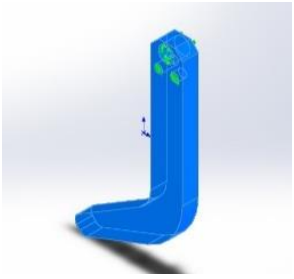	Name	Plain Carbon Steel
	Model type	Linear Elastic Isotropic
	Default breaking criterion	Unknown
	Breaking limit	2.20594e+008 N/m^2
	Breaking strength	3.99826e+008 N/m^2
	Mass density	7800 kg/m^3
	Elastic modulus	2.1e+011 N/m^2
	Poisson's ratio	0.28
	Thermal expansion coefficient	1.3e-005 /Kelvin

The chosen material (Plain Carbon Steel) is part of the materials library of SolidWorks program. For Autodesk Inventor program this material was introduced by the operator in the database.

Bearing

Bearing the structure or border conditions (or in the language of some software manufacturers that include modules of finite element method, linking conditions with external environment) are naturally required in the areas where the beam is mounted on the bearing structure - cylindrical surfaces of the three holes grouped at the top of the structure. The way in which the bearing is made is called mounting of the geometry in both programs we worked and is materialized in canceling translations of all meshing nodes located on the beam surfaces fixing holes on the bearing structure. In Fig.2 are given the representations of the bearing areas of the structure in both solving alternatives (the one that uses the SolidWorks program and the other that uses Autodesk Inventor).

Materialul ales (Plain Carbon Steel) face parte din biblioteca de materiale a programului SolidWorks. Pentru programul Autodesk Inventor acest material a fost introdus de operator in baza de date.

Rezemarea

Rezemarea structurii sau conditiile pe frontiera (sau in limbajul unora dintre producatorii de programe ce includ module de metoda elementului finit, conditiile de legatura cu mediul exterior), se impun in mod natural in zonele de prindere a barsei la structura portanta – suprafetele cilindrice ale celor trei gauri grupate la partea superioara a structurii. Modul in care se face rezemarea este numit fixare a geometriei in ambele programe in care s-a lucrat si se concretizeaza in anularea translatiilor tuturor nodurilor discretizarii situate pe suprafetele gaurilor de fixare a barsei pe structura portanta. In Fig. 2 se dau reprezentarile zonelor de rezemare a structurii in ambele variante de rezolvare (cea care foloseste programul SolidWorks si cea care foloseste programul Autodesk Inventor).

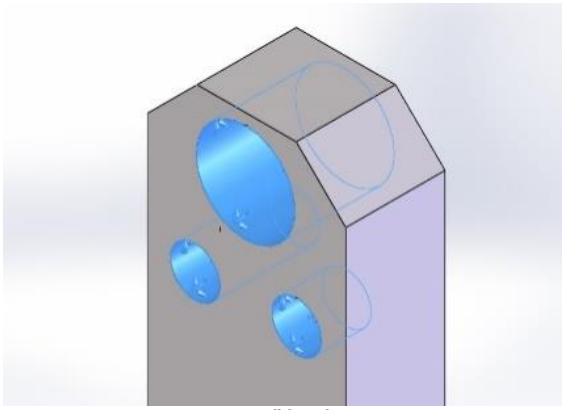

SolidWorks

Autodesk Inventor

Fig. 2 - Bearing the structure by canceling translations in all nodes on the hatched surfaces

Loading

Loading the structure or applying tasks can be done in various ways. In this paper are addressed issues of continue bodies mechanics, The loads may be the nature of forces, some pressures, moments or gravitational, possibly even all being able to participate to the complex loads.

In this example, the action of the soil on the soil working bodies found in the soil is shaped by a pressure to the intensity of 10^6 Pa, that was applied to all surfaces marked in fig.3 by arrows or / and by hatching.

Incarcarea

Incarcarea structurii sau aplicarea sarcinilor se poate face in diverse moduri. In aceasta lucrare fiind abordate probleme de mecanica corpurilor continue, incarcarile pot fi de natura unor forte, a unor presiuni, momente sau gravitationala, eventual chiar toate putand participa la solicitarile complexe.

Pentru acest exemplu, actiunea solului asupra organelor de lucru aflate in sol s-a modelat printr-o presiune cu intensitatea de 10^6 Pa, aplicata pe toate suprafetele marcate in fig.3 prin sageti sau/si prin hasurare.

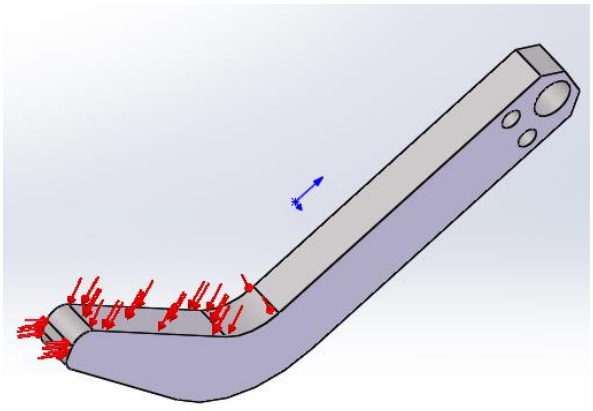

SolidWorks

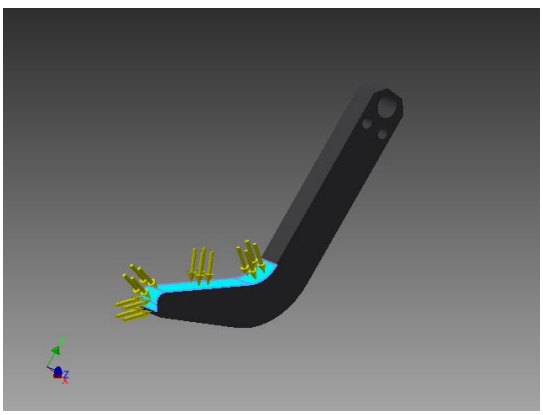

Autodesk Inventor

Fig.3 - Loading the structure with the pressure of 100000 Pa on the surfaces marked with arrows or hatched

Obviously, in order to model the soil – working body interaction can also be used other models extremely complicated in terms of bearing and loading.

Some alternative models are obtained very simply by reversing the loading areas with those of bearing or changing loads from pressures in forces. The complex models, often hybrid are obtained taking in consideration the soil and a part or all the bearing structure.

Meshing

Meshing in the two types of programs is graphically represented in Fig. 4 and the main characteristics in each of the variants are given below.

Evident, pentru modelarea interactiunii sol – organ de lucru, se pot folosi si alte modele extrem de complicate in ceea ce priveste rezemarea si incarcarea.

Unele modele alternative se obtin foarte simplu, inversand zonele de incarcare cu cele de rezemare sau schimband incarcarile din presiuni in forte. Modele complexe, de cele mai multe ori hibride, se obtin considerand si solul si o parte sau toata structura portanta.

Discretizarea

Discretizarea, in cele doua variante de programe este reprezentata grafic in Fig. 4 iar caracteristicile principale in fiecare dintre variante este tabelata mai jos.

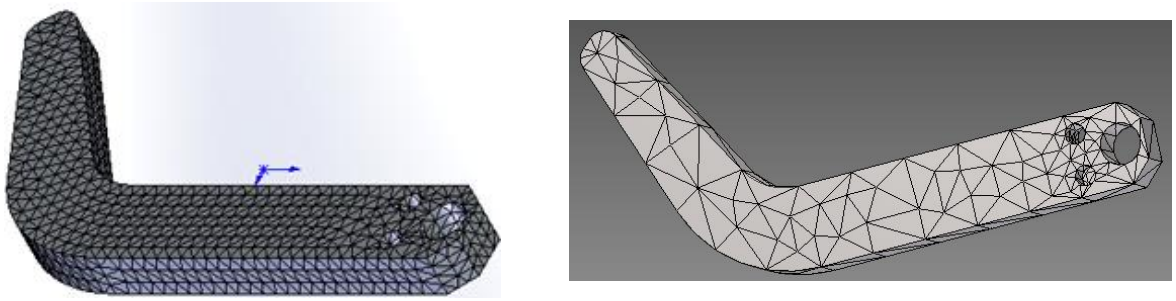

Fig.4 - The intersection of the structure meshing network with its border for each of the two programs used SolidWorks (right) and Autodesk Inventor

Meshing of the structure in both variants corresponds meshing on the two programs, automatically set to the established resolution by the software producers and their main characteristics appear in Table 2. These meshing can be refined or simplified, in order to obtain a more precise result or in a less time. A convergence analysis to refine the meshing networks is given in Table 5.

Discretizarile structurii, in ambele variante corespund la discretizarile pe care cele doua programe sunt setate automat la rezolutia stabilita de producatorii programelor si caracteristicile lor principale apar in Tabelul 2. Aceste discretizari se pot rafina sau se pot simplifica in vederea obtinerii unui rezultat mai exact sau in timp mai scurt. O analiza de convergenta la rafinarea retelelor de discretizare este data in Tabelul 5.

Table 2

The main characteristics of the meshing, automatically set for both programs used

Characteristic	SolidWorks	Autodesk Inventor
Number of nodes	12314	3027
Number of elements	7527	1665

RESULTS

The main results of the linear elastic structural analysis are: the values of the relative displacement vector, the values of specific deformation tensor and the Cauchy's stress tensor in each node of the meshing network.

With these values are calculated: the resultant relative displacement, the resultant specific deformation or its equivalent and the Von Mises equivalent stress [1], [2], [3], [4], [6]), terms in which is estimated the way how the structure meets the demands imposed. In this article, for economic reasons, at the static analysis we have discussed only the last three characteristics of the solution.

The main results of the analysis in frequency (or modal analysis, [6]) consist of the first n frequencies of own spectrum, the n number being set by the user and the deformed shapes of the structure being set when it vibrates on the selected frequencies of own spectrum.

The relative displacement

The relative displacement resulted is an important parameter of structures deformation. For agricultural machinery designed for tillage, a too high value of relative displacement can lead to a poor quality of agricultural works. The arrow of the sowing machines bearing structure should be limited, so not to alter the distances between seeded rows, for example.

REZULTATE

Principalele rezultate ale analizei structurale liniar elastice sunt: valorile vectorului deplasare relativa, valorile tensorului deformatie specifica si ale tensorului tensiune Cauchy, in fiecare nod al retelei de discretizare.

Cu aceste valori, se calculeaza deplasarea relativa rezultanta, deformatia specifica rezultanta sau echivalenta si tensiunea echivalenta (Von Mises, [1], [2], [3], [4], [6]), termeni in care se apreciaza masura in care structura face fata solicitarilor aplicate. Pentru acest articol, din motive de economie, la analiza statica s-au luat in discutie numai ultimele trei caracteristici ale solutiei.

Principalele rezultate ale analizei in frecvente (sau analiza modala, [6]) constau in primele n frecvente ale spectrului propriu, numarul n fiind setat de utilizator, si formele deformate ale structurii atunci cand aceasta vibreaza pe frecventele selectate ale spectrului propriu.

Deplasarea relativa

Deplasarea relativa rezultanta este un parametru important al deformarii structurilor. Pentru masinile agricole destinate lucrarilor solului, o valoare prea mare a acesteia putand conduce la calitatea necorespunzatoare a lucrarilor agricole. Sageata structurii portante a masinilor agricole de semanat trebuie sa fie limitata pentru a nu altera distantele dintre randurile semanate, de exemplu.

In fig.5 are given by comparison the states of the resultant relative displacement on the beam border, states provided by the two finite element analysis programs used. It is noted, the coincidence of the maximum values and the concordance of the distribution of the values of resultant relative displacement field.

In fig.5 sunt date comparativ starile de deplasare relativa rezultanta pe frontiera barsei, stari furnizate de cele doua programe de analiza cu elemente finite folosite. Se observa coincidenta valorilor maxime si concordanta distributiei valorilor campului de deplasare relativa rezultanta.

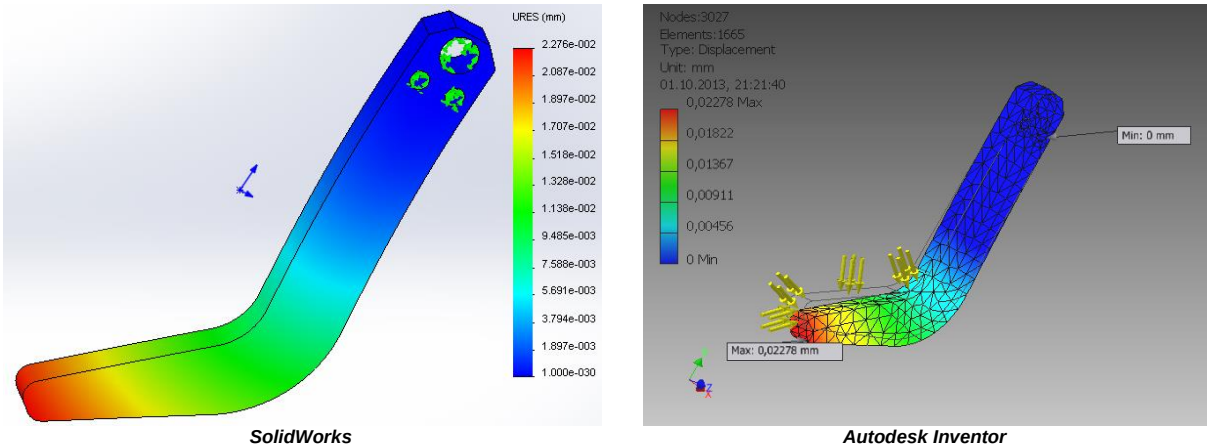

SolidWorks ***Autodesk Inventor***

Fig.5 - The map of the resultant relative displacement on the border structure provided by the finite element analysis module of each of the two programs

The convergence study of the solutions with meshing from Table 5 demonstrates, even more clearly, convergence of the solutions of the two programs.

The Von Mises equivalent stress

The Von Mises equivalent stress [1], [2], [3], [4], [6] is the measure of the stress in metal structures and is used for comparing with the yield strength, towards which, in order to functioning in elastic range, it must be smaller.

Studiul de convergenta a solutiilor cu discretizarea, din tabelul 5 demonstreaza inca si mai clar convergenta solutiilor celor doua programe.

Tensiunea echivalenta (Von Mises)

Tensiunea echivalenta (Von Mises), [1], [2], [3], [4], [6], este masura tensiunii in structurile metalice care se foloseste pentru compararea cu tensiunea limita de curgere, fata de care, in scopul functionarii in domeniul elastic, trebuie sa fie mai mica.

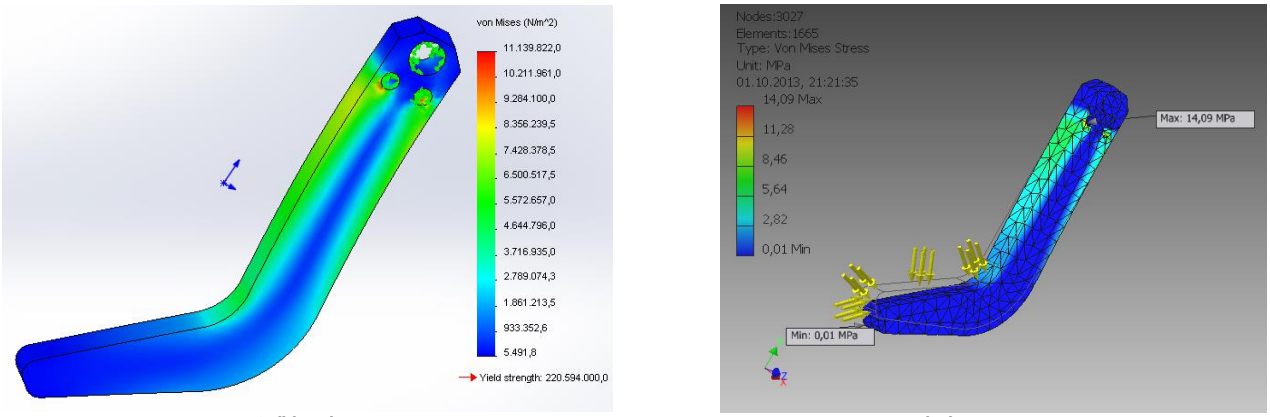

SolidWorks ***Autodesk Inventor***

Fig.6 - The map of the Von Mises equivalent stress on the structure border provided by the finite element analysis module of each of the two programs

In fig.6 are represented the equivalent stress fields on the beam border, fields resulted by using structural analysis programs, mentioned above. Although, as distribution in the structure, the two fields are similar, qualitatively, the maximum value indicated by the Autodesk Inventor program is by 26.48% higher than the maximum value indicated by SolidWorks program.

Since the difference is significant, a convergence study has been made, which results are given in Table 5, but this study raises new questions. These questions are not related to the training of the engineer, but can be setup details of the very complex numerical analysis.

In fig.6 sunt reprezentate campurile de tensiune echivalenta pe frontiera barsei, campuri rezultate prin folosirea programelor de analiza structurala sus mentionate. Desi ca distributie in structura, cele doua campuri se aseamana, calitativ, valoarea maxima indicata de programul Autodesk Inventor este cu 26,48 % mai mare decat valoarea maxima indicata de programul SolidWorks.

Deoarece diferenta este semnificativa s-a facut un studiu de convergenta ale carui rezultate sunt date in Table 5 si care nu face decat sa ridice noi semne de intrebare. Aceste intrebari nu tin insa de pregatirea inginerului utilizator neaparat, pot fi detalii de setare a analizei numerice deosebit de complexe.

The resultant specific deformation

The tensor of specific deformation is the gradient of the relative displacement in relation to spatial variables and its components and are used to calculate the components of Cauchy stress tensor, when the structure works in elastic linear field.

Deformatia specifica rezultanta

Tensorul deformatiei specifice este gradientul deplasarii relative in raport cu variabilele spatiale, iar componentele acestuia se folosesc pentru calculul componentelor tensorului tensiunilor Cauchy atunci cand structura lucreaza in domeniul elastic liniar.

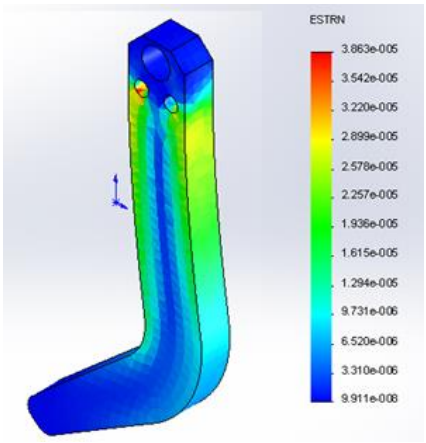

SolidWorks

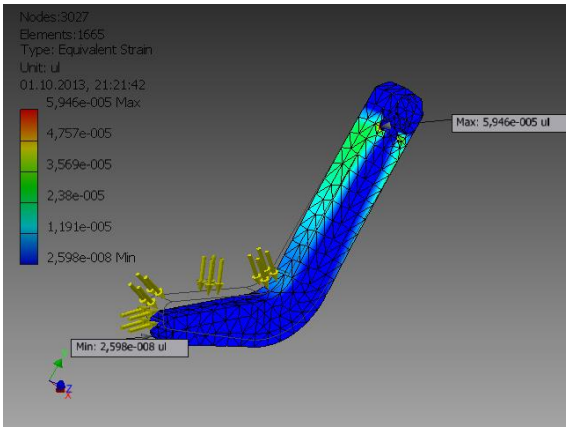

Autodesk Inventor

Fig.7 - The map of equivalent strain on the structure border provided by the finite element analysis module of each of the two programs

Using the components of the specific deformation tensor is calculated the equivalent specific or total deformation, which is a measure of the specific deformation in metallic structures. The distribution of the equivalent specific deformation on the structure border for both solutions is given in fig.7. As the equivalent stress, the specific deformation for the given solution using Autodesk Inventor program is approximately 28% higher.

The safety factor

The safety factor is calculated relatively to the yield strength stress and varies on the structure border in the two variants of solving, according to maps in Fig.8

Folosind componentele tensorului deformatie specifica se calculeaza deformatia specifica echivalenta sau totala, care este o masura a deformatiei specifice in structurile metalice. Distributia campului de deformatie specifica echivalenta pe frontiera structurii, pentru ambele solutii, este data in fig.7. Ca si tensiunea echivalenta, deformatia specifica la solutia data cu ajutorul programului Autodesk Inventor este cu aproximativ 28 % mai mare.

Factorul de siguranta

Factorul de siguranta se calculeaza relativ la tensiunea limita de curgere si variaza pe frontiera structurii, in cele doua variante de rezolvare, conform hartilor din fig.8.

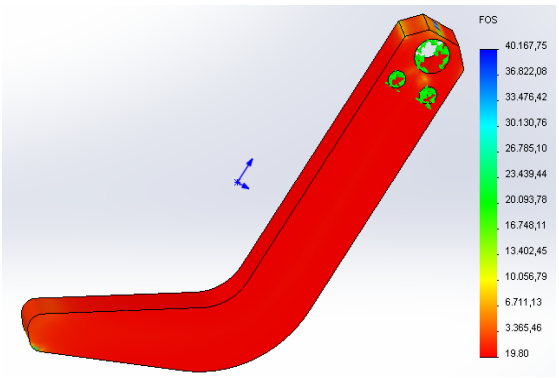

SolidWorks

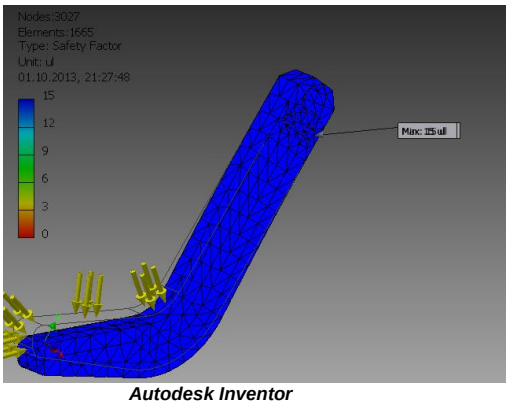

Autodesk Inventor

Fig.8 - The map of the safety factor on the structure border provided by the finite element analysis module of each of the two programs

Between the minimum values of the safety factor in the two variants of solving is transmited aproximately the same difference, as between the maximum values of the equivalent specific deformation and the equivalent stress.

For SolidWorks solution, the minimum safety factor is 19 and for the Autodesk Inventor solution, the minimum value of the safety factor is 15. Therefore, a difference of about 27%, comparable to that resulted from the maximum values of the specific deformation fields and the equivalent

Si intre valorile minime ale factorului de siguranta in cele doua variante de rezolvare, se transmite aproximativ aceeasi diferenta ca intre valorile maxime ale deformatiei specifice echivalente si tensiunii echivalente.

Pentru solutia SolidWorks factorul de siguranta minim este 19 iar pentru solutia Autodesk Inventor valoarea minima a factorului de siguranta este 15. Prin urmare, exista o diferenta de aproximativ 27%, comparabila cu cea rezultata din valorile maxime ale campurilor de

stress in the structure, exists.

Transmission of the error is completely natural, considering that works with the same material and the calculation relation is extremely simple for the safety factor.

Modal analysis

The modal analysis, [6], determines the own frequencies (first few) and own vibration modes of the structures. Knowledge of these features help to avoid some resonant regimes in determining by vizualization of some causes of vibration, or some malfunction of equipment, defects due to variation on a characteristic frequency of one of the components.

In fig.9…13 are presented the deformation forms of the beam, when it vibrates in its own first five modes.

deformatie specifica si tensiune echivalente in structura.

Transmiterea erorii este absolut fireasca tinand seama ca se lucreaza cu acelasi material si relatia de calcul este extrem de simpla pentru factorul de siguranta.

Analiza modala

Analiza modala, [6], determina frecventele proprii (primele cateva) si modurile proprii de vibratie ale structurilor. Cunoasterea acestor caracteristici ajuta la evitarea in lucru a unor regimuri rezonante, in determinarea prin vizualizare a unor cauze de vibratie, sau a unor defecte de functionare a unor instalatii, defecte datorate variatiei pe o frecventa proprie a uneia dintre componente.

In fig.9...13 sunt desenate formele de deformatie ale bârsei atunci cand aceasta vibreaza in primele cinci moduri proprii.

The first own frequency (fundamental)

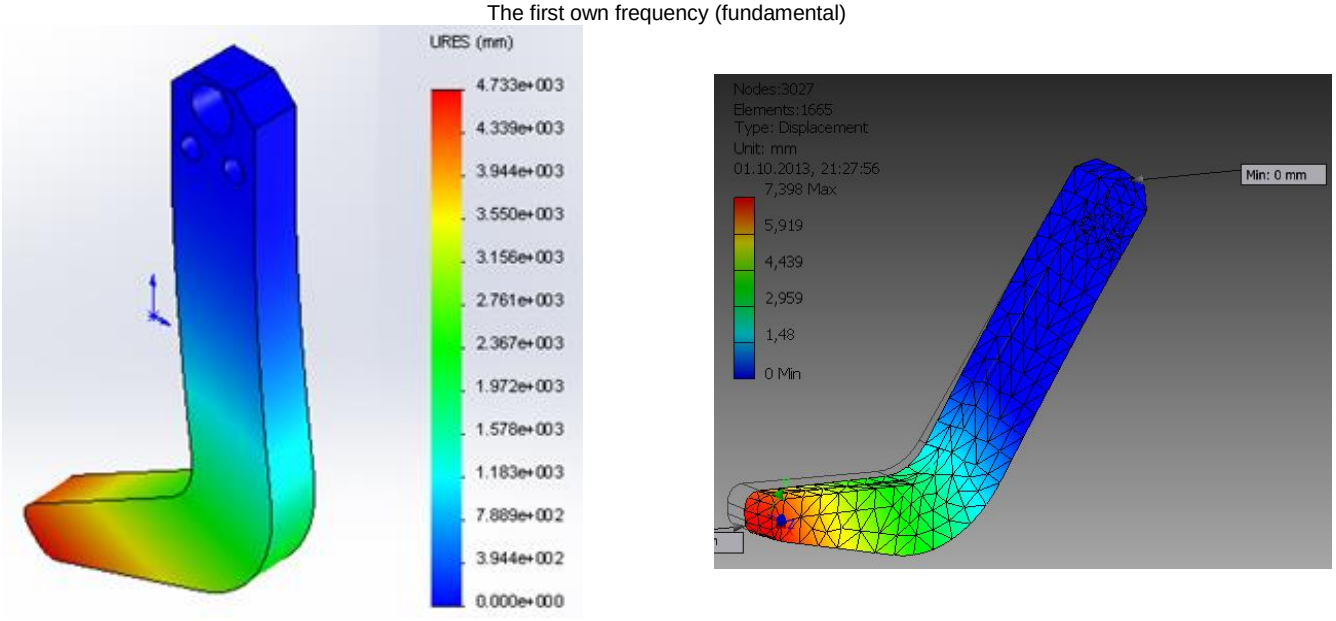

SolidWorks, f_1=534.41 Hz ***Autodesk Inventor, f_1=535.35 Hz***

Fig.9 - The deformed shape of the structure at vibration in its first own mode

A second own frequency

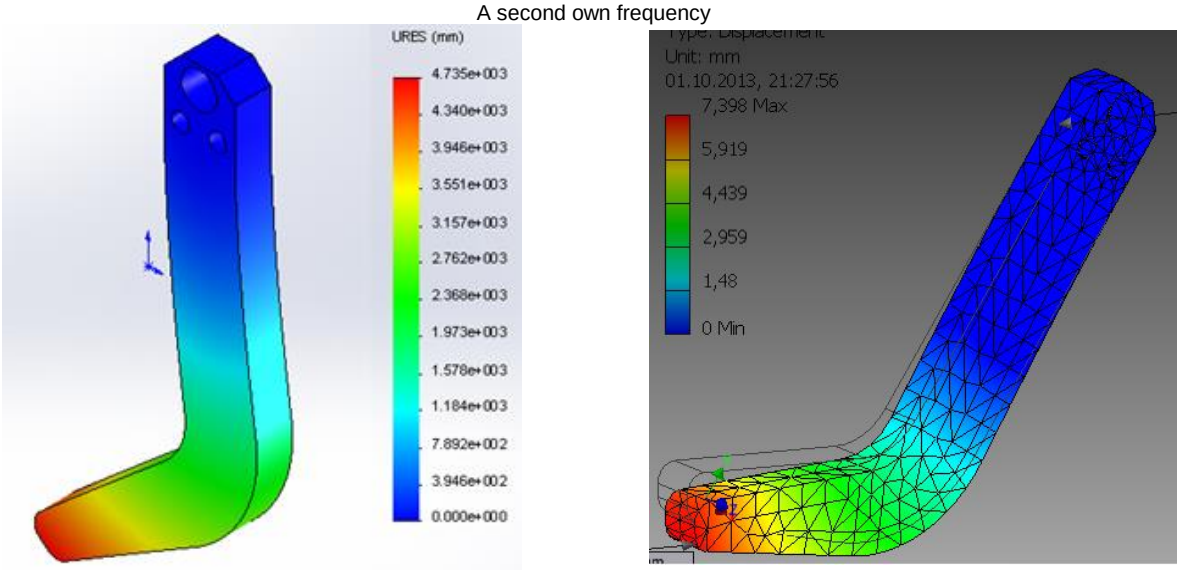

SolidWorks, f_2= 1024.50 Hz ***Autodesk Inventor, f_2= 1026.06 Hz***

Fig.10 - The deformed shape of the structure at vibration in the second own mode

A third own frequency

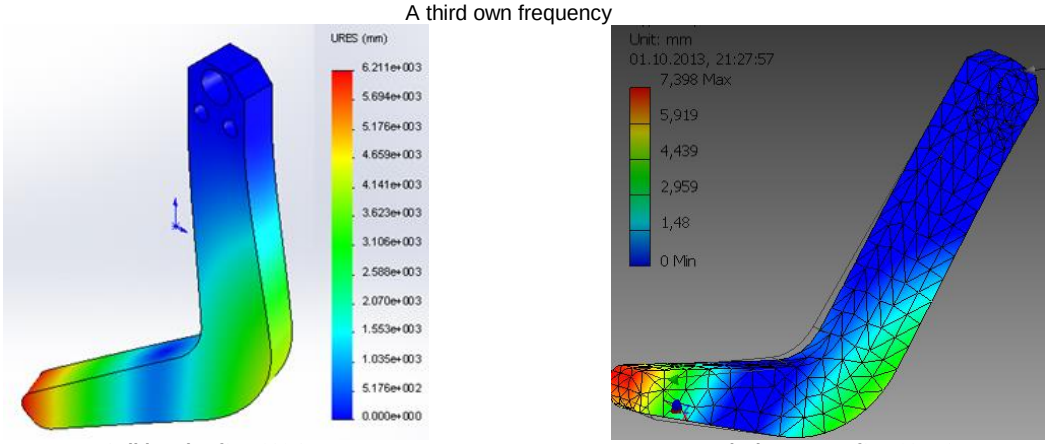

SolidWorks, f3= 1929.3Hz ***Autodesk Inventor, f3= 1934.43Hz***

Fig.11 - The deformed shape of the structure at vibration in the third own mode

A fourth own frequency

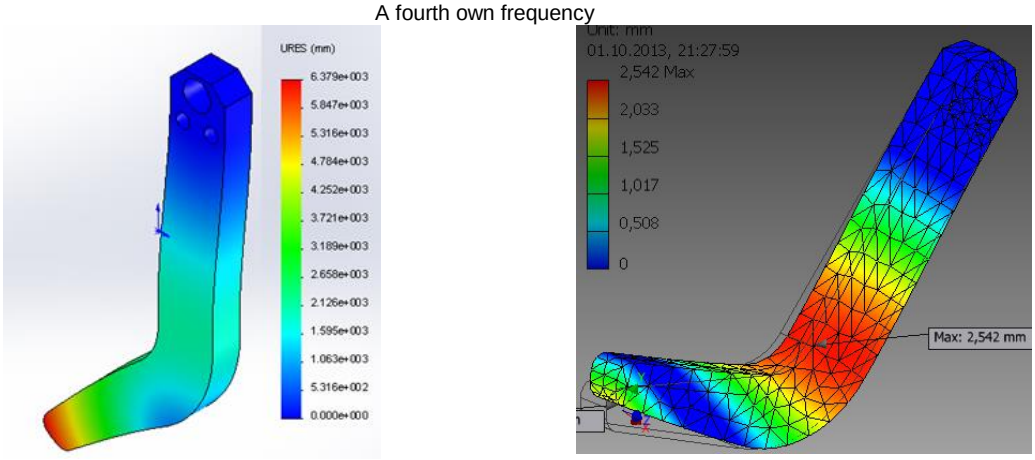

SolidWorks, f_4= 3853.80Hz **Autodesk Inventor, f_4= 3858.07Hz**

Fig.12 - The deformed shape of the structure at vibration in the fourth own mode

A fifth own frequency

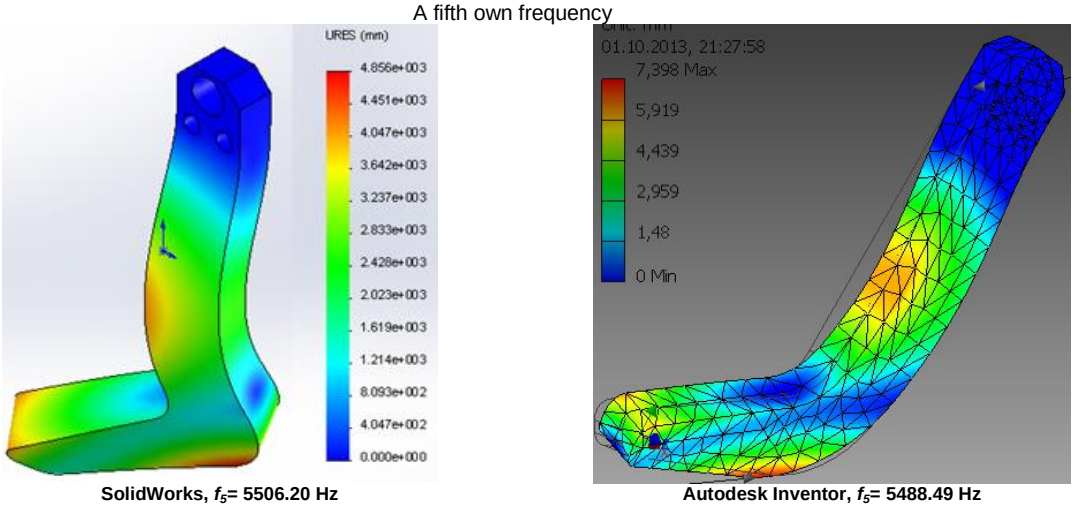

SolidWorks, f_5= 5506.20 Hz **Autodesk Inventor, f_5= 5488.49 Hz**

Fig.13 - The deformed shape of the structure at vibration in the fifth own mode

Comparative synthesis

An efficient comparison of the results of the two structural analysis programs for the same structrure under stress conditions in the same way can be done using Table 3 and Table 4.

Sinteza comparativa

O comparatie eficienta a rezultatelor celor doua programe de analiza structurala pentru o aceeasi structrura solicitata in acelasi mod, se poate face folosind tabelul 3 si tabelul 4.

Table 3

Autodesk Inventor Program

Number of nodes	Number of elements	Maximum equivalent stress [MPa]	Maximum resultant relative displacement [mm]
1459	760	14.00	0.02274
1664	888	15.45	0.02275
1713	910	12.04	0.02274
1962	1058	12.18	0.02276
2120	1144	13.79	0.02277
3027	1665	14.09	0.02278
4223	2420	15.84	0.02280
6939	4075	15.16	0.02280
20408	12971	15.47	0.02281
121907	82946	18.56	0.02282
778348	550974	30.23	0.02284

Table 4

SolidWorks Program

Number of nodes	Number of elements	Maximum equivalent stress [MPa]	Maximum resultant relative displacement [mm]
5230	2997	10.95	0.02275
8283	4914	10.39	0.02276
12314	7527	11.14	0.02276
17589	11023	11.14	0.02276
19331	12106	11.52	0.02278
21270	13431	12.08	0.02278
31512	20342	14.84	0.02279
33145	21381	11.62	0.02279
51821	34154	11.86	0.02279
53008	34925	12.21	0.02279
79171	52962	13.97	0.02281

Table 5

Comparative synthesis of results

Term	SolidWorks	Autodesk Inventor
Structure weight [kg]	0.215963	0.215963
Maximum resultant relative displacement [mm]	0.022760	0.0227788
Maximum equivalent stress [MPa]	11.14	14.095
Minimum safety factor	19.80	15.00
Fundamental natural frequency [Hz]	534.41	535.35

CONCLUSIONS

The structural analysis solutions of the beam for linear static analysis and modal analysis are partially satisfactory. If the modal analysis is more than satisfactory, the static analysis gives results only in terms of resultant relative displacement, but not satisfying enough, regarding the specific deformation and equivalent stress, namely, exactly in the most interesting part, from engineering point of view.These issues remain an open question to be studied at a deeper level, possibly contacting software manufacturers.

COSMOS/M structural analysis program, that is integrated in the current CAD SolidWorks program can give results (for a large number of types of finite elements with which it is working) both in nodes and on the elements.

The module of numerical solutions that solves the problem of finite element method in COSMOS program, evaluates stresses on each element of the module at a specific location within each element, in a point of the element (called Gaussian points or quadrature points). These points form the numerical basis of numerical integration schemes used in the finite elements codes. The number of selected points in this basis depends on the type and the quality of each element type.

The string of stresses obtained in the Gaussian points network inside each element are extrapolated in the nodes of each element.

CONCLUZII

Solutiile analizei structurale ale barsei la analiza static liniara si analiza modala sunt partial satisfacatoare. Daca analiza modala este mai mult decat satisfacatoare, analiza statica da rezultate convergente numai in termenii deplasarii relative rezultante, dar nu suficient de satisfacatoare in privinta deformatiei specifice si tensiunii echivalente, adica exact in partea cea mai interesanta din punct de vedere ingineresc. Aceste aspecte raman o problema deschisa care trebuie cercetata la un nivel mai profund, eventual contactand si producatorii programelor.

Programul de analiza structurala COSMOS/M care este integrat in actualul program CAD SolidWorks, poate da rezultatele (pentru o mare parte dintre tipurile de elemente finite cu care lucreaza) atat in noduri cat si pe elemente.

Modulul de solutii numerice care rezolva problema de metoda elementelor finite in programul COSMOS, evalueaza tensiunile pentru fiecare element al modelului la o locatie specifica in interiorul fiecarui element – intr-un punct al elementului (numite puncte Gaussiene sau puncte de cuadratura). Aceste puncte formeaza o baza numerica a schemelor de integrare numerica folosite in codurile elementelor finite. Numarul de puncte selectate in aceasta baza depinde de tipul si calitatea fiecarui tip de element.

Sirul tensiunilor obtinute in reteaua Gaussiana de puncte in interiorul fiecarui element sunt extrapolate in nodurile fiecarui element.

The nodal stress or stress in a some node is the average of all points from the Gaussian network, included in elements that have in one of the peaks the considered node.

The elemental stress or the stress in an element is the stress exactly calculated in the Gausiene points network (one and only one such point exists in each element). It is found that, the elemental values of the stress are the mean values of the nodal values from all element nodes. Most of the time, between the two types of stress values are differences, sometimes quite large, at least in some areas, usually in the most stressed.

The big difference between the nodal values and the elements shows that, the meshing should be refined to achieve the appropriate closeness or convergence.

REFERENCES

[1]. Ahrendts J. and collective (1995) - *Engineer Manual (Hutte. Die Grundlagen der Ingineurwissenschaften),* Technical Publishing House, Bucharest;
[2]. Buzdugan Gh. (1980) - *Strength of Materials*, Technical Publishing House, Bucharest;
[3]. Comănescu A., Suciu I., Weber Fr., Comănescu D., Mănescu T., Grecu B., Miklos I. (1982) - *Mechanics*, *Strength of materials and machine bodies,* Didactic and Pedagogic Publishing House, Bucharest;
[4]. Iacob C., Gheorghiţă I.S., Soare M., Dragoş L. (1980) - *Mechanical Dictionary*, Scientific and Encyclopedic Publishing House, Bucharest;
[5]. Letosnev M.N. (1959) - *Agricultural Machinery,* Agro-Forestry State Publishing House, Bucharest;
[6]. Marin C. (1997) - *Strength of materials and elasticity theory elements*, Biblioteca Publishing House,Târgovişte;
[7]. Ştefan A. & collective (1972) - *Dictionary of agricultural mechanics,* Publisher CERES, Bucharest;
[8]. Vedantham V. (2008) - *Nodal versus Elemental Stresses,* http://www.3dvision.com/wordpress2008/04/18/nodal-versus-elemental-stresses/

Tensiunea nodala, sau tensiunea intr-un nod oarecare, este media aritmetica a tuturor punctelor din reteaua gaussiana incluse in elementele care au intr-unul dintre varfuri nodul considerat.

Tensiunea elementala sau tensiunea intr-un element este exact tensiunea calculata in reteaua de puncte gausiene (cate un astfel de punct si numai unul exista in fiecare element). Se constata ca valorile elementale ale tensiunii sunt valorile medii ale valorilor nodale din toate nodurile elementului. De cele mai multe ori, intre cele doua tipuri de valori ale tensiunii exista diferente, uneori destul de mari, cel putin in anumite zone, de obicei cele mai tensionate.

Diferenta mare intre valorile nodale si elementale arata ca discretizarea trebuie rafinata pentru a atinge gradul de apropiere sau de convergenta convenabil.

BIBLIOGRAFIE

[1]. Ahrendts J. şi colectivul (1995) - *Manualul inginerului (Hutte. Die Grundlagen der Ingineurwissenschaften),* Editura Tehnică, Bucureşti;
[2]. Buzdugan Gh. (1980) - *Rezistenţa materialelor*, Editura Tehnică, Bucureşti;
[3]. Comănescu A., Suciu I., Weber Fr., Comănescu D., Mănescu T., Grecu B., Miklos I. (1982) - *Mecanica, Rezistenta materialelor si organe de masini*, Editura Didactică si Pedagogică, Bucuresti;
[4]. Iacob C., Gheorghiţă I.S., Soare M., Dragoş L. (1980) - *Dicţionar de mecanică,* Editura Stiinţifică şi Enciclopedică, Bucureşti;
[5]. Letosnev M.N. (1959) - *Masini Agricole*, Editura Agro-Silvica de Stat, Bucuresti;
[6]. Marin C. (1997) - *Rezistenţa materialelor şi elemente de teoria elasticităţii,* Editura Biblioteca, Târgovişte;
[7]. Ştefan A. & collective (1972) - *Dicţionar de mecanică agricolă*, Editura CERES, Bucureşti;
[8]. Vedantham V. (2008) - *Nodal versus Tensiuni Elementale*, http://www.3dvision.com/wordpress2008/04/18/nodal-versus-elemental-stresses/

STUDIES REGARDING A PNEUMATIC EQUIPMENT FOR SOWING SMALL SEEDS IN CUPS
/
STUDII PRIVIND REALIZAREA UNUI ECHIPAMENT PNEUMATIC PENTRU SEMĂNATUL SEMINŢELOR MICI ÎN ALVEOLE

Prof. Ph.D. Eng. Sărăcin I.[1)], Lect. Ph.D. Eng. Pandia O.[2)], Conf. Ph.D. Bozgă I.[2)], PhD. Eng. Ganea I.[3)]
[1)]University of Craiova, Faculty of Agriculture / Romania; [2)] University of Agricultural Sciences and Veterinary Medicine Bucharest / Romania; [3)]INMA Bucharest / Romania
Tel: 0762142949; E-mail: ion_saracin@yahoo.com

Abstract: *The paper presents theoretical studies and laboratory experiments regarding pneumatic equipment for sowing small seeds in cups, highlighting the advantages of this type of equipment with superior parameters obtained from the considered crops.*

Keywords: *seeds, distributor, ditch, cups, sowing*

INTRODUCTION

Utilization the equipment proposed for sowing small seeds in seedbeds decreases the volume of manual force required to do the work, decreases the amount of seed per surface unit, eliminates the execution of works thus reducing costs for obtaining seedlings. [3], [4].

It is also ensured the sowing depth and emerging uniformity of plants. To achieve the equipment plastic products or existing components of some installations and equipment that can be reused, are used.

Studies and experimental tests relating to the production index, consumption standard, the emerging degree and the plants percentage obtained will be continued. Based on the rules relating to the influencing factors for achieving optimal density can be established by species, the crop nature, the crop schemes implicitly expressing the productivity. [1], [2].

MATERIALS AND METHODS

Studies aim to achieve an equipment that can be used to set up small specific seed crops respectively forestry, flower, vegetable species and develop in the mechanization laboratories of the Faculty of Horticulture and Agriculture from Craiova. [6, 7]

Therefore, some of the methods used for sowing manually or mechanized the small seeds, existing in the country and abroad, were studied. (fig.1). [8]

Rezumat: *În lucrare se prezintă studiile teoretice şi experimentările din laboratoare privind realizarea unui echipament pneumatic pentru semănatul seminţelor mici în alveole, evidenţiind avantajele acestui tip de echipament prin parametrii superiori obţinuţi la culturile luate în calcul.*

Cuvinte cheie: *seminţe, distribuitor, rigolă, alveolă, semănat*

INTRODUCERE

Folosirea echipamentului propus pentru semănatul seminţelor mici în răsadniţe scade volumul de forţă manuală necesar pentru realizarea lucrării, scade cantitatea de seminţe pe unitatea de suprafaţă, elimină efectuarea unor lucrări reducând astfel cheltuielile pentru obţinerea răsadurilor. [3], [4].

De asemenea este asigurată adâncimea de semănat şi uniformitatea de răsărire a plantelor. Pentru realizarea echipamentului se folosesc mase plastice sau elemente componente ale unor instalaţii şi aparate existente care pot fi refolosite.

Studiile şi încercările experimentale referitoare la indici de producţie, norme de consum, gradul de răsărire şi procentul de plante obţinut vor continua. Pe baza regulilor referitoare la factorii de influenţă pentru realizarea unei densităţi optime se pot stabili pe specii, pe natură de culturi, pe scheme de cultură, implicit de producţie care exprimă în final productivitatea. [1], [2].

MATERIALE ŞI METODE

Studiile efectuate în vederea realizării unui echipament care să poată fi folosit la înfiinţarea culturilor specifice din seminţe mici respectiv specii silvice, floricole, legumicole au început şi se desfăşoară în laboratoarele de mecanizare ale Facultăţii de Horticultură şi Agricultură din Craiova. [6, 7]

În acest scop au fost studiate o parte din metodele folosite pentru semănatul seminţelor mici, manuale sau mecanizate existente în ţară şi în străinătate. (fig.1). [8]

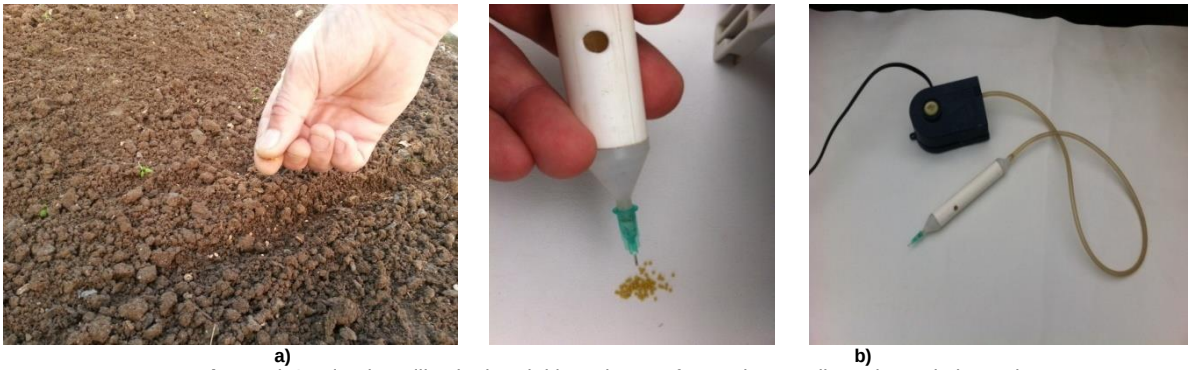

a) b)

Fig.1 - a) Sowing in gullies by hand; b) equipment for sowing small seeds, grain by grain

Also have been studied some characteristics of the seeds belonging to forestry, flower and vegetable species. [2]

Totodată au fost studiate şi unele caracteristici ale seminţelor din speciile silvice, floricole şi legumicole. [2]

Fig. 2 – Tabacco seeds covered by treating substances

Fig. 3 – Nude small and very small seeds

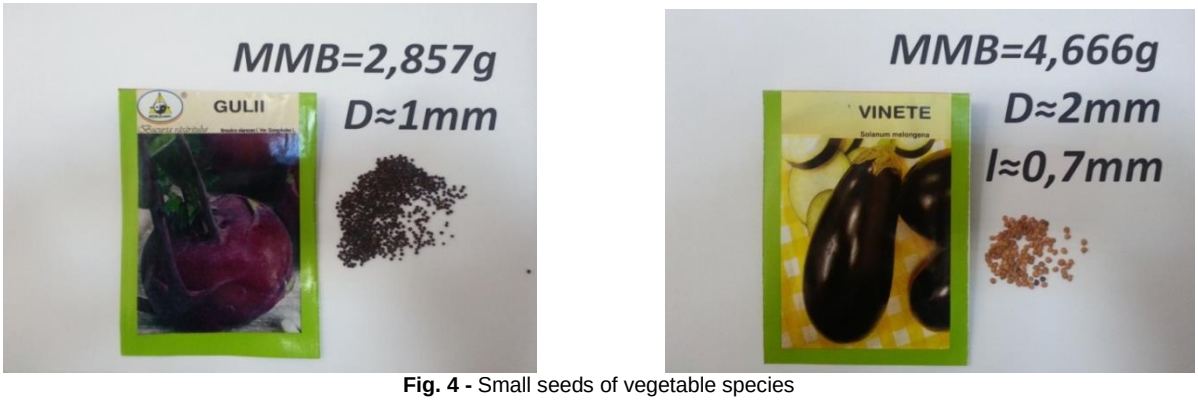

Fig. 4 - Small seeds of vegetable species

Documentation and studies consideration was given to the following:

- Direct sowing in cups;
- Consecutive sowing in several cups at the same time;
- Possibilities for sowing depth adjustment; [5]
- Automation possibilities for sowing small seeds in cups. [9], [10]

Based on the rules relating to the influencing factors for achieving optimal density, the production indexes, expressing the final productivity may be established on species, the crops nature on culture scheme.

Research and testing relating to the production indices at the consumption norms, will continue. [6], [7]

Following the results obtained recently through research, the consumption norms of the seeds sown in seedbeds should be set in relation to the average index of soil emergence, determined by laboratory germination, with plants maintenance index and the percentage of capable plants obtained. Sowing rate can be calculated as it follows:

a) Sowing rate in number of seeds per linear meter of the ditch channel, with the relation (1):

Documentarea şi studiile au luat în consideraţie şi următoarele:

- Semănatul direct în alveole;
- Semănatul consecutiv în mai multe alveole în acelaşi timp;
- Posibilităţile de reglare a adâncimii de semănat; [5]
- Posibilităţile de automatizare a semănatului a seminţelor mici în alveole. [9], [10]

Pe baza regulilor referitoare la factorii de influenţă în realizarea unor densităţi optime, se pot stabili pe specii, pe natură de culturi pe scheme de cultură, indicii de producţie care exprimă în final productivitatea .

Cercetările şi experimentările referitoare la indicii de producţie, la normele de consum, vor continua. [6], [7]

Ca urmare a rezultatelor obţinute în ultimul timp, prin cercetare, normele de consum de seminţe la semănăturile în răsadniţe trebuie să se stabilească în raport cu indicele mediu de răsărire în sol, cu germinaţia determinată în laborator, cu indice de menţinere a plantelor precum şi procentul de plante apte obţinute . Norma de semănat se poate calcula astfel:

a) *Norma de semănat în număr de seminţe la metru liniar de rigolă* , după relaţia (1):

$$n = i * \frac{100}{R} * \frac{100}{M} * \frac{100}{A} = I * \frac{1.000.000}{R * M * A} \text{ seeds/meter,}$$

or / sau:

$$n = \frac{I}{L} * \frac{1.000.000}{R*M*A} \text{ [seeds/m]}, \quad (1)$$

where:
n = consumption rate (sowing rate) in seeds number and seeds number to be sown per meter [pcs / m];
i = index of production per ditch meter [pcs/m];
R = index (percentage) of emerging;
G = technical germination or potency germination indicated in the analysis report [%];
M = index (percentage) of plant maintenance;
A = percentage of plants capable for planting.

b) *Sowing rate in grams of seed per meter,* with the relation (2):

în care:
n = norma de consum (norma de semănat) în număr de seminţe sau numărul de seminţe ce trebuie semănat la metru [buc/m];
i = indicele de producţie la metru de rigolă [buc/m];
R = indicele (procent) de răsărire;
G = germinaţia tehnică sau potenţa germinativă indicată în buletinul de analiză [%];
M = indicele (procent) de menţinere al plantelor;
A = procentul de plante apte de plantat.

b) *Norma de semănat în grame de seminţe la metru*, după relaţia (2):

$$q = n * \frac{G1000}{1000} * \frac{100}{P} = n * \frac{G1000}{10*P} \text{ [g/m]}$$

or / sau

$$q = \frac{I}{L} * \frac{1.000.000}{R*M*A} * \frac{G1000}{10*P} = I * \frac{1.000.000*G1000}{R*M*A*P} \text{ [g/m]} \quad (2)$$

where:
q = consumption rate (sowing rate), in grams of seeds or quantity of seeds in grams to be sown at linear meter;
G1000 = weight of 1000 seeds, indicated in the analysis report, stating the average number of seeds per kilogram - NK;
P = seeds purity [%], inidicated in analysis reports.

în care:
q = norma de consum (norma de semănat), în grame de seminţe sau cantitatea de seminţe în grame ce trebuie semănat la metrul liniar;
G1000 = greutatea a 1000 de seminţe, indicată în buletinele de analiză, ce menţionează şi numărul mediu de seminţe la kilogram – NK;
P = puritatea seminţelor [%], inidicată în buletinele de analiză.

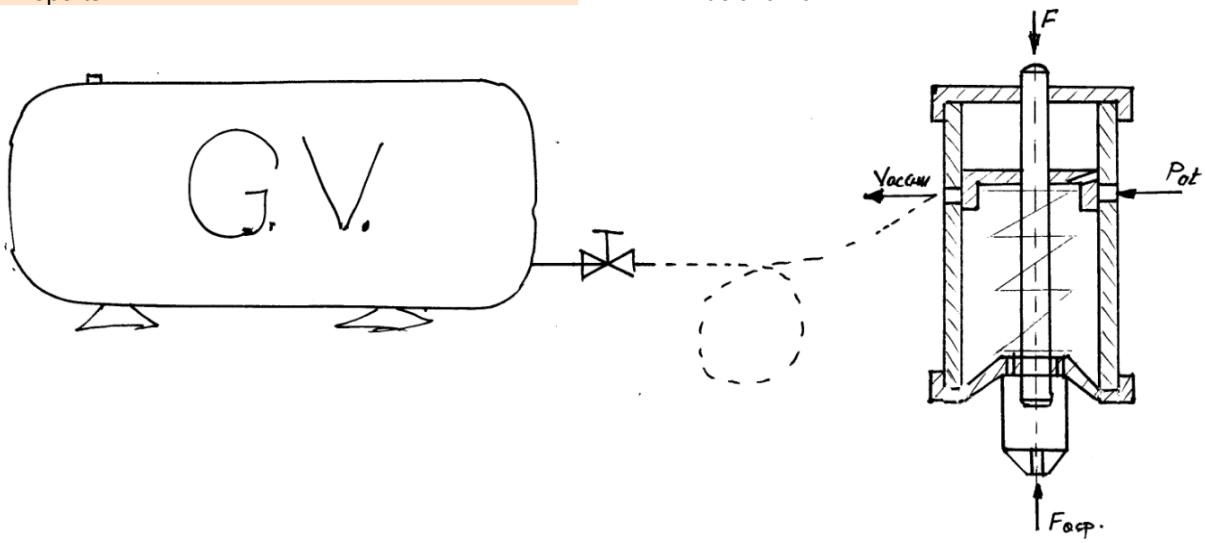

Fig. 5 – Functional diagram of the equipment

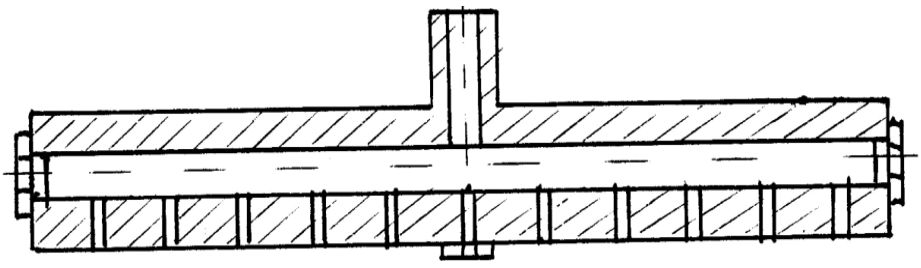

Fig. 6 – Distributor for 8 nozels

RESULTS

The results obtained in laboratory regarding the uniformity of distribution of turnip, eggplant and tabacco seeds are shown in fig. 7, 8 and 9:

REZULTATE

Rezultetele obţinute în laborator privind uniformitatea de distribuire pentru seminţele de gulie, vinete, respectiv tutun sunt prezentate în fig. 7, 8 şi 9:

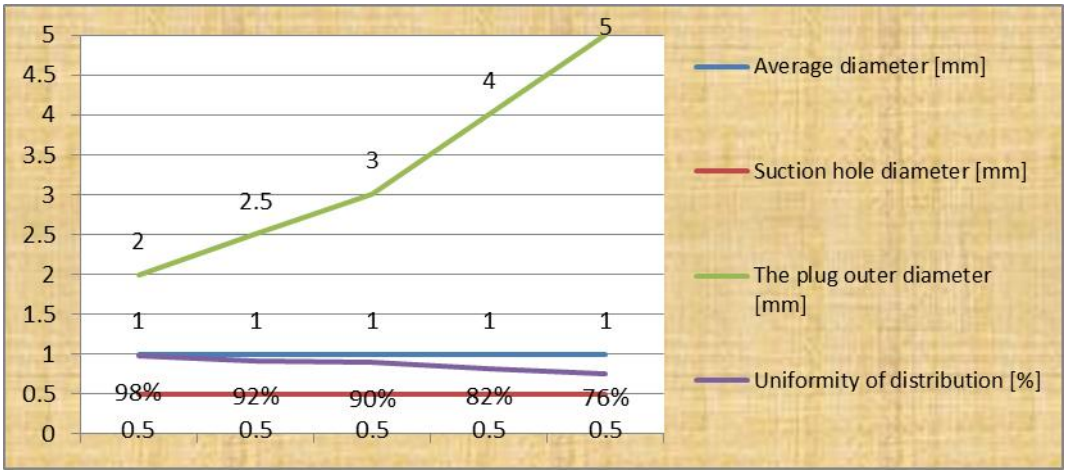

Fig.7 - Uniformity of distribution for turnip small grains average diameter of 1 mm and suction hole diameter of 0.5 mm

From the fig.7 it can be observed that the uniformity of seed distribution decreases with the outer diameter of the cone. This happens probably because the surface between the hole and the exterior of the cone allows setting more seeds on it during the aspiration.

Din fig.7 se observă că uniformitatea de distribuire a semințelor scade odată cu creșterea diametrului exterior al conului. Probabil datorită faptului că suprafața dintre orificiu și exteriorul conului permite așezarea mai multor semințe pe el în timpul aspirației.

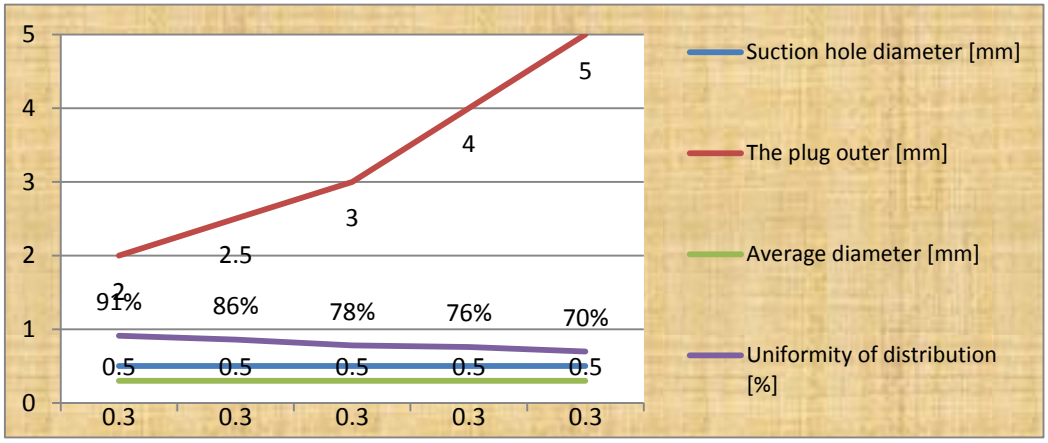

Fig.8 - Uniformity of distribution for small seeds of eggplants with average diameter of 1 mm and suction hole diameter of 0.5 mm

From the fig.8 it can be observed that the uniformity of seed distribution decreases with the outer diameter of the cone. This happens probably because the surface between the hole and the exterior of the cone allows setting more seeds conditioned by width during the aspiration.

Din fig.8 se observă că uniformitatea de distribuire a semințelor scade odată cu creșterea diametrului exterior al conului. Probabil că suprafața rezultată între orificiu și exteriorul conului permite așezarea mai multor semințe condiționate de lățime în timpul aspirației.

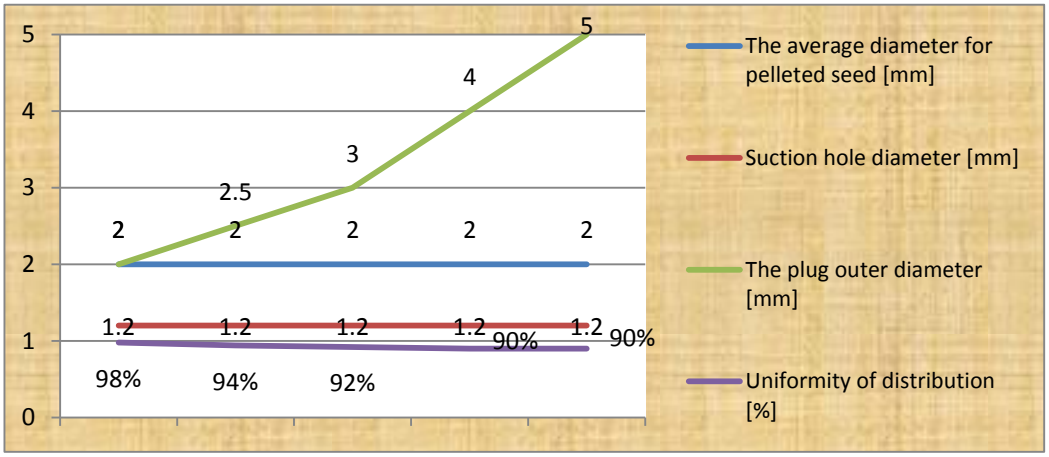

Fig.9 - Uniformity of distribution for small seeds of pelleted tobacco with average diameter of 1 mm and suction hole diameter of 0.5 mm

From the fig.9 it can be observed that the uniformity of seed distribution decreases with the outer diameter of the cone. This happens probably because the seeds outer diameter grows by pelleting and the surface between the cone and the hole does not allow setting more seeds during the aspiration.

CONCLUSIONS

For performing the production indexes the following technical indications related to compulsory minmum works to perform are imposed, such as:

- *When preparing the seeds*: verification of seeds quality, establishing the sowing norms, setting the sowing method, preparation of seeds according to each variety;
- *When sowing the seeds*: soil temperature, at the moment of sowing should be between +9ºC ... +15ºC;
- *When covering the seeds*: seeds covering with the humus-sand mixture prepared, slightly compressing the humus after soil covering;
- *Equipment can be used in narrower spaces, being easily to handle and use;*
- *Driving the vacuum generator can be done elctrically or thermically;*
- *Depression in installation does not require greater values, because of the seeds small mass;*
- *Nozzles holes should represent 0.5-0.6 out of the smallest size of seed;*
- *Nozzle peak should not allow placing more than one seed on the nozzle hole;*
- Seeds aspired within the sucking tube can be collected in lower cover, recovered and considered as innapropriate;
- By using this equipment, the productivity is increased, the space of establishing the seedlings is reduced, the seeds norm is diminished;
- The germinating, rising and development space of plants is assured;
- Equipment can be automated and built by minimum costs.

REFERENCES

[1]. Cristache A. et al., (1968) – *Forest species Culture quickly increasing*, Imprint Agrosylvicultural Bucharest.
[2]. Hulea A., (1962) – *Contributions on art culture in nurseries of some species of exotic,* Forest resinous,

Din fig.9 se observă că uniformitatea de distribuire a semințelor scade odată cu creșterea diametrului exterior al conului. Probabil că prin drajare diametul exterior al semințelor crește, iar suprafața dintre con și orificiu nu permite așezarea mai multor semințe în timpul aspirației.

CONCLUZII

Pentru realizarea indicilor de producţie se impune realizarea întocmai a următoarelor indicaţii tehnice privind lucrările minime obligatorii ce trebuie executate în răsadniţe astfel:

- *La pregătirea seminţelor*: verificarea calităţii seminţelor; stabilirea normelor de semănat; precizarea modului de semănare; pregătirea seminţelor conform specificului fiecărei specii;
- *La semănarea seminţelor*: temperatura solului, la data semănării trebuie sa fie intre +9ºC ... +15ºC;
- *La acoperirea seminţelor*: acoperirea seminţelor cu amestecul indicat de humus şi nisip pregătit; tasarea uşoară a humusului după acoperirea solului;
- *Echipamentul poate fi folosit în spaţii mici fiind uşor de manipulat şi folosit;*
- *Acţionarea generatorului de vacuum se poate face elctric sau cu motor termic;*
- *Depresiunea în instalaţie nu necesita valori mari datorita masei mici a seminţelor;*
- *Orificiile duzelor trebuie să reprezinte 0,5-0,6 din cea mai mică dimensiune a seminţei;*
- *Vârful duzei să nu permită aşezarea mai multor seminţe în acelaşi timp pe orificiul duzei;*
- Seminţele aspirate în interiorul tubului de aspiraţie pot fi colectate în capacul inferior, pot fi recuperate şi considerate necorespunzătoare;
- Prin utilizarea echipamentului se măreşte productivitatea, se micşorează spaţiul de înfiinţare al răsadniţelor, se micşorează norma de seminţe;
- Se asigură spaţiul de germinare, răsărire şi dezvoltare al plantelor;
- Echipamentul poate fi şi automatizat şi construit cu costuri minime.

BIBLIOGRAFIE

[1]. Cristache A. ş.a, (1968), *Cultură de specii forestiere cu creştere rapidă*, Imprint Agrosilvicultură, Bucureşti.
[2]. Hulea A., (1962), *Contribuţii privind artă cultivării în pepiniere a unor specii exotice,* Răşinoaşe forestiere,

Magazine no.9;
[3]. Mărdărescu R. şi colab (1968) – *Motoare pentru automobile şi tractoare,* Didactic and Pedagogical Publishing, Bucharest;
[4]. Oprean A., Fl. Ionescu, Al. Dorin., 1982 **–** *Acţionări hidraulice, elemente şi sisteme,* Technical Publishing, Bucharest, pp. 205-207;
[5]. Sărăcin I., Marin G., Olimpia P., Florea G. (2009) - *Baza energetică pentru agricultură, horticultură, silvicultură*, Aius Printed Publishing – Craiova;
[6]. Saracin I., Pandia O., Netoiu C., (2010) – *Theoretical study of achieving seeders for forestry nurseries of resinous*, Annals of the University of Craiova - Agriculture, Montanology, Cadastre Series, Vol. XL /2, pag. 556-560;
[7]. Saracin I., Pandia O., (2010) - *Sowing for small seeds*, Annals of the University of Craiova - Agriculture, Montanology, Cadastre Series, Vol. XL /2, pag. 561 - 565;
[8]. Sărăcin I., (2002-2004) - *Universal light sandy soils drill*, Contract CNCSIS, No.33451, University of Craiova;
[9]. Scripnic V., Babiciu P., (1979) – *Agricultural machines,* Publishing Ceres, Bucharest;
[10]. Toma D., (1975) - *Agricultural machines*, Didactic and Pedagogical Publishing, Bucharest.

Revista nr.9;
[3]. Mărdărescu R. şi colab (1968) – *Motoare pentru automobile şi tractoare,* Editura Didactică şi Pedagogică Bucureşti;
[4]. Oprean A., Fl. Ionescu, Al. Dorin., 1982 **–** *Acţionări hidraulice, elemente şi sisteme,* Editura Tehnică, Bucureşti, pag. 205-207;
[5]. Sărăcin I., Marin G., Olimpia P., Florea G. (2009) - *Baza energetică pentru agricultură, horticultură, silvicultură*, Editura Aius Printed – Craiova;
[6]. Saracin I., Pandia O., Netoiu C., (2010) – *Studiul teoretic privind realizarea unei maşini destinate plantațiilor forestiere de rasinoase*. Analele Universității din Craiova – Seria Agricultură, Montanologie, Cadastru, Vol. XL /2, pag. 556-560 ;
[7]. Saracin I., Pandia O., (2010) – *Semănătoare pentru semințe mici*, Analele Universității din Craiova Seria Agricultură, Montanologie, Cadastru, Vol.XL/2, pag.561-565 ;
[8]. Sărăcin I., (2002-2004) - *Semănătoarea uşoară universală pentru solurile nisipoase*, Ctr.CNCSIS, No.33451, Universitatea din Craiova ;
[9]. Scripnic V., Babiciu P., 1979 – *Maşini agricole,* Editura Ceres, Bucharest ;
[10]. Toma D., 1975 – *Maşini agricole*, Editura Didactică şi Pedagogică, Bucureşti.

THE DETERMINATION OF THE RESISTANT FORCES FOR DEEP LOOSENING OF SOIL MACHINES WITH ACTIVE ORGANS
/
DETERMINAREA FORTELOR REZISTENTE LA MASINILE DE AFÂNARE ADÂNCĂ A SOLULUI CU BRĂZDARE ACTIVE

PhD. Stud. Eng. David A. [1)], Prof. PhD. Eng. Voicu Gh. [2)], PhD. Stud. Eng. Persu C. [1)] Eng. Gheorghe G. [1)],
[1)]INMA Bucharest; [2)]P.U. Bucharest
Tel: 0720.569.365; E-mail: somy_alex_07@yahoo.com

Abstract: *This paper presents the calculation of the resistant forces that occur during the deep loosening works in a machine with active organs driven by the quadrilateral mechanism from the tractor PTO. By using the relations for calculating the resistance forces presented in the paper we determined the momentum necessary to drive the plowshares and compare it with the determined experimental values*

Keywords: *deep loosening of soil machines, resistant forces, soil.*

INTRODUCTION

Destruction of soil structure and compaction of the arable layer in depth reduces the water storage capacity, prevents soil aeration and spoils the aerohidric balance. In our contry the area occupied by soils that require deep loosening works represent approximately 19.8% of the total agricultural area [1].

Removing these shortcomings and increasing the efficiency of land works requires the application of complex improvement measures, where the deep soil loosening is very important.

The deep loosening soil machines with active organs have plowshares which are operated by a quadrilateral mechanism of the tractor PTO, cutting and loosening the soil [4].

Resisting forces acting on the main bodies of deep soil loosening machines driven by a quadrilateral mechanism are shown in figure 1.

-the resistant force to the displacement of the connecting rod (F_{RH});

-the resistant forces due to the breaking and accelerating of the soil by the plowshare found in oscillation(Q_i);

-the drag force (F_R).

Rezumat: *Lucrarea prezinta calculul forţelor rezistente ce apar în timpul lucrărilor de afânare adâncă a solului la masinile cu organele de lucru acţionate de un mecanism patrulater de la priza de putere a tractorului. Utilizând relaţiile de calcul al forţelor rezistente prezentate în lucrare se determina forţa de tracţiune şi momentul necesar acţionării brăzdarului şi se compară cu valorile determinate experimental.*

Cuvinte cheie: *maşina de afânarea adâncă a solului, forţe rezistente,sol.*

INTRODUCERE

Distrugerea structurii solului în stratul arabil şi compactarea lui în profunzime duce la reducerea capacităţii de acumulare a apei, la împiedicarea aerării solului si stricarea echilibrului aerohidric. Suprafaţa ocupată în ţara noastră de solurile care necesită lucrări de afânare adâncă este de circa trei milioane hectare, respectiv 19,8% din totalul suprafeţei agricole [1].

Inlăturarea acestor neajunsuri şi sporirea eficienţei lucrărilor de îmbunătăţiri funciare necesată aplicarea unui complex de măsuri agroameliorative, în cadrul cărora afânarea adâncă a solului prezintă o importantă deosebită.

Maşinile de afânare adâncă a solului cu organe de lucru active au brazdare care actionate de un mecanism patrulater de la prize de putere a tractorului produc taierea solului si totodata afânarea acestiua [4].

Forţele rezistente care actionează asupra principalelor organe ale maşinilor de afânare adânca a solului cu brăzdarele acţionate de un mecanism patrulater sunt prezentate în figura 1.

-forta rezistenta la deplasarea bielei (F_{RH});

-fortele rezistente datorate ruperii si accelerarii solului de catre brazdarul aflat in miscare de oscilatie(Q_i);

-forta rezistenta la inaintare (F_R).

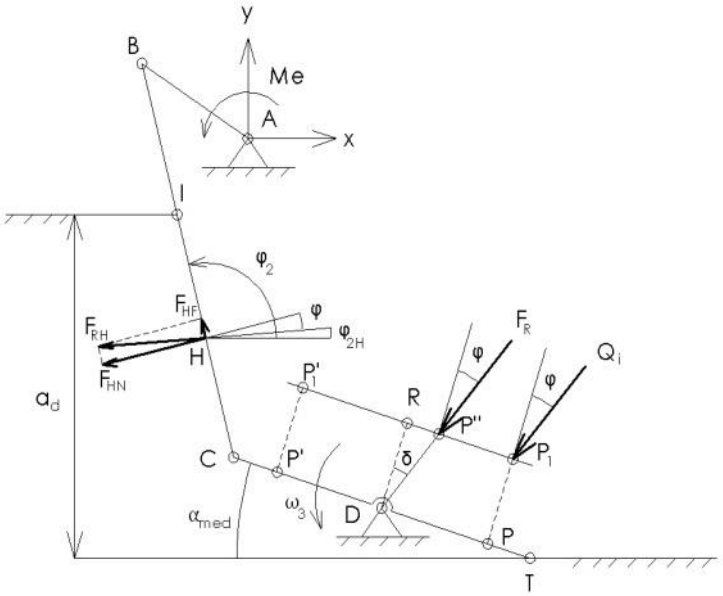

Fig. 1 - The resisting forces acting on deep soil loosening machine organs

MATERIALS AND METHODS

To determine the resistant force to the displacement of the connecting rod (F_{RH}), it can be assimilated with a double wedge (figure. 2) on which the normal forces F_N and N, and the soil friction forces μN and μF_n.

The normal forces of the rod on the inclined surface F_N and on the side surface are [1]:

$$F_N = k_1 \cdot S_1$$

where:

-k_1 is the specific resistance of soil deformation in the advancing direction

-k_2 is the specific resistance of soil deformation perpendicular to the advancing direction [2, 5];

-S_1, S_2 are the wedge surfaces, and the side surface of the connecting rod.

The total rezistent force, on the machines movement direction is :

MATERIALE ŞI METODE

Pentru determinarea forţei rezistente la deplasarea bielei (F_{RH}), aceasta poate fi asimilată cu o pană dublă (figura 2) asupra careia actionează fortele normale F_N şi N şi fortele de frecare μN şi μF_n.

Forţele normale pe suprafetele înclinate ale bielei F_N şi pe suprafetele laterale N sunt [1]:

$$N = k_2 \cdot S_2 \quad (1)$$

Unde:

-k_1 este rezistenţa specifică la deformarea solului pe direcţia de înaintare;

-k_2 este rezistenţa specifică la deformarea solului perpendiculară pe direcţia de înaintare [2, 5];

-S_1, S_2 suprafaţa penei, respectiv suprafaţa laterală a bielei.

Forţa rezistenta totala, pe directia de deplasare a maşinii este:

$$F = \frac{2 \cdot F_N \cdot \sin(\varphi + \frac{\alpha}{2})}{\cos\varphi} + 2 \cdot \mu \cdot N \quad (2)$$

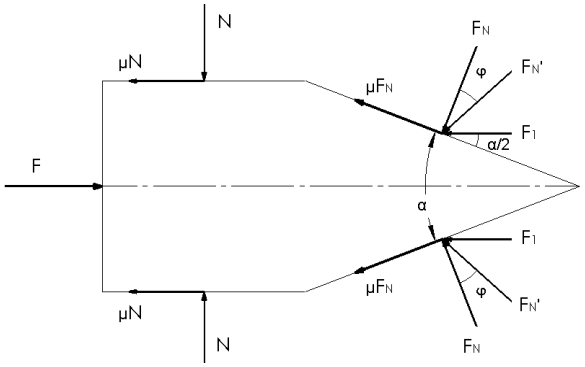

Fig. 2 - The forces acting on plowshares support [1]

The normal resistance force on the connecting rod F_{HN}, the soil friction forte with the connecting rod F_{HF} and the resultant force F_{RH} (figure 1) is determined by relations:

Forţa rezistentă normală pe biela F_{HN}, forţa de frecare a solului cu biela F_{HF} şi forţa rezultantă F_{RH} (figura 1) se determină cu relaţiile:

$$F_{HN} = \frac{F \cdot \cos\varphi}{\cos\varphi_{2H}} \qquad F_{HF} = \mu \cdot F_{HN} \qquad F_{RH} = \sqrt{F_{HN}^2 + F_{HF}^2} \quad (3)$$

The deep soil loosening machine has two working organs that dislocate the soil on a much larger width than the width of the plowshares. If dislocate soil is removed by a plowshare on a section perpendicular to the direction of movement, you optain a small isosceles trapezium base located at a depth approximately equal the width of plowshares l_b (figure 4). For working depth of 50 cm, the long side of the trapezoid located at ground level is 70 cm resulting in an tilt angle of the lateral aspect of the trapezium to the horizon β_1 = 1.03 rad = 59.036^0 (figure 3).

Maşina de afânare adânca a solului are doua organe de lucru care dislocă solul pe o laţime mult mai mare decât lăţimea brăzdarelor. Dacă se înlătură solul dislocat de un brăzdar, pe o porţiune perpendiculară pe direcţia de deplasare, se obţine un trapez isoscel cu baza mică aflată la adâncimea de lucru aproximativ egală cu lăţimea brăzdarului l_b (figura 4). Pentru adâncimea de lucru de 50 cm, latura mare a trapezului, aflată la nivelul solului, este de 70 cm rezultând un unghi de înclinare a laturilor laterale ale trapezului faţă de planul orizontal β_1 = 1.03 rad = 59.036^0 (figura 3).

Fig.3 - The transverse section shape of the soil displaced by a plowshare

The volume of soil displaced is shown in figure 4 [3]. In longitudinal section, the plowshare EF breaks the soil after a plan whose result, the median longitudinal vertical plane is inclined at an angle $\psi = 45^0$ [6]

The volume of soil displaced is :

$$V = \frac{a_d \cdot (S + s + \sqrt{S \cdot s})}{3} - \frac{EF^2 \cdot l_b \cdot cos\alpha_{med} \cdot sin\alpha_{med}}{2} \quad (4)$$

Where:

-α_{med} is the average angle of inclination from the horizontal plowshares

-$S = L \cdot (EF \cdot cos\alpha_{med} + EO) + \frac{\pi L^2}{8}$;

- $s = l_b \cdot EF \cdot cos\alpha_{med}$ is the large base area, respectively the lower base of the soil displacement;

-$EO = a_d \cdot ctg\psi - \frac{L}{2}$

- a_d – working depth;

- L - maximum working width of a plowshare.

When the plowshare rotates around the joint *D* with the angular velocity $\omega_3 > 0$ EF = DT (figure 1) and when $\omega_3 < 0$, FE =CD then the working depth is (a_d – CD·sinα_{med}).

The lateral area of the soil volume driven by the plowshare found in oscillation motion is calculated by the relationship.

Volumul de sol dislocat de brăzdar este prezentat în figura 4 [3]. În secţiune longitudinală, brăzdarul EF rupe solul după un plan a cărui urmă, în planul longitudinal vertical median, este înclinată cu un unghi $\psi = 45^0$ [6].

Volumul de sol dislocat este:

Unde:

-α_{med} - unghiul mediu de înclinare a brăzdarului faţă de orizontală;

-$S = L \cdot (EF \cdot cos\alpha_{med} + EO) + \frac{\pi L^2}{8}$;

- $s = l_b \cdot EF \cdot cos\alpha_{med}$ este suprafaţa bazei mari, respective a bazei mici a solului dislocat;

-$EO = a_d \cdot ctg\psi - \frac{L}{2}$

- a_d – adâncimea de lucru;

- L – latimea maxima de lucru a unui brazdar.

Atunci când brăzdarul se roteste în jurul articulaţiei *D* cu viteza unghiulară $\omega_3 > 0$ EF = DT (figura 1) iar atunci când $\omega_3 < 0$, FE =CD iar adâncimea de lucru este (a_d – CD·sinα_{med}).

Aria laterală a volumului de sol actionat de brăzdarul aflat în miscare de oscilatie se calculează cu relaţia.

$$A = \pi \cdot \frac{L}{2} \cdot \sqrt{\frac{L^2}{4} + a_d^2} + (2 \cdot a_d - EF \cdot sin\alpha_{med}) \cdot EF \cdot cos\alpha_{med} \quad (5)$$

For tearing the soil under the forces exerted by the plowshare, it is necessary to overcome the forces of cohesion that manifests between soil particles. These can be calculated using the equation:

$$F_{coez} = A \cdot (c + \sigma_n \cdot tg\varphi_0) \quad (6)$$

Where:

-*c* is the cohesion coefficient

-σ_n = 10–60 kPa is the normal tension (compresion) [7];

-$\mu_0 = tg\varphi_o = 0.35 \div 0.9$ [7] is the coefficient of internal friction of the soil.

Unde:

-*c* - este coeficientul de coeziune;

- σ_n = 10–60 kPa este tensiunea normală (de compresiune) [7];

-$\mu_0 = tg\varphi_o = 0.35 \div 0.9$ [7] este coeficientul de frecare internă a particulelor de sol.

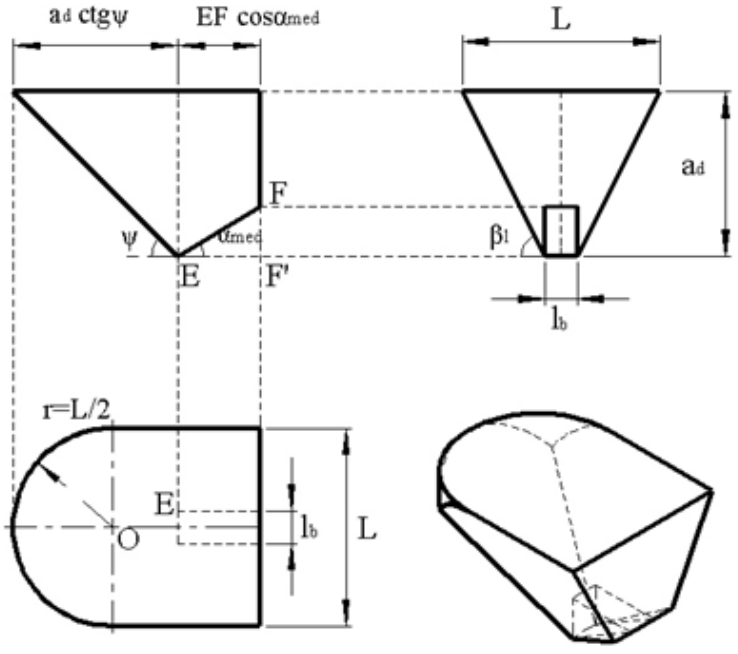

Fig.4 - Section through the soil displaced by plowshare

The normal cohesive force of the plowshare is calculatet using the equation:

Forţa de coeziune normală pe brăzdar se calculează cu relaţia:

$$F_{coezn} = F_{coezi} \cdot sin\beta_l \cdot \cos \propto_{med} \quad (7)$$

Where the inclined angle of the lateral side walls of the furrow is:

Unde unghiul de înclinare al pereţilor laterali ai brazdei este:

$$\beta_l = arctg \frac{2 \cdot a_d}{L - l_b} \quad (8)$$

Because the aggregate is moving with the working speed v_l , the speeds of the extreme points of the plowshare C and T (Figure 5), on the direction of movement, are :

Deoarece agregatul se deplasează cu viteza de lucru v_l, vitezele punctelor extreme ale brăzdarului C şi T (figura 5), pe direcţia de deplasare, sunt:

$$v_{c1x} = v_{cx} + v_l \qquad v_{t1x} = v_{t1x} + v_l \quad (9)$$

The speeds of the extreme points of the plowshare is determined by the relationship:

Vitezele punctelor extreme ale brăzdarului se determină cu relaţiile :

$$v_{c1} = \sqrt{v_{c1x}^2 + v_{cy}^2} \qquad v_{t1} = \sqrt{v_{t1x}^2 + v_{ty}^2} \quad (10)$$

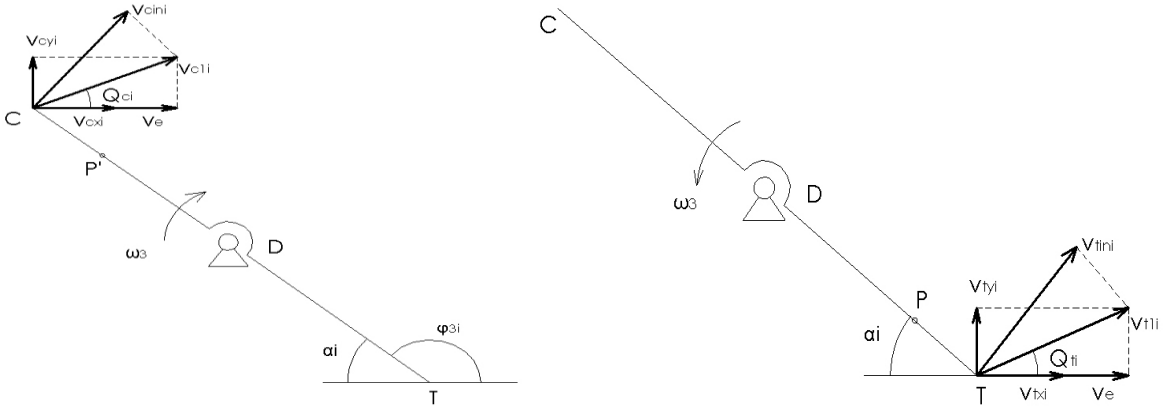

Fig.5 - The speeds of the extreme points of the plowshare

The normal speeds on the surface odthe plowshare in its extreme points are :

Vitezele normale pe suprafata brăzdarului în punctele extreme ale acestuia sunt:

$$v_{c1n} = v_{cx} \cdot \sin(\theta_c + \alpha_{med}) \qquad v_{t1n} = v_{tx} \cdot \sin(\theta_t + \alpha_{med}) \quad (11)$$

Where : $\theta_c = arctg \frac{v_{cy}}{v_{c1x}}$; $\theta_t = arctg \frac{v_{ty}}{v_{t1x}}$

Unde : $\theta_c = arctg \frac{v_{cy}}{v_{c1x}}$; $\theta_t = arctg \frac{v_{ty}}{v_{t1x}}$

Given that rotation speeds of the plowshore points are maximum in extreme and zero points in joint D, average speeds of rotation are applied at the point P for $\omega_3 > 0$ and P' for $\omega_3 < 0$, located at a distances d, and have the values:

Având în vedere că vitezele de rotaţie ale punctelor brăzdarului au valoarea maximă în punctele extreme şi zero în articulaţia D, vitezele medii de rotaţie sunt aplicate în punctul P pentru $\omega_3 > 0$, respectiv P' pentru $\omega_3 < 0$, aflate la distantele d, şi au valorile:

$$v_{ppn} = \frac{2}{3} \cdot v_{c1n} \qquad v_{pn} = \frac{2}{3} \cdot v_{t1n} \quad (12)$$

The plowshare forces acting on soil Q_v whose support through the point P if $\omega_3 > 0$ and the point P 'if $\omega_3 < 0$ causing its acceleration. To determine these forces we applied the kinetic energy theory [8].

Brăzdarul acţionează asupra solului cu forţele Q_v a căror suport trece prin punctul P dacă $\omega_3 > 0$ şi prin punctul P' dacă $\omega_3 < 0$ determinând accelerarea acestuia. Pentru determinarea acestor forţe se aplica teoria energii cinetice [8].

$$dL = dE \quad (13)$$

Where :
-*dL* is the variation of mechanical work forces Qv;
-*dE* is the variation of the kinetic energy of the soil dislodged plowshare.

Unde:
-*dL* este variaţia lucrului mecanic al fortelor Q_v ;
-*dE* este variaţia energie cinetice a solului dislocat de brăzdar.

$$Q_v \cdot d = \frac{V \cdot \rho_{sol} \cdot (v_{max}^2 - v_{min}^2)}{2} \quad (14)$$

Where :
ρ_{sol} is the soil density;
$v_{max} = v_{pnmax}$; $v_{min} = v_{pnmin}$; d = DP = 2/3 DT if $\omega_3 > 0$;
$v_{max} = v_{ppnmax}$; $v_{min} = v_{ppnmin}$; d = DP' = 2/3 DC if $\omega_3 < 0$;

Unde:
ρ_{sol} este densitatea solului;
$v_{max} = v_{pnmax}$; $v_{min} = v_{pnmin}$; d = DP = 2/3 DT daca $\omega_3 > 0$;
$v_{max} = v_{ppnmax}$; $v_{min} = v_{ppnmin}$; d = DP' = 2/3 DC daca $\omega_3 < 0$;

The plowshare normal force which causes the accelerated soil is calculated using the equation:

Forţa normală pe brăzdar, care determină accelerarea solului, se calculează cu relaţia:

$$Q_v = \frac{V \cdot \rho_{sol} \cdot (v_{max}^2 - v_{min}^2)}{2 \cdot d} \quad (15)$$

The normal resultant force on the plowshare, which causes tearing and the accelerated soil will be:

Forţa rezultantă normală pe suprafaţa brăzdarului, care determină ruperea şi accelerarea solului, va fi:

$$Q_r = Q_v + F_{coezn} \quad (16)$$

RESULTS

These forces acting in point P for $\omega_3 > 0$ and P' for $\omega_3 < 0$ causing the load the tractor PTO shaft.

The normal force on the plowshare Q_v and the rezultant force Q_r depends on the machines working depth a_d with values between 50 – 70 cm, on the working speed v_l and the angular velocity of the crank driven quadrangle mechanism. For the deep soil loosening machine EAA – 220 the normal force on a plowshare and the resultant angular speed of the plowshare $\omega_3 > 0$ and for $\omega_3 < 0$ were calculated for a working depth of a_d = 0.5 – 0.7m, work speeds of v_l = 0.2 – 1.5 m/s and angular velocity of the crank ω = 57.56 rad/s, the data are presented in table 1.

REZULTATE

Aceste forţe acţionează în punctul P pentru $\omega_3 > 0$ şi P' pentru $\omega_3 < 0$ determinând încarcarea arborelui prizei de putere a tractorului.

Forţa normală pe brăzdar Q_v şi forţa rezultantă Q_r depind de adâncimea de lucru a maşinii a_d cuprinsă intre 50 – 70 cm, de viteza de lucru v_l şi viteza unghiulară a manivelei mecanismului patrulater de acţionare. Pentru masina de afânare adânca a solului EAA – 220 s-a calculat forţa normală pe un brăzdar şi forţa normală rezultantă pentru viteza unghiulară a brăzdarului $\omega_3 > 0$ şi pentru $\omega_3 < 0$, pentru adâncimea de lucru a_d = 0.5 – 0.7m, viteza de lucru v_l = 0.2 – 1.5 m/s şi viteza unghiulara a manivelei ω = 57.56 rad/s, datele fiind prezentate în tabelul 1.

Tabel 1

The calculated values for the normal force on the plowshare Q_v and Q_r

Nr.	Depth/ [cm]	Work speed/ [km/h]	Q_v [daN] $\omega_3 > 0$	Q_v [daN] $\omega_3 < 0$	Q_r [daN] $\omega_3 > 0$	Q_r [daN] $\omega_3 < 0$
1	50	5.4	991	504	2025	1330
2	70	5.4	2284	1409	3929	2842
3	50	0.72	298	152	1333	979
4	70	0.72	687	426	2333	1859
5	70	4.32	1831	1122	3477	2554
6	50	4.32	795	401	1829	1228
7	60	4.32	1243	704	2571	1822
8	60	1.8	576	318	1904	1436
9	50	2.52	468	232	1502	1058
10	70	2.52	1077	648	2723	2080
11	60	5.4	1550	884	2879	2002
12	60	0.72	467	267	1795	1385
13	60	2.52	732	407	2060	1524

With the values in Table 1 we determined the multivariate function for calculating the normal forces on the plowshare when $\omega_3 > 0$ equation 17 and for $\omega_3 < 0$ equation prezented in figure 6 and figure 7.

Cu valorile din tabelul 1 s-au determinat funcţiile multivariabile pentru calculul fortei normale pe brăzdar pentru $\omega_3 > 0$ relaţia 17 şi $\omega_3 < 0$ relaţia 18 în figura 6 si figura 7 sunt reprezentate grafic aceste funcţii.

$$Q_v = 1964 - 63.251 \cdot a_d - 505.435 \cdot v + 0.609 \cdot a_d^2 + 9.814 \cdot a_d \cdot v + 26.542 \cdot v^2 \quad (17)$$

$$Q_v = 1571 - 52.165 \cdot a_d - 375.7 \cdot v + 0.491 \cdot a_d^2 + 6.864 \cdot a_d \cdot v + 17.389 \cdot v^2 \quad (18)$$

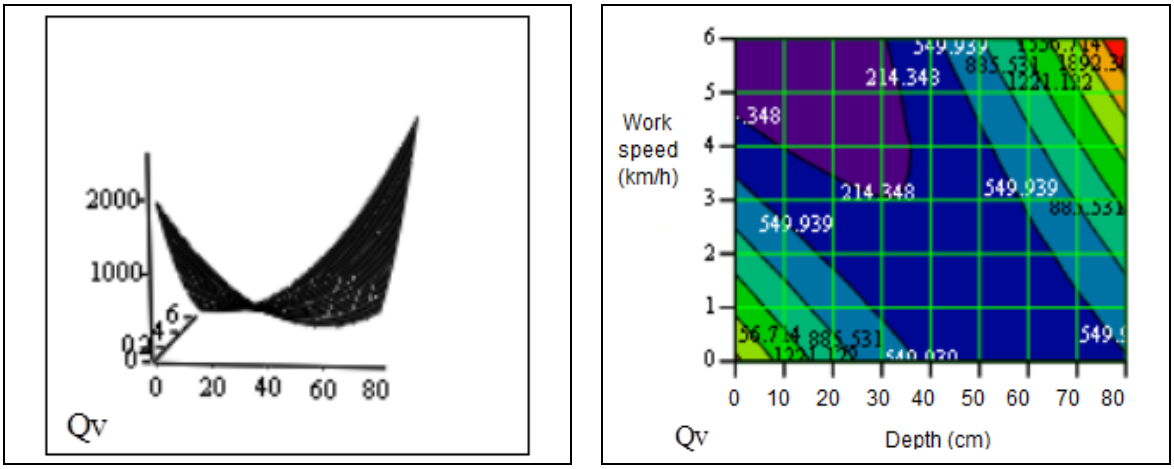

Fig.6 - The normal forces on the plowshare for $\omega_3 > 0$

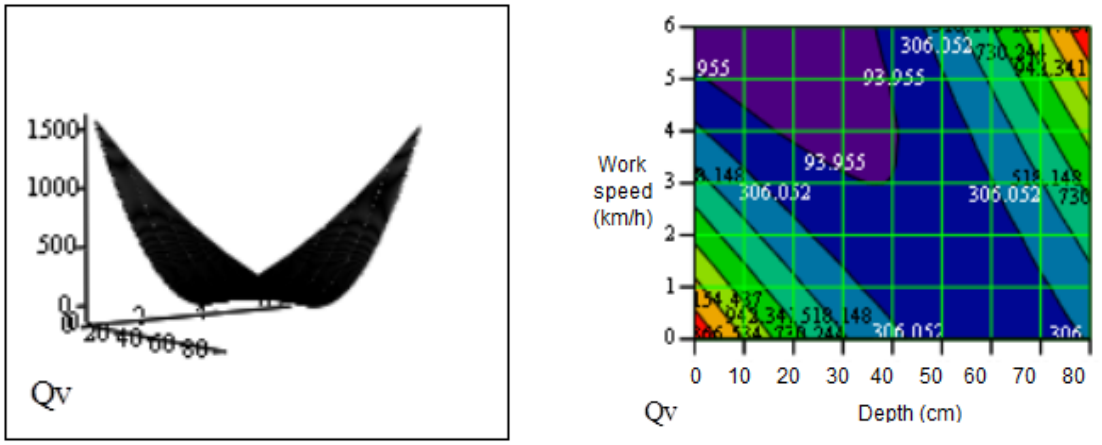

Fig.7 - The normal forces on the plowshare for. $\omega_3<0$

The resultant normal force on the plowshare for $\omega_3 > 0$ can be calculated using the equation19 and for $\omega_3 < 0$ using the equation 20. The graphical representation is shown in figure 8 and figure 9.

Forţa rezultantă normală pe brăzdar pentru $\omega_3 > 0$ se poate calcula cu relaţia 19 iar pentru $\omega_3 < 0$ cu relatia 20. Reprezentarea grafică a acestor funcţii este prezentată în figura 8 şi figura 9.

$$Q_r = 1883 - 46.845 \cdot a_d - 505.819 \cdot v + 0.727 \cdot a_d^2 + 9.816 \cdot a_d \cdot v + 26.581 \cdot v^2 \quad (19)$$

$$Q_r = 1293 - 35.885 \cdot a_d - 376.709 \cdot v + 0.607 \cdot a_d^2 + 6.868 \cdot a_d \cdot v + 17.507 \cdot v^2 \quad (20)$$

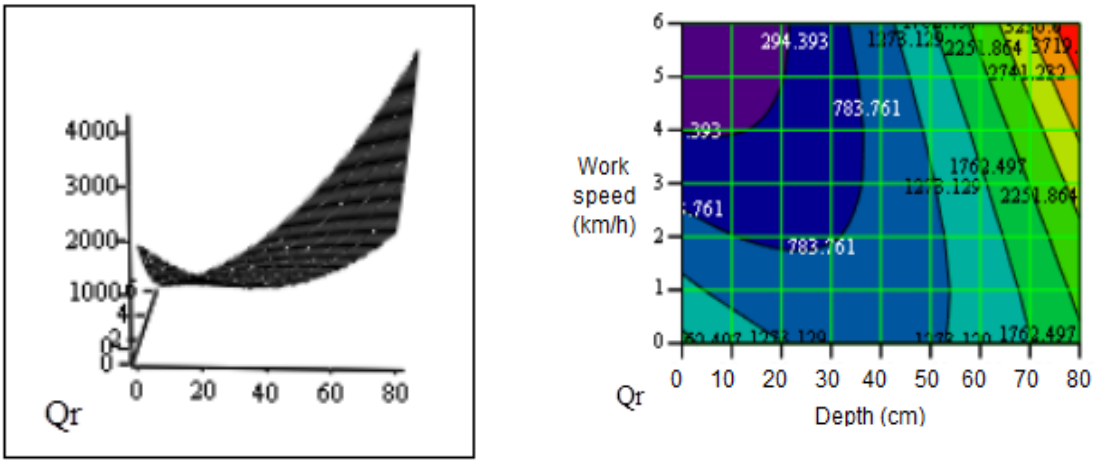

Fig.8 - The normal forces on the plowshare for $\omega_3 > 0$

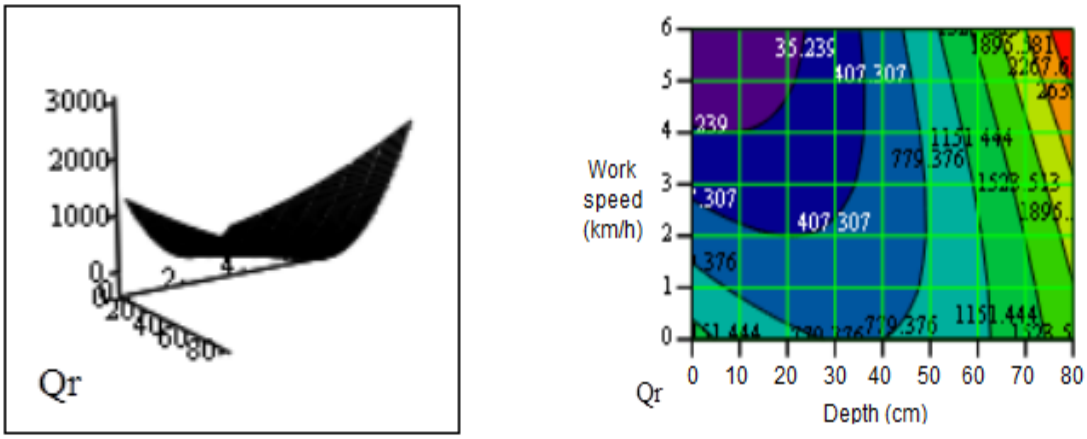

Fig.9 - The normal forces on the plowshare for $\omega_3 < 0$

The plowshare friction force Q_f and the resultant force Q are determined by the relations:

Forţa de frecare pe brăzdar Q_f şi forţa rezultantă Q se determină cu relaţiile:

$$Q_f = \mu \cdot Q_r \qquad Q = \sqrt{Q_r^2 + Q_f^2} \quad (21)$$

The drag force of the deep soil loosening machine can be calculated using the formula developed by V.P.Goreacikin. This force is considered proportional to loosened soil section:

$$F_i = k \cdot \frac{a_d \cdot (L + l_b)}{2} \quad (22)$$

Where : k is the plowing resistance coefficient;

The drag force for normal movment on the surface of the plowshare is:

$$F_{in} = \frac{F_i \cdot cos\varphi}{\sin(\alpha_i + \varphi)} \quad (23)$$

Where :
-φ is the angle of friction between soil and plowshare surface;
-α_i is the angle of inclination to the horizontal plan

The average drag force and the friction force on the surface of the plowshare is calculated using the equations:

$$F_{inmed} = \frac{\sum_1^n F_{in}}{n}$$

The resulting resistance force is:

$$F_f = \mu \cdot F_{inmed} \quad (24)$$

$$F_R = \sqrt{F_{inmed}^2 + F_f^2} \quad (25)$$

For the deep soil loosening machine EAA 220, for two working deeps, working speed v = 0.76 – 1.4 m/s , a soil density of 1500 kg/m^3 and plowing resistance coefficient k = 0.46 daN/cm^2 we calculated with the equations presented the strength and fracture resistance due to ground acceleration Q, the resistant force of the connection rods movement F_{RH}, the drag force F_R , the values calculated and the experimentally determined traction force F_t and the momentum necessary for operating the plowshare M_e.

The data are shown in Table 2.

Forţa rezistentă la înaintare a maşinii de afânare adâncă a solului F_t se poate calcula folosind formula elaborată de V.P.Goreacikin. Aceasta forţa se consideră proportională cu secţiunea solului afânat:

Unde: k – este coeficentul de rezistenţă la arat;

Forţa rezistentă la înaintare normală la suprafaţa brăzdarului este:

Unde:
-φ este unghiul de frecare dintre sol şi suprafata brăzdarului;
-α_i este unghiul de înclinare al brăzdarului faţă de planul orizontal.

Forţa rezistentă la înaintare normală medie şi forţa de frecare pe suprafata brăzdarului se calculează cu relatiile:

Forţa rezistentă rezultantă este:

Pentru maşina de afânare adâncă a solului EAA – 220, pentru doua adâncimi de lucru, viteza de lucru v = 0.76 – 1.4 m/s şi un sol cu densitatea de 1500 kg/m^3 şi coeficentul de rezistentă la arat k = 0.46 daN/cm^2 s-au calculat, cu relaţiile prezentate, forţa rezistentă datorată ruperii şi accelerării solului Q, forţa rezistentă la deplasarea bielei F_{RH}, forţa rezistentă la înaintare F_R precum şi valorile calculate şi cele determinate experimental pentru forţa de tracţiune F_t şi momentul necesar actionării brăzdarului M_e .

Datele sunt prezentate în tabelul 2.

Tabel 2

Theoretical and experimental forces and resistant moments

Nr. crt.	Depth [m]	Speed [m/s]	Q [daN]		F_{RH} [daN]	F_R [daN]	F_t [daN]		M_e [Nm]	
			$\omega_3 > 0$	$\omega_3 < 0$			Calc.	Exp.	Calc.	Exp.
1	0.6	0.76	2175	1620	629	1447	3603	3589	133	139
2		1.25	2924	1992			3980	4027	158	133
3	0.7	0.86	3246	2371	851	1908	4931	4003	188	150
4		1.4	4338	3043			5565	5472	230	223

CONCLUSIONS

From the data presented in Table 2 it results that the resistance forces were correctly determined considering that between the calculated and experimental values of traction and momentum required to operate the plowshare there are very small differences

Also:

-the resistant force to movement of the connecting rods F_{RH} and drag force F_R is independent of the work speed but it depends only on the working depth and soil characteristics;

-the resistant force due to the tear and accelerating soil has different values depending on the angle of rotation of the crank handles operating mechanism ω_3;

-the small difference between the calculated and experimentally determined values for traction force and momentum required to operate the plowshare enables us to say that the assumptions considered in calculating the resistant forces are correct.

CONCLUZII

Din datele prezentate în tabelul 2 rezultă că forţele rezistente au fost corect determinate având în vedere că între valorile calculate şi cele experimentale ale forţei de tracţiune şi momentul necesar acţionării brăzdarului diferentele sunt foarte mici.

De asemenea:

-forţele rezistente la deplasarea bielei F_{RH} şi forţa rezistentă la înaintare F_R nu depind de viteza de lucru ci numai de adâncimea de lucru şi caracteristicile solului;

-forta rezistenţa datorată ruperii şi accelerării solului are valori diferite în funcţie de unghiul de rotaţie al manivelei mecanismului de acţionare ω_3;

-diferenţa mică dintre valorile calculate şi cele determinate experimental pentru forţa de tracţiune şi momentul necesar actionării unui brăzdar ne permite să afirmăm că ipotezele avute în vedere la calculul fortelor rezistente sunt corecte.

REFERENCES

[1]. Balaci C. (1998) - PhD thesis - *Contributions to the active organ work refining deep soil* Bucharest;

[2]. Caproiu S. (1982) - *Machines, agricultural tillage, sowing and crop maintenance*, Didactic and Pedagogic Publishing House, Bucharest;

[3]. Jeno Balaton Gonczi Attila, (2012) - *On the tensile strength and sizing calculation refining soil bodies*, Proceedings of the scientific communications meeting of Aurel Vlaicu University of Arad, Volume 4;

[4]. Kofoed S., (1969) - *Kinematics and Power Requirement of Oscillating Tillage Tools,* Journal of Agricultural Engineering Research, No.14;

[5]. Marin E., Pirnă I., Sorică C., Manea D., Cârdei P. (2012) - *Studies on structural analysis of resistance structure as a component of equipment with active working parts driven to deeply loosen the soil*, INMATEH Agricultural Engineering, Vol.36, No.1;

[6]. Sineokov G.N., (1965) - *Designing of tillage machines,* Masinostroenie Publishing House, Moscow

[7]. University of Pretoria (1995) - Kosisira Publishing House, LL, 2005 Transylvania, Cluj – Napoca;

[8]. Voinea R., Voiculescu D., Ceausu V., (1975) - *Mechanics*, Didactic and Pedagogic Publishing House, Bucharest.

BIBLIOGRAFIE

[1]. Balaci C., (1998) - Teza de doctorat – *Contribuţii la studiul organelor active pentru lucrarile de afânare adâncă a solului,* Bucuresti,

[2]. Caproiu S. (1982) - *Maşini agricole de lucrat solul, semănat şi întretinere a culturilor*, Editura Didactica si Pedagogica, Bucuresti ;

[3]. Jeno Balaton, Attila Gonczi, (2012) - *Cu privire la calculul rezistenţei la tracţiune şi dimensionarea organelor de afânare a solului*, Lucrările reuniunii comunicarilor ştiinţifice Aurel Vlaicu Universitatea din Arad, volumul 4;

[4]. Kofoed S., (1969) - *Cinematica şi puterea necesara ale echipamentelor vibratorii de lucrat solul,* Jurnalul ingineresc al cercetarilor agricole, nr.14;

[5]. Marin E., Pirnă I., Sorică C., Manea D., Cârdei P. (2012) - *Studii privind analiza structurală a structurii de rezistenţă, componentă a echipamentului tehnic cu organe active antrenate pentru lucrarea de afânare în profunzime a solului*, INMATEH - Inginerie Agricolă, Vol.36, No.1;

[6].Sineokov G.N. (1965) - *Proiectarea maşinilor de cultivat*, Editura: Maşinostroenie, Moscova;

[7]. Universitatea din Pretoria (1995) - Editura Kosisira, LL, 2005 Transilvania, Cluj – Napoca;

[8]. Voinea R., Voiculescu D., Ceausu V., (1975) - *Mecanica*, Editura Didactica si Pedagogica, Bucuresti.

EXPERIMENTAL RESEARCH ON MOISTURE TRANSMITTING RATE BETWEEN HUMIDITY SENSITIVE MATERIAL AND THE EXTERNAL ENVIRONMENT
/
水分在湿敏材料与外界环境间传输速率的试验研究

Lect. Ph.D. Chen Zhongjia[1)], Lect. Ph.D. Yuan Xiangyue[*1)], Prof. Ph.D. Eng. Yu Guosheng[1)], Prof. Ph.D. Eng. Grigu Kaunyon [2)]

[1)] School of Technology, Beijing Forestry University, Beijing / China;
[2)] Laboratory for Advanced Agricultural Technology R&D, MOAD Companies Group, Inc., Takatsuki / Japan
Tel: +861062338144; Email: shirley_yxy2001@163.com

Abstract: *Shortage of water resources has become a serious problem of the world. With the growing increasingly reduction of water and energy resources, the agricultural irrigation method of water-saving and energy-saving should be adopted. In developed countries, control and monitoring of agricultural water-saving irrigation products are mostly dependent on computer technology, which need an external power source, and the price of the whole irrigation system is very expensive. So, it is not suitable to remote forest areas in China. In this paper, a new type of water-saving valve was introduced and is characterized by high automation, low costs and is capable of controlling without power supply. In order to make the valve to be used better in agricultural irrigation, experiments on moisture transmission rate between humidity sensitive materials and the external environment were conducted. And the results showed that the control unit of the valve could realize the irrigation automatically and timely according to the transmission rate between humidity sensitive material and the external environment, which would provide theoretical and experimental basis for the accurate control of the valve. It would play an important role for expanding agricultural water-saving irrigation and accelerating the speed of rational use of water resources.*

Keywords: *Water-saving valve; Humidity sensitive material; Transmission rate; Agricultural irrigation; Water Crisis*

摘要: *水资源短缺已经成为全世界面临的严重问题。随着水资源和能源的日益减少，必须发展农业节水节能灌溉技术。在发达国家，农业节水灌溉产品的监控系统大多依赖计算机技术，它需要有外部电源供给，且整个系统的价格非常昂贵，因此不适用于中国的偏远地区。本文介绍了一种新型的节水阀门，它具有高自动化高、低成本且能实现无电源控制的特点。为了使该阀门能更好地应用于农业生产灌溉，本文进行了水分在湿敏材料与外界环境间传输速率的试验研究。试验结果表明，阀门的控制单元能根据湿敏材料和外部环境之间水分传输的速率实现自动和及时的灌溉，这将为阀门的精准控制提供理论和试验依据。对于发展农业节水灌溉和加速水资源的合理利用也能起到重要的作用。*

关键词: *节水阀门; 湿敏材料; 传输速率;农业灌溉; 水资源危机*

INTRODUCTION

Water is the most important limited resources among all the natural resources, thus it should be tapped and utilized rationally. China accounts for only 9% of arable land resources in the world, and even a less percent of 6% of world's water resources. At the same time, half of more than 600 cities in China are deficient in water resources. What's more, the distribution of water resources in China is not even. For example, North China and Northeast account for 40% of national population with only about 5% of national water resources, and the 25% fresh water resources in North China is from South China. At present, the water supply is only 6180 billion cubic meters in China [9], while it is estimated that water demand will amount to 8180 billion cubic meters by 2030. In addition, China is an agricultural country and 40% arable land needs irrigation [10]. Therefore, agricultural water-saving and energy-efficient irrigation has become an irresistible trend to relief the water resource crisis and realize agricultural modernization.

In recent years, agricultural water-saving irrigation equipment in the world still faces many problems in spite of certain development. In China, the automation level of water-saving irrigation equipment especially in remote

引言

在所有自然资源中，水是最重要的有限资源，必须合理开发和利用。中国耕地资源占世界总量的 9%，然而，水资源更加紧缺，仅占世界总量的 6%。同时，在中国 600 多个城市中，一半的城市存在水资源匮乏问题。另外，中国的水资源在全国范围内分布不均匀，例如，华北和东北虽然人口占全国人口的 40%，但水资源仅占全国总量的 5%左右，华北的淡水资源仅为华南的 25%，预计到 2030 年，中国的需水量预计达到 8180 亿立方米。目前，供水量仅有 6180 亿立方米[9]。除此之外，中国作为一个农业大国，其中 40%的耕地面积需要通过灌溉来完成生产[10]。因此，采用农业节水、节能的灌溉方法已成为中国灌溉技术发展的总趋势，推广节水灌溉也已成为中国为缓解水资源危机和实现农业现代化的必然选择。

近年来，国内外的农业节水灌溉设备虽有一定的发展，但仍存在不少的问题。国内尤其在偏远地区的节水设备自

areas is so poor that they are generally controlled manually by installing all kinds of valves. Currently, micro-irrigation equipment is only applied to such cash crops as fruits and vegetables, and still needs development for field crops, while foreign equipment with a high overall level, whose automatic control system are realized mostly by using computers, sensors and remote sensing and telemetry and etc. [7], which means a high cost beyond the reach of most farmers or foresters in China. In the early 1940s, L. A. Richards, the Doctor of Cornell University in the USA, invented a tension meter measuring the flow of water. Although it could replace the dripper in drip irrigation and realize the control without power supply, it also had disadvantages caused by its complex structure, high cost and low sensitivity [6]. In 1980s, L.Ornstein, the professor of Washington State University developed a kind of intelligent water-saving valve named Irristat, which could meet the requirement of being cost-effective, energy-saving and of high automation without power supply. However, the inappropriate structure of Irristat made the installation and monitor difficult to be conducted during the irrigation process, thus it was unfit for promotion [8]. Currently, such a water-saving irrigation equipment characterized by low cost, energy efficiency, high automation is urgent needed in China [1].

A new type of intelligent water-saving valve without power supply had been developed since 2006 by the research team of Beijing Forestry University in China. It was characterized by high automation, low costs and no electronic control. As the core of the water-saving valve, control unit could employ the feature of water swelling and drying shrinkage of the humidity sensitive materials to open or close the inlet port to guide the irrigation. Whether to open or close the valve in time laid in timely moisture exchange between the humidity sensitive materials and soil around. Therefore, mastering the exchange rate and law between humidity sensitive materials and external environment in control unit, is of great importance to make the valve to be used better in irrigation and production.

The structure of the new type valve was shown in figure 1. The water inlet port 11 and outlet port 10 were connected at the very start. After the valve was inserted into the soil, water from outlet 10 outflowed into the soil, then penetrated to the control element 3, which meant humidity sensitive materials had absorbed water and swelled. Soon spool 7 was moved upward under the thrust caused by material expansion. Water would no longer flow into the valve when the inlet 11 was completely blocked by the conical nose of the spool 7, and then the irrigation stopped. After that, the moisture in the soil would gradually decrease with the absorption and evaporation of plants, and the moisture in the control unit 3 also would reduce because of the dehydration of material. When the material volume shrank, spool 7 would move back under the action of the back-moving spring 9, inlet 11 was gradually opened, and water flowed out again from the outlet 10 to soil. In addition, the amount of water required from plants could be controlled through the adjusting screw 1 at the rear of the valve to meet multiple needs of water for various plants in different seasons and soils, and therefore increased yields [2-4].

动化水平较低，大都是通过安装各种各样的阀，靠手工调节来控制灌溉。微灌设备的适应范围比较窄，目前的微灌设备主要集中在果菜等经济作物中，适合大田作物的微灌设备亟待研究解决。国外的微灌设备整体水平比较高，其自动控制系统大都通过采用计算机、传感器、遥感遥测等来实现[7]。虽然实现了高水平的灌溉自动化，但成本都比较高，不适合中国大部分农民使用。早在 20 世纪 40 年代，美国康奈尔大学的 L.A.Richards 博士就发明出了一种测试水势的张力计，它虽然能够取代滴灌系统中的滴头，并实现无源控制，但结构比较复杂，造价太高，而且灵敏度不高[6]。1980 年，美国华盛顿州立大学的 L.Ornstein 教授研制的无源智能控制阀 Irristat 能够实现低成本、节能、无源高自动化的要求，但由于 Irristat 自身结构的问题，使得在灌溉过程中的安装和监测比较麻烦，不适合推广普及[8]。目前，兼具低成本、节能、高自动化和适合推广普及的节水灌溉设备在国内外仍是一个亟待解决的问题[1]。

北京林业大学（中国）的研究团队从 2006 年开始研制一种新型的无需电源供给的智能节水阀门，它具有高自动化、低成本和无需电控的特点。控制单元是无电源节水阀门的核心部位，它利用其控制单元中湿敏材料吸水膨胀失水收缩的特性来开启或关闭阀门进水口，从而指导灌溉。阀门能否及时开启或关闭的关键在于控制单元内的湿敏材料与外界水分能否及时的交换，因此，掌握水分在控制单元内的湿敏材料与外界环境的交换速率及规律，对该阀门应用于生产灌溉极其必要。

无电源智能节水阀门是利用湿敏材料吸水膨胀失水收缩的特性来控制阀门的关闭和打开，结构如图 1 所示，初始时进水口和出水口为连通状态。阀门插入土壤中，水从出水口流出进入土壤后，控制元件 3 即湿敏材料吸水膨胀，阀芯 7 在材料膨胀推力的作用下向上移动，当其锥形头部将进水口 11 完全堵上时，水就不再进入设备，从而停止灌溉。土壤中的水分随着植物的吸收和蒸发会渐渐减少，根据水分平衡原理，控制元件 3 中的水分也随之减少，材料失水体积收缩，从而阀芯 7 在复位弹簧 9 的作用下反向移动，进水口渐渐打开，水从出水口流出。另外，还可以根据作物的需水量来调节阀门的调节螺钉 1，满足不同作物在不同季节、不同质地的土壤中的水分需求，进而提高作物产量[2-4]。

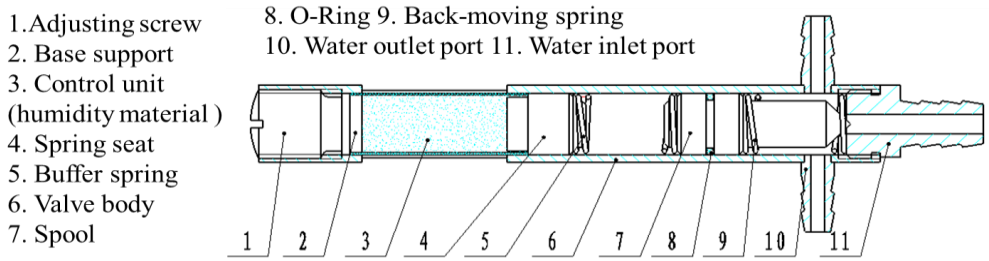

Fig.1- The structure of the intelligent water-saving valve

MATERIALS AND METHODS

Purpose of the experiment

The following experiments were designed to measure the moisture transmitting rate between humidity sensitive materials and the external environment. It has mainly studied the transmission rate between moisture and external environment at different ratio of humidity sensitive materials and different distances between the dripper and valve body. The experiment focused on the time to close the valve and to open it again at the above conditions.

Rate conversion of the experiment

The common way to get moisture transmission rate was to calculate the relationship between time and soil moisture content by using soil moisture sensor and data collector, and then obtain the result through data analysis. However, the requirement of connection between soil moisture sensor and computer made the whole system heavy and hard to operate, and the circuit was complex with limited application (shown in the figure 2, part A). So the common way was unfeasible upon all these conditions. A new way(shown in figure 2, part B) was adopted to convert the moisture transmitting rate between humidity sensitive materials and external environment to the rising rate of the valve's spool, which could also be converted to the relationship between the time and the distances (from the dripper to valve body, named C in figure2, part B). So the moisture transmitting rate would be obtained by calculating the relationship between distances and time measured from opening the dripper to closing the corresponding valve.

材料与方法

试验目的

本试验的目的主要是测量水分在湿敏材料与外界环境间的传输速率，主要研究无电源智能节水阀体中放置不同配比的湿敏材料以及节水阀滴口距离阀门不同距离时，水分与外界环境间的传输速率。重点在于上述条件下节水阀门的关闭和再次打开的时间。

试验速率转换

测量水分传输速度的一般做法是利用土壤水分传感器和数据采集器进行试验得出土壤含水率与时间的关系，进而进行数据分析得出试验结果，而在本试验中，由于土壤水分传感器需要与电脑连接，整个设备变得非常笨重，不便操作并且电路比较复杂，且该系统应用范围有限（见图 2，A 部分）。因此，采用了一种全新的思路（见图 2，B 部分），就是将水分在湿敏材料与外界环境间的传输速率转换为节水阀阀芯上升的速率，而节水阀阀芯上升的速率可以转换为节水阀滴口与阀门之间的距离与时间的关系。所以试验中通过采用不同的滴口与阀门距离（用 C 表示，见图 2，B 部分）进行试验，测出相应节水阀门关闭的时间，得出它们的关系，也就得出了水分在湿敏材料与外界环境间的传输速率。

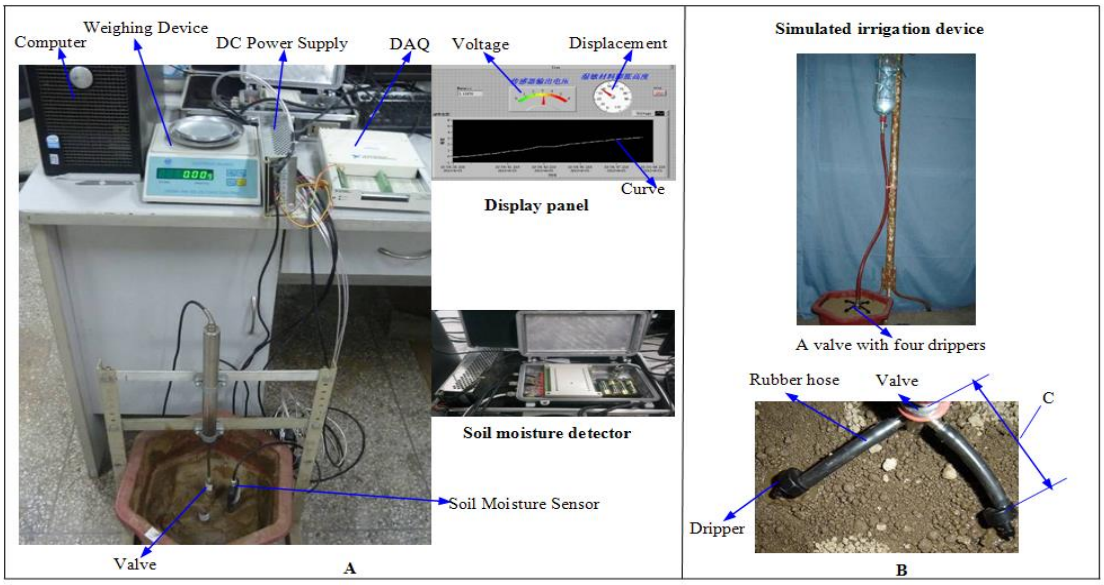

Note: A. Common method of measuring system; B. A new way to get transmission rate; C. Distance between Valve body and Drippers

Fig.2 - Common and new method of measuring transmission rate

Summary of the experimental field

The experiment was conducted in vehicle internship center of Beijing Forestry University (located in Haidian District, Beijing) with the accurate position of 39 degrees north latitude, 116 degrees east longitude and the altitude of 20m to 60m. This place has a warm temperate, semi-humid and semi-arid monsoon climate with an annual mean temperature of 11～13℃, annual precipitation of 600～700mm and an annual average sunshine time of 2780.2 hours.

Experiment materials

Known from previous researchers, a kind of France water-retaining agent, named SNF, has better comprehensive performance of water swelling and drying shrinkage. It is the copolymerization of acrylamide-acrylate, which can endure for about four years [11]. Based on early research, the mixture of SNF with the diameter of 0.5mm and sand with the diameter of 1~2mm was selected as the control unit in the valve so as to increase the rate of water absorption and loss [5]. Above mixed materials which volume ratio was 1:1 and 1:3 were selected in the following experiments. Total volume was 2ml or 4ml.

Three kinds of soil at Beijing were also involved, namely sand, loam and clay, with the clearance of sand being the biggest and of clay being the smallest. The loam was produced by mixing the sand and clay with the volume ratio of 1:1.

Experimental methods

Three kinds of soil, three distances, as well as the different mixture ratio, volume, and inserting depth of the mixed materials were involved in the experiments. The whole experiment was divided into 2 categories and 45 groups.

(1)Firstly, let half part of humidity sensitive materials in the valve exposed to the air.

a) Insert a valve with humidity sensitive materials into sand soil. The distances between the dripper and valve body were respectively set to 5cm，10cm，and 20cm.

b) Mixed materials at ratio of 1:1 and the total volume 2ml or 4ml were respectively put into the control unit of the valve. When irrigation experiment was starting, time to close and open the dripper (on the valve body, seen in the figure 2(B)) again should be observed carefully and be recorded. Moisture transmission rate could be calculated through the set distances and recorded time.

c) After that, mixed materials at ratio of 1:3 and the total volume 2ml or 4ml were put into the control unit. Data should be recorded as well.

d) According to the step (a-c), conducted the above experiments in the conditions of clay soil and loam soil in order, and recorded data.

(2)Then, let the whole mixed materials into soil isolated from air.

In contrast, experiments in three kinds of soil respectively at ratio of 1:1 and volume 2ml would be done in the condition of isolated from air, i.e., the control unit including humidity sensitive material was totally inserted into soil. Also observed the time to close and open the dripper again, and recorded data.

试验地概括

试验于北京市海淀区北京林业大学车辆实习中心进行。地理位置为北纬 39 度，东经 116 度，海拔为 20~60 米，气候条件为暖温带半湿润半干旱季风气候，全年平均气温为 11～13℃，年降水量 600～700 毫米之间，年平均日照 2780.2 小时。

试验材料

在前人的研究基础上，选用粒径为 0.5mm 的法国 SNF 保水剂作为试验材料，如图 2 所示。该保水剂属于丙烯酰胺-丙烯酸盐共聚交联物，使用寿命较长，可维持 4 年左右[11]。根据前期研究，选取粒径 1~2mm 的砂石与 SNF 混合作为阀门控制单元中的材料，以提高控制单元的吸水和失水速率[5]。本试验中选择的材料为：SNF 与砂石混合体积比为 1:1 和 1:3，总体积为 2ml 或 4ml。

试验中涉及三种土壤，分别是砂土，壤土和粘土，三种土壤中，砂土的间隙最大，粘土的间隙最小，壤土的间隙居中，并且壤土是砂土与粘土按体积 1:1 混合而得到的。

试验方法

试验中涉及三种土壤，三种距离，两种湿敏材料的配比，两种湿敏材料的体积，两种湿敏材料的插入深度，整个试验可分为 2 大类 45 组。

（1）先将湿敏材料的一半与空气接触进行试验。

a）具体操作：将节水阀插入砂土中，其滴口与阀体距离分别为 5cm，10cm，20cm。

b）将比例为 1:1 总体积为 2ml 或 4ml 的混合湿敏材料分别放入阀门的控制单元中。然后开始灌溉试验，仔细观察节水阀门关闭和再次打开的时间，并记录数据。通过预设的距离以及时间就可以计算出水分传输的速率。

c）接下来，选用比例 1:3 总体积为 2ml 或 4ml 的混合湿敏材料放入阀门的控制单元中，同样记录节水阀门关闭和再次打开的时间数据。

d）按照步骤（a-c），依次在上述条件下进行粘土和壤土的试验，并记录数据。

（2）然后，将整个阀门控制单元插入土中，即湿敏材料与空气完全隔离。

该部分作为对照组，进行的是节水阀中的湿敏材料与空气不接触，即阀体完全插入土壤中，混合湿敏材料比例为 1:1 总体积为 2ml，依次在上述三种土壤中的试验，观察节水阀门关闭时间和再次打开的时间并记录数据。

RESULTS AND DISCUSSIONS

Overall results of the experiment

The results of test (1) and (2) above were shown in Table 1 and Table 2. Analyses results were mainly reflected in the figure, shown in the following.

结果与分析

总体试验结果

表 1 和 2 列出了上述试验所得的结果。分析结果主要以下图表示。

Table 1

Data of test (1) in which half part of the humidity sensitive materials were exposed to the air

Serial No.	Volume ratio	Volume/ml	Distance between dripper and valve /cm	Type of soil	Time to close/h	Time to open/h	Temperature /humidity when closed	Temperature /humidity when opened
1	1:1	2	5	sand	3.5	89	11 °C 63%	12 °C/53%
2	1:1	2	10	sand	4.5	91	11 °C /75%	11 °C /52%
3	1:1	2	20	sand	8	109	12 °C /76%	13 °C /77%
4	1:1	4	5	sand	3	91	13 °C /77%	14 °C /89%
5	1:1	4	10	sand	5	95	14 °C /78%	11 °C /63%
6	1:1	4	20	sand	6	101	12 °C /65%	12 °C /76%
7	1:3	2	5	sand	4.5	87	11 °C /63%	12 °C /53%
8	1:3	2	10	sand	6	88.5	11 °C /75%	11 °C /52%
9	1:3	2	20	sand	9.5	104.5	12 °C /76%	13 °C /77%
10	1:3	4	5	sand	3.5	75	13 °C /77%	14 °C /89%
11	1:3	4	10	sand	5.5	78	14 °C /78%	13 °C /77%
12	1:3	4	20	sand	7	92	15 °C /89%	15 °C /89%
13	1:1	2	5	clay	6	97	13 °C /66%	12 °C /76%
14	1:1	2	10	clay	8	104	12 °C /65%	13 °C /77%
15	1:1	2	20	clay	10	121	13 °C /77%	11 °C /63%
16	1:1	4	5	clay	4.5	101	12 °C /65%	13 °C /66%
17	1:1	4	10	clay	7	109	12 °C /76%	14 °C /67%
18	1:1	4	20	clay	8	131	13 °C /66%	13 °C /77%
19	1:3	2	5	clay	7.5	95.5	13 °C /66%	12 °C /76%
20	1:3	2	10	clay	10	100	12 °C /65%	13 °C /77%
21	1:3	2	20	clay	12	117	13 °C /77%	11 °C /63%
22	1:3	4	5	clay	6.5	95	12 °C /65%	13 °C /66%
23	1:3	4	10	clay	8	107	12 °C /76%	14 °C /67%
24	1:3	4	20	clay	9.5	129.5	13 °C /66%	13 °C /77%
25	1:1	2	5	loam	4	95	11 °C /63%	12 °C /65%
26	1:1	2	10	loam	6	100	12 °C /65%	12 °C /53%
27	1:1	2	20	loam	9	118	11 °C /63%	13 °C /66%
28	1:1	4	5	loam	4	95	13 °C /77%	13 °C /77%
29	1:1	4	10	loam	6	102	14 °C /78%	14 °C /78%
30	1:1	4	20	loam	7	115	13 °C /77%	15 °C /89%
31	1:3	2	5	loam	6	89	11 °C /63%	12 °C /65%
32	1:3	2	10	loam	8	94	12 °C /65%	12 °C /53%
33	1:3	2	20	loam	10	110	11 °C /63%	13 °C /66%
34	1:3	4	5	loam	5	78	13 °C /77%	13 °C /77%
35	1:3	4	10	loam	7	90	14 °C /78%	15 °C /89%
36	1:3	4	20	loam	8	112	15 °C /89%	16 °C /89%

Table 2

Experimental data of humidity sensitive materials completely inserted into the soil in the control groups

Serial No.	Volume ratio	volume/ml	Distance between dripper and valve /cm	Type of soil	Time to close/h	Time to open/h	Temperature /humidity when closed	Temperature /humidity when opened
1	1:1	2	5	sand	5	92	15 °C /78%	15 °C /89%
2	1:1	2	10	sand	6.5	99	16 °C /89%	17 °C /90%
3	1:1	2	20	sand	9	115	15 °C /89%	16 °C /79%
4	1:1	2	5	clay	8	101	14 °C /78%	14 °C /78%
5	1:1	2	10	clay	9	112	15 °C /89%	15 °C /78%
6	1:1	2	20	clay	12	123	16 °C /89%	16 °C /89%
7	1:1	2	5	loam	7	97	16 °C /89%	16 °C /89%
8	1:1	2	10	loam	8	110	15 °C /78%	17 °C /90%
9	1:1	2	20	loam	10.5	122	17 °C /90%	15 °C /78%

The relationship between transmission rate and type of soil

From the data obtained from the experiment, it could be known the relationship between type of soil and moisture transmission rate between humidity sensitive materials and soils.

Figure 3 and 4 displayed the rising rate and falling rate of the valve's spool (that is, the rate of closing and opening the valve again) at the mixture ratio of 1:1 and volume 2ml when half of the humidity sensitive materials were contacted with air. In the figure, X-axis and Y-axis separately denoted the distance between dripper and valve body with unit cm and the time (to close and open the dripper again) with unit hour.

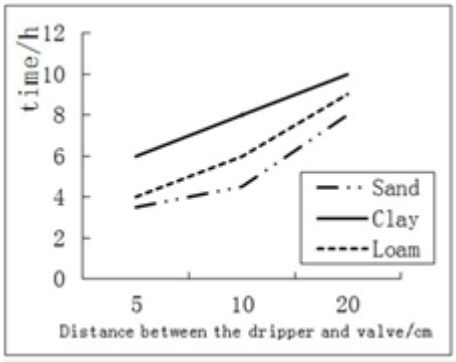

Fig.3- Rising rate of the spool

Seen from the figure 3 and 4, time to close the valve or open it again in sand soil was shortest while in clay soil was longest at the same distance between dripper and valve body, which illustrated that the fastest moisture transmission rate between humidity sensitive materials and soils could be found in sand and the slowest in clay. Same conclusion should be obtained after observing the data in Table 1 and Table 2 at different type of soil but with same ratio, volume and area contacted with air.

This phenomenon results from the different clearance of three types of soils. It was easy to find that the biggest clearance was in sand and the smallest in clay. So moisture transmission rate was the fastest in sand, and moisture could reach into the valve at the fastest speed and make humidity sensitive materials in valve swell quickly. But on the contrary, with transmission rate being

传输速率与土壤种类之间的关系

根据试验所得到的数据可以得知水分在湿敏材料与土壤之间的传输速率与土壤种类之间的关系。

图 3 和 4 表明了在混合比为 1:1、体积为 2ml、湿敏材料一半与空气接触的条件下，节水阀阀芯的上升和下降速率（即阀门关闭和再次打开的速率）。图中，X 轴表示滴口与阀门的距离，单位为 cm，Y 轴表示经历时间，即节水阀门关闭和再次打开的时间，单位为 h。

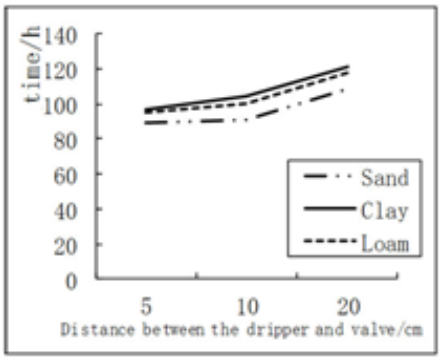

Fig.4- Falling rate of the spool

由图 3 和图 4 可以看出，在相同的滴口与阀体距离的条件下，在砂土中节水阀关闭所需时间最短，在粘土中阀门关闭所需时间最长，在壤土中居中。这说明了水分在湿敏材料与土壤间的传输速率，在砂土中最快，在粘土中最慢。通过观察表 1 和表 2 中的数据，在湿敏材料配比相同，体积相同，湿敏材料与空气的接触面积相同，而土壤种类不同的情况下，同样可以得到相同结论。

这样现象的产生，主要是因为三种土壤的间隙不同而导致的。我们可以很容易发现，三种土壤中，砂土的土壤间隙最大，水分在砂土中传输速率最快，所以水分可以以最快的速度到达节水阀中，并与湿敏材料接触，使得湿敏

the slowest in clay, humidity sensitive materials swell slowly. For the same reason, moisture evaporation speed was the fastest after the closure of the valve due to the big clearance in sand. Therefore, humidity sensitive materials had the fastest dehydration speed and the shortest time to open the valve again. However, the slow moisture evaporation rate caused by small clearance in clay would result in a longer time of dehydration and shrinkage, and a longer time to open the valve again. The clearance in loan fell somewhere between the sand and clay.

The relationship between transmission rate and ratio of humidity of sensitive materials

The relationship between transmission rate and ratio of humidity of sensitive materials would be analyzed by using the data obtained from the experiment. Figure 5-10 indicated the rising rate and falling rate of the valve's spool in three types of soils at the mixed ratio of 1:1 and volume 2ml when half of the humidity sensitive materials contacted with air.

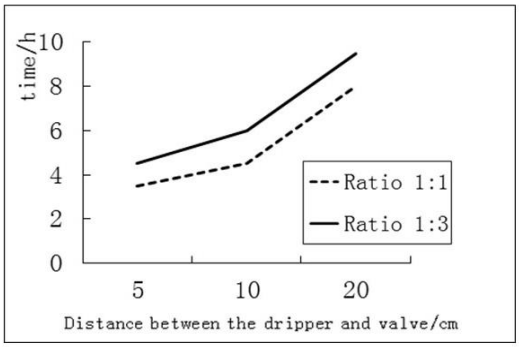

Fig.5 - The spool's rising rate in sand soil

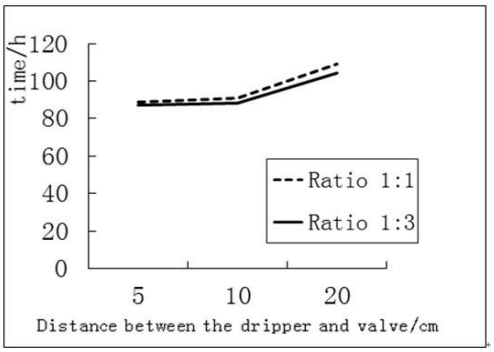

Fig.6 - The spool's falling rate in sand soil

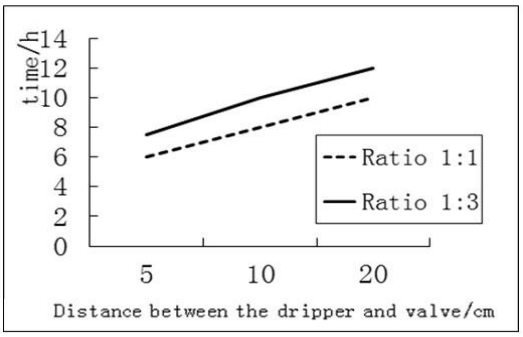

Fig.7 - The spool's rising rate in clay soil

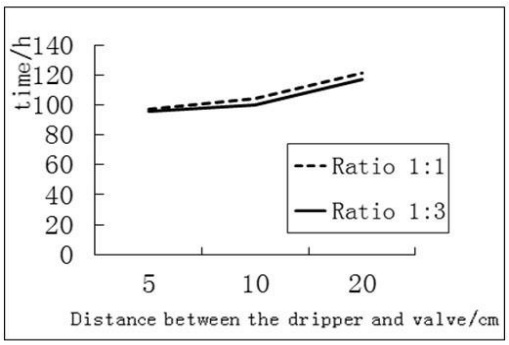

Fig.8 - The spool's falling rate in clay soil

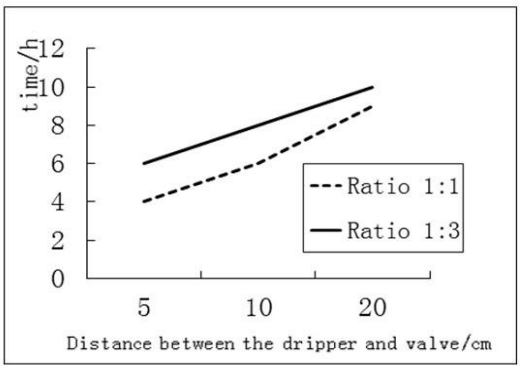

Fig.9 - The spool's rising rate in loam soil

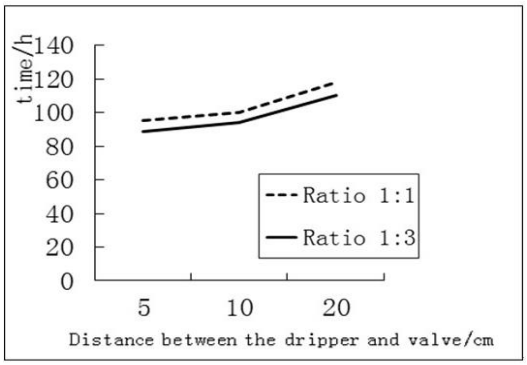

Fig.10 - The spool's falling rate in loam soil

It could be obtained from figure 5-10 that the spool has risen faster at the mixed ratio of humidity sensitive

材料最快膨胀；而粘土间隙最小，水分在粘土中传输速率最慢，所以湿敏材料膨胀速率最慢；同样的道理，因为砂土间隙大，所以在节水阀门关闭后，水分从砂土中蒸发的速度也最快，所以湿敏材料能最快脱水收缩，所以砂土中节水阀门再次打开所需的时间最短，而粘土则因间隙小，水分蒸发慢导致湿敏材料脱水收缩的时间变长，所以节水阀门再次打开的时间长，而壤土间隙介于二者之间，所以所需时间也处在砂土与粘土之间。

传输速率与湿敏材料配比之间的关系

利用试验所得到的数据可以分析出水分传输速率和湿敏材料配比的关系。图 5-10 表示在混合比为 1:1、体积为 2ml、湿敏材料一半与空气接触的条件下，节水阀阀芯在三种土壤类型中上升和下降速率。

由图 5-10 中可以看出，对于三种土壤，湿敏材料体积为 2ml，配比 1:1 与配比 1:3 比较，对于土壤达到相同的湿

materials 1:1 than that of 1:3, and fell slower when the ratio was 1:1 than that of 1:3 under the same conditions. The expansion amount of the mixture materials was larger because of more SNF at higher mixed ratio. Shrinkage was less because more SNF needed to dry in the valve, so time to open the valve again would be longer, and the spool had a slower moving.

The relationship between transmission rate and whether humidity sensitive materials exposed to the air

Based on the mixture materials contacting the air or not, an analysis was done comparatively to the condition of volume 2ml, ratio 1:1. Analysis results of the three types of soils were shown in figure 11-16.

度，在其他条件相同时，节水阀阀芯上升速率在配比 1:1 时比配比 1:3 时快，节水阀阀芯下降速率在配比 1:1 时比配比 1:3 时慢。因为在其他条件相同的情况下，比例越大，保水剂越多，吸水膨胀的越快。节水阀阀芯上升速率越快；同理，因为体积比大湿敏材料多，脱水收缩所需的时间变多，所以节水阀门再次打开所需时间增加，节水阀阀芯下降速率变慢。

传输速率与湿敏材料和空气接触与否的关系

针对湿敏材料与空气接触与否，在混合比为 1:1 体积 2ml 的条件下进行比对分析。三种土壤的分析结果如图 11-16 所示。

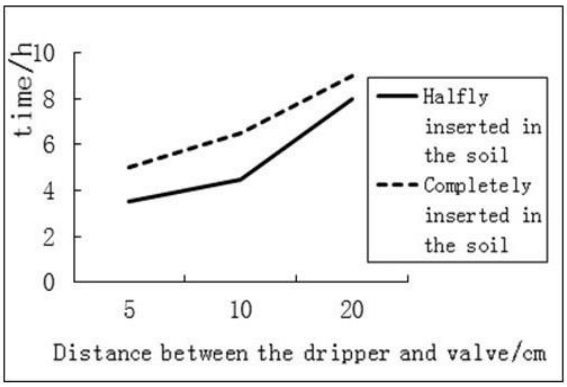

Fig.11 - The spool's rising rate in sand soil

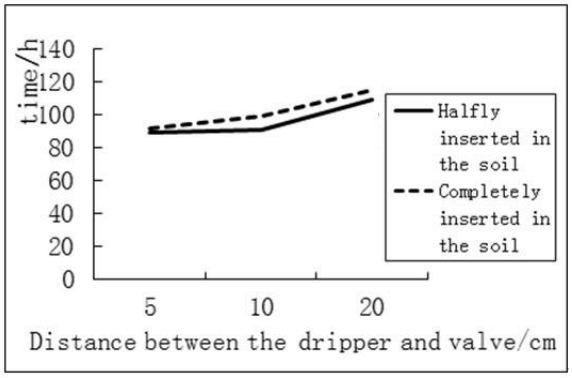

Fig.12 - The spool's falling rate in sand soil

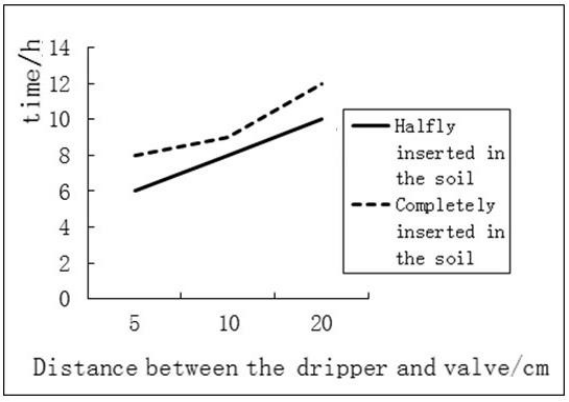

Fig.13- The spool's rising rate in clay soil

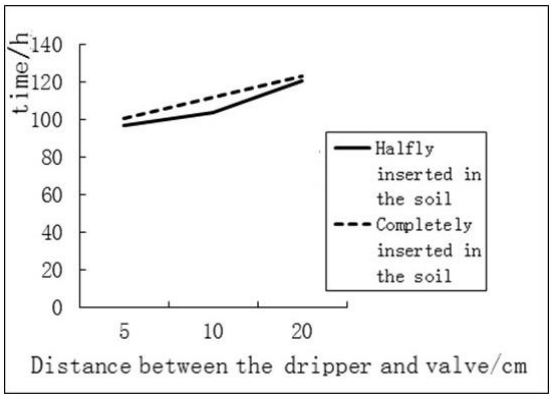

Fig.14- The spool's falling rate in clay soil

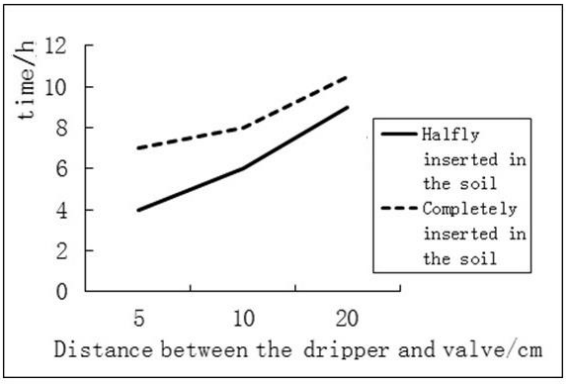

Fig.15 - The spool's rising rate in loam soil

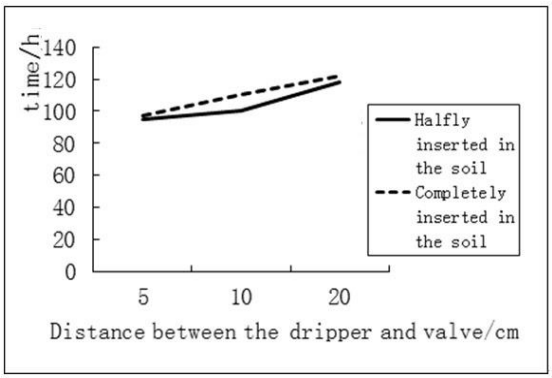

Fig.16 - The spool's falling rate in loam soil

It could be seen from figure 11-16 that the spool rose or fell faster when the mixture materials in valve contacted the air in all three soils at the mixing ratio of 1:1 and volume 2ml, which indicated that moisture transmission rate between humidity sensitive materials and external environment was faster when the valve half inserted into soil. It was mainly because that moisture needed evaporation after the closure of the valve caused by a certain degree of soil moisture, then the valve should be opened again. In the process, the humidity of air was less than that of soil, so humidity sensitive materials contacted with air had a faster dehydration speed, a shorter shrinkage time and a shorter time to open the valve again.

CONCLUSIONS

The new valve type was developed with the idea of water saving and energy conservation, which could control irrigation on-off without computer and sensors. It was especially suitable for popularization and promotion in agricultural and forestry irrigation of poor condition area.

Following conclusions were mainly found that moisture transmitting rate between humidity sensitive materials and the soils or the air was influenced by clearance of the soil, ratio of humidity sensitive materials, and whether exposure to the air through the above experiments and analyses.

(1)The fastest transmission rate of moisture between humidity sensitive materials and soil could be found in sand and the slowest in clay for different kinds of soils.

(2) The speed of material water-absorption was faster when its ratio was 1:1 than that of 1:3, and speed of material water-loss was slower at the ratio 1:1 than that of 1:3.

(3) The transmission rate of moisture was faster when contacting with air. Besides, a general time range (time to close the valve from 3 to 12 hours and time to open it again from 70 to 130 hours) could be summarized from the experimental data.

It would provide reference for the further application of the new water-saving valve, and it is helpful to develop rapidly water-and energy-efficient technologies to promote the steady and efficient development of agriculture and forestry products.

ACKNOWLEDGEMENT

The financial support of the Fundamental Research Funds for the Central Universities (No. YX2011-6) is gratefully acknowledged.

REFERENCES

[1]. Junjun Li. (2009) - *Study on Mechanical Properties of Control Unit of Control Valves without Power Supply*, Beijing Forestry University;

[2]. Junjun Li, Guosheng Yu. (2008) - *Experimental Study on Mechanical Proper ties of Control Unit of Control Valves without Power Supply*, Forestry Machinery & Woodworking Equipment. vol. 36, no.10, pp.12-15;

[3]. Ke Du, Xiangyue Yuan. (2011) - *Advances in Passive Control of Water Saving Irrigation Valve*, Hunan

从图 11-16 中可以看出，在其他条件相同时，湿敏材料体积 2ml，比例为 1:1 的情况下，对于三种土壤而言，湿敏材料有一半与空气接触时节水阀阀芯上升速率快于湿敏材料完全不与空气接触的情况，当湿敏材料有一半与空气接触时，节水阀阀芯下降的速率比湿敏材料完全不与空气接触时的快。也就是说明湿敏材料与空气接触时，则水分在湿敏材料与外界的传输速率越快。出现这样的结果，主要是因为当土壤湿润到一定程度，节水阀关闭后，水分需要蒸发，节水阀才能再次打开，此时空气的湿度小于土壤湿度，所以与空气接触的湿敏材料脱水速度变快，所以收缩的时间变短，节水阀再次打开所需时间变少。

结论

本文研制了一种无需计算机和传感器控制阀门开关的新型阀门，它以节水节能为本，尤其适于在落后条件的农业和林业地区推广和实施。

通过上述试验分析，可以得到无源智能节水阀门工作时，水分在湿敏材料与土壤和空气间传输速率与土壤间隙，湿敏材料配比，湿敏材料与空气接触与否三个影响因素的一些结论。

（1）对于不同的土壤种类，水分在湿敏材料和土壤之间传输速率在砂土中最快，而在壤土中最慢。

（2）对于湿敏材料的不同配比，对于材料吸水速率在配比 1:1 时比配比 1:3 时快，材料失水速率在配比 1:1 时比配比 1:3 时慢。

（3）对于湿敏材料是否与空气接触两种情况，与空气接触时的水分传输速率较快。同时，从试验数据可以总结出节水阀门关闭和再次打开大体有一个时间范围，基本上在 3 小时到 12 小时的范围内能够关闭，节水阀门再次打开也有一个范围大体上在 70 个小时到 130 个小时之间。

该研究可为新型节水阀门的进一步应用提供参考，同时，对于发展节水节能技术以提高农林业产品的稳步高效发展也很有帮助。

致谢

本文受到中央高校基本科研业务费专项资金资助（项目号：No. YX2011-6）。

参考文献

[1]. 李俊俊. (2009) - *无电源节水阀门控制单元性能研究[D]*. 北京林业大学机械设计及理论专业硕士论文, 中国, 北京;

[2]. 李俊俊, 俞国胜.(2008) - *无电源控制阀门控制单元力学性能实验研究*, 林业机械与木工设备, 第 36 卷, 第 10 期, 12-15;

[3]. 杜珂,袁湘月. (2011) - *无源控制节水灌溉装置研究进*

Agricultural Sciences, vol.23, no.11, pp.136-138;
[4]. Ke Du, Guosheng Yu, Xiangyue Yuan. (2013) - *Research on the Control Mechanism of Intelligent Water-saving Valve Control Elements*, Forestry Machinery & Woodworking Equipment, vol. 41, no. 9, pp.36-38;
[5]. Ke Du. (2013) - *Research in Wet Sensitivity of Humidity Control Component of Intelligent Water-saving Valve*, Beijing Forestry University.
[6]. Ornstein L. (1985) - *The Irristat: A moisture-sensitive self-regulating water valve for drip irrigation systems*, vol II, Proceedings Third International Drip/Trickly Irrigation Congress, Fresno, CA. ASAE, Nov. 17-21, pp.623-629;
[7]. Patamanska, G, Chehlarova-Simeonova, S. (2012)- *Changing existing irrigation systems and management in Bulgaria for sustainable use of water*, INMATEH - Agricultural Engineering, v 38, n 3, pp.73-78;
[8]. Robert G, Edward L, Marty W. (1986) - Water-sensitive valves for monitoring crop water use pattern, ASAE Technical Paper 86-2572. Presented at Winter Meeting of ASAE, Chicago, IL. Dec.16-19, pp.1-14;
[9]. Shuhui Luo. (2012) - *Face the Challenges of Water Resources*, WTO Economic Herald, no.5, pp.77-78;
[10]. Tingjun Wang, Weizhan Zhang. (2012) - *Status and Ways of Water Saving in Agriculture*, Beijing Agriculture, no.9, pp.149;
[11]. Xiaosan Liu, Chuan Ye, Guobin Xiao. (2012) - *Effect on the soil moisture and growth of autumn glutinous maize and polyacrylamide water retaining agent*, Chinese Agricultural Science Bulletin, no.30, pp.22-27.

展, 湖南农业科学, 第 23 卷, 第 11 期, 136-138;
[4]. 杜珂,俞国胜,袁湘月. (2013) - *智能节水阀门控制元件控制机理研究,* 林业机械与木工设备, 第 41 卷, 第 9 期, 36-38;
[5]. 杜珂. (2013) - *智能节水阀门湿敏控制元件湿感灵敏度的研究,* 北京林业大学机械设计及理论专业硕士论文, 中国, 北京.
[6]. Ornstein L. (1985) – *一种湿敏自调节滴灌阀门系统[A]*. 世界第三届滴灌会议第 2 卷[C], 美国加州夫勒斯诺市: 美国农业工程师协会,1985 年 12 月. 17-21, 623-629;
[7]. Patamanska, G, Chehlarova-Simeonova, S. (2012) - *改变灌溉系统和管理提高水资源可持续利用*, INMATEH - 农业工程, 第 38 卷, 第 3 期, 73-78;
[8]. Robert G, Edward L, Marty W. (1986) – *水分控制阀门监测作物需水模式 [A]*. 美国农业工程师协会冬季技术会议论文[C], 美国伊利诺伊州芝加哥: 美国农业工程师协会,1986 年 12 月 16 日-19 日, 1-14
[9]. 罗曙辉. (2012) - *应对水资源挑战,* WTO 经济导刊, 第 5 期, 77-78;
[10]. 王庭俊, 张伟战. (2012) - *我国农业用水现状及节水途径*, 北京农业, 第 9 期, 149;
[11]. 刘小三, 叶川, 肖国滨, 等. (2012) - *聚丙烯酰胺型保水剂对土壤水分及秋糯玉米生长的效应,* 中国农学通报, 第 28 卷, 第 30 期 , 22-27.

EFFECT OF ALTERNATE PARTIAL ROOT-ZONE IRRIGATION AND INFILTRATING IRRIGATION ON PHOTOSYNTHETIC CHARACTERISTICS AND YIELD OF JUJUBE TREES

/

渗灌和分根交替灌溉对枣树光合特性及产量的影响

Prof. Ph.D. Stud. Agr. Feng Y. [1,2)], Prof. Ph.D. Sci. Zhou J. [1*)], As. Ms. Agr. Wang Z. [2)], As. Ph.D. Agr. Zhang W. [3)], Ph.D. Agr. Yu.D. [4)]

[1)] School of Resources and Environment, Northwest A&F University / China; [2)] Institute of Fertilizer and Agricultural Water Conservation, Xinjiang Academy of Agricultural Sciences / China; [3)] College of Grassland and Environmental Sciences, Xinjiang Agricultural University / China; [4)] Department of Earth & Environmental Studies, Montclair State University / USA

Tel: +8618999973689; E-mail: fengyaozu@sina.com

Abstract: *At present, irrigation in Ziziphus Jujuba orchards around Tarim basin in Xinjiang Province, China, is mainly surface irrigation. Due to outdated irrigation technology and low irrigation efficiency, the fruit yields are low, which seriously affects sound development of local special forest fruit industry in Xinjiang. Infiltrating irrigation technology has favorable water-saving effects and studying its impact on the physiological and yield variation of Jujube trees would therefore greatly assist the development of the Jujube industry in Xinjiang China. Several ten-year-old Jujube trees were selected in Akesu area of Xinjiang to investigate the effects of different water-saving irrigation methods on their physiology and yield. Diurnal variation of photosynthetic capacity in Jujube leaves during florescence, young fruit and fruit expanding stages and Jujube yield were measured under 6000 m^3/ha of alternate partial root-zone irrigation and conventional infiltrating irrigation. The results indicated that: (1) the diurnal variation of net photosynthetic rate in Jujube leaves presented a bimodal curve with a midday depression phenomenon. The diurnal variation of transpiration rate appeared to single peak type. The diurnal variation of water use efficiency was a single-valley curve. The stomatal conductance varied during the growth season; (2) under conventional irrigation, the net photosynthesis rate, stomatal conductance and transpiration rate increased with increased irrigation volume; and (3) with the same irrigation volume, the root-divided alternative irrigation, compared with conventional irrigation, reduced leaf transpiration rate and increased leaf net photosynthesis rate and water use efficiency, resulting in an increase of Jujube yield by 11% per hectare. The study showed that root-divided alternative irrigation could save water consumption and increase Jujube yield*

Keywords: *jujube; root irrigation; root-divided alternative irrigation; photosynthesis*

INTRODUCTION

Jujube is the key industry of Xinjiang China, especially for the area around Tarim basin in South Xinjiang China. The region around Tarim basin has advantages in land, light and heat resources, but inadequate water is a major constraint affecting rapid development of the Jujube industry. Most irrigation system in orchards around Tarim basin use surface irrigation. As a result of outdated irrigation technology, extensive irrigation management, poor controllability of irrigating water quotas and low irrigation efficiency, The Chinese data are low and of inferior quality and low benefit fruit, which seriously affects sound development of this fruit industry. Therefore, study of the impact of different irrigation modes and volumes on the water utilization and yield of Jujube tree is necessary.

摘要： *目前，新疆环塔里木盆地枣园多采用地面灌溉方式，灌溉技术落后、效率低，导致枣树产量低，严重阻碍了新疆特色林果业健康发展。渗灌技术具有良好的节水效果，因此研究渗灌对枣树生理及产量变化影响，对发展新疆特色枣业具有科学指导意义。本研究以阿克苏地区实验林场九队10年树龄的灰枣为研究对象，利用Li-6400便携式光合仪，在6000$m^3 \cdot hm^{-2}$分根交替灌溉和不同灌溉量的渗灌条件下测定花期、幼果期和膨大期枣树叶片光合日变化，及其测定枣树产量。结果表明：（1）枣树叶片净光合速率日变化为双峰曲线，具有光合"午休"现象；蒸腾速率日变化曲线呈单峰型；水分利用效率日变化则呈单谷型；气孔导度随生育期的推进变化趋势不同。（2）常规渗灌条件下，随着灌溉量增加叶片净光合速率、气孔导度、蒸腾速率呈上升趋势。（3）同一灌溉量,与常规渗灌相比，分根交替灌溉能降低叶片蒸腾速率，提高叶片净光合速率、水分利用效率和枣树产量，且亩产量提高11%。初步证明，分根交替灌溉能够起到节水增产作用，为节约水资源，提高枣产量，促进特色枣产业的持续发展提供决策依据。*

关键词： *灰枣；渗灌；分根交替灌溉；光合特性*

引言

枣产业是新疆，特别南疆环塔里木盆地的重点产业，南疆环塔里木盆地具有得天独厚的土地和光热资源，但水资源不足是该区枣产业快速发展的主要制约因素之一。目前，南疆环塔里木盆地的大部分果园现大多采用地面灌溉，灌溉技术落后，灌溉管理粗放，灌水定额可控性差，灌溉效率低、导致果品产量少，品质差、效益低，严重阻碍了林果产业的健康发展。因此，研究不同灌溉方式和灌溉量对枣树水分利用与产量的影响具有重要的科学价值。

Photosynthesis has a close contact with the physiological and ecological indexes of plants, and it is the key factor affecting their yield and quality [10-12, 17]. Study of the diurnal variation of photosynthesis characteristics of potted mango seedlings under different soil water contents allowed determining the optimal soil water content range [16].Study of photosynthetic function of apple leaves under different irrigation modes by Ma et al [8] showed that alternate half root-zone irrigation was optimal. Chai et al [1] determined the diurnal variation of photosynthesis characteristics of fragrant pear during different growing periods. However, there are few reports concerning photosynthesis characteristics of Jujube trees under different moisture regulation. This study analyzed the diurnal variation of photosynthesis of Jujube leaves and yield during different growth periods under conditions of regular infiltrating irrigation and alternate partial root-zone irrigation (APRI). The results will provide a scientific foundation for saving water resources, increasing Jujube yield and accelerating the sustainable development of the Jujube industry.

MATERIALS AND METHODS

Study area

The study area located in Team 9 of Experimental Forest Farm, Akesu Prefecture, Xinjiang, China (80°20'E, 41°10'N; 1200 m). The area has a temperate continental climate, with long sunshine duration and large day–night temperature differences. The annual sunshine duration is 2800–3831 h. The total radiation amount is 6000 MJ/hm^2 and it is one of the areas with the most solar radiation in China. The annual frost-free season is 183–227 d, the annual average temperature is 9.9–11.5°C, and annual precipitation is 42.4–94 mm. Ten-year-old Jujube trees were selected in the study area, with planting interval of 2 m × 4 m. The surface soil texture is sandy, and the profile soil texture is sand over clay. The chemical characteristics of the soil profile are shown in Table 1.

光合作用与植物生理生态指标有着密切的关系，是影响植物产量和品质关键因素[10-12, 17]。姚全胜通过对不同土壤水分含量条件下杧果盆栽幼苗光合特性日变化规律的研究，确定最佳杧果盆栽的土壤含水量范围[16]；马怀宇通过对不同灌水方式下苹果叶片光合功能的研究，结果表明[8]，半根交替灌水为最佳灌溉方式；柴仲平[1]通过对梨树（香梨）不同生长期光合日变化研究，确定了梨树光合特性变化规律，但对水分调控下枣树光合特性研究鲜见报道。本研究在常规渗灌与分根交替灌溉条件下，结合当地环境因子变化特征，分析枣树不同生育期枣树叶片光合日变化规律和枣树产量变化规律，为节约水资源，提高枣产量，促进特色枣产业的持续发展提供决策依据。

材料与方法

试验地概况

试验地位于新疆阿克苏地区实验林场九队(80°20′E、41°10′N)，海拔 1200m。属温带大陆性气候，光照时间长，昼夜温差大，年日照时数为 2800-3831.35h,总辐射量 6000MJ·hm^{-2}，是全国太阳辐射量最多地区之一，全年无霜期为 183-227d，年平均气温为 9.9℃-11.5℃，年降水量 42.4-94mm。试验地枣树品种为 10 年树龄灰枣，枣树种植模式为 2m×4m，试验区土壤质地为沙土，质地构型为下粘上沙，土壤剖面肥力特征见表 1。

Table 1

Soil profile characteristics and nutrients of Jujube in the study area

Depth [cm]	Texture	Saturated moisture content [%]	Unit weight [g/cm^3]	Available nitrogen [mg/kg]	Phosphorus concentration [mg/kg]	Available kalium [mg/kg]	Organic content [%]	Salinity [g/kg]	pH
0–20	Sandy soil	28.18	1.46	6.15	14.20	35.52	0.52	1.85	7.64
20–40	Sand	27.34	1.49	2.46	16.54	31.48	0.28	1.23	7.42
40–60	Clay	31.76	1.48	9.83	9.47	73.34	0.72	1.45	7.44
60–80	Clay	31.83	1.50	2.46	3.78	21.31	0.13	1.34	7.73

Material of infiltrating irrigation tube

The infiltrating irrigation tube was constructed of special rolled steel, with a pipe diameter of 32 mm, an aperture of 2 mm and a pitch of holes of 1.0 m (fig.1).

渗灌管材料

渗灌管材选用特制 Cr12 钢材，管径 32mm，孔径：2mm；孔距 1.0m（图 1）。

Fig.1 - Section of infiltrating irrigation tube

Experimental design

Two irrigation modes including regular infiltrating irrigation and Alternate Partial Root-zone Irrigation (APRI) were adopted. The regular infiltrating irrigation used three irrigation quotas: 3000 m3/hm2, 6000 m3/hm2 and 9000 m^3/hm^2 abbreviated as W1, W2 and W3, respectively. The laying method was two rows of infiltrating irrigation tubes placed under one row of fruit trees. The distance between the infiltrating irrigation tubes and trees was 70 cm, and placement depth was 25 cm.

The APRI used only one irrigation quota of 6000 m^3/hm^2. The laying method was three rows-6 tubes. From east to west, tube no.. 1, 4 and 5 were water supply system 1, while tube no. 2, 3 and 6 were system 2, and these two systems supplied irrigation alternately. The water volume was controlled by water meter and the total fertilizer amount was 1995 kg/hm^2 (Table 2), with each treatment having three replications.

试验设计

试验采用常规渗灌和分根交替灌溉两种灌溉方式，常规渗灌设置 3 个灌溉总额：3000 m^3/hm^2、6000 m^3/hm^2 和 9000 m^3/hm^2，分别记为 W1，W2，W3，铺设方式一行果树下铺设两行渗灌管，渗灌管距树 70cm，埋深 25cm；分根交替灌溉（APRI）设置一个灌水总额 6000 m^3/hm^2，铺设方式为 3 行 6 管，自东向西 1、4、5 管为一号供水系统，2、3、6 管为二号供水系统，一、二号供水系统交替灌溉；水量由水表控制，施肥总量为 1995kg/hm^2，每个处理 3 次重复，具体施肥见表 2。

Table 2

Fertilizer design

Total fertilizing amount		**1995[kg/hm^2]**				
Fertilizer variety		Fertilizing amount	Base fertilizer amount	Additional fertilizer before flowering		Additional fertilizer after flowering
N	[kg/hm^2]	997.5	72	587.1		334.5
P_2O_5		726	276	162		270
K_2O		262.5	37.5	37.5		187.5
Growth period		Budding period	Full-blossom period	Fruitlet period	Expanding period	Mature period
Additional fertilizer 11 times		1	4	3	2	1

Determination and control of soil moisture

A TRIME instrument was used to measure moisture before and after irrigation during the growth period, while a SM100 Soil Moisture Timing Collector was also used to measure before and after rainfall. Five points were fixed in two sides by taking the pipeline as the center, i.e., the horizontal perpendicular distances between the pipeline and the five points were respectively 0, ±35, ±70, ±105, and ±140 cm. In addition, six points were fixed in the vertical direction of the ground to monitor soil moisture variation (of vertical depths of 0, 20, 40, 60, 80 and 120 cm) giving a monitoring depth of 0–120 cm, Then, soil was extracted using a soil auger, dried and measured by TRIME instrument and SM100 Soil Moisture Timing Collector.

The following formula is used for calculating the irrigation period.

土壤水分测定及控制

采用随机取样的方法，生育期内灌前灌后水分监测采用 trime 仪观测、sm100 土壤水分定时采集器，降雨前后加测。以管道为中心两边分别定 5 个点，即在垂直管道距离为 0cm、±35cm、±70cm、±105cm，±140cm，5 个点，垂直地面 6 个深度，即垂直地面向下 0cm、20cm、40cm、60cm、80cm、120cm、6 个深度监测土壤含水变化，监测深度 0-120cm。土钻取土、烘干对 trime 仪和 sm100 进行校核。

灌水周期:

$$T = m / ET_a \quad (1)$$

Where, *T* is irrigation period (d), *m* is irrigation quota (m^3/hm^2) and ET_a is daily water consumption (m^3/hm^2). The detailed moisture adjustment program is shown in Table 3.

式中：T-灌水周期（天）； m-灌水定额 m^3/hm^2；ET_a-日耗水量 m^3/hm^2，具体水分调控方案见表 3 。

Table 3

The root penetration irrigation systems in Jujube orchard

Irrigation quota: 3000、6000、9,000 [m^3/hm^2]						
	Total	**Budding period**	**Full-blossom period**	**Fruitlet period**	**Expanding period**	**Mature period**
Irrigation quota	100%	5%	35%	30%	25%	5%
Irrigation frequency	26	3	6	7	6	4
Irrigation period	6.2 days	8 days	6 days	5 days	6 days	8 days

Determination of photosynthetic rate and physiological index

The Li-6400 Portable Photosynthesis Meter equipped with red and blue light (6400-02B) was used to determine the following indices of environmental factors during the flowering period (30 May 2012), the fruit period (25 June) and the expanding period (25 July), including photosynthetic active radiation (PAR) and atmospheric CO_2 concentration (Ca). The following photosynthetic physiological indices were also been determined: net photosynthetic rate (Pn), stomatal conductance (Gs) and evaporation rate (Evap). Three plants were selected in each treatment with relatively consistent growth and two healthy leaves from the middle and upper parts of young shoots were measured on cloudless days. The average value of three reading values of each leaf was regarded as the measured value. The period of time was 09:00–21:00, with one measurement every 2 h. The limiting value of water use efficiency (WUE) was calculated using the obtained parameters, using the formula: WUE= Pn/Evap

Determination of meteorological factors

A Vantage Pro2 wired automatic meteorological station was used to measure precipitation (P), solar radiation (Rs), air temperature (Ta), relative humidity (RH) and wind speed (Ws).

Yield determination

During the harvest time of Jujube, five plants were randomly selected in each treatment respectively, and the statistic was made by taking the plot as a unit. The quantity and weight of fruit, average weight of single fruit and total yield in each treatment were recorded to calculate the yield per hectare in accordance with single-plant yield and planting density.

Data processing

Excel 2010 and SPSS 18.0 were used for data processing and statistical analysis.

RESULTS AND ANALYSIS

Environmental factor analysis of Jujube orchard

Under natural conditions, variation in Rs, PAR, Ca, Ta, RH and other environmental factors all affected the photosynthesis characteristics of Jujube leaves. Rs and PAR among measured external environmental indices increased gradually with time from 9:00, reached peaks

光合速率及生理指标测定

于花期（2012 年 5 月 30 日）、幼果期（6 月 25 日）、膨大期（7 月 25 日），采用 Li-6400 便携式光合仪，配备红蓝光源（6400-02B），测定环境因子指标：光合有效辐射（*RAR*）和大气 CO_2 浓度（*Ca*），光合生理指标：净光合速率（*Pn*）、气孔导度（*Gs*）、和蒸腾速率（*Evap*）。每处理选取生长较为一致的植株 3 株，选光照较好的新梢中上部健康叶 2 片并标记，每叶片以 3 次读数的平均值作为测定值，时间为 09:00-21:00,每隔两个小时测定一次。根据所获取的参数计算水分利用效率 *WUE*，公式为 *WUE=Pn/Evap*。

气象因子测定

采用 Vantage Pro2 有线自动气象站测定降雨量（precipitation, P）和太阳辐射（solarradiation，Rs），气温（airtemperature，Ta），相对湿度（relative humidity, RH）和风速（wind speed，Ws）.

产量测定

在红枣收获期，每个处理随机选取 5 株进行单采单收，以小区为单位进行统计。采收时，记载各处理的果实数目、果实重量，平均单果重及总产量，根据单株产量和栽植密度计算出每亩产量。

数据处理

本文采用 Excel 2010 与 SPSS 18.0 进行数据处理与统计分析。

结果与分析

枣园环境因子分析

自然条件下，太阳辐射、光合有效辐射、大气 CO_2 浓度、大气温度以及大气相对湿度等环境因子的变化都会给果树叶片的光合特性带来影响。由表 4 可知，在测定的外界环

around 15:00 and then dropped gradually (Table 4). Rs and PAR in different growth periods increased gradually from 30 May, reached peaks on 25 June and dropped on 25 July. Ta presented a variation trend of initial increase followed by a decrease, with peak values all at 17:00. Diurnal variation amplitudes of Ta on 30 May, 25 June and 25 July were 20.6°C, 17.2°C and 19.8°C, respectively. That of the earlier growth period was higher than the latter, mainly because Ta at 9:00 was low in the earlier growth period.

This showed that large day–night temperature differences, strong Rs and low RH are typical climatic features of this desert-oasis zone. However, great variation in temperature and RH could improve the yield and quality of fruit trees as it increased the carbon assimilation capacity of plants in daytime and decreased the consumption of dry matter by plant respiration at night.

境指标中，太阳辐射和光合有效辐射从 9:00 开始随时间的推移逐渐升高，15:00 左右达到峰值，之后逐渐降低；不同生育期太阳辐射和光合有效辐射从 5 月 30 日开始逐渐增高，6 月 25 达到最高值，7 月 25 日有所下降。大气温度呈呈现先升高后降低的变化趋势，均在 17：00 温度达到最高值，5 月 30 日、6 月 25 日和 7 月 25 日的气温日变幅为 20.6℃、17.2℃、19.8℃，生育初期的日气温变幅高于后期，主要是因为生育初期 9:00 的大气温度偏低的。

可见，昼夜温差大，太阳辐射强，空气湿度低等气候特征为荒漠绿洲区的典型气候特征，而温湿度变化大的特点，可以提高植物白天的碳同化能力并且降低夜间的植物呼吸作用对干物质的消耗，从而提高果树果实的产量及品质。

Table 4

Daily changes of environmental factors in different growth periods

Date	Indices	Determined time						
		9:00	11:00	13:00	15:00	17:00	19:00	21:00
30 May	Solar radiation [W/m^2]	92	275	603	764	631	443	188
	Air temperature [^{o}C]	11.7	20.1	26.2	32	32.3	30.1	29.3
	Relative humidity [%]	73	43	31	13	15	16	21
	Photosynthetic active radiation [μmol/(m^2·s)]	597.33	1,490.00	1,640.00	1,928.00	1,640.00	751.50	429.33
	Atmospheric CO_2 concentration[μmol/mol]	404.67	393.30	396.83	397.00	398.70	401.57	404.43
25 June	Solar radiation [W/m^2]	127	261	774	854	653	456	283
	Air temperature [^{o}C]	18.1	25.8	28.6	34.5	35.3	34.1	30.8
	Relative humidity [%]	51	38	33	18	21	23	22
	Photosynthetic active radiation [μmol/(m^2·s)]	1,397.67	1,940.00	2,123.67	2,400.00	1,998.00	1,840.00	1,674.00
	Atmospheric CO_2 concentration [μmol/mol]	409.57	402.83	383.33	387.60	392.43	388.57	395.60
25 July	Solar radiation[W/m^2]	104	191	687	807	660	456	169
	Air temperature [℃]	16.6	24.4	29.3	36.4	37.6	36.4	33.1
	Relative humidity [%]	75	58	40	20	27	28	35
	Photosynthetic active radiation [μmol/(m^2·s)]	673.67	1,515.33	2,050.33	2,155.00	1,600.67	1,531.00	1,274.00
	Atmospheric CO_2 concentration(μmol/mol)	437.53	367.10	361.77	379.60	384.90	388.57	395.60

Note: The former three items were from the observed results of the meteorological station (observation once every 15 min), while the latter two were from the measured results of the photosynthesis meter.

Diurnal variation of photosynthesis under infiltrating irrigation

1) Diurnal variation of net photosynthetic rate

The diurnal variation of Pn of jujube leaves at different growth periods presented an 'M' shape (Fig. 2), with the peak value usually at 11:00 and 17:00; and it always showed a 'noon break' appearance during 14:00–16:00, especially under W1 treatment. Under regular infiltrating irrigation, the Pn of Jujube leaves showed a steady increasing trend with increased irrigation volume. For the daily average Pn on 30 May (Table 5), that of W1 significantly decreased by 23% compared with that of W3 (P < 0.05). Meanwhile, the difference in Pn between W2 and APRI was not significant, and the Pn of APRI increased slightly compared with that of W2. On 25 June, the Pn of W1 significantly decreased by 21.2% compared

渗灌条件下光合特性日变化规律

1)净光合速率(Pn)的日变化规律

由图 2 可知，不同生育期枣树叶片净光合速率日变化呈"M"型，峰值基本都出现在 11:00 和 17:00，14:00-16:00 均出现"午休"现象，W1 处理下"午休"现象最明显。常规渗灌下随着灌溉量的增加，叶片的光合速率呈明显的稳定上升的趋势。5 月 30 日的日平均光合速率（表 5）W1 与 W3 相比降低 23%，差异显著（P<0.05），W2 和 APRI 净光合速率差异不显著；APRI 和 W2 相比略有上升。6 月 25 日 W1 与 W3 相比降低了 21.2%，差异显著

with that of W3 (P < 0.05). On 25 July, the Pn of W1 and W2 decreased by 33% and 13%, respectively, compared with that of W3 (P < 0.05). The Pn of APRI increased by 14% compared with that of W2 (P < 0.05). Thus APRI significantly increased the Pn of Jujube leaves under the same irrigation volume compared to regular infiltrating irrigation.

（P<0.05）。7 月 25 日 W1、W2 与 W3 相比分别降低了 33%和 13%，差异显著（P<0.05）；APRI 与 W2 相比上升了 14%，差异显著（P<0.05），表明同一灌溉量，APRI 能够显著提高枣树叶片净光合速率。

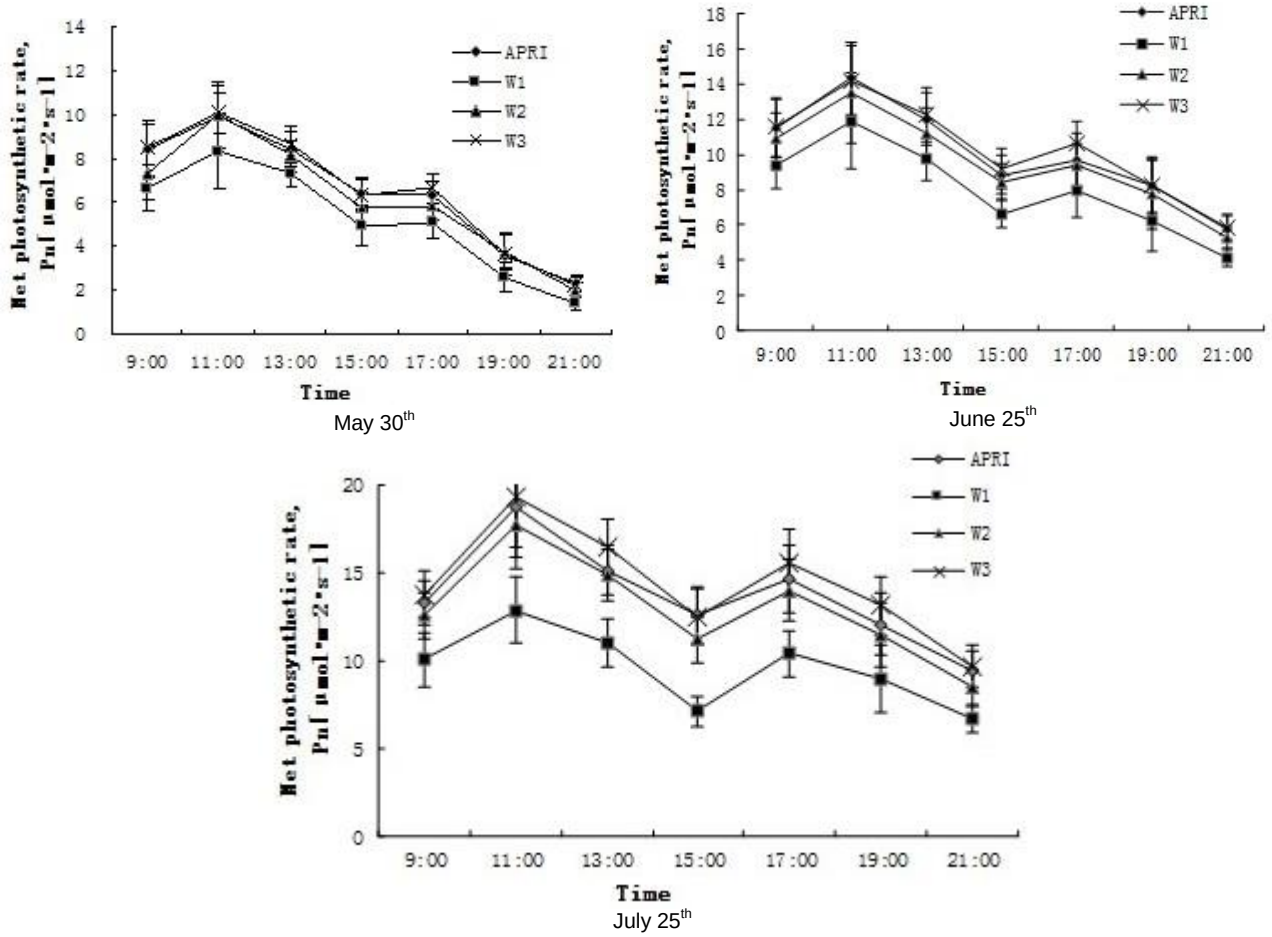

Fig.2 Diurnal variation of net photosynthetic rate of jujube leaves under infiltrating irrigation

Table 5

Daily average values of all photosynthetic indexes under infiltrating irrigation conditions

Date	Treatment	Net photosynthetic rate [μmol/·m^{2}·s]	Evaporation rate [mmol/·m^{2}·s]	Water use efficiency [μmol/mmol]	Stomatal conductance [mol/m^{2}·s]
30 May	APRI	6.48±0.52^{a}	1.86±0.24^{ab}	3.46±0.39^{a}	71.52±19^{ab}
	W1	5.19±0.47^{b}	1.69±0.21^{b}	3.00±0.40^{b}	45.52±16^{b}
	W2	6.45±0.54^{a}	2.04±0.22^{a}	3.13±0.47^{b}	79.05±19^{a}
	W3	6.59±0.53^{a}	2.15±0.26^{a}	3.04±0.36^{b}	84.67±20^{a}
25 June	APRI	9.97±1.0^{a}	3.64±0.32^{a}	2.85±0.18^{a}	150.5714±39^{a}
	W1	7.87±0.95^{b}	3.37±0.37^{b}	2.45±0.22^{b}	114.4286±38^{b}
	W2	9.23±0.97^{a}	3.84±0.39^{a}	2.55±0.19^{b}	162.714±38^{a}
	W3	10.13±1.00^{a}	4.19±0.40^{a}	2.50±0.17^{b}	168±40^{a}
25 July	APRI	14.33±1.20^{a}	3.24±0.73^{b}	5.25±0.82^{a}	172.08±52^{a}
	W1	9.60±0.82^{c}	2.82±0.56^{c}	4.40±0.88^{b}	123.57±37^{b}
	W2	12.54±1.09^{b}	3.43±0.64^{ab}	4.68±0.90^{b}	198.22±48^{a}
	W3	14.36±1.16^{a}	3.86±0.75^{a}	4.50±0.78^{ab}	205.18±53^{a}

Notes: Different letters (i.e. a, b and c) indicate significant difference at P < 0.05.

2) Diurnal variation of evaporation rate

Evaporation is an important physiological index reflecting the water status of plants. The ability of plants to adapt to arid environments is strong when Evap is low[2]. The diurnal variation curves of Evap were uniformly of unimodal type under different treatments during main growth periods, with the peak values always during 14:00–16:00 (Fig.3). Under regular infiltrating irrigation, the Evap increased gradually with increased irrigation volume. The daily average Evap (Table 5) of W1 were all significantly different ($P < 0.05$) on 30 May, 25 June and 25 July compared with those of W3, while the corresponding values of APRI decreased by 9%, 6% and 7% compared with those of W2. Thus APRI decreased the Evap of jujube leaves under the same irrigation level compared to regular infiltrating irrigation.

2) 蒸腾速率(Evap)的日变化规律

蒸腾速率是反映植物水分状况的重要生理指标，蒸腾速率越低则代表植物适应干旱环境的能力越强[2]，由图 3 可知，主要生育期不同处理下蒸腾速率日变化曲线趋势相同呈单峰型，峰值均出现在 14:00-16:00 之间。常规渗灌下随着灌溉量的增加，蒸腾速率逐渐升高。5 月 30 日、6 月 25 日和 7 月 25 日 W1 的日平均蒸腾速率（表 5）与 W3 相比均较表现为差异显著（$P<0.05$）；APRI 与 W2 相比分别下降了 9%、6%和 7%，表明同一灌溉水平 APRI 降低了叶片蒸腾速率。

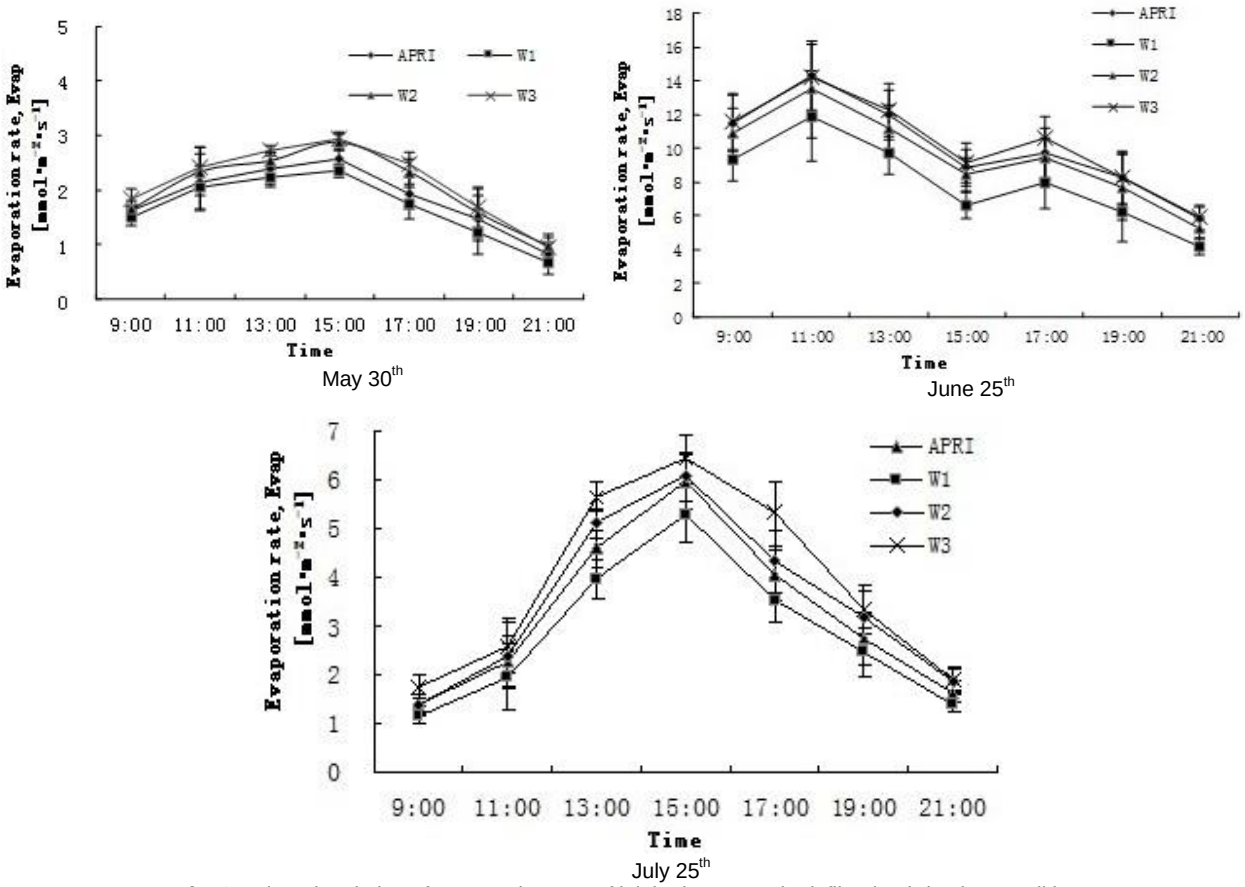

Fig. 3 - Diurnal variation of evaporation rate of jujube leaves under infiltrating irrigation conditions

3) Diurnal variation of water use efficiency

The WUE reflects the short-term or instantaneous behavior of plant leaves to water conditions. To some extent, it reflects the water consumption of plants and their adaptability to an arid environment[9].The diurnal variation curves of WUE of Jujube leaves presented a single-valley shape during main growth periods (Fig. 4). WUE reached a maximum at 9:00. The main reasons for this phenomenon include that the Pn of leaves increased with increased PAR (external environmental factor) by this time, the stomatal aperture of leaves was larger, the RH of air was still high and the Evap had not reached a maximum. WUE of plants was high, and dropped to a minimum at 15:00. The daily average WUE of leaves of W2 and APRI on 30 May increased by 3% and 14% compared with that of W3, they thereafter increased by

3) 水分利用率(WEU)的日变化规律

水分利用率是反映植物叶片对水分条件的短期或瞬间反应行为在一定程度上反映植物的耗水性和对干旱的适应性[9]。由图 4 可看出，枣树主要生育期内叶片的水分利用效率日变化曲线呈单谷型，9:00 时水分利用率达到最大，主要是因为此时叶片的净光合速率会随着外部环境因子光合有效辐射的上升而增加，且此时的叶片气孔开度较大，空气的相对湿度还较高，蒸腾速率还未达到最大，所以植物的水分利用效率高。15:00 是水分利用率降到最低值。5 月 30 日 W2 和 APRI 处理下叶片水分利用率日均值比 W3 分别提高了 3%和 14%， 6 月 25 日 W2 和 APRI 处理下叶片水分利用率日均值

2% and 14% on 25 June, and by 2% and 15% on 25 July. The results implied that slight moisture loss could improve the WUE of leaves. The daily average WUE of leaves of APRI on 30 May, 25 June and 25 July increased by 11%, 12% and 13%, respectively, compared with those of W2. Thus APRI significantly increased the WUE of Jujube leaves under the same irrigation level.

比 W3 分别提高了 2%和 14%。7 月 25 日 W2 和 APRI 处理下叶片水分利用率日均值比 W3 分别提高了 2%和 15%，说明轻度的水分亏损会提高叶片水分利用率。5 月 30 日、6 月 25 日和 7 月 25 日 APRI 处理下的叶片水分利用率日均值比 W2 分别提高 11%、12%和 13%，表明同一灌溉水平 APRI 能够显著提高叶片水分利用率。

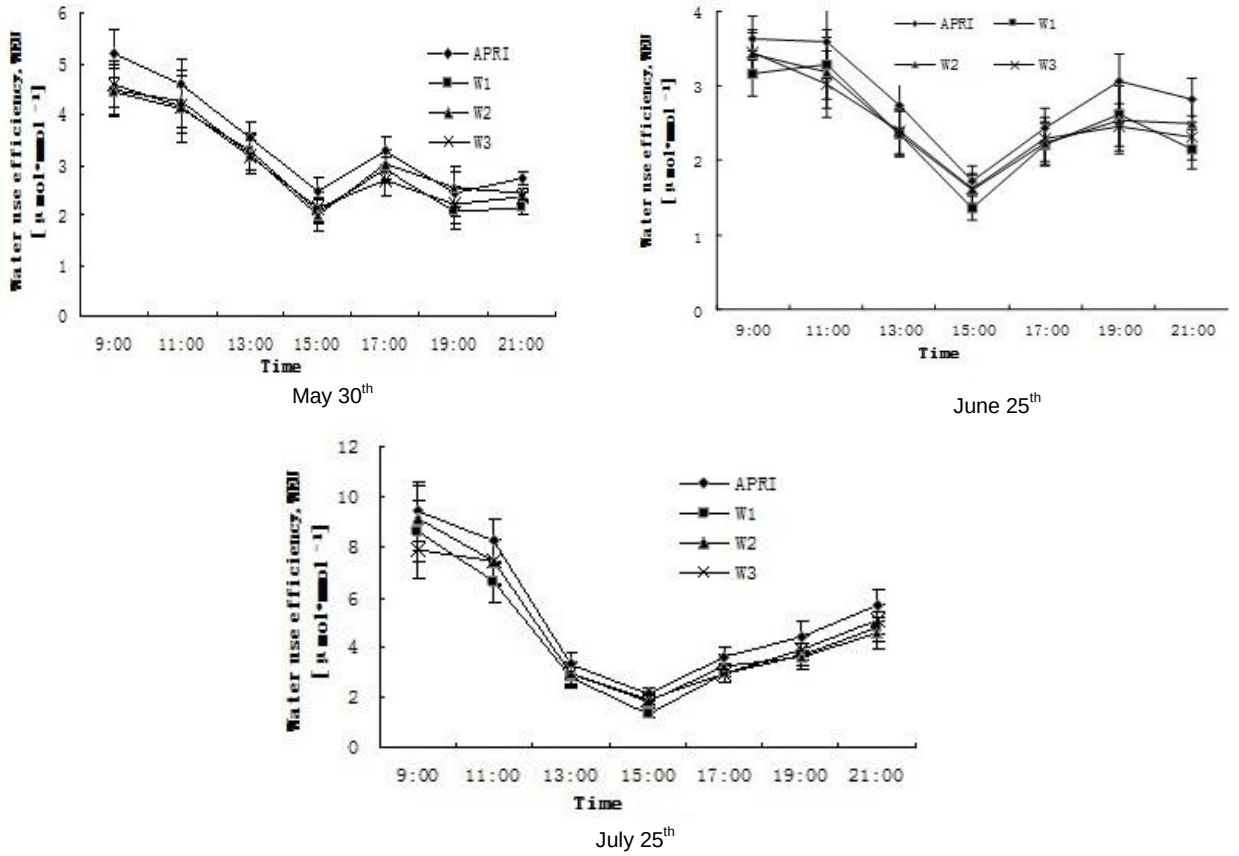

May 30th　　June 25th

July 25th

Fig. 4 - Diurnal variation of water use efficiency of Jujube leaves under infiltrating irrigation conditions

4) Diurnal variation of stomatal conductance

The Gs of leaves reached a maximum on 9:00 on May 30 (Fig.5) and then declined gradually and remained stable after 15:00. The main reason for the aforesaid phenomenon is that PAR was relatively low in the morning and the air RH was high, which led to high stomatal apertures, and then Gs decreased gradually with increasing PAR and decreasing RH. The daily average value of Gs of W1 was notably lower than those of other treatments ($P < 0.05$). The variation trends of Gs and Pn of Jujube leaves were similar, both with a bimodal pattern on 25 June, and peak values always at 11:00 and 17:00. The Gs of treatments all showed a trend of initially high followed by low values. The daily average value of Gs of W1 decreased by 31% compared with that of W3 ($P < 0.05$). The diurnal variation curve of Gs of Jujube leaves showed a bimodal pattern on 25 July, and peak values occurred at 13:00 and 17:00 with the former higher than the latter. The daily average values of Gs of W1 and APRI decreased by 39% and 16%, respectively, compared with those of W3. The daily average values of Gs of APRI on 30 May, 25 June and 25 July decreased by 9%, 7% and 12%, respectively, compared with those of W2 ($P < 0.05$).

4) 气孔导度（Gs）的日变化规律

由图 5 可知，5 月 30 日叶片气孔导度在 9:00 达到最大，随后逐渐降低，15:00 后趋于平缓，主要原因是早上太阳光合有效辐射较低，空气湿度较高，导致气孔高度开放，随后随着光合有效辐射升高和空气湿度降低气孔导度逐渐降低；W1 处理下气孔导度日均值显著低于其他处理（$P<0.05$）。6 月 25 日叶片气孔导度变化趋势与净光合速率一致，呈双峰型，峰值出现在 11:00 和 17:00 点，不同处理气孔导度均呈现前高后低的趋势， W1 的叶片气孔导度日均值比 W3 下降了 31%，差异显著（$P<0.05$）；7 月 25 枣树叶片的气孔导度日变化曲线呈双峰型。气孔导度峰值出现在 13:00 和 17:00。第一次峰值明显高于第二次，与 W3 气孔导度日均值相比 W1 和 APRI 分别下降了 39%和 16%，5 月 30 日、6 月 25 日和 7 月 25 日 APRI 处理下的叶片气孔导度日均值比 W2 分别降低了 9%、7%和 12%，差异不显著（$P<0.05$）。

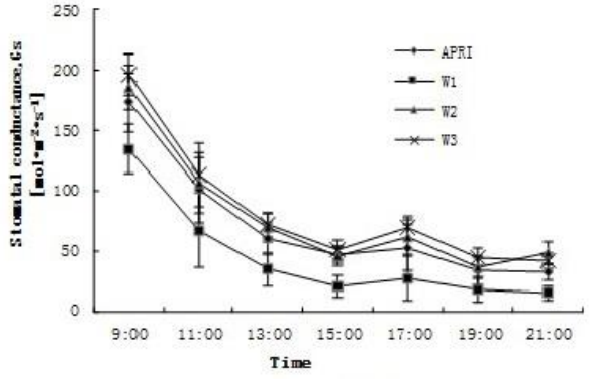

May 30th

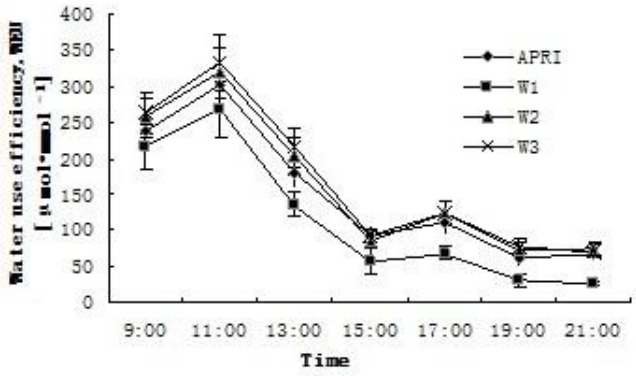

June 25th

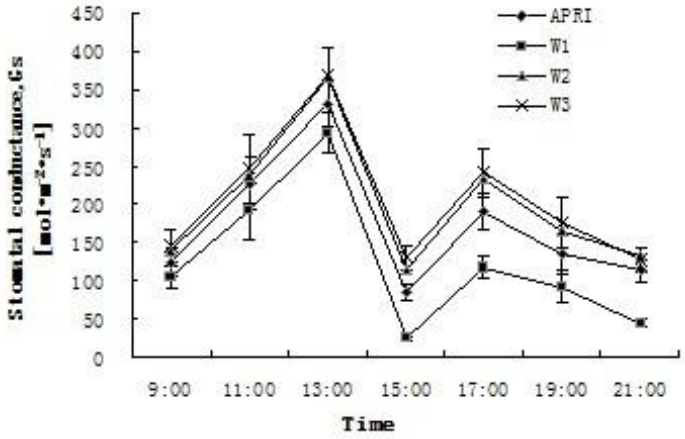

July 25th

Fig.5 Diurnal variation rule of stomatal conductance

Influence of infiltrating irrigation and APRI on yield of Jujube

The weight of fresh fruit, weight of dry fruit, fruit setting quantity, fruit width and yield per hectare all increased gradually with increased irrigation volume under regular infiltrating irrigation (Table6). APRI increased weight of fresh fruit, weight of dry fruit, fruit setting quantity and fruit width of Jujube under the same irrigation level compared to regular infiltrating irrigation. The yield per hectare of APRI increased by 11% compared with that of W2, showing that APRI could save water and increase yield.

渗灌和 APRI 对枣树果实产量影响

由表 6 可知，常规渗灌条件下随着灌溉量的增加枣树的鲜果重、坐果数、干果重、果径和亩产量均逐渐增加，同一灌溉水平，APRI 有利于提高枣树的鲜果重、坐果数、干果重和果径，与 W2 亩产量相比, APRI 的亩产量提高了 11%，表明 APRI 能够达到节水增产的作用。

Table 6

Yield analysis of Jujube

Treatment	Irrigation quota [m^3/hm^2]	Weight of fresh fruit [g]	Weight of dry fruit [g]	Fruit setting quantity [Thousand piece]	Fruit width [cm^2]	Yield [kg/hm^2]
APRI	6000	5.19	3.17	212.22	3.60	16426 a
W1	3000	4.15	2.67	201.65	3.40	12147 b
W2	6000	4.70	3.15	207.40	3.50	14703 b
W3	9000	5.25	3.14	216.29	3.80	17100 a

DISCUSSIONS AND CONCLUSIONS

For Jujube trees in the area around Tarim basin in South Xinjiang of China, the daily average values of Pn in the later growth period were higher than that of

结论与讨论

南疆环塔里木盆地生长后期净光合速率日均值高于果实生长前期，本文中7月25 日和6月25日的净光合速率明显

earlier periods. The Pn values of this study on 25 June and 25 July were higher than that on 30 May. This phenomenon was possibly due to the peak values of PAR on 30 May, 25 June and 25 July, which were 1928, 2400 and 2155 W/m^2, respectively. Moreover, Ta difference might also cause different photosynthetic rates. Excessive Ta can decrease the photosynthetic rate of plant leaves [6-7, 14] and generate the photosynthetic 'noon break' phenomenon. Low temperature at night can also improve Pn during the day, as research results of McDonald and Paulsen [9] showed that the Pn of pea and other plants under a diurnal temperature of 30/25°C was lower than that of 30/15°C. The decrease of RH and Ta could reduce respiration and consumption by weakening the dark respiration rate. Thus, the fruit setting rate and yield could be improved.

Different irrigation treatments had a significant impact on Pn of Jujube trees, which rose with increased irrigation volume. Under the same meteorological conditions, the lack of soil moisture could result in decreases of Gs and Evap. Thus, the Pn of leaves and the WUE could also be reduced [4-5,18-19]. This study showed that the WUE of leaves decreased under W1 irrigation treatment. During each growth period, the Pn, Gs and Evap for the W2 treatment were lower than those for W3, but the difference was not significant. However, the WUE for W2 was higher than that for W3 treatment, showing the decrease of irrigation volume to some extent did not decrease the Pn, Gs and Evap, but improved the WUE and enabled the Jujube trees to possess certain drought resistant ability [15, 3] .

Under the same irrigation level, the Pn of APRI on 30 May and 25 June increased slightly compared with that of W2, while the Pn and WUE under APRI treatment on 25 July were apparently higher than those of W2, and the Pn and WUE under APRI and W2 treatments were 14.33, 12.54, 5.25 and 4.50 μmol·mmol^{-1}, respectively. The main reason for this phenomenon was the abundant secondary roots produced by jujube under alternate stress of the APRI treatment, and then the absorbing ability of root systems for water and fertilizer was enhanced, and so WUE improved and Pn also increased, the yield therefore also increased. The Evap under APRI treatment in each growth period was higher than that of W2, but the Gs was lower. This was mainly because some roots were in an area of dry soil under APRI, and so the Jujube roots likely formed plenty of abscisic acid due to water stress, which was transferred to leaves to reduce stomatal apertures and water consumption by evaporation. Some roots were in area with irrigated soil, so as to meet the normal physiological activities.

APRI improved the fruit setting rate and yield of Jujube trees under the same irrigation level as regular infiltrating irrigation. The fruit setting rates and yields of APRI and W2 treatments were 212220 and 207400, and 16426 and 147036 kg/hm^2, respectively. Pn increased when Jujube trees suffered alternate stress under the APRI treatment, and so the fruit setting rate and total yield improved.

Under the same irrigation level, the APRI reduced Evap and Gs, and improved Pn, WUE and yield per hectare and significantly (P < 0.05) improved the yield by 11% compared with regular infiltrating irrigation. The yield per hectare of Jujube showed no difference (P < 0.05) under the APRI compared with W3. The APRI

高于5月30日。造成这一现象的原因可能是由于5月30日、6月25日和7月25 日、的光合有效辐射的峰值分别为1928、2400和2155W/m^2，但空气温度的差异则导致其光合速率的不同，过高的空气温度会导致植物叶片光合速率的降低，且会产生"光合午休"现象[6-7, 14]。夜间的低温也会提高白天的光合速率，McDonald 等的研究结果表明豌豆等作物昼夜温度为30/25℃时的光合速率会低于30/15℃时的光合速率[9]。大气相对湿度 和空气温度的降低则导致暗呼吸速率的减弱，从而降低呼吸消耗，提升坐果率和产量。

不同灌水处理对枣树的净光合速率有着显著的影响，随着灌水量的增加枣树叶片净光合速率呈上升趋势。在同样的气象条件下，土壤水分的亏缺会导致气孔导度和蒸腾速率的降低，从而降低净光合速率[4-5,18-19]，并降低叶片水分利用效率，本文在W1灌溉处理下叶片水分利用效率下降，与该文章结论相一致。不同时期W2处理下的净光合速率、气孔导度和蒸腾速率低于W3处理差异不显著，但W2处理下的水分利用效率高于W3处理，表明一定程度上降低灌水量并不会显著降低净光合速率、气孔导度和蒸腾速率，但会提高水分利用效率，具有一定的抗旱能力[15, 3]。

同一灌溉水平，5 月 30 日和 6 月 25 日 APRI 的净光合速率高于 W2，但不显著；7 月 25 日 APRI 处理下的净光合速率和水分利用效率显著高于 W2，APRI 和 W2 处理下的净光合速率和水分利用效率分别为 14.33μmol·m^{-2}·s^{-1} 、 12.54μmol·m^{-2}·s^{-1} 和 5.25μmol·mmol $^{-1}$ 、 4.50 μmol·mmol $^{-1}$，造成这一现象的原因可能是因为 APRI 使枣树根部受到交替胁迫后次生根大量增加，根系吸水吸肥能力增加，水分利用效率明显提高，净光合速率也随之增加，最终产量也得到提升。各时期 APRI 处理下的蒸腾速率高于 W2，气孔导度低于 W2，但差异不显著，主要是因为 APRI 使部分根系处于土壤干燥的区域，枣树受到水分胁迫，根部形成大量脱落酸，传送到叶片，气孔开度减少，降低蒸腾耗水量；还有部分根系处于灌水的区域中，以满足正常的生理活动。

本文中，同一灌溉水平，APRI 能够提高枣树坐果率和枣树产量。APRI 和 W2 处理下的坐果率高和产量分别为 212220 个、207400 个和 16426kg/hm^2、147036 kg/hm^2，APRI 处理下果树受到一定交替胁迫能够提高净光合速率进而提高坐果率，产量得到提升。

在同一灌溉水平下，分根交替灌溉降低枣树叶片蒸腾速率、气孔导度；提高枣树叶片的净光合速率、水分利用率，最终提高枣树达11%，与常规渗灌相比达到显著水平（P<0.05），与W3相比，分根交替灌溉条件下红枣亩产量

improved Pn and yield on the basis of water saving. This study demonstrated an effective irrigation mode for development of the jujube industry in Xinjiang, and provided a decision basis for saving water resources, increasing Jujube yield and accelerating the sustainable development of this industry.

ACKNOWLEGEMENT

The study was supported by the Program for International S&T Cooperation Projects (2010DFA92720-11), National Sci-tech Support Program (2009BADA4B03), Xinjiang Water Conservancy Sci-tech Special Project (2013T04), (2013T05) and (2014T16).

REFERENCES

[1]. Chai Z P, Wang X M, Chen B L, et al.(2013) – *Research on Diurnal Variations of Photosynthetic Characteristics Pyrusbretschneideri Under Different Growth Stages.* Northern Horticulture, vol.6, pg.1-5;

[2]. Chai Z P, Wang X M, Sun X, et al.(2011) – *Influence of Different Application Ways of Biogas Waste Fertilizer on Photosynthetic Characteristics and Yield of Zizyphus jujube.* Acta Agriculturae Boreali-occidentalis Sinica, vol.20, no.2, pg.170-173;

[3]. Fang Q X, Chen Y H, Li Q Q, et al. (2006) – *Effects of soil moisture on radiation utilization during late growth stages and water use efficiency of winter wheat.* Acta Agronomica Sinica, vol.32, no.6, pg. 861-866;

[4]. Guo C F, Sun Y, Zhang M Q.(2008) – *Effect of soil water stress on photosynthetic light response curve of teaplant.* Chinese Journal of Eco-Agriculture, vol.16, no.6, pg.1413-1418;

[5]. Jiao J Y, Yin C Y, Chen K. (2011) – *Effects of soil water and nitrogen supply on the photosynthetic characteristics of Jatropha curcas seedlings.* Acta Phytoecologica Sinica, vol.35, no.1, pg.91-99;

[6]. Li T L, Yan A D, Luo X L, et al.(2010) – *Temperature modified model for single-leaf net photosynthetic rate of greenhouse tomato.* Transactions of the Chinese Society of Agricultural Engineering, vol.26, no.9, pg. 274-279;

[7]. Li T L, Li M. (2009) – *Effect of short-term daytime sub-high temperature stress on photosynthesis of tomato leaves.* Transactions of the Chinese Society of Agricultural Engineering, vol.25, no.9, pg.220-225;

[8]. Ma H Y, Lü D G, Liu G C, et al.(2012) – *Effects of different irrigation modes on the photosynthetic function and antioxidant enzyme activities of 'Hanfu' apple leaves.* Chinese Journal of Ecology, vol.31,no.10,pg.2534- 2540;

[9]. McDonald G K, Paulsen G M. (1997) – *High temperature effects on photosynthesis and water relations of grain legumes.*Plant Soil. Vol.196,no.1, pg.47-58;

[10]. Ou L J, Hu A S, Li B H, et al.(2012) – *Photosynthesis and physiological characteristics of rice with floating culture method.* Transactions of the Chinese Society of Agricultural Engineering, vol.28, no.12, pg.127-133;

[11]. Papastylianou I. (1995) – *Yield components in relation to grain yield losses of barley fertilized with nitrogen*. European Journal of Agronomy, vol.4, no.1, pg. 55－63;

未表现出差异（*P*<0.05），表明分根交替灌溉能够达到节水提高净光合速率和产量作用；为新疆枣产业的发展提供有效的灌溉方式，为节约水资源，提高枣产量，促进特色枣产业的持续发展提供科学依据。

致谢

国家国际科技合作项目（2010DFA92720-11），国家科技支撑项目（2009BADA4B03），新疆水利科技专项（2013T04），（2013T05）和（2014T16）。

参考文献

[1]. 柴仲平, 王雪梅, 陈波浪, 等. (2013) – *香梨不同生长期光合特性日变化研究.* 北方园艺, 第 6 卷, 1-5;

[2]. 柴仲平, 王雪梅, 孙霞, 等. (2011) – *沼肥不同施用方式对枣树光合特性与产量的影响.* 西北农业学报, 第 20 卷, 第 2 期, 170-173;

[3]. 房全孝, 陈雨海, 李全起, 等. (2006) – *土壤水分对冬小麦生长后期光能利用及水分利用效率的影响.* 作物学报,第 32 卷, 第 6 期, 861-866.

[4]. 郭春芳, 孙云, 张木清. (2008) – *土壤水分胁迫对茶树光合作用-光响应特性的影响.* 中国生态农业学报, 第 16 卷, 第 6 期, 1413-1418;

[5]. 焦娟玉, 尹春英, 陈珂. (2011) – *土壤水、氮供应对麻疯树幼苗光合特性的影响.* 植物生态学报, 第 35 卷, 第 1 期, 91-99;

[6]. 李天来, 颜阿丹, 罗新兰, 等. (2010) – *日光温室番茄单叶净光合速率模型的温度修正.* 农业工程学报, 第 26 卷, 第 9 期, 274-279;

[7]. 李天来, 李淼. (2009) – *短期昼间亚高温胁迫对番茄光合作用的影响.* 农业工程学报, 第 25 卷, 第 9 期, 220-225;

[8]. 马怀宇, 吕德国, 刘国成, 等. (2012) – *不同灌水方式对'寒富'苹果叶片光合功能和抗氧化酶活性的影响.* 生态学杂志, 第 31 卷, 第 10 期, 2534-2540;

[9]. McDonald G K, Paulsen G M. (1997) –*高温对谷物豆科植物的光合作用和水分关系的影响.* 植物与土壤, 第 196 卷, 第 1 期, 47-58;

[10]. 欧立军, 胡爱生, 李必湖, 等. (2012) – *水上浮床种植水稻的光合特性及生理特点.* 农业工程学报, 第 28 卷, 第 12 期, 127-133;

[11]. Papastylianou I. (1995) – *施氮条件下产量组分与产量损失之间的关系.* 欧洲农学杂志, 第 4 卷, 第 1 期, 55-63;

[12]. Wei L, Xiong Y C, Bao L M,et al.(2011) – *Photosyn - thetic characterization and yield of summer corn during grain filling stage under different planting pattern and population densities.* Acta Ecologica Sinica, vol.31, no.9, pg.2524- 2531;
[13]. Wei R F, Zhuang F, Fan Y Y, et al. (2012) – *Effect of Soil Water Content on Photosynthetic Characteristics and Transpiration Water Consumption of Jujube.* Journal of Irrigation and Drainage, vol.31, no.2, pg.107-111;
[14]. Wolleweber B, Porter J R, Schellberg J.(2003) – *Lack of interaction between extreme high-temperature events at vegetative and reproductive stages in wheat.* Journal of Agronomy and Crop Science, vol.189, no.3, pg.142-150;
[15]. Xu J Z, Peng S Z, Wei Z, et al. (2012) – *Character-istics of rice leaf photosyntetic light response Curve with different water and nitrogen regulation.* Transactions of the Chinese Society of Agricultural Engineering, vol.28, no.2, pg.72-76;
[16]. Yao Q s, Lei X T, Wang Y C, et al.(2006) – *Effects of different water moisture on photosynthesis, transpiration and stoma conductance of potted mango seedlings.* Journal of Fruit Science, vol.23, no.2, pg.223-226;
[17]. Zhu R, Yao Li X, Ma W Y, et al. (2010) – *Status and Prospect of Zizyphus jujube Producing in Sinkiang*. Hei long jiang Agricultural Sciences, vol.6, pg.158-163;
[18]. Zhu Y Y, He K Q, Tang D F, et al.(2007) – *Response to light of ulmus pumila in different soil Moisture.* Research of Soil and Water Conservation, vol.14, no.2, pg. 92-94;
[19]. Zhu J J, Kang H Z, Li Z H, et al. (2005) – *Impact of water stress on survival and photosynthesis of Mongolian pine seedlings on sandy land.* Acta Ecologica Sinica, vol.25,no.10, pg.2527-2533.

[12]. 卫丽, 熊友才, Bao luo Ma, 等. (2011) – *不同群体结构夏玉米灌浆期光合特征和产量变化.* 生态学报, 第 31 卷, 第 9 期, 2524- 2531;
[13]. 魏瑞锋, 庄飞, 范阳阳, 等. (2012) – *土壤水分对枣树光合特性及耗水量的影响.* 灌溉排水学报, 第 31 卷, 第 2 期, 107-111;
[14]. Wolleweber B, Porter J R, Schellberg J. (2003) – *小麦营养生长和生殖阶段期间极端高温事件影响无较强的的持续性.* 农作物科学, 第 189 卷, 第 3 期, 142-150;
[15]. 徐俊增, 彭世彰, 魏征, 等. (2012) – *不同供氮水平及水分调控条件下水稻光合作用光响应特征.* 农业工程学报, 第 28 卷, 第 2 期, 72-76;
[16]. 姚全胜, 雷新涛, 王一承, 等. (2006) – *不同土壤水分含量对杧果盆栽幼苗光合作用、蒸腾和气孔导度的影响.* 果树学报, 第 23 卷, 第 2 期, 223-226;
[17]. 朱锐, 姚立新, 马雯彦, 等. (2010) – *新疆枣树生产的现状与展望.* 黑龙江农业科学, 第 6 卷, 158-163;
[18]. 朱艳艳, 贺康宁, 唐道锋, 等. (2007) – *不同土壤水分条件下白榆的光响应研究.* 水土保持研究, 第 14 卷, 第 2 期, 92－94;
[19]. 朱教君, 康宏樟, 李智辉, 等. (2005) – *水分胁迫对不同年龄沙地樟子松幼苗存活与光合特性影响.* 生态学报, 第 25 卷, 第 10 期, 2527-2533.

A KINEMATIC ANALYSIS AND SIMULATION BASED ON *ADAMS* FOR EGGPLANT PICKING ROBOT
/
基于 ADAMS 的茄子采摘机器人运动学分析与仿真

Prof. Peng Zhang[1)], Prof. Jian Song[1)], Stud. Shenglei Gong[1)], Prof. Bo Jiang[2)] , Prof. Muham, D. Polar[3)]
[1)] School of Machanical-electronic and Vehicle Engineering in University of Weifang, Weifang / China; [2)] College of Medicine, University of Saskatchewan, Saskatchewan / Canada; [3)] Advanced Machine Engineering and Automation Center of CCB Corp, Singapore
Tel: +86-536-8785603; E-mail: sjian11@hhit.edu.cn

Abstract: *Eggplant picking robot is a type of complex optical-mechanical-electrical equipment in greenhouse environment. Its structure and control are more exigent than traditional industrial robot. Optimization design method was utilized for the design of the eggplant picking robot body structure parameters in accordance with the eggplant growth and distribution space. In order to determine the spatial position relationship between the eggplant picking robot components and the end effector, the theoretical model of robot was established by virtue of Denavit-Hartenberg approach and the positive solution of the kinematic equation is obtained. Premultiplication decoupling of* A_i^{-1} *and matrix* ${}^0T_4$ *were adopted to solve inverse kinematic solution with the help of Matlab software. Pro/E software was used to establish 3-D simulation model, and ADAMS (Automatic Dynamic Analysis of Mechanical Systems) simulation software was imported for the kinematics simulation analysis. It was indicated by the simulation results that the kinematic model established by D-H approach reflects the real motion conditions of the robot, and both the positive and inverse kinematic solutions are correct. Structure of four degrees freedom eggplant picking robot was reasonable, it could meet the requirements of eggplant picking in the greenhouse cultivation pattern.*

Keywords: *Eggplant picking robot, ADAMS, Kinematic simulation, four degrees of freedom, Agricultural machinery*

INTRODUCTION

Harvesting or picking is the most effort-requiring and time-consuming procedure in eggplant production operation, which, according to statistics, approximately accounts for from 50% to 70% of all the amount of working [7]. Moreover, it requires timely picking to guarantee the product quality, making it as the hardest work in the whole operation [5]. With the rapid development of agricultural mechanization, considering the problems with aging of population and the decrease of agricultural labor force, it is more and more significant to research and develop fruit and vegetable picking robot [8]. Since the mid 1980s, researches on automatic fruit and vegetable picking have been started in the western developed countries represented by Japan, and some vegetable picking robots with certain intelligence were experimented and developed [9,10,11]. In the intelligent tomato picking robot end effector based on multi-sensor information fusion and open control system designed by Jizhan Liu, etc, the vacuum chuck device of the execution system could separate the fruit from the fruit bunch, its finger gripper mechanism could grasp the tomato firmly, and the fruit stem disconnecting device could cut off the fruit stem with laser [4]. Peng Cui proposed a bionic manipulator which was applied to the apple picking robot end effector and the simple fixture was replaced with the tendon-driven bionic manipulator, enhancing the adaption of the end effector to grab apple in complex environment [6]. Wei Lu designed an original orange picking robot arm and end effector,

摘要: *茄子采摘机器人是一种工作在复杂的温室中的复杂的光机电一体化设备，它的结构和控制系统比一般的工业机器人要求更加苛刻。本文根据茄子的生长分布空间，利用优化设计方法进行了茄子采摘机器人本体结构参数的设计。借助 Denavit-Hartenberg 法建立了采摘机器人的理论模型，得到机器人的运动学方程的正解，确定机器人各运动构件与末端执行器在空间位置之间的关系。采用* A_i^{-1} *与矩阵* ${}^0T_4$ *左乘解耦，借助 Matlab 软件求出运动学逆解。利用 pro/e 建立茄子采摘机器人三维模型，导入 ADAMS 仿真软件进行运动学仿真分析。仿真结果表明：D-H 法建立的运动学模型反映了采摘机器人的真实运动情况，采摘机器人运动学正逆解正确。设计开发的 4 自由度采摘机器人结构设计的合理，能够满足温室栽培模式下茄子采摘的要求。*

关键词: *茄子采摘机械手， ADAMS，运动学仿真，四自由度，农业机械化*

引言

在果蔬生产作业中，收获采摘是费力最大、耗时最多的一个环节。据统计，约占整个作业量的 50～70％[7]。而且为了保证产品的质量，必须做到适时采摘，是整个作业中最辛苦的工作[5] 。随着人口的老龄化和农业劳动力的减少，研究开发果蔬采摘机器人具有越来越重要的意义[8]。从 20 世纪 80 年代中期开始，日本等西方发达国家开始了自动化收获水果蔬菜的研究，试验开发了一些具有一定智能的蔬菜采摘机器人[9,10,11]。刘继展等设计的基于多传感器信息融合和开放式控制的智能型番茄采摘机器人末端执行器，其执行系统的真空吸盘装置使果实从果束中分离，手指夹持机构对番茄可靠抓持,果梗切断装置利用激光对果梗进行切断[4]。崔鹏等提出了一种应用于苹果采摘机器人末端执行器的仿生机械手，采用腱传动式仿生机械手取代了简单的夹具,提高了末端执行器在复杂环境中抓取苹果的适应性[6]。卢伟等针对柑橘树冠较高,果梗木质化程度高、短且坚硬的特点,设计了新颖的柑橘采摘机器人手臂和末端执行器[12]。

considering the tall crown of citrus tree, and the high degree of lignification of its short and stiff fruit stem [12].

However, the above-described robots are still far from practical application owing to the influence factors from technology, market, and price and so on[1]. It can be seen from the analysis of literatures at home and abroad that these researches on the picking robot are mainly focused on identifying, positioning and sorting the target fruit via the vision system [14], while there are rare researches on the basic machine of the picking robot [3].

Robot kinematics is an important constituent part of robotics, whose purpose is to establish the relationships among spatial positions of the robot components and end effectors so as to provide theoretical basis and technical parameters for the optimized control of the robot [2]. However, it requires establishing mathematic model of the robot arm movements to finish most of these tasks, which have tedious process, heavy computation burden, and are error-prone [13]. In this paper, ADAMS simulation software was used for kinematics analysis and simulation study on the eggplant picking robot, which could solve the above-mentioned problem in the course of kinematics analysis in traditional multi-rigid-body system and meanwhile show intuitively the kinematic performance of the robot movement components in the diagram and simulation animation form, providing a powerful guarantee for follow-up programming of robot motion trail and verification of the structure parameter rationality.

MATERIALS AND METHODS

Structure parameter of picking robot

The articulated robot with four degrees of freedom is selected to be the basic machine of the picking robot because the picking object of the eggplant picking robot is the eggplant whose fruit is cylindrical.

The robot structure parameters mainly include the robot arm length and the rotation angle scope,etc. and these parameters determine the work space of the robot. The optimization design of the eggplant picking robot structure parameters is to use optimal method to analyze and calculate the mechanism size in accordance with the eggplant growth and distribution space.

The purpose of the optimization design is to obtain the most compact mechanical structure. The upper arm length x_1 and the forearm x_2 of picking robot are regarded as the design variables, and the actually work space of picking robot is optimization objective. The objective function is shown as follow:

但是由于技术、市场和价格等因素的影响，离实际应用还有很大距离[1]。综合国内外研究文献，对于采摘机器人的研究大多集中在视觉系统对果实采摘与分拣目标的识别和定位上[14]，而对于采摘机器人机械本体的研究较少[3]。

机器人运动学是机器人学的重要组成部分，研究机器人运动学的目的就是建立机器人各运动构件与末端执行器在空间位置之间的关系，为机器人的优化控制提供理论依据和技术参数[2]。但完成这些工作大都需要建立机器人手臂运动的数学模型，过程繁琐、计算量大、容易出错[13]。本文运用 ADAMS 仿真软件对茄子采摘机器人进行运动学分析与仿真研究，解决了传统多刚体系统运动学分析过程所产生的上述问题，同时能将机器人各个运动机构的运动性能通过图表和模拟动画的形式直观表现出来，为后续机器人的运动轨迹进行规划，结构参数的合理性验证提供有力保证。

材料与方法

采摘机器人结构参数

由于茄子采摘机器人的采摘对象是茄子，其果实呈圆柱形。所以，选用具有四自由度关节式机器人作为采摘机器人的机械本体。

机器人结构参数，主要包括机械臂的长度及其转角范围等。机器人的结构参数决定了机器人的工作空间。茄子采摘机器人结构参数的优化设计是根据茄子生长分布空间，利用优化方法进行机构尺寸分析与计算。

优化设计的目的是得到最紧凑的机械结构。优化设计变量为大臂长 x_1，小臂长 x_2，优化目标是采摘机器人的实际工作空间。目标函数如下式所示：

$$\min f(X)=\frac{1}{4}\pi(x_1+x_2)^2+\frac{1}{2}\pi x_2^2-\frac{1}{2}(x_1^2+x_2^2-2x_1x_2\cos 30^\circ) \quad (1)$$

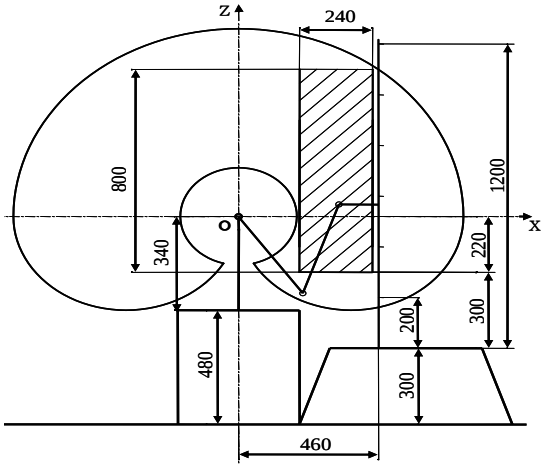

Fig. 1 - The working space of eggplant picking robot

The working space of eggplant picking robot is shown as Fig.1.The constraint condition is that it should be the minimum value under the required rectangle work space conditions, i.e., the rectangle work space required by the picking manipulator operation must be confined in the real work space. Using the optimization toolbox of Matlab software for programming, calculating and operation, the optimization result can be obtanined as follow:

图 1 表示了茄子采摘机器人实际需要的工作空间。约束条件为使其在包容所要求的矩形工作空间条件下为最小值，就是必须使采摘机械手作业要求的矩形工作空间包含在实际工作空间内。使用 Matlab 软件的优化工具箱进行编程计算，运行得到优化结果为：

$$X = [312, 335] \tag{2}$$

With an overall consideration, it confirms that $x_1 = x_2 = 350mm$. The height of pedestals is 340mm, rotation angle of the waist θ_1 is $\pm 180^\circ$; the upper arm length x_1 is 350mm, rotation angle θ_2 is $\pm 90^\circ$; the forearm length x_2 is 350mm, rotation angle θ_3 is $\pm 150^\circ$

综合考虑，确定 $x_1 = x_2 = 350mm$ 。最后确定底座高为 340mm，腰部回转角 θ_1 为±180°；大臂长 350mm，回转角度 θ_2 为±90°；小臂长 350mm，回转角度 θ_3 为±150°。

Model based on kinematic theory

D-H model is an approach proposed by Denavit-Hartenberg for the expression and modeling of robot joints and connecting rods, which adopts 4×4 homogeneous transformation matrix to describe the spatial position relationship of the adjacent robot rod pieces, thus translates the complicated kinematic question into 4×4 equivalence transformation matrix of the coordinate system of the end effectors and reference coordinate system. As shown in Fig.2, the coordinate system of connecting rods of 4-DOF picking robot is established according to D-H approach.

运动学理论模型

D-H 模型是 Denavit 和 Hartenberg 提出的对机器人关节和连杆进行表示和建模的方法。它采用 4×4 齐次变换矩阵来描述相邻机器人杆件的空间位置关系，将复杂的运动学问题转化为末端执行器的坐标系与参考坐标系的 4×4 等价变换矩阵。如图 2 所示，按照 D-H 法建立四自由度采摘机器人各连杆坐标系。

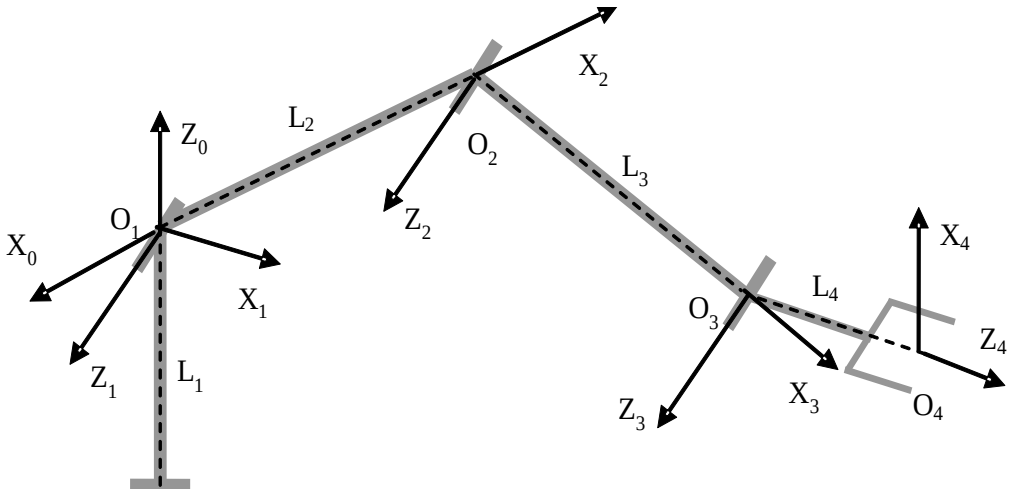

Fig.2 - Coordinate system of connecting rods of eggplant picking robot

Matrix A_i represents 4-order homogeneous transformation matrix between the connecting rod coordinate systems, and is usually expressed as follow:

矩阵 A_i 表示连杆坐标系之间的 4 阶齐次变换矩阵，一般表达为：

$$A_i = Rot(z,\theta_i)\times Trans(a_i,0,0)\times Rot(x,\alpha_i) = \begin{bmatrix} \cos\theta_i & -\sin\theta_i\cos\alpha_i & \sin\theta_i\sin\alpha_i & a_i\cos\theta_i \\ \sin\theta_i & \cos\theta_i\cos\alpha_i & -\cos\theta_i\sin\alpha_i & a_i\sin\theta_i \\ 0 & \sin\alpha_i & \cos\alpha_i & d_i \\ 0 & 0 & 0 & 1 \end{bmatrix} \tag{3}$$

The parameters of the picking robot joint connecting rods can be obtained according to the coordinate system of connecting rods of picking robot in Fig.2, as shown in Table1.

依据图 2 建立的采摘机器人各连杆坐标系可以得到各关节连杆参数，如表 1 所示。

Table 1

Connecting rod parameters of picking robot joint

i	θ_i	α_i	a_i	d_i	Variable Range	Link parameters(mm)
1	θ_1	90°	0	0	±180°	L_1=340mm
2	θ_2	0	L_2	0	±90°	L_2=350mm
3	θ_3	0	L_3	0	±150°	L_3=350mm
4	θ_4	90°	L_4	0	±120°	L_4=180mm

In Table1, θ_i is the included angle between the two common perpendiculars in a plane perpendicular to joint i axis. a_i is the distance of two end joints from i to $i+1$ along the common perpendicular. α_i is the included angle between the two joint axes in a plane perpendicular to a_i . d_i is the distance of the two common perpendiculars along joint i axis. L_1 is the height of stand column of the solid of revolution pedestal, L_2 the length of the upper arm, L_3 the length of the fore arm, while L_4 is the distance from the central point of the hand gripper to the wrist reference point.

在表 1 中，θ_i 是垂直于关节 i 轴线的平面内两个公垂线的夹角。a_i 是是两端关节 i 和 $i+1$ 沿公垂线的距离。α_i 是垂直于 a_i 的平面内两个关节轴线的夹角。d_i 是沿关节 i 轴线的两个公垂线的距离。L_1 回转体底座立柱高度，L_2 为大臂的长度，L_3 为小臂长度，L_4 为手爪中心点到腕部参考点的距离。

Positive kinematic solution

The positive kinematic solution is to obtain the pose of the end effector in the given coordinate system with known joint variables and geometric parameters of the rod pieces. The expression (4) of the end effector pose of the picking robot in the reference coordinate system can be obtained when the parameters in Table 1 are substituted into formula (3).

运动学正解

机器人的运动学正问题是已知杆件的关节变量和几何参数求末端执行器在给定坐标系中的位姿。将表 1 中的参数代入公式（3）可以得到采摘机器人末端执行器在基坐标系中的位姿表示式（4）。

$$ {}^{0}T_4 = A_1A_2A_3A_4 = \begin{bmatrix} -C_1S_{234} & S_1 & C_1C_{234} & C_1(C_{234}L_4 + C_{23}L_3 + C_2L_2) \\ -S_1S_{234} & -C_1 & -S_1C_{234} & S_1(C_{234}L_4 + C_{23}L_3 + C_2L_2) \\ C_{234} & 0 & S_{234} & S_{234}L_4 + S_{23}L_3 + S_2L_2 \\ 0 & 0 & 0 & 1 \end{bmatrix} \quad (4) $$

Wherein, $C_1=\cos\theta_1$, $S_1=\sin\theta_1$,
$C_{23}=\cos(\theta_2+\theta_3)$, $S_{23}=\sin(\theta_2+\theta_3)$,
$C_{234}=\cos(\theta_2+\theta_3+\theta_4)$, $S_{234}=(\theta_2+\theta_3+\theta_4)$.

The coordinate system of the end effector is established with the hand gripper center as the origin of coordinates. Axis Z is represented with vector $\bar{a}$ in the direction that the end effector approaches object, axis Y is represented with vector $\bar{o}$ in the direction of the connecting line of the two fingers, and axis X is determined to be represented with vector $\bar{n}$ in accordance with the right-hand rule. The end effector posture is determined by vectors $\bar{n}$, $\bar{o}$ and $\bar{a}$. The gripper's posture is ensured by the rotation vector ${}^{0}_{T}R$, as shown in expression (5).

其中，$C_1=\cos\theta_1$, $S_1=\sin\theta_1$,

$C_{23}=\cos(\theta_2+\theta_3)$, $S_{23}=\sin(\theta_2+\theta_3)$,

$C_{234}=\cos(\theta_2+\theta_3+\theta_4)$, $S_{234}=(\theta_2+\theta_3+\theta_4)$.

取手抓中心为坐标原点，建立末端执行器坐标系。Z 轴取在末端执行器接近物体方向用矢量 $\bar{a}$ 表示，Y 轴设在两手指的连线方向用矢量 $\bar{o}$ 表示，X 轴根据右手法则确定用矢量 $\bar{n}$ 表示，矢量 $\bar{n}$ 、$\bar{o}$ 和 $\bar{a}$ 确定末端执行器的姿态。手爪的姿态由旋转矩阵 ${}^{0}_{T}R$ 规定，如式（5）所示。

$$ {}^{0}_{T}R = \begin{bmatrix} \bar{n} & \bar{o} & \bar{a} \end{bmatrix} \quad (5) $$

The gripper's position is stipulated by its origin of coordinates and described with position vector $\bar{p}$. The four vectors added to scale factor are expressed in a 4×4 homogeneous matrix as shown in expression (6).

手爪的位置由其坐标系的原点规定，用位置矢量 $\bar{p}$ 描述。将这四个矢量加入比例因子写成 4×4 齐次矩阵如式（6）所示。

$$ {}^{0}T_4 = \begin{bmatrix} n_x & o_x & a_x & p_x \\ n_y & o_y & a_y & p_y \\ n_z & o_z & a_z & p_z \\ 0 & 0 & 0 & 1 \end{bmatrix} \tag{6} $$

Inverse kinematic solution

The inverse question of robot kinematics is to obtain the joint variables with the known pose of the end effector in the given coordinate system and the known geometrical parameters of the rod pieces. There are many methods for inverse robot kinematic solution. In this paper, premultiplication decoupling of A_i^{-1} and matrix ${}^{0}T_4$ is adopted to the solution with the help of Matlab software, and hence:

运动学逆解

机器人运动学的逆问题是已知末端执行器在给定坐标系中的位姿和杆件的几何参数求关节变量。求解机器人运动学逆解的方法很多，本文采用 A_i^{-1} 与矩阵 ${}^{0}T_4$ 左乘解耦，借助 Matlab 软件求解得：

$$ \begin{cases} \theta_1 = \arctan\left(\dfrac{P_y}{P_x}\right) \\ \quad = \arctan\left(\dfrac{P_y}{P_x}\right) + 180^{\circ} \\ \theta_2 = -\arctan\left(\dfrac{m}{n}\right) \pm \arctan \dfrac{m^2 + n^2 - L_3^{\,2} + L_2^2}{2L_2\sqrt{n^2+m^2} - \left(\dfrac{m^2+n^2-L_3^2+L_2^2}{2L_2}\right)} \\ \theta_3 = \pm \arctan \dfrac{\sqrt{4L_3L_2 - (n^2+m^2-L_3^2-L_2^2)}}{n^2+m^2-L_3^2-L_2^2} \\ \theta_4 = -(\theta_3 + \theta_2) \end{cases} \tag{7} $$

It can be observed from expression (7) that $\theta_1, \theta_2, \theta_3$ have two solutions respectively, there exist 8 different sets of inverse solutions in this mechanical system, which are usually selected according to the principle of the shortest route or more small movement of joint and less movement of large joint.

由式（7）我们可以观察到 $\theta_1, \theta_2, \theta_3$ 分别有两个解，即此机械系统存在 8 组不同的逆解，通常根据最短行程或多移动小关节少移动大关节的原则选择。

RESULTS ANALYSIS AND DISCUSSION WITH KINEMATIC SIMULATION

结果分析与讨论

Establishment of 3-D simulation model

3-D 仿真模型的建立

The mechanical structure of the 4- DOF picking robot consists of the pedestal, the waist between the upper arm and electrical machine box, the elbow between the upper arm and the fore arm, the wrist between the fore arm and the end effector, and the end effector. The interconnection of the components forms the four rotating joints, namely, waist, shoulder, elbow, and wrist joints. The three preceding joints determine the position of the end effector in the work space, while the last joint determines its pose. Although ADAMS software possesses powerful kinematic and dynamic solution function, it is comparatively weak in the aspect of 3-D solid model building. Therefore, the robot virtual prototype is built in virtue of pro/E software which has powerful 3-D solid model building function in line with the picking robot structure. During the course of modeling, the main solid components are retained while such detailing components as the circular beads, chamfers, gears, bearings and electrical machine are ignored on the premise that the simulated analysis requirements are satisified, and 3-D simulation model of the eggplant picking robot is built as the following Fig.3.

四自由度采摘机器人机械结构由底座、大臂与电机箱体之间的腰部、大臂与小臂之间的肘部、小臂与末端执行器之间的腕部、末端执行器构成，构件之间相互连接形成的腰、肩、肘、腕 4 个旋转关节，前三个关节决定末端执行器在工作空间的位置，后一个关节决定末端执行器在工作空间的姿态。虽然 ADAMS 软件具有强大的运动学动力学求解功能但在三维实体建模方面相对薄弱，因而根据采摘机器人结构借助三维实体建模功能强大的 pro/e 软件来构建机器人虚拟样机。建模过程中在满足仿真分析要求的前提下，忽略模型的圆角、倒角、齿轮、轴承、电机等细化的部件，保留主要的实体部件，建立茄子采摘机器人三维仿真模型如下图 3。

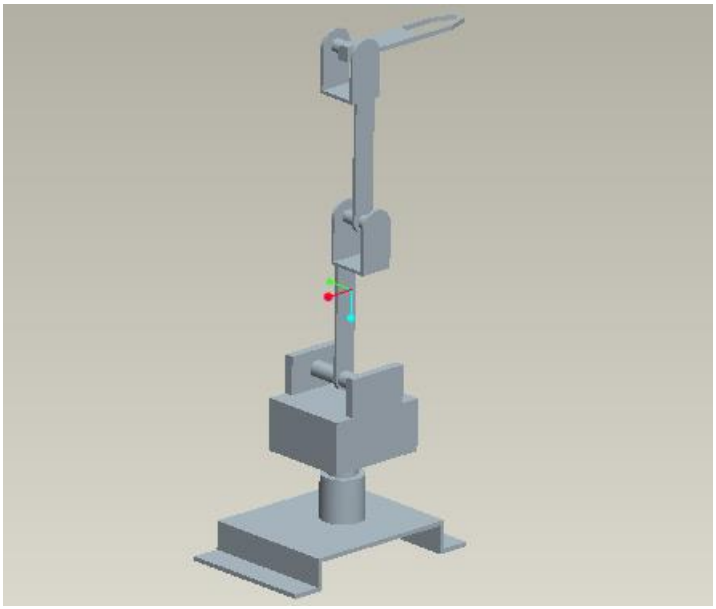

Fig. 3 - 3-D simulation model of the picking robot

Pretreatment for simulation

The model built in pro/E software is saved as intermediate format parasolid, and then is imported into ADAMS simulation software. ADAMS motion toolkit is used to add constraint to the imported 3-D simulation model as follows:

Fixed joints are added to between the bed and the ground, revolute joints are added to the waist, shoulder, and elbow and wrist part.

ADAMS drive toolkit is used to add drive to the imported 3-D simulation model as follows:

仿真预处理

将在 pro/e 中建立的模型保存为中间格式 parasolid，然后导入 ADAMS 仿真软件中。运用 ADAMS 运动工具集对导入的三维仿真模型添加约束，如下：

底座与大地之间添加固定副，腰、肩、肘、腕部添加旋转副。

运用 ADAMS 驱动工具集导入的三维仿真模型添加驱动，如下：

$$waist(time) = 180 * \sin(75d * time - 90d) + 180d \quad (7)$$

$$shoulder(time) = -45 * \sin(180d * time - 90d) - 45d \quad (8)$$

$$elbow(time) = -30d * \sin(145d * time - 90d) - 30d \quad (9)$$

$$wrist(time) = 80d * \sin(145d - time - 90d) + 80d \quad (10)$$

With the above mentioned tasks completed, the virtual prototype model of the picking robot is established as in Fig.4.

完成上述各项工作就建立了采摘机器人虚拟样机模型，如图 4 所示。

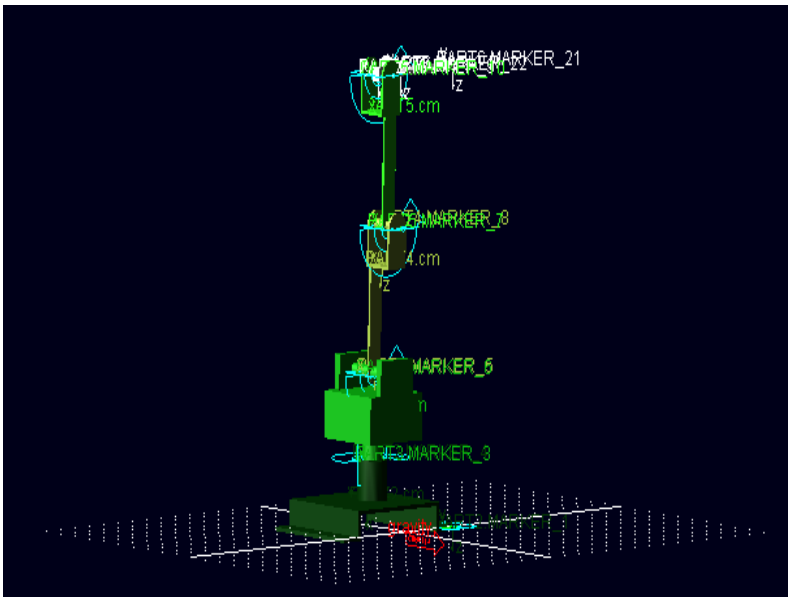

Fig. 4 - Virtual prototype model of the picking robot

Model Self-test

Before the simulating calculation, inquire the degree of freedom of the system, the components with mass undefined and over-constraint through "model verify" function in "tools" menu. Information such s as "model verified successfully" and "degrees of freedom for model..1" are displayed as shown in Fig.5, which indicates the modeling is correct and the kinematic simulation can be conducted for the next step.

模型自检

在仿真计算之前，通过 tools 菜单中的 model verify 功能对系统的自由度、未定义质量的构件和过约束情况进行查询，如图 5 信息显示"model verified successfully"和"0 degrees of freedom for model.1"说明建立模型正确，可以进行下一步的运动学仿真。

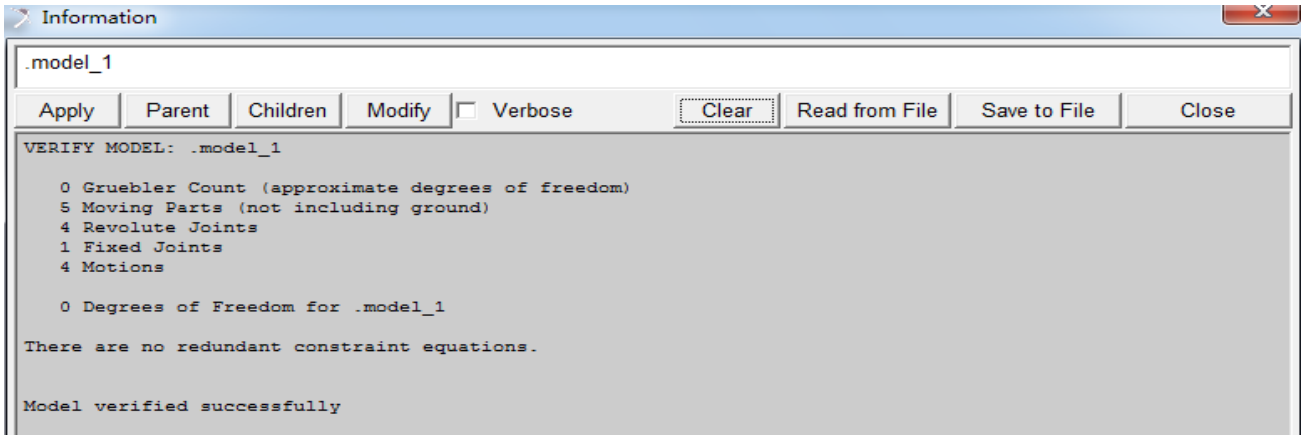

Fig. 5 - Self-test interface

Simulation analysis

The mark point mark-21, which is fixed joint to the centroid part6.cm of the end effector, is taken as the object of study. To study its position relative to fixed coordinate system, the rotational speed of each joint is set as $30^{\circ}/s$, simulation time is set as 5s, and simulation calculation is performed. After the simulation is completed, "postprocess" interface for post-processing is entered as shown in Fig.6.

仿真分析

以固连在末端执行器质心 part6.cm 上的标记点 mark-21 为研究对象，研究其相对于固定坐标系的位置，设定每个关节的转动速度为 $30^{\circ}/s$，设定仿真时间为 5s，进行仿真运算。仿真结束后进入 postprocess 界面后处理，如图 6 所示。

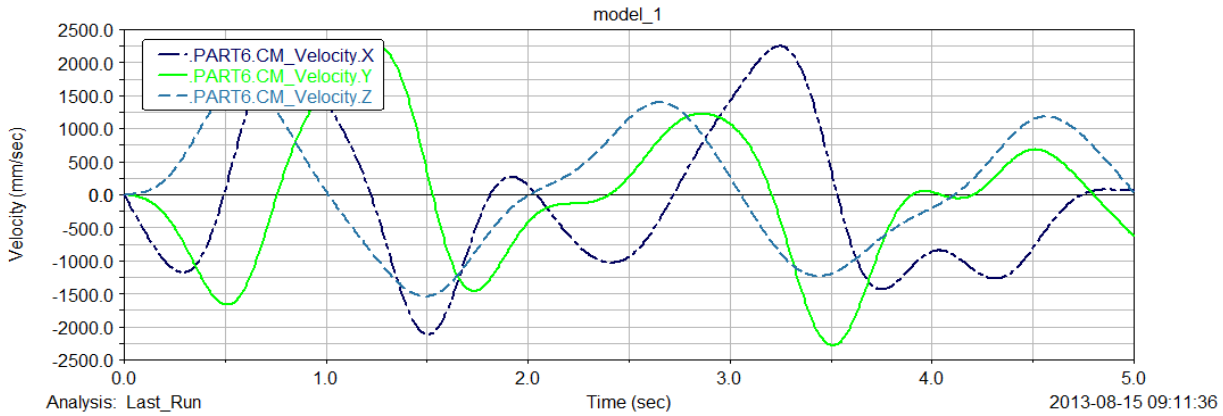

Fig. 6 - Speed graph

The solid line, the long broken line and the short broken line in the figure represent respectively the speed in the X, Y and Z directions. It is observed from Fig.6 that the change-in- speed is smooth and steady at the centroid part6.cm of the end effector, which does not generate strenuous vibration phenomenon during the whole course of movement, meeting the task requirements.

图中实线表示 X 方向的速度，长虚线表示 Y 方向速度，短虚线表示 Z 方向的速度，从图 6 中可以看出末端执行器质心 part6.cm 处速度变化相对平稳，末端执行器在整个运动过程中没有产生剧烈震动现象，达到工作要求。

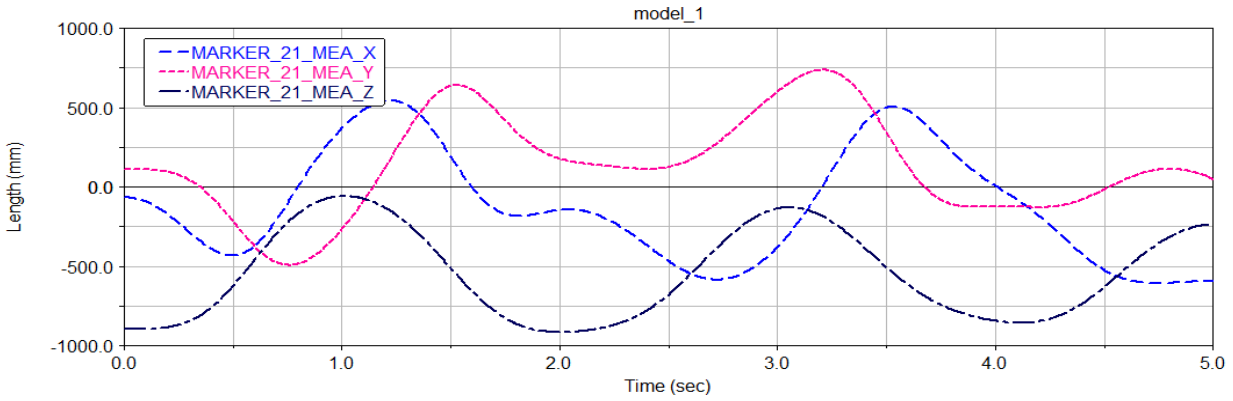

Fig. 7 - Displacement curve

As shown in Fig.7, the long broken line, the short broken line and the dot-dash line represent respectively the displacement in the X, Y and Z directions. In the postprocessing interface, it can be obtained by virtue of measurement button that the displacement of marker-21 at the initial position is x =-66mm， y=113mm， z=-897mm when t=0, which is consistent with the initial conditions of the manipulator. When the manipulator moves to the point of t=5s, the displacement of marker-21 on the three coordinates is x=-591mm，y=50，z=-236. Through test and verification, the theoretical calculation results from expression (4) and (5) in the D-H coordinate system are identical with the simulation results. The graph of Displacement and speed can reflect the real motion conditions and apply to picking robot control.

CONCLUSIONS

The application of picking robot in agricultural production can effectively reduce the number of harvest labors and increase the income of farmers, and also has great significance to improve the level of automation and intelligentization for agricultural machinery. In this paper, by applying virtual prototype technology into the design of agricultural machines, the product design cycle can be effectively shortened and product performance can be improved. As a modern design approach, the virtual design technology will have a significant impact to the development of agricultural equipment.

Eggplant picking robot with 4 degrees of freedom is developed in order to improve the economy and adaptability of the picking robot and it adopts 4-DOF open motion chain which is formed by connecting the waist, the upper arm, the fore arm and the wrist in series through the rotational joints. The robot completes the picking operation through movements of each joint. The objective of studying robot kinematics is to establish the relationship of the spatial position between the robot motion components and the end effector, to build mathematic model of the robot arm movements, and to provide theoretical basis and technical parameters for agricultural robotic control.

The optimized design of structure and path planning is based on the kinematics analysis of the manipulator. In order to determine the spatial position relationship between the robot components and the end effector, the theoretical model is established by virtue of Denavit-Hartenberg approach and the positive solution of the kinematic equation is obtained. Premultiplication decoupling of A_i^{-1} and matrix ${}^0T_4$ is adopted to obtain

如图 7 所示，长虚线代表 X 方向的位移，短虚线代表 Y 方向的位移，点划线代表 Z 方向的位移，在后处理界面借助测量按钮出可得出当 t=0 时 marker-21 在初始位置的位移为 x =-66mm，y=113mm，z=-897mm，与机械手原始状态相吻合。当机械手运动到 t=5s 时 marker-21 在三个坐标上的位移是 x=-591mm，y=50，z=-236，经验证与 D-H 坐标系中联立式（4），（5）所得理论计算结果与仿真结果相同。位移和速度曲线图能够反映真实运动情况，可以应用于采摘机器人的控制。

结论

采摘机器人在农业生产中的应用，大量的减少了收获用工，增加了农民的收入，对于提高农业机械的自动化和智能化水平具有重要意义。本文的研究，将虚拟样机技术应用于农业机械的设计，缩短了设计周期，提高了产品质量。虚拟设计技术作为一种的现代化设计手段，必将对农业装备发展产生重要影响。

为了提高采摘机器人经济性和适应性，开发了 4 自由度茄子采摘机器人。其采用 4 自由度的开式运动链，由腰部、大臂、小臂和手腕通过转动关节串联而成。机器人是通过各个关节的运动，来完成采摘作业。研究机器人运动学的目的就是建立机器人各运动构件与末端执行器在空间位置之间的关系，建立机器人手臂运动的数学模型，为机器人的控制提供理论依据和技术参数。

机械手的运动学分析是结构优化设计、轨迹规划的基础。为了确定机器人各运动构件与末端执行器在空间位置之间的关系，借助 Denavit-Hartenberg 法建立了理论模型，得到运动学方程的正解。采用 A_i^{-1} 与矩阵 ${}^0T_4$ 左乘解

inverse kinematic solution with the help of Matlab software. Pro/e software is used to establish 3-D simulation model of the picking robot, whose functions are experimented and tested by means of ADAMS, a dedicated virtual prototype develop tool. ADAMS simulation software is introduced for the kinematics simulation analysis. It is illustrated by the simulation results that the kinematic model established by D-H approach reflects the real motion conditions of the robot, and both the positive and inverse kinematic solutions are correct. The structural design of 4 DOF picking robot designed and developed is rational and it can meet the requirements of eggplant picking in the greenhouse cultivation pattern.

ACKNOWLEDGEMENT

The paper was the systematically extended version of the authors' synoptic paper in Chinese "Kinematics Analysis and Working Space Simulation of Picking Robot for Eggplant", which has been published with abstract in Vol.8, No.4, 2008 of Journal of Weifang University. This work was supported by Shandong province science and technology development project (No.2011YD03048) and Shandong Provincial Natural Science Foundation, China (No.Y2008 G32).

REFERENCES

[1]. Arima S., Kondo N. (2009) – *Cucumber harvesting robot and plant training system*. Journal of Robotics and Mechatronics, vol. 11, no. 3, pp. 208-212;
[2]. Denavit, J., Hartenberg, R.S.. (1955) – *A Kinematic Notation for Lover pair Mechanisms based on matrices*. Journal of Applied Mechanics, vol. 22, no.6, pp.102-108;
[3]. Jian S., Tiezhong Z., Liming Xu. (2006) – *Research Actuality and Prospect of Picking Robot for Fruits and Vegetables*. Transactions of the Chinese Society for Agricultural Machinery, vol. 37, no.5, pp.158-162;
[4]. Jizhan L., Pingping L., Zhiguo L. (2008) – *Hardware Design of the End-effector for Tomato-harvesting Robot*. Transactions of the Chinese Society for Agricultural Machinery, Vol. 39, no.3, pp.109-112;
[5]. Kondo N., Monta M. Fujiura T.(1996) – *Fruit harvesting robot in Japan.* Advances in Space Research , vol.18, no.2, pp.181-184;
[6]. Peng C., Zhen C. Xiaochao. (2011) – *Statics Analysis of Apple-picking Robot Humanoid Manipulator*. Transactions of the Chinese Society for Agricultural Machinery, vol. 42, no. 2, pp.149-153;
[7]. Xiuying T., Tiezhong Z. (2005) – *Robotics for Fruit and Vegetable Harvesting: a Review.* Robot, vol.27, no.1, pp.90-96;
[8]. Shigehiko H., Katsunobu G., Yukitsugu I. (2002) – *Robotic Harvesting System for Eggplants*. Japan Agricultural Research Quarterly, vol.36,no.6, pp.163-168;
[9]. Song J. (2011) – *Target Identification Based on Improved Wavelet Edge Detection for Eggplant Picking Robot*. International Review on Computers and Software, Vol.6, no.5, pp.710-714;
[10]. Ting Y., Wei L., Yuzhi T. (2009) – *Information Acquisition for Cucumber Harvesting Robot in Greenhouse.* Transactions of the Chinese Society for Agricultural Machinery, vol.40, no.10, pp.151-155;
[11]. Van Henten E.J., Van Tuijl B.A J., Hemming J. (2002) – *Field Test of an Autonomous Cucumber Picking Robot*. Biosystems Engineering, vol. 86, no.4, pp.305–313.

耦，借助 matlab 软件求出运动学逆解。利用 pro/e 建立采摘机器人三维模型，借助于专用虚拟样机开发工具 ADAMS 试验和测试功能，导入 ADAMS 仿真软件进行运动学仿真分析。仿真结果表明：D-H 法建立的运动学模型反映了机器人的真实运动情况，运动学正逆解正确。设计开发的 4 自由度采摘机器人结构设计的合理，能够满足温室栽培模式下茄子采摘的要求。

致谢

本文是作者对其出版在《潍坊学院学报》2008 年第 8 卷第 4 期的文章的深度扩展与系统分析。本研究受到山东省科技发展计划项目(No.2011YD03048) 和山东省自然科学基金(No.Y2008G32)的资助。

参考文献

[1]. Arima S., Kondo N. (2009) — *黄瓜收获机器人与种植培育系统*. 机器人与机械系统期刊, 第 11 卷, 第 3 期, 208-212;
[2]. Denavit, J., Hartenberg, R.S.. (1955) —*基于矩阵的双联机构运动学方法*. 应用机械学期刊, 第 22 卷, 第 6 期, 102-108;
[3]. 宋健, 张铁中, 徐丽明. (2006) — *果蔬采摘机器人研究进展*. 农业机械学报, 第 37 卷, 第 5 期, 158-162;
[4]. 刘继展, 李萍萍, 李智国. (2008) —*番茄采摘机器人末端执行器的硬件设计*. 农业机械学报, 第 39 卷, 第 3 期, 109-112;
[5]. Kondo N., Monta M. Fujiura T.(1996) — *日本的蔬菜收获机器人*. 空间技术研究进展, 第 18 卷, 第 2 期, 181-184;
[6]. 崔鹏, 陈志, 张晓超. (2011) —*苹果采摘机器人仿生机械手静力学分析与仿真*. 农业机械学报, 第 42 卷, 第 2 期, 149-153;
[7]. 汤修映, 张铁中.(2005) —*果蔬收获机器人研究综述*. 机器人. 第27卷, 第1期, 90-96;
[8]. Shigehiko H., Katsunobu G., Yukitsugu I. (2002) — *茄子机器人采摘系统*. 日本农业研究季刊, 第 36 卷, 第 6 期, 163-168;
[9]. 宋健. (2011) — *基于改进的小波边缘提取的茄子采摘机器人目标识别*. 国际计算机和软件进展, 第 6 卷, 第 5 期, 710-714;
[10]. 袁挺,李伟,谭豫之. (2009) —西红柿采摘机器人末端执行器硬件设计. 农业机械学报, 第 40 卷, 第 10 期, 109-112;
[11]. Van Henten E.J., Van Tuijl B.A J., Hemming J. (2002) — *黄瓜采摘机器人现场试验*. 生物系统工程, 第 86 卷, 第 4 期,305–313;

[12]. Wei L., Aiguo Song., Jianrong C. (2011) – *Structural design and kinematics algorithm research for orange harvesting robot*. Journal of Southeast University, vol. 41, no.1, pp.95-100;
[13]. Xifeng L., Xiangwen M., Saorong C. (2005) – *Kinematics Optimizing and Simulation Test of Tomato Picking Manipulator*. Transactions of the Chinese Society for Agricultural Machinery, vol. 36, no.7, pp.96-100;
[14]. Xu, L., You, Z., Wu, S., et al. (2013)–*Development and experiment on automatic grading equipment for kiwi*. INMATEH- Agricultural Engineering, vol. 41, no.3, pp.55-64.

[12]. 卢伟, 宋爱国, 蔡健荣. (2011) —*柑橘采摘机器人结构设计及运动学算法*. 东南大学学报, 第 41 卷, 第 1 期, 95-100;
[13].梁喜凤,苗香雯, 崔绍荣. (2005) — *番茄收获机械手运动学优化与仿真试验*. 农业机械学报, 第 36 卷, 第 7 期, 96-100;
[14]. 许丽佳, 尤志坤, 武胜 等. (2013) —*猕猴桃自动分级设备的研制与试验*. 国际农业工程期刊, 第 41 卷, 第 3 期, 55-64.

THEORETICAL ARGUMENTATION OF PARAMETERS OF A WINDROVER STEMS DRIVING AND EVACUATING WORKING PART
/
ARGUMENTAREA TEORETICĂ A PARAMETRILOR ORGANULUI DE ANTRENARE ŞI EVACUARE A TULPINILOR UNUI VINDROVER

PhD. Eng. Cerempei V.
Institute of Agricultural Machinery "Mecagro" Chisinau / Moldova
E-mail: institut@mecagro.md

***Abstract**: In order to assure the optimum operating conditions for the combine of harvesting thick stem plants, the constructive and kinematic parameters of windrower part performing the stems cut driving, evacuating and transporting to the feeding apparatus, are explained.*

***Keywords**: windrower,thick stems, driving, evacuating, transporting, constructive and kinematic parameters*

INTRODUCTION

Efficiency of operating system of combine designed to thick plants harvesting (corn, sorghum saccharate, sunflower) depends on the quality of a whole series of technological phases. Cutting part parameters are explained in paper [1]. Also, the argumentation of parameters of element performing cut stems driving, evacuating from the row and transporting to the feeding apparatus is of a great importance.

MATERIALS AND METHODS

In order to appropriately cut and securely driving with reduced energy consumption the stem should be cut and completely introduced within the disc driving space before contacting the working surface of driving tooth. When the drum tooth top contacts the stem, the correlation between the combine speed V_{com} and drum angular speed ω_{ant} should meet the following condition: the stem must penetrate the driving space at equal or bigger distance than its diameter, before being touched by the next tooth wall (fig.1). In this case, the combine will run the distance:

***Rezumat**: Pentru asigurarea condiţiilor optime de funcţionare a combinei de recoltat plante cu tulpini groase sunt argumentaţi parametrii constructivi şi cinematici ai organului vindroverului, care execută antrenarea, evacuarea din rând şi transportarea tulpinilor tăiate către aparatul de alimentare.*

***Cuvinte cheie**: vindrover, tulpini groase, antrenare, evacuare, transportare, parametrii constructivi şi cinematici*

INTRODUCERE

Eficienţa funcţionării combinei de recoltat plante cu tulpini groase (porumb, sorg zaharat, floarea soarelui) depinde de calitatea executării a unui şir întreg de faze tehnologice. Parametrii organului de tăiere sunt argumentaţi în lucrarea [1]. Nu mai puţin importantă este argumentarea parametrilor organului, care execută antrenarea, evacuarea din rând şi transportarea tulpinilor tăiate către aparatul de alimentare.

MATERIALE ŞI METODĂ

Pentru tăierea ireproşabilă şi antrenarea sigură cu consum redus de energie este necesar ca tulpina, până a intra în contact cu suprafaţa de lucru a dintelui de antrenare, să fie tăiată şi introdusă complet în spaţiul de antrenare al discului. Din momentul contactului vârfului dintelui din tambur cu tulpina, corelaţia dintre viteza combinei V_{com} şi viteza unghiulară a tamburului ω_{ant} trebuie să corespundă următoarei condiţii: tulpina pînă să fie atinsă de peretele următorului dinte trebuie să intre în interiorul spaţiului de antrenare la distanţă egală sau mai mare decât diametrul acesteia (fig.1). În acest caz combina va parcurge distanţa:

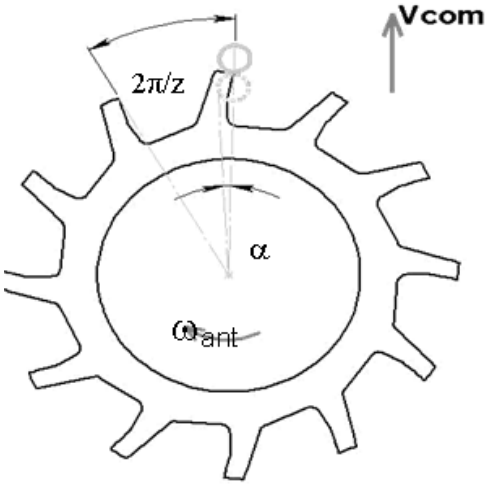

Fig. 1 – Scheme of driving and evacuating the stem from the row

$$S = \hat{i} + d \quad (1)$$

Where:
$\hat{i}$ is the stem curving; d – stem diameter.
For running the distance S, the time period is necessary.

Unde:
$\hat{i}$ este încovoierea tulpinii; d – diametrul tulpinii.
Pentru parcurgerea distanţei S este necesară durata de timp:

$$\tau = \frac{S}{V_{com}} = \frac{\hat{i} + d}{V_{com}}. \quad (2)$$

Concomitantly, at the same period of time the drum will rotate at angle (fig.1):

Concomitent, în aceeaşi perioadă de timp tamburul se va roti la unghiul (fig.1):

$$\theta - \alpha = \frac{2\pi}{z} - arctg\frac{r}{R-r}, \quad (3)$$

where z is the drum teeth number; r – stem radius ; R – drum radius. Then, the time necessary for driving the stem will be equal.

unde z este numărul de dinţi ai tamburului; r – raza tulpinii; R – raza tamburului. Atunci perioada de timp necesară pentru antrenarea tulpinii va fi egală:

$$\tau = \frac{\theta - \alpha}{\omega_{ant}} = (\frac{2\pi}{z} - arctg\frac{r}{R-r}) / \omega_{ant} = \frac{\hat{i} + d}{V_{com}}. \quad (4)$$

As the stem diameter *d* of corn, sorghum is much smaller than drum diameter (dmax ≈30…40 mm<<D_{min} ≈550 mm), and plants stems curving in normal conditions approches 0 (î→0), formula (2,4) of time period simplifies:

Deoarece diametrul tulpinii *d* al porumbului, sorgului este mult mai mic decâT diametrul tamburului (dmax ≈30…40 mm<<D_{min} ≈550 mm), iar încovoierea tulpinilor plantelor menţionate în condiţiile normale se apropie de 0 (î→0), formule (2,4) a duratei de timp se simplifică:

$$\tau = \frac{2\pi}{z\omega_{ant}} sau \tau = \frac{d}{V_{com}}, \text{ de unde } \frac{V_{com}}{z\omega_{ant}} = \frac{d}{2\pi} \text{ sau } z\omega_{ant} = \frac{2\pi V_{com}}{d} \quad (5)$$

As a general rule, if the stem is placed between the drum teeth when starting the cutting, the constructive and kinematic parameters ratio should correspond to:

Pentru cazul general, când tulpina în momentul iniţierii tăierii se află între dinţii tamburului, raportul parametrilor constructivi şi cinematici trebuie să corespundă:

$$z\omega_{ant} \le 2\pi V_{com} / d \quad (6)$$

Immediately after the stem cutting, it is necessary to consecutively perform the following operations: evacuating the stem from the row, moving, reorienting from vertical position to horizontal one and its driving towards the relevant assembly rollers. When running a distance of 1 meter, the combine windrower has to cut plant stems (corn, saccharate sorghum, sunflower etc.) in each row and within the period of time $\tau' = 1/V_{com}$.

Imediat după tăierea tulpinii este necesar de efectuat consecutiv următoarele operaţiuni: evacuarea tulpinii din rând, deplasarea, reorientarea din poziţia verticală în cea orizontală şi antrenarea acesteia către tăvălugii ansamblului respectiv. La parcurgerea distanţei de 1 metru liniar vindroverul combinei trebuie să taie m tulpini de plante (porumb, sorg zaharat, floarea-soarelui etc.) în fiecare rând şi în perioada de timp $\tau' = 1/V_{com.}$

RESULTS

Evacuation of stems in row. Having in view the request of *an operative evacuation of the stems from the row,* each tooth of driving-evacuating drum should transport at the most one plant for each row (fig.1). In this case, for evacuating the stems the drum will rotate with an angle which value will be:

REZULTATE

Evacuarea tulpinilor din rând. Având în vedere *cerinţa evacuării operative a tulpinilor din rând,* fiecare dinte al tamburului de antrenare-evacuare trebuie să transporte maximum câte o plantă din fiecare rând (fig. 1). În acest caz pentru evacuarea m tulpinilor tamburul se va roti la un unghi, a cărui valoarea integrală va fi:

$$\varphi' = \frac{2\pi}{z} \cdot m \quad (7)$$

where *z* is the number of teeth on drum disc; *m* – number of harvested stems in a row at 1 linear meter. For achieving the angle above φ', the disc needs a similar period of time:

unde *z* este numărul de dinţi pe un disc al tamburului; **m** – numărul de tulpini recoltate într-un rând la 1 metru liniar. Pentru a parcurge unghiul menţionat φ' discul are nevoie de aceiaşi perioadă de timp:

$$\tau' = \varphi' / \omega_{ant} = 2\pi m / z\omega_{ant} \quad (8)$$

where ω_{ant} is the angular speed of driving drum.

Operative evacuation of stems from the row requires that the drum runs the angle φ' within a less period of time than the time necessary for the combine to cross 1 linear meter distance, namely:

unde ω_{ant} este viteza unghiulară a tamburului de antrenare.

Evacuarea operativă a tulpinilor din rând necesită ca tamburul să parcurgă unghiul φ' într-o perioadă de timp mai mică, decât cea necesară combinei pentru a traversa distanţa de 1 metru liniar, adică:

$$2\pi m / z\omega_{ant} \leq 1/V_{com}. \quad (9)$$

From inequality (9) results that, for operatively evacuating the stems in row, the drum constructive and kinematic parameters ration should be:

Din inegalitatea (9) reiese, că pentru evacuarea operativă a tulpinilor din rând raportul parametrilor constructivi şi cinematici ai tamburului trebuie să fie:

$$z\omega_{ant} \geq 2\pi m V_{com} \quad (10)$$

Respecting both efficient operating conditions of windrower (safely driving the stems to the drum teeth and evacuating them) determines the drum driving parameters as follows:

Respectarea ambelor condiţii de funcţionare eficientă a vindroverului (antrenarea sigură a tulpinilor de către dinţii tamburului şi evacuarea operativă a lor din rând) determină parametrii tamburului de antrenare în felul următor:

$$2\pi V_{com} m \leq z\omega_{ant} \leq 2\pi V_{com} / d \quad (11)$$

For efficiently driving the stems requires that the drum teeth pitch (fig.1) be: $P = \frac{2\pi(R-r)}{z}$ and circular speed of drum $V = \omega_{ant}(R-r)$ assures the displacement period from a tooth to another contacting the stem within a greater period of time than the necessary for cutting a stem: $\frac{2\pi(R-r)}{z} / \omega_{ant}(R-r) \geq \frac{d}{V_{com}}$, from here

Condiţia antrenării eficiente a tulpinilor impune ca pasul dinţilor din tambur (fig.1) $P = \frac{2\pi(R-r)}{z}$ şi viteza circulară a tamburului $V = \omega_{ant}(R-r)$ să asigure durata deplasării de la un dinte până la altul din contact cu tulpina într-o perioadă de timp mai mare decât cea necesară pentru tăierea unei tulpini: $\frac{2\pi(R-r)}{z} / \omega_{ant}(R-r) \geq \frac{d}{V_{com}}$, de aici

$$z\omega_{ant} \leq 2\pi V_{com} / d \quad (12)$$

where *R, r* represents the drum radius and respectively the stem radius $(r = d/2)$.

The last inequality (12) confirms the correctness of formula (11) and allows to set the dimensions of driving space of drum disc.

Stems evacuation and driving. As mentioned before, during the working process, the drum teeth perform a complex movement: they rotate along with the drum with angular speed ω_{ant} and moves with the combine with linear speed V_{com} (fig.2).

Taking into account the recommendations [2], [3], from the scheme shown (fig. 2) can be obtained the ecuations of displacement of different points of evacuating disc:

unde *R, r* reprezintă raza tamburului şi respectiv a tulpinii $(r = d/2)$.

Ultima inegalitate (12) confirmă corectitudinea formulei (11) şi permite precizarea dimensiunilor spaţiului de antrenare a discului din tambur.

Plenitudinea evacuării şi antrenării tulpinilor. După cum s-a menţionat anterior, în procesul de lucru dinţii tamburului efectuează o mişcare complexă: se rotesc împreună cu tamburul cu viteza unghiulară ω_{ant} şi se mişcă consecvent împreună cu combina cu viteza liniară V_{com} (fig.2).

Ţinând cont de recomandări [2], [3], din schema prezentată (fig. 2) pot fi obţinute ecuaţiile deplasării diferitor puncte ale discului de evacuare:

the tooth AB: $Y_A = V_{com} \cdot \tau_1 + R \sin\omega_{ant}\tau_1,\ X_A = R\cos\omega_{ant}\tau_1,$ (13)

$$Y_B = V_{com}\tau_1 + (R-b)\sin\omega_{ant}\tau_1,\ X_B = (R-b)\cos\omega_{ant}\tau_1 \quad (14)$$

the tooth CD: $Y_c = V_{com}\tau_2 + (R-b)\sin\omega_{ant}\tau_2,\ X_c = (R-b)\cos\omega_{ant}\tau_2$ (15)

$$Y_D = V_{com}\tau_2 + R \sin\omega_{ant}\tau_1,\ X_D = R\cos\omega_{ant}\tau_2, \quad (16)$$

where *R* is the drum radius; *b* – tooth working width.

Scheme analysis (fig. 2) demonstrates that *efficient and complete evacuation of stems* can be reached when $Y_{A_1} \geq Y_{C_1}$. Taking into consideration the necessity of

unde *R* este raza tamburului; *b* – lăţimea de lucru a dintelui.

Analiza schemei (fig. 2) demonstrează că *antrenarea şi evacuarea eficientă şi completă* a tulpinilor poate fi în cazul când $Y_{A_1} \geq Y_{C_1}$. Luând în consideraţie necesitatea

diminishing the energy consumption, the variant is optimum when $Y_{A_1} = Y_{C_1}$. In this case:

minimizării consumului de energie, este optimă varianta când $Y_{A_1} = Y_{C_1}$.În acest caz:

$$\tau_1 = \varphi_1 / \omega_{ant} = \pi / 2\omega_{ant}, \quad (17)$$

$$\tau_2 = \varphi_2 / \omega_{ant} = (\frac{\pi}{2} + \frac{2\pi}{z}) / \omega_{ant} = \frac{\pi}{2\omega_{ant}} + \frac{2\pi}{z\omega_{ant}} = \frac{\pi z + 4\pi}{2z\omega_{ant}} = \frac{\pi(4+z)}{2z\omega_{ant}} \quad (18)$$

From formulae (13, 15) it follows:

Din formulele (13, 15) urmează:

$$Y_{A_1} = V_{com}\frac{\pi}{2\omega_{ant}} + R\sin\omega_{ant}\frac{\pi}{2\omega_{ant}} = \frac{\pi V_{com}}{2\omega_{ant}} + R,$$

$$Y_{C_1} = V_{com}\frac{\pi(4+z)}{2z\omega_{ant}} + (R-b)\sin\omega_{ant}\frac{\pi(4+z)}{2z\omega_{ant}} \quad (19)$$

$$\frac{\pi V_{com}}{2\omega_{ant}} + R = \frac{\pi V_{com}(4+z)}{2z\omega_{ant}} + (R-b)\sin\frac{\pi(4+z)}{2z}$$

Ecuation (19) describes the ratio between the constructive (*R,b,z*) and kinematic (V_{com}, ω_{ant}) parameters of windrower in case of safe evacuation of stems in row. After modification the ecuation (19) has the following form:

Ecuaţia (19) descrie raportul dintre parametrii constructivi (*R,b,z*) şi cinematici (V_{com}, ω_{ant}) ai vindroverului pentru cazul evacuării sigure a tulpinilor din rând. După modificare ecuaţia (19) are următorul conţinut:

$$\frac{2\pi V_{com}}{z\omega_{ant}} = R - (R-b)\sin\frac{\pi(4+z)}{2z} = R - (R-b)\sin(\frac{2\pi}{z} + \frac{\pi}{2}). \quad (19)$$

If we note the angular pitch between the drum disc teeth $\frac{2\pi}{z} = \theta$, then:

Însemnăm pasul unghiular dintre dinţii discului tamburului $\frac{2\pi}{z} = \theta$, atunci:

$$\frac{2\pi V_{com}}{z\omega_{ant}} = R - (R-b)\sin(\theta + \frac{\pi}{2}) \text{ sau } \frac{2\pi V_{com}}{\omega_{ant}} = z\cdot\left[R - (R-b)\sin\left(\theta + \frac{\pi}{2}\right)\right]$$

$$\frac{V_{com}}{\omega_{ant}} = \frac{R - (R-b)\sin(\theta + \frac{\pi}{2})}{\theta}. \quad (20)$$

From the obtained equations (20) results, that increasing the combine displacement speed V_{com} requires, in case of fixed constructive parameters (*z, R, b*) a relevant increment of drum angular frequency ω_{ant}. More rationally would be to determine values of parameters *z, R, b* and speed ω_{ant}, which assures the complete driving and evacuation of stems according to translation speed of combine V_{com}.

Degree of driving the stems in the drum lateral space. The windrower rotative disc below ensures the stems cutting according to rotation angle φ from 0 to π (fig.2). Rotative drum, placed above the cutting disc, can perform the efficient driving of stems when the angle is narrower ($0<\varphi<\pi$). This range may be precised by analyzing the scheme of stems driving (fig.3). From the scheme mentioned it results that for driving a stem of d diameter, at a certain moment, it is necessary that the distance between projections on x axis (perpendicular on

Din ecuaţiile obţinute (20) reiese, că majorarea vitezei de deplasare a combinei V_{com} necesită, în cazul parametrilor constructivi ficşi (*z, R, b*) o mărire respectivă a vitezei unghiulare ω_{ant} a tamburului. Mai raţională însă este determinarea valorilor parametrilor *z, R, b* şi a vitezei ω_{ant}, care asigură plenitudinea antrenării şi evacuării tulpinilor în diapazonul de lucru al vitezei de translaţie a combinei V_{com}.

Diapazonul de antrenare a tulpinilor în spaţiul lateral al tamburului. La vindrover discul rotativ de jos asigură tăierea tulpinilor în diapazonul unghiului de rotaţie φ de la 0 până la π (fig.2). Tamburul rotativ, amplasat deasupra discului de tăiere, poate executa antrenarea eficientă a tulpinilor în diapazonul mai îngust al unghiului ($0<\varphi<\pi$). Acest diapazon poate fi precizat, analizând schema antrenării tulpinilor (fig.3). Din schema menţionată reiese, că pentru antrenarea la momentul dat a unei tulpini, care are diametrul d, este necesar ca distanţa dintre proiecţiile pe axa x (perpendiculară direcţiei de mişcare a combinei) vârfurilor a doi dinţi vecini să fie mai mare decât diametrul

combine moving direction) of two close teeth tops be bigger than stem diameter:

tulpinii:

$$X_{\tilde{n}} - X_{a} = R\cos\left(\omega_{ant}\tau - \frac{2\pi}{z}\right) - R\cos\omega_{ant}\tau \rangle d, \qquad \cos(\omega_{ant}\tau - \theta) - \cos\omega_{ant}\tau \rangle \frac{d}{R} \tag{21}$$

$$\text{sau } \cos(\varphi - \theta) - \cos\varphi \rangle \frac{d}{R}.$$

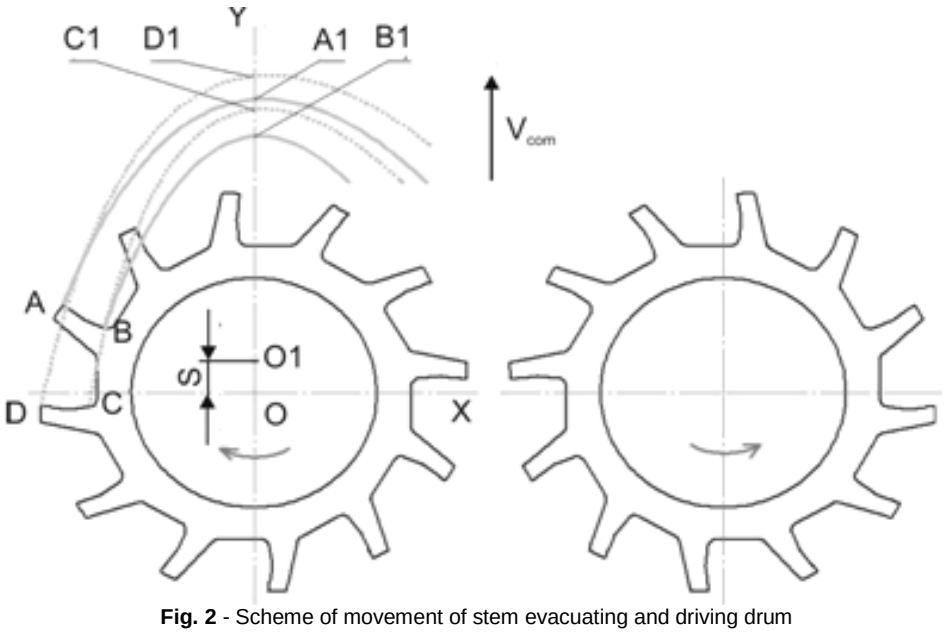

Fig. 2 - Scheme of movement of stem evacuating and driving drum

Knowing the values of stems diameter *d*, of drum constructive parameters (radius *R*, angular pitch θ *of teeth*), can be calculated the angle φ determining the *minimum driving conditions of stems*, position of lateral and central dividers .

Action of forces acting in stems driving and evacuating. Previous analysis of processes of cutting, driving and evacuating the stems in the windrower was based on kinematic and constructive parameters. For assuring the windrower efficient operation, it is necessary to analyze the forces acting on stems and respectively on windrower working parts (*study of process dynamics*).

As previously mentioned, during the working process the combine moves with the translation speed V_{com}, and windrower working parts co-axially placed, rotate at different speed: lower cutting disc – by speed ω_t, upper drum with discs for stems evacuating – by speed ω_{ant}.

Previous calculations based on formula (11) demonstrate that drum linear rotation speed will be up to 5m/s [5]. Therefore, cutting speed value (V_t ≥30 m/s) is much higher than driving speed value ($V_t >> V_{ant}$).

The complex operating process of windrower consists in following stages:

a) cutting (stem is subjected to cutting disc action and, in certain cases, during a short period of time,to lower driving disc; in this stage, the stem remains connected to the root);

Cunoscând valorile diametrului tulpinilor *d*, ale parametrilor constructivi ai tamburului (raza *R*, pasul unghiular θ al dinţilor), se poate calcula unghiul φ care determină *condiţii minime de antrenare a tulpinilor*, poziţia divizorilor laterali şi a celui central .

Acţiunea forţelor în procesul de antrenare şi evacuare a tulpinilor. Analiza precedentă a proceselor de tăiere, antrenare şi evacuare a tulpinilor în vindrover a fost bazată pe parametrii cinematici şi constructivi. Pentru asigurarea funcţionării eficiente a vindroverului este necesară analiza forţelor, care acţionează asupra tulpinii şi respectiv asupra organelor de lucru ale vindroverului (*studiul dinamicii procesului)*.

După cum s-a menţionat anterior, în procesul de lucru combina se deplasează cu viteza de translaţie V_{com}, iar organele de lucru ale vindroverului amplasate coaxial execută mişcare de rotaţie cu diferite viteze: discul inferior de tăiere – cu viteza ω_t, tamburul superior cu discuri pentru antrenarea şi evacuarea tulpinilor – cu viteza ω_{ant}.

Calculele prealabile în baza formulei (11) demonstrează, că viteza liniară de rotaţie a tamburului va fi de până la 5m/s [5]. Prin urmare, valoarea vitezei de tăiere (V_t ≥30 m/s) este mult mai mare decât cea a vitezei de antrenare ($V_t >> V_{ant}$).

După cum reiese din descrierea modelului fizic, procesul complex de funcţionare a vindroverului constă din următoarele etape:

a) *tăierea* (tulpina este supusă acţiunii discului de tăiere şi, în unele cazuri pe o perioadă scurtă, dintelui discului inferior de antrenare; la etapa aceasta tulpina rămâne în legătură cu rădăcina);

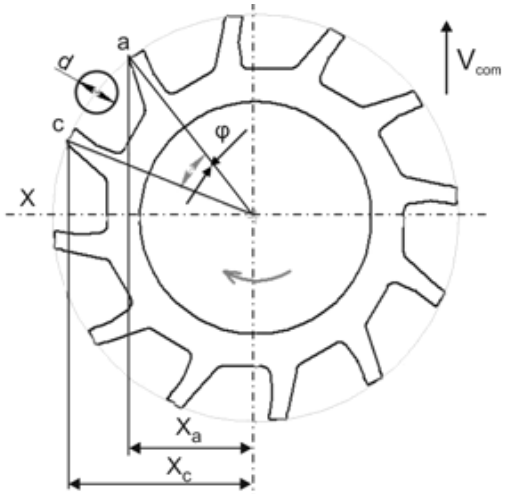

Fig.3 - Scheme of stem lateral driving to the drum teeth

b) driving (the cut stem is placed in inner space between the drum teeth and is driven by cutting disc and drum teeth);
c) evacuation (the stem is in the same space as teeth and is subdued to drum teeth).

As the first stage, practically does not influence the driving-evacuating process, we shall analyze the forces applied to stem in the following two stages. The stem, immediately after the cutting is in vertical position within the space between the drum (fig.4) and is subjected to action of following forces: gravity force P(P =mg), force of stem friction on the cutting disc towards the rotation movement $F_1(F_1 = f_1P)$, force of inertia $F_{i2}(F_{i2} = ma_2)$, determined by combine translation movement by speed V_{com}. Under these forces action the stem begins a complex movement: simoultaneously, towards the cutting disc rotation and rotation pin. As a result, the reactive forces appear: respectively, inertia forces $F_{i1}(F_{i1} = ma_1)$ and friction forces $F_2(F_2 = f_1P)$. After initiating the stem movement, subjected to force F_1 the centrifugal force appears F_{cf}^t , $(F_{cf}^t = m\omega_{pt}^2 R)$. Angular speed ω_{pt} of stem foot is the same as the cutting disc speed (in terms of direction) ω_t , but ω_{pt} has a smaller value, which depends on the friction coefficient f_1. Ratio of forces F_{cf}^t şi F_{i2} determines the direction and value of friction force F_2, which is always inversely to the stem movement direction and maintains its position.

If projecting the forces above on axes X,Y the following results will be obtained:

*b) antrenarea (*tulpina tăiată se află în spaţiul interior între dinţii tamburului de antrenare şi este acţionată de discul de tăiere şi dinţii tamburului);
c) evacuarea (tulpina se află în acelaşi spaţiu şi sub acţiunea preponderentă a dinţilor tamburului).

Deoarece prima etapă practic nu influenţează asupra procesului de antrenare-evacuare, vom analiza forţele aplicate asupra tulpinii în următoarele două etape. Tulpina imediat după tăiere se află în poziţia verticală în spaţiul dintre dinţii tamburului (fig.4) şi este supusă acţiunii următoarelor forţe: gravitaţională P(P =mg), de frecare a piciorului tulpinii pe discul de tăiere în direcţia rotaţiei $F_1(F_1 = f_1P)$, de inerţie $F_{i2}(F_{i2} = ma_2)$, cauzată de mişcarea de translaţie a combinei cu viteza V_{com}. Sub acţiunea acestor forţe tulpina începe o mişcare complexă: simultan în direcţia rotaţiei discului de tăiere şi spre axa de rotaţie. Drept rezultat apar forţele reactive: respectiv de inerţie $F_{i1}(F_{i1} = ma_1)$ şi de frecare $F_2(F_2 = f_1P)$. După iniţierea deplasării tulpinii sub acţiunea forţei F_1 apare forţa centrifugală F_{cf}^t , $(F_{cf}^t = m\omega_{pt}^2 R)$. Viteza unghiulară ω_{pt} a piciorului tulpinii coincide după direcţie cu viteza discului de tăiere ω_t , însă ω_{pt} are o valoare mai mică, care depinde de coeficientul de frecare f_1. Raportul forţelor F_{cf}^t şi F_{i2} determină direcţia şi valoarea forţei de frecare F_2, care totdeauna este îndreptată împotriva direcţiei de mişcare a tulpinii şi serveşte pentru menţinerea poziţiei acesteia.

Proiectarea forţelor menţionate pe axele X,Y dă următoarele rezultate:

$$\text{axa } X \rightarrow F_1 = F_{i1}, \quad f_1 mg = ma_1, \quad f_1 g = a_1, \tag{22}$$

axY→at first stage

axY→ at first stage

$$F_{i2} = F_2 + F_{cf}^t, \quad ma_2 = f_1 mg + m\omega_{pt}^2 R, \quad a_2 = f_1 g + \omega_{pt}^2 R,$$

axY →at final stage may be (if)

axaY →la etapa finală poate fi (în cazul dacă)

$$F_{i2} + F_2 = F_{cf}^t, \quad ma_2 + f_1 mg = m\omega_{pt}^2 R; \quad a_2 + f_1 g = \omega_{pt}^2 R, \quad \omega_{pt}^2 R = a_2 + a_1, \tag{23}$$

where *m* is stem mass, *g* – acceleration of natural fall; a_1, a_2 – acceleration of stem towards the circular direction and respectively to the combine direction; f_1 – coefficient of friction of stem on cutting disc surface; ω_{pt} – angular speed of stem foot on the cutting disc; *R* – radial coordinate of stem placement.

In the second driving stage the stem foot approches the rear surface of tooth (fig. 4 b). In this case, the following forces act upon the stem: gravity force P, centrifugal force $F_{cf}^{ant}(F_{cf}^{ant} = m\omega_{ant}^2 R)$, friction force of stem foot on the cutting disc F_1, F_2 and tooth rear surface $F_3(F_3 = f_3 R_1 \cos\alpha)$, reactive force R_1,where ω_{ant} is the angular speed of stem and driving drum, f_3 – coefficient of friction, α – angle between the tooth rear surface and centrifugal speed vector.

Because of friction force F_1 l existing when acting the cutting disc, the energy consumed is of a power of:

unde *m* este masa tulpinii, *g* – accelerarea de cădere liberă; a_1, a_2 – accelerarea tulpinii în direcţia circulară şi respectiv în direcţia deplasării combinei; f_1 – coeficientul de frecare a materialului tulpinii pe suprafaţa discului de tăiere; ω_{pt} – viteza unghiulară a piciorului tulpinii pe discul de tăiere; *R* – coordonata radială de amplasare a tulpinii.

În faza a doua de antrenare piciorul tulpinii se apropie de suprafaţa din spatele dintelui (fig. 4 b). În acest caz asupra tulpinii acţionează următoarele forţe: gravitaţională P, centrifugală $F_{cf}^{ant}(F_{cf}^{ant} = m\omega_{ant}^2 R)$, de frecare a piciorului tulpinii pe discul de tăiere F_1, F_2 şi pe suprafaţa din spatele dintelui $F_3(F_3 = f_3 R_1 \cos\alpha)$, reactivă R_1, unde ω_{ant} este viteza unghiulară a tulpinii şi tamburului de antrenare, f_3 – coeficientul de frecare, α – unghiul dintre suprafaţa din spate a dintelui şi vectorul vitezei centrifugale.

Din cauza existenţei forţei de frecare F_1, la acţionarea discului de tăiere se consumă energie a cărei putere este:

$$N = F_1 R(\omega_t - \omega_{ant}), \quad (24)$$

where ω_t, ω_{ant} is angular speed of cutting disc and respectively of driving drum.

Reducing energy consumption is possible, if the stem foot will detach from cutting disc surface and support on the lower driving disc. In this case, the centrifugal force F_{cf}^{ant} and friction forces F_3 of upper stem parts act on surface of contact of driving drum teeth.

Following the analyses of schemes (fig. 4) it results that the danger of untimely throwing the stem away from the driving space, comes from centrifugal forces F_{cf}^{t} (at first stage, when supporting the stem on cutting disc) and F_{cf}^{ant} (at second stage, when the stem is supported on drum). Force F_{cf}^{t} may have higher values in comparison with force F_{cf}^{ant} because of bigger speed of cutting disc.

Diminishing the negative effect of centrifugal forces can be obtained by the following methods:

- Reducing the friction coefficient f_1 of stem foot on the cutting disc and respectively the angular speed ω_{pt};
- Increasing the translation speed of the combine V_{com} and respectively of inertia force F_{i2};
- Maintaining the optimum range of drum rotation speed, drum assuring the vegetal matter efficient evacuation, by avoiding an early pushing out;
- Using on rear surface of lower disc teeth driving particular profile which interromps the stem foot evacuation [2];
- Creating the conditions of going up and supporting the stem foot on rear surface of teeth, by assuring the minimum gap between the lower disc and cutting disc, cutting the faces on rear surface [2];
- Utilization of guiding bars of stems within the driving and evacuating space.

unde ω_t, ω_{ant} este viteza unghiulară a discului de tăiere şi respectiv a tamburului de antrenare.

Reducerea consumului de energie este posibilă, dacă piciorul tulpinii se va desprinde de la suprafaţa discului de tăiere şi se va sprijini pe discul inferior de antrenare. În acest caz asupra tulpinii acţionează forţa centrifugală F_{cf}^{ant} şi forţele de frecare F_3 ale piciorului, părţilor superioare ale tulpinii pe suprafeţele de contact ale dinţilor tamburului de antrenare.

Din analiza schemelor (fig. 4) reiese, că pericolul expulzării înainte de vreme a tulpinii din spaţiul de antrenare provine de la forţele centrifugale F_{cf}^{t} (la prima etapă în cazul sprijinului tulpinii pe discul de tăiere) şi F_{cf}^{ant} (la etapa a doua, când tulpina este sprijinită pe tamburul de antrenare). Forţa F_{cf}^{t} are posibilitatea de a avea valori mai înalte în raport cu forţa F_{cf}^{ant} din cauza vitezei mai mari a discului de tăiere.

Minimizarea efectului negativ al forţelor centrifugale poate fi obţinută prin următoarele metode:

- reducerea coeficientului de frecare f_1 a piciorului tulpinii pe discul de tăiere şi respectiv a vitezei unghiulare ω_{pt};
- majorarea vitezei de translaţie a combinei V_{com} şi respectiv a forţei de inerţie F_{i2};
- menţinerea în diapazonul optim a vitezei de rotaţie a tamburului de antrenare, care asigură antrenarea şi evacuarea eficientă a masei vegetale fără expulzarea ei înainte de termen;
- utilizarea pe suprafaţa din spate a dinţilor discului inferior de antrenare profilului special, care frânează expulzarea piciorului tulpinii [2];
- crearea condiţiilor de urcare şi sprijinire a piciorului tulpinii pe suprafaţa din spate a dintelui prin asigurarea jocului minim dintre discul inferior de antrenare şi discul de tăiere, tăierea faţetelor pe suprafaţa din spate [2];
- utilizarea tijelor de ghidare a tulpinilor în spaţiul de antrenare şi evacuare.

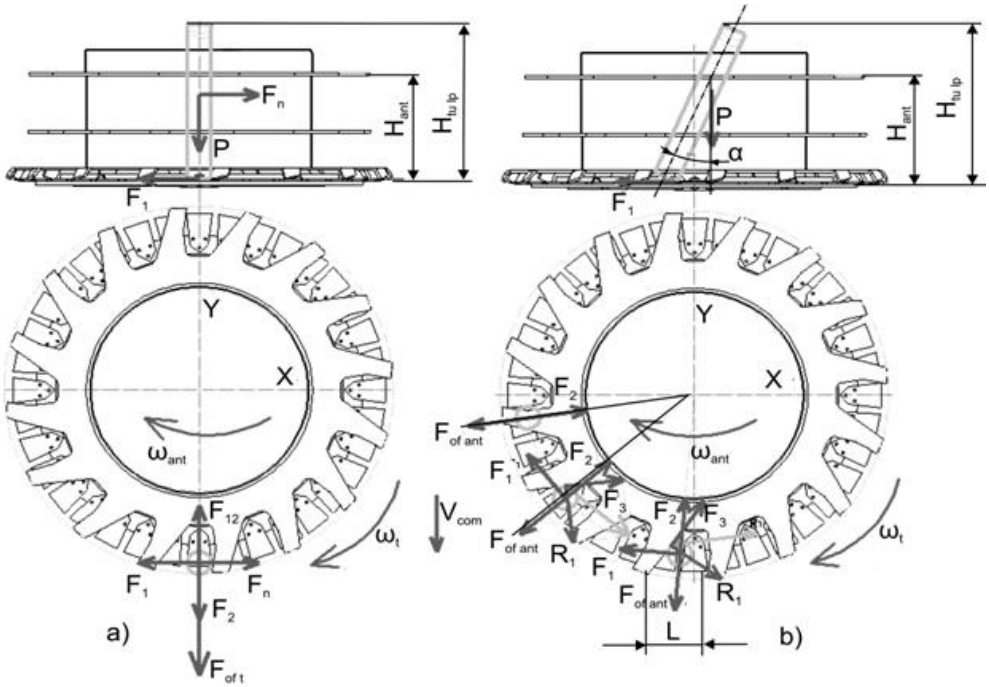

Fig. 4 - Scheme of forces acting on windrower stems
a) initial phase; b) final driving phase

Driving the stem by means of guiding bar. During a drum rotation cycle, it is necessary to meet two different conditions (fig.5):

a) after cutting, as recently mentioned, in the upper sectors I, II have to be created the conditions appropriate for a safe driving and displacement of stems by drum teeth;

b) after the stems, vegetal wastes arriving in windrower feeding chamber (sector III), they have to leave the drum teeth to the feeding rollers.

From the scheme presented (fig.5) comes out that one of main conditions for the correct operating of windrower is to assure the stem driving within the inner space of tooth, when stem cross section diameter is on disc edge.. În this case, the forces acting on stem are perpendicularly on working surfaces of guiding bar (force N_1) and tooth (forţa N_2).

Displacement of stem in driving space results in friction forces appearing:

*Antrenarea tulpinii cu ajutorul tijei de ghidare***.** Pe durata unui ciclu de rotaţie a tamburului de antrenare - evacuare a tulpinilor este necesar de respectat două condiţii cu totul diferite (fig.5):

c) după tăierea tulpinilor, după cum s-a menţionat recent, trebuie de creat în sectoarele anterioare I, II condiţii pentru antrenarea şi deplasarea sigură a tulpinilor de către dinţii tamburului;

d) după nimerirea în camera de alimentare a vindroverului (sectorul III), tulpinile, resturile vegetale ale buruienilor trebuie să elibereze complet dinţii tamburului şi simultan să fie antrenate de către tăvălugii de alimentare.

Din schema prezentată (fig.5) reiese, că una din principalele condiţii pentru funcţionarea eficientă a vindroverului este asigurarea antrenării tulpinii în spaţiul interior al dintelui atunci cînd diametrul secţiunii transversale a tulpinii se află pe periferia discului. În acest caz asupra tulpinii acţionează forţe, îndreptate perpendicular pe suprafeţele de lucru a tijei de ghidare (forţa N_1) şi a dintelui (forţa N_2).

Deplasarea tulpinii în spaţiul de antrenare are drept consecinţă apariţia forţelor de frecare:

$$F_1=N_1\cdot f_1, \qquad F_2=N_2\cdot f_2\ , \tag{25}$$

where f_1,f_2 are the friction coefficients of stem on working surface of guiding bar and respectively of drum tooth.

For determining the conditions of driving the stem between drum tooth and guiding bar, we project on axes X,Y the forces applied:

unde f_1,f_2 sunt coeficienţii de frecare a tulpinii pe suprafaţa de lucru a tijei de ghidare şi respectiv a dintelui tamburului.

Pentru determinarea condiţiilor de antrenare a tulpinii între dintele tamburului şi tija de ghidare, proiectăm pe axele X,Y forţele aplicate:

$$\text{axis X: } N_2\cdot\sin\gamma = F_1 + F_2\cdot\cos\gamma \tag{26}$$

$$\text{axis Y: } N_1 = N_2\cdot\cos\gamma + F_2\cdot\sin\gamma \text{ sau } N_1 = N_2\cdot\cos\gamma + N_2\cdot f_2\cdot\sin\gamma \tag{27}$$

Displacement of stem within the drum space imposes that: $N_2\cdot\sin\gamma \geq N_1\cdot f_1 + N_2\cdot f_2\cdot\cos\gamma$.

Using in the last inequality, the value N_1 from formula (27), we obtain after modification:

Deplasarea tulpinii în interiorul spaţiului tamburului impune ca: $N_2\cdot\sin\gamma \geq N_1\cdot f_1 + N_2\cdot f_2\cdot\cos\gamma$.

Utilizând în ultima inegalitate valoarea N_1 din formula (27), obţinem după modificare:

$$\sin\gamma \geq \cos\gamma \cdot f_1 + f_2 \cdot \sin\gamma \cdot f_1 + f_2 \cdot \cos\gamma$$

$$tg\gamma \geq f_1 + f_1 \cdot f_2 \cdot tg\gamma + f_2,\ tg\gamma(1 - f_1 \cdot f_2) \geq f_1 + f_2,\ tg\gamma \geq \frac{f_1 + f_2}{1 - f_1 \cdot f_2} \quad (27)$$

Because $f_1 = tg\varphi_1$, $f_2 = tg\varphi_2$ (φ_1, φ_2 - (friction angles), we obtain:

Deoarece $f_1 = tg\varphi_1$, $f_2 = tg\varphi_2$ (φ_1, φ_2 - unghiuri de frecare), obţinem:

$$tg\gamma(1 - tg\varphi_1.tg\varphi_2) \geq tg\varphi_1 + tg\varphi_2, \quad tg\gamma \geq \frac{tg\varphi_1 + tg\varphi_2}{1 - tg\varphi_1 \cdot tg\varphi_2} = tg(\varphi_1 + \varphi_2), \quad \gamma \geq \varphi_1 + \varphi_2. \quad (28)$$

It results that, for safely driving and moving the stem within the drum with diminished energy consumption, it is necessary that the coefficients of friction f_1, f_2 should be reduced, and angle γ between the working surfaces of guiding bar and permanent drum tooth be higher than $\varphi_1 + \varphi_2$ sum. At the same time, the working width of driving space b_{ant} (fig. 5) should meet the following condition:

De aici reiese că, pentru antrenarea sigură şi deplasarea tulpinii în interiorul tamburului cu consum redus de energie, este necesar ca coeficienţii de frecare f_1, f_2 să fie micşoraţi, iar unghiul γ dintre suprafeţele de lucru a tijei de ghidare şi a dintelui tamburului permanent să fie mai mare decât suma $\varphi_1 + \varphi_2$. Totodată, lăţimea de lucru a spaţiului de antrenare b_{ant} (fig. 5) trebuie să corespundă următoarei condiţii:

$$b_{ant} \geq 2d_{tulp} + d_{tg}, \quad (29)$$

where d_{tulp} is stem diameter; d_{tg} – diameter of guiding bar.

Ejecting the stems from the drum. Taking into account the forces and speed applied on the stem (fig. 5), as well as the condition that the minimum distance is on axis X, the ejecting plates upper part (cleaning) should be placed at the end of sector II.

We shall analyze the conditions of evacuating the stems from the drum in sector III (fig.5). Forces N_1, N_2, F_1, F_2, applied on stem in this sector are identical with those from sectors I, II. Projecting the forces above on X,Y axes gives the results:

unde d_{tulp} este diametrul tulpinii; d_{tg} – diametrul tijei de ghidare.

Expulzarea tulpinilor din tambur. Luând în calcul forţele şi vitezele aplicate asupra tulpinii (fig. 5), precum şi condiţia că distanţa minimă dintre două tambururi este pe axa X, începutul plăcilor de expulzare (curăţire) trebuie să fie amplasat la terminarea sectorului II.

Vom analiza condiţiile expulzării tulpinilor din tambur în sectorul III (fig.5). Forţele N_1, N_2, F_1, F_2, aplicate asupra tulpinii în acest sector, sunt identice celor din sectoarele I, II. Proiectarea forţelor menţionate pe axele X,Y dă următoarele rezultate:

axis X – $N_2 \cdot \sin\gamma = F_1 + F_2 \cdot \cos\gamma$, axis Y – $N_1 = N_2 \cdot \cos\gamma + F_2 \cdot \sin\gamma$

Formulae obtained are similar to formulae (26), (27), which allows to conclude: safe stems evacuation is performed if the angle γ between the working surfaces of drum teeth and ejecting plates is bigger than the sum of stem friction coefficients on respective working surfaces ($\gamma \geq \varphi_1 + \varphi_2$).

For increasing the probability of ejecting the stems and vegetal wastes, it is necessary that the length of area where teeth and plates interact be maximum.

Taking into consideration the fact that the angle between the working surfaces of driving teeth and vector of combine translation speed V_{com} changes from 90° when entering the sector III (fig. 5) up to 0° when leaving sector III, the ejecting plates along of area of teeth will be inclined towards the optimum speed vector V_{com}. This will allow to maintain the optimum condition of evacuation (formula 28) and to increase the length of ejecting contact of stems in sector III ($\xi_2 > \xi_1$, fig.5 b). Plates may have right linear or curvelinear shape. For assuring the appropriate evacuation conditions of vegetal matter on the whole length of area where teeth interact with plates, the last ones should be convex.

For ensuring of favorable conditions for vegetal mass expulsion on the entire length of the interaction between the driving teeth and the expulsion plates, the plates shape must be convex. Based on the expulsion scheme of the stalks (Fig. 5) can be calculated the duration of the expulsion:

Formulele obţinute coincid cu formulele (26), (27), ceea ce permite să se tragă următoarea concluzie: expulzarea sigură a tulpinilor se efectuează dacă unghiul γ dintre suprafeţele de lucru ale dinţilor tamburului şi plăcilor de expulzare va fi mai mare decât suma coeficienţilor de frecare a tulpinii pe suprafaţele de lucru respective ($\gamma \geq \varphi_1 + \varphi_2$).

Pentru majorarea probabilităţii de expulzare a tulpinilor şi resturilor vegetale este necesar ca lungimea zonei de interacţiune a dinţilor şi plăcilor să fie maximal posibilă.

Luând în consideraţie faptul că unghiul dintre suprafeţele de lucru ale dinţilor de antrenare şi vectorul vitezei de translaţie a combinei V_{com} se schimbă de la 90° la intrare în sectorul III (fig. 5) până la 0° la ieşire din sectorul III, plăcile de expulzare pe lungimea contactului cu dinţii de antrenare vor fi înclinate spre vectorul vitezei V_{com}. Aceasta a permite menţinerea condiţiei optime de expulzare (formula 28) şi majorarea lungimii contactului de expulzare a tulpinilor în sectorul III ($\xi_2 > \xi_1$, fig.5 b). Plăcile de expulzare pot să aibă forma dreptliniară sau curbiliniară.

Pentru asigurarea condiţiilor favorabile de expulzare a masei vegetale pe toată lungimea interacţiunii dinţilor de antrenare şi plăcilor ultimele mai bine să fie de forma convexă. În baza schemei de expulzare a tulpinilor (fig. 5) se poate calcula durata expulzării:

$$\tau_{\exp} = \frac{\xi}{\omega_{ant}}, \quad (30)$$

from which results the ratio of the expulsion durations for the angles ξ_1, ξ_2: $\frac{\tau_1}{\tau_2} = \frac{\xi_1}{\xi_2}$.

Because $\xi_2 > \xi_1$, consequently $\tau_2 > \tau_1$. stalks travel speed across the surface from the front of the driving tooth is equal to:

de unde reiese raportul duratelor de expulzare pentru unghiuri ξ_1, ξ_2: $\frac{\tau_1}{\tau_2} = \frac{\xi_1}{\xi_2}$.

Deoarece $\xi_2 > \xi_1$, prin urmare $\tau_2 > \tau_1$. Viteza deplasării tulpinilor de-a lungul suprafeţei din faţa dintelui de antrenare este egală:

$$V_{\exp} = \frac{b_{ant}}{\tau} \quad (31)$$

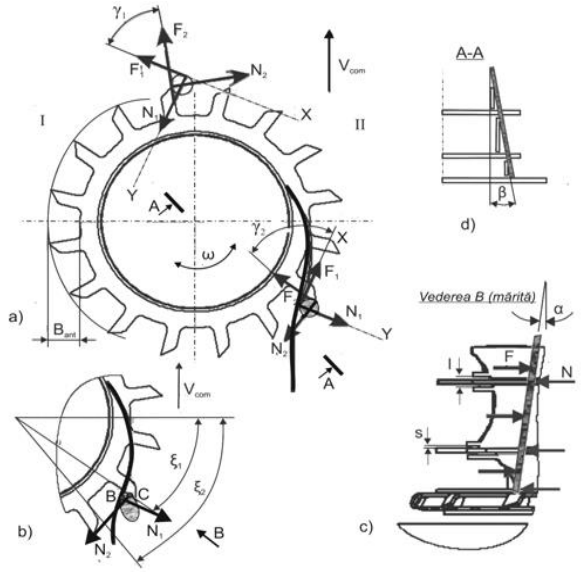

Fig. 5 - The placement scheme of guiding rods of stalks and plates for cleaning the teeth

It is obvious that $V_{exp2} < V_{exp1}$, which for ξ_2 favors the expulsion of the stems.

The geometrical parameters of driving drum in the vertical plane also affect the conditions of evacuation of the stalks.

As mentioned, in the process of expulsion on the stalk act the frictional forces between the working surfaces of the expulsion plates and teeth. For the compensation of these forces on the stalk are applied the normal forces N. Under the action of forces N (fig. 5c) occurs the bending of stalks, whose value can be determined from the strength of materials formula.

Este evident că $V_{exp2} < V_{exp1}$, ceea ce pentru ξ_2 favorizează expulzarea tulpinilor.

Parametrii geometrici ai tamburului de antrenare în planul vertical de asemenea influenţează condiţiile de evacuare a tulpinilor.

După cum s-a mai menţionat, în procesul expulzării asupra tulpinii acţionează forţele de frecare cu suprafeţele de lucru a plăcilor de expulzare şi a dinţilor. Pentru compensarea acestor forţe asupra tulpinii se aplică forţele normale N. Sub acţiunea forţelor N (fig. 5c) se produce încovoierea tulpinilor, a cărei valoare se poate determina din formula cunoscută în rezistenţa materialelor

$$\hat{\imath} = \frac{FlS^2(1 - S/l)^2}{3EI}, \quad (32)$$

where l – is the distance between the expulsion plates; S – clearance between the plate and tooth in the vertical plane; E – the elasticity modulus; I – the moment of inertia of the cross-section of the stalk; F – actuation force. Minimization of stalk bending is welcomed for its expulsion and it is possible, as demonstrates the formula (32), first of all, by reducing the friction forces and respectively of driving forces F (dependent on the the normal forces), of the clearance S and the increase the moment I, that depends on the geometrical parameters of the cross-section of the stalk (for example, for: the round shape $I = \frac{\pi D^4}{64}$, tubular shape $I = \frac{\pi}{64}(D^4 - d^4)$, where D,d – the outer diameter and respectively inner of the cross-section of the stalk).

unde l – este distanţa dintre plăcile de expulzare; S – jocul dintre placă şi dinte în planul vertical; E – modul de elasticitate; I – momentul de inerţie a secţiunii transversale a tulpinii; F – forţa de acţionare.

Minimizarea încovoierii tulpinii este binevenită pentru expulzarea ei şi este posibilă, după cum demonstrează formula (32), în primul rând prin reducerea forţelor de frecare şi respectiv a forţelor de acţionare F (dependente de forţele normale), jocului S şi majorarea momentului I, care depinde de parametrii geometrici ai secţiunii transversale a tulpinii (de exemplu, pentru: forma rotundă – $I = \frac{\pi D^4}{64}$, tubulară – $I = \frac{\pi}{64}(D^4 - d^4)$, unde D, d – diametrul exterior şi respectiv interior al secţiunii transversale a tulpinii).

The distance *l* between the plates influences less the bending of stalk, at the same time with the simultaneous reduction *l* and *S* takes place the essential decrease of bending *î*. The minimum value of the clearance S is determined by the technological possibilities of windrover manufacturing. The distance *l* depends primarily on the thickness δ of the driving teeth, which in its turn is determined by the need to ensure the rigidity of the disk and the exclusion of cutting the stalk ($\delta > \delta_t$ where δ_t- is the thickness of the tooth with which it starts cutting the of stalks). According to the data [6], the optimal thickness of the blade knife is 0.02 ... 0.04 mm, being allowed 0.1 mm. According to the preliminary results, in order to obtain enough rigidity the minimum thickness of the driving disk must be at least 3 ... 4 mm, that is 30 ... 40 times higher than allowable value for cutting. Therefore, the distance $l \geq \delta_{\min} + S_{\min}$.

As mentioned, at the stage of stalks movement in the sector III (fig.5) it is necessary to concomitantly perform their expulsion from the drum and reorient from the vertical to the horizontal position. Therefore, distance L between the driving teeth (fig.4) must be enough to assure the change of the stalk position from vertical to the horizontal one. Angle α of inclination of the stalk will depend on the drum geometrical parameters in the following way:

Distanţa *l* dintre plăci influenţează mai puţin asupra încovoierii tulpinii, totodată cu reducerea simultană *l* şi *S* are loc diminuarea esenţială a încovoierii *î*. Valoarea minimă a jocului S este determinată de posibilităţi tehnologice de confecţionare a vindroverului. Distanţa *l* depinde în primul rînd de grosimea δ a dinţilor de antrenare, care la rîndul său este determinată de necesitatea asigurării rigidităţii discului şi excluderii tăierii tulpinii ($\delta > \delta_t$ unde δ_t- este grosimea dintelui, cu care se începe tăierea tulpinilor). Conform datelor [6], grosimea optimă a lamei cuţitului este 0,02...0,04 mm, se admite 0,1 mm. Conform rezultatelor prealabile, pentru obţinerea rigidităţii suficiente grosimea minimă a discului de antrenare trebuie să fie de cel puţin 3...4mm, adică de 30...40 ori mai mare decît valoarea admisibilă pentru tăiere. Prin urmare, distanţa $l \geq \delta_{\min} + S_{\min}$.

După cum s-a mai menţionat, la etapa mişcării tulpinilor în sectorul III (fig.5) este necesară concomitent expulzarea lor din tambur şi reorientarea din poziţia verticală în cea orizontală. Pentru aceasta distanţa L dintre dinţii de antrenare (fig.4) trebuie să fie suficientă pentru asigurarea schimbării poziţiei tulpinii din verticală în cea orizontală. Unghiul α de înclinare a tulpinii va depinde de parametrii geometrici ai tamburului în felul următor:

$$tg\alpha = \frac{L-d}{h_{ant}}, \quad (33)$$

where d is the diameter of the stalk, h_{ant}– the height of the stalk driving.

More favorable conditions for the reorientation of stalks provide inclination in the vertical plane of the drum teeth (the angle α, fig. 4b; 5c) and of the expulsion plates (the angle β, fig. 5d). In this case the foot of the stalk comes out faster from the drum and arrives by its lifting between the supplying rollers.

Inclination of surfaces referred improves not only the conditions for the reorientation of stalks, but also for their expulsion because size and the profile of cross section of the stalk in the plane of interaction and plates of the drum teeth and the expulsion plates (fig. 5a,b)change. The round shape of the the cross section (fig. 5a) changes into ellipsoidal (fig. 5b). Therefore, it increases the area of the section and respectively the moment of inertia I, the resistance to bending. Concomitantly changes the position of the points of application of the normal forces N_1, N_2 (points B,C, fig. 3.13b), favoring the expulsion of stalks.

CONCLUSIONS

1) For ensuring the conditions for qualitative cutting, driving safely and operative evacuation of all of stalks into windrover with the vertical axis of rotation of the working bodies, was established the dependence between the agrotechnical parameters of the stalks (the diameter, the number m to 1 meter in the row), the constructive parameters (the number of teeth of the drum *z*) and kinematic parameters (combine speed V_{com}, the speed of rotation of the driving drum ω_{ant}). There have been determined the positions of the lateral dividers and of the central one in relation to the driving drum in order to obtain reliable driving of the stalks.

unde d este diametrul tulpinii, h_{ant}– înălţimea antrenării tulpinii.

Condiţii mai favorabile pentru reorientarea tulpinilor asigură înclinarea în plan vertical a dinţilor tamburului (unghiul α, fig. 4b; 5c) şi plăcilor de expulzare (unghiul β, fig. 5d). În acest caz piciorul tulpinii iese mai repede din tambur şi nimereşte prin ridicarea sa între tăvălugii de alimentare.

Înclinarea suprafeţelor menţionate îmbunătăţeşte nu numai condiţiile pentru reorientarea tulpinilor, dar şi pentru expulzarea lor, deoarece se schimbă mărimea şi profilul secţiunii transversale a tulpinii în planul interacţionării dinţilor tamburului şi plăcilor de expulzare (fig. 5a,b). Forma rotundă a secţiunii transversale (fig. 5a) se schimbă în elipsoidală (fig. 5b). Prin urmare, se măreşte suprafaţa secţiunii şi respectiv momentul de inerţie I, rezistenţa la încovoiere. Concomitent se schimbă poziţia punctelor de aplicare a forţelor normale N_1, N_2 (puncte B,C, fig. 3.13b), favorizând expulzarea tulpinilor.

CONCLUZII

1) Pentru asigurarea condiţiilor de tăiere calitativă, antrenare sigură şi evacuare operativă a tulpinilor din rînd în vindrover cu axa verticală de rotaţie a organelor de lucru, s-a stabilit dependenţa dintre parametrii agrotehnici ai tulpinilor (diametrul, numărul m la 1 metru liniar în rînd), parametrii constructivi (numărul de dinţi ai tamburului *z*) şi cinematici (viteza combinei *Vcom,* viteza de rotaţie a tamburului de antrenare *ωant*). Au fost determinate poziţiile divizorilor laterali şi a celui central în raport cu tamburul de antrenare cu scopul obţinerii antrenării sigure a tulpinilor.

2) The analysis of the forces acting on the stalk in the windrover has shown that the danger of untimely expulsion of the stalk from the area of driving comes from the centrifugal forces. Methods are proposed to minimize the negative influence of centrifugal forces. For safely driving and moving of the stalk inside the drum with low energy consumption is required that the coefficients of friction of the stalk on the surfaces of drum teeth f_2 and of guiding bars *f1* to be minimal, and the angle **γ** between the working surfaces of the guiding bar and of the drum tooth to be permanently greater than the sum $\varphi_1+\varphi_2$. Also the working width of the driving space (the working length of the driving tooth) must be greater than or equal to the sum of two diameters of stalk and a diameter of the guiding rod.
3) The reliable expulsion of the stalks in the reception chamber is performed,if the angle *γ* between the the working surfaces of the drum teeth and the expulsion plates is greater than the sum of the coefficients of friction of stalk on the respective working surfaces ($\gamma \geq \varphi_1+\varphi_2$). For increasing the probability of expulsion of stalks and of vegetal remains it is necessary that the length of the zone of interaction of the teeth and plates to be the maximum possible. The convex shape of the expulsion plate provides favorable conditions for vegetal mass expulsion on the entire length of the interaction of the driving teeth and the plates.
4) The expulsion of stalks from the drum and their reorientation from the vertical to the horizontal position inside the reception chamber depend on the the constructive parameters not only in the horizontal plane but also in the the vertical one (angles of inclination of the drum teeth α and of the expulsion plates *β*). The angles *α* and *β* change the size and the profile of (from round in the ellipsoidal) of the cross section of the stalk in the plane of the drum teeth and plates interaction, changes the position of the points of application of the normal forces, favoring the expulsion of stalks from drum in the reception room of the windrover.

REFERENCES

[1]. Hăbăşescu I., Cerempei V. şi alţii (2009) - *Energy from biomass: technologies and technical means*, Bons Offices Chisinau Publishing House, pp.368;
[2]. Hăbăşescu I., Cerempei V., Balaban N., Raicov V. -, *Reaping Machine For Harvesting Of Crops With Thick Stalks*, Patent MD 395;
[3]. Klepin N., Sakun V. (1980) - *Agricultural and ameliorative machines*, Kolos Publishing House Moscow, pp. 671;
[4]. Osobov V., Vasiliev G. (1983) - *Machines and units for hay harvesting*, Agricultural Machines, Moscow, p.304;
[5]. Raikov V. (2011) - *Calculation of cutting and orientation mechanisms of rotor type windrover*, Collection "Technologies And Technical Means For Agriculture" Publishing House Bons Offices Chisinau, pp.146 -160;
[6]. Reznik N. (1975) - *Theory of blade cutting and the bases of cutting devices calculation*, Agricultural Machines, Moscow, p.340.

2) Analiza forţelor care acţionează asupra tulpinii în vindrover a demonstrat că pericolul expulzării înainte de vreme a tulpinii din spaţiul de antrenare provine de la forţele centrifugale. Sunt propuse metode de minimizare a influenţei negative forţelor centrifugale. Pentru antrenarea sigură şi deplasarea tulpinii în interiorul tamburului cu consum redus de energie este necesar ca coeficienţii de frecare a tulpinii pe suprafaţele dinţilor tamburului *f2* şi tijelor de ghidare *f1* să fie minimi, iar unghiul **γ** dintre suprafeţele de lucru tijei de ghidare şi a dintelui tamburului să fie permanent mai mare decât suma $\varphi_1+\varphi_2$.Totodată, lăţimea de lucru a spaţiului de antrenare (lungimea de lucru a dintelui de antrenare) trebuie să fie mai mare sau egală cu suma a două diametre ale tulpinii şi un diametru al tijei de ghidare.
3) Expulzarea sigură a tulpinilor în camera de recepţie se efectuează, dacă unghiul **γ** dintre suprafeţele de lucru ale dinţilor tamburului şi plăcilor de expulzare va fi mai mare decât suma coeficienţilor de frecare a tulpinei pe suprafaţele de lucru respective ($\gamma \geq \varphi_1+\varphi_2$). Pentru majorarea probabilităţii de expulzare a tulpinilor şi resturilor vegetale este necesar ca lungimea zonei de interacţiune a dinţilor şi plăcilor să fie maximal posibilă. Forma convexă a plăcii de expulzare asigură condiţii favorabile pentru expulzarea masei vegetale pe toată lungimea interacţiunii dinţilor de antrenare şi plăcilor.
4) Expulzarea tulpinilor din tambur şi reorientarea lor din poziţia verticală în cea orizontală în camera de recepţie depind de parametrii constructivi nu numai în plan orizontal, dar şi în cel vertical (unghiuri de înclinare a dinţilor tamburului *α* şi plăcilor de expulzare *β*). Unghiurile *α* şi *β* modifică mărimea şi profilul (din rotund în elipsoidal) secţiunii transversale a tulpinii în planul interacţionării dinţilor tamburului şi plăcilor de expulzare, schimbă poziţia punctelor de aplicare a forţelor normale, favorizând expulzarea tulpinilor din tambur în camera de recepţie a vindroverului.

BIBLIOGRAFIE

[1]. Hăbăşescu I., Cerempei V. şi alţii (2009) - *Energie din biomasă: tehnologii şi mijloace tehnice*, Editura Bons Offices Chişinau, 368 p;
[2]. Hăbăşescu I., Cerempei V., Balaban N., Raicov V. -, *Secerătoare pentru recoltarea culturilor cu tulpini groase*, Brevet MD 395;
[3]. Klepin N., Sakun V. (1980) - *Maşini agricole şi ameliorative*, Editura Kolos Moscova, 671p;
[4]. Osobov V., Vasiliev G. (1983) - *Maşini şi echipamente pentru recoltarea fânului*, Maşini Agricole, Moscova, 304p;
[5]. Raikov V. (2011) - *Calculul mecanismelor de tăiere şi orientare ai vindroverului de tip rotor*, Culegere „Tehnologii şi mijloace tehnice pentru agricultură", Editura Bons Offices Chişinău, p.146 ÷160;
[6]. Reznik N. (1975) -*Teoria tăierii cu lamă şi bazele calculării aparatelor de tăiere*, Maşini Agricole, Moscova, 340p.

KINEMATIC ANALYSIS OF THE DRIVING MECHANISM OF ECCENTRIC SEPARATOR AS A COMPONENT PART OF MACHINE OF HARVESTING MISCANTHUS RHIZOMES
/
ANALIZA CINEMATICĂ A MECANISMULUI DE ACTIONARE A SEPARATORULUI CU EXCENTRIC AFLAT IN COMPONENTA ECHIPAMENTULUI TEHNIC DE RECOLTARE A RIZOMILOR DE MISCANTHUS

Ph.D. Stud. Eng. Sorică E.[1)], **Prof. Ph.D. Eng. Pirnă I.**[1)], **Ph.D. Eng. Sorică C.**[1)], **Prof. Ph.D. Eng. David L.**[2)]
[1)] INMA Bucharest / Romania; [2)] Politehnica University of Bucharest / Romania
Tel: 0722 / 487.889; E-mail: postelnicu.elena@yahoo.com

Abstract: *The paper presents the kinematic analysis of mechanism which drives the eccentric separator comprised by the technical equipment of harvesting Miscanthus rhizomes, where the positions, speed and accelerations of component elements, are determined.*
The kinematic analysis of the mechanism which drives the eccentric separator allows to identify the functional and constructive parameters which have to be operated for improving the mechanism structure and performance.

Keywords: *kinematic analysis, numerical study, eccentric separator, optimization, functional and constructive parameters*

INTRODUCTION

Within the crop technology of Miscanthus energetic plant, rhizomes harvesting represents one of the most important operations, which greatly influences the quality of seeds , necessary to establish a new crop.

Majority of technical equipment for harvesting the root vegetables generally, comprises extracting working parts and separating working parts. In case of tehnical equipment with fix inclined blade-type extracting working parts, the harvesting quality is mainly influenced by the separating parts.

Therefore, knowing the kinematic parameters of these separating parts, represents an objective necessary to be fulfilled for constructively and functionally optimize the respective equipment..

The technical equipment for harvesting Miscanthus rhizomes (fig. 1) comprises a separator with eccentric driven by a quadrilateral mechanism formed of handle, connecting rod and balance lever, represented by separator's rods.

Eccentric separator (fig. 2) is designed to clean by shaking and transport the extracted Mischantus rhizomes towards the machine rear part. The machine comprises two oscillating grates which take over the soil dislocated mass together with the rhizomes and an oscillating mechanism with eccentric which performs an optimum vibratory effect so that the soil detaches from rhizomes and falls between the grate rods.

Rezumat: *Lucrarea prezintă analiza cinematică a mecanismului de actionare a separatorului cu excentric aflat in componenta echipamentului tehnic de recoltare a rizomilor de Miscanthus, în care sunt determinate poziţiile, vitezele şi acceleraţiile elementelor componente.*
Analiza cinematică a mecanismului de acţionare a separatorului cu excentric permite identificarea parametrilor funcţionali şi constructivi asupra cărora să se acţioneze în scopul optimizării construcţiei şi funcţionării acestuia.

Cuvinte cheie: *analiză cinematică, studiu numeric, separator cu excentric, optimizare, parametrii funcţionali şi constructivi*

INTRODUCERE

In cadrul tehnologiei de cultura a plantei energetice Miscanthus, recoltarea rizomilor reprezinta una din cele mai importante operatii [1], [2], [3], [5], [6], [7], [9] cu influenta majora asupra calitatii materialului saditor, necesar infiintarii unei noi culturi.

Majoritatea echipamentelor tehnice de recoltat radacinoase, in general, au in componenta organe de dislocat si organe de separat. In cazul echipamentelor tehnice cu organe de dislocat de tip lama inclinata fixa, calitatea lucrarii de recoltare este influentata preponderent de organele de separare.

In acest context, cunoasterea parametrilor cinematici ai acestor tipuri de organe de separare, reprezinta un obiectiv necesar a fi indeplinit in scopul optimizarii constructive si functionale a echipamentelor respective.

Echipamentul tehnic de recoltare a rizomilor de Miscanthus (fig. 1) are in componenta un separator cu excentric actionat prin intermediul unui mecanism patrulater format din manivela, biela si balansier, reprezentat de vergelele separatorului.

Separatorul cu excentric (fig. 2) este destinat pentru curăţirea de pământ, prin scuturare şi transport a rizomilor de Miscanthus dislocaţi, spre spatele maşinii. Acesta are în componenţă două grătare oscilante care preiau masa de sol dislocată împreună cu rizomii şi un mecanism oscilant cu excentric care realizează un efect vibrator optim astfel încât solul să se desprindă de rizomi şi să cadă pe sol printre vergelele grătarului.

Fig. 1 - Equipment for harvesting Miacanthus rhizomes, ERM

Fig. 2 - Eccentric separator

MATERIALS AND METHODS

Mechanism of driving the eccentric separator as a component of technical equipment for Miscanthus rhizomes harvesting, is a quadrilateral mechanism (fig. 3) made of handle *1*, rod *2*, balance lever *3* and four rotation couplings (*R*).

MATERIALE ŞI METODE

Mecanismul de acţionare a separatorului cu excentric, parte componenta a echipamentului tehnic de recoltat rizomi de Miscanthus, este un mecanism patrulater (fig. 3) compus din: manivela *1*, biela *2*, balansierul *3* şi patru cuple de rotaţie (*R*).

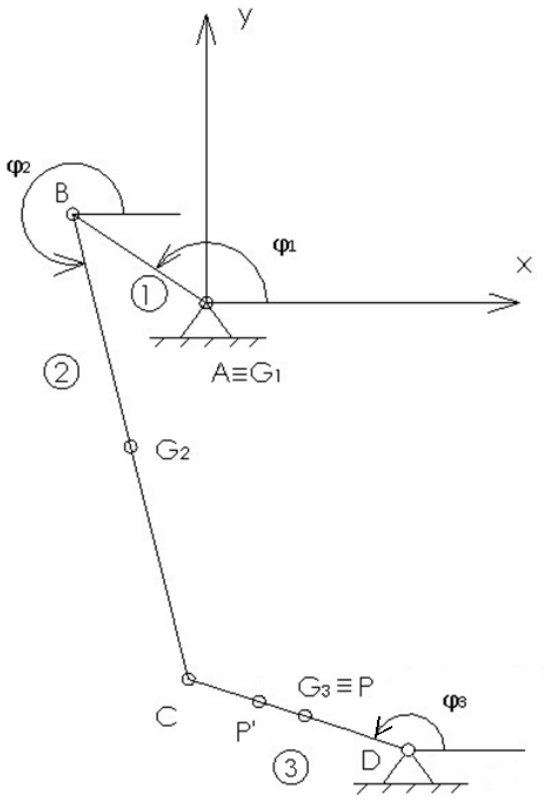

Fig. 3 - Scheme of quadrilateral mechanism which drives the eccentric separator

Point B coordinates are:

Coordonatele punctului B sunt:

$$\begin{cases} x_b = AB \cdot \cos\varphi_1 \\ y_b = AB \cdot \sin\varphi_1 \end{cases} \quad (1)$$

Speed and accelerations of point B are obtained by differentiation related to time

Vitezele şi acceleraţiile punctelor B se obţin prin derivarea în raport cu timpul:

$$\begin{cases} v_{bx} = -AB \cdot \omega_1 \cdot \sin\varphi_1 \\ v_{by} = AB \cdot \omega_1 \cdot \cos\varphi_1 \\ a_{bx} = -AB \cdot \omega_1^2 \cdot \cos\varphi_1 \\ a_{by} = -AB \cdot \omega_1^2 \cdot \sin\varphi_1 \end{cases} \quad (2)$$

For 3R modular group made of connecting rod 2, balance lever 3 and rotation couplings B,C and D, it can be written:

Pentru grupa modular 3R formată din bielă 2, balansierul 3 şi cuplele de rotaţie B, C şi D se poate scrie:

$$\overline{AB} + \overline{BC} = \overline{AD} + \overline{DC} \quad (3)$$

We are designing this vector equation on coordinates axes and obtain the equation system:

Proiectăm această ecuaţie vectorială pe axele de coordonate şi obţinem sistemul de ecuaţii:

$$\begin{cases} BC \cdot \cos\phi_2 - CD \cdot \cos\phi_3 - (x_d - x_b) = 0 \\ BC \cdot \sin\phi_2 - CD \cdot \sin\phi_3 - (y_d - y_b) = 0 \end{cases} \quad (4)$$

Linear equation system, in unknown φ_2 şi φ_3, can be solved by eliminating the φ_3 angle between the two equations of non linear system:

Sistemul de ecuaţii liniare, în necunoscutele φ_2 şi φ_3, se pot rezolva prin eliminarea unghiului φ_3 între cele două ecuaţii ale sistemului neliniar:

$$\begin{cases} BC \cdot \cos\phi_2 - (x_d - x_b) = CD \cdot \cos\phi_3 \\ BC \cdot \sin\phi_2 - (y_d - y_b) = CD \cdot \sin\phi_3 \end{cases} \quad (5)$$

The following notations are made

Se fac următoarele notaţii:

$$\begin{cases} k = x_d - x_b \\ h = y_d - y_b \end{cases} \quad (6)$$

The equation system will be: Sistemul de ecuaţii va fi:

$$\begin{cases} BC \cdot \cos\phi_2 - k = CD \cdot \cos\phi_3 \\ BC \cdot \sin\phi_2 - h = CD \cdot \sin\phi_3 \end{cases} \quad (7)$$

We are raising to square the two equations: Ridicăm la pătrat cele două ecuaţii:

$$\begin{cases} BC^2 \cdot \cos^2\phi_2 + k^2 - 2 \cdot BC \cdot k \cdot \cos\phi_2 = CD^2 \cdot \cos^2\phi_3 \\ BC^2 \cdot \sin^2\phi_2 + h^2 - 2 \cdot BC \cdot h \cdot \sin\phi_2 = CD^2 \cdot \sin^2\phi_3 \end{cases} \quad (8)$$

We are summing up the two equations and obtain: Adunăm cele două ecuaţii şi obţinem:

$$BC^2 + k^2 + h^2 - 2 \cdot BC \cdot k \cdot \cos\varphi_2 - 2 \cdot BC \cdot h \cdot \sin\varphi_2 = CD^2 \quad (9)$$

The following notations are made: Se fac următoarele notaţii:

$$\begin{cases} a = 2 \cdot BC \cdot k \\ b = 2 \cdot BC \cdot h \\ c = BC^2 - CD^2 + k^2 + h^2 \end{cases} \quad (10)$$

The circular function equation is obtained: Se obţin ecuaţia trigonometrică:

$$b \cdot \sin\varphi_2 + a \cdot \cos\varphi_2 + c = 0 \quad (11)$$

Solution of circular function equation is Soluţia ecuaţiei trigonometrice este:

$$\begin{cases} \sin\varphi_2 = \dfrac{b \cdot c - a\sqrt{a^2 + b^2 - c^2}}{a^2 + b^2} \\ \cos\varphi_2 = \dfrac{a \cdot c + b\sqrt{a^2 + b^2 - c^2}}{a^2 + b^2} \\ \sin\varphi_3 = \dfrac{BC \cdot \sin\varphi_2 - h}{CD} \\ \cos\varphi_3 = \dfrac{BC \cdot \cos\varphi_2 - k}{CD} \end{cases} \quad (12)$$

Rotation angles of connecting rod and balance lever are Unghiurile de rotaţie ale bielei şi balansierului sunt:

$$tg\varphi_2 = \frac{\sin\varphi_2}{\cos\varphi_2} \qquad \varphi_2 = arctg(\varphi_2) \quad (13)$$

$$tg\varphi_3 = \frac{\sin\varphi_3}{\cos\varphi_3} \qquad \varphi_3 = arctg(\varphi_3) \quad (14)$$

For determining the angular speed of rod and balance lever, the equation system is derived from relation (4) in relation with time:

Pentru determinarea vitezelor unghiulare a bielei şi balansierului se derivează sistemul de ecuaţii din relaţia (4) în raport cu timpul:

$$\begin{cases} -BC \cdot \dot{\varphi}_2 \cdot \sin\varphi_2 + CD \cdot \dot{\varphi}_3 \sin\varphi_3 = \dot{k} \\ BC \cdot \dot{\varphi}_2 \cdot \cos\varphi_2 - CD \cdot \dot{\varphi}_3 \cos\varphi_3 = \dot{h} \end{cases} \quad (15)$$

Where: unde:

$$\begin{cases} \dot{k} = \dot{x}_d - \dot{x}_b \\ \dot{h} = \dot{y}_d - \dot{y}_b \end{cases} \quad (16)$$

Matrix of unknowns coefficients is Matricea coeficienţilor necunoscutelor este:

$$\omega = \begin{vmatrix} -BC \cdot \sin\varphi_2 & CD \cdot \sin\varphi_3 \\ BC \cdot \cos\varphi_2 & -CD \cdot \cos\varphi_3 \end{vmatrix} \quad (17)$$

The equations system (15) in unknowns $\dot{\varphi}_2$ şi $\dot{\varphi}_3$, is solved by means of inverse matrix method and we obtain:

Sistemul de ecuaţii (15) în necunoscutele $\dot{\varphi}_2$ şi $\dot{\varphi}_3$, se rezolvă folosind metoda mătricii inverse şi se obţine:

$$\begin{Vmatrix} \dot{\varphi}_2 \\ \dot{\varphi}_3 \end{Vmatrix} = w^{-1} \begin{Vmatrix} \dot{k} \\ \dot{h} \end{Vmatrix} \tag{18}$$

For determining the angular accelerations, the equations (15) are derived in relation with time and we obtain:

Pentru determinarea acceleraţiilor unghiulare se derivează în raport cu timpul ecuaţiile (15) şi se obţine:

$$\begin{cases} -BC \cdot \ddot{\varphi}_2 \cdot \sin\varphi_2 - BC \cdot \dot{\varphi}_2^{\,2} \cos\varphi_2 + CD \cdot \ddot{\varphi}_3 \sin\varphi_3 + CD \cdot \dot{\varphi}_3^2 \cos\varphi_3 = \ddot{k} \\ BC \cdot \ddot{\varphi}_2 \cdot \cos\varphi_2 - BC \cdot \dot{\varphi}_2^{\,2} \sin\varphi_2 - CD \cdot \ddot{\varphi}_3 \sin\varphi_3 + CD \cdot \dot{\varphi}_3^2 \sin\varphi_3 = \ddot{h} \end{cases} \tag{19}$$

Where:

unde:

$$\begin{cases} \ddot{k} = \ddot{x}_d - \ddot{x}_b \\ \ddot{h} = \ddot{y}_d - \ddot{y}_b \end{cases} \tag{20}$$

The following notations are made :

Se fac următoarele notaţii:

$$\begin{cases} A_1 = \ddot{k} + BC \cdot \dot{\varphi}_2^2 - CD \cdot \dot{\varphi}_3^2 \cos\varphi_3 \\ A_2 = \ddot{h} + BC \cdot \dot{\varphi}_2^2 \sin\varphi_2 - CD \cdot \dot{\varphi}_3^2 \sin\varphi_3 \end{cases} \tag{21}$$

System of equations (19) becomes:

Sistemul de ecuaţii (19) devine:

$$\begin{cases} -BC \cdot \sin\varphi_2 \cdot \ddot{\varphi}_2 + CD \cdot \sin\varphi_3 \cdot \ddot{\varphi}_3 = A_1 \\ BC \cdot \cos\varphi_2 \cdot \ddot{\varphi}_2 - CD \cdot \cos\varphi_3 \cdot \ddot{\varphi}_3 = A_2 \end{cases} \tag{22}$$

System of linear equations in unknowns $\ddot{\varphi}_2$ and $\ddot{\varphi}_3$ is solved by inverse matrix method:

Sistemul de ecuaţii liniare în necunoscutele $\ddot{\varphi}_2$ şi $\ddot{\varphi}_3$ se rezolva cu metoda matricii inverse:

$$\begin{Vmatrix} \ddot{\varphi}_2 \\ \ddot{\varphi}_3 \end{Vmatrix} = w^{-1} \begin{Vmatrix} A_1 \\ A_2 \end{Vmatrix} \tag{23}$$

For C rotating torque, the position, velocity and angular speed are determined with relations:

Pentru cupla de rotaţie C se determină poziţia, viteza şi acceleraţia unghiulară cu relaţiile:

$$\begin{cases} x_c = x_d + CD \cdot \cos\varphi_3 \\ y_c = y_d + CD \cdot \sin\varphi_3 \\ v_{cx} = -CD \cdot \dot{\varphi}_3 \cdot \sin\varphi_3 \\ v_{cy} = CD \cdot \dot{\varphi}_3 \cdot \cos\varphi_3 \\ a_{cx} = -CD \cdot \dot{\varphi}_3^2 \cdot \cos\varphi_3 - CD \cdot \ddot{\varphi}_3 \cdot \sin\varphi_3 \\ a_{cy} = -CD \cdot \dot{\varphi}_3^2 \cdot \sin\varphi_3 + CD \cdot \ddot{\varphi}_3 \cdot \cos\varphi_3 \end{cases} \tag{24}$$

RESULTS

Kinematic analysis is based on a series of values considered constant, representing the actual dimensions of the handle, connecting rod, balance lever, respectively A and D rotating torque positions. Considering the origin of the coordinate system XAY in point A, we will have the following constants:

AB=0.013 m;
BC=0.456 m;
CD=0.329 m;
X_d=0.135 m;
Y_d=-0.43 m.

Kinematic analysis for the quadrilateral mechanism was performed using a program developed in MathCad 14.

In order to limit the data volume that would result by calculating the kinematic parameters in each crank position (0...360°) were considered 37 intermediate positions, in which position 1 and 37 are equivalent and correspond to 0 respectively 360°.Therefore, it will be determined the kinematic parameters in these intermediate points while kinematic analysis will be achieved by reference to the mentioned positions.

The AB handle separator of the acting mechanism is driven by hydraulic engine coupled to the tractor hydraulic system. For numerical simulation using the mentioned computer program, was considered an average hydraulic motor shaft speed of 250 rot/min. The variation of velocity components of point B on the axis of coordinates depending on the angle of rotation φ1 (crank position) is shown in Figure 4.

REZULTATE

Analiza cinematica are la baza o serie de valori considerate constante, reprezentand dimensiunile reale ale manivelei, bielei, balansierului, respectiv pozitiile cuplelor de rotatie A si D. Considerand originea sistemului de coordonate XAY in punctul A, vom avea urmatoarele constante:

AB=0,013 m;
BC=0,456 m;
CD=0,329 m;
X_d=0,135 m;
Y_d=-0,43 m.

Analiza cinematica a mecanismului patrulater s-a efectuat cu ajutorul unui program realizat in MathCad 14.

Pentru a limita volumul mare de date care ar fi rezultat prin calcularea parametrilor cinematici in fiecare pozitie a manivelei (0...360°), s-au considerat 37 de pozitii intermediare, in care pozitia 1 si 37 sunt echivalente si corespund valorii de 0 respectiv 360°. Ca urmare, se vor determina parametrii cinematici in aceste puncte intermediare iar analiza cinematica se va realiza prin raportare la pozitiile amintite.

Manivela AB a mecanismului de acţionare a separatorului este acţionată prin intermediul motorului hidraulic cuplat la instalatia hidraulica a tractorului. Pentru simularea numerica utilizand programul de calcul amintit, s-a considerat o valoare medie a turatiei la axul motorului hidraulic de 250 rot/min. Variaţia componentelor vitezei punctului B pe axele de coordonate în funcţie de unghiul de rotaţie φ_1 (poziţia manivelei) este prezentat în figura 4.

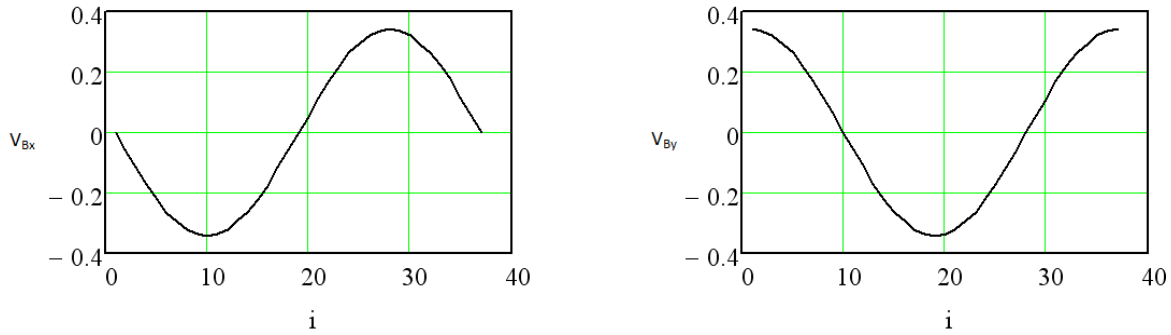

Fig. 4 - Variation of component velocity at point B

Absolute velocity of point B has a value of 0.340 m/s.

The connecting rod BC rotates with angle φ_2. Changes in the rotating angle of the connecting rod on the crank position shown in Figure 5.

Viteza absoluta a punctului B are valoarea 0.340 m/s.

Biela BC se roteşte cu unghiul φ_2. Variaţia unghiului de rotaţie a bielei în funcţie de poziţia manivelei este prezentată în figură 5.

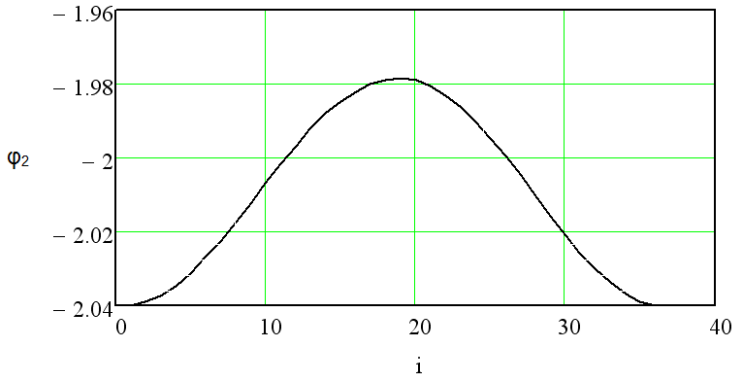

Fig. 5 - Variation of the rod BC rotating angle

Maximum value of rotating angle φ_2= - 1.978 rad is obtained for the position i = 19 (rotation of the crank with φ_1 = 3.142 rad) when the crank is in the horizontal position at 180 degrees. The minimum value of the angle of rotation of the rod φ_2 = - 2.04 rad corresponds to position 1

Valoarea maximă a unghiului de rotaţie φ_2 = - 1.978 rad se obţine pentru poziţia i=19 (rotaţia manivelei cu φ_1 = 3.142 rad) atunci când manivela se află în poziţia orizontala, la 180 grade. Valoarea minimă a unghiului de rotaţie a bielei φ_2 = - 2.04 rad corespunde poziţie 1 sau 37

or 37 (crank rotation with φ_1 = 0 rad or 6283 rad) when the crank is in the horizontal position at 0 or 360 degrees. Changes in the angular velocity of the rod ω_2 and ε_2 angular acceleration of the rod are shown in Figure 6.

(rotaţia manivelei cu φ_1 = 0 rad sau 6.283 rad) atunci când manivela se află în poziţia orizontala, la 0 sau 360 grade. Variaţia vitezei unghiulare a bielei ω_2 şi acceleraţiei unghiulare ε_2 a bielei este prezentată în figura 6.

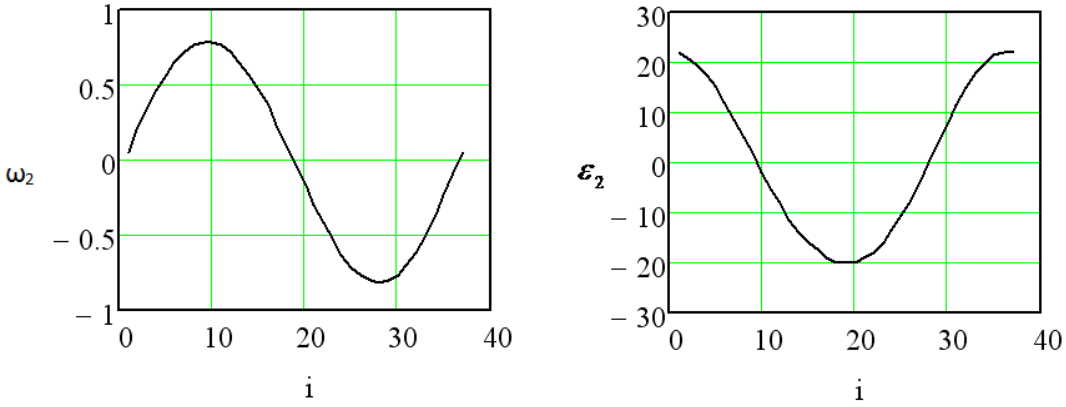

Fig. 6 - Variation of rod angular velocity and acceleration / *Variaţiei vitezei şi acceleraţiei unghiulare a bielei*

Figure 7 shows the variation in the speed component of point C of on axes of the connecting rods and the speed variation point C in Figure 8 depending on the position of the crank.

În figură 7 se prezintă variaţia componentelor vitezei punctului C al bielei pe axele de coordonate iar în figură 8 variaţia vitezei punctului C în funcţie de poziţia manivelei.

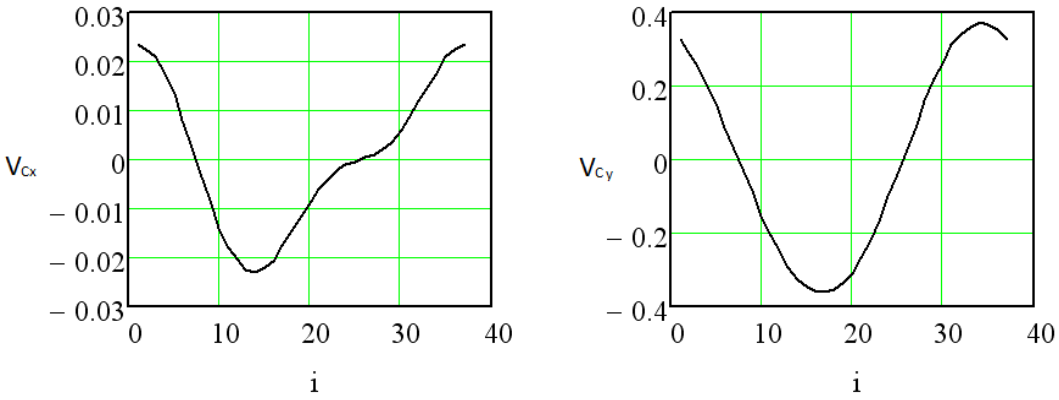

Fig. 7 - Variation of velocity components of point C

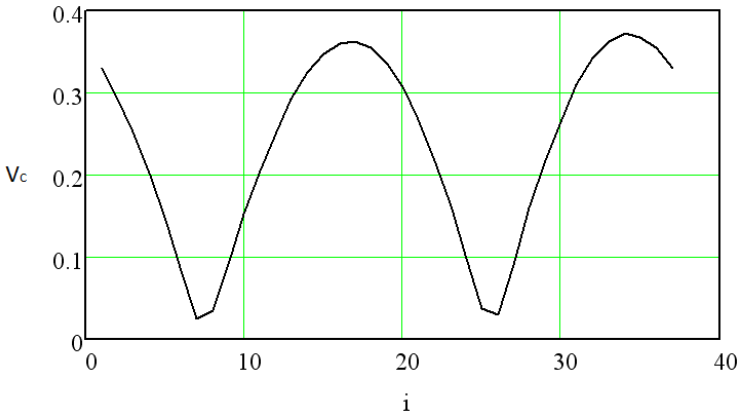

Fig. 8 - Variation of absolute velocity of point C

It is observed that the extreme positions of point C correspond to position i = 7 and i = 34 of the crank, speed of point C having the minimum v_c = 0.026 m / s and maximum v_c = 0.372 m / s

Se observă că poziţiile extreme ale punctului C corespund poziţiilor i= 7 şi i= 34 ale manivelei, viteza punctului C avand valoarea minimă v_c = 0.026 m/s respectiv maxima v_c = 0.372 m/s.

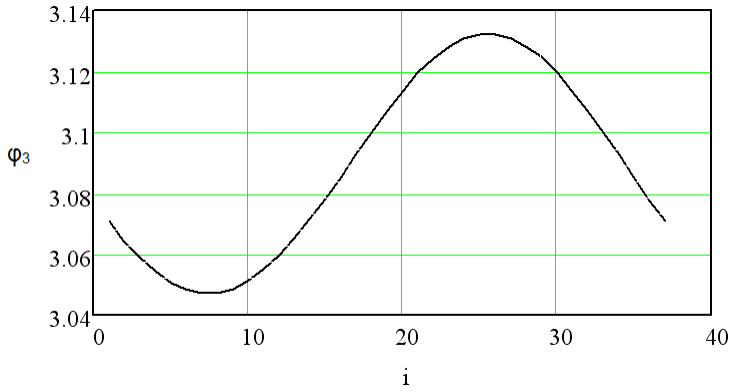

Fig. 9 - Variation in the rotating angle of balance wheel

Maximum rotation angle value is φ_3 = 3.132 rad, the minimum value φ_3 = 3.047 rad and the variation of this angle is 0.085 rad. These values correspond to the extreme positions of the point C.

Variation in velocity and angular acceleration of balance lever is shown in Figure 10.

Valoarea maximă a unghiului de rotaţie este φ_3 = 3.132 rad, valoarea minimă φ_3 = 3.047 rad iar variaţia acestui unghi este de 0.085 rad. Aceste valori corespund poziţiilor extreme ale punctului C.

Variaţia vitezei şi acceleraţia unghiulară a balansierului este prezentă în figură 10.

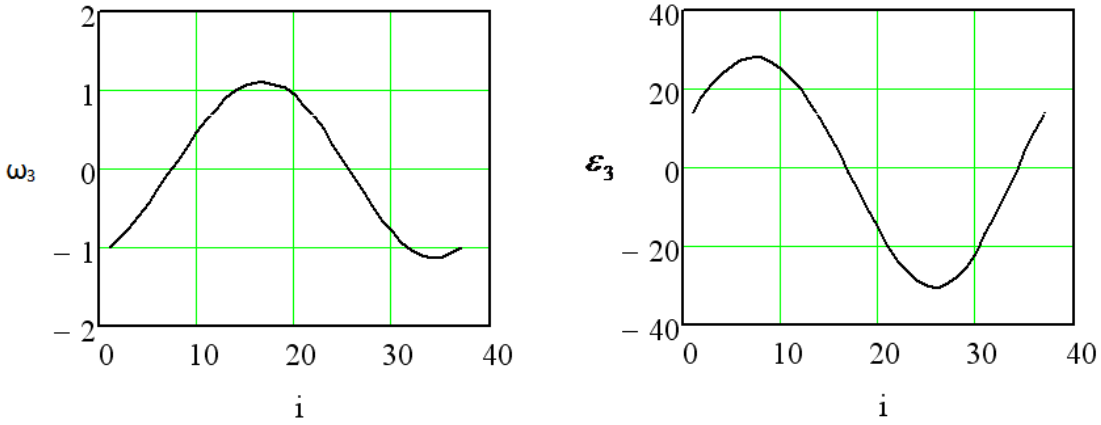

Fig. 10 - Variation of angular velocity and acceleration balance lever

CONCLUSIONS

Through kinematic analysis program of mechanism operating the eccentric separator can be determined positions, velocities and accelerations components.

Velocities can be analytically determined by the two axes of the considered coordinate system as well as the absolute velocities of points B and C, in m / s

Also, can be determined the maximum and minimum rotation angle φ_2, which can be correlated with the positions of the crank at a certain moment.

Variation of rotating angle φ_3 between the maximum and minimum, provide information regarding extreme positions of point C, respectively the amplitude and oscillation frequency of the balance lever, allowing the identification of functional and constructive parameters having to be adjust in order to optimize the construction and operation of the separator with eccentric.

REFERENCES

[1]. Atkinson C. J. (2009) - *Establishing perennial grass energy crops in the UK: A review of current propagation options for Miscanthus*, Biomass and Bioenergy, Volume 33, Issue 5, Pages 752–759;

[2]. Boersma N. N., Heaton E. A. (2014) - *Propagation method affects Miscanthus × giganteus developmental morphology*, Industrial Crops and Products, Volume 57, June 2014, Pages 59–68;

CONCLUZII

Prin intermediul programului de analiză cinematică a mecanismului de acţionare a separatorului cu excentric, se pot determina poziţiile, vitezele si acceleraţiile elementelor componente.

Se pot determina analitic atat vitezele pe cele doua axe ale sistemului de coordonate considerat, cat si vitezele absolute ale punctelor B si C, in m/s.

De asemenea, se pot determina valorile maxima si minima a unghiului de rotaţie φ_2, putand fi corelate cu pozitiile manivelei la un anumit moment.

Variatia unghiului de rotaţie φ_3, intre valoarea maxima si minima, furnizeaza informatii privind poziţiile extreme ale punctului C, respectiv amplitudinii si frecventei de oscilatie a balansierului, permitand identificarea parametrilor funcţionali şi constructivi asupra cărora să se acţioneze în scopul optimizării construcţiei şi funcţionării separatorului cu excentric.

BIBLIOGRAFIE

[1]. Atkinson C. J. (2009) - *Stabilirea culturilor energetice perene în Marea Britanie: O trecere în revistă a opțiunilor actuale de propagare pentru Miscanthus,* Biomasă și Bioenergie, Volum 33, Nr.5, Pag.752–759;

[2]. Boersma N. N., Heaton E. A. (2014) - *Metoda de propagare afecteaza Miscanthus-ul x morfologie de dezvoltare gigantică,* Culturi industriale și produse, Volum 57, iunie 2014, Pag.59–68;

[3]. Huisman W, Kortleve W. J. (1994) - *Mechanization of crop establishment, harvest, and post-harvest conservation of Miscanthus sinensis Giganteus*, Industrial Crops and Products, Volume 2, Issue 4, September 1994, Pages 289–297;
[4]. Manolescu N., Kovacs Fr., Orănescu A. (1972) - *Theory of machines and mechanisms*, Didactic and Pedagogic Publishing House, Bucharest;
[5]. O'Flynn M. G., Finnan J. M., Curley E. M., McDonnell K. P. (2014) - *Reducing crop damage and yield loss in late harvests ofMiscanthus × giganteus*, Soil and Tillage Research, Volume 140, July 2014, Pages 8–19;
[6]. Postelnicu E., Sorică C., Grigore I., Ludig M., Niţu M. (2012) - *Methods for obtaining seedling material in order to promote energy plant Miscanthus,* Annals of the University of Craiova - Agriculture, Montanology, Cadastre Series, Vol. XLII 2012/2, pp. 419-423, Craiova;
[7]. Sorică C., Voicu E., Manea D (2009) - *Technology for promotion in Romania of energy crop Miscanthus, as renewable resource to increase energy competitiveness in independence purposes*, INMATEH no. 29 (2009 - III), pp.19-26, Bucharest, ISSN 1583-1019, http://www.inma.ro/inmateh;
[8]. Sorică E. (2014) – *Kinematic and kinetostatic analysis of the working process of technical equipment for harvesting Miscanthus rhizomes*, Report No.3, PhD School;
[9]. Voicu E., Pirnă I., Ciurel G., Chiţoiu M., Brkic M. (2010) - *Researches on harvesting of Miscanthus crop with the forage harvester*, INMATEH no. 32 (2010 - III), pp. 37-42, Bucharest, ISSN 1583-1019, http://www.inma.ro/inmateh

[3]. Huisman W, Kortleve W. J. (1994) - *Mecanizarea înființării culturii, recoltare, conservare și post-recoltare de Miscanthus sinensis Giganteus,* Culturi industriale și produse, Volum 2, Nr.4, septembrie 1994, Pag.289–297;
[4]. Manolescu N., Kovacs Fr., Orănescu A. (1972) - *Teoria mecanismelor şi a maşinilor*, Ed. Didactică şi Pedagogică, Bucureşti;
[5]. O'Flynn M. G., Finnan J. M., Curley E. M., McDonnell K. P. (2014) - *Reducerea vătămării culturilor și pierderii randamentului în ultima perioadă de recoltare a Miscanthus × giganteus*, Cercetări privind solul şi recoltarea, Volum 140, Pag.8–19;
[6]. Postelnicu E., Sorică C., Grigore I., Ludig M., Niţu M. (2012) - *Metode de obținere a materialului săditor in scopul promovării plantei energetice Miscanthus*, Analele Universităţii din Craiova, seria Agricultură – Montanologie – Cadastru, Vol. XLII 2012/2, pag. 419-423, Craiova;
[7]. Sorică C., Voicu, E., Manea, D (2009) - *Tehnologie pentru promovarea în România a plantei energetice Miscanthus ca sursă regenerabilă în scopul creşterii competitivităţii şi securităţii energetice*, in revista INMATEH Nr. 29 (2009-III), pag. 19-26, Bucureşti, ISSN 1583-1019, http://www.inma.ro/inmateh;
[8]. Sorică E. (2014) – *Analiza cinematica si cineto-statica a procesului de lucru a echipamentului tehnic de recoltat rizomi de Miscanthus*, Referat nr.3, Scoala doctorala;
[9]. Voicu E., Pirnă I., Ciurel G., Chiţoiu M., Brkic M. (2010) - *Cercetări privind recoltarea culturii de Miscanthus cu combina de furaje*, in revista INMATEH Nr. 32 (2010-III), pag.37-42, Bucureşti, ISSN 1583-1019, http://www.inma.ro/inmateh

RESEARCHES REGARDING THE SOLAR RADIATION USE AS HEATING SOURCE IN HAY VENTILATING INSTALLATIONS
/
CERCETĂRI PRIVIND UTILIZAREA RADIAŢIEI SOLARE CA SURSĂ DE ÎNCĂLZIRE A AERULUI UTILIZAT DE INSTALAŢIILE DE VENTILARE A FÂNULUI

Ph.D. Eng. Nedelcu A., Ph.D.Eng. Ciuperca R., Ph.D.Eng. Popa L, Ph.D.Eng. Voicu E., Eng. Zaica A.
- INMA Bucuresti - Romania
Tel: 0212693250; E-mail: nedelcuus@yahoo.com

Abstract: *Solar radiation is a natural heat source with multiple uses on farms, for example, heating the air used in drying fruit technology and for domestic hot water or artificial drying of forage crops in order to obtain the hay. The paper presents the results of researches performed with a plane solar collector particular type, which is made of common materials and is designed to heat the air within special fodder ventilating installations for obtaining high quality hay and reducing conventional energy consumption. During this research, it has been measured and continuously monitored the following parameters: meteorological parameters (solar radiation, temperature, humidity), the temperature in the panel at various times of the day, TPS, air velocity in the panel, VPS, temperature variation during the panel ventilation, ∆ T solar collector efficiency, η.*

Keywords: *hay, hot air ventilation, solar radiation, solar collectors*

INTRODUCTION

Through harvesting, preparation and preserving various forms of fodder on grasslands and fodder crops it aims to achieve a final product with a nutritional value as close as possible to the original green fodder, starting from the premise that it fulfills a high quality feed, both in terms of botanical composition (balanced mix of perennial grasses with vegetables) and in the harvesting phenophase [2], [3], [5].

Harvesting, preparation and preserving as hay form represents the traditional method used in our country to capitalize the fields with feed and fodder crops, especially in the hilly and mountainous areas. In the plain regions, the hay is produced on agricultural land planted with annual or perennial forage crops, natural grasslands occupying smaller areas.

In order to reduce the drying time and implicitely the losses of nutritive substances, many harvesting, preparing and conserving methods of hay have been developed, drying representing an operation of great importance, with the biggest implications in the final quality of hay. The most known fodder drying methods are: traditional (natural) drying in stubble field; drying on supports; fodder drying by cold air ventilation; fodder drying by hot air ventilation; green fodder drying by thermal dehydration in special drying and briquetting stations, [4].

The biggest losses of nutritive substances are determined by hay traditional drying in stubble. These losses might reach, in bad weather conditions, even 50..60%, the drying period coming up to 6-8 days [7].

When hay of 35-45% moisture is gathered from the field, it is stored in hay stores or platforms endowed with drying installation, where is achieved cold or warm air ventilation up to conservation humidity (under 7%) and consequently, losses may be reduced up to

Rezumat: *Radiaţia solară este o sursă de căldură naturală cu multiple utilizări în fermele agricole, spre exemplu încălzirea aerului utilizat în tehnologia de uscare a fructelor, pentru prepararea apei calde menajere sau pentru uscarea artificială a plantelor furajere şi în vederea obţinerii fânului. Lucrarea prezintă rezultate ale cercetarilor efectuate cu un tip special de captatoare solare plane, construite din materiale uzuale, pentru încălzirea aerului utilizat de instalaţiile speciale pentru ventilarea furajelor în vederea obţinerii unui fân de calitate şi reducerea consumului de energie convenţională. În cadrul cercetărilor au fost masurati si monitorizaţi permanent următorii parametri: parametrii meteorologici (radiaţia solară, temperatura, umiditate), temperatura aerului din panou la diverse ore ale zilei, T_{PS}, viteza aerului în panou, V_{PS}, variaţia temperaturii în panou în timpul procesului de ventilare, ∆T, randamentul captatorilor solari, η.*

Cuvinte cheie: *fân, ventilare cu aer cald, radiaţie solara, captatori solari*

INTRODUCERE

Prin recoltarea, pregătirea şi conservarea sub diferite forme a furajelor de pe pajişti şi din culturile furajere se urmăreşte realizarea unui produs final cu o valoare nutritiva cât mai apropiată de cea iniţială a furajului verde, plecându-se de la premisa că acesta îndeplineşte condiţiile unui furaj de foarte bună calitate, atât în ceea ce priveşte compoziţia sa botanică (amestec echilibrat de graminee cu leguminoase perene), cât şi în cea referitoare la fenofaza de recoltare [2], [3], [5].

Recoltarea, pregătirea si conservarea sub formă de fân reprezintă metoda traditională folosită în ţara noastră pentru valorificarea furajelor de pe pajiştile şi culturile furajere, în special de pe suprafeţele din zona colinară şi montana. În regiunile de câmpie, fânul se produce pe terenurile agricole cultivate cu plante furajere anuale sau perene, pajiştile naturale ocupând suprafeţe mai mici.

Pentru reducerea timpului de uscare şi implicit a pierderilor de substanţe nutritive s-au dezvoltat mai multe metode de recoltare, pregătire şi conservare a fânului, uscarea reprezentand o operatie de mare importanta, cu cele mai mari implicatii in calitatea finala a fanului. Metodele de uscare a furajelor cunoscute sunt: uscarea tradiţională (naturală) pe mirişte; uscarea pe suporţi; uscarea furajelor prin ventilare cu aer rece; uscarea furajelor prin ventilarea cu aer cald; uscarea furajelor verzi prin deshidratare termică în staţii speciale de uscare şi brichetare etc. [4].

Pierderile cele mai mari de substanţe nutritive se obţin la uscarea tradiţională pe mirişte a fânului. Aceste pierderi ajung, în caz de vreme nefavorabilă (prin mucegairea fânului), chiar la 50…60 %, timpul de uscare crescând la peste 6…8 zile [7].

Atunci când fânul strâns din câmp la umiditatea de 35-45% este depozitat pe fânarele sau platformele prevăzute cu instalaţie de uscare, unde se face definitivarea uscării fânului prin ventilare cu aer rece sau cald, până la umiditatea de păstrare (sub 17%), se pot

15-20% [8].

Installations for hay warm air drying based on conventional energy consumption: fossile fuels and electric energy are complex, expensive and difficult to redeem in small and medium-sized farms in unfavourable areas. Because of necessity to reduce conventional energy consumption, new solutions for non-polluting and cheap air heating solar installations have been sought [9], [10], [11].

MATERIALS AND METHODS

The hay drying installation tested comprises the solar collector (fig.1), storage platform, technical equipment with axial fan and two circuits for air absorbtion humidity and temperature measuring sensors and a command board equiped with micro PLS, where the venting programs were set according to methodology elaborated for the installation testing.

The paper presents solutions designed to heat the air in solar collectors assembled as a panel placed on the ground, next to the drying platform.

The constructive solutions allow the users to move the drying installation from a store platform to another, on the spot, where hay final drying is needed. Also, the panel may be adapted for mounting on the roof deposits.

The solar panel (fig.1) is a main assembly of air ventilation installation of bulk hay and because it is built as a modular structure, the users may adjust their installation according to the farm needs [6].

reduce pierderile cu până la 15-20% faţă de tehnologia clasica de uscare naturala in brazda [8].

Instalaţiile pentru uscarea fânului cu aer cald bazate pe consumul de energie convenţională: combustibili fosili, energia electrică sunt complexe, scumpe şi greu de amortizat în fermele mici şi mijlocii din zonele defavorizate. Din necesitatea reducerii consumului de energie convenţionala s-au căutat soluţii pentru încălzirea aerului în instalaţii solare, cu preţ de cost mai mic şi nepoluante [9], [10], [11].

MATERIALE ŞI METODE

Instalatia de uscare a fânului utilizată in cadrul experimentarilor a fost construită din panoul solar (fig.1), platforma de depozitare, echipament tehnic cu ventilator axial şi doua circuite pentru absorţia aerului, senzori pentru masurarea umidităţii şi temperaturii şi un tablou de comadă echipat cu micro PLS, în care au fost setate programele de ventilare conform metodologiei elaborate pentru testarea instalaţiei.

Lucrarea prezintă soluţii pentru încălzirea aerului în captatoare solare asamblate sub forma unui panou amplasat pe sol, în apropierea platformei de uscare.

Soluţiile constructive permit utilizatorilor mutarea panoului solar de la o platforma de depozitare, la alta, acolo unde este necesară definitivarea uscării fânului. De asemenea, panoul poate fi adaptat pentru montarea pe acoperişul depozitelor.

Panoul solar (fig.1) este un ansamblu principal al instalaţiei de ventilare cu aer a fânului vrac, şi deoarece este construit într-o structură modulară utilizatorii îşi pot configura instalaţia de uscare conform necesarului din fermă. [6].

Fig.1 - Assembled solar panel

1 - End collector; 2 - Intermediary collector; 3 - Admission and pressing collector; 4 - Air intake hole in the panel; 5 - Air exhausting hole; 6 - Tubes

The solar panel of installation studied comprises five solar collectors designed to heat the air, serially mounted one after the other, on a frame made of metallic profiles. The solar collectors are light, made of pressed wood. The frontal wall through which the light passes is made of transparent material. Within the space designed to heat the air, in the relevant collectors have been mounted intermediary longitudinal walls, creating this way, the space to lead the air in a zigzag movement, on all the collectors surface, in order to obtain a maximum heating yield.

The air to be ventilated is heated in the panel collectors by means of greenhouse effect. During the air ventilating, the atmospheric air is absorbed through a hole - 4, passes through the solar panel in a zigzag course, it is heated and after that is exhausted through a special hole - 5 of solar panel, continuing its way through the flexible tubing - 6 towards the fan admission hole to the drying platform levelling chamber.

A very important performance indicator of solar plane panel is given by the solar collectors yield, η., calculated with relation (1), [1]:

Panoul solar al instalaţie studiate**,** este format din cinci captatori solari de încălzire a aerului, montaţi în serie unul după celălalt pe un cadru din profile metalice. Captatorii solari sunt de tipul uşor, în cazul de faţa cu pereţii din OSB. Peretele frontal de admisie a radiatiei solare este din plexiglass transparent. În spaţiul de încălzire al aerului, în captatorii înseriaţi s-au montat pe lungime pereţi longitudinali intermediari, creându-se trasee pentru dirijarea aerului în zig-zag, pe toată suprafaţa captatorilor, pentru obţinerea unui randament maxim de încălzire.

Aerul necesar ventilării este încălzit în captatorii solari ai panoului prin efectul de seră. In timpul ventilării, se absoarbe aerului rece atmosferic prin orificiu - 4, acesta parcurge panoul solar pe traseul în zig - zag, se încălzeşte, şi se evacuează prin orificiul special - 5 al panoului solar, continuând traseul prin tubulatura de aspiraţie flexibilă - 6, către orificiul de admisie al ventilatorului până în camera de uniformizare a platformei de uscare.

Un indicator de performanţă important pentru panoul solar plan este randamentul colectorilor solari, η, calculat cu relaţia (1), [1]:

$$\eta = \eta_0 - \frac{q_p}{I_g} \quad (1)$$

where:
- η_0 - optical yield;
- q_p - density of thermal flow dissipated in environment, from thermal agent, [W/m^2];
- I_g - density of global solar radiation, [W/m^2];
- η_0 and q_p are determined from relations (2) respectively (3):

unde:
- η_0 - randament optic;
- q_p - densitatea fluxului termic pierdut în mediul ambiant, de la agentul termic, [W/m^2];
- I_g - densitatea fluxului radiaţiei solare globale, [W/m^2];
- η_0 şi q_p se determină din relaţiile (2), respectiv (3):

$$\eta_0 = \tau \cdot \alpha \quad (2)$$

$$q_p = k \cdot \Delta t \quad (3)$$

where:
- τ - transmission factor of transparent material, τ = 0.8...0.87 values recommended for glass, plexiglass;
- α - factor of absorbtion of absorbing material,
- $\alpha \approx 0.9$ value recommended for black enamel;
- k - global coefficient of thermal transfer between collector and environment, [W/m^2 K]; usual known values k = 2…4 [W/m^2 K];
- Δt - difference between collector average temperature and environment, [° C].

Introducing relations (2) and (3) into (1), results the relation (4), used for determining the yield of installation plane collectors, results:

unde:
- τ - factorul de transmisie al materialului transparent, τ = 0,8...0,87 valori recomandate pentru sticla, plexiglass;
- α - factorul de absorbţie al materialului absorbant,
- $\alpha \approx 0.9$ valoare recomanda pentru email negru;
- k - coeficientul global de transfer termic între colector şi mediul ambiant, [W/m^2 K]; valori uzuale cunoscute k = 2…4 [W/m^2 K];
- Δt - diferenţa dintre temperatura medie a colectorului şi mediul ambiant, [° C].

Introducând relaţiile (2) şi (3) în (1) rezulta relaţia (4) utilizată în determinarea randamentului captatorilor plani ai instalaţiei cercetate:

$$\eta = \eta_0 - k\frac{\Delta t}{I_g} \quad (4)$$

expressing:
ΔT - growing indicator of panel air temperature [°C];
ΔT_v - difference between panel air temperature before venting and air temperature in the panel after hot ventilation of hay stored for drying, [°C]:

ΔT and ΔT_v depend on air temperature in solar panel, respecivelly on air temperature in the panel, after fodder venting, as one can see in relations (5) and (6):

exprimând:
ΔT - indicatorul de creştere a temperaturii aerului în panou, [°C];
ΔT_v - diferenta dintre temperatura aerului din panou solar înainte de ventilare şi temperatura aerului din panou după ventilarea cu aer cald a fânului depozitat pentru uscare, [°C].

ΔT şi ΔT_v depind de temperatura aerului in panoul solar, respectiv de temperatura aerului în panou, după ventilarea furajului, asa cum se poate vedea si in relatiile (5) si (6):

$$\Delta T = T_P - T_a \quad (5)$$

$$\Delta T_V = T_P - T_{Pv} \quad (6)$$

where:
T_P - air temperature in solar panel, [° C];
T_{Pv} - air temeperature in the panel after hot air venting of fodder, [° C].

A digital thermometer with transducer measuring the panel temperature, INMA Bucharest professional agrometeorological station designed to control meteo parameters and a TESTOVENT 4000 type anemometer for determining wind speed in the panel when ventilating, were all used for tests.

în care:
T_P - temperatura aerului în panoul solar, [° C];
T_{Pv} - temperatura aerului în panou după ventilarea furajelor cu aer cald, [° C].

La experimentări s-au utilizat: un termometru digital cu traductor pentru măsurarea temperaturii în panoul solar, staţia meteo profesională agro-meteoreologică pentru monitorizarea parametrilor meteo, termohigrometru şi anemometru tip TESTOVENT 4000 pentru determinarea vitezei aerului în panou în momentul ventilării.

Fig. 2 - Measuring the temperature and the air speed
1 - Temperature inside panel; 2 - Air speed at the inlet in panel; 3 - Air speed at the outlet in panel

RESULTS

Equipment for converting solar radiation, solar collectors planar panel is covered with transparent materials that are being crossed by solar radiation on the road to conversion element represented by the absorbing surface made of OSB material painted in black enamel.

Transparent cover panel was made of Plexiglas known as acrylic glass or stiplex with high transparency such as glass and has a high impact resistance.

The measurements were performed between the hours 8 in the morning and 16 in the afternoon. The parameters of atmospheric air and inside the captors, determined by measurement or calculation, are presented in Table 1, values measured being specific to a cloudy day of June.

REZULTATE

Echipamentul de conversie a radiaţiei solare, panoul cu captatori solari plani, este acoperit cu materiale transparente, care sunt traversate de radiaţia solară, în drumul spre elementul de conversie reprezentat de suprafaţă absorbantă realizată din OSB vopsită cu email negru. Capacul transparent al panoului a fost realizat din plexiglass cunoscut si sub denumirea de sticla acrilică sau stiplex, cu transparenta asemanatoare sticlei şi rezistenta la impact mare.

Masuratorile s-au efectuat în intervalul orar 8...16. Parametrii aerului atmosferic şi din interiorul captatorilor, determinati prin masurare, sau prin calcule, sunt prezentati in tabelul 1, valorile sunt specifice unei zile cu cer variabil din luna iunie.

Table 1

Air solar panel parameters

Parameter	UM	Hour								
		8	9	10	11	12	13	14	15	16
Solar radiation, *Ig*	kW/m^2	0.425	0.562	0.525	0.219	0.798	0.203	0.159	0.073	0.055
Atmospheric humidity, *Ua*	%	72.243	65.075	64	61.287	59.392	54.477	53.094	58.419	72.243
Atmospheric temperature, *Ta,*	^{0}C	23	24.89	26.31	26.5	27.36	27.44	27.78	26.89	23
Temperature in the panel, *Tp*	^{0}C	24.6	28	40	45	66	65	56	55	55
Indicator of panel temperature increasing, $\Delta T_.$	^{0}C	1.6	3.11	13.69	18.5	38.64	37.56	28.22	28.11	32
Panel temperature after 15 ventilating min. T_{Pv}[^{0}C]	^{0}C	23	26	30	33	38	36	30	29	27
Temperature variation during the ventilation, ΔT_V	^{0}C	1,6	2	10	12	28	29	28	25	28

The absoption process of solar radiation on absorbing surface of solar collectors, is characterized by the absorption coefficient of the absorbing material. Thus, the black enamel in which the collector was peinted has an absorption coefficient of α = 0.9 which means that 90% of solar radiation that reaches this material is converted into heat [1].

For the average yield calculation of the solar collector it has been used the equations (1), (2), (3), (4) and the following coefficient values [1]:

- transmission factor for glass or Plexiglas: $\tau \approx 0.835$;
- absorption factor for black enamel: $\alpha = 0.9$;
- global heat transfer coefficient between collector and the environment *k = 2.5* W/m^2 K;

From Table 1 it have resulted the recorded average values for the following parameters:

- difference between average temperature of the collector and the ambient temperature: Δt = 22,27°C.
- Global solar radiation density flux during the experiments: I_g = 335 W/m^2.

From the calculation it has resulted:

- optical yield: η_0 = 75%;
- average yield of solar collectors on the experimenting day: $\eta = 58\%$

Procesul de absorbţie a radiaţei solare pe suprafaţa absorbantă a colectorilor solari, este caracterizat de coeficientul de absorbţie al materialului absorbant. Astfel emailul negru cu care a fost vopsit captatorir, are un coeficient de absorbţie α=0,9 ceea ce înseamnă că 90% din radiaţia solară care ajunge pe acest material, este transformată în căldură [1].

Pentru calculul randamentului mediu al colectorilor solari s-au utilizând relaţiile (1),(2),(3),(4) şi următoarele valori pentru coeficienţi, [1]:

- factor de transmisie pentru sticla sau plexiglass: $\tau \approx$ 0,835;
- factorul de absorbţie pentru email negru: $\alpha = 0.9$;
- coeficientul global de transfer termic între colector şi mediul ambiant, *k = 2,5* W/m^2 K;

Din tabelul 1 au rezultat valorile medii înregistrate pentru următorii parametri:

- diferenţa dintre temperatura medie a colectorului şi cea a mediului ambiant: Δt = 22,27°C.
- densitatea fluxului radiaţiei solare globale în timpul experimentărilor: I_g = 335 W/m^2

Din calcul au rezultat:

- randament optic: η_0 = 75%;
- randamentul mediul al colectorilor solari în ziua experimentărilor: $\eta = 58\%$.

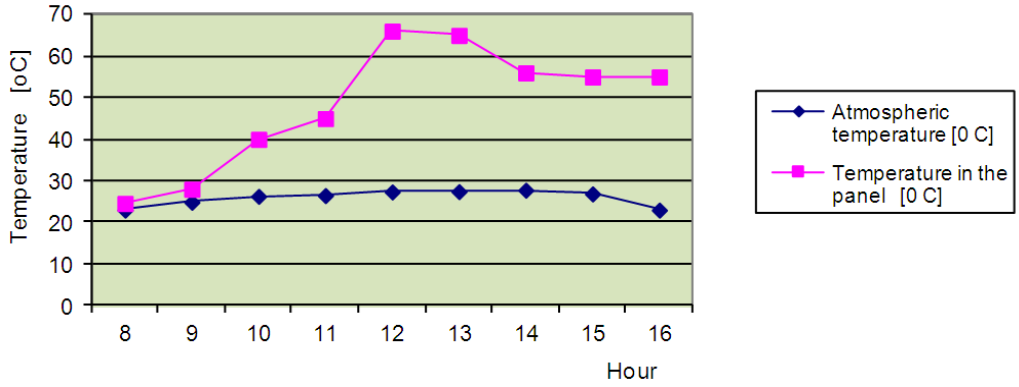

Fig.3 - The air temperature variation in the atmosphere and solar sensors

The temperature and air humidity variation of the solar panel according to the atmospheric parameters are shown in Figures 3 and 4.

Variaţia temperaturii şi umiditatii aerului din panoul solar în funcţie de parametrii atmosferici este arătată în figurile 3 şi 4.

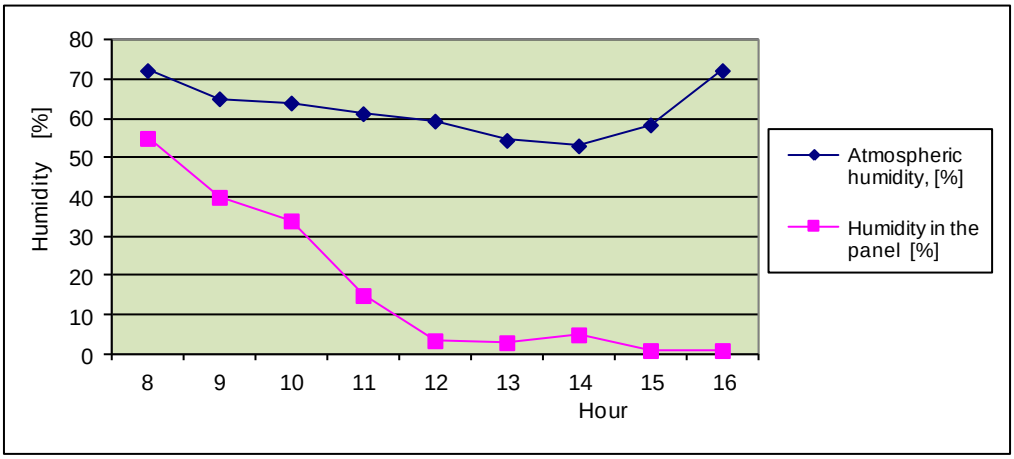

Fig.4 – The atmospheric humidity variation and solar sensors

During fodder ventilation by air heated in solar collectors studied, the installation axial fan absorbs the air, leads it through tube system to the drying platform levelling chamber, from where air penetrates into the fodder mass through the grating of drying platform and ventilating channels designed for this purpose.

The solar panel air velocities at different times of ventilation are shown in Table 2.

În timpul ventilării furajelor cu aerul încalzit în captatorii solari studiaţi, ventilatorul axial al instalaţiei absoarbe aerul, îl dirijeaza prin tubulaturi în camera de uniformizare a platformei de uscare, iar de aici pătrunde în masa de furaje prin grătarul-plasă al platformei de uscare şi canalele de ventilare special amenajate pe platforma de uscare.

Vitezele aerului în panoul solar în diverse momente ale ventilării sunt prezentate în tabelul 2.

Table 2

The panel air velocities during the ventilating process

Parameter	Hour			
	8	10	12	14
Air speed [m/s/]	1.61	1.71	1.84	1.84
Air speed when entering the panel [m/s/]	2.4	2.5	2.4	2.4
Air speed when leaving the panel [m/s/]	2.5	2.5	2.4	2.5

CONCLUSIONS

After the researches, the following appreciacions and conclusions can be formulated:

- In order to reduce hay qualitative and quantitative losses, determined by long time exposure to sun and atmospheric factors after mowing and leaves losses by shaking, the technology of gathering the fodder on field at 35-45% humidity, their storing in special dryers or hay special stores and the final drying up to appropriate conservation humidity (about 18%) by warm air ventilation, were assured;

CONCLUZII

În urma cercetărilor se pot formula următoarele concluzii şi aprecieri:

- Pentru reducerea pierderilor calitative şi cantitative ale fânului, datorate expunerii îndelungate la factorii atmosferici după cosire şi pierderilor de frunze prin scuturare s-a introdus tehnologia de strângere a furajelor din câmp la umidităţi de 35…40%, depozitarea acestora în uscătoare sau fânare speciale şi definitivarea uscării până la umiditatea de păstrare (cca.18%) prin ventilare cu aer rece sau cald;

- For small farms has been achieved and studied the hay drying installation by ventilating the air heated in panel comprising the solar collectors, for reducing the electric and mechanical energy consumption;
- Temperature in panel is influenced by solar radiation and atmospheric air temperature. Analyzing the panel temperature increasing indicator, it has been found that between 8..9 hours the temperature raises up to 3°C, and between 10…16 hours the temperature reaches up to 39°C. Maximum values are registered within 14-16 hour interval;
- The solar panel construction and ventilation installation make the air speed in the panel to be almost steady during ventilation process;
- The average yield of the solar panel , η=58%, is within the values indicated in the literature;
- The solar panel studied assures the heated air necessary to achieve the hay dehydrating by ventilation

Acknowlegement

Paper is financed by MADR – Sectoral Programme ADER 2020, Financing Contract no.65/2011.

REFERENCES

[1]. Balan M., (2007) - *Renewable energy*, UT PRES Publishing, ISBN: 978-973-662-350-9, Cluj Napoca Romania, http://www.termo.utcluj.ro/regenerabile/;
[2]. Hermenean I., Mocanu V. (2008) - *Technologies, machines and installations for pasture fodder harvesting and conservation as hay*, Transilvania University Publishing, Braşov;
[3]. Horrocks R.D., Vallentine J.F., (1999) - *Field-Harvesting Hay* - chapter 13, Harvested Forages, pp. 245-277;
[4]. Horrocks R.D., Vallentine J.F., (1999) - *Processing and Storing Hay* - chapter 16, Harvested Forages, pp. 315–323;
[5]. Neculăiasa V., Dănilă I. (1995) - *Working processes and harvesting machines*, Publishing "A92", Iaşi;
[6]. Nedelcu A, Lazăr G., Dragan R., Ciobanu V. (2012) - *Dimensioning IVF-0 installation for fodder plants drying by air ventilation*, ACTA TECHNICA CORVINIENSIS - BULLETIN of ENGINEERING, fascicle V, ISSN 2067 - 3809;
[7]. Mănişor P., Bălan V. (1991) - *Technologies and equipment for bulk fodder valorisation in industrial flow,* CERES Publishing, Bucharest;
[8]. M.A.D.R. (2010) - *Systems designed to store fodder. Farm standards*.
[9]. Rusănescu C.O., Paraschiv G., Murad E., Duţu M.F. (2013), *Monitoring Solar Radiation Intensity With Sun-Earth Angle In The Year 2011 In The North West Of Bucharest,* INMATEH - Agricultural Engineering, Vol.40. No.2, pp. 97...102;
[10]. Yang D.J., Yuan Z.F., Lee P.H., Yin H.M. (2012) - *Simulation and experimental validation of heat transfer in a novel hybrid solar panel*, Original Research Article, International Journal of Heat and Mass Transfer, Volume 55, Issue 4, 3, pp. 1076-1082;
[11]. Zhong Hao., Guihua Li., Runsheng T., Wenli D. (2011) - *Optical performance of inclined south - north panels three-positions related tracked*, Energy. The International Journal Volume 36, Issue 2, February, pp.1171 - 1179.

- Pentru fermele mici s-a realizat şi studiat instalaţia de uscare a fânului prin ventilare cu aer încălzit în panou realizat din captatoare solare, pentru reducerea costurilor sub aspectul consumului de energie electrică sau mecanică;
- Temperatura din panou este influenţată de radiaţia solară şi temperatura aerului atmosferic. Analizând indicatorul de creştere a temperaturii în panou, se constată că între orele 8..9 creşterea temperaturii este de cca.3°C, iar între orele 10…16 cu până la 39°C. Valorile maxime s-au înregistrat în intervalul orar 14…16;
- Construcţia panoului solar şi instalaţia de ventilare fac ca în panou viteza aerului sa fie aproape constantă în procesul de ventilare;
- Randamentul mediu al panoului solar, η=58%, se incadrează in valorile indicate de literatura de specialitate;
- Panoul solar cercetat asigură aerul cald necesar definitivării uscării fânului prin ventilare.

Recunoaştere

Lucrarea este finanţată de către MADR - Program Sectorial ADER 2020, Contract de finanţare nr.65/2011.

BIBLIOGRAFIE

[1]. Balan M. (2007) - *Energii regenerabile*, Editura UT PRES, ISBN: 978-973-662-350-9, Cluj Napoca Romania, http://www.termo.utcluj.ro/regenerabile/;
[2]. Hermenean I., Mocanu V. (2008) - *Tehnologii, maşini şi instalaţii pentru recoltarea şi conservarea sub formă de fân a furajelor de pe pajişti*, Editura Universităţii Transilvania din Braşov;
[3]. Horrocks R.D, Vallentine J.F., (1999) - *Domeniul-Recoltarea fânului* - cap. 13, Recoltarea furajelor, pag. 245 - 277;
[4]. Horrocks R.D., Vallentine J.F., (1991) - *Prelucarea şi depozitarea fânului* - cap. 16, Recoltarea furajelor, pag. 315 – 323;
[5]. Neculăiasa V., Dănilă I. (1995) - *Procese de lucru şi maşini agricole de recoltat*, Editura A92, Iaşi;
[6]. Nedelcu A, Lazăr G., Dragan R., Ciobanu V. (2012) - *Dimensionarea instalaţiei IVF-0 pentru uscarea plantelor ierboase prin ventilare cu aer*, ACTA TECHNICA CORVINIENSIS – BULLETIN of ENGINEERING, fascicul V, ISSN 2067-3809;
[7]. Mănişor P., Bălan V. (1991) - *Tehnologii şi utilaje pentru valorificarea furajelor de volum în flux industrial,* Ed. CERES, Bucureşti;
[8]. M.A.D.R. (2010) - *Sisteme pentru depozitarea furajelor. Standarde de fermă*;
[9]. Rusănescu C.O., Paraschiv G., Murad E., Duţu M.F. (2013) - *Monitorizarea intensităţiii radiatiei solare in anul 2011 in partea de nord-vest a orasului bucuresti cu ajutorul unghiurilor soare-pământ,* INMATEH - Agricultural Engineering, vol.40, .nr.2, pag. 97...102;
[10]. Yang D.J., Yuan Z.F., Lee P.H., Yin H.M. (2012) - *Simulare şi validarea experimentală a transferului de căldură într-un nou panou solar hibrid,* Articol de cercetare originala, Jurnalul International de Transfer de căldură şi masă, volumul 55, nr. 4, 3, pag.1076 – 1082;
[11]. Zhong Hao., Guihua Li., Runsheng T., Wenli D. (2011) - *Performanţă optică a unor panouri solare înclinate sud-nord urmărite dupa trei directii,* Energie, Jurnal International, vol.36, nr.2, februarie, pag.1171 - 1179.

CONTRIBUTIONS TO THE MODELING AND SIMULATION OF HYDRAULIC SERVOSYSTEMS FOR TRACTORS AND AGRICULTURAL MACHINERY

CONTRIBUŢII LA STUDIUL MODELĂRII ŞI SIMULĂRII SERVOMECANISMELOR HIDRAULICE PENTRU TRACTOARE ŞI MAŞINI AGRICOLE

Ph.D. Stud. Eng. Anghel Stelian
- P. U. Bucharest – Faculty of Biotechnical Engineering Systems – Romania –
Tel: 0726342501; E-mail: stelica_anghel@yahoo.com (Str. Dorobanti Nr.2, bl. F 26, et. 1, ap. 5, Buzau)

Abstract: *The purpose of this study is to achieve, in general, modeling and simulation of hydraulic servosystems, encountered in tractors and agricultural machinery. Due to their compact design and good controllability, position-controlled hydraulic servo drives are used in the automation of a great number of agricultural machines . The analysis starts from the functional model and then the simulation model is built using a specialized software. The paper demonstrates that the simulation software SimulationX can be effectively used to investigate complex problems of hydraulic drive structures in relation to the mechanical elements and the control loop in early development stages of new hydraulic systems. The graphically-interactive and object-oriented concept of SimulationX facilitates a friendly modeling and quick analysis of technical systems for the user.*

Keywords: *hydraulic servo drive, closed - loop system, simulation software, piston stroke, pump, control valve, relief valve*

INTRODUCTION

The theoretical and experimental research of the elements of hydraulic systems represents the fundamental components of their analysis and synthesis realised in order to know the performances of static and dynamic quality. Experimental analysis is preponderant especially, when the system is known, and the theoretical (analytical) analysis for the case where the synthesis is done (system design).

The direct study of a system is more difficult to be carried out because of high cost or because it does not exist, but that is to be designed and carried out. For this reason the modeling is used. The model of a real system is also a system that presents analogies with the system modeled, on which basis conclusions on some properties of the real system can be drawn.

The description of the instructions for behavioral data generation, as well as a description model of a system, assume the existence and the use of a certain language. It may be a natural language, a mathematical language or a programming language, depending on which the model described may be called informal model, mathematical model (formal) or simulation model.

Possessing a number of advantages, numerical simulation has established itself in recent years, especially after elaboration and implementation of simulation languages, which allow rapid simulation of the operation of any system whose mathematical model for the operation in dynamic regime is known [1]. The paper presents the mathematical models of some major components of hydraulic systems [6].

Hydraulic motor model

In developing mathematical model for linear hydraulic model, it starts from the shape in fig.1, comprising the loading scheme and multivariable model of fig.2.

Rezumat: *Scopul acestui studiu este de a realiza, in general, modelarea şi simularea unor servomecanisme hidraulice, întâlnite la tractoare şi maşini agricole. Datorită configuraţiei lor compacte şi bunei maniabilităţi, servomecanismele hidraulice cu controlul poziţiei sunt utilizate în automatizarea unui mare număr de maşini din agricultura. Analiza pleacă de la modelul funcţional şi se construieşte apoi modelul de simulare cu ajutorul unui program specializat. Studiul demonstrează că programul de simulare SimulationX poate fi utilizat efectiv pentru a investiga problemele complexe ale structurilor transmisiilor hidraulice în raport cu elementele mecanice şi bucla de comandă în stagiile premergătoare de dezvoltare a unor noi sisteme hidraulice. Conceptul grafic-interactiv şi orientare pe obiect al lui SimulationX facilitează utilizatorului o modelare accesibilă şi o analiză rapidă a sistemelor tehnice.*

Cuvinte cheie: *servomecanism hidraulic, sistem buclă închisă, program de simulare, cursa pistonului, pompă, distribuitor, supapă de siguranţă,*

INTRODUCERE

Cercetarea teoretică şi experimentală a elementelor sistemelor hidraulice reprezintă componentele fundamentale ale analizei şi sintezei acestora realizată în scopul cunoaşterii performanţelor de calitate statice şi dinamice. Analiza experimentală este preponderentă în special atunci când sistemul este cunoscut, iar cea teoretică (analitică) pentru cazul când se face sinteza (proiectarea sistemului).

Studierea directă a unui sistem real este mai dificilă de realizat din cauza costului ridicat sau pe motiv că acesta nu există, că urmează a fi proiectat şi realizat. Pentru acest motiv, se recurge la modelare. Modelul unui sistem real este la rândul lui un sistem ce prezintă analogii cu sistemul modelat, pe baza cărora se pot trage concluzii asupra unor proprietaţi ale sistemului real.

Descrierea instrucţiunilor de generare a datelor comportamentale, precum şi descrierea modelului unui sistem, presupun existenţa şi utilizarea unui anume limbaj. Acesta poate fi un limbaj natural, limbaj matematic sau un limbaj de programare, în funcţie de care modelul descris poate fi denumit model neformal, model matematic (formal) sau model de simulare.

Posedând o serie de avantaje, simularea numerică s-a impus în ultimii ani, mai ales după elaborarea şi implementarea limbajelor de simulare, care permit simularea rapidă a funcţionarii oricărui sistem la care este cunoscut modelul matematic de funcţionare în regim dinamic [1]. În cele ce urmeaza sunt prezentate modelele matematice ale unor componente importante ale sistemelor hidraulice [6].

Modelul motorului hidraulic

In elaborarea modelului matematic pentru motorul hidraulic liniar, se porneşte de la schiţa din fig.1, cuprinzând schema de încărcare şi modelul multivariabil din fig.2.

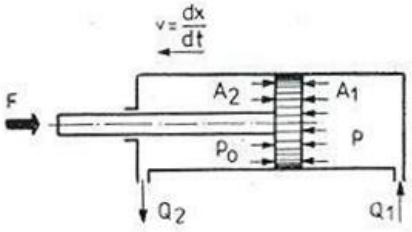

Fig.1 - The loading diagram

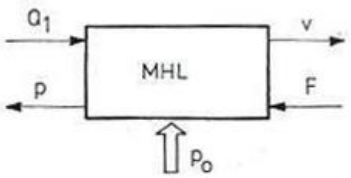

Fig.2 - Linear hydraulic motor model

In figures above, it is noted: F - strength force in [N]; A_1 and A_2 - active areas of the piston $[m^2]$; Q_1, Q_2 - input flow-rates ,or output flow rate $[m^3/s]$; p and p_0 - the input instantaneous pressures, respectively output ones $[N/m^2]$; M - the mass(reduced to piston rod) [kg].

Starting from the equation of rates and moments the mathematical model of linear motor operating in dynamic stage is written (without Q_2's equation) in the form:

In figurile de mai sus s-au notat: F – forţa rezistentă în [N]; A_1 si A_2 - ariile active ale pistonului $[m^2]$; Q_1, Q_2 - debitele de intrare, respectiv de ieşire $[m^3/s]$; p si p_0 - presiunile instantanee de intrare, respectiv de ieşire $[N/m^2]$; M - masa (redusă la tija pistonului) [kg].

Plecând de la ecuaţia de debite şi momente, se scrie modelul matematic de funcţionare a motorului liniar în regim dinamic (fară ecuaţia lui Q_2) sub forma:

$$Q_1 = \frac{dx}{dt}\cdot A_1 + a_M(p - p_0) + \frac{V_0 + x\cdot A_1}{E}\cdot\frac{dp}{dt} \quad (1)$$

$$M\cdot\frac{d^2x}{dt^2} + b_M\cdot\frac{dx}{dt} + c_{fp}\cdot\frac{x}{|x|}\cdot(A_1\cdot p - A_2\cdot p_0) + F = p\cdot A_1 - p_0\cdot A_2 \quad (2)$$

Where a_M is the linearised coefficient of the loss of flow to the piston, proportional to the pressure $[(m^3/s)/N/m^2)]$; V_o - the initial volume of liquid in engine chamber under the pressure p $[m^3]$; b_M - the linearised coefficient of losses of forces proportional to speed [$N/(m/s)$]; c_{fp} - coefficient of dry friction (adimensional).

To avoid the nonlinearity originating from the product of two variables, namely the factor $\frac{v_o + x\cdot A_2}{p}\cdot\frac{dp}{dt}$, the following replacement is made:

unde a_M este coeficientul liniarizat de pierderi de debit la piston, proporţionale cu presiunea $[(m^3/s)/N/m^2)]$; V_o - volumul iniţial de lichid aflat în camera motorului sub presiunea p $[m^3]$; b_M - coeficientul liniarizat al pierderilor de forţe proporţionale cu viteza $N/(m/s)$]; c_{fp} - coeficientul de frecare uscată (adimensional).

Pentru evitarea neliniarităţii provenite din produsul a două variabile, este vorba de factorul $\frac{v_o + x\cdot A_2}{p}\cdot\frac{dp}{dt}$, se face înlocuirea:

$$\frac{V_0 + x\cdot A_1}{E} \approx \frac{V_0 + \frac{L}{2}A_1}{E} = \frac{V_0'}{E}, \quad (3)$$

where L is the piston stroke.

In view of the new notations, substituting then $dx/dt=V$ and by applying transformed Laplace, in null initial conditions, the relationship (1) and (2) become:

unde L este cursa pistonului.

Având în vedere noile notaţii, înlocuind apoi $dx/dt=V$ şi aplicând transformata Laplace, în condiţii iniţiale nule, relaţiile (1) si (2) devin:

$$Q_1(s) = V(s)\cdot A_1 + a_M\cdot[p(s) - p_0(s)] + \frac{V_0'}{E}\cdot p(s)\cdot s \quad (4)$$

$$M\cdot V(s)\cdot s + b_M\cdot V(s) + c_{fp}\cdot\frac{x(s)}{|x(s)|}\cdot[A_1\cdot p(s) - A_2\cdot p_0(s)] + F(s) = p(s)\cdot A_1 - p_0(s)\cdot A_2 \quad (5)$$

Control valve model

Being widespread in hydraulic drive systems, discrete manifolds provide connections of the body pressure source to mobile component, or various combinations and connections between pipes, by relative displacement between the spool and the valve body (fig.3) [2].

Modelul distribuitorului hidraulic

Având o largă răspândire în sistemele hidraulice de acţionare, distribuitoarele discrete asigură conexiunile sursei de presiune cu organul motor, sau diverse combinaţii şi legaturi între conducte, prin deplasarea relativă dintre sertar şi corp (fig.3) [2].

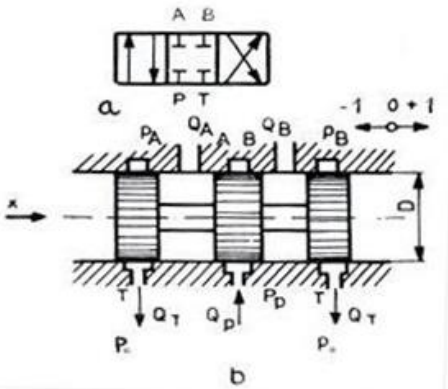

Fig.3 - The scheme of a control valve with three positions

Considering a control valve with three positions with positive coverage (blockage in the middle position) and negligible losses, it results for: $x = +1(P_p \to A,\ B \to T);\ Q_p = Q_A;\ Q_B = Q_T,$
and Ohm's law for turbulent flow (the case most frequently encountered), we can write:

Considerând un distribuitor cu trei poziţii cu acoperire pozitivă (blocaj în poziţie mediană) şi pierderi neglijabile, rezultă, pentru: $x = +1(P_p \to A,\ B \to T);\ Q_p = Q_A;\ Q_B = Q_T,$ iar conform legii lui Ohm pentru curgere turbulentă (cazul cel mai frecvent intâlnit), se poate scrie:

$$P_p - P_A = R \cdot Q_A^2 - R \cdot Q_p^2 \quad (6)$$

$$P_B - P_0 = R \cdot Q_B^2 - R \cdot Q_T^2 \quad (7)$$

For $x = 0$; $Q_A = 0$; $Q_B = 0$ and $Q_T = 0$, and for $x = -1$, $Q_p = Q_B$ and $Q_A = Q_T$, it results:

Pentru $x = 0$; $Q_A = 0$; $Q_B = 0$ şi $Q_T = 0$, iar pentru $x = -1$, $Q_p = Q_B$ şi $Q_A = Q_T$, rezultă:

$$P_p - P_B = R \cdot Q_B^2 = R \cdot Q_p^2 \quad (8)$$

$$P_A - P_0 = R \cdot Q_A^2 = R \cdot Q_T^2 \quad (9)$$

In the above notations and relations was considered, *x = +1* - displacement (opening) from left to right; *x = 0* - middle position (spool not tripped); *x = - 1* – displacement (opening) from right to left; Neglecting the switching time (*0.03 – 0.1 s*) the switching is done outside working phases; *R* is the hydraulic resistance ($R = \rho/2 \cdot C_D \cdot \pi \cdot D \cdot x$); where ρ is the density of the liquid [kg/m^3]; C_D - flow coefficient (dimensionless); *D* – spool diameter [*m*], and *x* – fixed displacement of the spool valve.

Starting from the relationships from the data presented for the case x = +1, abstract model (quadrupole) has the form of fig.4.

În notaţiile şi relaţiile prezentate anterior, s-a considerat, *x = +1*– deplasarea (deschiderea) de la stânga la dreapta; *x = 0* - poziţie mediană (sertar neacţionat); *x = - 1* – deplasare (deschidere) de la dreapta spre stânga. Se neglijează timpul de comutare (*0,03 – 0,1 s*); Comutarea se face în afara fazelor de lucru; *R* este rezistenţa hidraulică ($R = \rho/2 \cdot C_D \cdot \pi \cdot D \cdot x$), unde ρ este densitatea lichidului [kg/m^3]; C_D - coeficient de debit (adimensional); *D* – diametrul sertarului [*m*], iar *x* – deplasarea fixă a sertarului.

Plecând de la datele şi relaţiile prezentate pentru cazul *x* = +1, modelul abstract (cvadripolul) are forma din fig.4.

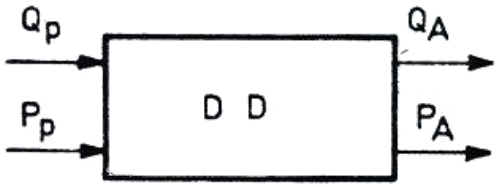

Fig.4 - Hydraulic control valve model

The simulation software used for hydraulic systems is based on functional models of these systems, connecting components to each other and establishing parameters for each component. Modeling can be called as object oriented.

A virtual instrument for modeling and simulation of hydrostatic systems called SimulationX, has been used.

The fluid power models in SimulationX consider extreme nonlinearities such as pressure, temperature, nonlinear valve properties and cavitation, as well as volumetric and mechanical yields.

The fluid power libraries interact with models from *Mechanics*, *Power Transmission* and *Controls*. This permits the simulation of complex multi-physics models [7].

I chose this simulation software for its performance and the existence of a large number of libraries and numerous mechanic elements, control signals, transfer functions etc.

It is true that not all pumps, valves or other devices of hydrostatic category, will be represented by the same mathematical models and consequently the same virtual instruments, but hydrostatic elements with constructive-functional features, in one category or another, will be analyzed with special virtual instruments tailored for the respective particularities. Each virtual instrument of dynamic analysis of a hydrostatic drive, comes with its functional, constructive parameters as input size and the characteristic size as outputs.

Under these circumstances, it appears that it may consider any hydraulic system, based on common

Programele de simulare utilizate pentru sistemele hidraulice se bazează pe schemele funcţionale ale sistemelor respective, conectarea componentelor unul cu celălalt şi stabilirea parametrilor pentru fiecare component. Modelarea poate fi denumită ca fiind orientată pe obiect.

S-a utilizat în acest studiu un instrument virtual pentru modelarea si simularea sistemelor hidrostatice numit SimulationX.

Modelele hidraulice în SimulationX iau în considerare neliniarităţile extreme ale presiunii, temperaturii, proprietăţilor distribuitorului şi cavitaţia, precum şi randamentele volumice şi mecanice.

Biblioteca de simboluri hidraulice interacţionează cu modelele din *Mecanică*, *Transmisii* şi *Control*. Acest lucru permite simularea modelelor multifizice complexe [7].

Am ales acest soft de simulare pentru performanţe şi existenţa unui număr mare de biblioteci şi al unui număr mare de elemente mecanice, semnale de comandă, funcţii de transfer etc.

Este adevarat că nu toate pompele, supapele sau o altă categorie de aparatura hidrostatică, vor putea fi reprezentate prin aceleaşi modele matematice şi implicit aceleaşi instrumente virtuale, dar elementele hidrostatice cu particularităţi constructiv-funcţionale, dintr-o categorie sau alta, vor putea fi analizate cu instrumente virtuale speciale, adaptate particularităţilor respective. Fiecare instrument virtual de analiză dinamică a unui element hidrostatic de acţionare, este însotit de parametrii săi funcţional-constructivi, ca mărimi de intrare şi de mărimile caracteristice corespunzătoare, ca mărimi de ieşire.

În aceste condiţii, reiese că se poate analiza orice sistem hidraulic, pornind de la părţile componente

component parts and entering the corresponding parameters for different types of pumps, control valves, valves, hydraulic cylinders etc.. Another approach may be that approach where it starts from a certain hydraulic scheme, at which index features will be analyzed, modifying afterwards the structure by adding new elements and analyzing index features obtained [3].

MATERIALS AND METHODS

The hydraulic drive system, as shown in figure 5, consists of a hydraulic cylinder and a 4/3 control valve (control element of the control circuit) in a closed position control loop.

For the position control loop in this example, a P-controller is used.

For the modeling of the hydraulic components such as, hydraulic cylinder, 4/3 proportional directional control valve, pressure supply, and reservoir, the corresponding model objects of the *Hydraulics* library of SimulationX are selected and positioned on the worksheet.

The mechanical mass *mass considers* the mass of the piston rod (with rigidly coupled load mass). The weight force of the piston rod and the load mass is performed by an external force.

The position of the rod is measured by a sensor block that takes over the mechanical state values and the mechanical connections. The absolute position of the rod is detected and compared to the command value.The subtraction yields the error signal .

The signal for controlling the valve is obtained in the P controller (proportional amplification of the error signal with the gain factor "*kp*").

Once created the model structure shown in figure, we can enter parameters and activate elements of protocol attributes of the variables which we want to plot after simulation (table 1).

comune şi introducând parametrii corespunzatori pentru diferite tipuri de pompe, distribuitoare, supape, cilindri hidraulici etc. Un alt mod de abordare poate fi acela în care se porneşte de la o anumita schemă hidraulică, la care se vor analiza caracteristicile indiciale, modificându-se apoi structura prin adăugarea unor elemente şi analizând noile caracteristici indiciale obţinute [3].

MATERIALE ŞI METODE

Sistemul de acţionare hidraulică, aşa cum se arată în figura 5, constă dintr-un cilindru hidraulic şi un distribuitor proporţional (element de control al circuitului de comandă), într-o buclă închisă de control al poziţiei.

Pentru bucla de control de poziţie in acest exemplu, este utilizat un controler de tip P (proporţional).

Pentru modelarea componentelor hidraulice, cum ar fi, cilindru hidraulic, distribuitor proporţional 4/3, sursă de presiune, şi rezervor, sunt selectate obiectele corespunzătoare modelului din biblioteca Hidraulică a lui SimulationX şi poziţionate pe foaia de lucru.

Masa mecanică *mass* consideră masa tijei pistonului (cu masa de încărcare cuplate rigid). Forţa de greutate a tijei pistonului şi încărcarea sunt realizate de forţa externă .

Poziţia tijei este masurată de un senzor care preia valorile parametrilor de stare mecanici şi conexiunile mecanice. Poziţia absoluta a tijei este detectată şi comparată cu valoarea de comandă. Diferenţa dă semnalul de eroare.

Semnalul pentru comanda distribuitorului proporţional este obţinut în controllerul de tip P (amplificare proporţională a semnalului de eroare cu factorul "*kp*").
Odată creată structura modelului conform figurii , se pot introduce parametrii elementelor şi se activează atributele de protocol ale variabilelor pe care dorim să le reprezentăm grafic după simulare (tabelul 1).

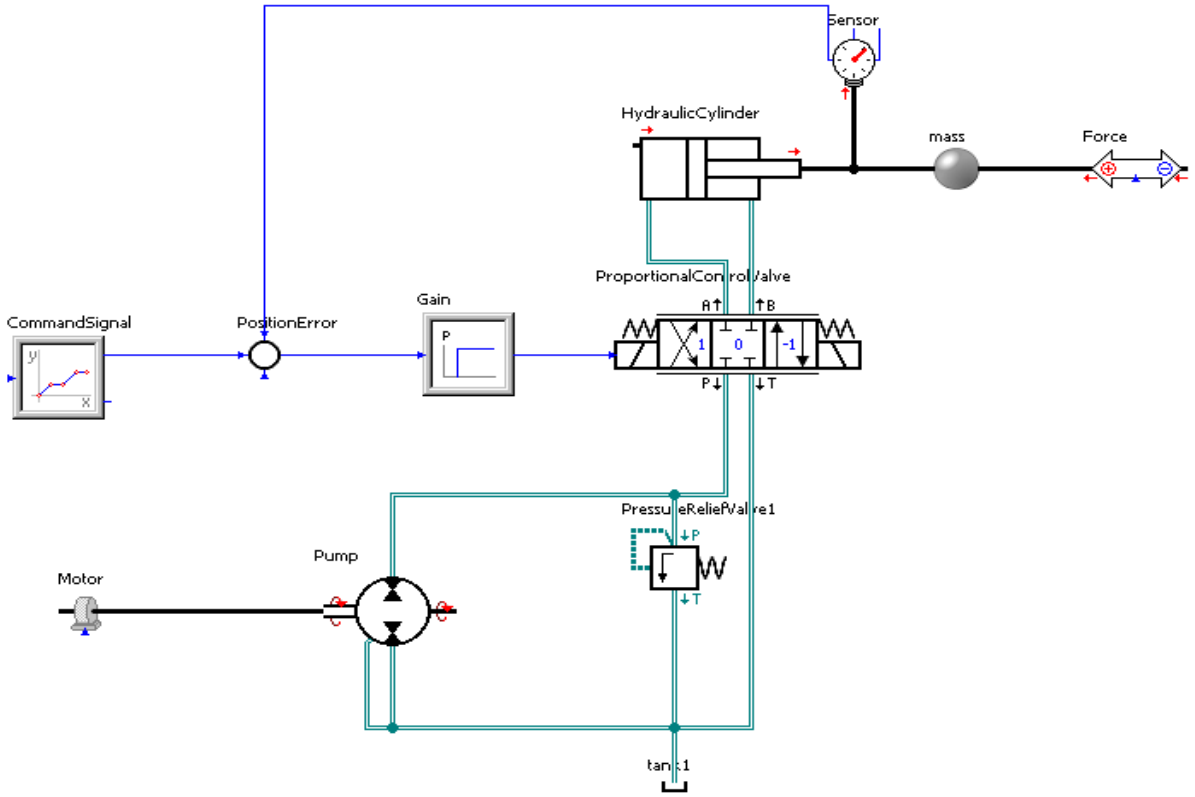

Fig.5 - Model of the hydraulic system

Table 1

Elements Elemente	Input parameters Parametri de intrare
Cilindru Cylinder 	Cylinder Dimensions Maximum Stroke maxStroke: 94 mm Piston Diameter dPiston: 90 mm Rod Diameter dRod: 30 mm Transfer of Coordinates dxh: -47 mm Friction Description cylFriction: No Friction Losses Pressure Chamber A pA: bar Pressure Chamber B pB: bar Pressure Drop A -> B pAB: bar Volume Flow Port A (Meter-in Flow) QA: l/min Volume Flow Port B (Meter-in Flow) QB: l/min
Pompă Pump 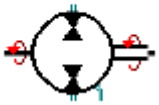	Displacement Volume Vd: 12.6 cm³ Friction Description frKind: No Friction Losses Leakage Description lKind: No Leakage Volume at Port A VA: cm³
ReliefValve 	Pressure Drop P->T pPT: bar Volume Flow (Meter-In Side) Q: l/min Mass Flow mdot: kg/s Power Dissipation Pdiss: kW
Motor 	Kind kind: Rotational Speed Rotational Speed om: 2200 rpm Torque T: Nm Power Pe: Nm/s
ProportionalControlValve 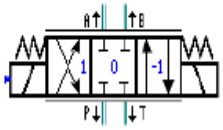	Stroke Signal strokeDescr: Normalized Signal (-1 … 1) Type of Edges edgesEnum: Identical Edges

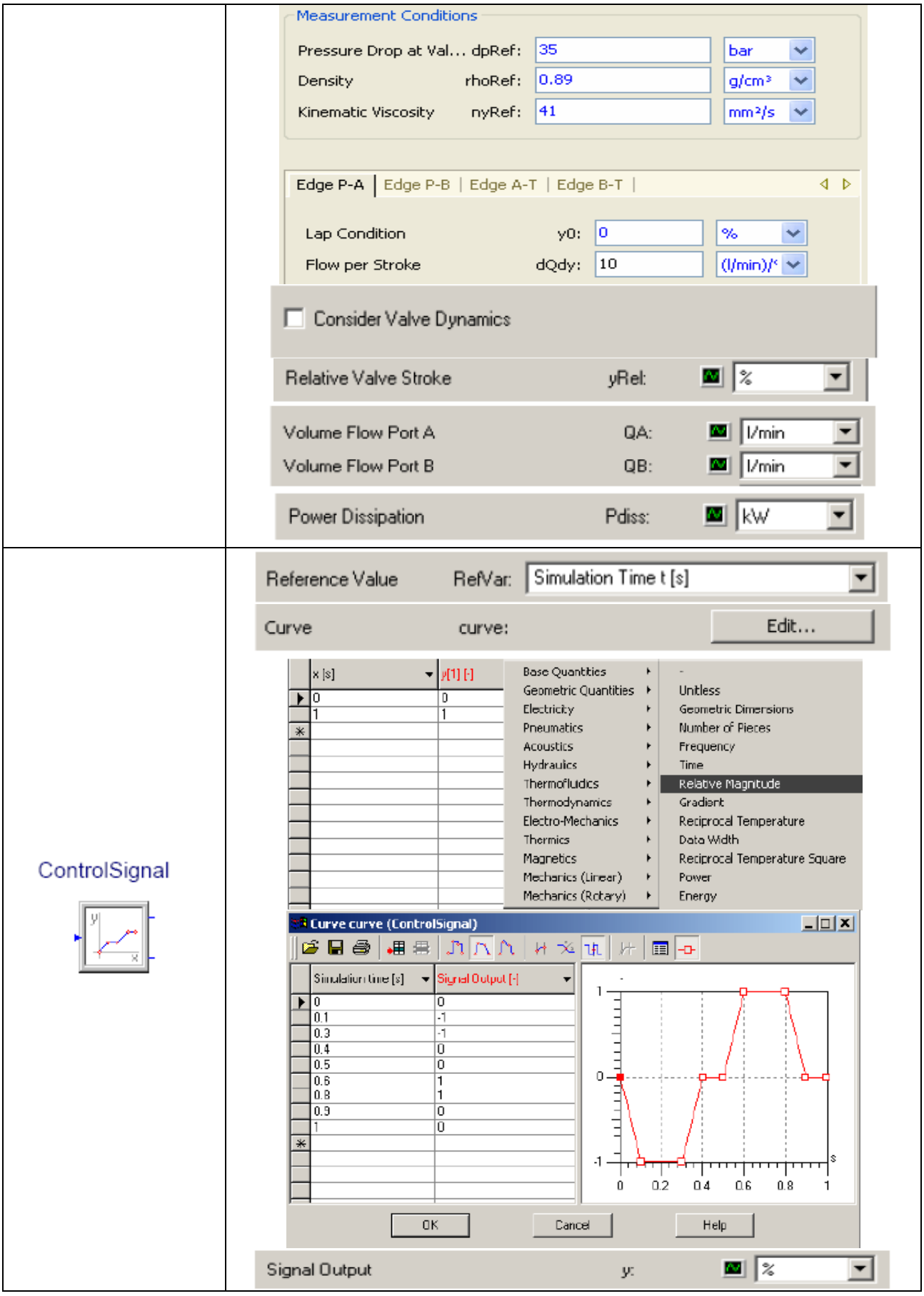

For this simulation we have used the technical characteristics of U -650 M tractor power steering [8]; [9].

Pentru simulare s-au folosit caracteristicile tehnice ale servodirecţiei tractorului U-650 M [8]; [9].

RESULTS

Once we have introduced the model parameters, the simulation may be started and the results can be observed, and, at the same time the type of oil may be changed by double-clicking on the connection and selecting a liquid [5].

The control signal shows the specified characteristics. If the stroke signal for the valve is negative, the pump is connected to port A of the cylinder and the piston is moved to the right.

The flow at port A and B of the valve is somehow proportional to the stroke signal (fig.6):

REZULTATE

Odată ce s-au introdus parametrii modelului, se poate porni simularea şi se pot observa rezultatele, se poate schimba tipul uleiului prin comanda „dublu click" pe conductă şi selectarea uleiului [5].

Semnalul de comandă arată caracteristicile specifice. Dacă cursa distribuitorului este negativă, pompa este conectată la orificiul A al cilindrului şi pistonul este deplasat spre dreapta.

Debitul la orificiile A si B ale distribuitorului este într-o oarecare masură proporţional cu alura semnalului (fig.6):

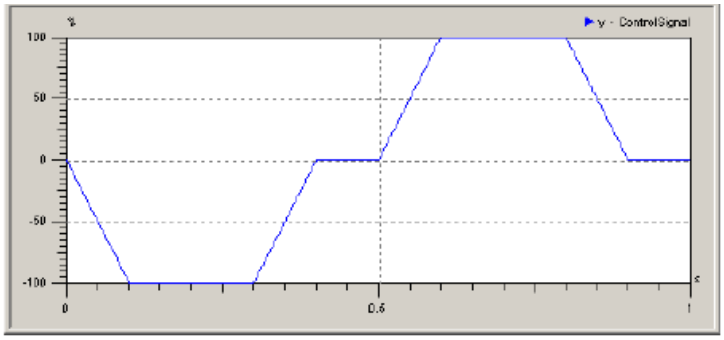

Fig.6 - Shape of the control signal

Because we have a differential cylinder, the flow shows an unsymmetrical behavior. The maximum positive flow can not exceed 10 l/min, which is the flow of the pump (fig.7).

Din cauza faptului că avem un cilindru diferenţial, debitul prezintă un comportament asimetric. Dacă s-a stabilit debitul pompei la 10 l/min, atunci debitul maxim pozitiv nu poate depăşi această valoare (fig.7).

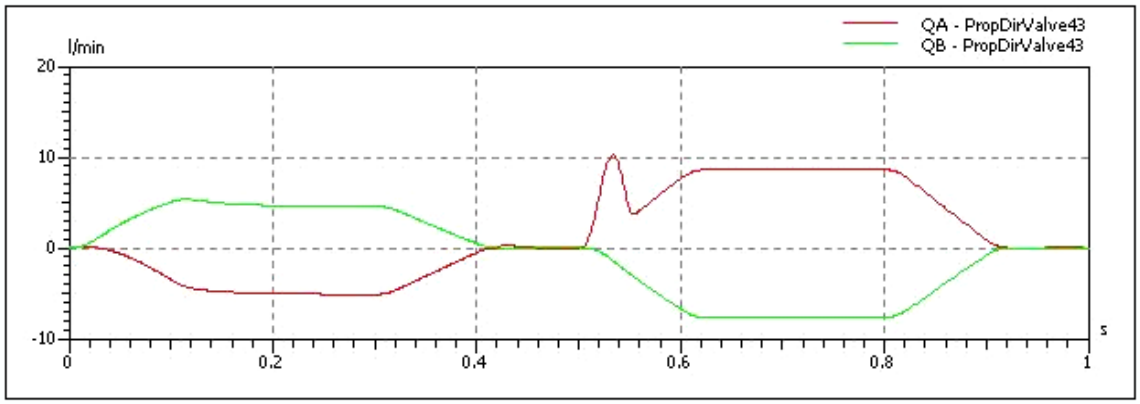

Fig.7 - Variation of proportional directional control valve flow

The pressure can not exceed 100 bar (at the pressure set for the relief valve), and at full negative opening of the control valve, the pump pressure will drop up to 32 bar, since the pump cannot deliver enough flow (fig.8):

Presiunea nu poate să depaşească 100 bar (la presiunea setată pentru supapa de siguranţă), la deschiderea maxima negativă a distribuitorului, presiunea va scădea la 32 bar, deoarece pompa nu poate furniza suficient debit (fig.8):

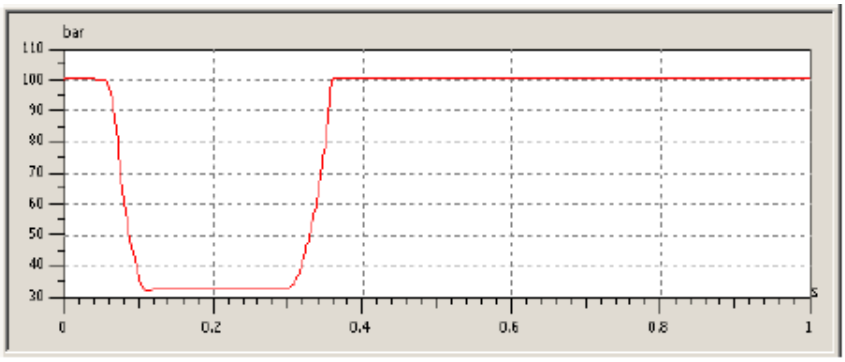

Fig.8 - Variation of pressure in relief valve

The velocity of the piston is proportional to the flow in the valve, and if the pump pressure drops from 100 bar to 32 bar, the velocity also decreases slightly. When the control valve is closed, the piston oscillates because of the oil compressibility noticing that the piston velocity begins to oscillate with high frequency after 0.2 s (fig.9).

From the simulation study made, it was observed that the transitional time ranges between approximately 0.12 s and 4 s. It was noted that the hydrostatic execution elements that provide a translational movement of the load present higher transient periods.

For simulation of the pressure it was chosen a longer time (5 s) to view the corresponding pressure variation for a certain period of operation. If we examine the variation of the pressure in the hydraulic cylinder , we find an oscillation of the front of the stroke due to the oil compressibility.

Likewise, the pressure does not exceed 80 bar which is the maximum pressure of pump (fig.10) .

Viteza pistonului este proporţională cu debitul distribuitorului, iar dacă presiunea pompei scade la 32 bar, viteza va scădea de asemenea. Când distribuitorul este închis, pistonul oscilează din cauza compresibilităţii uleiului, observandu-se că viteza pistonului începe să oscileze cu o frecvenţă inaltă după 0,2 s (fig.9).

Din studiul simulărilor efectuate, s-a observat că timpul tranzitoriu, variază între aproximativ 0,12 s şi 4 s. S-a remarcat că elementele hidrostatice de execuţie, care asigură o mişcare de translaţie a sarcinii, prezintă durate mai mari ale regimului tranzitoriu.

Pentru simularea presiunii s-a ales un timp mai lung (5 s), pentru a putea vizualiza variaţia presiunii corespunzătoare unei anumite perioade de funcţionare. Dacă se examinează variaţia presiunii din cilindrul hidraulic, se constată pe prima parte a cursei o oscilaţie a acesteia datorită compresibilitaţii uleiului.

De asemenea presiunea nu poate depăşi 80 bar care este presiunea maximă a pompei (fig.10).

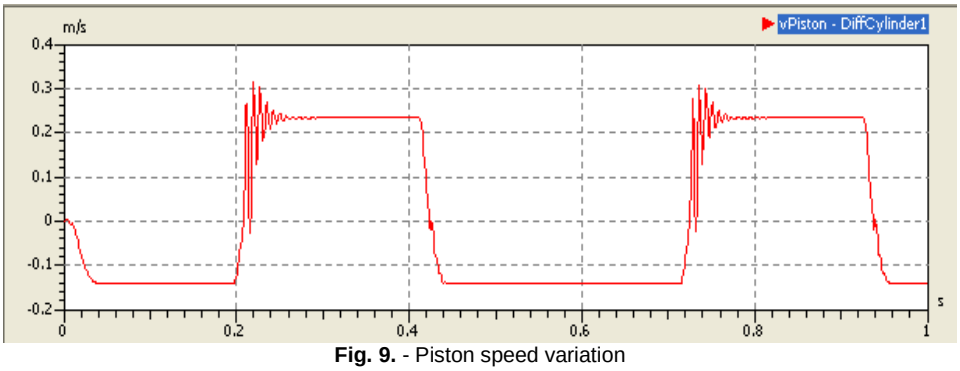

Fig. 9. - Piston speed variation

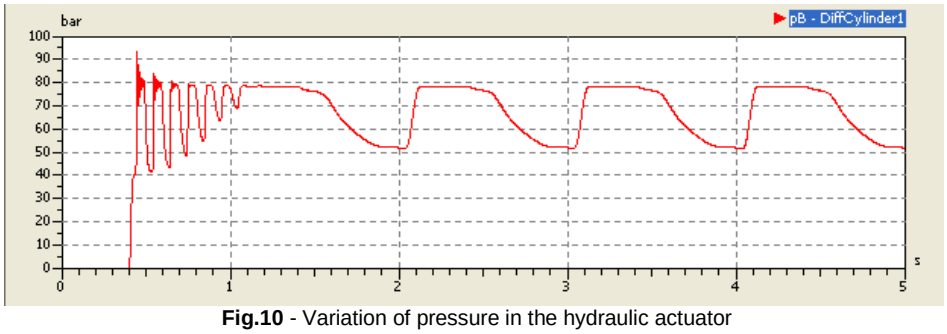

Fig.10 - Variation of pressure in the hydraulic actuator

In this model, the dynamic behavior of the propotional directional control valve has been neglected.It is, therefore desirable to include parameters corresponding to the proportional contol valve (fig.11) [4].

If we restart the simulation with the inclusion of dynamic behavior of the proportional control valve, it will be observed that the system shows a stable state (fig.12 and fig.13).

În acest model s-a neglijat comportarea dinamică a distribuitorului. De aceea este de dorit să includem parametrii corespunzători pentru distribuitorul proporţional (fig.11) [4].

Dacă se porneşte din nou simularea cu includerea comportamentului dinamic al distribuitorului proporţional, se va observa că sistemul arată o stare stabilă (fig.12 si fig.13).

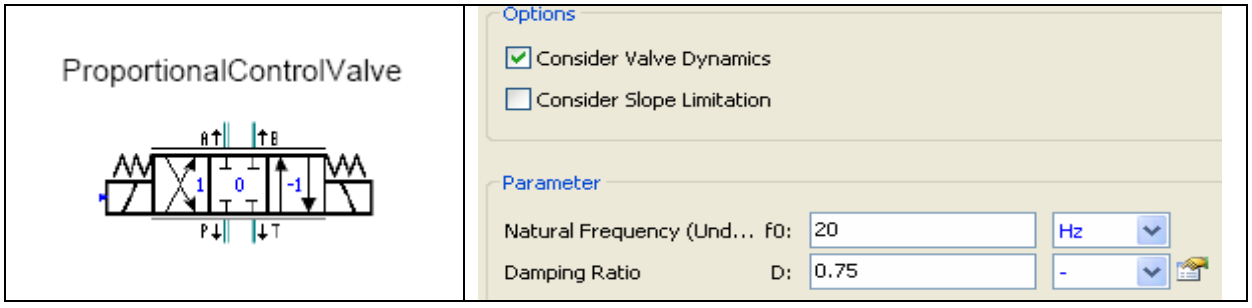

Fig.11 - Consider the dynamic behavior of hydraulic proportional control valve

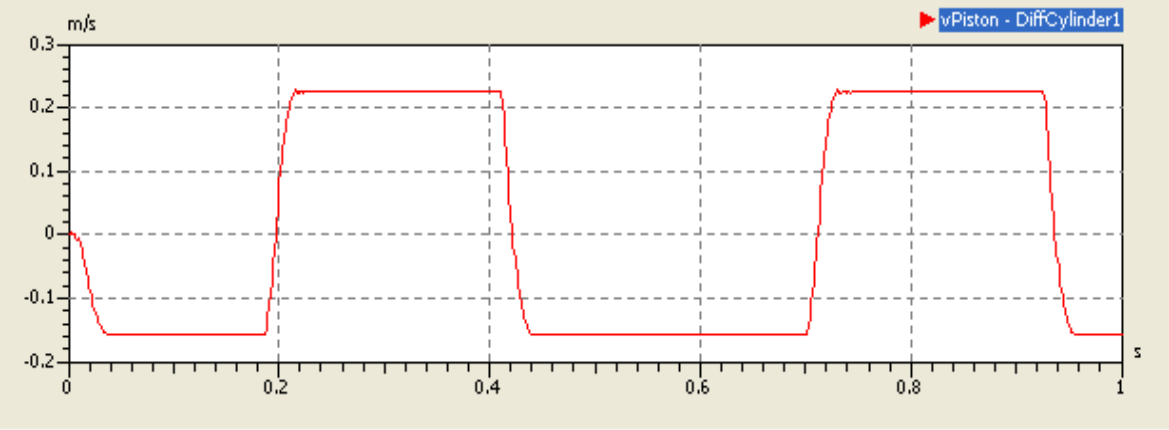

Fig.12 - Piston speed variation considering the dynamic behavior of the proportional control valve

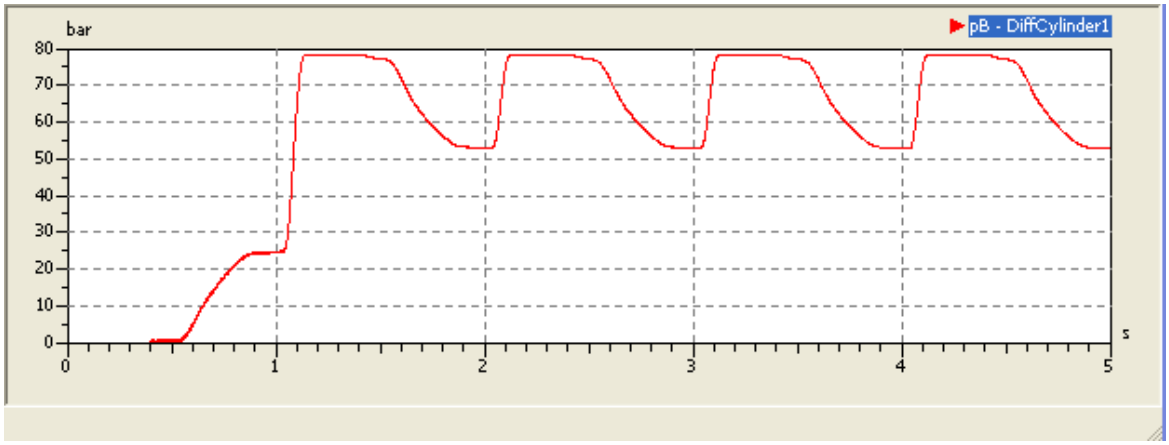

Fig.13 - Hydraulic actuator pressure variation considering the dynamic behavior of the proportional control valve

CONCLUSIONS

In the case of the hydraulic system studied, it was observed an instability of the piston speed , which starts to oscillate with high frequency after 0.2 s , due to oil compressibility .

It has also been observed that in the range 0 to 0.2s, when the maximum negative opening of the proportional control valve pressure drops to 32 bar, the piston speed also decreases .

Folowing the hydraulic actuator pressure variation it has been observed, that in the time interval from 0 to 1 the pressure has large oscillations which occur with greater frequency. This is because the hydrostatic elements that provide a translational movement of the load (such as hydraulic cylinders), show greater transient periods; after about 1 second the varying of the pressure becoming uniform.

If one takes into account the dynamic behavior of the proportional control valve, then the piston speed and cylinder pressure become stable and present an steady variation.

Comparing modern study opportunities with traditional treatment, we can make the following observations:

- Loading elements can be performed in various conditions, operations and requirements being determined as evolution in time as compared with traditional research using static models based on the maximum strength;
- Use of modeling and simulation software offers a simple answer to mathematical issues involved in research.

CONCLUZII

În cazul sistemului hidraulic studiat s-a observat o instabilitate a vitezei pistonului, care au început să oscileze cu o frecvenţă înaltă dupa 0,2 s, datorită compresibilităţii uleiului.

De asemenea s-a observat că în intervalul 0 – 0,2 s când, la deschiderea maximă negativă a distribuitorului, presiunea scade la 32 bar, viteza pistonului scade şi ea.

Urmărind variaţia presiunii în servomotorul hidraulic, pe intervalul de timp 0 – 1 s, presiunea are oscilaţii mari care se produc cu o frecvenţă mare. Acest lucru se datorează faptului că elementele hidrostatice, care asigură o mişcare de translaţie a sarcinii (de tipul cilindrilor hidraulici), prezintă durate mai mari ale regimului tranzitoriu; după aproximativ 1 secundă variaţia presiunii devine uniformă.

Dacă se ţine seama şi de comportamentul dinamic al distribuitorului, viteza pistonului şi presiunea din cilindru devin stabile şi cu o variaţie uniformă.

Comparând posibilitaţile de studiu moderne, cu tratarea tradiţională, rezultă:

- Încărcarea elementelor se poate face în diverse condiţii, funcţionarea şi solicitările fiind determinate ca evoluţie în timp, comparativ cu cercetarea tradiţională care utilizează modelul calculului static, pe baza unor forţe maxime;
- Utilizarea programelor de modelare şi simulare oferă un răspuns simplu la aspectele matematice care intervin în cercetare.

REFERENCES
[1]. Burrows, C. R. - (1998) *Fluid Power Systems – An Academic Perspective*. JHPS Journal of Fluid Power Systems, January 1998, 29(1), pp.26-32;
[2]. DeRose D., - (2003) *Proportional and Servo Valve Technology*, Fluid Power Journal, March/April (2003);
[3]. Jelali M. and Kroll A, - (2003) *Hydraulic Servo Systems - Modelling, Identification & Control*, Springer, 2003;
[4]. Kuo B.C. and Golnaraghi F., - (2003) *Automatic Control Systems*, Wiley, 2003;
[5]. Schwarzenbach J. and Gill K.F., - (1992) *System Modelling & Control*, Edward Arnold, 1992;
[6]. Oprean .A. and others – (1989) *Hydraulic drives and automation* (*modeling , simulation , test*), Technical Publishing House , Bucharest, 1989;
[7]. *** Documentation ITI SimulationX;
[8]. ****Technical documentation Plopeni Mechanical Plant*;
[9]. *** *Technical note of U -650 M tractor*.

BIBLIOGRAFIE
[1]. Burrows, C. R. - (1998) *Sistemele Hidraulice – O Perspectivă Academică*. JHPS Journal of Fluid Power Systems, Ianuarie 1998, 29(1), pag.26-32;
[2]. DeRose D., - (2003) *Tehnologia Distribuitoarelor Proporţionale*, Fluid Power Journal, Martie/Aprilie 2003;
[3]. Jelali M. şi Kroll A, - (2003) *Servomecanisme Hidraulice – Modelare, Identificare şi Control*, Springer, 2003;
[4]. Kuo B.C. and Golnaraghi F., - (2003) *Sisteme de Reglare Automată*, Wiley, 2003;
[5]. Schwarzenbach J. and Gill K.F., - (1992) *Modelarea si Reglarea Sistemelor*, Edward Arnold, 1992.;
[6]. Oprean. A. şi alţii – (1989) *Acţionări şi automatizări hydraulice (Modelare, simulare, încercare),* Editura Tehnică, Bucureşti, 1989;
[7]. *** *Documentaţie ITI SimulationX*;
[8]. *** *Documentaţie tehnică Uzina Mecanică Plopeni*;
[9]. *** *Notiţa tehnică a tractorului U – 650 M*.

RESEARCHES REGARDING APPLES SORTING PROCESS BY THEIR SIZE
/
CERCETĂRI PRIVIND PROCESUL DE SORTARE A MERELOR DUPĂ DIMENSIUNI

Ph.D. Eng. Popa L., Ph.D. Eng. Ciupercă R., Ph.D. Eng. Nedelcu A.,
Ph.D. Eng. Voicu E., Eng. Ştefan V., Eng. Petcu A.
INMA Bucharest / Romania
Tel: 021.269.32.76; E-mail: lucretia_popa@yahoo.com

Abstract: *Article comprises the results of theoretical and experimental researches related to apple sorting process by size. Apple calibration allows to sell them at an appropriate price by dimensional groups, according to standards which define fruits by categories. Apples may be designed to direct consumption (Extra category, I-st Category, II-nd Category) and consumption after being industrially processed (apple jus, apple vinegar, jams etc.). Experimental researches have been performed by means of a sorting equipment with spiral profiling rolls, which operates according to principle of longitudinal movement of fruit under action of rolls and apples falling within the correspondence area between apple size and sorting slot size between the two rolls.*

Keywords: *apples sorting, calibration*

INTRODUCTION

Romania's accession to E.U. has imposed certain responsabilities, among which the compliance to specific norms regarding fresh fruits and vegetables sale, if the producer wants to capitalize his merchandise on a common market [7]. Products traded on these markets should meet certain conditions related to: minimum quality requirements (be whole, sain, without lesions, foreign odour and/or taste, etc.), minimum characteristics of maturity, tolerance (±10% out of products number or weight), origin marking.

As for the calibration the European regulations provide for apples sold for direct consumption a minimum size of 60 mm. In order to guarantee the fruit size homogeneity, it is necessary that the diameter difference between fruits belonging to the same parcel should be limited to ±5 mm for fruits from «Extra» category and for those from I-st and II-nd category presented by rows and superposed layers and to ±10 mm for fruits from I-st category-as bulk, parcel or selling package [8].

The market harsh competition has led to the necessity of sorting the fruits according to European regulations. Romania has complied with these regulations and, therefore the apples sold in stores should fulfil the requirements of regulation [8].

At world level, numerous researches on fruit sorting were achieved [1]…[6], which represent a permanent concern, sorting resulting in homogenous products with greater marketability.

In the context of ones previously mentioned, INMA Bucharest has designed and achieved a sorting equipment for apples by size, designed to subsistence fruit growing farms, namely a profiling rolls equipment.

MATERIALS AND METHODS

Equipment was designed in 3D, by means of SolidWorks program, which allowed the modelling and theoretically determining the rolls position, in order to determine the sorting slots dimensions (fig.1).

Rezumat: *Articolul cuprinde rezultate ale cercetărilor teoretice şi experimentale privind procesul de sortare a merelor după dimensiuni. Calibrarea merelor permite vânzarea acestora la un preţ adecvat pe grupe dimensionale, cunoscându-se faptul că există standarde care definesc fructele pe categorii. Merele pot fi pentru consum direct (categoria Extra, Categoria I, Categoria II) şi pentru consum după industrializare (suc de mere, oţet de mere, gemuri ş.a.) Cercetările experimentale s-au realizat cu ajutorul unui echipament de sortare cu valţuri profilate tip spirală, care funcţionează pe principiul avansului longitudinal al fructelor sub acţiunea valţurilor şi căderii libere a merelor în zona de corespondenţă dintre dimensiunea mărului şi dimensiunea fantei de sortare dintre cele două valţuri.*

Cuvinte cheie*: sortare-calibrare mere*

INTRODUCERE

Intrarea României în U.E. impune anumite responsabilităţi, printre care şi respectarea unor norme specifice privind vânzarea fructelor şi legumelor în stare proaspătă, dacă producătorul doreşte să-şi valorifice producţia în cadrul unor pieţe comune [7]. Produsele comercializate în aceste pieţe trebuie să respecte nişte condiţii privind: cerinţe minime de calitate (întregi, sănătoase, fără boli, fără miros şi/sau gust străin etc.), caracteristici minime de maturitate, toleranţă (±10% din numărul sau greutatea produselor), marcarea originii.

În ceea ce priveşte calibrarea, reglementările europene prevăd pentru merele care se vând pentru consumul direct, un calibru minim de 60 mm. Pentru a garanta omogenitatea de calibru a fructelor se impune ca diferenţa de diametru dintre fructele din acelaşi colet să fie limitată la: ±5 mm pentru fructele din categoria «Extra» şi pentru fructele din categoriile I şi II prezentate pe rânduri şi în straturi suprapuse şi ±10 mm pentru fructele din categoria I prezentate în vrac, în colet sau în ambalajul de vânzare [8].

Concurenţa din ce în ce mai acerbă conduce la necesitatea sortării fructelor conform reglementărilor europene. România s-a aliniat acestor reglementări şi merele care se vând în magazine trebuie să respecte cerinţele din standard [8].

Pe plan mondial s-au efectuat numeroase cercetări privind sortarea fructelor [1]…[6], constituind o preocupare permanentă, sortarea conducând la obţinerea unor produse omogene şi cu vandabilitate mai mare.

În contextul celor prezentate anterior, INMA Bucureşti a proiectat şi realizat un echipament de sortare mere după dimensiuni, destinat fermierilor din fermele pomicole de semi-subzistenţă, echipament cu valţuri profilate.

MATERIALE SI METODE

Echipamentul a fost proiectat în 3D, cu ajutorul programului SolidWorks, ceea ce a permis modelarea şi determinarea teoretică a poziţiei valţurilor, pentru definirea dimensiunilor fantelor de sortare (fig.1).

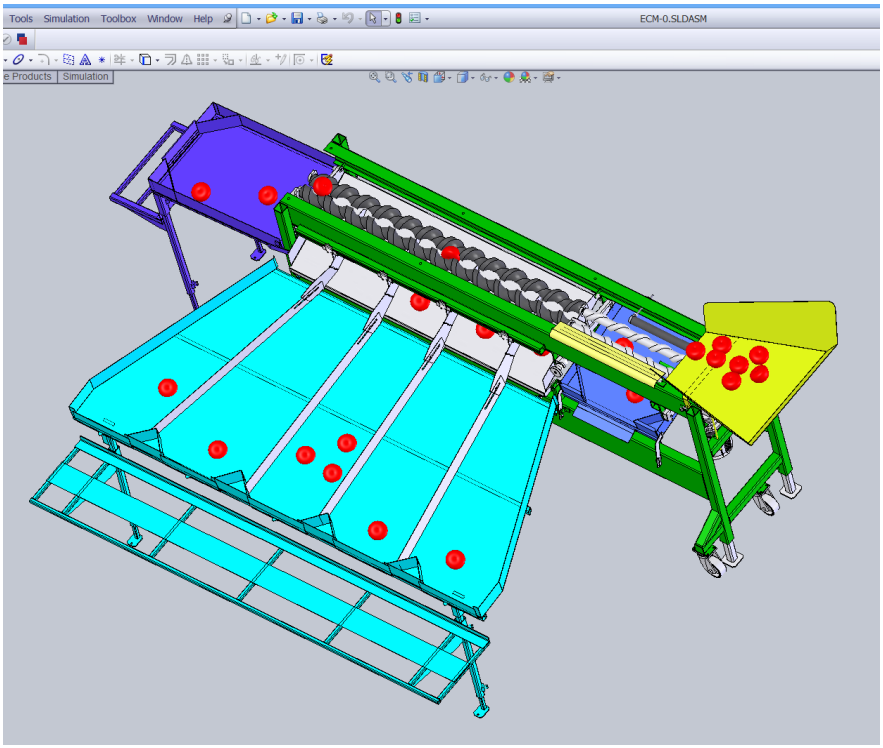

Fig.1 - Echipamentul cu valţuri profilate destinat sortării merelor după dimensiuni

Certain constructive and functional characteristics were determined since the design phase, which were subsequently checked during the testing stages of equipment.

Equipment has been tested both in laboratory and exploitation conditions.

Theoretical determination of sorting capacity

Determination was made by taking into account the main sorts of apples in Romania: Ionathan, Golden Delicious and Idared.

Calculation was made during an ideal feed flow with apples, which is continous and uniform.

In reality, feeding breaks or auxiliary times necessary to load the apples tray, may appear, which determine a smaller real working capacity of this equipment than its theoretical capacity.

Sorting is made from small diameters to bigger ones per 7 sorting groups:

Dimensional sorting groups

- < 60 mm;
- 60…65 mm
- 65…70 mm;
- 70…75 mm;
- 75…80 mm;
- 80…85 mm;
- > 85 mm.

Apples fall on rolls in primary area where sorting of apples which size is less than 60 mm, takes place (fig.1 and fig.2). Then, they are displaced towards central area, by opposite rotation of rolls until they reach the area where the apple dimension is similar to dimension of slot between rolls and they fall on collecting trays. Rolls are disposed at a certain angle, which can be adjusted by changing the supporting bearings position. The apples designed to direct consumption are gathered both on a central and a final tray, where apples over 85 mm size are collected, but which have a smaller share in the apple mass sorted.

Apples with sizes less than 60 mm are intended to be consumed after processing as juice, vinegar, jam etc.

În faza de proiectare, s-au determinat anumite caracteristici constructive şi funcţionale, care au fost verificate ulterior în etapele de testare a echipamentului.

Echipamentul a fost testat atât în condiţii de laborator cât şi în condiţii de exploatare.

Determinarea teoretică a capacităţii de sortare

Determinarea s-a făcut luând în considerare principalele soiuri de mere din România: Ionathan, Golden Delicios şi Idared.

Calculul s-a făcut în condiţiile unui flux ideal de alimentare cu mere, continuu şi uniform.

În realitate, au loc întreruperi ale alimentării, apar timpi auxiliari necesitaţi de încărcarea masei de alimentare cu mere, ceea ce face ca, pentru aceste echipamente, capacitatea de lucru reală să fie mai mică decât cea teoretică.

Sortarea se face de la diametre mici spre diametre mari, pe 7 grupe de sortare:

Grupe dimensionale de sortare:

- < 60 mm;
- 60…65 mm
- 65…70 mm;
- 70…75 mm;
- 75…80 mm;
- 80…85 mm;
- > 85 mm.

Merele cad pe valţuri în zona primară, unde are loc sortarea merelor cu dimensiuni mai mici de 60 mm (fig.1 şi fig.2). Apoi sunt deplasate spre zona centrală, prin rotaţia valţurilor în sensuri opuse, până ce ajung în zona în care dimensiunea mărului coincide cu fanta dintre valţuri şi merele cad pe tăvile de colectare. Valţurile sunt dispuse la un anumit unghi ce se poate regla, prin modificarea poziţiei lagărelor de sprijin. Colectarea merelor pentru consumul direct se face pe masa centrală cât şi pe masa finală, unde sunt colectate merele cu dimensiuni de peste 85 mm dar care au o pondere mai mică în volumul de mere sortat. Merele cu dimensiuni mai mici de 60 mm sunt destinate a fi consumate după procesare sub formă de suc, oţet de mere, gem etc.

RESULTS

Apple specific mass is determined according to structure, texture and chemical composition, elements which at their turn depend on other factors, such as: soil and climate conditions, agro-technique applied, apple ripening level.

From specialty literature it has been found that apples have a specific weight ranged between 0.6512...0.9583 kg/cm^3, their state being able to be variable, an average specific mass of fresh apples being taken into account for calculations.

$$\gamma_{fresh\ apples} \cong 830\ kg/m^3$$

where γ_m =apples specific mass

In order to calculate an apple mass, it has been considered the apples shape, which is not spherical, but there is a ratio *K,* between apple dimension on two perpendicular directions (height and equatorial diameter)*:*

$$K = \frac{H}{D} \quad (1)$$

where:

K is the ratio between the apple dimensions on two perpendicular directions ;

H – apple height, mm

D – apple equatorial diameter , mm.

For the three sorts of apple this ratio has the following values:

Ionathan sort	*K = 0.82…0.86*
Golden sort	*K = 0.90…0.96*
Idared sort	*K = 0.78…0.80*

Following the determinations performed, it has been found that for Golden Delicious sort the ratio between height and diameter is almost unitary, while for the other two sorts, the apple diameter is bigger than its height.

Average mass of an apple was calculated by formula

$$m = \gamma_m \cdot V_{mar} = \gamma_m \cdot \frac{4}{3} \cdot \pi \cdot \left(\frac{D}{2}\right)^3 \cdot K \quad (2)$$

where:

γ_m is apple specific mass

V_{mar} – apple volume;

Following the determinations performed and taking into account an average value of *K* ratio, mass *m for* 1 apple resulted, depending on apple sort and size, according to table 1:

REZULTATE

Masa specifică a merelor este determinată de structură, textură şi compoziţia chimică, elemente care la rândul lor sunt dependente de alţi factori cum sunt: condiţiile pedo-climatice, agrotehnica aplicată, gradul de maturare la care este mărul.

Din literatura de specialitate a reieşit că merele au greutatea specifică cuprinsă între 0,6512...0,9583 kg/cm^3, starea acestora putând fi variabilă, pentru calcule luându-se în considerare o masă specifică medie, pentru merele în stare proaspătă.

$$\gamma_{mere\ proaspete} \cong 830\ kg/m^3$$

unde γ_m =masa specifică a merelor

Pentru calculul masei unui măr, s-a luat în considerare faptul că forma merelor nu este sferică, ci există un raport, *K,* între dimensiunea mărului pe două direcţii perpendiculare (înălţime şi diametru ecuatorial)*:*

unde:

K este raportul dintre dimensiunile mărului pe cele două direcţii;

H – înălţimea mărului, mm

D – diametrul ecuatorial al mărului, mm.

Pentru cele trei soiuri de măr, acest raport are valorile:

Soiul Ionathan	*K = 0,82…0,86*
Soiul Golden	*K = 0,90…0.96*
Soiul Idared	*K = 0,78…0,80*

Din determinările efectuate s-a constatat că la soiul Golden Delicios raportul între înălţime şi diametru este aproape unitar, pe când la celelalte două soiuri, diametrul mărului este mai mare decât înălţimea.

Masa medie a unui măr s-a calculat cu formula:

unde:

γ_m este masa specifică a merelor

V_{mar} - volumul mărului;

Din determinările efectuate, luând în calcul o valoare medie a raportului *K*, a rezultat masa *m* pentru 1 măr, funcţie de soi şi dimensiuni, conform tabelului 1:

Tabel 1

Theoretical mass of an apple according to apple sort and equatorial diameter, *D*

D (mm)	Masa medie pentru 1 măr, *m* (kg)		
	Ionathan	Golden Delicios	Idared
60	0.079	0.087	0.074
65	0.100	0.111	0.094
70	0.125	0.139	0.118
75	0.154	0.170	0.145
80	0.187	0.207	0.176
85	0.224	0.248	0.211

Friction between apples and coils surface is neglectable, as the displacement is made by apples rolling between rolls coils, fig.2, coefficient of rolling friction being almost 0; therefore the apple displacement speed on rolls is equal to axial displacement speed, which depends on rolls rotative speed and coil pitch, according to relation:

Frecarea dintre mere şi suprafaţa spirelor este neglijabilă, deoarece deplasarea se face prin rostogolirea merelor între spirele valţurilor, fig.2, coeficientul de frecare de rostogolire fiind aproape 0, de aceea viteza de deplasare a mărului pe valţuri este egală cu viteza de deplasare axială, care este funcţie de turaţia valţurilor şi de pasul spirei, conform relaţiei:

$$v = \frac{p \cdot n}{60} \quad [\text{mm/s}] \tag{3}$$

where:
v is axial speed, mm/s
p = pitch of coil, mm. *p=120 mm*
n = rolls rotative speed, rot/min. *n=88.7 rot/min*

unde:
v este viteza axială, mm/s
p = pasul spirei, mm. *p=120 mm*
n = turaţia valţurilor, rot/min. *n=88,7 rot/min*

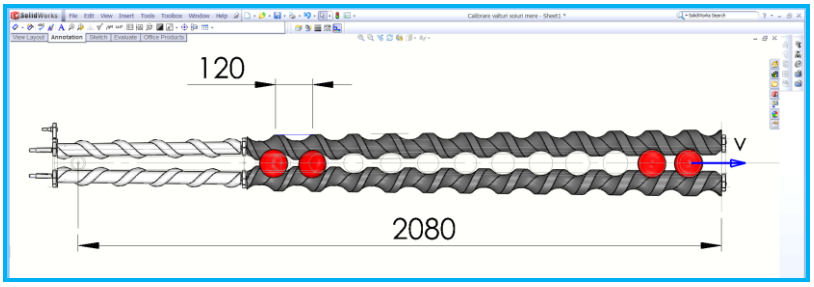

Fig.2 - Scheme of sorting parts of spiral rolls type with profiling surface

Calculations were performed based on certain simplifying hypotheses:
- the apples are considered to be homogenous as size;
- the apples feeding is continuous so that the rolls should be uniformly loaded, an apple being put in each cell.

Time of displacement of an apple on rolls was calculated by formula:

Calculele s-au efectuat luând în considerare anumite ipoteze simplificatoare:
- se consideră că merele sunt omogene ca dimensiune;
- alimentarea cu mere se face continuu, astfel că valţurile sunt încărcate uniform, în fiecare alveolă fiind câte un măr.

Timpul de deplasare a unui măr pe valţuri s-a calculat cu formula:

$$t = \frac{L}{v} \quad [\text{s}] \tag{4}$$

where:
t is apple displacement time to the falling area, [s];
L = space covered by apple from fall on rolls till the sorting area, [mm];
v = axial displacement speed of apple [mm/s]

unde:
t este timpul de deplasare a mărului până la zona de cădere, [s];
L = spaţiul parcurs de măr de la căderea pe valţuri şi până la zona în care este sortat, [mm];
v = viteza de deplasare axială a mărului, [mm/s]

Calibration tolerance

Tolerance of calibration is determined for each dimensional group, as a ratio between the number of products from the plot considered, which have not fulfilled the respective group requirements and the total number of apples collected per dimensional group analyzed, from plots considered, expressed in percentages.

Toleranţa de calibrare

Toleranţa de calibrare se determină pe fiecare grupă dimensională, ca raport între numărul de exemplare din lotul considerat, care nu îndeplinesc cerinţele privind calibrul grupei dimensionale respective şi numărul total de exemplare colectate pe grupa dimensionala analizată, din loturile considerate, exprimat în procente.

$$c = \frac{N_c}{N_g} \cdot 100 \quad [\%] \tag{5}$$

where:
N_c is the number of apples from considered plot, which do not meet the requirements of dimensional group size;
N_g – total number of apples collected per dimensional group analyzed, from the considered plot.

unde:
N_c este numărul de mere din lotul considerat, care nu îndeplinesc cerinţele privind calibrul grupei dimensionale respective;
N_g – numărul total de mere colectate pe grupa dimensională analizată, din lotul considerat.

At the same time, among the apples which do not meet the size requirements of dimensional group analyzed, the number of apples with maximum diameter of equatorial section smaller by, at least 5 mm, comparing to lower limit of respective group, will be noted.

Apples displacement speed on rolls is constant, whatever the apple size is, depending only on rolls rotative speed and coil pitch:

De asemenea, dintre exemplarele care nu îndeplinesc cerinţele privind calibrul grupei dimensionale analizate, se va nota numărul de exemplare cu diametrul maxim al secţiunii ecuatoriale mai mic cu cel puţin 5 mm faţă de limita inferioară a grupei dimensionale respective.

Viteza de deplasare a merelor pe valţuri este constantă, nefiind dependentă de dimensiunile mărului ci doar de turaţia valţurilor şi de pasul spirei:

$$v = \frac{p \cdot n}{60} = \frac{120 \cdot 88.7}{60} = 177.4 \quad \text{mm/s} \tag{6}$$

Replacing the speed value *v* from relation (6) in relation (4), we shall obtain:

Înlocuind valoarea vitezei *v* din relaţia (6) în relaţia (4), vom avea:

$$t = \frac{60 \cdot L}{p \cdot n} = \frac{L}{177.4} \quad [\text{s}] \tag{7}$$

If all apples were over 85 mm, they would cross all the rolls length and be gathered on the final tray.

Time necessary for an apple to cover the whole length of rolls would be t_t and for covering the distance appropriate to a coil pitch- would be t_{1p}:

Dacă toate merele ar avea dimensiuni de peste 85 mm, ar parcurge toată lungimea valţurilor şi ar fi colectate pe masa finală.

Timpul necesar unui măr pentru a parcurge întreaga lungime a valţurilor va fi t_t iar pentru parcurgerea distanţei corespunzătoare unui pas al spirei, timpul necesar va fi t_{1p}:

$$t_t = \frac{2080}{177.4} = 11.73 \text{ s} \quad (8)$$

$$t_{1p} = \frac{120}{177.4} = 0.68 \text{ s} \quad (9)$$

To determine t_t, it was taken into account the total length of the rolls, L_t=*2080 mm,* and for the time t_{1p} it was considered L_{1p}=*120 mm* as time crossed by a coil pitch.

Taking into consideration the average mass of an apple depending on its sort and the results of t_t and t_{1p}, after calculations, the conclusion reached was that the equipment has a theoretical sorting capacity according to table 2, if in each slot of every dimensional group one apple falls.

Pentru determinarea timpului total t_t s-a luat în calcul lungimea totală a valţurilor, L_t=*2080 mm* iar pentru timpul t_{1p} s-a considerat spaţiul L_{1p}=*120 mm*.

Luând în considerare masa medie a unui măr, funcţie de soi precum şi rezultatele timpilor t_t şi t_{1p}, după calcule, s-a ajuns la concluzia că echipamentul are o capacitate teoretică de sortare conform tabelului 2, dacă în fiecare fantă din fiecare grupă dimensională ar cădea câte un măr:

Tabel 2

Theoretical sorting capacity related to apple sort and equatorial diameter, D

Theoretical sorting capacity (kg/h)		
Ionathan Sort	**Golden Delicios Sort**	**Idared Sort**
655	682	580

Values in table 2 are ideal values, which is not in compliance with reality, the apple share within the total volume to be sorted not being uniform.

Experimental researches made with 3 apple sorts, the same which were previously taken into account, have led to results closer to reality.

First, the sorting rolls were adjusted by adjusting the median distance related to dimensional group, the setting being made at the beginning and the end of rolls.

An aspect during the experimental researches is shown in fig.3.

Valorile din tabelul 2 sunt nişte valori ideale, ceea ce în practică nu este real, proporţia merelor în volumul total ce necesită a fi sortat nefiind uniformă.

Cercetările experimentale efectuate cu 3 soiuri de mere, aceleaşi cu cele luate în calcul anterior au condus la nişte rezultate mai apropiate de realitate.

În prealabil s-a făcut reglajul valţurilor de sortare, reglându-se distanţa mediană, aferentă grupei dimensionale, reglajul făcându-se la începutul şi la sfârşitul valţurilor.

În fig.3 se observă un aspect din timpul cercetărilor experimentale.

Fig.3 - Aspect during the experimental researches

The experimental researches found by measurements that the equipment has a real capacity sorting cca.450 kg/h.

As for the calibration tolerance, after having performed the measurements, taking into consideration the equatorial diameter of the apples, the following average results were obtained:

În urma cercetărilor experimentale s-a constatat prin măsurători că echipamentul are o capacitate reală de sortare de cca.450 kg/h.

În ceea ce priveşte toleranţa de calibrare, în urma efectuării măsurătorile după diametrul ecuatorial al merelor, s-au obţinut următoarele rezultate medii:

Tabel 3

Calibration tolerance

Dimensional group [mm]	Quantity [buc]	Quantity from quality category [pcs]	D_{max}-D_{min} from quality category	Quantity not framing within dimensional group [pcs] / [%]	Quantity for which D≤ (Lower limit-5)
60…65	0	0	0	0	0
65…70	5	5	9	3 / 60,0	0
70…75	13	13	6	2 / 15,3	0
75…80	12	12	13	7 / 58,3	0
80…85	6	6	10	1 / 16,6	0
>85	4	4	3	1 / 25,0	0

CONCLUSIONS

After experimental research have drawn the following conclusions:

- It has been found that sorting is not always made by diameter, but by the smallest size between height and diameter, also depending on the apple position in respective area, the manner in which it rotates, so that the sorting should be performed either by diameter or by height, according to their value, or ratio between the two values, H/D.
- A more precise adjustment of rolls slots, as well as an increment of sorting limits should be achieved, having in view the fact that the difference between the maximum limit and minimum limit is of only 5 mm and apples have a random behaviour, which determine a non-eloquent tolerance to calibration.
- Equipment will be useful if the sorting limits are modified, the dimensional groups diminishing up to max.3: <60 mm; 60-85 mm; >85 mm.

REFERENCES

[1]. Nasir M.H.A. (2011) - *Fruit Recognition Based on Color Features*, Technologic University of Malaysia;
[2]. Lee D.J., Archibald J.K.; Xiong G., (2011) - *Rapid Color Grading for Fruit Quality Evaluation Using Direct Color Mapping*, Automation Science and Engineering, IEEE Transactions on Volume:8, Issue: 2, pp.292…302;
[3]. Lee D.J., Chang Y, Archibald J.K., Greco C.G., (2008) - *Color quantization and image analysis for automated fruit quality evaluation*, Automation Science and Engineering, IEEE International Conference, pp.194…199;
[4]. Pla F., Sanchiz J.M., Sánchez J.S., Ugolini N., Diaz M., (2001) - *A machine vision system for on-line fruit colour classification*, Spanish Symposium on Pattern Recognition and Image Analysis;
[5]. Dintwa E., Zeebroeck M., Ramon H., Tijskens E., (2008) - *Finite element analysis of the dynamic collision of apple fruit,* Postharvest Biology and Technology No.49 pp.260…276;
[6]. Treeamnuk K., Pathaveerat S., Terdwongworakul A., Bupata C., (2010) - *Design of machine to size java apple fruit with minimal damage,* Biosystems Engineering, No.107, pp.140…148;
[7]. *** - *Regulation (CE) no.1221/2008 of CE regarding the trading standards in fruits and vegetables field*
[8]. *** - *SR 2714:2003 Fresh fruits and vegetables*.

CONCLUZII

În urma cercetărilor experimentale s-au tras următoarele concluzii:

- S-a constatat că sortarea nu se face întotdeauna după diametru, ci după dimensiunea cea mai mică, dintre înălţime şi diametru, depinzând şi de poziţia în care se află mărul în spaţiul respectiv, de modul în care s-a rotit, astfel încât este posibil ca sortarea să se facă fie după diametru, fie după înălţime, funcţie de valoarea acestora, de raportul între cele două valori, H/D.
- Se impune o reglare mai precisă a deschiderii valţurilor precum şi creşterea limitelor de sortare, având în vedere că diferenţa între limita maximă şi cea minimă este doar de 5 mm iar comportamentul merelor s-a dovedit unul aleatoriu, ceea ce face ca toleranţa la calibrare să nu fie elocventă.
- Echipamentul poate fi util dacă se modifică limitele de sortare reducându-se grupele dimensionale la max.3: <60 mm; 60-85 mm; >85 mm.

BIBLIOGRAFIE

[1]. Nasir M.H.A. (2011) - *Recunoaşterea fructelor după catacteristicile de culoare*, Univ. Tehnologică din Malaezia;
[2]. Lee D.J., Archibald J.K., Xiong G., (2011) - *Sortarea rapidă după culoare pentru evaluarea calităţii fructelor prin utilizarea mapării directe după culoare*, Automatizare şi Inginerie, Lucrările IEEE Volum 8, Nr.2, pag.292…302;
[3]. Lee D.J., Chang Y., Archibald J.K., Greco C.G., (2008) - *Cuantificarea culorii şi analiza imaginii pentru evaluarea automată a calităţii fructelor*, Conferinţa Internaţională IEEE, pag.194…199;
[4]. Pla F., Sanchiz J.M., Sánchez J.S., Ugolini N., Diaz M., (2001) - *Un sistem de vizualizare pentru clasificarea on-line a fructelor după culoare*, Simpozionul Spaniol Pentru Recunoaşterea Formei şi Analiza Imaginii;
[5]. Dintwa E., Zeebroeck M., Ramon H., Tijskens E., (2008) - *Analiza prin metoda elementelor finite a coliziunii dinamice a merelor,* Biologia şi Tehnologia Post-recoltare No.49, pag.260…276;
[6]. Treeamnuk K., Pathaveerat S., Terdwongworakul A., Bupata C., (2010) - *Proiectarea unei maşini pentru sortarea după dimensiuni a merelor Java, cu vătămări minime,* Ingineria Biosistemelor, Nr.107, pag.140…148;
[7]. *** - *Regulamentul (CE) nr.1221/2008 al CE în sectorul fructelor şi legumelor privind standardele de comercializare;*
[8]. *** - *SR 2714:2003 Fructe şi legume proaspete.*

HIGH –SPEED CONVEYOR PARAMETERS OPTIMIZATION / *ОПТИМІЗАЦІЯ ПАРАМЕТРІВ ШВИДКОХІДНИХ ТРАНСПОРТЕРІВ*

B. M. Hevko, O.L. Lyashuk, L.R.Rohatynska, Y.M. Tarasyuk
Ternopil Ivan Pul'uj National Technical University, Ruska str., 56, Ternopil, Ukraine
E-mail: Oleg-lashyk@rambler.ru

Abstract: *The procedure of high-speed conveyers optimization based on nonlinear problem where the minimization of materials consumption of high-speed spiral conveyors is achieved at initial absolute choice of kinematic and dynamic parameters minimizing the conveyor power capacity is developed.*
The parameters change is restricted by range of definition, represented by generalized function. The calculation procedure of rational constructional parameters and conveyors-mixers operating regimes is developed. It consists of ten main stages including derived analytical dependences.

Key words: *vertical screw (spiral) conveyor, optimization, objective (target function), constraints function.*

INTRODUCTION

Screw conveyors are getting more and more widespread in manufacturing processes dealing with granular material transporting as they are characterized by simple construction, and correspondingly, high reliability, easy use and adjustment when applied in automated systems, environmental friendliness due to their tightness [1],[3],[4],[10]. High-speed conveyors are applied for versatile unloading-loading units aimed at load transporting both on horizontal, inclining and vertical paths. The existing methods of their calculations are based on a number of theoretical and experimental investigations [1],[3],[4],[10], and also on statistical data analysis of their operating results. [1],[2],[3],[4],[9],[10]. The statement and solution of the problem to choose optimal parameters of flexible conveyor providing its material [4], [5] and power [6, 7] consumption minimizing are well known. But this statement doesn't allow to get a solution of optimization problem of screw conveyors as interconnected system.

The problems of different machine parts optimization are considered in the research of A. Hryhorjev [3], B. Hevko, R. Rohatynsky [4], V. Loveikin [6], O. Rohatynska [7], I. Hevko [8] and others. Nevertheless, taking into consideration variety of technological processes and design of screw transporting- technological mechanisms, the problem of optimization needs further study and specification of various parameters having theoretical and practical value.

The purpose of the paper is to develop a complex task of parameter optimization where minimization of material consumption of high-speed screw conveyor is achieved at initial absolute choice of kinematic and dynamic parameters, minimizing the conveyor power capacity.

MATERIALS AND METHODS

The important factor while choosing conveyors for versatile transfer complexes is to determine the sphere of their usage, namely dealing with transportation of certain granular materials. As, according to [7], minimal limit of energy intensity of screw conveyor is defined by coefficient of load friction to spiral surface, then the main

Резюме: *Розроблено методику оптимізації швидкохідних транспортерів на основі нелінійної задачі в якій мінімізація матеріаломісткості швидкохідного гвинтового конвеєрів досягається при попередньому безумовному виборі кінематичних та динамічних параметрів, що мінімізують енергоємність конвеєра.*

На зміну параметрів накладено обмеження які задають область визначення, яка представлена узагальненою функцією. Розроблено методику розрахунку раціональних конструктивних параметрів і режимів роботи конвеєрів змішувачів у вигляді десяти основних етапів з виведеними аналітичними залежностями.

Key words: *вертикальний гвинтовий конвеєр , оптимізація, цільова функція, функції обмеження.*

ПЕРЕДМОВА

Для технологічних операцій переміщення сипкого вантажу велике розповсюдження набули гвинтові конвеєри, які характеризуються простотою конструкції та, відповідно, високою надійністю, простотою в користуванні та легкістю адаптування при використанні в автоматизованих системах, екологічністю використання внаслідок їх герметичності [1],[3],[4],[10]. Для універсальних розвантажувально-завантажувальних комплексів, які призначені для транспортування вантажу, як по горизонтальних, похилих, так і вертикальних трасах, використовують швидкохідні гвинтові конвеєри. Існуючі методи їх розрахунку ґрунтуються на ряді теоретичних та експериментальних досліджень [1],[3],[4],[10], а також аналізі статистичних даних за результатами їх експлуатації [1],[2],[3],[4],[9],[10]. Відомі постановка та розв'язок задачі вибору оптимальних параметрів ГК з умови мінімізації його матеріаломісткості [4], [5] та енергоємності [6, 7]. Проте така постановка не дозволяє отримати розв'язок оптимізаційної задачі гвинтових конвеєрів, як взаємопов'язаної системи.

Питанням оптимізації різних механізмів машин присвячені праці Григор'єва А.М. [3], Гевко Б.М., Рогатинського Р.М. [4], Ловейкіна В.С. [6], Рогатинської О.Р. [7], Гевко І.Б. [8] та інших. Однак, враховуючи різноманітність технологічних процесів і конструктивного виконання ГТТМ, питання оптимізації потребує подальших досліджень і уточнень різних параметрів теоретичного й практичного значення.

Мета роботи є розроблення комплексної задачі параметричної оптимізації в якій мінімізація матеріаломісткості швидкохідного гвинтового конвеєрів досягається при попередньому безумовному виборі кінематичних та динамічних параметрів, що мінімізують енергоємність конвеєра.

МАТЕРІАЛ І МЕТОДИКА

Важливою умовою при виборі конвеєрів для універсальних перевантажувальних комплексів є встановлення області їх використання, зокрема щодо транспортування певного діапазону сипких вантажів. Оскільки, згідно [7], мінімальна межа енергоємності гвинтових конвеєрів визначається коефіцієнтом тертя вантажу до поверхні спіралі,

requirement of conveyor design is its ability to transport load under unfavorable conditions. In such a case we'll consider the most unfavorable, for power consumption purpose, is vertical position of screw conveyor.

Efficiency of load transportation by screw conveyors, according to [1], [3], [10], is determined by the dependence $N=\rho_\pi g Q (W_L L+H)$, either for vertical screw $N=\rho_\pi g Q W_H$ where ρ_π - volume mass (bulk density) of load in flow; g- gravity acceleration; Q- conveyor volume output; W_L and W_H - coefficient of resistance of load transportation; L and H - transportation length and height of load lifting accordingly, for vertical conveyors $L=H$.

The energy intensity w is given, which determines energy consumption to transport a unit of load mass per unit of length accordingly, for vertical screw conveyors:

то визначальною умовою при проектуванні конвеєра є його спроможність транспортувати вантаж з несприятливими властивостями. При цьому будемо розглядати найбільш несприятливе, з точки зору енергетичних затрат, є вертикальне розміщення гвинтового конвеєра.

Потужність транспортування вантажу гвинтовими конвеєрами, згідно [1], 3], [10], визначають за залежністю $N=\rho_\pi gQ(W_L L+H)$, чи для вертикальних шнеків $N=\rho_\pi gQW_H$, де ρ_π - об'ємна маса (насипна густина) вантажу в потоці; g - прискорення земного тяжіння; Q - об'ємна продуктивність конвеєра; W_L та W_H - коефіцієнт опору переміщенню вантажу; L та H- відповідно довжина транспортування та висота підйому вантажу, для вертикальних ГК $L=H$. Приведена енергоємність w, що визначає енергетичні затрати для переміщення одиниці маси вантажу на одиницю довжини, відповідно для вертикального гвинтового конвеєра буде:

$$w = N/(Q \cdot L) = \rho_{\Pi} g W_H \quad (1)$$

In expanded form the energy intensity factor for vertical screw conveyors the formula is:

В розгорнутому вигляді для вертикальних гвинтових конвеєрів коефіцієнт опору записується виразом:

$$W_H = \frac{\mu_2 P_S (\mathrm{tg}\alpha + \mathrm{tg}\beta_{\Pi})\cos\beta_{\Pi}}{\mathrm{tg}\alpha \cdot \mathrm{tg}\beta_{\Pi}}, \quad (2)$$

where β_{Π} - flow angle of arrival under gravity influence; $P_S = D\omega_{\Pi}^2/(2g)$ - flow specific speed, determined by load rotational speed in flow ω_{Π} against screw axle of diameter D. The above-mentioned factor is connected with conveyor specific speed coefficient $P_k = D\omega^2/(2g)$ by the dependence $P_s = PC_\beta^2/(1+C_\beta)^2$. Here C_β - the coefficient (number) of kinematic similitude of screw transportation $C_\beta = \mathrm{tg}\alpha \cdot \mathrm{tg}(\alpha+\varphi_1)$, where φ_1 - angle of friction of cargo to the screw surface.

The paper [7] shows that the minimal possible theoretical level of power capacity factor W_H depends only on the load friction factor on the screw surface μ_1 and for its change interval $0{,}3 \le 0\mu_1 \le 1$ is approximated by the dependence.

де β_{Π} - кут нахилу траєкторії потоку під впливом тяжіння; $P_S = D\omega_{\Pi}^2/(2g)$ - коефіцієнт швидкохідності потоку, що визначається кутова швидкість обертання вантажу в потоці ω_{Π} відносно осі шнека діаметром D, що пов'язаний із коефіцієнтом швидкохідності конвеєра $P_k = D\omega^2/(2g)$ залежністю $P_s = PC_\beta^2/(1+C_\beta)^2$. Тут C_β - коефіцієнт кінематичної подібності гвинтового транспортування, $C_\beta = \mathrm{tg}\alpha \cdot \mathrm{tg}(\alpha+\varphi_1)$, де φ_1 — кут тертя вантажу до гвинтової поверхні.

В роботі [7] показано, що мінімально можливий теоретичний рівень критерію енергоємності W_H залежить тільки від коефіцієнту тертя вантажу по гвинтовій поверхні шнека μ_1 і для інтервалу його зміни $0{,}3 \le 0\mu_1 \le 1$ апроксимується залежністю.

$$W_H = 2{,}30 + 6{,}64\mu_1 + 19{,}16\mu_1^2 \quad (3)$$

Such a minimal value is achieved under condition when dimensionless criterion of dynamic similitude $Sc_{\Pi} = \omega_k/\omega$, where ω_k - conveyor critical angle speed and screw lifting angle with external diameter α are [7]:

Таке мінімальне значення досягається за умови, коли безрозмірний критерій динамічної подібності $Sc_{\Pi} = \omega_k/\omega$, де ω_k - критична кутова швидкість конвеєра та кут підйому гвинта за зовнішнім діаметром α набувають значень [7]:

$$Sc_{\Pi}(\mu) = 0{,}3 + 0{,}1\mu_1; \qquad \mathrm{tg}\alpha = f(\mu) = 0{,}25 - 0{,}1\mu_1. \quad (4)$$

Accordingly, all other dimensionless criteria of screw transportation, namely the coefficient (number) of kinematic similitude C_β, minimizing the conveyor power capacity, will also definitely be determined by the friction factor $\mu_1 = \mathrm{tg}\varphi_1$. Taking into consideration all above mentioned we'll optimize vertical screw conveyors according to their material consumption under condition of minimal power consumption of load screw transportation.

Відповідно і значення всіх інших безрозмірні критеріїв гвинтового транспортування , зокрема критерію кінематичної подібності C_β, які мінімізують енергоємність конвеєра, будуть також однозначно визначатись такою характеристикою вантажу, як коефіцієнтом тертя $\mu_1 = \mathrm{tg}\varphi_1$. З врахуванням викладеного проведемо оптимізацію швидкохідного вертикального конвеєра за його матеріаломісткістю за умови мінімальної енергоємності гвинтового транспортування вантажу.

За критерій матеріаломісткості гвинтової транспортно-

As material consumption factor of screw transporting-technological system, similarly to [4], [5], we'll take the ratio value of conveyor-mixer mass to the unit length of the given efficiency Q. Material consumption factor at the given efficiency is used for the case when this criterion is one of the principal (for mobile systems) and the transportation function is the basic one. In this case the problem of conveyor material consumption minimization is determined according to the criterion

технологічної системи, аналогічно [4], [5] приймаємо величину відношення маси конвеєра-змішувача одиничної довжини заданої продуктивності Q. Критерій за матеріалоємністю, для випадку заданої продуктивності, використовується для випадку, коли такий фактор є одним із визначальних (для мобільних систем) і функція транспортування є домінуючою. В цьому випадку задача мінімізації матеріалоємності (вартості) конвеєра визначається за критерієм

$$F_0 = \alpha_1 V_1 + \alpha_2 V_2 + \alpha_3 V_3 \to \min, \quad (5)$$

where V_1, V_2, V_3 – volumes of mixer sleeve, helical spiral and center shaft correspondingly; ρ_i - material density (or their prime cost) of which α_1 - sleeve, α_2 - helical spiral and α_3 - center shaft are made. Volumes of sleeve, helical spiral and mixer center shaft of unit length are found according to [4]:

де V_1, V_2, V_3 – відповідно об'єми кожуха змішувача; гвинтової спіралі та центрального вала; ρ_i - густини матеріалів (чи їх собівартість), з якого виготовлені α_1 - кожух, α_2 - гвинтова спіраль та α_3 - центральний вал. Об'єм кожуха, гвинтової спіралі та центрального вала змішувача одиничної довжини, відповідно визначається аналогічно [4]:

$$V_1 = \pi S_K D(1 + 2k_z + S_K / D); \quad V_2 = HD(1 - k_d)\sqrt{1 + 1/k_T} \quad ; V_3 = \pi S_d D(k_d - S_d / D), \quad (6)$$

where S_K - sleeve wall thickness; S_d - hollow shaft wall thickness; H - spiral thickness; k_z - gap (between spiral and кожухом) factor, according to load characteristics is assumed that $k_z = 2z / D = 0{,}21 - 0{,}23$; k_T - helix lead factor T, $k_T = T / D = \pi \operatorname{tg}\alpha$; k_d - coefficient estimated by the ratio of internal d and external D diameters of helical spiral $k_d = d / D$.

The following technological, constructional and license limitations are in the form of inequations $f_i \le 0$ and equations $g_j = 0$ to determine the optimal parameters of vertical high-speed screw conveyors. In particular, technological constraints are described in [4], [5] in detail, so we use main of them without any change:

1. The necessary condition for the efficiency we need Q is found from the known dependence:

де S_K - товщина стінки кожуха; S_d - товщина стінки пустотілого вала; H - товщина спіралі; k_z - коефіцієнт зазору між спіраллю та кожухом, приймається згідно характеристик вантажу $k_z = 2z / D = 0{,}21 - 0{,}23$; k_T - коефіцієнт кроку T спіралі, $k_T = T / D = \pi \operatorname{tg}\alpha$; k_d - коефіцієнт, що оцінюється відношенням внутрішнього d і зовнішнього D діаметрів гвинтової спіралі, $k_d = d / D$. На визначення оптимальних параметрів вертикальних швидкохідних гвинтових конвеєрів накладаються такі технологічні, конструктивні та експлуатаційні обмеження у вигляді нерівностей $f_i \le 0$ та рівнянь $g_j = 0$. Зокрема технологічні обмеження детально описані в [4], [5] і тому використовуємо основні з них без змін:

1.Умова забезпечення потрібної продуктивності Q визначається із відомої залежності :

$$f_1 = -D^{2,5}(1 - k_d^2) + \frac{8Q}{k_T \varphi_н \omega} \le 0, \quad (7)$$

where $\Pi_н$ - coefficient of efficiency, in the first approximating of the conveyor-mixer space filling which also takes into account the кожуха diameter increase comparing to the spiral diameter; ω - screw angular velocity.

2. Technological requirement of spiral fabrication of strip breakdown [4], [5]:

де $\varphi_н$ - коефіцієнт продуктивності, в першому наближенні наповнення простору конвеєра-змішувача, що враховує також збільшення діаметра кожуха, порівняно із діаметром спіралі; ω - кутова швидкість шнека.

2.Технологічна умова формоутворення спіралі із полосової заготовки, [4], [5]:

$$f_2 = -k_d + \sqrt{\pi^2 + 1 - \phi_{доп}^2} / \pi\phi_{доп} \le 0, \quad (8)$$

where $f_2 = -k_d + \sqrt{\pi^2 + 1 - \phi_{доп}^2} / \pi\phi_{доп} \le 0,$ - permissible coefficient of metal elongation inequality, determined by coefficient of elongation $\phi_{доп} = (1 + 2\delta_5)^2$.

3. Technological requirement of providing the strip resistance while spiral making is known [4], [5]:

де $f_2 = -k_d + \sqrt{\pi^2 + 1 - \phi_{доп}^2} / \pi\phi_{доп} \le 0,$ - допустимий коефіцієнт нерівномірності видовження металу, що визначається коефіцієнтом видовження $\phi_{доп} = (1 + 2\delta_5)^2$.

3.Технологічна умова забезпечення стійкості смуги при виготовлені спіралі є відомою [4], [5]:

$$f_3 = D(1-k_d) - \frac{2H}{\delta} \le 0, \quad (9)$$

where δ - permissible specific thickness of a helical spiral workpiece after rolling δ = *0.02…0.03* after winding δ = *0.05…0.07*

4. For long conveyors the condition is introduced to provide hollow sleeve endurance at rotation by torsional moment on stiff shaft $T_2 = N/\omega$:

де δ - допустима питома товщина заготовки гвинтової спіралі, отриманої прокатуванням $\delta = 0{,}02...0{,}03$, отриманої навиванням $\delta = 0{,}05...0{,}7$.

4. Для довгих конвеєрів вводять умову забезпечення міцності пустотілого вала при крученні крутильним моментом $T_2 = N/\omega$ на валу:

$$f_4 = -S_d(k_d D)^2(1 + k_d S_d / D) + \frac{T_2}{\pi[\tau_{кр}]} \le 0, \quad (10)$$

where $[\tau_{кр}]$ - permissible torsional stress of shaft material.

5. Providing condition of helical spiral endurance while in operation:

де $[\tau_{кр}]$ - допустиме напруження кручення матеріалу вала.

5. Умова забезпечення стійкості гвинтової спіралі в процесі роботи:

$$f_5 = \frac{K_{CT} D H^3 E(1-k_d)}{\sqrt{1+k_T}} - T_2 \le 0\,, \quad (11)$$

where K_{CT} – trial coefficient; E –Young's modulus.

6. Condition for the calculated friction factor μ_1 choice, taking into account the most unfavorable conditions:

де K_{CT} - експериментальний коефіцієнт; E - модуль Юнга.

6. Умова вибору розрахункового значення коефіцієнта тертя μ_1, виходячи із найбільш несприятливих умов:

$$f_7 = \mu_1 - \mu_{\max} \le 0\,. \quad (12)$$

Constraints $g_j = 0$, imposed on design and technological parameters of screw conveyor are: Compatibility of screw surface lead angle and minimal power consumption condition (4). Compatibility of dynamic similitude factor and minimal power consumption condition

Обмеження $g_j = 0$, що накладаються конструктивні та технологічні параметри гвинтового конвеєра мають такий вигляд.

Відповідність кута підйому гвинтової поверхні умові мінімальної енергоємності згідно (4). Відповідність критерію динамічної подібності умові мінімальної енергоємності

$$g_3 = \mu_2 P_k S c_{\Pi}^2 - k_P \operatorname{tg}(\alpha + \varphi_1) = 0\,. \quad (13)$$

After transformations the given condition looks like

Після перетворень дана умова набуває вигляду

$$g_3 = \mu_2 D\omega^2(0{,}3 + 0{,}1\mu_1)^2(1 - 0{,}25\mu_1 + 0{,}1\mu_1^2) - 2gk_P(0{,}25 + 0{,}9\mu_1) = 0\,. \quad (13a)$$

where k_P - flow reduction coefficient, is observed and in the first approximation is adopted $k_P = 1$.

As basic design and technological parameters of screw conveyors, i.e. as independent changeable components in screw conveyors optimization we'll take those as in the known optimization models: $x_1 = D$ - sleeve external parameters; $x_2 = \omega$ - angular rate of rotation of helical spiral $x_3 = \operatorname{tg}\alpha = T/(\pi D)$ - helix angle tg determined by helical spiral pitch T ; $x_4 = k_d = d/D$ - coefficient estimated by correlation of internal *d* and external *D*diameters of helix spiral; $x_5 = H$ - helix spiral thickness. Besides, we'll introduce the parameter determining the characteristics of screw transporting schedule $x_6 = \mu_1 = \operatorname{tg}\varphi_1$ - calculated value of load friction factor to spiral surface.

Search of parameters x_k optimizing the objective function F_0 at constraints $f_i \le 0$, $g_j = 0$ is similarly to

де k_P - коефіцієнт приведення до потоку, визначається експериментально і в першому наближені приймається $k_P = 1$.

За основні конструктивні і технологічні параметри гвинтових конвеєрів, тобто за незалежні змінні при оптимізації гвинтових конвеєрів приймемо такі, як і у відомих оптимізаційних моделях: $x_1 = D$ - зовнішній діаметр кожуха; $x_2 = \omega$ - кутова швидкість обертання гвинтової спіралі $x_3 = \operatorname{tg}\alpha = T/(\pi D)$ - тангенс кута підйому витка, що визначається кроком гвинтової спіралі T ; $x_4 = k_d = d/D$ - коефіцієнт, що оцінюється відношенням внутрішнього d і зовнішнього D діаметрів гвинтової спіралі; $x_5 = H$ - товщина гвинтової спіралі. Крім цього, введемо параметр, що визначає характеристики режиму гвинтового транспортування $x_6 = \mu_1 = \operatorname{tg}\varphi_1$ - розрахункове значення коефіцієнта тертя вантажу до поверхні спіралі.

[4, 5], using Kuhn-Tucker conditions, when for the nonlinear programming problem in the given setting there are the following multipliers $u_i \geq 0$, i = 1, 2, …n, that $u_i f_i = 0$ and $\partial\varphi(x_i, u_i)/\partial x_j = 0$, where $\varphi(x_j, u_i) = F_0 + \sum_{i=1}^{n} u_i f_i$.

Constraints $g_j = 0$ are used for the problem order reduction, i.e. for the independent parameters number reduction.

Objective function (factor of quality) in the given nonlinear programming problem, taking into account (5) and (6), is put down in this way:

Пошук параметрів x_k, що оптимізують цільову функцію F_0 при заданих обмеженнях $f_i \leq 0$, $g_j = 0$ шукаємо, аналогічно [4, 5], з використанням умов Куна-Такера, за якими для задачі нелінійного програмування в даній постановці існують такі множники $u_i \geq 0$, *i* = 1, 2, …*n*, що $u_i f_i = 0$ і $\partial\varphi(x_i, u_i)/\partial x_j = 0$, де $\varphi(x_j, u_i) = F_0 + \sum_{i=1}^{n} u_i f_i$.

Обмеження $g_j = 0$ використовуємо для зменшення розмірності задачі, тобто для зменшення кількості незалежних параметрів.

Функція мети (критерій якості) в даній задачі нелінійного програмування, з врахуванням (5) та (6), запишемо в такому вигляді:

$$F_0 = \pi x_1[\alpha_1 S_K(1 + k_z + S_K/x_1) + \alpha_2 x_5(1 - x_4)\sqrt{1 + 1/x_3} + \pi\alpha_3 S_d x_1(x_4 - S_d/x_1)]. \quad (14)$$

Thereafter, the parameters satisfying the optimum conditions and unknown parameters can be found from the equations set.

$$\partial\varphi(x_j, u_i)/\partial x_j = \frac{\partial F_0}{\partial x_j} + \sum_{i=1}^{n}(u_i + \frac{\partial f_i}{\partial x_j}) = 0;\ u_i f_i = 0.$$

Відповідно, параметри, що задовольняють умови оптимуму та невідомі коефіцієнти, шукаємо із системи рівнянь

$$\partial\varphi(x_j, u_i)/\partial x_j = \frac{\partial F_0}{\partial x_j} + \sum_{i=1}^{n}(u_i + \frac{\partial f_i}{\partial x_j}) = 0;\ u_i f_i = 0.$$

RESULTS AND DISCUSSION

New conditions introduction $g_j=0$, providing low energy-consuming operating modes of conveyor, which allow to have a new parameter $x_2=\omega$ out the linear programming problem solution, so it doesn't change the solution structure of the very optimization model and calculation schemes for determining the optimal parameters, shown in [4], [5], but only makes them more specific. Accordingly, we are finding the solution of the optimization problem similar to [4], according to two calculation schemes with primal constraints on conveyor capacity and additional constraints on technology of spiral making and on the shaft strength (for long conveyors). Accordingly, we define the following order of searching of optimal design values and technological parameters of high-speed screw conveyor:

1. According to technical specifications of transportation to provide all load nomenclature processing $f_7 = 0$, therefore.

РЕЗУЛЬТАТИ

Введення нових умов $g_j = 0$, що забезпечують малоенергоємні режими роботи конвеєра, дозволяє вивести новий параметр $x_2 = \omega$ за межі розв'язку задачі лінійного програмування а тому не змінює структуру розв'язку самої оптимізаційної моделі та розрахункові схеми визначення оптимальних параметрів, наведеної в [4], [5], а тільки конкретизує їх. Відповідно, розв'язок оптимізаційної задачі проводимо аналогічно [4], за двома розрахунковими схемами з основним обмеженням за продуктивністю конвеєрами і додатковим обмеженням за технологією виготовлення спіралі и за міцністю вала (для довгих конвеєрів). Відповідно, визначаємо такий порядок пошуку оптимальних конструктивно-технологічних параметрів швидкохідного гвинтового конвеєра:

1. За технічними умовами транспортування для забезпечення переробки всієї номенклатури вантажів приймають $f_7 = 0$, звідки

$$\mu_1 = \mu_{1\max}. \quad (15)$$

From situation $g_1=0$ angle of screw ascent is determined $\alpha = 0.25$ on external diameter, minimizing the power parameters of transportation and lead coefficient.

Визначають із умови $g_1 = 0$ кут підйому гвинта $\alpha = 0{,}25$ по зовнішньому діаметру, що мінімізує енергосилові параметри транспортування та коефіцієнт кроку

$$\mathrm{tg}\alpha = 0{,}25 - 0{,}1\mu_{1\max}. \quad (16)$$

$$k_T = T/D = \pi\,\mathrm{tg}\alpha. \quad (17)$$

In case, when $k_T \leq k_{Tmin}$, we adopt that $tg\ \alpha = k_T/\pi$.

If purpose-built conveyor is designed for transportation of only one kind of load with friction factor μ_1, then $tg\ \alpha = 0.25\text{-}0.1\mu_1$ is adopted.

2. From situation $g_2=g_3=0$ conveyor power speed coefficient is determined:

У випадку, коли $k_T \leq k_{T\min}$, приймаємо $\mathrm{tg}\alpha = k_T/\pi$. Якщо проектується спеціалізований конвеєр для транспортування тільки одного виду вантажу з коефіцієнтом тертя μ_1, то приймають $tg\ \alpha = 0.25\text{-}0.1\mu_1$.

2. Із умови $g_2=g_3=0$ визначають коефіцієнт швидкохідності конвеєра:

$$P_k = \frac{k_P \operatorname{tg}(\alpha+\varphi_1)}{\mu_2 Sc_{\Pi}^{\ 2}} = \frac{k_P(0{,}25+0{,}9\mu_1)}{\mu_2(0{,}3+0{,}1\mu_1)^2(1-0{,}25\mu_1+0{,}1\mu_1^2)}, \quad (18)$$

3. From technological situation $f_1=0$ the ratio k_d of screw internal and external diameters is found

3. Із технологічної умови $f_1=0$ визначають співвідношення k_d між внутрішнім і зовнішнім діаметрами спіралі

$$k_d = \sqrt{\pi^2+1-\phi_{доп}^2}/\pi\phi_{доп} \le 0, \quad (19)$$

4. From the equation set solution $f_1=0$ and $g_3=0$ at the given efficiency rotating speed is found:

4. Із розв'язку системи рівнянь $f_1=0$ та $g_3=0$ за заданою продуктивністю визначають кутову швидкість:

$$\omega = \left[\frac{\pi\varphi_н g^3 \operatorname{tg}\alpha \cdot P_k^{\ 3}(1-k_d^2)(1-Sc_{\Pi})}{Q(1+C_\beta)}\right]^{\frac{1}{5}} = \sqrt[5]{\frac{\varphi_н g^3(1-k_d^2)}{\mu_2^3 Q}} K_\omega(\mu_1), \quad (20)$$

where $K_W(\mu_1)$ - depends only on μ_1 and is found by simplification of the previous one taking into account the values P_k, Sc_π, and C_β.

де $K_W(\mu_1)$ - вираз, що залежить тільки від μ_1 і отримується спрощенням попереднього із врахуванням значень P_k, Sc_π, та C_β.

5. Screw internal and external diameters are found

5. Визначають зовнішній і внутрішній діаметр спіралі

$$D = \sqrt{2P_k g/\omega^2} = \frac{g^{1/5} Q^{1/10} K_D(\mu_1)}{\mu_2^{1/5} \varphi_н^{1/10}(1-k_d^2)^{1/10}}. \quad (21)$$

6. Lead of a helix is determined by the dependence

6. Крок спіралі визначається за залежністю

$$T = k_T D. \quad (22)$$

7. Spiral internal diameter (shaft diameter), as such

7. Внутрішній діаметр спіралі (діаметр вала), відповідно

$$d = k_d D = D\sqrt{\pi^2+1-\phi_{доп}^2}/\pi\phi_{доп}. \quad (23)$$

8. Spiral thickness from the situation $f_3 = 0$

8. Товщина спіралі із умови $f_3 = 0$

$$H = \delta(D-d)/2. \quad (24)$$

For specific spirals, namely for elastic spirals, values $H=\delta(D-d)/2$ are inspected on the conformance to situation $f_5 \le 0$.

Для спеціальних спіралей, зокрема для спіралей з еластичних матеріалів, значення $H=\delta(D-d)/2$ перевіряють на відповідність умові $f_5 \le 0$.

9. Axial velocity of load transportation according to [6], [7] is determined by the dependence

9.Осьова швидкість транспортування вантажу згідно [6], [7] визначається за залежністю

$$v_{\Pi} = \frac{T\omega}{2\pi} \cdot \frac{1-Sc_{\Pi}}{1+C_\beta}. \quad (25)$$

10. Vertical conveyor transportation capacity, providing the efficiency Q of length L at load transporting, by bulk density ρ_π

10. Потужність транспортування вертикального конвеєра, що забезпечує продуктивність Q довжиною L при транспортуванні вантажу, насипною густиною ρ_π

$$N = \rho_{\Pi} gQLW = \frac{\rho_{\Pi} gQLC_\beta (Sc_{\Pi}+C_\beta)^3}{Sc_{\Pi}(1+C_\beta)(1-Sc_{\Pi})\operatorname{tg}^2\alpha\sqrt{(Sc_{\Pi}+C_\beta)^2+(1-Sc_{\Pi})^2\operatorname{tg}^2\alpha}}. \quad (26)$$

Behavior of vertical screw conveyor angular velocity and its spiral diameter, minimizing the conveyor power capacity at different rheological properties of load, is shown on fig.1.

Характер зміни кутової швидкості вертикального гвинтового конвеєра та діаметру його спіралі, що мінімізують енергоємність конвеєра при різних реологічних властивостях вантажу, наведений на рис.1.

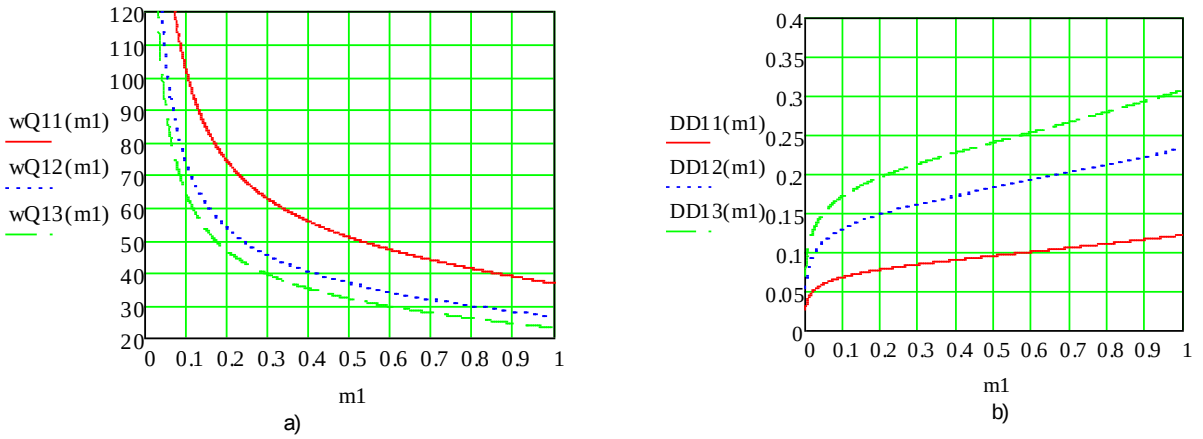

Fig. 1. Change of rational value of angular velocity $\omega(\mu_1) = wQ(m1)$, c-1 (a) and spiral external screw diameter $D(\mu_1) = DD(m1)$, м (b) from load friction ratio to the spiral (sleeve) surface, $\mu_1 = \mu_2$, for the given conveyor efficiency

In case of long screw conveyors their shafts bear heavy torsion load, hence the received values d are tested on limits.

At its violation the internal diameter is determined by the approximating dependence

Для довгих гвинтових конвеєрів їх вали несуть значні крутні навантаження, а тому отримані значення d перевіряють на відповідність обмеженню .

При його порушенні внутрішній діаметр визначають по наближеній залежності

$$d = \sqrt{\frac{2k_M M_{кр}}{\pi S_d [\tau_{кр}]}} . \quad (27)$$

Further the spiral external diameter is specified

В подальшому уточнюють зовнішній діаметр спіралі

$$D_i = \sqrt[3]{d^2 D_{i-1} + \frac{8Q}{k_T \varphi_н \omega_{i-1}}} , \quad (28)$$

where values D_{i-1} and ω_{i-1} are taken from the previous calculations.

At significant difference of values D_{i-1} and D_i the coefficient $k_d=d/D$ is specified and calculated value of angular velocity ω is specified according to dependence (20).

For horizontal and low falling high-speed screw conveyors there is no critical angular speed, hence the parameter $Sc=0$, and a rational angle of helical spiral lifting versus friction factor is determined graphically, e.g. according to [8].

In case of loading-unloading transporting screw systems, having two screw conveyors – loading and unloading, the normal working condition is to provide more efficient unloading conveyor Q_2 than a loading one Q_1 at any conditions, that is

де значення D_{i-1} та ω_{i-1} беруть із попередніх розрахунків.

При значному розходженні значень D_{i-1} та D_i уточнюють коефіцієнт $k_d=d/D$ та уточняють розрахункове значення кутової швидкості ω згідно залежності (20).

Для горизонтальних та низько нахилених швидкохідних гвинтових конвеєрів не існує критичної кутової швидкості, а тому параметр $Sc=0$, а раціональний кут підйому гвинтової спіралі в залежності від коефіцієнту тертя визначається графічно, наприклад згідно [8].

У випадку завантажувально-розвантажувальної транспортної гвинтової системи, яка має два гвинтових конвеєри – забірний і вивантажувальний, умова її нормальної роботи полягає в забезпеченні продуктивності вивантажувального конвеєра Q_2 більшої ніж забірного Q_1 за всяких умов, тобто

$$Q_{2\min} \geq \lambda Q_{1\max} , \quad (29)$$

where
λ - safety margin λ =1.2…1.3 depending on the working conditions.
Q_{1max} - is reached at horizontal position of loading conveyor, and Q_{2min} - at vertical one of unloading conveyor.

Situation (29) in the first approximating is:

де
λ - коефіцієнт запасу λ =1,2…1,3 залежно від умов роботи.
Q_{1max} - досягається при горизонтальному розміщенні забірного конвеєра, а Q_{2min} - при вертикальному вивантажувального.

Умова (29) в першому наближенні буде

$$\frac{\varphi_{и2} D_2^2 \omega_2 \operatorname{tg}\alpha_2 (1 - Sc_{П2})}{1 + \operatorname{tg}\alpha_2 \operatorname{tg}(\alpha_2 + \varphi_2)} \geq \frac{\lambda \varphi_{и1} D_1^2 \omega_1 \operatorname{tg}\alpha_1}{1 + \operatorname{tg}\alpha_1 \operatorname{tg}(\alpha + \varphi_1)} \quad (30)$$

The ratio we received allow to calculate with high accuracy the optimal constructional and technological parameters of screw conveyors (SC), providing the necessary mixture quality at high efficiency of transportation process.

CONCLUSION

Theoretical basis of optimization of high-speed conveyers for granular materials transportation is developed. The nonlinear programming problem is solved using Kuhn-Tucker conditions.

The procedure of calculations of rational constructional parameters and conveyors-mixers operating regimes is developed. It consists of ten main stages with derived analytical dependences.

REFERENCES

[1]. Alecsandrov M. P., (1974) - *Handling machines*. Mechanical Engineering, Moscow, pp.503;

[2]. *Augers for agricultural machines.* (1973) GOST 2705 - 73: Publishing House of the standards, Moscow, 16 c.

[3]. Hrigoriev A.M., (1972) - *Screw conveyers.* Mashynostrojenije, Moscow, pp.286;

[4]. Hevko B.M. Rohatynsky R.M. (1989) - *Screw feeding mechanisms of agricultural machines.* High school, Lviv, pp.175;

[5]. Hevko B. M. Rohatynsky R.M., (1987) - *Optimization of the design parameters of the screw conveyors*. Math. Universities, Engineering-No.5 Moscow, pp.109–114;

[6]. Loveykin V. S., Rohatynska O.R., (2004) - *Optimization of screw conveyors.* - Handling Machinery. No.2, pp. 8-15.

[7]. Rohatynka O.R., Dudun Y.V., Rohatynka L. R., Klendiy M. B., (2006) - *Optimization of design parameters and vertical screw conveyors.* - Journal of Kharkov Petro Vasilenko National Technical University of Agriculture, Vol 2, No.44 "Mechanization of agriculture." Harkiv, pp.258-264,

[8]. Rohatynsky R.M., Hevko I.B., Dyachun A.E., (2014) - *Research and application basics of screw transport and technological mechanisms.* - TNTU Ivan Pul'uj, Ternopil, pp.278.

[9]. *Standard Screw conveyors for feed* (1980) Basic information: GOST 23976 - 80. Publishing House of the standards, Moscow, with19.

[10]. Volkov P. A., Gnutov A. N., Diachkov V.K. et all (1984) *Conveyors* - Mechanical Engineering, Leningrad, pp.367.

Отримані співвідношення дозволяють з високою точністю обчислити оптимальні конструктивні й технологічні параметри гвинтових конвеєрів (ГК), при яких забезпечується потрібна якість суміші при високій ефективності процесу транспортування.

ВИСНОВОК

Розроблено теоретичні основи оптимізації швидкохідних транспортерів для транспортування сипких матеріалів. Розв'язано задачу нелінійного програмування з використанням умов Куна-Таккера.

Розроблено методику розрахунку раціональних конструктивних параметрів і режимів роботи гвинтових конвеєрів у вигляді десяти основних етапів з виведеними аналітичними залежностями.

БІБЛІОГРАФІЯ

[1]. Александров М. П. (1974) - *Подъемно-транспортные машины*. – Машиностроение., – 503 с., Москва;

[2]. ГОСТ Шнеки для сельскохозяйственных машин : ГОСТ 2705 - 73. - Изд-во стандартов 1973, 16с., - (Національні стандарти України);

[3]. Григорьев А.М. (1972) - *Винтовые конвееры*. Машиностроение., - 286 с., Москва;

[4]. Гевко Б.М., Рогатынский Р.М. (1989) - *Винтовые подающие механизмы сельскохозяйственных машин.* Выща школа, – 175 с., Львов.

[5]. Гевко Б.М. Рогатынский Р.М. (1987) - *Оптимизация конструктивных параметров шнековых конвейеров.* Машиностроение., – №5. – С. 109 – 114 - Москва;

[6]. Ловейкін В.С., Рогатинська О.Р. (2004) *Оптимізація режимів роботи гвинтових конвеєрів* / Підйомно-транспортна техніка. № 2,.- С. 8-15.;

[7]. Рогатинська О. Р., Дудін Ю. В, Рогатинська Л. Р., Клендій М. Б. (2006.) - *Оптимізація режимів роботи та конструктивних параметрів вертикальних гвинтових конвеєрів.* - Вісник Харківського національного технічного університету сільського господарства імені Петра Василенка. – Т. 2, № 44 „Механізація сільськогосподарського виробництва". – С. 258-264. – Харків;

[8]. Рогатинський Р.М., Гевко І.Б., Дячун А.Є. (2014) - *Науково-прикладні основи створення гвинтових транспортно-технологічних механізмів.* – ТНТУ імені Івана Пулюя, – 278 с., Тернопіль.

[9]. ГОСТ Конвейеры винтовые для кормов. Основные параметры: ГОСТ 23976 - 80. – Изд-во стандартов 19 с. - (Національні стандарти України);

[10]. Конвейеры: (1984) - Справочник [Волков Р .А., Гнутов А. Н., Дьячков В .К. и др.] ; под общ. ред. Ю.А. Пертена. Машиностроение, – 367 с., Ленинград.

THEORETICAL ASPECTS RELATED TO THE AIR FLOW THROUGH THE SEED LAYER ON THE PNEUMATIC-VIBRATING MACHINE SURFACE
/
ASPECTE TEORETICE PRIVIND CIRCULAŢIA CURENTULUI DE AER, PRIN STRATUL DE SEMINŢE DE PE SUPRAFAŢA MAŞINII PNEUMO-VIBRATOARE

Prof. Ph.D Eng. Căsăndroiu T., Eng. Buciuman F.V.
POLITEHNICA University of Bucharest / Romania
Tel: 0728833188; E-mail: florina_buciuman@yahoo.com

Abstract: *The thesis presents the main theoretical elements related to the air flow going through granular bed under vibrating motion. It draws the hypothesis of analogy between the vibrating granular layer and the stationary layer, having in view that the seeds speed on the machine table are relatively low and consequently their influence upon air flow through layer can be neglected. It is emphasized that in this case can be utilized with good results, the Ergun equation as a link between pressure downfall (-ΔP) on the thickness of the seed layer and air speed for a global laminar turbulent way through layer. On this basis have been presented theoretical studies for two different machines used in the concrete work practice for wheat and barley seeds. Experimental results obtained regarding the pressure downfall (-ΔP) subject to the fans air flow of these machines have been compared to those evaluated by calculation and there is reasonable difference (errors ±5%).*

Keywords: *pressure downfall (-ΔP), stratification, global laminar- flow, minimum fluidization speed*

INTRODUCTION

One of the necessary operations for sorting seeds, often used, is sorting seeds by their density. The pneumatic vibrating machines [6, 7] are used for sorting seeds by density. The flat working surfaces of such machine which carry out segregation are represented schematically in fig.1.

By means of this method the selection is realized as an effect of a combined action of a continuous air flow which is homogeneous, upward, of constant pressure and goes through the seed layer situated on a cobweb or wire net surface and due to the vibrations at which this surface is subject. [2,3,4].

As a result of air flow together with the agitation caused by vibrations of the surface, the particle mixture on the sorting surface will get loose the particles arriving in the air flow in suspension condition and a stratification by density of the seeds is obtained, fig 2.

The stratification effect is favored if during the air circulation through seed layer, such layer will get loose up to fluidization limit, an increasing of the porosity of the seed layer, respectively, [6].

As proved by experimental researches [2, 4] the air circulation through seed layer situated on the flat surface of the pneumatic vibrating machine plays an important role in seeds stratification.

Rezumat: *În lucrare se prezintă principalele elemente teoretice legate de curgerea aerului prin medii granulare în stare de mişcare vibratorie. Se formulează ipoteza analogiei între stratul granular vibrator cu stratul în stare staţionară, având în vedere că vitezele de deplasare a seminţelor pe masa maşinii sunt relativ mici şi în consecinţă influenţa acestora asupra curgerii aerului prin strat se poate neglija. Se evidenţiază faptul că în această situaţie se poate utiliza, cu bune rezultate, ecuaţia lui Ergun, de legătură între căderea de presiune (-ΔP) pe grosimea stratului de seminţe şi viteza curentului de aer, pentru o curgere globală laminar-turbulentă prin strat. Pe această bază s-au prezentat studii de caz pentru două maşini diferite existente în practică, în condiţii concrete de lucru pentru seminţele de grâu şi orz. Datele experimentale obţinute, referitoare la căderea de presiune (-ΔP) în funcţie de debitul de aer al ventilatoarelor existente la aceste maşini au fost comparate cu cele evaluate prin calcul, diferenţele încadrându-se în limite rezonabile (în domeniul erorilor ±5%).*

Cuvinte cheie: *căderea de presiune (-ΔP), stratificare, curgere globală laminar-turbulentă, viteză minimă de fluidizare*

INTRODUCERE

Una din operaţiile necesare de sortare a seminţelor, este adesea şi separarea acestora după densitatea lor. Pentru separarea după densitate a seminţelor se utilizează maşinile pneumo-vibratoare, [6, 7]. Schematic, suprafeţele plane de lucru ale acestor maşini care efectuează separarea sunt reprezentate în fig.1.

Prin această metodă separarea se realizează ca efect al acţiunii combinate a unui curent de aer continuu, uniform, ascendent, de presiune constantă, care străbate stratul de seminţe ce se află pe o suprafaţă din ţesătură fină sau plasă de sârmă şi a vibraţiilor la care aceasta este supusă, [2, 3, 4].

Sub acţiunea curentului de aer şi a agitaţiei provocate de oscilaţiile suprafeţei, amestecul granular de seminţe de pe suprafaţa de separare se afânează, particulele acestuia ajungând în stare de suspensie în curentul de aer, având loc şi o stratificare după densitate a seminţelor, fig.2.

Efectul de stratificare este favorizat dacă la curgerea curentului de aer prin stratul de seminţe se produce o afânare a acestuia până la starea limită de fluidizare, respectiv o creştere a porozităţii stratului de seminţe, [6]. Aşa cum au arătat şi cercetările experimentale, [2, 4] un rol esenţial în fenomenul stratificării îl joacă circulaţia curentului de aer prin stratul de seminţe de pe suprafaţa plană a maşinii pneumo-vibratoare.

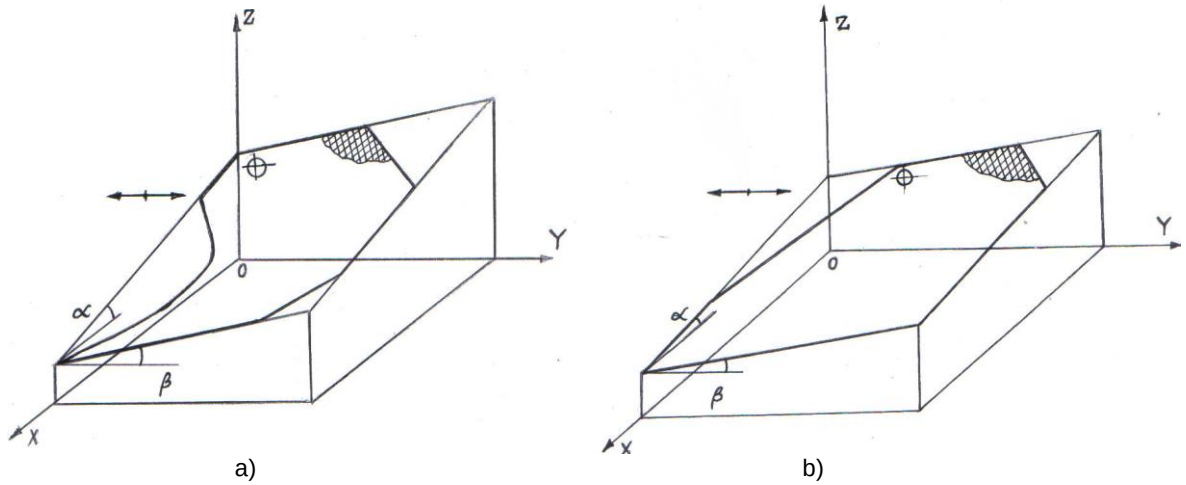

a) b)

Fig.1 - Scheme of surfaces for pneumatic vibrating segregation by seeds density
a) - scheme of wheat machine doubled inclined table
b) - scheme of barely seeds machine double inclined table

The information furnished by specialty literature regarding the relevant theoretical aspects is quite poor. Therefore, in this thesis, appropriate mathematical models regarding the air circulation through seed layer under vibrations effect, were developed, the model with experimental data obtained on a machine in working process was tested and on this basis a theoretical study with concrete data was performed.

În literatura de specialitate informaţiile referitoare la aspectele teoretice corespunzătoare sunt sărace. De aceea în această lucrare s-au dezvoltat modele matematice adecvate fenomenului circulaţiei de aer prin stratul de seminţe supus vibraţiilor, s-a testat modelul cu datele experimentale obţinute la o maşină existentă în lucru şi s-a efectuat, pe această bază, un studiu de caz aplicat pe datele concrete.

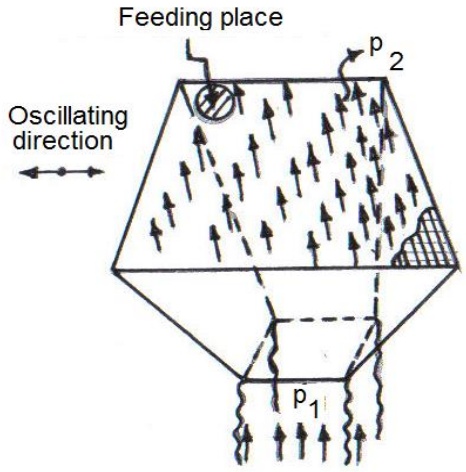

Fig 2 - Diagram of vibrating surface with one seed layer segregated by particles' density

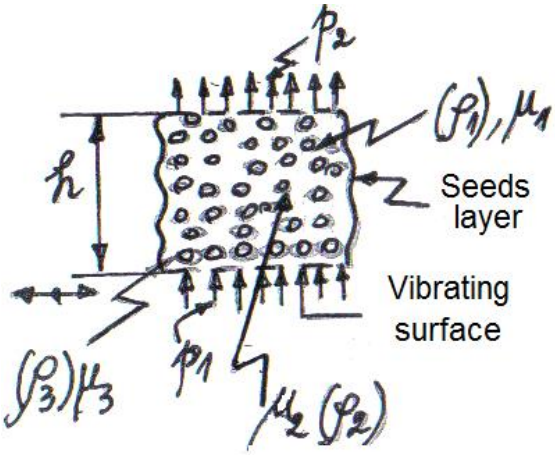

Fig. 3-Cross section detail drawing, on seed layer's height (h) at segregation state by particles density, ($\rho_1 < \rho_2 < \rho_3$)

MATERIALS AND METHODS

According to specialty literature, in order to assure the air circulation through seed layer, a pressure downfall (-ΔP) on the thickness of seed layer is evaluated, as presented in fig. 2 and fig. 3.

The theoretical basis of the seed stratification due to air circulation through layer by analogy with air circulation through granular, porous, stationary bed, [6], to which is assimilated, is hereby presented.

As a consequence of stratification there is a differentiation as regards the seeds friction coefficient on the relevant supporting surfaces. Thus, the interaction between seeds is reduced and decreases towards zero, which makes motion possible within the mixing layer, on its thickness.

The heavy particles, with high density, fall to the base of the mixing layer (getting in contact with the segregation surface) and the lighter particles, with lower

MATERIALE ŞI METODE

Potrivit literaturii de specialitate pentru asigurarea circulaţiei aerului prin stratul de seminţe se apreciază necesitatea unei anumite căderi de presiune (-ΔP) pe grosimea stratului, aşa cum este prezentat schematic în fig. 2 şi fig. 3.

Se va prezenta baza teoretică a stratificării seminţelor datorată curgerii aerului prin strat, prin analogie cu fenomenul circulaţiei aerului prin medii granulare poroase staţionare, [6] cu care acesta este asimilat.

Consecinţa stratificării este o diferenţiere a coeficientului de frecare a seminţelor pe suprafeţele corespunzătoare de sprijin. În acest fel se va micşora interacţiunea între particule până la anulare, ceea ce le asigură posibilitatea deplasării în interiorul stratului de amestec, pe grosimea sa.

Particulele grele, de densitate mare, coboară la baza stratului de amestec (ajungând în contact cu suprafaţa de separare), iar particulele mai uşoare, de densitate mai

density, move to the upper part of the layer, getting loose, with a more reduced interaction with the lower layers comparing to the one of heavy particles with segregation surface, see fig.3.

The presence of air layers between segregated lines, causes, probably, a decrease in friction coefficient value, lower values for those in the upper layer, together with particle density decrease, as in fig.3.

We will consider applicable the fluid flow theory through solid particles bed, which does not change its characteristics during process, thus representing an approximation of real case when seeds move with relative low speeds on the vibrating surface.

Therefore, we will analyze, only the fluid (air) flow through seed layer (solid particles) in stationary condition. The seed bed is considered as stationary when its characteristics remain unchanged.

During air circulation through seed layer are considered to be plausible three flow type: laminar flow, turbulent flow and global laminar turbulent flow, [5].

Out of these, the last flow is most probable. We shall present synthesized the three flow modes.

Laminar flow

The flow is laminar if air flow through existing channels within seeds bed is laminar. After making several considerations and calculations, which are to be presented in details in item [6], Fanning equation for each channel can be written as follows:

mică, se deplasează spre partea superioară a stratului şi ies la suprafaţa acestuia, găsindu-se în stare afânată, cu o interacţiune mai redusă cu păturile inferioare în raport cu aceea a particulelor grele cu suprafaţa de separare, vezi fig.3. Existenţa păturilor de aer între straturile stratificate determină, probabil o scădere a coeficientului de frecare de la baza stratului spre partea lui superioară, odată cu scăderea densităţii particulelor, ca în fig.3.

Se va considera aplicabilă teoria curgerii fluidelor prin patul de particule solide care nu-şi schimbă caracteristicile în timpul procesului, ceea ce reprezintă o aproximare a cazului real în care seminţele se deplasează cu viteze, relativ mici, pe suprafaţa vibratoare. De aceea se va analiza numai curgerea fazei fluidului (aerului) prin stratul de seminţe (particule solide) în stare staţionară. Patul de seminţe este considerat staţionar, când caracteristicile acestuia nu variază.

La curgerea aerului prin stratul de seminţe sunt plauzibile trei regimuri de curgere: curgere laminară, curgere turbulentă şi curgere globală laminar-turbulentă, [5]. Dintre acestea, ultimul regim de curgere este cel mai probabil. Vom prezenta în sinteză cele trei regimuri de curgere.

Curgerea laminară

Curgerea este laminară dacă fluxul de aer prin canalele existente în patul de seminţe este laminar. După o serie de consideraţii şi calcule, prezentate în detaliu în [6], ecuaţia lui Fanning pentru fiecare canal poate fi pusă sub forma:

$$\frac{(-\Delta P)}{\rho_a} = \frac{64}{\mathrm{Re}} \cdot \frac{h' \cdot v^2{}_c}{2 \cdot D_e} \tag{1}$$

where Reynolds number, i.e. v_c is presented in the formulae:

unde numărul lui Reynolds, respectiv v_c sunt prezentate în formulele:

$$\mathrm{Re} = \frac{\rho_a \cdot v_c \cdot D_e}{\eta} \tag{2}$$

$$v_c = v \cdot \frac{h'}{h \cdot \varepsilon} \tag{3}$$

The symbols used in these equations are as follows: ρ_a - air density; v_c - air speed through channel; v - conventional air speed through cross section equal with table surface covered with seeds; D_e - channel equivalent diameter; h` - channel length (as a rule, lower than seed layer thickness h); ε - seed layer porosity.

After making several considerations and calculations presented detailed in [1], we get final form of eq. (1):

Semnificaţia mărimilor din aceste ecuaţii este: ρ_a - densitatea aerului; v_c - viteza aerului prin canal ; v - viteza convenţională a aerului prin secţiunea egală cu suprafaţa mesei acoperită cu seminţe; D_e - diametrul echivalent al canalului; h` - lungimea canalului (de regulă mai mic decât grosimea h a stratului de seminţe); ε - porozitatea stratului de seminţe.

După o serie de consideraţii şi calcule, prezentate în detaliu în [1], ec. (1) devine în forma finală:

$$v = \frac{(-\Delta P)}{\eta \cdot h} \cdot \frac{\varepsilon^3}{K''(1-\varepsilon)^2 (a_{so})^2} \tag{4}$$

The equation (4) is known as Kozeny-Carman equation. where: *K"* - Kozeny constant which depends on porosity and specific surface and was experimentally established, *K"* = 5±0,5; a_{so} - specific surface of the particle, defined by a_{so} - (particle surface) / (particle volume); η - air dynamic viscosity; (- ΔP) pressure downfall on thickness layer.

Turbulent flow

If air flow through channels is the turbulent one, the Fanning equation can be applied, [5].

Ecuaţia (4) este cunoscută sub numele de ecuaţia Kozeny-Carman. unde: *K"* - constanta lui Kozeny care depinde de porozitate şi suprafaţa specifică şi a fost găsită experimental, *K"*=5±0,5; a_{so} - aria specifică a particulei, definită prin a_{so} - (suprafaţa particulei) / (volumul particulei); η - este vâscozitatea dinamică a aerului; (- ΔP) căderea de presiune pe grosimea stratului.

Curgerea turbulentă

Dacă circulaţia aerului prin canale este turbulentă, se poate aplica ecuaţia lui Fanning, [5].

$$\frac{(-\Delta P)}{\rho_a} = 4f \cdot \frac{h' \cdot v^2{}_c}{2 \cdot D_e} \quad (5)$$

where: f is the friction coefficient:
In conformity with item, [5] above:

unde: f este factorul de frecare:
În conformitate cu consideraţiile din, [5]:

$$D_e = \frac{4 \cdot \varepsilon}{a_{so}(1-\varepsilon)}, \quad a_{so} = \frac{6}{d_e} \quad (6)$$

Having in view the item (3), (6) above, which are included in item (5) and after making calculation, the result is:

Având în vedere relaţiile (3), (6) care se includ în (5) şi după efectuarea calculelor se obţine:

$$\frac{(-\Delta P)}{h} = 3(K')^3 \cdot f \cdot \frac{\rho_a v^2 (1-\varepsilon)}{d_e \varepsilon^3} \quad (7)$$

where: K' = h´/ h is so called bed tortuousness coefficient and d_e is particle equivalent diameter. If we make notation $f' = f \cdot (K')^3$, a modified friction coefficient, then the equation (7) becomes:

unde: K' = h´/ h este aşa numitul coeficient de tortuozitate a patului şi d_e este diametrul echivalent al particulei., Dacă se notează: $f' = f \cdot (K')^3$, un factor de frecare modificat atunci ecuaţia (7), devine:

$$\frac{(-\Delta P)}{h} = 3f' \cdot \frac{\rho_a v^2 (1-\varepsilon)}{d_e \varepsilon^3} \quad (8)$$

This equation is known as Burke-Plummer equation and value of f' to be obtained experimentally and depends on Reynolds number, [5].

Această ecuaţie este cunoscută sub numele de ecuaţia lui Burke-Plummer, iar valoarea lui f' se obţine experimental şi depinde de numărul lui Reynolds, [5].

Global laminar- turbulent flow

This is the real case, most plausible, in which both flow types through seed layer exist simultaneously. The characterization of air flow is defined by Reynolds number modified for particle:

Curgerea globală laminar - turbulentă

Acesta este cazul real, cel mai plauzibil, în care sunt prezente simultan ambele regimuri de curgere al aerului prin stratul de seminţe. Caracterizarea regimului de curgere se face prin numărul lui Reynolds modificat pentru particule:

$$\mathrm{Re}_p = \frac{\rho_a \cdot v \cdot d_e}{\eta} \quad (9)$$

where v is not the real speed but conventional speed.
As per item [5] data, if: Re_p < 40 then flow mode is laminar and for Re_p > 40 the flow mode is turbulent or global-turbulent. In accordance with certain considerations, detailed in item [5], it is recommended for estimations, in case of solid granular materials (seeds) the following equation to be applied:

unde v nu este viteza reală ci viteza convenţională.
Conform datelor din [5], dacă: Re_p < 40 atunci regimul de curgere este laminar şi pentru Re_p > 40 regimul de curgere este turbulent sau global laminar-turbulent. După unele consideraţii, prezentate în detaliu în [5], se recomandă pentru estimări, în cazul materialelor granulare solide (seminţele) utilizarea ecuaţiei:

$$\frac{(-\Delta P)}{h} = 150 \cdot \frac{(1-\varepsilon)^2 \eta}{\varepsilon^3 d^2{}_e} \cdot v + 1{,}75 \cdot \frac{(1-\varepsilon)\rho_a}{\varepsilon^3 d_e} \cdot v^2 \quad (10)$$

known as Ergun equation.
This equation can be used to estimate not only pressure downfall (-ΔP), at the air circulation through seed layer, independent of flow type, if all parameters on the right side of the equation can be evaluated, but also conventional speed v when pressure downfall (-ΔP) is estimated.

cunoscută sub numele de ecuaţia lui Ergun.
Această ecuaţie poate fi folosită la estimarea, atât a căderii de presiune (-ΔP), la curgerea curentului de aer prin stratul de seminţe, independent de tipul curgerii, dacă toţi parametrii din dreapta ecuaţiei pot fi evaluaţi, cât şi a vitezei convenţionale v când se estimează căderea de presiune (-ΔP).

Minimum speed at fluidization

It is important to know the point when fluidization takes place, defined by minimum speed of fluidization. In this point takes place the dynamic equilibrium between weight forces (F_G) and those exerted by air (F_P) upon particles:

Viteza minimă de fluidizare

Este important de cunoscut punctul la care are loc fluidizarea, definit prin viteza minimă de fluidizare. În acest punct are loc echilibrul dinamic între forţele de greutate (F_G) şi cele exercitate de aer (F_P) asupra particulelor:

$$F_G = (\rho_p - \rho_a) S \cdot h(1-\varepsilon) g \quad (11)$$

where: ρ_p - particles density; S - vibrating surface (equal to cross surface of the column having same surface); g - gravity acceleration. The force due to air pressure on the particles from layer of cross section, is:

unde: ρ_p - este densitatea particulelor; S - este aria suprafeţei vibratoare (egală cu suprafaţa transversală a unei coloane cu această suprafaţă); g - acceleraţia gravitaţională. Forţa datorită presiunii aerului asupra particulelor din strat din secţiunea transversală este:

$$F_p = (-\Delta P)\cdot S \quad (12)$$

where: (-ΔP) - is pressure downfall of the air when goes through the seed layer, which depends on its flow. The minimum speed on which fluidization takes place, corresponds to the equality between the two forces, $F_G = F_P$ and resulting:

unde: (-ΔP) - este căderea de presiune a aerului la trecerea prin stratul de seminţe, care depinde de curgerea acestuia. Viteza minimă la care are loc fluidizarea, corespunde egalităţii între cele două forţe, $F_G = F_P$, de unde rezultă:

$$\frac{(-\Delta P)}{h} = (\rho_p - \rho_a)(1-\varepsilon)g \quad (13)$$

and for pressure downfall Ergun equation to be applied (10), resulting the below equation:

iar pentru căderea de presiune se foloseşte ecuaţia lui Ergun (10), obţinându-se ecuaţia

$$(\rho_p - \rho_a)(1-\varepsilon)g = 150\cdot\frac{(1-\varepsilon)^2\eta}{\varepsilon^3 d^2_e}v_m + 1{,}75\cdot\frac{(1-\varepsilon)\rho_a}{\varepsilon^3 d_e}v^2_m \quad (14)$$

where: v_m - minimum speed at fluidization.

It is correct to apply the equation (14) if the particles Reynolds number from equation (9) meet the requirement of turbulent flow, $Re_p > 40$, [5]. On the basis of these equations, with practical data for wheat and barley seeds, the values of pressure downfall and air speed under different working conditions will be evaluated, on theoretical studies, applicable to the two types of machines existing in practice.

unde: v_m - este viteza minimă la fluidizare.

Utilizarea ecuaţiei (14) este corectă dacă numărul lui Reynolds pentru particule din ecuaţia (9) satisface cerinţa curgerii turbulente, $Re_p > 40$, [5]. Pe baza acestor ecuaţii, cu date practice pentru seminţele de grâu şi orz, vor fi evaluate, pe studii de caz, cu aplicaţie la două tipuri de maşini existente în practică, valorile căderilor de presiune şi vitezelor curentului de aer în diferite condiţii de lucru.

RESULTS

Theoretical study

Theoretical study will make reference to the estimation of conventional air speed under seed layer not only for wheat seeds but for barley seeds, in the segregation process by density and compare them to the customary values utilized in practice for Cimbria Gravity Separator GA71 machine, for wheat seeds, and Jubus MJ-S 120 machine, for barley seeds.

In order to evaluate the pressure downfall and air speed under different working conditions we will refer to the Glosa species of native wheat seeds, crop of year 2011 and 2012 selected by densitometry machine Gravity Separator with an active vibrating surface of S = 1.5 m^2, [1].

During our experimental studies, the wheat seeds layer during the machine working process had a height, experimentally measured by us, h = 25 mm in a loose condition having a porosity greater than the one when air does not circulate through system. In repose condition, the wheat seeds porosity was ε = 0.35 - 0,4.

It was taken into account the sphericity coefficient (for shape), ψ = 0.85, [5]. On the basis of the known formula, the equivalent diameter of wheat seeds is, [1]: $d_e = \psi (6/\pi)^{1/3}(m_p/\rho_p)^{1/3}$ where: m_p - seeds mass (0.04 g - average value); ρ_p - seeds density (1,25 g/cm^3 - average value), after making calculations we get d_e=3.35 mm, [1].

Also, it was taken into account for pressure downfall (-ΔP) the average value experimentally determined, [4] of: (-ΔP) = 7.5 mm H_2O = 73.5 Pa, for air density and dynamic viscosity under normal conditions (t =20°C and atmospheric pressure 760 mm. Hg.col.), ρ_a = 1.21 kg/m^3 and η = 2.12 ·10^{-5} Pa· s, [2].

Substituting above data in Ergun equation (10) and making calculation, we obtain the second order equation in v: v^2 + 0,269v - 0,496 = 0, valid for a positive result of equation only, for air speed under seed layer v = 0.58 m/s. The regime of air circulation against particles is checked and Reynolds number modified with eq.(9) is calculated. The result is, Re_p = 111, $Re_p > 40$, thus

REZULTATE

Studiul de caz

Studiul de caz se va referi la evaluările vitezelor convenţionale ale aerului sub stratul de seminţe, atât pentru seminţele de grâu cât şi pentru seminţele de orz, în cazul procesului de separare după densitate şi compararea acestora cu valorile uzuale utilizate în practică în cazul maşinii Cimbria Gravity Separator GA71, utilizată pentru seminţele de grâu, iar pentru seminţele de orz maşina Jubus MJ-S 120.

Pentru evaluarea căderilor de presiune şi a vitezelor curentului de aer în diferite condiţii de lucru ne vom referi la seminţele de grâu din soiul autohton Glosa, din producţia anului 2011 şi 2012 sortate cu maşina densimetrică Cimbria Gravity Separator având o suprafaţă vibratoare activă S = 1,5 m^2, [1].

La experimentările noastre stratul de seminţe de grâu în timpul lucrului maşinii avea o înălţime măsurată experimental de noi, h = 25 mm într-o stare afânată cu o porozitate mai mare ca aceea când aerul nu circulă prin sistem. În starea de repaus, porozitatea seminţelor de grâu a fost ε = 0,35 - 0,4.

S-a considerat coeficientul de sfericitate (de formă), ψ = 0,85, [5]. Diametrul echivalent al seminţelor de grâu este, pe baza relaţiei cunoscute, [1]: $d_e = \psi (6/\pi)^{1/3}(m_p/\rho_p)^{1/3}$ unde: m_p - masa seminţei (0,04 g - valoare medie); ρ_p - densitatea seminţei (1,25 g/cm^3 - valoare medie), după efectuarea calculelor a rezultat d_e=3,35 mm, [1].

De asemenea s-a considerat pentru căderea de presiune (-ΔP) valoarea medie determinată experimental, [4] de: (ΔP) = 7,5 mm H_2O = 73,5 Pa, pentru densitatea aerului şi vâscozitatea dinamică în condiţii normale (t =20°C şi presiunea atmosferică 760 mm. col. Hg), ρ_a = 1,21 kg/m^3 şi η = 2,12 ·10^{-5} Pa· s, [2].

Înlocuind datele de mai sus în ec. lui Ergun (10) şi efectuând calculele rezultă ecuaţia numerică de gradul II în v: v^2 + 0,269v - 0,496 = 0, valabilă numai soluţia pozitivă a ecuaţiei pentru viteza aerului sub stratul de seminţe v=0,58m/s. Se verifică regimul de curgere al aerului faţă de particule, calculându-se numărul lui Reynolds modificat cu ec.(9). Se obţine, Re_p = 111, $Re_p >$

means that the air flow is turbulent, and the utilization of Ergun equation is completely justified.

In conformity with technical description of the machine Q = 1 m^3/s, S_a = 1.5 m^2 the conventional speed used during machine working process is v=Q/S_a=0.67 m/s, which means a deviation from estimated speed of Ergun equation (0.58 m/s), of (-13.4%), such value being accepted in technical conditions.

Also, during machine working process the pressure downfall was measured by piezometric method by means of a glass pipe, connected to machine, as shown in [1], resulting the value (-ΔP=10 mm col.H_2O). The pipe was filled with distilled water at the environment temperature and the pressure downfall represents the gauge difference after reading on the paper, attached to the latch plate, [1]. The value experimentally determined is 10 mm col.H_2O as against those evaluated by calculation 9.51 mm col.H_2O.

Using Ergun equation (10) for value of air flow speed during machine working process (v = 0.67 m/s) and for the values of the above mentioned parameters for wheat, after making calculation we obtain (-ΔP)=93.2 Pa. In this case, the estimated error between calculated value and measured value is 4.9 %, such deviation justifies the validity of Ergun equation.

Also, the pressure downfall and air flow speed were evaluated for barley seeds, separated by gravity machine Jubus MJ-S 120, with an active surface S_a = 3.36 m^2 [6], this machine is used in practice in Constanta country. During experimental studies, have been used Maresal species of native barley seeds, from Constanta country, from 2011 crop.

During experimental studies, the barley layer had a height experimentally measured by us h = 25 mm, at a porosity ε = 0.45, [1], seeds average dimensions being l = 10mm, b = 3.5mm, c = 3mm where: l, b, c (length, width, and thickness of barley seed). For barley designed to sowing, it is necessary to sort seeds by their density in order to obtain the most vigorous material.

Drawing an analogy between the shape of barley seeds and an oblate spheroid, with length l, big semi axis x=l/2=5mm and small semi axis: y = (b+c)/4 = 1.625mm, and making relevant calculations we obtain a sphericity coefficient ψ=0,839, [1] and the equivalent diameter of barley seeds is, on the basis of the known formula, [1]: $d_e = \psi\,(6/\pi)^{1/3}(m_p/\rho_p)^{1/3}$ where: m_p - seed mass (0.05 g - average value); ρ_p - seed density (1.3 g/cm^3 - average value),after making calculation: d_e= 3.51 mm, [1].

Input these data into Ergun equation (10), and considering pressure downfall (-ΔP)=7.5mm H_2O=73.5Pa, and for air density and dynamic viscosity under normal conditions (t=20°C and atmospheric pressure 760 mm. Hg col), ρ_a=1.21kg/m^3 and $\eta=2.12\cdot10^{-5}$Pa·s, [2], after making calculations we obtain the second order equation in v: v^2+0,235v-0,807=0, valid for the positive result for air speed under the seed layer, only v=0.79m/s. The regime of air flow against particles is checked and Reynolds number modified with eq.(9) can be calculated. The result is, Re_p=158 (Re_p > 40) that means the air flow is turbulent, the utilization of Ergun equation is completely justified.

This value of the speed allows to estimate the flow of machine's fan during working process, Q=v·S_a, obtaining Q=0.79·3.36=2.654m^3/s, such value being used to make an initial adjustment of the machine.

40, circulaţia aerului fiind turbulentă, ceea ce justifică utilizarea ec. Ergun.

Din datele tehnice ale maşinii Q = 1 m^3/s, S_a = 1,5 m^2 rezultă viteza convenţională utilizată în timpul lucrului maşinii de v=Q/S_a=0,67 m/s, ceea ce înseamnă o abatere faţă de viteza estimată din ecuaţia lui Ergun (0,58 m/s), de (-13,4 %), valoare acceptată în condiţii tehnice.

De asemenea s-a procedat la măsurarea căderii de presiune în timpul lucrului maşinii, prin metoda piezometrică cu ajutorul unui tub din sticlă, conectat la maşină, aşa cum se arată în [1], obţinându-se valoarea (-ΔP = 10 mm col.H_2O). În tub s-a introdus apă distilată la temperatura mediului iar căderea de presiune reprezintă diferenţa de nivel ce s-a citit pe hârtia milimetrică, ataşată plăcii de sprijin, [1]. Valoarea determinată experimental este de 10 mm col. H_2O faţă de cea evaluată prin calcul de 9,51 mm col. H_2O.

Utilizând ec. lui Ergun (10) pentru valoarea vitezei curentului de aer din timpul lucrului maşinii (v = 0,67 m/s) şi pentru valorile parametrilor specificaţi anterior în cazul grâului, după efectuarea calculelor se obţine (-ΔP)=93,2 Pa. În acest caz eroarea estimată pentru calcul faţă de valoarea măsurată, obţinută este de 4,9 %, eroare ce justifică valabilitatea aplicabilităţii ec. lui Ergun în acest caz.

De asemenea au fost evaluate căderile de presiune şi viteza curentului de aer, în cazul seminţelor de orz, sortate cu maşina densimetrică Jubus MJ-S 120, având o suprafaţă activă S_a = 3,36 m^2 [6], utilizată în practică în cadrul jud. Constanţa. La încercările experimentale s-au folosit seminţe de orz soiul autohton Mareşal, din jud. Constanţa din producţia anului 2011.

În timpul experimentărilor stratul de seminţe de orz avea o înălţime măsurată experimental de noi de h = 25 mm, la o porozitate ε = 0,45, [1], dimensiunile medii ale seminţelor fiind l = 10mm, b = 3,5mm, c = 3mm unde: l, b, c (lungimea, lăţimea, grosimea seminţei de orz). Pentru orzul destinat însămânţării este necesară o separare după densitate a seminţelor pentru obţinerea fracţiei cu seminţele cele mai viguroase.

Asimilându-se forma reală a seminţelor de orz cu un elipsoid de revoluţie, cu lungimea l, semiaxa mare x=l/2=5mm şi semiaxa mică: y = (b+c)/4 = 1,625mm, efectuând calculele se obţine un coeficient de sfericitate ψ=0,839, [1] şi diametrul echivalent al seminţelor de orz este, pe baza relaţiei cunoscute, [1]: $d_e = \psi\,(6/\pi)^{1/3}(m_p/\rho_p)^{1/3}$ unde: m_p - masa seminţei (0,05 g - valoare medie); ρ_p - densitatea seminţei (1,3 g/cm^3 - valoare medie), după efectuarea calculelor va fi: d_e = 3,51 mm, [1].

Cu aceste date introduse în ecuaţia lui Ergun (10), şi considerând căderea de presiune (-ΔP)=7,5mm H_2O=73,5Pa, iar pentru densitatea aerului şi vâscozitatea dinamică în condiţii normale (t=20°C şi presiunea atmosferică 760 mm.col. Hg), ρ_a=1,21kg/m^3 şi $\eta=2,12\cdot10^{-5}$Pa·s, [2], după efectuarea calculelor se obţine ecuaţia numerică de gradul II în v: v^2+0,235v-0,807=0, valabilă numai soluţia pozitivă a ecuaţiei pentru viteza aerului sub stratul de seminţe v=0,79m/s. Se verifică regimul de curgere al aerului faţă de particule, calculându-se numărul lui Reynolds modificat cu ec.(9). Se obţine, Re_p=158 (Re_p > 40) care arată că circulaţia aerului este turbulentă, deci ceea ce justifică utilizarea ec. Ergun.

Această valoare a vitezei permite, estimarea debitului ventilatorului maşinii, în timpul lucrului, Q=v·S_a, obţinându-se Q=0,79·3,36=2,654m^3/s, valoare utilizată pentru efectuarea unui reglaj iniţial al maşinii.

CONCLUSIONS

This thesis states that stratification effect is enabled if during air flow circulation through seed layer, the seed layer will get loose up to fluidization level, respectively an increase of layer porosity and surface vibrations which are conveyed to the layer of seeds.

Also, it is emphasized the important part in elaborating the technological separation flow within the machine of pressure downfall (-ΔP) on the layer thickness which allows the air flow circulation through porous bed , and, respectively the air speed circulation.

During seeds segregation process by density with pneumatic vibrating machines, the vibrating motion of the planned double inclined surface of the machine plays an important role together with vertical air flow circulation through seed layer on the surface which has a stratification effect.

It was developed a mathematical model of the air flow going through seeds vibrating layer on the basis of theory of analogy between this and flowing through bed of solid particles in stationary condition, considering that under real condition, the particles (seeds) movements take place with a speed, relatively low, on the vibrating surface.

Data are useful for the real case of air flow going through seed layer which is global laminar turbulent flow where the two flow modes exist simultaneously; thus allows Ergun's equation (eq.10) to be applied in order to create a link between pressure downfall (-ΔP) and the speed of air flow through layer seeds.

Mathematical model of the air flow circulation through vibrating seed layer, in the form of Ergun (ec.10) equation, was applied for concrete situation in two theoretical studies, and the estimated values for pressure downfall (-ΔP), have been compared to experimental data obtained through measurements, and they were highly satisfactory.

Both values of conventional speed (v=0.58 m/s) obtained for air circulation under layer of wheat seed with thickness h=25 mm, porosity ε=0.4 which is plausible, and experimental confirmation of value of estimated pressure downfall (-ΔP), allow us to appreciate that we can use the Ergun equation with good results not only to determine speed v and consequently the fan's rate flow if the pressure downfall is known, but also for evaluate pressure downfall (-ΔP) if speed v is known (from fan's rate flow formula).

Also, the value of speed (v=0.79m/s) for air circulation under barley seed layer with thickness h=25mm and a porosity ε = 0.45 is plausible, being one more proof that Ergun equation can be utilized with good results, to evaluate not only the speed v but also the pressure downfall (-ΔP) for various situation arisen during working process of machine in discussion.

These data are very useful for research and engineering activities in the field of pneumatic-vibrating machines for sorting seeds by density and also contribute to enrich the bank of scientific data in this domain.

REFERENCES

[1]. Buciuman F.V., (2013) - *Contribution to optimization of selection, cleaning and segregation systems for grains*, Doctorate thesis, Bucharest PU; Bucharest, Romania;
[2]. Căsăndroiu T., (1993) - *Machinery for initial processing and preserving the agricultural products,* Course, vol. 1, Bucharest Politechnic University,

CONCLUZII

În această lucrare se constată că efectul de stratificare este favorizat dacă la curgerea curentului de aer prin stratul de seminţe se produce o afânare a acestuia până la starea limită de fluidizare, respectiv o creştere a porozităţii stratului şi de vibraţia suprafeţei transmisă şi ea stratului de seminţe.

De asemenea, se evidenţiază rolul fundamental în elaborarea fluxului tehnologic de separare optim în interiorul maşinii, a căderii de presiune (-ΔP), pe grosimea stratului de seminţe care asigură circulaţia aerului prin patul poros cu care acesta este asimilat şi respectiv a vitezei de circulaţie a aerului.

În procesul separării seminţelor după densitate cu ajutorul maşinilor pneumo-vibratoare un rol însemnat îl are, pe lângă mişcarea vibratorie a suprafeţei plane dublu înclinate a maşinii şi circulaţia curentului de aer vertical ascendent prin stratul de seminţe de pe suprafaţă, cu efect de stratificare.

S-a dezvoltat modelul matematic al curgerii aerului prin stratul de seminţe vibrator pe baza ipotezei analogiei între aceasta şi curgerea prin patul de particule solide în stare staţionară, considerându-se că în starea reală deplasările particulelor (seminţelor) au loc cu viteze relativ mici, pe suprafaţa vibratoare.

Curgerea globală laminar-turbulentă este cazul real de curgere a aerului prin stratul de seminţe în care sunt prezente simultan ambele regimuri de curgere ceea ce a permis utilizarea ecuaţiei lui Ergun (10) pentru legătura între căderea de presiune (-ΔP) şi viteza convenţională a curentului de aer prin seminţele din strat.

Modelul matematic al curgerii aerului prin stratul de seminţe vibrator sub forma ecuaţiei lui Ergun (ec.10) a fost utilizat în situaţii concrete în două studii de caz, comparându-se valorile estimate pentru căderea de presiune (-ΔP), cu datele experimentale obţinute la măsurători, care au dat deplină satisfacţie.

Atât valoarea vitezei convenţionale (v=0,58 m/s) obţinută pentru circulaţia aerului sub stratul de seminţe de grâu de grosime h=25 mm şi o porozitate ε=0,4 care este plauzibilă, cât şi confirmarea experimentală a valorii estimate a căderii de presiune (-ΔP), ne permit să apreciem că se poate utiliza cu bune rezultate ecuaţia lui Ergun fie pentru determinarea vitezei v şi de aici a debitului ventilatorului dacă se ştie căderea de presiune (-ΔP), fie pentru evaluarea căderii de presiune (-ΔP), dacă se cunoaşte viteza v (din cunoaşterea debitului respectiv al ventilatorului).

De asemenea valoarea vitezei (v=0,79m/s) obţinută pentru circulaţia aerului sub stratul seminţelor de orz de grosime h=25 mm şi o porozitate ε=0,45 este plauzibilă, încă o dovadă că se poate utiliza cu bune rezultate ecuaţia lui Ergun la evaluări fie ale vitezei v, fie ale căderii de presiune (-ΔP), pentru diferitele situaţii posibile în timpul lucrului maşinilor considerate.

Aceste date sunt utile în activităţile de cercetare şi inginereşti din sfera maşinilor pneumo-vibratoare pentru separare densimetrică a seminţelor contribuind la îmbogăţirea băncii de informaţii ştiinţifice din acest domeniu.

BIBLIOGRAFIE

[1]. Buciuman F.V., (2013) - *Contribuţii privind optimizarea sistemelor de sortare, curăţire şi separare a materialelor agricole,* Teză de doctorat, Universitatea Politehnică Bucureşti, Bucureşti, România;
[2]. Căsăndroiu T., (1993) - *Utilaje pentru prelucrarea primară şi păstrarea produselor agricole,* Curs, vol. 1, Universitatea Politehnică Bucureşti, Bucureşti, România;

[3]. Căsăndroiu T. (1976) - *Laboratory guide for sorting, conditioning machines and primary work of the agricultural products,* Bucharest PI;
[4]. Iaremenco M.K. (1952) - *The study of pneumatic segregation table* - The Study of Scientific Research for Agricultural Mechanization - Volume 17, Moscow;
[5]. Ibartz A., Gustavo V. Barbosa - Canovas (2003) - *Unit Operations in Food Engineering, Circulation of Fluid through Porous Beds: Fluidization,* CRC Press, Publishing House, pg. 205-235;
[6]. *** - *Prospects, Manual of Instruction*: Densimetric Machine Jubus M-JS-30/120;
[7]. *** - www.cimbria.com *Cimbria Gravity Separator GA71.*

[3]. Căsăndroiu T., (1976) - *Îndrumar de laborator pentru maşini de sortat, condiţionat şi prelucrarea primară a produselor agricole,* IPB, Bucureşti;
[4]. Iaremenco M.K., (1952) - *Studiul mesei pneumatice de sortare* - Lucrarea Institutului de Cercetari Stiintifice de Mecanizare a Agriculturii - Volumul 17, Moscova;
[5]. Ibartz A., Gustavo V. Barbosa-Canovas (2003) - *Aparatură pentru industria alimentară, Circulaţia fluidului prin paturi poroase: fluidizare*, Editura CRC Press, pag.205-235;
[6]. *** *Prospecte, Manual de instrucţiuni*: Maşina densimetrică Jubus M-JS-30/120;
[7]. *** - www.cimbria.com *Cimbria Gravity Separator GA71.*

PHYSICAL PROPERTIES OF THE GRIST FRACTIONS AT THE SECOND REDUCTION PASSAGE OF A MILLING PLANT
/
PROPRIETĂŢILE FIZICE ALE FRACŢIILOR DE MĂCINIŞ LA AL DOILEA PASAJ DE MĂCINARE AL UNEI MORI DE GRÂU

As. Ph.D. Eng. Constantin G.A., Prof. Ph.D. Eng. Voicu Gh., Lect. Ph.D. Eng. Stefan E.M., Prof. Ph.D. Eng. Paraschiv G., Lect. Ph.D. Eng. Muşuroi G.
„Politehnica" University of Bucharest, Faculty of Biotechnical Systems Engineering / Romania
Tel: 0727651064; E-mail: gabriel_alex99@yahoo.com

Abstract: *Choosing the functional and constructive characteristics of the equipment on the technological flow of a milling plant is influenced primarily by the physical properties of grist intermediate products. In the paper are presented the results of experimental researches concerning the physical properties of grist (the coefficient of static friction - on three types of surfaces, angle of natural slope, bulk density, density, specific surface, porosity) at plansifter compartment of the reduction roller mill for a milling plant of 4.2 t/h from Romania.*

Keywords: *wheat milling, grist, plansifter compartment, physical properties, grinding phase, reduction roller mill*

INTRODUCTION

Manufacture of wheat flour involves repeated grinding and sieving operations, for endosperm to be separated from the bran. Grinding of wheat is made into two separated technological phases: crushing of wheat seeds (breakage phase) and grinding of semolina (reduction phase). In wheat milling plant, breakage / reduction and sifting are complementary operation forming together individual technological phases. After each grinding stage, a sorting on fractions (sifting) of the grist within a plansifter compartment, is performed.

According to several papers from the specialty literature [1, 7, 10, 11], sifting of intermediate products is affected by several factors, the most important being: size and shape of the grist particles, character of the relative motion of the particles on the sieve surface, characteristics of sifting sieve fabric, revolution of plansifter, and the amount of material reaching the sieve.

To properly correlate the technical characteristics of equipment used in the milling process flow is particularly important to know the granulometric characteristics, as well as physical characteristics of grist intermediate products. Thus, operating parameters of equipment on the technological flow, and proper selection of fabrics from inside of plansifters or semolina machines, are influenced by the physical properties of grist.

Coefficient of static friction and angle of natural slope of grist intervene in the movement of grist particles on different types of surfaces, in the sorting on fractions and in the characterization of separation on fractions process, [3].

As described in the paper [5], it is important to know the physical properties of wheat seeds (size and shape, bulk density, density, and mechanical properties, among which hardness and elastic modulus) because they influence the processes of grinding and sifting, grist

Rezumat: *Alegerea caracteristicilor funcţionale şi constructive ale echipamentelor de pe fluxul tehnologic al oricărei unităţi de morărit este influenţată în primul rând de proprietăţile fizice ale produselor intermediare de măciniş. În lucrare sunt prezentate rezultatele unor cercetări experimentale privind proprietăţile fizice ale măcinişului (coeficientul de frecare static – pe trei tipuri de suprafeţe, unghiul de taluz natural, masa volumică, densitatea, suprafaţa specifică, porozitatea) la compartimentul de sită plană al celui de-al doilea măcinător pentru o unitate de morărit de 4,2 t/h din România.*

Cuvinte cheie: *mărunţirea grâului, măciniş, compartiment de sită plană, proprietăţi fizice, faza de măcinare, măcinător*

INTRODUCERE

Fabricarea făinii de grâu presupune operaţii repetate de măcinare şi cernere, pentru ca endospermul să fie separat de tărâţă. Mărunţirea grâului se face în două faze tehnologice separate: zdrobirea seminţelor de grâu (faza de şrotare) şi măcinarea grişurilor (faza de măcinare). În morile de grâu şrotarea / măcinarea şi cernerea sunt operaţii complementare formând împreună pasaje tehnologice individuale. După fiecare etapă de mărunţire se face o sortare pe fracţii (cernere) a măcinişului în cadrul unui compartiment de sită plană.

Conform mai multor lucrări din literatura de specialitate [1, 7, 10, 11], cernerea produselor intermediare este afectată de mai mulţi factori, cei mai importanţi fiind: mărimea şi forma particulelor de măciniş, caracterul mişcării relative a particulelor de material pe suprafaţa sitei, caracteristicile ţesăturii sitei de cernere, turaţia sitei plane, dar şi cantitatea de material care ajunge pe sită.

Pentru corelarea corectă a caracteristicilor tehnice ale utilajelor folosite în cadrul fluxului tehnologic de morărit este deosebit de importantă cunoaşterea caracteristicilor granulometrice, precum şi a proprietăţilor fizice ale produselor intermediare de măciniş. Astfel, parametrii de lucru ai echipamentelor de pe fluxul tehnologic, precum şi alegerea corectă a ţesăturilor din interiorul sitelor plane sau ale maşinilor de griş, sunt influenţate de proprietăţile fizice ale măcinişului.

Coeficientul de frecare static, precum şi unghiul de taluz natural al măcinişului, intervin în mişcarea particulelor de măciniş pe diferite tipuri de suprafeţe, în procesul de sortare pe fracţii şi în caracterizarea procesului de separare pe fracţii, [3].

După cum se arată în lucrarea [5], este importantă şi cunoaşterea proprietăţilor fizice ale seminţelor de grâu (formă şi mărime, masă volumică, densitate, precum şi proprietăţi mecanice, între care duritatea şi modulul de elasticitate) deoarece acestea influenţează procesele de

properties being correlated with those of the seeds from which it came. Among these, wheat seeds hardness imposes functional and constructive characteristics of the roller mills, as well as shape and size of grist particles which influence the choice of fabrics for sorting on fractions of grist.

Processes of drying, ventilation, heating and cooling of wheat seeds, efficient use of storage places (especially, at seeds and final products of the grinding process), but also process of modeling of air flow through the mass of material particles are affected by the porosity of the wheat seeds and intermediate grist products, [6]. Also, porosity of grist fractions and density of particles influence the stratification of grist on the frames inside of plansifter compartment.

Taking into account the importance of knowing the physical properties of grist products, obtained after each stage of sifting within a plansifter compartment, this paper presents the results of experimental research on the physical properties of the fractions separated at compartment of reduction roll 2 of a milling plant of 4.2 t/h.

MATERIALS AND METHODS

Samples used in the experimental measurement of the physical characteristics of grist were taken on the technological flow of unit S.C. Spicul S.A., Roşiorii de Vede, Teleorman, Romania. There were experimentally determined: coefficient of static friction, angle of slope, bulk density and density of particles of each fraction and were calculated the specific surface and porosity of grist fraction at plansifter compartment C2 for passage M1B from the reduction phase of the milling plant. In fig.1 is presented the flow diagram for reduction phase of semolina at the reminded milling plant.

mărunţire şi cernere, proprietăţile măcinişului fiind corelate cu cele ale seminţei din care provine. Dintre acestea, duritatea seminţelor de grâu impune caracteristicile funcţionale şi constructive ale cilindrilor de mărunţire, precum şi forma şi mărimea particulelor de măciniş care influenţează alegerea ţesăturilor pentru sortarea fracţiilor de măciniş.

Procesele de uscare, ventilare, încălzire şi răcire a seminţelor de grâu, ocuparea eficientă a locurilor de depozitare (în special, la seminţe şi produsele finite ale procesului de mărunţire), dar şi procesul de modelare a fluxului de aer prin masa de particule de material sunt influenţate de porozitatea seminţelor de grâu şi a produselor intermediare de măciniş, [6]. De asemenea, porozitatea fracţiilor de măciniş şi densitatea particulelor influenţează stratificarea măcinişului pe ramele compartimentelor de sită plană

Dată fiind importanţa cunoaşterii proprietăţilor fizice a produselor de măciniş, obţinute după fiecare fază de cernere în cadrul unui compartiment de sită plană, în această lucrare se prezintă rezultatele unor cercetări experimentale asupra proprietăţilor fizice ale fracţiilor separate la compartimentul măcinătorului 2 al unei unități de morărit de 4,2 t/h.

MATERIALE ŞI METODE

Probele utilizate în determinările experimentale ale caracteristicilor fizice ale măcinişului au fost prelevate de pe fluxul tehnologic al unităţii S.C. Spicul S.A., Roşiorii de Vede, Teleorman, România. Au fost determinate experimental: coeficientul de frecare static, unghiul de taluz natural, masa volumică şi densitatea particulelor fiecărei fracţii şi au fost calculate suprafaţa specifică şi porozitatea fracţiilor de măciniş la compartimentul C2 de sită plană aferent pasajului M1B din faza de măcinare a morii. În fig.1 este prezentată diagrama fazei de măcinare a grişurilor la unitatea de morărit amintită.

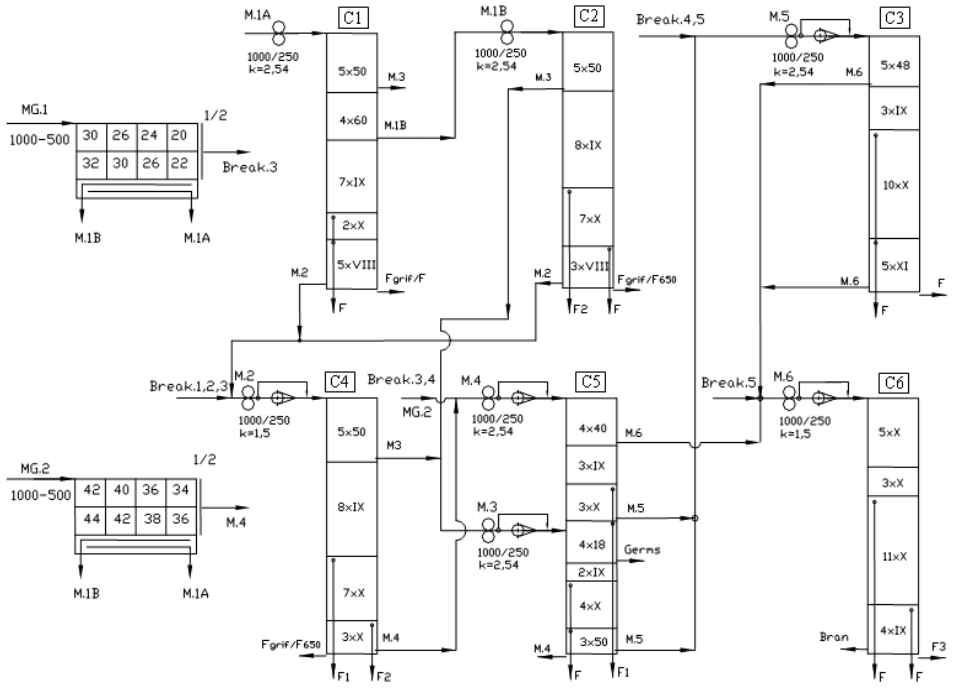

Fig. 1 – The flow diagram of the wheat reduction phase in a milling plant with the capacity of 4.2 t/h / C1–C6 – plansifter compartments; Break 1–5 – break rolls; MG1, MG2 – semolina machines; M1A, M1B, M2–M6 – reduction rolls; F, F1, F2 – flour

For technological diagram of the analyzed mill, equivalence between number of mesh and mesh size, as are indicated in the diagram, is presented in table 1.

Bulk density of a granular mixture is defined as the mass of the material reported to the total volume that it occupies in its natural state.

Pentru diagrama tehnologică a morii analizate, echivalenţa dintre numărul sitei şi dimensiunea ochiurilor acesteia, aşa cum sunt ele precizate în diagramă, este prezentată în tabelul 1.

Masa volumică a unui amestec granular este definită ca fiind masa materialului raportată la volumul total pe care acesta îl ocupă acesta în starea sa naturală.

Table 1

Equivalence between the mesh number and mesh size

Mesh number	18	20	26	36	40	46	48	50	54	56	60	VIII	IX	X	XI
Mesh size [mm]	1.17	1.05	0.78	0.52	0.47	0.39	0.37	0.35	0.32	0.31	0.28	0.18	0.17	0.15	0.13

This property is considered as one of base qualitative indices used in establishing of extraction flour, [4]. Yield of flour is closely related to the bulk density. To determine the bulk density was used the method of graduated cylinder.

Density represents the ratio between the mass of the sample and the volume occupied by the particles of it. In paper, determination of density of the grist fractions was made through pycnometric method using xylene as working fluid (ρ_x=825,44 kg/m^3).

Methodology for determining the bulk density and density used in this paper is given in detail in the papers [2, 8] and corresponds to the standard method.

In the paper was performed also particle size analysis of each grist fraction. Fineness of grist, assessed by the *mean diameter* d_m of grinded particles, determined with sieve shaker, was calculated with relation:

Această proprietate este considerată ca unul din indicii calitativi de bază folosindu-se în stabilirea extracţiei de făină, [4]. Randamentul în făinuri este strâns legat de valoarea masei volumice. Pentru determinarea masei volumice s-a utilizat metoda cilindrului gradat.

Densitatea reprezintă raportul dintre masa probei şi volumul ocupat de particulele din aceasta. În lucrare, determinarea densităţii fracţiilor de măciniş s-a făcut prin metoda picnometrică utilizând ca lichid de lucru xilenul (ρ_x=825,44 kg/m^3).

Metodologia de determinare a masei volumice şi a densităţii utilizată în lucrarea de faţă este dată în detaliu în lucrările [2, 8] şi corespunde cu metoda standard.

În lucrare s-a efectuat şi analiza granulometrică a fiecărei fracţii de măciniş. Fineţea măcinişului, apreciată prin *diametrul mediu* d_m al particulelor mărunţite, determinat cu clasificatorul cu site, s-a calculat cu relaţia:

$$d_m = \frac{\sum p_i \cdot d_i}{\sum p_i}, \text{ [mm]} \quad (1)$$

where:

p_i represents percentage of material on the sieve of the sieve shaker (i = 0, 1, 2,…, 5); Σp_i = 100 – sum of the percentages of material on sieves; d_i – average particle size of each intermediate fractions, considered as an arithmetic mean of sieves size apertures surrounding the respective fraction $d_i = (l_i+l_{i+1})/2$. Classifier sieves were chosen to meet the estimated relationship $l_{i+1} = \sqrt{2} \cdot l_i$, from the topper to the lower sieve.

Knowing the average diameter of newly formed particles, their *specific external surface* $S_{e.m}$ can be evaluated by the relation (2):

unde:

p_i reprezintă procentul de material pe sita i a clasificatorului (i = 0, 1, 2,…, 5); Σp_i = 100 – suma procentelor de material de pe site; d_i – dimensiunea medie a particulelor fiecărei fracţii intermediare, considerată ca medie aritmetică a dimensiunii orificiilor sitelor care încadrează fracţia respectivă $d_i = (l_i+l_{i+1})/2$. Sitele clasificatorului au fost alese astfel încât să respecte cât mai bine cerinţa $l_{i+1} = \sqrt{2} \cdot l_i$, pornind de la sita de sus către sita cea mai de jos a clasificatorului.

Cunoscând diametrul mediu al particulelor nou formate, *suprafaţa exterioară specifică* $S_{e.m}$ a acestora se poate evalua cu relaţia (2):

$$S_{e.m} = \frac{6}{\rho \cdot d_m}, \text{ [m}^2\text{/kg]} \quad (2)$$

where:

ρ is the density of analyzed fraction, determined with the pycnometer.

Porosity represents the property of granular materials not to overlay the whole storage volume, existing a intergranular space. Knowing the values of bulk density and density of grist, porosity was determined by the relation (3), [2], [8]:

unde:

ρ este densitatea particulelor fracţiei analizate, determinată cu picnometrul.

Porozitatea reprezintă proprietatea materialelor granulare de a nu ocupa întregul volum de depozitare, existând un spaţiu intergranular. Cunoscând valorile masei volumice şi a densităţii măcinişului, porozitatea a fost determinată cu relaţia (3), [2], [8]:

$$\varepsilon = \left(1 - \frac{\rho_V}{\rho}\right) \cdot 100 \text{ , [\%]} \quad (3)$$

The angle of the natural slope is the angle that is made by a free surface of a mass of granular material poured onto a surface, with the horizontal plane. To determine the angle of natural slope was used the material cone method, [2].

Coefficient of static friction, determined by the usual method of the inclined plane [9], was carried out on three types of surfaces: fiber glass, steel sheet and cotton canvas.

RESULTS

The experimental data which characterize the physical properties of the grist obtained at reduction roll M1B of the technological diagram of milling plant, and sorted on fraction in afferent plansifter compartment, are shown in table 2.

According to the technological diagram, wheat semolina ground in reduction roll M1B are sorted on fractions inside of plansifter compartment C2 (see fig.1), consisting of four frame packages with metallic fabric or from plastic material with mesh size in correlation with type of fabric and with number of wires per unit length (table 1).

From the analysis of fig. 1, it has been found that the first five sieves are disposed within a package, have no. 50 (i.e. mesh size of 0.35 mm) and transmit the packet refusal to reduction roll M3, while the sifting of the frames is directed to second package with eight sieve frames (flour sieves, having the fabric no. IX, ie mesh size 0.1 mm). Refusal of the second package feeds the frames of the third package that has seven sieve frames no. X, with mesh size of 0.15 mm (flour sieve). Sifting of sieve frames from packages 2 and 3 is evacuated from compartment as flour, and their refusal passes to fourth package equipped with five frames no. VIII (also flour sieve), with mesh size of 0.18 mm. Sifting of this frames is a semolina flour and is evacuated as such, while the refusal of the package is redirected to reduction roll M2.

All fractions extracted at compartment C2 – afferent to reduction roll M1B were analyzed and the coefficient of static friction and angle of natural slope were determined (table 2).

Unghiul de taluz natural reprezintă unghiul pe care îl face suprafaţa liberă a unei mase de material granular turnat pe o suprafaţă, cu planul orizontal. Pentru determinarea unghiului de taluz natural a fost utilizată metoda conului de material, [2].

Coeficientul de frecare static, determinat prin metoda uzuală a planului înclinat [9], s-a efectuat pe trei tipuri de suprafeţe: fibră de sticlă lucioasă, tablă din oţel şi pânză din bumbac.

REZULTATE

Datele experimentale ce caracterizează proprietăţile fizice ale măcinişului obţinut la măcinătorul M1B al diagramei tehnologice a unităţii de morărit, sortat pe fracţii în compartimentul de sită plană aferent, sunt prezentate în tabelul 2.

Conform diagramei tehnologice, grişurile de grâu mărunţite la măcinătorul M1B sunt clasificate pe fracţii în interiorul compartimentului C2 (vezi fig. 1), alcătuit din patru pachete de rame cu ţesături metalice sau din material plastic cu dimensiunile orificiilor sitelor în corelaţie cu tipul ţesăturii şi cu numărul de fire pe unitatea de lungime (tabelul 1).

Din analiza figurii 1 se constată că primele cinci site, sunt dispuse în cadrul unui pachet, au nr. 50 (adică dimensiunile orificiilor 0,35 mm) şi transmit refuzul pachetului către măcinătorul M3, în timp ce cernutul ramelor este dirijat către pachetul al doilea cu opt rame de sită (site de făină, având ţesătura nr. IX, adică orificii de dimensiune 0,1 mm). Refuzul pachetului al doilea alimentează ramele pachetului al treilea care are şapte rame de sită numărul X, cu orificiile ţesăturii de 0,15 mm (site de făină). Cernuturile ramelor de sită de la pachetele 2 şi 3 sunt evacuate din compartiment sub formă de făină, iar refuzul acestora trece la pachetul al patrulea prevăzut cu 5 rame nr. VIII (de asemenea, site de făină), cu orificii de 0,18 mm. Cernutul acestor rame este o făină grifică şi este evacuată ca atare, în timp ce refuzul pachetului este redirijat la măcinătorul M2.

Toate fracţiile de măciniş extrase la compartimentul C2 – aferent măcinătorului M1B au fost analizate şi s-a determinat coeficientul de frecare şi unghiul de taluz natural (tabelul 2).

Table 2

Values of coefficient of static friction and angle of natural slope

Grist fraction	Static friction coefficient, μ			Angle of natural slope, ψ
	Steel sheet	Cotton canvas	Fiber glass	
C2 Entrance	0.576÷0.723	1.470÷>1.760	0.676÷1.000	38.320
C2 M3	0.611÷0.900	>1.760÷>1.760	0.782÷1.535	41.152
C2 M2	0.835÷1.176	>1.760÷>1.760	>1.760÷>1.760	49.927
C2 Fgrif	0.688÷1.035	>1.760÷>1.760	0.829÷>1.760	38.767
C2 F2	0.653÷0.941	>1.760÷>1.760	>1.760÷>1.760	41.081
C2 F	0.676÷1.400	>1.760÷>1.760	>1.760÷>1.760	46.178

From Table 2 it can be seen that the values of the coefficient of static friction, on steel sheet and fiber glass, are within the limits described in the specialty literature. Values of friction coefficient obtained for cotton canvas also falls within the range of values presented in other papers, being somewhat higher, because of humidity, of equivalent average diameter of particles quite small, which makes them adhere to work surface used in experiments, and to high content of endosperm of grist fractions analyzed.

Using experimental values, presented in table 2, were drawn charts of variation of the average values for the coefficient of static friction and the angle of natural slope for the six grist fractions analyzed, using MS Excel program version 12 (fig.2).

Values of bulk density, specific surface, porosity and mean diameter of the grist fractions analyzed are presented in table 3.

Based on the data obtained and presented in table 3, were graphically drawn, the variations of bulk density, density, specific surface and porosity of grist intermediate products analyzed.

As can be seen from the analysis of data from table 3, and of charts in figure 3, bulk density of fractions resulted when sorting grist in plansifter compartment C2 has a random variation, depending on the type of sieve frame fabric, and the size of apertures of the working sieve, but also of the initial granulation of grist or of shell content, adhesive on the semolina particles subjected to grinding.

Din tabelul 2 se poate observa că valorile coeficientului de frecare static, pe tablă de oţel şi fibră de sticlă, sunt în limitele prezentate în literatura de specialitate. Valorile coeficientului de frecare obţinute pentru pânza din bumbac se încadrează şi ele în limitele largi ale valorilor prezentate în alte lucrări ştiinţifice, fiind însă ceva mai mari, datorită umidităţii, diametrului mediu echivalent al particulelor destul de mic, care face ca acestea să adere la suprafaţa de lucru folosită în experimente, cât şi conţinutului ridicat de endosperm al fracţiilor de măciniş analizate.

Folosind valorile experimentale, prezentate în tabelul 2, au fost trasate graficele de variaţie a valorilor medii pentru coeficientul de frecare static şi pentru unghiul de taluz natural pentru cele şase fracţii de măciniş analizate, utilizând programul MS Excel versiunea 12 (fig.2).

Valorile masei volumice, densităţii, suprafeţei specifice, porozităţii şi a diametrului mediu al fracţiilor de măciniş analizate sunt prezentate în tabelul 3.

Pe baza datelor obţinute şi prezentate în tabelul 3, au fost trasate, grafic, variaţiile masei volumice, densităţii, suprafeţei specifice şi a porozităţii produselor intermediare de măciniş analizate.

După cum se observă din analiza datelor din tabelul 3, cât şi a graficelor din figura 3, masa volumică a fracţiilor rezultate la sortarea măcinişului în compartimentul de sită plană C2 are o variaţie aleatoare, ea depinzând, atât de tipul ţesăturii ramei de sită, cât şi de dimensiunea orificiilor sitelor de lucru, dar şi de granulaţia iniţială a măcinişului sau de conţinutul de înveliş aderent pe particulele de griş supuse mărunţirii.

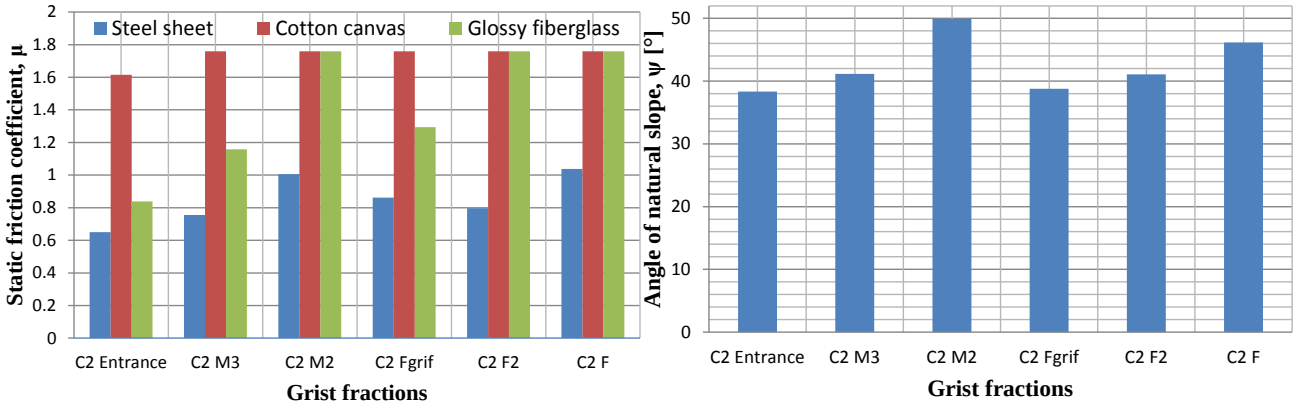

Fig. 2 - Variations of the average values of static friction coefficient for six grist fractions, on 3 types of surface (steel sheet, cotton canvas and fiber glass) and of natural slope angle

Table 3

Values of density, bulk density, specific surface, porosity and average diameter for grist fractions resulting at C1 compartment (from technological diagram)

Grist fractions	Average diameter	Bulk density	Density	Specific surface	Porosity
	[mm]	[g/dm^3]	[g/dm^3]	x 10^3 [m^2/kg]	[%]
C2 Entrance	0.160	499.000	1371.970	27.333	63.629
C2 M3	0.420	463.000	1334.897	10.702	65.316
C2 M2	0.210	426.000	1389.644	20.560	69.345
C2 Fgrif	0.140	463.000	1371.312	31.253	66.237
C2 F2	0.130	460.000	1377.551	33.504	66.607
C2 F	0.090	440.000	1382.717	48.214	68.179

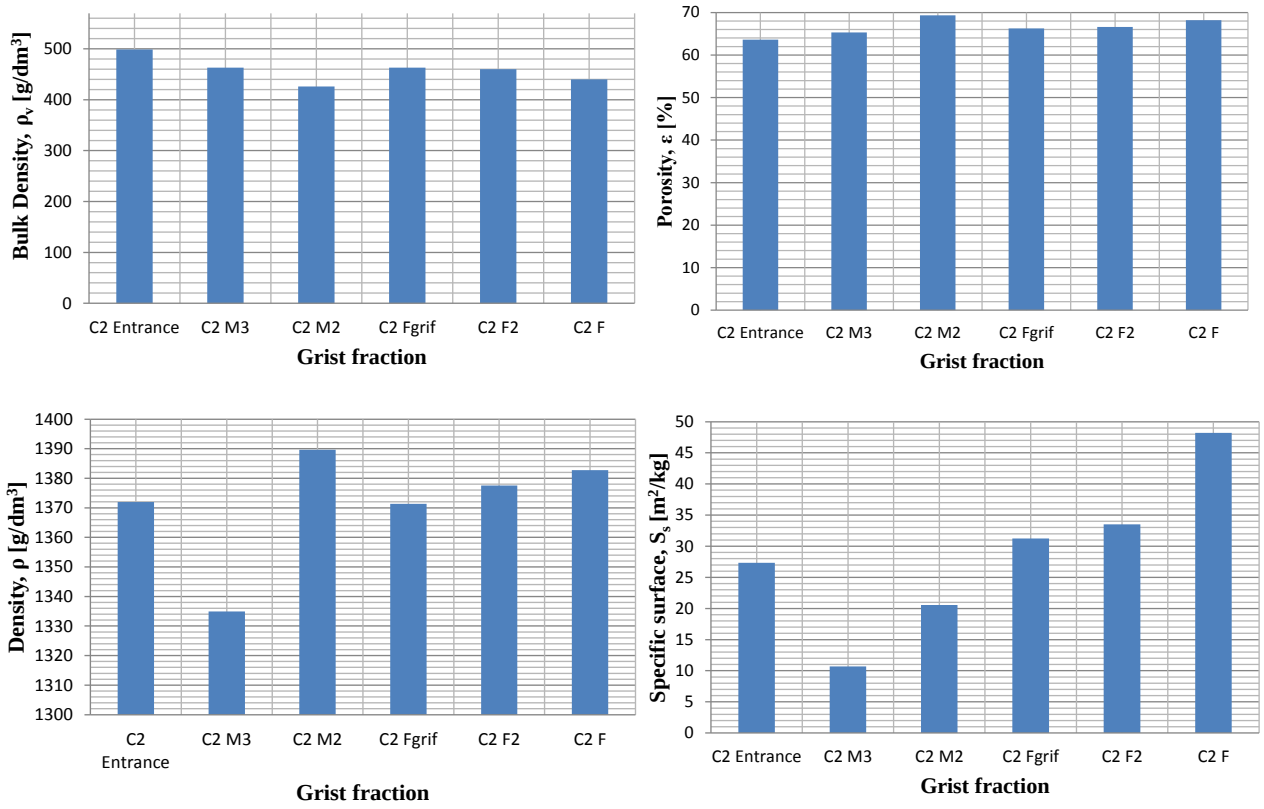

Fig. 3 - Variations of bulk density, porosity, density and specific surface values, depending on six grist fractions analyzed

Also, when grist is separated on fractions, the porosity of each fraction is changing, and this will influence the bulk density value of the resulting material.

However, it has been noticed that fractions C2-M3 and C2-Fgrif have the highest bulk density value (about 463 kg/m^3 for both). Nevertheless,it appears, that porosity of flours has relatively high values, in the inverse relationship with bulk density (about 65.3% for C2-M3, respectively 66.2% for C1-Fgrif).

It has been also noted, that fraction which has the lowest bulk density (fraction C2-M2, which is a dunst) presents the higher porosity (having 426 kg/m^3 bulk density and 69.3% porosity), in the same inverse ratio as the other fractions of compartment.

Related to the surface area of the grist fractions of compartment C2 of the second reduction roll, it is found that the flour fractions have the highest values (31.2 for m^2/kg C2-Fgrif, 33.5 m^2/kg for C2-F2 respectively 48.2 m^2/kg for m^2/kg).

It is found that fraction C2-M3 (with a high content of shell) has a lower specific surface (about 10.7 m^2/kg), even if the porosity is high.

Regarding the fraction C2-M2 classified as dunst, it has a specific surface, with value of about 20.5 m^2/kg, in linear relationship with the porosity of the material.

It has been also noticed that flours (consisting of the endosperm of the wheat seeds) have high values of density with values over 1371 kg/m^3.

De asemenea, la separarea pe fracţii a măcinişului, porozitatea fiecărei fracţii se modifică, iar aceasta va influenţa valoarea masei volumice a materialului rezultat.

Totuşi, se observă că fracţiile C2-M3 şi C2-Fgrif au cea mai mare valoare a masei volumice (circa 463 kg/m^3 pentru ambele). Se constată, însă, că porozitatea făinurilor are valori relativ ridicate, în relaţie invers proporţională cu masa volumică (circa 65,3% pentru C2-M3, respectiv 66,2% pentru C1-Fgrif).

Este de remarcat, de asemenea, că fracţia care are cea mai mică masă volumică (fracţia C2-M2, care reprezintă un dunst), prezintă cea mai mare valoare a porozităţii (având 426 kg/m^3 masa volumică şi 69,3% porozitatea), în aceeaşi relaţie invers proporţională ca şi celelalte fracţii ale compartimentului.

Legat de suprafaţa specifică a fracţiilor de măciniş sortate la compartimentul C2 al celui de-al doilea măcinător, se constată că fracţiile de făină au valorile cele mai ridicate (31,2 m^2/kg pentru C2-Fgrif, 33,5 m^2/kg pentru C2-F2 respectiv 48,2 m^2/kg pentru C2-F).

Se constată că fracţia C2-M3 (cu un conţinut ridicat de înveliş) are o suprafaţă specifică scăzută (circa 10,7 m^2/kg), chiar dacă valoarea porozităţii este mare.

În ceea ce priveşte fracţia C2-M2, clasificată în categoria dunsturilor, aceasta are o suprafaţă specifică, cu valoarea aprox. 20,5 m^2/kg, în relaţie direct proporţională cu porozitatea materialului.

Se remarcă, de asemenea, că făinurile (constituite din endospermul seminţelor de grâu) au valori ridicate ale densităţii cu valori de peste 1371 kg/m^3.

CONCLUSIONS

The physical characteristics of grist intermediate products determine the functional characteristics of the passages technological equipment (breakage or reduction) from milling plant.

The analysis and interpretation of data obtained for the 6 samples, coming from the input and 5 outputs of the plansifter compartment C2 (fig. 1), show the following:

- fraction C2-M2, having a high content of shell (bran), compared with the other analyzed fractions that have a high content of endosperm, has a lower bulk density (~426 g/dm^3);
- semolina flour extracted at this compartment (C2-Fgrif) together with fraction C2-M3 have the highest bulk density (both ~463 g/dm^3);
- also, it can be observed that, although the mass of grist mixture that feeds the plansifter compartment C2 has a porosity of 63.62 %, after sorting, the porosity changes considerably reaching 68.18 % for flour fraction C1-F and 69.35 % for dusnt that feeds reduction roll M2 (fraction C2-M2).

For all plansifter compartments of a milling plant, from the wheat reduction phase, it is important to know the average size of particles of separated fractions, because it re-enters into the grinding process, and structural characteristics of the roller mills and their operating parameters must be correlated with these.

At the analyzed mill, physical properties of grist, average size of particles of fractions at plansifter compartments and their particle size distribution fall within the limits shown in other specialty papers.

The data presented can be important for all specialists and workers in the milling and grinding of wheat, referring, firstly, to reduction phase of technological process.

ACKNOWLEDGEMENT

The work has been funded by the Sectoral Operational Programme of Human Resources Development 2007-2013 of the Romanian Ministry of Labour, Family and Social Protection through the Financial Agreement POSDRU/107/1.5/S.76903.

REFERENCES

[1]. Allen T., (2003) –*Particle size analysis by sieving. Powder Sampling and Particle Size Determination*, Elsevier, pp. 208 – 250, Ch.4;
[2]. Căsăndroiu T., David L., (1994) – *Equipment for primary processing and preservation of agricultural products. Guidelines for laboratory work,* Polytehnic University of Bucharest;
[3]. Coskuner Y., Karababa E., (2007) – *Physical properties of coriander seeds (Coriandrum Sativum L.),* Journal of Food Engineering, Volume 80, Issue 2, pp. 408-416;
[4]. Costin I., (1988) – *Miller book,* Technical Publishing, Bucharest;
[5]. Dziki D., Laskowsky J., (2005) – *Wheat seeds physical properties and milling process*, Acta Agrophysica. 6(1), pp: 59-71;

CONCLUZII

Caracteristicile fizice ale produselor intermediare de măciniş determină caracteristicile funcţionale ale echipamentelor din pasajele tehnologice (de şrotare sau măcinare) din morile de grâu.

Din analiza şi interpretarea datelor obţinute pentru cele 6 probe, care provin de la intrarea şi cele 5 ieşiri ale compartimentului de sită plană C2 (fig.1), se constată următoarele:

- fracţia C2-M2, având un conţinut mai ridicat de înveliş (tărâţă), faţă de celelalte fracţii analizate ce au un conţinut mai ridicat de endosperm, are o masă volumică mai mică (~426 g/dm^3);
- făina grifică extrasă la acest compartiment (C2-Fgrif) împreună cu fracţia C2-M3 au masa volumică cea mai mare (ambele ~463 g/dm^3);
- de asemenea, se poate observa că, deşi masa amestecului de măciniş ce alimentează compartimentul de sită plană C2 are o porozitate de 63,62%, după sortarea pe fracţii porozitatea se modifică considerabil ajungând până la 68,18% pentru fracţia de făină C1-F şi 69.35% pentru dunstul ce alimentează măcinătorul M2 (fracţia C2-M2).

Pentru toate compartimentele de sită plană ale unei mori, din faza de măcinare a grâului este important a se cunoaşte dimensiunile medii ale particulelor fracţiilor separate, distribuţia după dimensiuni şi compoziţia fizică a acestora, deoarece ele reintră în procesul de mărunţire, iar caracteristicile constructive ale cilindrilor de măcinare, precum şi parametrii funcţionali ai acestora trebuie să fie corelate cu acestea.

La moara analizată, proprietăţile fizice ale măcinişurilor, dimensiunile medii ale particulelor fracţiilor la compartimentele sitei plane şi distribuţia după mărime a acestora se încadrează în limitele prezentate şi în alte lucrări ştiinţifice de specialitate.

Datele prezentate pot fi importante pentru toţi specialiştii şi lucrătorii în domeniul morăritului şi măcinării grâului, cu referire, în primul rând, la faza de măcinare a procesului tehnologic.

RECUNOAŞTERE

Rezultatele prezentate în acest articol au fost obţinute cu sprijinul Ministerului Muncii, Familiei şi Protecţiei Sociale prin Programul Operational Sectorial Dezvoltarea Resurselor Umane 2007-2013, Contract nr. POSDRU/107/1.5/S/76903.

BIBLIOGRAFIE

[1]. Allen T., (2003) – *Analiza granulometrică prin cernere*, *prelevarea de materiale granulare şi determinarea dimensiunii*, Elsevier, pag. 208 – 250, Ch.4;
[2]. Căsăndroiu T., David L., (1994) – *Utilaje pentru prelucrarea primară şi păstrarea produselor agricole. Îndrumar pentru lucrări de laborator,* Universitatea Politehnica Bucureşti;
[3]. Coskuner Y., Karababa E., (2007) – *Proprietăţile fizice ale seminţelor de coriandru (Coriandrum Sativum L.),* Revista de Inginerie Alimentară, Volum 80, Nr.2, pag. 408-416;
[4]. Costin I., (1988) - *Cartea morarului,* Editura Tehnică, Bucureşti;
[5]. Dziki D., Laskowsky J., (2005) – *Proprietăţile fizice ale seminţelor de grâu şi procesul de morărit*, Acta Agrophysica. 6(1), pag. 59-71;

[6]. Karimi M., Kheiralipour K., Tabatabaeefar A., Khoubakht G., Naderi M., Heidarbeigi K., (2009) – *The efect of moisture content on physical properties of wheat*, Pakistan Journal of Nutrition, 8 (1), pp. 90-95;
[7]. KeShun Liu, (2009) – *Some factors affecting sieving performance and efficiency,* Powder Technology, 193, pp. 208-213;
[8]. Mohsenin N.N., (1970) – *Physical properties of plant and animal materials, vol. I (Structure, physical characteristics and mechanical properties),.* Gordon and Breach Science Publishers, N.Y.;
[9]. Orăşanu N., Voicu Gh., Ungureanu N., (2009) – *Determination of the static and dynamic friction coefficients for the milling products and their variation with respect to some parameters,* Modelling and optimization in the machines building field, MOCM. Vol. 15/3, pp.44-50;
[10]. Standish N., (1985) – *The kinetics of batch sieving,* Powder Technology 41, pp.57 – 67;
[11]. Sultanbawa F.M., Owens W.G., Pandiela S.S., (2001) - *A new approach to the prediction of particle separation by sieving in flour milling*, Transactions of IchemE, 79 (Part C), pp. 201-218;
[12]. Voicu Gh., Biris S.S., Stefan E.M., Constantin G.A., Ungureanu N., (2013) – *Grinding characteristics of wheat in industrial mills*, Chapter 15 in Food Industry Book, Edited by InTech Europe, University Campus STeP Ri, Rijeka, Croatia, pp: 323-354.

[6]. Karimi M., Kheiralipour K., Tabatabaeefar A., Khoubakht G., Naderi M., Heidarbeigi K., (2009) – *Efectul conţinutului de umiditate asupra proprietăţilor fizice ale seminţelor de grâu*, Revista de Nutriție din Pakistan, 8 (1), pag.90-95;
[7]. KeShun Liu (2009) – *Unii factori care afectează performanţa şi eficienţa cernerii,* Tehnologia Pulberilor, 193, pag: 208-213;
[8]. Mohsenin N.N., (1970) – *Proprietăţile fizice ale materialelor animale şi vegetale, vol. I (Structură, caracteristici fizice şi proprietăţi mecanice).* Editura Ştiințifică „Gordon and Breach", N.Y.;
[9]. Orăşanu N., Voicu Gh., Ungureanu N. (2009) – *Determinarea coeficientului de frecare static şi dinamic pentru măcinişuri şi variaţia lor cu anumiţi parametri,* Modelare şi optimizare in domeniul construcției de maşini, MOCM. Vol. 15/3, pag: 44-50;
[10]. Standish N., (1985) – *Cinematica unui pachet de cernere,* Powder Technology 41, pag.57 – 67;
[11]. Sultanbawa F.M., Owens W.G., Pandiela S.S. (2001) - *O nouă abordare a predicţie de separare a particulelor prin cernere, în morărit*, Lucrări ale IchemE, 79 (Partea C), pag. 201-218;
[12]. Voicu Gh., Biriş, S.S., Ştefan E.M., Constantin G.A., Ungureanu N., (2013) – *Caracteristicile de măcinare a grâului în morile industriale*, Capitolul 15 in Manualul pentru industrie alimentară, Editat de InTech Europa, Campusul STeP Ri Universității, Rijeka, Croaţia, pag: 323-354.

THE EFFECT OF ULTRASOUND TREATMENT ON SELECTED MAIZE AND BUCKWHEAT EXTRUDATES PARAMETERS / *WPŁYW ULTRADŹWIĘKÓW NA WYBRANE PARAMETRY EKSTRUDATÓW KUKURYDZIANYCH I GRYCZANYCH*

PhD. Eng. Żelaziński T., PhD. Eng. Ekielski A., PhD. Stud. Eng Zdanowska P., PhD. Stud. Eng. Florczak I.
Warsaw University of Life Sciences, Faculty of Production Engineering, Warsaw / Poland
Tel: +48 22 59 345 00; e-mail: tomasz_zelazinski@sggw.pl

Abstract: *This study attempted to understand the influence of ultrasound pretreatment on quality of extrudates. The maize and buckwheat seeds were subjected to low power ultrasound at 40kHz frequency. The pretreated material was processed using extrusion cooking technology. The effect of the ultrasound waves on quality of extrudates produced from pretreated seeds and its grinds were investigated. Typical quality standard parameters like sectional expansion, volumetric expansion indices, water solubility index and water absorption index of extrudates were investigated by using central composition design. For all extrudates samples inner cells structure was also determined. The inner texture of extrudate as structure and configuration of pores were described using mean size of pores, their number on cross section unit, geometric orientation of pores. The extrudates produced from pretreatment materials were compared with extrudates obtained from non-treated material. Extrudates made from pretreated material showed different texture properties than produced from ultrasound untreated ones.*

Keywords: *ultrasound, food extrusion, buckwheat, maize*

INTRODUCTION

Extrusion is one of the most extensively used and promising method for ready-to-eat cereals and other processed food production. It is a process where a mixture of food ingredients is forced to flow through a die. Moisture, high shear, mass temperature and pressure applied during extrusion make it possible to convert raw starchy material for variety end uses (Desrumaux et al., 1998, Chang et al., 2001, Ekielski et al., 2007a). The pre-treatment of raw materials in conditioners used in extrusion line is able to reduce energy consumption and improve the final product quality (Ekielski et al., 2007b, Wójtowicz and Mościcki, 2008). One of the interesting pretreatment methods is the ultrasound radiation used for starchy raw materials directly before extrusion process. Depending on the intensity and frequency of the ultrasonic waves it can be utilized for preparation of new and improved products as well as used to facilitate testing the quality of manufactured food products, especially in the on-line monitoring of the quality of extruded products (Owolabi et al., 2008, Awad et al., 2012).

Ultrasounds are widely studied and used in variety of food processing operations and processes like freezing, drying, sticky products cutting, meat crumbling, wine and whiskey aging, cheeses ripening, sterilization, extraction, emulsification, and many more (Soria and Villamiel, 2010, Chang et al., 2012). Effect of ultrasound is used mainly for cavitation and improves mass and heat transfer. Using ultrasounds, food processing processes can be done several times faster, with high degree of reproducibility at reduced processing costs, simplifying the operations performed and yielding a higher purity of the final product, thereby eliminating the process of treating and purifying waste water (Hromádková et al., 2003; Chemat et al., 2011; Chandrapala et al., 2012; Karkani et al., 2013).

Abstrakt: *W pracy przedstawiono wyniki badań procesu ekstruzji nasion gryki i kukurydzy, które poddano wcześniej wstępnej obróbce ultradźwiękowej w całości i po zmieleniu. Celem badań było określenie wpływu pola akustycznego o niskiej częstotliwości 40kHz na jakość wytworzonych produktów. Wyznaczono wskaźniki ekspandowania radialnego i objętościowego oraz wskaźniki wodochłonności WAI i rozpuszczalności wodnej WSI z zastosowaniem doświadczenia z centralnym planowanem kompozycyjnym. Dla wszystkich próbek wyznaczono również porowatość ekstrudatu. Rozkład porów został opisany poprzez średnią wielkość porów i ich liczbę na jednostkę powierzchni przekroju poprzecznego oraz orientację geometryczną porów. Ekstrudaty otrzymane z materiału poddanego ultradźwiękom porównano z ekstrudatami z materiału nie poddanego żadnej obróbce, otrzymując odmienne właściwości teksturalne.*

Słowa kluczowe: *ultradźwięki, ekstruzja żywności, gryka, kukurydza*

WSTĘP

Ekstruzja jest obecnie jedną z najczęściej stosowanych metod wytwarzania produktów żywościowych gotowych do spożycia oraz wielu innych wyrobów. Jest to proces, w którym mieszanina składników spożywczych przeciskana jest pod wpływem wysokiego ciśnienia przez dyszę wylotową ekstrudera. Na skutek występujących w trakcie procesu wysokich temperatur oraz sił ścinanajacych w połaczeniu z odpowiednią wilgotnością w surowcu skrobiowym zachodzą przemiany umożliwiające powstawanie zupełnie nowych produktów (Desrumaux in. 1998, Chang i in. 2001, Ekielski in., 2007a). W procesie ekstruzji stosowana jest często wstępna obróbka surowców w kondycjonerach, której celem jest zmniejszenie zużycia energii oraz poprawa jakości produktu końcowego (Ekielski i wsp., 2007b, Wójtowicz i Mościcki, 2008). Podobne korzyści może przynieść zastosowanie w procecie ekstruzji technologii ultradźwiękowej. Odpowiedni dobór mocy i częstotliwości fal ultradźwiękowych może umożliwić wytwarzanie ulepszonych lub też zupełnie nowych wyrobów ekstrudowanych. Może także umożliwić monitorowanie jakości produktów on-line (Owolabi i wsp., 2008, Awad i wsp., 2012).

Ultradźwięki są szeroko zbadane i wdrożone do produkcji w takich operacjach i procesach jak mrożenie, suszenie, krojenie lepkich produktów, kruszenie mięsa, starzenie wina i whiskey, dojrzewanie serów, sterylizacja, ekstrakcja, tworzenie emulsji i wiele innych (Chang i wsp., 2012, Soria i Villamiel, 2010). Działanie ultradźwięków znajduje zastosowane przede wszystkim dzięki zjawisku kawitacji i polepszeniu transferu masy. Z pomocą ultradźwięków procesy przetwórstwa żywności mogą być realizowane kilkakrotnie krócej, z wysoką powtarzalnością, przy jednocześnie obniżonych kosztach przetwarzania. Ich zastosowanie upraszcza wykonywane czynności i daje wyższą czystość końcowego produktu, co eliminuje obróbkę po procesie i oczyszczanie ścieków (Hromádková i wsp., 2003, Chemat i wsp., 2011, Chandrapala i wsp., 2012, Karkani i wsp., 2013).

Some studies also support the use of ultrasound in the extrusion process to improve the flow and to reduce the resistance of highly viscous and sticky material transported from the inside of the extruder and the modification of its structure. To this end, the ultrasound source was located at right angles to the cylinder to impart a radial vibration (Akbari et al., 2007). From the standpoint of extrusion process used directly on grains important effect of sonication is the degradation of the polymers, including carbohydrates. Depolymerization occurring due to cavitation phenomenon may be related to the physical collapsing of cavitation bubbles or chemical changes produced by the action of radicals on the polymer chain. Ultrasounds were tested on the starch of many different plants. The first work in this area was established in 1933. Many studies demonstrated that ultrasounds alter the rheological properties of food: disturb the arrangement of crystalline grains of maize and potato starch, the starch gelatinization, increase the water absorption capacity and the solubility of the starch grains of corn and increase wheat proteins solubility, reduce viscosity, improve foaming properties (Vinatoru et al., 1999; Jambrak and et al., 2010; Chemat et al., 2011; Zhu et al., 2012; Hernouxa et al., 2013; Sujka and Jamroz, 2013).

The objective of the present investigation was to study the effect of ultrasound waves pre-treatment on extrudate properties obtained through the single screw extrusion cooking of maize and buckwheat seeds.

MATERIALS AND METHODS

Maize (Credo varieties) and buckwheat (Luba varieties) grains which were procured from the local market have been used in the investigation. For investigation of the ultrasound effect for maize and buckwheat, the two group of raw materials have been prepared: ultrasound treated and untreated. Treated samples have been prepared as suspension in the water.

Suspension has been prepared by stirring the appropriate amount of grain (grain sample mass=5 kg) and water in 1:1 mass ratio.

Ultrasound treatment

Separately maize-water and buckwheat-water suspension have been treated with ultrasonic waves. The ultrasound transducer has been located in the container filled with suspension. The ultrasound 40kHz generator (Inter Sonic 37P, Poland) was attached to the transducer, irradiated the 40kHz frequency waves with 60W power. Samples were treated for 20 minutes.

Determination of ultrasound power

Ultrasonic power transmit to suspension, which is considered as mechanical energy, is partly dissipated and converted on thermal energy. Since the suspension temperature grows up, the ultrasound power is able to estimate by measurement of suspension temperature changes. The equation (1) describes this functional relationship shown below (Margulis, 2003):

$$P = m \cdot c_p \cdot \left(\frac{dT}{dt} \right); \quad (1)$$

where: m - the mass of the sonicated liquid (g), c_p - the specific heat of medium at a constant pressure dependent on composition and volume of medium ($J \cdot g \cdot K^{-1}$), dT/dt - the slope of the suspension temperature changes in observe time curve.

Ultrasound intensity is expressed in watts per unit volume suspension. In the experiment ultrasound intensity P=11.5 $W \cdot cm^{-3}$ was obtained.

Podejmowano również próby zastosowania ultradźwięków przy wspomaganiu procesu ekstruzji do poprawy przepływu i redukowania oporu silnie lepkiego i kleistego materiału transportowanego z wnętrza ekstrudera oraz modyfikacji jego struktury. W tym celu źródło ultradźwięków lokalizowano pod kątem prostym do cylindra, aby nadać mu promieniowe drgania (Akbari i wsp., 2007). Z punktu widzenia procesu ekstruzji stosowanej bezpośrednio na ziarna zbóż ważnym efektem działania ultradźwięków jest degradacja polimerów, w tym węglowodanów. Depolimeryzacja zachodząca na skutek zjawiska kawitacji, może być związana z fizycznym zapadaniem się pęcherzyków kawitacyjnych lub z chemicznymi zmianami spowodowanymi działaniem rodników na łańcuch polimerowy. Ultradźwięki były badane na skrobi pochodzącej z wielu różnych roślin. Pierwsza praca z tego zakresu powstała w 1933 roku. W wielu pracach dowiedziono, że ultradźwięki zmieniają właściwości reologiczne żywności: zaburzają układ krystaliczny ziaren skrobiowych kukurydzy i ziemniaka, żelatynizację skrobi, zwiększają zdolność absorpcji wody i rozpuszczalność ziaren skrobiowych kukurydzy, a także zwiększają rozpuszczalność białek pszenicy, redukują lepkość, polepszają właściwości pianotwórcze (Jambrak i wsp., 2010; Chemat i wsp., 2011, Zhu i wsp., 2012, Hernouxa i wsp., 2013, Sujka i Jamroz, 2013).

Celem pracy było zbadanie wpływu działania fal ultradźwiękowych na parametry jakościowe ekstrudatów otrzymywanych z kukurydzy i gryki wytwarzanych na ekstruderze jednoślimakowym.

MATERIAŁ I METODYKA

Podstawowym materiałem wykorzystywanym w badaniach było ziarno kukurydzy odmiany Credo oraz ziarno gryki odmiany Luba. Materiał podzielono na dwie grupy: poddane obróbce i nie poddane obróbce. Obróbka wstępna ziaren przeznaczonych do przetwarzania w procesie ekstruzji polegała na poddawaniu ich działaniu fal ultradźwiękowych. Surowiec przed obróbką ultradźwiękową został zalany wodą w stosunku 1:1, tworząc zawiesinę. Jednorazowo działaniu ultradźwięków poddawano próbkę o masie 5 kg.

Obróbka ultradźwiękami

Ziarno kukurydzy i gryki poddano działaniu fal ultradźwiękowych o natężeniu 40 kHz za pomocą generatora ultradźwięków z przetwornikiem (Inter Sonic 37P, Poland) o mocy nominalnej 60 W umieszczonego w pojemniku z zawiesiną. Czas działania ultradźwięków wynosił 20 min.

Określenie mocy ultradźwięków

Moc ultradźwięków podawana do zawiesiny materiału z wodą, traktowana jako energia mechaniczna, jest częściowo rozpraszana i zamieniana na energię cieplną. Ponieważ temperatura zawiesiny wzrastała moc ultradźwięków mierzono poprzez zmiany temperatury zawiesiny. Równanie (1) opisujące tę zależność funkcyjną przedstawiono poniżej (Margulis, 2003):

gdzie: m – masa cieczy poddanej obróbce (g), c_p – ciepło właściwe czynnika przy stałym ciśnieniu w zależności od składu i ilości czynnika ($J \cdot g \cdot K^{-1}$), dT/dt – krzywa zmian temperatury zawiesiny w danym okresie czasu.

Natężenie ultradźwięków wyrażona jest w watach na jednostkę objętości zawiesiny. W badaniach uzyskano natężenie równe P=11,5 $W \cdot cm^{-3}$.

Experiment

The single 5 kg mass of corn or buckwheat grain sample before experiment was placed in the glass container filled with water in 1:1 ratio. The samples were treated for 20 minutes by the ultrasonic generator and transducer. Figure 1 shows the experimental stand for ultrasound processing.

Grains after ultrasound treatment were dried to 15% w/w (buckwheat) and 25% w/w (maize) moisture content with a drum dryer. The final moisture content was measured in moisture analyser WPS 210 (Poland). Half of the ultrasound treated material was ground in grinder RUD-216 (Poland) equipped with 20 mesh screen.

A single screw extruder KZM-2 (modified Russian one), with outer diameter of the extruder screw of 100 mm, was used. The length to diameter (L/D) ratio of the extruder was 8:1, the screw speed - 200 rpm. The extruder was provided with a temperature control facility (in two separate zones), and digital display for measuring electrical power consumption developed during extrusion. The temperature of the extruder at sections (starting from the feed end) was maintained at 80, 125 ^{0}C by fuzzy algorithm controller (Ekielski, 2006). Feeding of the raw material to the extruder was accomplished by using single screw volumetric feeder. The extrusion trials were repeated three times.

Quality indices

Water absorption and water solubility indices. Water absorption (WAI) and water solubility (WSI) indices were detemined by the method of Anderson et al. (1969). The extrudates were first milled to a mean size of 180-250 µm. A 2.5g sample was dispersed in 25 ml of distilled water. The plastic stem had been used to break up any lumps, next start to stir for 20 minutes. Four dispersion samples were rinsed into centrifuge pockets and then centrifuged at 4500 rpm for 15 minutes. The supernatant was decanted for determination of its solids content and sediment was weighted. Collected supernatant had been dried in 105°C in laboratory dryer for 24 hours. The residues solids had been weighted on the precision electronic scale, mass determined with 0,001 g accuracy. WAI and WSI were calculated from the equations (2) and (3):

$$WAI = \frac{m_o}{m_e} \cdot 100[-] \quad (2)$$

$$WSI = \frac{m_n}{m_e} \cdot 100[\%] \quad (3)$$

where: m_o - mass of sediment, m_e - mass of dry solids (mass of dry milled extrudate), m_n – mass of dissolved solids in supernatant.

The inner structure of extrudate

Porosity tests were performed on the test image analysis with a light chamber equipped with fluorescent light TL-D DeLuxe Pro 18 W/965 (Philips manufactured) with color emitted temperature 6500K, presented the color index Ra=90%. Images have been taken by CCD camera (model FD30, Hitachi) and grabber image software saved the pictures on computer HDD. The pictures saved in TIFF format were treated and analysed by National Instrument NI Vision 7.1.1 software. Porosity was determined for using the method described by Gosselin and Rodrigue (2005) where an irregular boundary for the analyzed group of air pores in cut view , was used.

Color cut view images obtained during experiment were then transposed to the monochrome color space. The resulting images 8-byte grayscale (256 levels) in next step were converted to binary bitmaps. The threshold T transformations were selected automatically as the result of the function (4):

Przebieg badań

Przed rozpoczęciem eksperymentu każdą próbę surowca o masie 5 kg kukurydzy lub gryki umieszczano w szklanym pojemniku z wodą w stosunku 1:1. Następnie próbki poddawano obróbce ultradźwiękowej przez okres 20 minut.

Ziarna po obróbce ultradźwiękowej suszono w suszarce bębnowej do wilgotności 15% (gryka) i 25% (kukurydza). Wilgotność końcową mierzono w wagosuszarce WPS 210 (Polska). Połowa materiału po obróbce była mielona w rozdrabniaczu RUD-216 (Polska), i przesiewana na sicie o oczkach 20 mesh.

Następnie materiał ekstrudowano na ekstruderze jednoślimakowym KZM-2 (modyfikacja rosyjskiego ekstrudera), o średnicy zewnętrznej ślimaka 100 mm. Stosunek długości do średnicy (L/D) wytłaczarki wynosił 8:1, prędkość obrotowa ślimaka wynosiła 200 obr.·min^{-1}. Wytłaczarka była wyposażona w regulator temperatury (w dwóch oddzielnych strefach) oraz cyfrowy miernik z wyświetlaczem zużycia energii elektrycznej w trakcie wytłaczania. Temperaturę wytłaczarki w sekcjach (licząc od końca zasilającego) utrzymywano na poziomie 80°C i 125°C z użyciem regulatora ustawionego za pomocą algorytmu rozmytego (Ekielski, 2006). Podawanie surowca do wytłaczarki zachodziło przy użyciu jednoślimakowego podajnika objętościowego. Próby wykonano w 3 powtórzeniach.

Wskaźniki jakościowe

Wskaźniki wodochłonności WAI i **rozpuszczalności WSI.** Wodochłonność i rozpuszczalność określano metodą Andersona i wsp. (1969). Metoda pomiaru polegała na wymieszaniu 2,5 g rozdrobnionego ekstrudatu (wielkość cząsteczek 180-250 µm) w 25 ml destylowanej wody i oddzieleniu nadmiaru wody od osadu po upływie 20 minut poprzez odwirowanie w wirówce przy prędkości obrotowej 4500 obr·min^{-1} przez 15 min. Uzyskany w ten sposób nadsącz zlewano na płytki Petriego i suszono w temperaturze 105^{o}C przez 24 godz. Odsączoną próbkę ważono na wadze elektronicznej z dokładnością 0,001g. Współczynniki WAI i WSI obliczono z zastosowaniem poniższych równań (2) i (3):

gdzie: m_o – masa nasączonej próbki, m_e - masa suchej próbki (masa suchego rozdrobnionego ekstrudatu), m_n – masa wysuszonego nadsączu.

Struktura wewnętrzna ekstrudatu

Badania porowatości wykonano na stanowisku badawczym do analizy obrazu z komorą świetlną wyposażoną w świetlówki światła dziennego TL – D De Luxe Pro 18W/965 o temperaturze barwowej 6500 K i współczynniku odwzorowywania barw Ra - 90% firmy Philips oraz kamerę CCD KP – FD30 firmy HITACHI i oprogramowanie do analizy zdjęć. Zdjęcia zapisywano w formacie TIF. Porowatość określano według metody Gosselin i Rodrigue (2005) stosując nieregularną obwiednię analizowanej grupy porów powietrznych na analizowanych zdjęciach. Do analizy zdjęć zastosowano program firmy National Instrument NI Vision 7.1.1. Uzyskane kolorowe zdjęcia transponowano do przestrzeni monochromatycznej.

Otrzymane obrazy o 8-bajtowej skali szarości (256 odcieni) przekształcano w dwuwartościowe mapy bitowe. Wartość progową T przekształcenia dobierano automatycznie jako wynik funkcji (4):

$$T = su_p\{A_T\} \quad (4)$$

where: A_T – presented the set values for the number of pore recognized, for the threshold values equal T∈<0-255>. After calculating the value of T, set the number of pore per unit area [cm^2] and the average pore size were counted.

gdzie: A_T – zbiór przedstawiający wartości liczby rozpoznawalnych por dla wartości progowej T∈<0-255>. Po obliczeniu wartości T wyznaczono liczbę por na jednostkę powierzchni [cm^2] oraz średni rozmiar por.

Physical extrudate properties

Expansion indexes. The sectional, volumetric indexes of the extrudates were assigned according to the methods developed by Alvarez Martinez et al. (1988).

The sectional expansion (SEI) was calculated by dividing the cross-sectional areas of the extrudates (S_e) by the cross sectional of the die opening (S_d). The volumetric expansion index (VEI) is the apparent raw material density (□m) to apparent extrudate density after expansion (□e). Expansion indexes were expressed as (5) and (6):

Właściowości fizyczne ekstrudatów

Wskaźniki ekspansji. Wskaźniki ekspandowania objętościowego i radialnego obliczano według poniższych wzorów (Alvarez-Martinez i wsp. 1988).

Wskaźnik ekspandowania radialnego (SEI) był obliczany jako stosunek przekroju ekstrudatu (S_e) do pola przekroju poprzecznego otworu matrycy (S_d). Wskaźnik ekspansji objętościowej (VEI) obliczano jjako stosunek gęstości materiału wejściowego (ρ_m) do gęstości ekstrudatu (ρ_e). Indeksy ekspansji wyrażono jako (5) i (6):

$$SEI = \frac{S_e}{S_d} \quad (5)$$

$$VEI = \frac{\rho_m}{\rho_e}\frac{(1-MC_m)}{(1-MC_e)} \quad (6)$$

where:
MC_m and MC_e are the moisture contents of the raw material before extrusion proces, and moisture content of the extrudates, respectively.

gdzie:
MC_m i MC_e to odpowiednio zawartość wilgoci w suchym materiale przed ekstruzją i zawartość wilgoci w ekstrudacie.

Apparent extrudate density. The expanded extrudate density (□e) was calculated as the mass of extrudate sample (m_e) is divided by the equivalent volume of extrudates (V_e). The sample was weighted on the laboratory scale (RADWAG WPS 300) with an accurancy of 0.001g. The volume of extrudates (V_e) was determined with water displacement method developed by Ekielski (Ekielski and Osiak 2003). The extrudate sample was immersed in container filled with rapeseed oil to impregnate. After removing the samples from the oil container, the extrudate was dried of excess oil and immersed into the tank filled with water. The water volume increase was read from the scale on the side of the vessel.

Gęstość ekstrudatu. Gęstość ekstrudatu (ρ_e) obliczono jako stosunek masy eukstrudatu (m_e) do objętości ekstrudatu (V_e). Próbki ważono na wadze laboratoryjnej firmy RADWAG WPS 300 z dokładnością 0,001g. Objętość ekstrudatu (V_e) określono metodą wypornościową opracowaną przez Ekielskiego (Ekielski i Osiak, 2003). Próbka ekstrudatu zanurzana była w pojemniku wypełnionym olejem rzepakowym do impregnacji. Po usunięciu próbki ze zbiornika oleju, ekstrudat odsączano z nadmiaru oleju i zanurzano w zbiorniku z wodą. Następnie odczytywano objętośść wody. Różnica objętości wody odpowiadała mierzonj objętości ekstrudatu.

Statistical analysis

The experiments were designed using standard design (SD) 2**(2-0) with selectivity R=Full (three repetitions). Standard design comprising two independent processing parameters at two different levels. SD was chosen for designing the experiments, because it is a correct tool for optimization and it also reduces the number of experiments. Data were analysed using DOE module, SD design in the Statistica 10 program (table 1).

Analiza statystyczna

W badaniach zastosowano plan standardowy 2**(2-0) o rozdzielczości R=FULL z trzema powtórzeniami o oliczbie wielkości wejściowych dwa na dwóch różnych poziomach. W celu poprawnego przeprowadzenia eksperymentu (SD - standard design) wielkości wejściowe sprowadzono do wartości liczbowej. Dane poddano analizie w programie Statistica 10 z wykorzystaniem modułu planowania doświadczeń DOE (tab.1).

Table 1

Treatment coded and the plan of experiments generated by standard design (SD) in Statistica 10

	Treated by	**Code**
Seed	non-ground seeds (whole seed)	-1
	ground seeds	1
	40 kHz ultrasound treated	-1
	without ultrasound treatment	1
Rep.	**Mechanical treated material code**	**Ultrasound treated material code**
1	-1	-1
1	1	-1
1	-1	1
1	1	1
2	-1	-1
2	1	-1
2	-1	1
2	1	1
3	-1	-1
3	1	-1
3	-1	1
3	1	1

To determine the significance of the quality parameters extrudates ANOVA variance analysis was applied.

RESULTS

The influence of ultrasonic pretreatment on the quality parameters of corn and buckwheat extrudate indicates that ultrasound treatment results in qualitative changes in the products obtained. This relationship was confirmed by the results of empirical research and statistical significance tests carried out for each of the extrudate quality parameters (tab. 2). When one had looked on the results shown, it should be noted that in some cases the results of significance test for corn and buckwheat clearly differ, which might be primarily due to the different chemical composition of these materials, as well as the various physical characteristics of whole seeds undergoing a process of extrusion. Particular attention had been paid to WAI parameter, where statistical analysis clearly shows the importance of changes in both the corn and buckwheat extrudate.

The obtained experiment results during testing of influence of ultrasonic treatment on the corn and buckwheat extrudate quality parameters are shown in Figures (1-6). Analyzing the graph (figure 1), it can be observed that the water absorption (WAI) extrudates varied depending on the method of pretreatment. The values of this index were the highest (5.60 - corn and 5.23 - buckwheat) for extrudates obtained from whole grains and treated with ultrasound. In the case of grounded grains and subjected to ultrasonic treatment were lower WAI values for extrudates obtained from whole grains. Extrudates obtained from untreated material were characterized by ultrasound and the lowest water absorption and WAI values ranged from 5.04 to 4.66 for buckwheat and corn.

Istotność parametrów jakościowych ekstrudatów określono z wykorzystaniem analizy wariancji ANOVA.

WYNIKI BADAŃ

Wyniki badań wpływu obróbki ultradźwiękowej na parametry jakościowe ekstrudatu kukurydzianego i gryczanego wskazują, że fale ultradźwiękowe powodują zmiany jakościowe uzyskiwanych produktów. Zależność tą potwierdzają zarówno wyniki badań empirycznych, jak i statystyczne testy istotności przeprowadzone dla poszczególnych parametrów jakościowych ekstrudowanych wyrobów (tab. 2). Należy zwrócić uwagę, że wyniki testu istotności dla kukurydzy i gryki w niektórych przypadkach wyraźnie się różnią, co może wynikać głównie z różnego składu chemicznego tych surowców, jak również z różnych cech fizycznych całych ziaren poddawanych procesowi ekstruzji. Szczególną uwagę zwraca parametr WAI, gdzie analiza statystyczna wyraźnie wskazuje na istotność zmian zarówno w ekstrudacie kukurydzanym, jak i gryczanym.

Wyniki badań wpływu obróbki ultradźwiękowej na parametry jakościowe ekstrudatu kukurydzianego i gryczanego przedstawiono na rysunkach (1-6). Analizując wykres (rys. 1) można zaobserwować, że wodochłonność surowca (WAI) zarówno dla kukurydzy, jak i gryki jest największa (5,60 – kukurydza i 5,23 – gryka) dla ekstrudatów uzyskanych z całych ziaren oraz poddanych działaniu ultradźwięków. W przypadku ziaren poddanych obróbce ultradźwiękowej oraz rozdrobnionych wartości WAI były mniejsze w stosunku do ekstrudatów uzyskanych z całych ziaren. Ziarna niepoddane obróbce ultradźwiękowej odznaczały się natomiast najmniejszą wodochłonnością pomiędzy 5,04 to 4,66 dla gryki i kukurydzy.

Table 2

ANOVA variance analysis results

	Maize Volume expansion indices (VEI) [-]					Buckwheat Volume expansion indices (VEI) [-]				
	SS	**df**	**MS**	**F**	**p**	**SS**	**df**	**MS**	**F**	**p**
Ground (1)	0.0179	1	0.0179	13.2762*	0,0066	0.2809	1	0.2809	0.7672	0.4066
Ultrasound treated (2)	0.0514	1	0.0514	38.1771*	0.0003	0.0390	1	0.0390	0.1066	0.7524
1 vs. 2	0.0212	1	0.0212	15.7945*	0.0041	0.1273	1	0.1273	0.3477	0.5717
Error	0.0108	8	0.0013			2.9293	8	0.3662		
Overall SS	0.1012	11				3.3766	11			
	The sectional expansion indices (SEI) [-]					**The sectional expansion indices (SEI) [-]**				
Ground (1)	0.0068	1	0.0068	0.1054	0.7538	0.0578	1	0.0578	0.6255	0.4518
Ultrasound treated (2)	0.2137	1	0.2137	3.2968	0.1070	0.4972	1	0.4972	5.3841*	0.0489
1 vs. 2	0.0440	1	0.0440	0.6782	0.4341	0.0202	1	0.0202	0.2189	0.6524
Error	0.5185	8	0.0648			0.7387	8	0.0923 / *0,0923*		
Overall SS	0.7829	11				1.3138	11			
	WAI [-]					**WAI [-]**				
Ground (1)	0.3624	1	0.3624	19.6290*	0.0022	0.1007	1	0.1007	112.8312*	0.00005
Ultrasound treated (2)	0.9307	1	0.9307	50.4122*	0.0001	0.0822	1	0.0822	92.1038*	0.00001
1 vs. 2	0.3624	1	0.3624	19.6290*	0.0022	0.1281	1	0.1281	143.6149	0.00002
Error	0.1477	8	0.0185			0.0071	8	0.0009		
Overall SS	1.8032	11				0.3181	11			
	WSI [%]					**WSI [%]**				
Ground (1)	5.2260	1	5.2260	25.3445*	0.0010	0.4019	1	0,4019	0.19654	0.6693
Ultrasound treated (2)	0.5931	1	0.5931	2.87623	0.1283	0.0216	1	0.0216	0.01054	0.9208
1 vs. 2	5.2260	1	5.2260	25.3445*	0.0010	0.1192	1	0.1192	0.0583	0.8153
Error	1.6496	8	0.2062			16.3575	8	2.0447		
Overall SS	12.6947	11				16.9001	11			

	Porosity [amount pores in cm^2]					Porosity [amount pores in cm^2]				
Ground (1)	310.083	1	310.0833	9.81794*	0.0139	20.0208	1	20.0208	4.9031	0.0577
Ultrasound treated (2)	444.083	1	444.0833	14.0607*	0.0056	25.5208	1	25.5208	6.2500*	0.0369
1 vs. 2	374.083	1	374.0833	11.8443*	0.0088	35.0208	1	35.0208	8.5765*	0.0190
Error	252.667	8	31.5833			32.6667	8	4.0833		
Overall SS	1380.92	11				113.2292	11			
	Average of size pores [mm^2]					**Average of size pores [mm^2]**				
Ground (1)	0.0050	1	0.0050	0.0444	0.8383	20.0208	1	20.0208	4.9031	0.0577
Ultrasound treated (2)	0.0760	1	0.0760	0.6765	0.4346	25.5208	1	25.5208	6.2500*	0.0369
1 vs. 2	0.0012	1	0.0012	0.0107	0.9201	35.0208	1	35.0208	8.5765*	0.0190
Error	0.8984	8	0.1123			32.6667	8	4.0833		
Overall SS	0.9806	11				113.2292	11			

* - significant at 5% (p ≤0,05)

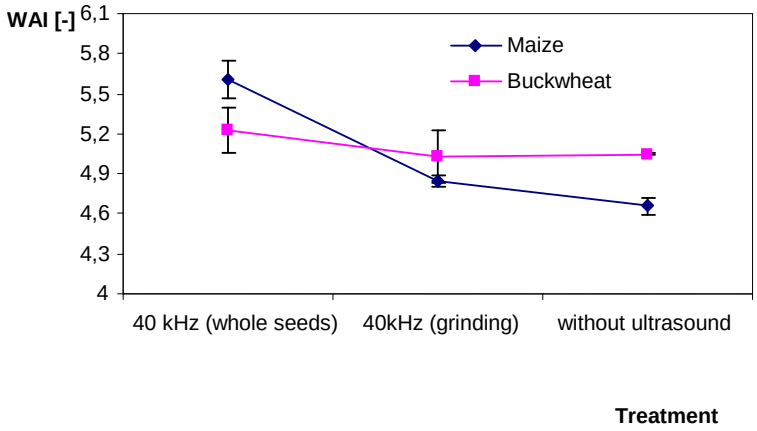

Fig. 1 - The water absorption indices (WAI) changes for corn and buckwheat extrudates according to material pre-treatment

Analyzing figure 2 showing WSI parameter change, it can be observed that the course of the graph is reversed in relation to the WAI graph. The highest values for WSI amounting 22.63% were recorded for buckwheat extrudate obtained from raw material without utrasonic pre-treatment. In the case of corn extrudate similar trend was also observed. This course of the graph can indicate that the degradation of the extrudate due to the conditions prevailing in the cylinder of the extruder was the highest. Increased degradation of starch, in turn, could be caused by an uncontrolled increase of shear and temperature of the extruder barrel as a result of the processing of grain with intact cell structure. According to Mason and Zhao (1994) and Kobus (2006) ultrasonic waves can disrupt plant cells. According to the authors, the cell content is released into the extraction solvent. Such a phenomenon occurs mainly in products with a high degree of hydration. Such a statement may be grounds to believe that the phenomenon took place in the case of raw materials subjected to sonication and led to a decrease in solubility.

Analizując wykres (rys. 2) przedstawiający zmiany wartości parametru WSI można zaobserwować, że przebieg wykresu jest odwrotny w stosunku do wykresu WAI. Największe wartości parametru WSI dla ekstrudatu (22,63%) uzyskanego z surowca niepoddanego działaniu ultradźwięków (gryka) mogą wskazywać, że degradacja ekstrudatu na skutek warunków panujących w cylindrze ekstrudera była największa. Mogło to być z kolei wynikiem niekontrolowanego zwiększenia sił ścinających i temperatury w cylindrze ekstrudera na skutek przetwarzania ziarna z nienaruszoną strukturą komórkową. Według Mason i Zhao (1994) i Kobus (2006) fale ultradźwiękowe mogą rozrywać komórki roślinne. Według autorów zawartość komórek uwalniana jest do rozpuszczalnika ekstrakcyjnego. Takie zjawisko zachodzi głównie w produktach o dużym stopniu uwodnienia. Stwierdzenie to może dać podstawy do podejrzeń, że zjawisko takie miało miejsce w przypadku surowców, które poddano działaniu ultradźwięków i doprowadziło do spadku rozpuszczalności.

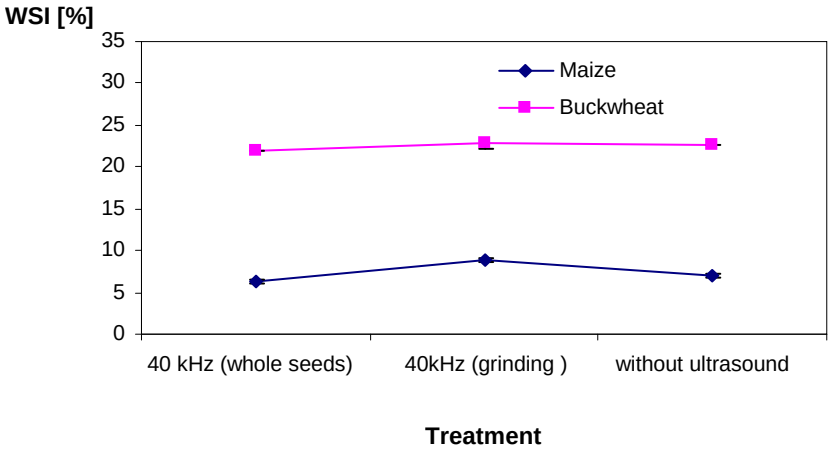

Fig. 2 - The water solubility indices (WSI) changes for corn and buckwheat extrudates according to material pretreatment

The qualitative parameter, which undergoes significant changes as a result of sonication was also extrudate porosity and average pore size measured on the surface of the extrudate cross-section. It was found that the porosity was the highest in the case of extrudates obtained from whole grains treated with ultrasound and time - 66.33 pores in cm^{-2} for corn and 42.33 pores in cm^{-2} for buckwheat. The lowest porosity characterized grounded while extrudates treated with ultrasound and extrudates obtained from whole grains and roasted effect of ultrasonic waves, reaches values are: 40.66 - 42.33 pores in cm^{-2} for both extrudated researched (Figure 3). According to Lanuay et al, (1983), Ekielski and Żelaziński (2012), the high porosity is usually a positive attribute of extruded materials and can provide a high homogeneity of the sample. Low porosity can be translated on the formation of large pores of irregular shape. The Figure 4 shows the variation in average pore size in the examined extrudates. The diagram of buckwheat treated with ultrasound can point to such a relationship.

Parametrem jakościowym, który ulegał istotnym zmianom na skutek działania ultradźwięków była również porowatość ekstrudatu oraz średni rozmiar por ekstrudatu mierzony na powierzchni jego przekroju poprzecznego. Stwierdzono, że porowatość była największa w przypadku ekstrudatów uzyskanych z całych ziaren poddanych działaniu ultradźwięków – 66,33 pory w cm^2 dla kukurydzy i 42,33 pory w cm^2 dla gryki. Taką tendencję można zaobserwować zarówno dla ekstrudatów kukurydzianych, jak i gryczanych. Najmniejszą porowatością charakteryzowały się natomiast ekstrudaty niepoddane działaniu fal ultradźwiękowych (rys. 3). Według badań Lanuay i wsp. (1983), Ekielskiego i Żelazińskiego (2012) wysoka porowatość jest zwykle cechą pozytywną dla ekstrudowanych surowców i może świadczyć o dużej jednorodności próbki. Niska porowatość może się natomiast przekładać na powstawanie dużych porów o nieregularnym kształcie. Na wykresie (rys. 4) przedstawiono zmiany średniego rozmiaru por w ekstrudatach poddnych badaniom. Przebieg wykresu gryki poddanej działaniu ultradźwięków może wskazywać na taką zależność.

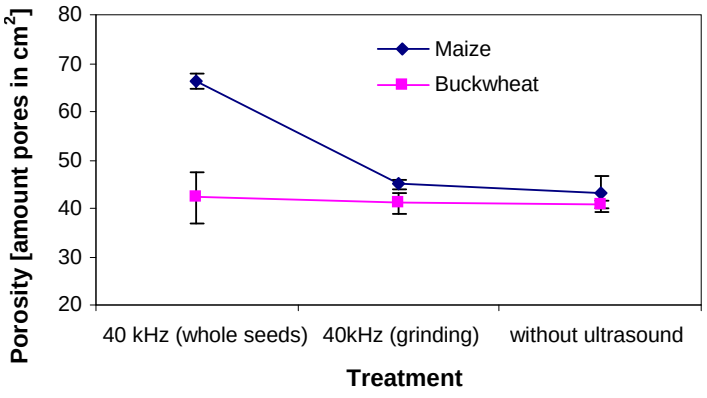

Fig. 3 - The porosity indices changes for corn and buckwheat extrudates according to material pre-treatment

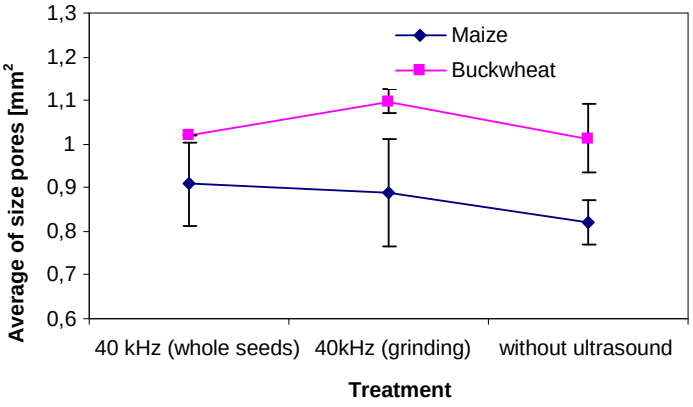

Fig. 4 - The porosity indices changes for corn and buckwheat extrudates according to material pre-treatment

The volume expansion index (VEI) and sectional expansion index (SEI) shown only a slight change in the values of these indicators (Fig. 5 and 6). It should be noted, however, that the tendency of the changes, as in the case of a WAI or porosity decrease also. The smallest values volumetric expansion indices of the samples obtained were characterized with whole grains treated with ultrasonic waves. In the case of a sectional expansion ratio small differences also appear, however, the trend shown on the chart in comparison to the volume expansion ratio is reversed.

Badania stopnia ekspandowania objętościowego i radialnego (SEI) wskazują tylko na niewielkie zmiany wartości tych wskaźników (rys. 5 i 6). Należy jednak zaznaczyć, że najmniejszymi wartościami EO tego parametru zarówno dla gryki i kukurydzy (całe ziarna poddane falom ultradźwiękowym) natomiast największymi głównie kukurydza niepodana działaniu ultradźwięków. W przypadku Ekspansji radialnej różnice również wydają się niewielkie jednakże tendencja przebiegu wykresu w porównaniu do ekspansji objętośiowej jest odwrotna.

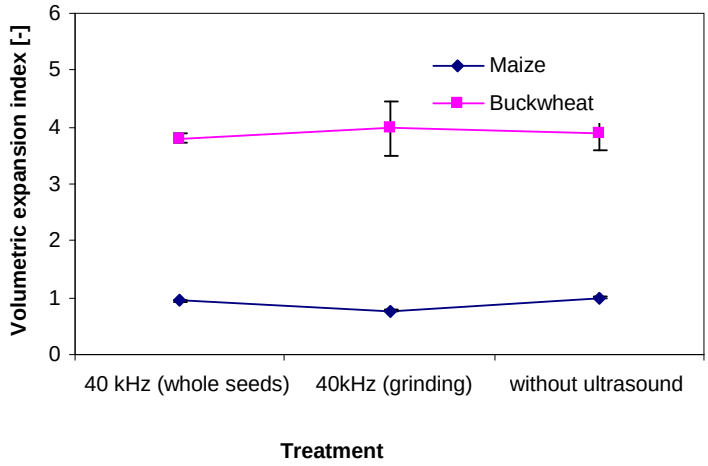

Fig. 5 - The volume expansion indices (VEI) changes for corn and buckwheat extrudates according to material pre-treatment

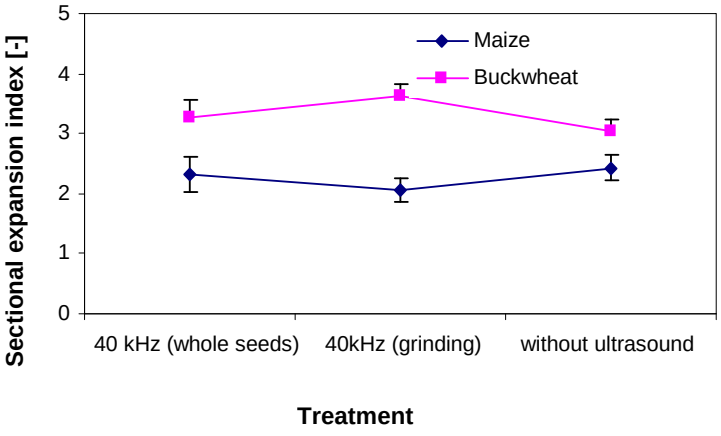

Fig. 6 - The sectional expansion indices (SEI) changes for corn and buckwheat extrudates according to material pre-treatment /

CONCLUSIONS

In conclusion, it should be noted that the effect of 40kHz ultrasonic waves can contribute to improving the quality of extrudates, both corn and buckwheat. It is called for high values of the WAI and WSI also low, indicating a high degree of gelation of starch and, at the same time, low degree in comparison to other materials used in the study of WSI, the high porosity of the extrudates which can continue to provide a high sensory qualities of such materials (Lui and Peng (2005) and Desrumaux et al., (1998) Lanuay et al., (1983), Żelaziński and Ekielski, 2011) and slightly progressive changes in the indices of volume and sectional expansion. This may be a positive feature of such behavior of these indicators because the indicators value often depends on eg. the shape of the products themselves.

When using a raw material treated with ultrasound may not be necessary to reprogram extruder's control systems to produce the same product as the native material. This may, however, require a number of additional tests using other types of extruders.

REFERENCES

[1]. Akbari Mousavi S. A. A, Feizi H., Madoliat R., (2007) - *Investigations on the effects of ultrasonic vibrations in the extrusion process*. Journal of Materials Processing Technology, pp.187–188, 657–661;
[2]. Alvarez-Martinez L., Kondury K. P., Harper J. M., (1988) - *A general model for expansion of extruded products.* Journal of Food Science, 53, pp.609-615;
[3]. Anderson R. A., Conway H. F., Pfeifer V. F., Griffin E. L. (1969) - *Roll and extrusion-cooking of grain sorghum grits.* Cereal Science Today, 14, pp.372-375, 381;
[4]. Awad T. S., Moharram H. A., Shaltout O. E., Asker D., Youssef M. M. (2012) - *Applications of ultrasound in analysis, processing and quality control of food. A review.* Food Research International, 48, pp.410–427;
[5]. Chandrapala J., Oliver C., Kentish S., Ashokkumar M., (2012) - *Ultrasonics in food processing*. Ultrasonics Sonochemistry, 19, 975–983;
[6]. Chang H.-J., Xu X.-L., Zhou G.-H., Li C.-B., Huang M., (2012) - *Effects of characteristics changes of collagen on meat physicochemical properties of beef semitendinosus muscle during ultrasonic processing.* Food and Bioprocess Technology, 5 (1), pp.285–297.
[7]. Chang M., Peng J.-C., Wei K., (2001) - *The study of optimum conditions of die diameter and buckwheat content for the development of extruded corn food.* Mechanical Engineering, 10 (1-4), pp.43-57;
[8]. Chemat F., Huma Z., Khan M. K., (2011) - *Applications of ultrasound in food technology. Processing, preservation and extraction.* Ultrasonics Sonochemistry, 18, pp.813–835;
[9]. Desrumaux A., Bouvier J. M., Burri J., (1998) - *Corn grits particle size and distribution effect on the characteristic of expanded extrudates.* Journal of Food Science Engineering Processing, 63 (5), 857-863;
[10]. Ekielski A., (2006) - *Use of fuzzy c in optimization of operation of a line for extrusion of plant products.* Inżynieria Rolnicza. Nr 7 (82). s. 145-153;
[11]. Ekielski A., Majewski Z., Żelaziński T., (2007) - *Effect of extrusion conditions on physical properties of buckwheat–maize blend extrudate.* Polish Journal of Food and Nutrition Sciences, 57, 2(A), 57-61;
[12]. Ekielski A., Majewski Z., Żelaziński T., (2007) - *Effect of die hole diameter in the extruder on energy consumption and quality indices of maize-buckwheat extrudate.* Polish Journal of Food and Nutrition Sciences, 57, 2(A), 53-56;

WNIOSKI

Podsumowując należy zaznaczyć, że działanie fal ultradźwiękowych 40kHz może przyczyniać się do poprawy jakości ekstrudatów, zarówno kukurydzianych i gryczanych. Przemawiają za tym wysokie wartości WAI, a zarazem niskie wartości WSI, co świadczy o wysokim stopniu zżelifikowania skrobi. Niewielke wartości parametru WSI i wysoka porowatość, a także w niewielkim stopniu postępujące zmiany wskaźników stopnia ekspandowania objętościowego i radialnego ekstrudatów, mogą świadczyć o wysokich walorach sensorycznych takich produktów (Żelaziński i Ekielski, 2011, Lui i Peng, 2005, Desrumaux i wsp., 1998, Lanuay i wsp., 1983). Może być to cecha pozytywna takiego zachowania się analizowanych wskaźników, ponieważ od ich wartości zależy często np. kształt samych produktów.

Przy zastosowaniu surowców poddanych działaniu ultradźwięków być może nie będzie potrzebne przeprogramowanie ekstruderów w celu uzyskania takiego samego produktu, jak z surowca natywnego. Wymagać to może jednak wielu dodatkowych prób z wykorzystaniem innych typów ekstruderów.

LITERATURA

[1]. Akbari Mousavi S. A. A, Feizi H., Madoliat R., (2007) – *Badania nad wpływem drgań ultradźwiękowych w procesie wytłaczania*. Journal of Materials Processing Technology, 187–188, 657–661;
[2]. Alvarez-Martinez L., Kondury K. P., Harper J. M., (1988) – *Ogólny model ekspansji wyrobów ekstrudowanych.* Journal of Food Science, 53, 609-615;
[3]. Anderson R. A., Conway H. F., Pfeifer V. F., Griffin E. L., (1969) – *Ekstruzyjne gotowoanie i walcowanie rozdrobnionego ziarna sorgo.* Cereal Science Today, 14, 372-375, 381;
[4]. Awad T. S., Moharram H. A., Shaltout O. E., Asker D., Youssef M. M., (2012) – *Zastosowanie ultradźwięków w analizie, przetwarzaniu i kontroli jakości żywności.* A review. Food Research International, 48, 410–427;
[5]. Chandrapala J., Oliver C., Kentish S., Ashokkumar M., (2012) – *Ultradźwięki w przetwórstwie żywności*. Ultrasonics Sonochemistry, 19, 975–983;
[6]. Chang H.-J., Xu X.-L., Zhou G.-H., Li C.-B., Huang M., (2012) – *Wpływ charakterystycznych zmian kolagenu na właściwości fizykochemiczne mięsa wołowego z mięśnia półścięgnistego podczas obróbki ultradźwiękami.* Food and Bioprocess Technology 5 (1), 285–297;
[7]. Chang M., Peng J.-C., Wei K., (2001) – *Badanie optymalnych parametrów średnicy dyszy i zawartości gryki na rozwój kukurydzianej żywności ekstrudowanej.* Mechanical Engineering, 10 (1-4), 43-57;
[8]. Chemat F., Huma Z., Khan M.K., (2011) – *Zastosowanie ultradźwięków w technologii żywności. Przetwarzanie, konserwowanie i ekstrakcja.* Ultrasonics Sonochemistry, 18, 813–835;
[9]. Desrumaux A., Bouvier J. M., Burri J., (1998) – *Wpływ wielkości i rozkładu cząstek kaszy kukurydzianej na charakterystykę ekstrudatów.* Journal of Food Science Engineering Processing, 63 (5), 857-863;
[10]. Ekielski A., (2006)- *Wykorzystanie sterowników rozmytych do optymalizacji pracy linii do ekstrudowania produktów roślinnych. Inżynieria Rolnicza.* Nr.7 (82). s.145-153;
[11]. Ekielski A., Majewski Z., Żelaziński T. (2007) – *Wpływ parametrów ekstruzji na własciwości fizyczne ekstrudatów z mieszanki gryka-kukurydza.* Polish Journal of Food and Nutrition Sciences, 57, 2(A), 57-61;
[12]. Ekielski A., Majewski Z., Żelaziński T., (2007) – *Wpływ średnicy otworu dyszy ekstrudera na zużycie energii i wskaźniki jakościowe ekstrudatów kukurydzino-gryczanych.* Polish Journal of Food and Nutrition Sciences, 57, 2(A), 53-56;

[13]. Ekielski A., Osiak J., (2003) - *The effect of extruder wear parts on selected parameters of extrusion process.* Inżynieria Rolnicza, 7(49), 39-46;
[14]. Ekielski A., Żelaziński T., (2012) - *Influence of porosity on textural properties of wheat extrudates)*. Inżynieria Rolnicza, 3 (138), 35-42;
[15]. Gosselin R., Rodrigue D., (2005) - *Cell morphology analysis of density polymer foams.* Polymer Testing, 24, 1027-1035;
[16]. Hernouxa A., Lévęquea J., Lassi U., Molina-Boisseaud S., Maraisd M., (2013) - *Conversion of a non-water soluble potato starch waste into reducing sugars under non-conventional technologies.* Carbohydrate Polymers, 92, 2065– 2074;
[17]. Hromádková Z., Ebringerová A., (2003) - *Ultrasonic extraction of plant materials—investigation of hemicellulose release from buckwheat hulls.* Ultrasonics Sonochemistry, 10, 127–133;
[18]. Jambrak A. R., Herceg Z., Šubaric´ D., Babic´ J., Brnc˘ic´ M., Brnc˘ic´ S.R., Bosiljkov T., C˘ vek D., Tripalo B., Gelo J., (2010) - *Ultrasound effect on physical properties of corn starch*. Carbohydrate Polymers, 79, 91–100;
[19]. Karkani O. A., Nenadis N., Nikiforidis C. V., Kiosseoglou V., (2013) - *Effect of recovery methods on the oxidative and physical stability of oil body emulsions.* Food Chemistry, 139, 640–648;
[20]. Kobus Z., (2006) - *Temperature Changes of carrot pulp during Sonification.* Inżynieria Rolnicza, 7 (82), 255-261;
[21]. Lanuay B., Lisch J. M., (1983) - *Twin-screw extrusion cooking of starch pastes, expansion and mechanical properties of extrudates.* Journal of Food Engineering, 9 (2), 259–280;
[22]. Lui W.-B., Peng J., (2005) - *Effects of operating conditions on degradable cushioning extrudate's cellular structure and the specific heat.* Journal of Food Engineering, 70 (2), 171–182;
[23]. Margulis M. A., Margulis I. M., (2003) - *Calorimetric method for measurement of acoustic power absorbed in a volume of a liquid.* Ultrasonic Sonochemistry, 10, 343–345.
[24]. Mason T. J., Zhao Y., (1994) - *Enhanced extraction of tea solids using ultrasound.* Ultrasonics, 32, 375-377;
[25]. Owolabi G. M., Bassim M. N., Page J. H., Scanlon M. G., (2008) - *The influence of specific mechanical energy on the ultrasonic characteristics of extruded dough.* Journal of Food Engineering, 86, 202–206;
[26]. Soria A. C., Villamiel M., (2010) - *Effect of ultrasound on the technological properties and bioactivity of food: a review. Trends in Food Science & Technology 21, 323 - 331*;
[27]. Sujka M., Jamroz J., (2013) - *Ultrasound-treated starch: SEM and TEM imaging, and functional behaviour.* Food Hydrocolloids, 31, 413-419;
[28]. Vinatoru M., Toma M., Mason T.J., (1999) - *Ultrasonically assisted extraction of bioactive principles from plants and the constituents.* Advances in Sonochemistry, 5, 216;
[29]. Wójtowicz A., Mościcki L., (2008) - *Energy consumption during extrusion-cooking of precooked pasta.* Teka Komisji Motoryzacji i Energetyki Rolnictwa PAN, 2, 311-318;
[30]. Zhu J., Li L., Chen L., Li X., (2012) - *Study on supramolecular structural changes of ultrasonic treated potato starch granules*. Food Hydrocolloids, 29, 116-122;
[31]. Żelaziński T., Ekielski A., (2012) - *Sensory investigation covering maize-buckwheat extrudate.* Postępy techniki przetwórstwa spożywczego, 1, 50-54.

[13]. Ekielski A., Osiak J., (2003) - *Wpływ stopnia zużycia elementów ekstrudera na wybrane parametry ekstruzji.* Inżynieria Rolnicza, 7(49), 39-46;
[14]. Ekielski A., Żelaziński T., (2012) - *Wpływ porowatości na cechy teksturalne ekstrudatów zbożowych.* Inżynieria Rolnicza. Nr 3 (138). s. 35-42;
[15]. Gosselin R., Rodrigue D. (2005) – *Analiza morfologiczna komórek zagęszczonych pianek polimerowych.* Polymer Testing, 24, 1027-1035;
[16]. Hernouxa A., Lévęquea J., Lassi U., Molina-Boisseaud S., Maraisd M., (2013) – *Przekształcanie odpadowej nierozpuszczalnej skrobi ziemniaczanej na cukry redukujące w ramach technologii niekonwencjonalnych.* Carbohydrate Polymers, 92, 2065– 2074;
[17]. Hromádková Z., Ebringerová A., (2003) - *Ultradźwiękowa ekstrakcja surowców roślinnych - badanie uwalniania hemicelulozy z łuski gryki*. Ultrasonics Sonochemistry, 10, 127–133;
[18]. Jambrak A. R., Herceg Z., Šubaric´ D., Babic´ J., Brnc˘ic´ M., Brnc˘ic´ S. R., Bosiljkov T., C˘ vek D., Tripalo B., Gelo J., (2010) – *Wpływ ultradźwięków na fizyczne własciwości skrobi kukurydzianej*. Carbohydrate Polymers, 79, 91–100;
[19]. Karkani O. A., Nenadis N., Nikiforidis C. V., Kiosseoglou V., (2013) – *Wpływ metod uzyskania oleju na właściwości utleniające i fizyczną stabilność olejowych emulsji do ciała.* Food Chemistry, 139, 640–648;
[20]. Kobus Z., (2006) - *Zmiany temperatury miazgi marchwiowej podczas procesu sonifikacji.* Inżynieria Rolnicza, 7 (82), 255-261;
[21]. Lanuay B., Lisch J. M., (1983) – *Dwuślimakowa ekstruzja makaronów skrobiowych, ekspansja i mechaniczne własciwosci ekstrudatów.* Journal of Food Engineering, 9 (2), 259–280;
[22]. Lui W.-B., Peng J., (2005) – *Wpływ warunków procesu na właściwości amortyzujace struktury komórkowej i ciepło właściwe ekstrudatów.* Journal of Food Engineering, 70 (2), 171–182;
[23]. Margulis M. A., Margulis I. M., (2003) – Kalorymetryczna metoda pomiaru mocy akustycznej zaabsorbowanej w objętości cieczy. Ultrasonic Sonochemistry, 10, 343–345.
[24]. Mason T.J., Zhao Y., (1994) – *Ulepszona ekstrakcja ciał stałych z herbaty za pomocą ultradźwięków.* Ultrasonics, 32, 375-377;
[25]. Owolabi G. M., Bassim M. N., Page J. H., Scanlon M. G., (2008) – *Wpływ właściwej energii mechanicznej na charakterystykę ultradźwiękową ekstrudowanego ciasta.* Journal of Food Engineering, 86, 202–206;
[26]. Soria A. C., Villamiel M., (2010) – Wpływ ultradźwięków na właściwosci technologiczne i bioaktywność żywności: przegląd. *Trends in Food Science & Technology 21, 323 -331*;
[27]. Sujka M., Jamroz J., (2013) – *Skrobia traktowana ultradźwiękami: obrazowanie SEM i TEM oraz właściwości funkcjonalne.* Food Hydrocolloids, 31, 413-419;
[28]. Vinatoru M., Toma M., Mason T. J. (1999) – Wspomagana ultradźwiękami ekstrakcja cząstek bioaktywnych z *roślin i ich części.* Advances in Sonochemistry, 5, 216;
[29]. Wójtowicz A., Mościcki L., (2008) – Energochłonność ekstruzji podgotowanego makaronu. Teka Komisji Motoryzacji i Energetyki Rolnictwa PAN, 2, 311-318;
[30]. Zhu J., Li L., Chen L., Li X., (2012) – *Badanie zmian supramolekularnych strukturalnych zmian cząstek skrobi poddanych obróbce ultradźwiękowej*. Food Hydrocolloids, 29, 116-122;
[31]. Żelaziński T., Ekielski A., (2012) - *Badania sensoryczne ekstrudatów kukurydzian-gryczanych.* Postępy techniki przetwórstwa spożywczego, 1, 50-54.

THE EFFECT OF EXTRUDATE FINENESS ON THE SHAPE OF PARTICLES OBTAINED / *WPŁYW STOPNIA ROZDROBNIENIA EKSTRUDATU NA KSZTAŁT UZYSKANYCH CZĄSTEK*

PhD. Eng. Ekielski A., PhD. Eng. Żelaziński T., PhD. Stud. Eng Zdanowska P., PhD. Stud. Eng. Florczak I.
Warsaw University of Life Sciences, Faculty of Production Engineering, Warsaw / Poland
Tel: +48 22 59 345 00; e-mail: adam_ekielski@sggw.pl

Abstract: *The aim of this study was to investigate the influence of the grounded extrudate fraction on the obtained particles' shape and attempt to link these characteristics with the quality of the extrudate from which they were originated. The material used in the study was the wheat-corn extrudate produced in the twin-screw extruder at 130, 140 and 150°C. The extrudates were grounded in the hammer shredder and then particles were separated on a laboratory sieve sifter. It was extrudate porosity and ground particle shape investigated. It was found that the products obtained in the twin-screw extruder at different temperatures of the process are distinguished by the variable internal structure which can affect obtaining extrudate fractions with varying percentage of particles and the shape of the extrudate after grinding. It was observed that the smallest and largest extrudate fractions were ground the most. Elongation factor showed an increase in the length of the fraction obtained with the reduction of extrudate particles size. Differentiation of the shape could be important because of the sensory evaluation of the products carried by consumers, and consequently it could be a very valuable insight for future producers of such products.*

Keywords: *food extrusion, grinding, breadcrumbs, shape*

INTRODUCTION

A characteristic feature of extruded products is mostly the porous, expanded and highly differentiated internal structure. The pores in these products may have a different size, shape, occuring in varying numbers in a defined area, or differing with wall thickness. Their quality depends on many factors, which is the subject of many research works (Hayter et al., 1986; Mezreb et al., 2003; Włodarczyk-Stasiak, Jamroz, 2009; Crowley et al., 2010; Żelazinski, 2011; Bisharat et al., 2013).

It has been proven that the pores surrounding the outside of the extrudate are flattened, which may be due to the influence of the walls of the matrix outlet channel and the high speed of heat and mass transfer occurring in the surface layer. As approaching the center, the internal pore structure of the extrudate is usually symmetrical, but their size and shape can varied (Desrumaux et al., 1998, Ekielski, Żelaziński 2012). According to Lui and Peng (2005) and Desrumaux et al. (1998), changes in porosity affect the textural characteristics of extruded products. Lanuay et al. (1983) noted that the porosity has also a significant impact on the sensory evaluation - with increase of the pore size product crispness increases. This process is not entirely understood and still raises the interest of many authors (Desrumaux et al, 1998; Ays¸e et al., 2004; Lui and Peng, 2005; Biller et al., 2005; Biller, 2006; Agbisit et al., 2007; Wojtowicz et al., 2010; Żelaziński, 2011).

Therefore, the distinctive structure of the products obtained by extrusion can have a significant effect on further processing, e.g. by grinding for breadcrumbs. Currently, these products pose a number of requirements

Abstrakt: *Celem pracy było zbadanie wpływu stopnia rozdrobnienia ekstrudatu na kształt uzyskanych cząstek i próba powiązania tych cech z jakością ekstrudatu z którego powstały. Materiałem wykorzystywanym w badaniach był ekstrudat pszenno-kukurydziany wyprodukowany na współbieżnym ekstruderze dwuślimakowym w temperaturze 130, 140 i 150 °C. Wytworzone ekstrudaty rozdrobniono na rozdrabniaczu bijakowym, a następnie przeprowadzono separację cząstek na laboratoryjnym przesiewaczu sitowym. Badano porowatość ekstrudatu oraz kształt cząstek rozdrobnionego ekstrudatu. Stwierdzono, że produkty uzyskane na ekstruderze dwuślimakowym w różnych temperaturach procesu wyróżniają się zmienną strukturą wewnętrzna, co może mieć wpływ na uzyskanie frakcji ekstrudatu o różnym procentowym udziale oraz na kształt cząstek ekstrudatu po ich rozdrobnieniu. Zaobserwowano, że najmniejsze i największe frakcje ekstrudatu były najbardziej okrągłe. Współczynnik wydłużenia wskazywał natomiast na wzrost długości uzyskanych frakcji wraz ze zmniejszeniem cząstek ekstrudatu. Zróżnicowanie kształtu może być istotne ze względu na ocenę sensoryczną produktów dokonywaną przez odbiorców, w konsekwencji może być to niezwykle cenne spostrzeżenie dla przyszłych producentów tego typu produktów.*

Słowa kluczowe: *ekstruzja, rozdrobnienie, panier, kształt*

WSTĘP

Cechą charakterystyczną wyrobów ekstrudowanych jest głównie porowata, rozwinięta i bardzo zróżnicowana wewnętrzna struktura. Pory w tych produktach mogą posiadać różny rozmiar, kształt, występować w różnej liczbie na określonej powierzchni, czy też różnić się grubością ścianek. Ich jakość uzależniona jest od wielu czynników, co jest tematem wielu prac badawczych (Hayter i in., 1986; Mezreb i in., 2003; Włodarczyk-Stasiak i Jamroz, 2009; Crowley i in., 2010; Żelazinski, 2011; Bisharat i in., 2013).

Udowodniono, że pory otaczające zewnętrzną część ekstrudatu są spłaszczone, co może być efektem oddziaływania ścianek kanału wylotowego matrycy oraz dużej szybkości wymiany ciepła i masy występującej w warstwie przypowierzchniowej. W miarę zbliżania się do środka ekstrudatu struktura wewnętrzna porów jest zwykle symetryczna, ale ich rozmiar i kształt może się zmieniać (Desrumaux i in., 1998, Ekielski i Żelaziński 2012). Według Lui i Peng (2005) oraz Desrumaux i in. (1998) zmiany porowatości wpływają na cechy teksturalne ekstrudowanych produktów. Lanuay i in. (1983) zauważyli, że porowatość istotnie wpływa również na ocenę sensoryczną - wraz ze wzrostem wielkości porów wzrasta chrupkość produktów. Proces ten nie jest do końca poznany i ciągle budzi zainteresowanie wielu autorów (Desrumaux i In., 1998; Ays¸e i in., 2004; Lui i Peng, 2005; Biller i in., 2005; Biller, 2006; Agbisit i in., 2007; Wojtowicz i in., 2010; Żelaziński, 2011).

Charakterystyczna budowa produktów uzyskanych na drodze ekstruzji może mieć zatem istotny wpływ na dalszą obróbkę np. poprzez rozdrobnienie z przeznaczeniem na panier spożywczy. Obecnie tego

including both appropriately selected composition and sensory characteristics. The same shape of such products particles can be also essential. Ultimately, it may be relevant for the breadcrumbs classification for a particular product type. In the literature, there are no tests found on breadcrumbs obtained from the extrudate as yet. In the context of the extrusion process it has been considered the particle size of the material to be extruded with its effects on the physicochemical properties and digestibility of the product (Al-Rabadi et al., 2011; Al-Rabadi et al., 2012).

Therefore, the objective of this study was to investigate the influence of the extrudate fineness degree on the obtained particles' shape and an attempt to link these characteristics with the quality of the extrudate from which they were originated.

MATERIALS AND METHODS

The material used in the study was the wheat-corn extrudate (20% wheat, 80% maize), produced in the twin-screw co-extruder with a length to screw diameter L/d=27. At the head of the extruder die was used with a multiple outlet nozzles of 3 mm. Screw rotation speed of 300 rpm, and temperature profiles viewed from extruder's die, were: {130/130/100°C}, {140/140/100°C} and {150/150/100°C } Celsjus degrees. The temperature was controlled in the first and second section of the extruder using the PID controller.

Porosity was determined by the method of Gosselin and Rodrigue (2005), using an irregular boundary of the analyzed group of air pores in the analyzed images. The porosity analysis was lead with the use of LabView 7.1 package with visionary libraries and Vision Asistant 7.1.1 program, where the images were transposed to the monochrome area and were treated with specialized photo retouch. Then, the obtained images of byte grayscale (256 levels) were converted to divalent bitmaps and appropriate shades of gray thresholds were chosen in the range of 1-255 (treshold).

The resulting extrudates were ground in a hammer grinder with a sieve on the output of 3 mm. This was followed by separation of the particles on the laboratory sieve analyzer: Laboratory siever type LP2E-2e (MULTISERV) according to DIN ISO 3310-1, amplitude of 60, frequency of 2.00 Hz, duration of 10 minutes, sieve sizes: 2.0, 1.6, 1,0, 0.8, 0.5, 0.25, 0.1, <0.05 mm.

Individual breadcrumbs fractions were spread out on black paper, then photographed using a CCD camera KP-FD30 HITACHI in the light chamber, illuminated with fluorescent light TL-D De Luxe Pro 18W/965, with a color temperature of 6500K (Philips) and visual analysis was given using the Visio Assistant 7.1 program. This program allowed for the calculation of coefficients which characterize the particles shape according to the following formulas (1), (2), (3), (4), (5):

typu produktom stawia się szereg wymagań obejmujących zarówno odpowiednio dobrany skład, jak i cechy sensoryczne. Istotny może być również sam kształt cząstek takich produktów, który docelowo może mieć znaczenie przy zakwalifikowaniu panieru do danego typu produktu. W literaturze nie znaleziono jak dotąd badań przeprowadzanych na panierze spożywczym uzyskanym z ekstrudatu. W kontekście procesu ekstruzji rozpatrywano jak dotąd wielkość cząstek materiału poddawanego ekstruzji wraz z jego wpływem na cechy fizykochemiczne i strawność produktu (Al- Rabadi i in., 2011; Al-Rabadi i in., 2012).

Celem pracy było zatem zbadanie wpływu stopnia rozdrobnienia ekstrudatu na kształt uzyskanych cząstek i próba powiązania tych cech z jakością ekstrudatu z którego powstały.

MATERIAŁ I METODYKA

Materiałem wykorzystywanym w badaniach był ekstrudat pszenno-kukurydziany (20% pszenica, 80% kukurydza), wyprodukowany na współbieżnym ekstruderze dwuślimakowym o stosunku długości do średnicy ślimaków L/d=27. Na głowicy ekstrudera zastosowano wielootworową matrycę z dyszami wylotowymi 3 mm. Prędkość obrotowa ślimaków wynosiła 300 obr•min^{-1}, a profil temperaturowy procesu w cylindrze ekstrudera, patrząc od ekstrudrera do matrycy wynosił: {130,/130/100°C}, {140,/140/100°C}, {150,/150/100°C} stopni Celcjiusza. Temperaturę utrzymywano w dwóch pierwszych sekcjach ekstrudera utrzymywano za pomocą sterownika PID.

Porowatość określano według metody Gosselin i Rodrigue (2005), stosując nieregularną obwiednię analizowanej grupy porów powietrznych na analizowanych zdjęciach. Do analizy porowatości wykorzystano pakiet LabView 7.1 z bibliotekami wizyjnymi oraz programem Vision Asistant 7.1.1, gdzie zdjęcia transponowano do przestrzeni monochromatycznej i poddawano specjalistycznej obróbce graficznej. Następnie otrzymane obrazy o bajtowej skali szarości (256 odcieni) przekształcano w dwuwartościowe mapy bitowe i dobierano odpowiednie wartości progowe odcieni szarości z zakresu od 1–255 (treshold).

Wytworzone ekstrudaty rozdrobniono na rozdrabniaczu bijakowym z sitem na wyjściu 3 mm. Następnie przeprowadzono separację cząstek na analizatorze laboratoryjnym: przesiewacz laboratoryjny typ LP2E-2e (Multiserv) wg normy DIN ISO 3310-1, amplituda 60, częstotliwość 2,00 Hz, czas 10 minut, wielkości sit: 2,0; 1,6; 1,0; 0,8; 0,5; 0,25; 0,1; <0.05 mm.

Poszczególne frakcje panieru rozkładano na czarnym papierze, następnie fotografowano za pomocą kamery CCD KP–FD30 firmy HITACHI w komorze bezcieniowej, oświetlonej świetlówkami światła dziennego TL–D De Luxe Pro 18W/965, o temperaturze barwowej 6500K firmy Philips i podawano analizie wizyjnej, wykorzystując program Visio Assistant 7.1. Wspomniany program pozwalał na obliczenie współczynników charakteryzujących kształt cząstek według poniższych wzorów (1), (2), (3), (4):

Elongation Factor $$\frac{F}{RF_b} \quad (1)$$

Heywood Circularity Factor $$\frac{P}{2\sqrt{\pi A}} \quad (2)$$

Compactness Factor $$\frac{A}{W \cdot H} \quad (3)$$

Type factor $$\frac{A^2}{4\pi\sqrt{I_{xx} - I_{yy}}} \quad (4)$$

where:
F – Max Feret; RF_b – Feret (Rect Short Side); P - Perimeter; A – Area of the particle ; W – Bounding Rect Width; H – Bounding Rect Height;
I_{xx} – Moment of Inertia XX - $\sum_{xx} - \frac{\sum_x^2}{A}$,
I_{yy} - Moment of Inertia YY $\sum_{yy} - \frac{\sum_y^2}{A}$.

The experiment was planned by the Central Compositional Plan / Design of Experiments (DOE) - the number of input values: 2, number of blocks: 1, number of circuits: 24 with repetition. Different variables were coded as numeric values: -1, 0, 1. Furthermore, the additional repeat was applied at a central point. The plan was created using the Statistica 10, which was then used to obtain a response surface. Variable analysis of significance was performed using analysis of variance ANOVA and statistical evaluation of the fit quality of surface response equations - a coefficient of determination R^2 and mean square error MSE (Mean Square Error).

RESULTS

Samples from twin-screw extruder had a uniform structure and visually, despite the use of three extrusion temperature t={130, 140, 150}°C, did not differ significantly from each other. Mounted multi-hole die with a holes diameter of 3mm and a knife cutting device made it possible to produce extrudates in the shape of a cylinder with a diameter of about 4mm and a length of about 6 mm (Fig.1).

gdzie: F – maksymalny rozmiar Fereta; RF_b – krótszy wymiar prostokątny Fereta; P – Obwód cząsteczki A – Pole rzutu cząstki ; W – szerokość cząstki ; H – długość cząstki;
I_{xx} – Moment bezwładności osi xx - $\sum_{xx} - \frac{\sum_x^2}{A}$,
I_{yy} - Moment bezwładności osi yy $\sum_{yy} - \frac{\sum_y^2}{A}$.

Eksperyment zaplanowano za pomocą Centralnego Planu Kompozycyjnego (DOE) - liczba wielkości wejściowych: 2, liczba bloków: 1, liczba układów: 24 z powtórzeniem. Poszczególne zmienne zakodowano jako wartości liczbowe: -1, 0, 1. Zastosowano ponadto dodatkowe powtórzenia w punkcie centralnym. Plan utworzono z wykorzystaniem programu Statistica 10, służącego następnie do uzyskania powierzchni odpowiedzi. Analizę istotności zmiennych przeprowadzono za pomocą analizy wariancji ANOVA, a ocenę statystyczną jakości dopasowania równań powierzchni odpowiedzi – za pomocą współczynnika determinacji R^2 oraz błędu średnio kwadratowego MSE (ang. Mean Square Error).

WYNIKI BADAŃ

Próbki uzyskane na dwuślimakowym ekstruderze charakteryzowały się jednorodną budową i wizualnie, pomimo zastosowania trzech temperatur procesu ekstruzji t={130, 140, 150}°C, nie różniły się znacząco od siebie. Zamontowana wielootworowa matryca o średnicy otworów 3mm z nożem obcinającym pozwoliła na wytworzenie ekstrudatów w kształcie walca o średnicy około 4mm i długości około 6mm (rys.1).

The extrudate sample view / *Widok próbki ekstrudatu*

Extrudate cross-section view obtained in a particular temperature

t =130°C **t=140°C** **t=150°C**

Fig.1 - View of whole-samples and cross-section of the samples obtained under different temperature conditions

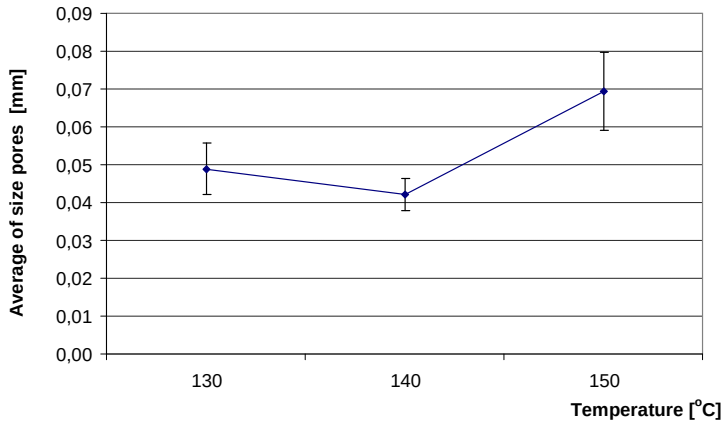

Fig.2 - Effect of extrusion temperature on the average of size of pores designated in cross-section of extrudate

Samples produced under these conditions differed significantly by the construction of the internal structure, which confirmed the results of empirical research. It was found that the samples obtained at the highest temperature (150°C) had the greatest pores, with the average size of about 0.07 mm^2. The average pore size obtained at 130 and 140°C ranged from 0.042 to 0.051 mm^2 (Fig.2).

The graph (Fig.3) shows the additional parameters determining the porosity of the resulting products, i.e. the number of pores in mm^2 in the extrudate cross-sectional area and the total surface pores, expressed as a percentage of pore surface in relation to the analyzed surface of the extrudate. It was found that the fewest number of pores (2 pores•mm^{-2}) was in the extrudate made in a temperature of 150°C, while other samples prepared at lower temperatures contain as low as 4.5 to 5.5 pores in mm^2. The total area of pores in the analyzed extrudate samples is in the range from about 16% to 24%, as shown in Figure 3.

Wytworzone w tych warunkach próbki różniły się jednak znacząco budową struktury wewnętrznej, co potwierdziły wyniki badań empirycznych. Stwierdzono, że próbki uzyskane w najwyższej temperaturze (150°C) posiadały największe pory, których średnia powierzchnia wynosiła około 0,07 mm2. Średni rozmiar porów uzyskanych w temperaturze 130 i 140°C zawierał się w przedziale od 0,042 do 0,051 mm^2 (rys. 2).

Na wykresie (rys. 3) przedstawiono dodatkowe parametry określające porowatość uzyskanych produktów tj. liczbę porów w mm^2 powierzchni przekroju ekstrudatu oraz ogólną powierzchnię porów wyrażoną jako procentowy udział powierzchni porów w stosunku do analizowanej powierzchni ekstrudatu. Stwierdzono, że najmniejszą liczbę porów (2 pory•mm^{-2}) posiadał ekstrudat wytworzony w temperaturze 150 °C, podczas gdy pozostałe próbki wytworzone w niższych temperaturach zawierały w mm^2 nawet od 4,5 do 5,5 pora. Ogólna powierzchnia porów w analizowanych próbkach ekstrudatu zawierała się w przedziale średnio od 16% do 24%, co przedstawiono na rysunku 3.

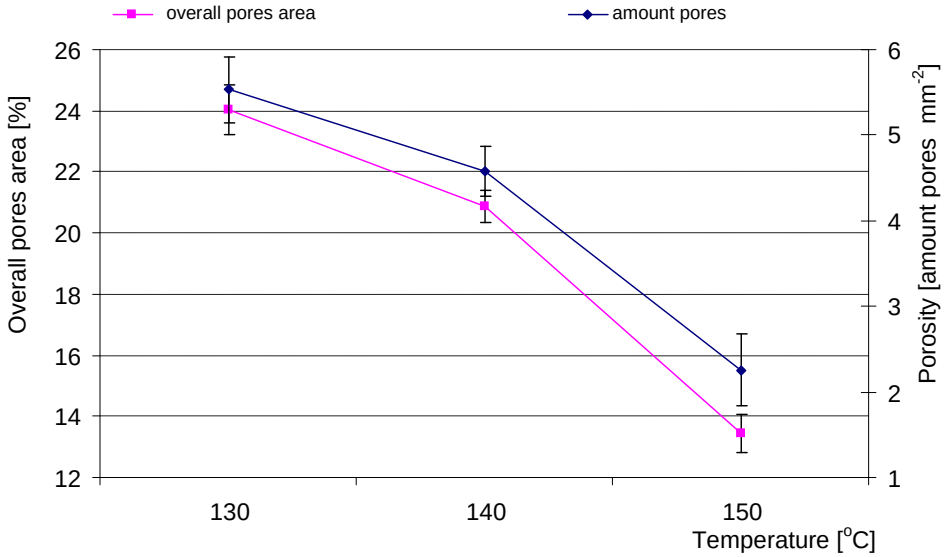

Fig.3 - Effect of extrusion temperature on the overall pores area and the number of pores in the extrudate cross-section

As porosity of the obtained results showed that the individual extrudate samples obtained at different temperatures differed distinctly, one could assume that they behave in different ways when subjected to the action of hammer mill. Therefore, below in Table 1 there are summarized the results of the percentage distribution of the fractions obtained. Based on preliminary

Ponieważ uzyskane wyniki badań porowatości wykazały, że poszczególne próbki ekstrudatu uzyskane przy różnych temperaturach wyraźnie się różniły, można było założyć, że w różny sposób będą się zachowywały po poddaniu ich działaniu rozdrabniacza bijakowego. Dlatego poniżej w tabeli 1. zestawiono wyniki procentowego rozkładu uzyskanych frakcji. Na podstawie wstępnej analizy można stwierdzić, że procentowy udział

examination it can be concluded that the percentage fraction of the extrudate varies depending on the sieve used, as well as the extrusion temperature employed.

frakcji ekstrudatu zmienia się w zależności od zastosowanego sita, jak również od zastosowanej temperatury procesu ekstruzji.

Table 1

Percentage of crushed extrudate fractions for different temperature conditions

Sieve mesh size # DIN ISO 3310-1 [mm]	130 °C	140 °C	150 °C
0,05 <	2.33	2.79	0.86
0.1	10.52	17.02	2.32
0.25	15.75	24.34	4.32
0.5	13.05	16.96	8.52
0.8	4.10	5.26	4.88
1.0	23.19	20.53	33.02
1.6	22.54	9.77	36.73
2.0	8.53	3.34	9.36

Additionally, it can be observed that the individual fractions of particulate ground extrudate distinguished not only by fragmentation but also by the shape of the resulting particles. Carry out a preliminary analysis of the image allowed for the characterization of particles shape with the four coefficients of the shape described in the methods. Below, there are some sample images of particulate extrudate samples fraction analyzed (Fig. 4).

Dodatkowo można było zaobserwować, że poszczególne frakcje rozdrobnionego ekstrudatu wyróżniały nie tylko stopieniem rozdrobnienia, ale dodatkowo kształtem uzyskanych cząstek. Przeprowadzenie wstępnej analizy obrazu pozwoliło na scharakteryzowanie kształtu uzyskanych cząstek na podstawie czterech współczynników kształtu, opisanych w metodyce pracy. Poniżej przedstawiono wybrane przykładowe zdjęcia frakcji analizowanych próbek rozdrobnionego ekstrudatu (rys. 4).

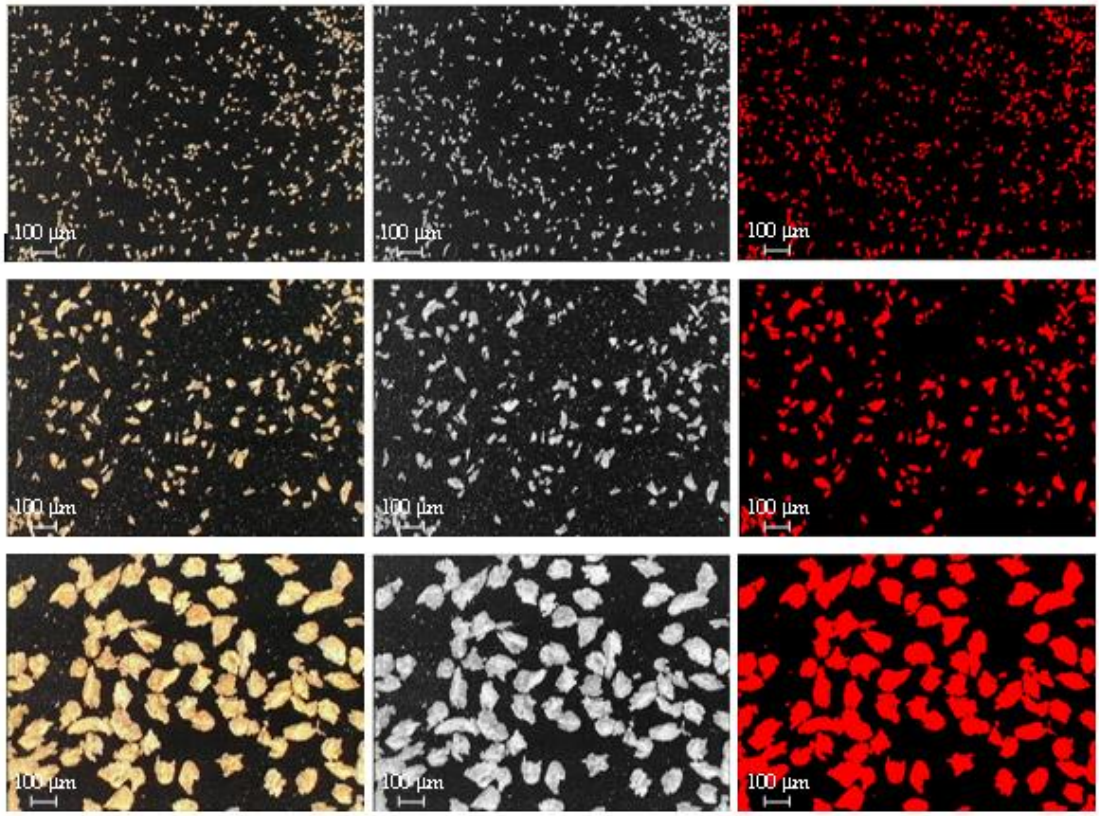

Fig.4 - Example analysis of the ground fraction of the extrudate. a) the fraction of 0.1, b) the fraction of 0.25, c) the fraction of 0.8.

On the basis of the statistical analysis it was found that the only important parameter influencing on the particle shape obtained during experiment is the degree of the extrudate fragmentation, obtained after separation of the ground extrudate to the appropriate fractions. The analysis of variance ANOVA indicated the importance of first and second order factor in analyzing elongation, roundness and compactness factor. In the case of the surface development factor (Type Factor) there were both temperature and fragmentation of the second row significant.

Na podstawie przeprowadzonej analizy statystycznej stwierdzono, że jednym istotnym parametrem mającym wpływ na kształt uzyskanych cząstek jest stopień rozdrobnienia ekstrudatu, uzyskany po rozdzieleniu rozdrobnionego ekstrudatu na odpowiednie frakcje. Przeprowadzona analiza wariancji ANOVA wskazała na istotność pierwszego i drugiego rzędu przy analizowaniu współczynnika wydłużenia, okrągłości i współczynnika upakowania. W przypadku współczynnika rozwinięcia powierzchni (Type Factor) istotnymi okazały się zarówno temperatura, jak i rozdrobnienie drugiego rzędu.

Table 2

Anova table with important factors for p<0.05

	SS	df	MS	F	p
Elongation factor, R^2 = 0.258, MS = 0.008, *R^2 = 0,558, MS = 0,008*					
Temperature *(L)*	0.0131	1	0.0131	0.1712	0.6837
Temperature *(Q)*	0.0531	1	0.0531	0.6963	0.4144
Grinding *(L)*	0.3654	1	0.3654	4.7881	0.0414
Grinding *(Q)*	0.0287	1	0.0287	0.3759	0.5471
Error	1.4500	19	0.0763		
Overall SS	1.9542	23			
Roundness factor, R^2 = 0.687, MS = 0.008					
Temperature *(L)*	0.0348	1	0.0348	4.3298	0.0512
Temperature *(Q)*	0.0008	1	0.0008	0.1052	0.7493
Grinding *(L)*	0.0008	1	0.0008	0.0992	0.7562
Grinding *(Q)*	0.2943	1	0.2943	36.6754	0.0000
Error	0.1525	19	0.0080		
Overall SS	0.4874	23			
Compactness factor, R^2 = 0.584, MS = 0.003					
Temperature *(L)*	0.0102	1	0.0102	2.9790	0.1006
Temperature *(Q)*	0.0110	1	0.0110	3.1980	0.0897
Grinding *(L)*	0.0103	1	0.0103	2.9990	0.0995
Grinding *(Q)*	0.0523	1	0.0523	15.2418	0.0010
Error	0.0652	19	0.0034		
Overall SS	0.1568	23			
Type factor, R^2 = 0.463, MS = 0.001 / *Współczynnik rozwinięcia, R^2 = 0,563, MS = 0,001*					
Temperature *(L)*	0.0051	1	0.0051	3.6954	0.0697
Temperature *(Q)*	0.0164	1	0.0164	11.8644	0.0027
Grinding *(L)*	0.0021	1	0.0021	1.5249	0.2319
Grinding *(Q)*	0.0063	1	0.0063	4.5219	0,0468
Error	0.0263	19	0.0014		
Overall SS	0.0592	23			

The values of the factors as a function of the analyzed fineness (obtained fraction) and the temperature of the extrusion process are shown in the form of three-dimensional response surface plots generated in Statistica 10. It was found that the smallest and largest extrudate fractions were close to unity, so were the most round. In the case of the middle fraction roundness values significantly increased, suggesting that the obtained fractions were less round and may have an irregular or elongated shape (Fig. 5).

Wartości analizowanych współczynników w funkcji rozdrobnienia (uzyskanych frakcji) oraz temperatury procesu ekstruzji przedstawiono w postaci trójwymiarowych wykresów powierzchni odpowiedzi wygenerowanych w programie Statistica 10. Stwierdzono, że najmniejsze i największe frakcje ekstrudatu zbliżone były do jedności, zatem były najbardziej okrągłe. W przypadku frakcji środkowych wartości współczynnika okrągłości wyraźnie wzrastały, co sugeruje, że uzyskane frakcje były mniej okrągłe i mogły posiadać nieregularny lub wydłużony kształt (rys. 5).

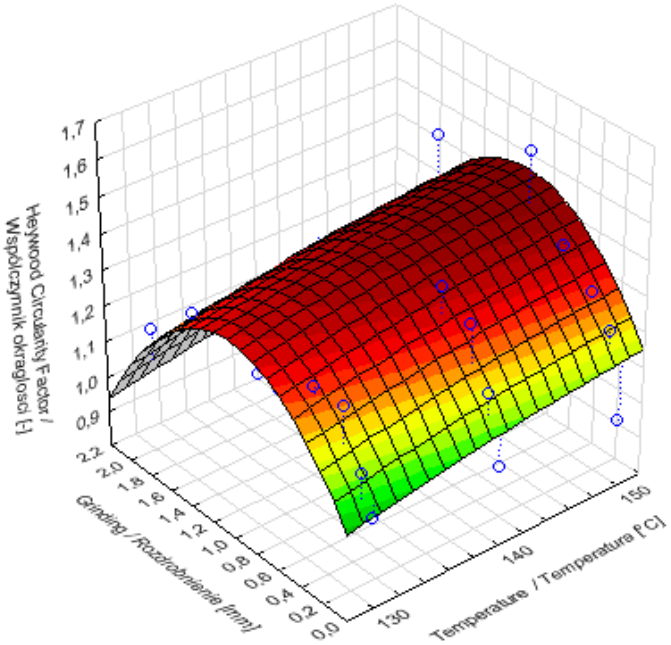

$$z = -1{,}485 + 0{,}032 \cdot x - 0{,}0001 \cdot x^2 + 0{,}597 \cdot y - 0{,}292 \cdot y^2$$

Fig. 5 - Effect of extrusion temperature and the degree of extrudate fineness into roundness factor of breadcrumbs particles obtained

Elongation factor (Fig.6) showed an increase in the length of the fraction obtained with the reduction of extrudate particle size. Therefore, the greatest length had the particles retained on a sieves of 0.25, 0.1 and less than 0.05 mm. Extension of the fine particles is due to the fact that their main ingredients are shredded pieces of the pore walls structure. While, in the case of larger particles, the main component are whole extrudate's pore fragments, creating a more rounded structure. This phenomenon can be explained physically - by the presence of pore wall fragments, and chemically - different chemical composition of extrudate fractions - bonds between the plant fibers and grain protein in given particles. The diversity of shape is important because of the sensory evaluation of the products obtained from the consumers. This can be extremely valuable insight for future producers of such products.

Współczynnik wydłużenia (rys.6) wskazywał natomiast na wzrost długości uzyskanych frakcji wraz z zmniejszeniem cząstek ekstrudatu. Największą długość posiadały zatem cząstki zatrzymane na sitach 0,25; 0,1 oraz poniżej 0,05 mm. Wydłużenie drobnych cząstek jest spowodowane tym, że głównym ich składnikiem są rozdrobnione fragmenty struktury ścianek porów. Podczas gdy, w przypadku większych cząstek, głównym ich składnikiem są całe fragmenty porów ekstrudatu, tworząc bardziej obłe struktury. Takie zjawisko można uzasadnić zarówno fizycznie - obecnością fragmentów ścianek por, jak i zróżnicowanym składem chemicznym frakcji ekstrudatu - wiązaniami między włóknami roślinnymi a białkiem zbóż w danych cząstkach. Zróżnicowanie kształtu jest istotne ze względu na ocenę sensoryczną uzyskiwanych produktów przez odbiorców. Może być to niezwykle cenne spostrzeżenie dla przyszłych producentów tego typu produktów.

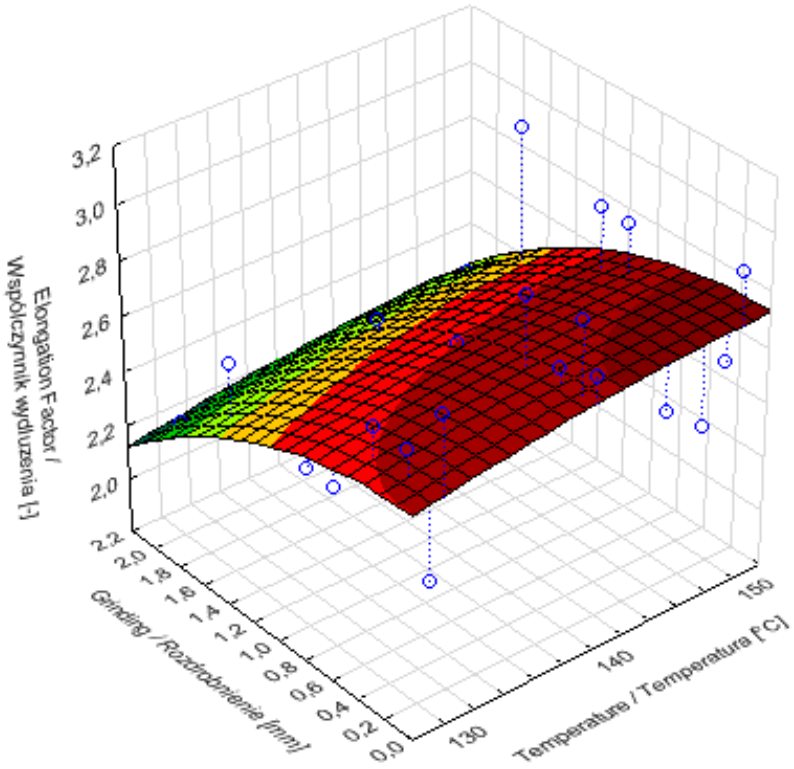

$$z = -1{,}638 + 0{,}056 \cdot x - 0{,}0001 \cdot x^2 + 0{,}015 \cdot y - 0{,}106 \cdot y^2$$

Fig. 6 - Effect of extrusion temperature and the degree of extrudate fineness into elongation factor of breadcrumbs particles obtained

Analysis of compatness factor showed that this parameter varies inversely than a roundness factor (Fig. 7). It was found that the lowest value of this ratio ranged from 0.5 to 0.6, indicating that the particles of such form in the slightest degree fill a rectangular boundary included in the calculated dependence (formula 3).

Analiza współczynnika upakowania (compatness factor) wykazała, że parametr ten zmienia się odwrotnie niż współczynnik okrągłości (rys. 7). Stwierdzono, że najmniejsze wartości tego współczynnika zawierały się w przedziale 0,5-0,6, co świadczy, że cząstki o takim kształcie w najmniejszym stopniu wypełniają obwiednię prostokątną uwzględnioną w obliczanej zależności (wzór 3).

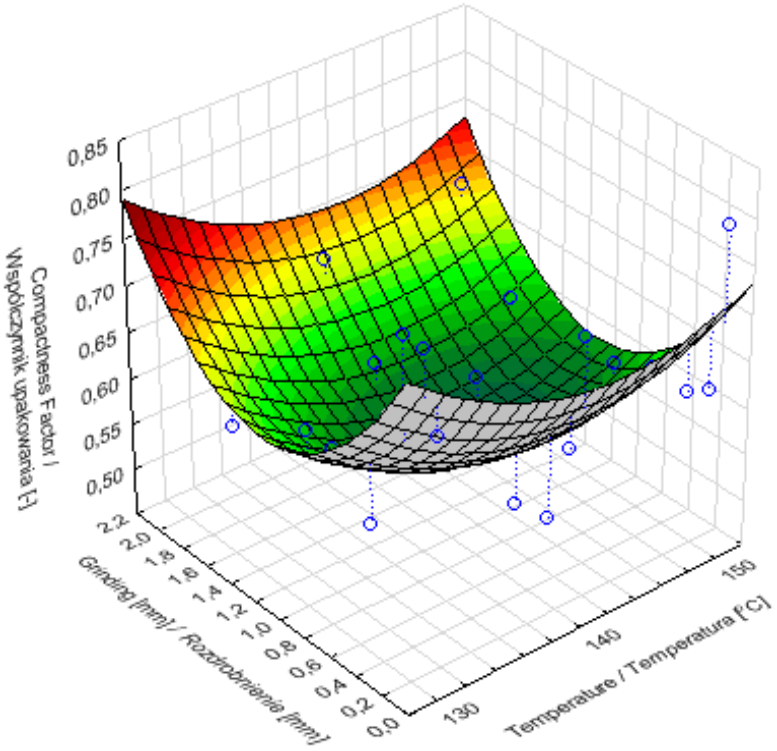

$$z = 9{,}697 + 0{,}0126 \cdot x + 0{,}0004 \cdot x^2 - 0{,}287 \cdot y + 0{,}129 \cdot y^2$$

Fig. 7 - Effect of extrusion temperature and the degree of extrudate fineness into compactness factor of breadcrumbs particles obtained

Graph showing the type factor (Fig.8) as a function of temperature and fineness have a course close to the compactness factor.

Wykres przedstawiający współczynnik rozwinięcia powierzchni Type Factor (rys. 8) w funkcji rozdrobnienia i temperatury posiadał przebieg zbliżony do współczynnika upakowania (Compactness Factor).

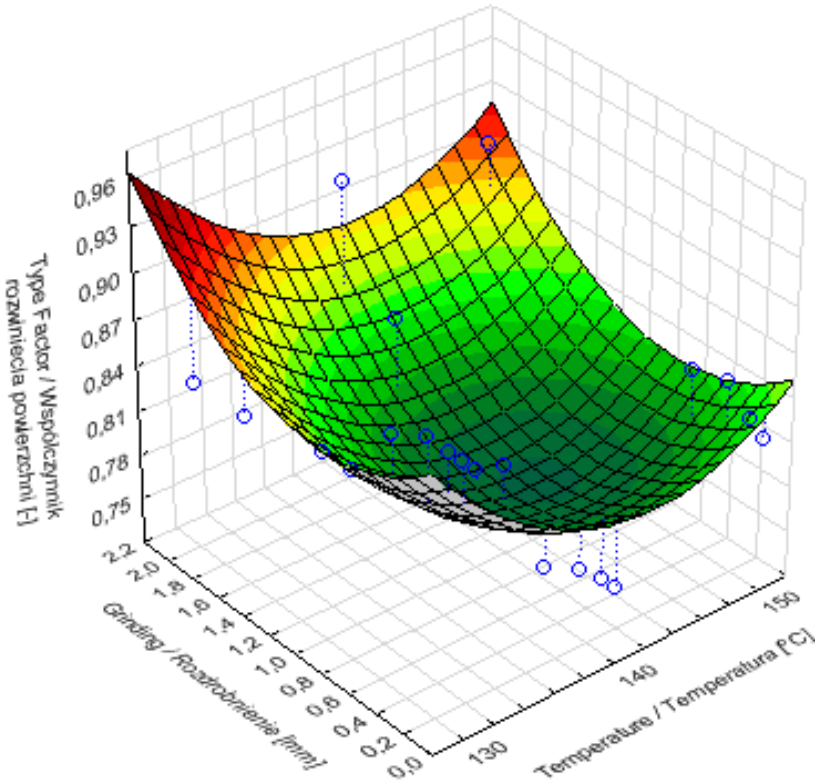

$$z = 9{,}789 - 0{,}126 \cdot x + 0{,}0004 \cdot x^2 - 0{,}0812 \cdot y + 0{,}05 \cdot y^2$$

Fig. 8 - Effect of extrusion temperature and the degree of extrudate fineness into type factor of breadcrumbs particles obtained

CONCLUSIONS

Extrudates obtained in the twin-screw extruder at different temperatures of the process have distinguished by a variable internal structure, which may have an impact on obtaining extrudate fraction with different percentage of the particles and the shape of the extrudate particles after their fragmentation.

Analyzed shape ratios are clearly different depending on the obtained sieved extrudate fractions. This may have a technological importance in the case of each fraction destination for selected food products. Such a relationship can be very useful in, for example, the design of breadcrumbs extrudates production lines intended for different products.

Further research requires the link between the chemical composition, sensory analysis with the shape and size of the particles of obtained breadcrumbs.

REFERENCES

[1]. Agbisit R., Alavi S., Cheng E., Herald T., Trater A., (2007) – *Relationships between microstructure and mechanical properties of cellular cornstarch extrudates*. Journal of Texture Studies, 38, pp.199-219;
[2]. Al-Rabadia G. J., Torleyb P. J., Williamsa B. A., Bryden W. L., Gidleya M. J., (2011) – *Effect of extrusion temperature and pre-extrusion particle size on starch digestion kinetics in barley and sorghum grain extrudates.* Animal Feed Science and Technology, 168, pp.267-279;
[3]. Al-Rabadia G. J., Torleyb P. J., Williamsa B. A., Bryden W. L., Gidleya M. J., (2012) – *Particle size heterogeneity in milled barley and sorghum grains: Effects on physico-chemical properties and starch digestibility*. Journal of Cereal Science, 56, pp.396-403;
[4]. Biller E. (2006) – *Dynamics of color changes during thermal processing of wheat bread, depending on the time of dough kneading.* Agriculture Engineering, 7(82), pp.43-50;
[5]. Biller E., Ekielski A., (2005) – *Modeling of wheat bread texture using the index of surface color changes dynamics during thermal processing.* Agriculture Engineering, 10(70), pp.23-31;
[6]. Bisharat G.I., Oikonomopoulou V.P., Panagiotou N.M., Krokida M. K., Maroulis Z. B., (2013) – *Effect of extrusion conditions on the structural properties of corn extrudates enriched with dehydrated vegetables.* Food Research International, 53, pp.1-14;
[7]. Chuang G. C.-C., Yeh A.-I., (2004) – *Effect of screw profile on residence time distribution and starch gelatinization of rice flour during single screw extrusion cooking.* Journal of Food Engineering, 63 (6), 21–31;
[8]. Crowley P., Grau H., Arendt E. K., (2000) – Influence of Additives and Mixing Time on Crumb Grain Characteristics of Wheat Bread. Cereal Chemistry, 77(3), pp.370-375;
[9]. Desrumaux A., Bouvier J. M., Burri J., (1998) – *Corn grits particle size and distribution effect on the characteristic of expanded extrudates.* Journal of Food Science Engineering Processing, 63 (5), pp.857-863;
[10]. Ding Q.B., Ainsworth P., Plunkett A., Tucker G., Marson H., (2006) – *The effect of extrusion conditions on the functional and physical properties of wheat-based expanded snacks.* Journal of Food Engineering, 73 (2), pp.142–148;
[11]. Ekielski A., (2011) – *Effect of selected parameters of double-screw extruder operation on fractal dimensions of the extrudate.* Annals of Warsaw University of Life Sciences-SGGW, 57, pp.41-47;

WNIOSKI

Ekstrudaty uzyskane na ekstruderze dwuślimakowym w różnych temperaturach procesu wyróżniała zmienna struktura wewnętrzna, co mogło mieć wpływ na uzyskanie frakcji ekstrudatu o różnym procentowym udziale oraz kształcie cząstek ekstrudatu po ich rozdrobnieniu.

Analizowane współczynniki kształtu wyraźnie różnią się w zależności od uzyskanej przesiewanej frakcji ekstrudatu. Może mieć to znaczenie technologiczne w przypadku przeznaczenia poszczególnych frakcji dla wybranych produktów żywnościowych. Taka zależność może być bardzo przydatna w przypadku np. projektowania linii technologicznych produkcji panieru ekstrudowanego z przeznaczeniem dla różnych produktów.

Dalszych badań wymaga również powiązanie składu chemicznego, analizy sensorycznej z kształtem i wielkością cząstek otrzymanego panieru.

LITERATURA

[1]. Agbisit R., Alavi S., Cheng E., Herald T., Trater A., (2007) – *Związki między mikrostrukturą i właściwościami mechanicznymi ekstrudatów z komórkowej skrobi kukurydzianej.* Journal of Texture Studies, 38, 199-219;
[2]. Al-Rabadia G. J., Torleyb P. J., Williamsa B. A., Bryden W. L., Gidleya M. J., (2011) – *Wpływ temperatury procesu ekstruzji i wielkością cząstek materiału przed ekstruzją na kinetykę rozkładu skrobi w ekstrudacie z jęczmienia i sorgo.* Animal Feed Science and Technology, 168, 267-279;
[3]. Al-Rabadia G. J., Torleyb P. J., Williamsa B. A., Bryden W. L., Gidleya M. J., (2012) – *Zróżnicowanie wielkości cząstek zmielonego jęczmienia i ziarna sorgo: Wpływ na właściwości fizyko-chemiczne i strawność skrobi.* Journal of Cereal Science, 56, 396-403;
[4]. Biller E., (2006) – *Dynamika zmian barwy podczas obróbki termicznej pieczywa pszennego w zależnosci od czasu miesienia ciasta.* Inżynieria Rolnicza, 7(82), 43-50;
[5]. Biller E., Ekielski A., (2005) – *Modelowanie cech teksturalnych pieczywa pszennego z wykorzystaniem wskaźnika dynamiki zmian barwy powierzchni w czasie obróbki termicznej.* Inżynieria Rolnicza, 10(70), 23-31;
[6]. Bisharat G.I., Oikonomopoulou V.P., Panagiotou N.M., Krokida M. K., Maroulis Z. B., (2013) – *Wpływ warunków wytłaczania na właściwości strukturalne ekstrudatów z kukurydzy wzbogaconych suszonymi warzywami.* Food Research International, 53, 1-14;
[7]. Chuang G. C.C., Yeh A.I., (2004) – *Wpływ profilu ślimaka ekstrudera na rozkład czasu przebywania i żelowania skrobi z mąki ryżowej podczas ekstruzji w ekstruderze jednoślikakowym.* Journal of Food Engineering, 63 (6), 21–31;
[8]. Crowley P., Grau H., Arendt E. K., (2000) – *Wpływ dodatków i czasu mieszania na charakterystykę miękiszu chleba pszennego.* Cereal Chemistry, 77(3), 370-375;
[9]. Desrumaux A., Bouvier J. M., Burri J., (1998) – *Wpływ wielkości cząstek kaszy kukurydzianej i ich dystrybucji na cechy fizyczne ekspandowanych ekstrudatów.* Journal of Food Science Engineering Processing, 63 (5), 857-863;
[10]. Ding Q.B., Ainsworth P., Plunkett A., Tucker G., Marson H., (2006) – *Wpływ warunków procesu ekstruzji na funkcjonalne i fizyczne właściwości ekspandowanych przekąsek pszenicznych.* Journal of Food Engineering, 73(2), 142–148;
[11]. Ekielski A., (2011) – *Wpływ wybranych parametrów pracy dwuślimakowego ekstrudera na fraktalne wymiary ekstrudatu.* Annals of Warsaw University of Life Sciences-SGGW, 57, 41-47;

[12]. Ekielski A., Majewski Z., Żelaziński T., (2007) – *Effect of extrusion conditions on physical properties of buckwheat –maize blend extrudate*. Polish Journal of Food and Nutrition Sciences, 57, 2(A), pp.57-61;
[13]. Emir Aysˌe O˝ zer • Sˌenol I˙ banogˇlu • Paul Ainsworth, Cahide Yagˇmur., (2004) – *Expansion characteristics of a nutritious extruded snack food using response surface methodology.* European Food Research and Technology, 218, 5, pp.474-479;
[14]. Girish M., Ganjyal G. M., Milford A., Hanna M. A., (2004) – *Effect of extruder die nozzle dimension on expansion and micrographic characterization during extrusion of acetylated starch*. Starch, 56, pp.108-117;
[15]. Girish M., Ganjyal G. M., Milford A., Hanna M. A., (2006) – *Digital image processing for measurement of residence time distribution in a laboratory extruder*. Journal of Food Engineering, 75 (2), pp.237–244;
[16]. Gosselin R., Rodrigue D., (2005) – *Cell morphology analysis of density polymer foams.* Polymer Testing, 24, pp.1027-1035;
[17]. Hayter A. L., Smith A. C., Richmond P., (1986) – *The physical properties of extruded food foams,* Journal of Materials Science, 21 (10), pp.3729-3736;
[18]. Lanuay B., Lisch J. M., (1983) – *Twin-screw extrusion cooking of starch pastes, expansion and mechanical properties of extrudates.* Journal of Food Engineering, 9 (2), pp.259–280;
[19]. Lui W.-B., Peng J., (2005) – *Effects of operating conditions on degradable cushioning extrudate's cellular structure and the specific heat.* Journal of Food Engineering, 70 (2), pp.171–182;
[20]. Mezreb K., Goullieu A., Ralainirina R., Queneudec M., (2003) - *Application of image analysis to measure screw speed influence on physical properties of corn and wheat extrudates.* Journal of Food Engineering, 57, pp.145-152;
[21]. Mościcki L., Mitrus M., Wójtowicz A., (2007) - *Extrusion technique in food industry.* PWRiL, Warszawa;
[22]. PN-ISO 6564:1999 – *Sensory analysis - Methodology - Methods of flavor profiling*;
[23]. Robin F., Engmann J., Pineau N., Chanvrier H., Bovet N., Della Valle G., (2010) – *Extrusion, structure and mechanical properties of complex starchy foams*. Journal of Food Engineering, (98), pp.19-27;
[24]. Singh N., Smith A.C. (1997) – *A Comparison of wheat starch. Whole wheat meal and oat flour in the extrusion cooking process.* Journal of Food Engineering, 34, pp.15-32;
[25]. Włodarczyk-Stasiak M., Jamroz J., (2009) – *Specific surface area and porosity of starch extrudates determined from nitrogen adsorption data.* Journal of Food Engineering, 93, pp.379-385;
[26]. Wójtowicz A., Moscicki L., Mitrus M., Oniszczuk T., (2010) – *Effect of plasticizing system configuration on selected properties of extruded whole-grain pasta.* Agriculture Engineering, 4(122), pp.291-297;
[27]. Żelaziński T. (2010) – *Research of extrusion process involving mixtures of buckwheat and corn.* Zeszyty Problemowe Postępów Nauk Rolniczych, 546, pp.375-381;
[28]. Żelazinski T. (2011) – *Investigaton on porosity of extrudates at various buckwheat content in the mixture.* Annals of Warsaw University of Life Sciences-SGGW, 57, 49-55;
[29]. Żelazinski T., Ekielski A., (2012) – *Sensory analysis of corn-buckwheat extrudates.* Postępy Techniki Przetwórstwa Spożywczego, 1, pp.50-54.

[12]. Ekielski A., Majewski Z., Żelaziński T., (2007) – *Wpływ warunkw procesu ekstruzji na właściwości fizyczne ekstrudatu z mieszanki gryka-kukurydza.* Polish Journal of Food and Nutrition Sciences, 57, 2(A), 57-61;
[13]. Emir Aysˌe O˝ zer • Sˌenol I˙ banogˇlu • Paul Ainsworth, Cahide Yagˇmur., (2004) – *Charakterystyka ekspansji odżywczych ekstrudowanych przekąsek z użyciem metody powierzchni odpowiedzi.* European Food Research and Technology, 218, 5, 474-479;
[14]. Girish M., Ganjyal G. M., Milford A., Hanna M. A. (2004) – *Wpływ wymiaru dyszy wylotowej wytłaczarki na ekspansję i mikrograficzną charakterystykę podczas ekstruzji skrobi acetylowanej.* Starch, 56, 108-117;
[15]. Girish M., Ganjyal G. M., Milford A., Hanna M. A., (2006) – *Cyfrowe przetwarzanie obrazu do pomiarów rozkładu czasu przebywania w laboratoryjnym ekstruderze.* Journal of Food Engineering, 75 (2), 237–244;
[16]. Gosselin R., Rodrigue D., (2005) – *Analiza morfologiczna komórek gęstych pianek polimerowych*. Polymer Testing, 24, 1027-1035;
[17]. Hayter A. L., Smith A. C., Richmond P. (1986) – *Właściwości fizyczne ekstrudowanych pianek spożywczych,* Journal of Materials Science, 21 (10), 3729-3736;
[18]. Lanuay B., Lisch J. M., (1983) – *Dwuślimakowa ekstruzja past skrobiowych, ekspansja i właściwości mechaniczne ekstrudatu.* Journal of Food Engineering, 9 (2), 259–280;
[19]. Lui W.-B., Peng J., (2005) – *Wpływ warunków pracy na degradowalną gąbczastą strukturę komórkową ekstrudatów i ciepło właściwe.* Journal of Food Engineering, 70 (2), 171–182;
[20]. Mezreb K., Goullieu A., Ralainirina R., Queneudec M., (2003) - *Zastosowanie analizy obrazu do pomiaru wpływu prędkości ślimaka na właściwości fizyczne kukurydzianych i pszenicznych ekstrudatów.* Journal of Food Engineering, 57, 145-152;
[21]. Mościcki L., Mitrus M., Wójtowicz A., (2007) - *Technika ekstruzji w przemyśle rolno-spożywczym.* PWRiL, Warszawa;
[22]. PN-ISO 6564:1999; *Analiza sensoryczna – Metodologia – Metody profilowania smakowitości*;
[23]. Robin F., Engmann J., Pineau N., Chanvrier H., Bovet N., Della Valle G., (2010) – *Ekstruzja, struktura i właściwości mechaniczne złożonych skrobiowych pianek.* Journal of Food Engineering, (98), 19-27;
[24]. Singh N., Smith A.C., (1997) – *Porównanie skrobi pszennej. Mąka pełnoziarnista i mąka owsiana w procesie ekstruzji.* Journal of Food Engineering, 34, 15-32;
[25]. Włodarczyk-Stasiak M., Jamroz J., (2009) – *Powierzchnia właściwa i porowatość ekstrudatów skrobiowych wyznaczona na podstawie adsorpcji azotu.* Journal of Food Engineering, 93, 379-385;
[26]. Wójtowicz A., Moscicki L., Mitrus M., Oniszczuk T., (2010) – *Wpływ konfiguracji układu plastyfikujacego na wybrane cechy ekstrudowanych makaronów pełnoziarnistych.* Inżynieria Rolnicza, 4(122), 291-297;
[27]. Żelaziński T., (2010) – *Badania procesu ekstruzji mieszanek z udziałem gryki i kukurydzy.* Zeszyty Problemowe Postępów Nauk Rolniczych, 546, 375-381;
[28]. Żelazinski T., (2011) – *Badanie porowatości ekstrudatów w zależności od zawartości gryki w mieszance.* Annals of Warsaw University of Life Sciences-SGGW, 57, 49-55;
[29]. Żelazinski T., Ekielski A., (2012) – *Badania sensoryczne ekstrudatów kukurydziano-gryczanych.* Postępy Techniki Przetwórstwa Spożywczego, 1, 50-54.

ALGORITHM FOR DETERMINATION OF CHARACTERISTIC PARAMETERS OF FILTERING PROCESS IN GRANULAR MATERIAL INCOMPRESSIBLE LAYER
/
ALGORITM PENTRU DETERMINAREA INDICILOR CARACTERISTICI AI PROCESULUI DE FILTRARE PRIN STRAT INCOMPRESIBIL DE MATERIAL GRANULAR

Lect. Ph.D. Eng.Safta Victor Viorel, As. Ph.D Student Eng. Dilea Mirela, As. Ph.D Student Eng.Constantin Gabriel Alexandru
POLITEHNICA University of Bucharest, Faculty of Biotechnical Systems Engineering
Tel: 0724017310; E-mail: saftavictorviorel@yahoo.com

Abstract: *This paper presents the algorithm used to perform computations related to processing of results obtained in laboratory experiments for determining the characteristic parameters of filtering process in incompressible layer of granular material in a quick and convenient way.*

Keywords: *filtering process, material layer, specific resistances, algorithm, program.*

INTRODUCTION

Filtration is the separation process of a heterogeneous liquid-solid system in constituent phases with the aid of a porous filter medium [1, 2].

The driving force which imposes the filtering process is usually the difference between the pressures on free surfaces of heterogeneous systems and filter medium.

Under the action of driving force the fluid from heterogeneous systems passes through the filter medium pores separating as filtered product while the solid particles in suspension in heterogeneous environment are retained by the filter medium especially on its surface, but also in its pores.

Thus, as the filtering process takes place, on the filter medium surface forms a wet solid particles cake which will act as an additional filter medium, its percentage in the filtering process being greater as the thickness increases .

Because of the large number of factors that interfere with filtration process, it is very difficult to develop a mathematical model to simulate the process framework. Therefore, models of filtering process for specific cases were developed.

For analysis of more complex cases we started from the basic models which have been developed and completed by results of experimental determinations [2].

MATERIALS AND METHODS

For filtering process, a base case from which it usually starts is filtering through incompressible porous media with incompressible solid particles cake formation, media that exhibit a constant resistance to filtrate passing through them.

In almost all cases the filtrate flow through this media is laminar. Thus, was obtained an equation (Darcy's filter equation) experimentally confirmed, where filtration rate, w_f, is directly proportional to the pressure difference acting as a driving force and inversely proportional to fluid viscosity and the resistances which oppose the filter medium and the solid particles cake at flow of filtrate [2],[4]:

Rezumat: *Această lucrare prezintă algoritmul pentru calculele aferente prelucrării rezultatelor obţinute în urma experimentelor de laborator pentru determinarea indicilor caracteristici ai procesului de filtrare prin strat incompresibil de material granular.*

Cuvinte cheie: *proces de filtrare, material granular, rezistenţe specifice, algoritm, program.*

INTRODUCERE

Filtrarea este procesul de separare a unui sistem eterogen lichid – solid în fazele constituente cu ajutorul unui mediu de filtrare poros [1, 2].

Forţa motrice care impune procesul de filtrare este de obicei diferenţa dintre presiunile exercitate pe suprafeţele libere ale sistemului eterogen şi ale mediului de filtrare. Sub acţiunea forţei motrice lichidul din sistemul eterogen trece prin porii mediului de filtrare separându-se sub formă de filtrat în timp ce particulele solide aflate în suspensie în mediul eterogen sunt reţinute de mediul filtrant, pe suprafaţa sa în special, dar şi în porii săi într-o oarecare măsură. Astfel, pe măsură ce procesul de filtrare are loc, pe suprafaţa mediului filtrant se formează un strat de precipitat umed care la rândul său va acţiona ca un mediu de filtrare suplimentar, ponderea sa în procesul de filtrare fiind din ce în ce mai mare, pe măsură ce grosimea sa creşte.

Datorită numărului foarte mare de factori ce intervin în procesul de filtrare este foarte greu de elaborat un model matematic care să simuleze procesul în cadru general. De aceea, s-au elaborat modele ale procesului de filtrare pentru cazuri particulare elementare. Pentru analiza cazurilor mai complexe s-a plecat de la modelele elementare care au fost dezvoltate şi completate cu rezultatele unor determinări experimentale [2].

MATERIALE ŞI METODE

Pentru procesul de filtrare, un caz de bază de la care se pleacă de regulă îl constituie filtrarea prin medii poroase incompresibile cu formare de precipitat de asemenea incompresibil, medii care opun o rezistenţă constantă la trecerea filtratului prin ele. Aproape în toate cazurile curgerea filtratului prin aceste medii este laminară. Pe baza acestui fapt s-a ajuns la o relaţie (relaţia lui Darcy) confirmată şi experimental, potrivit căreia viteza w_f de filtrare este direct proporţională cu diferenţa de presiune care acţionează ca forţă motrice şi invers proporţională cu vâscozitatea lichidului şi rezistenţele pe care le opun mediul de filtrare şi stratul de precipitat la curgerea filtratului [1], [4]:

$$w_f = \frac{\dot{V}}{A} = \frac{\Delta p}{(R_p + R_m)\cdot \eta} \quad (1)$$

where: $\dot{V} = dV/dt$ [m^3/s] – derived of filtrate volume separated in relation with time, namely the filtrate flow rate separated;
A [m^2] – filter area;

în care: $\dot{V} = dV/dt$ [m^3/s] – derivata volumului de filtrat separat în funcţie de timp, adică debitul volumic de filtrat separat;
A [m^2] – suprafaţa mediului de filtrare;

Δp [Pa] – differential pressure across the free surfaces of heterogeneous system and the filter medium;
R_p [m^{-1}] – the resistance of solid particles cake deposited on the filter surface to the passing filtrate;
R_m [m^{-1}] – the filter medium resistance opposed to filtrate passing;

Taking into account the resistance of the solid particles cake deposited on the filter surface , the filtrate passing can be expressed by the following expressions:

Δp [Pa] - presiunea diferenţială care se exercită pe suprafeţele libere ale sistemului eterogen şi mediului de filtrare;
R_p [m^{-1}] – rezistenţa stratului de precipitat depus pe suprafaţa de filtrare opusă la trecerea filtratului;
R_m [m^{-1}] – rezistenţa mediului de filtrare opusă la trecerea filtratului;

Ţinând seama că rezistenţa opusă de stratul de precipitat depus pe suprafaţa de filtrare la trecerea filtratului mai poate fi exprimată cu următoarele expresii [3]:

$$R_p = \alpha \cdot h = \alpha \cdot \frac{c_p}{\rho_p} \cdot \frac{V}{A} = \alpha \cdot y \cdot \frac{V}{A} \quad (2)$$

where: α [m^{-2}] – specific solid particles cake resistance deposited on the filter surface;
h [m] – filter cake thickness deposited on the filter surface;
c_p [kg/m^3] – mass concentration of suspension from heterogeneous system;
ρ_p [kg/m^3] – solid particles cake density deposited on the filter surface;
V [m^3] – filtrate volume;
A [m^2] – filter area;
y – solid content of the suspension.

and that the resistance R_m, opposed by the filter medium is usually noted with β [m^{-1}], resulting the following expression known as the fundamental differential equation of filtration through incompressible filter medium, with solid particles cake incompressible formation:

în care: α [m^{-2}] – rezistenţa specifică a stratului de precipitat depus pe suprafaţa de filtrare;
h [m] – grosimea stratului de precipitat depus pe suprafaţa de filtrare;
c_p [kg/m^3] – concentraţia masică a suspensiilor din sistemul eterogen supus filtrării;
ρ_p [kg/m^3] – densitatea stratului de precipitat depus pe suprafaţa de filtrare;
V [m^3] – volumul de filtrat separat;
A [m^2] – suprafaţa mediului de filtrare;
y – fracţia volumică a fazei solide din suspensie

şi de faptul că rezistenţa R_m, opusă de mediul de filtrare la trecerea filtratului, se notează de regulă cu β [m^{-1}], rezultă următoarea expresie cunoscută şi ca ecuaţia diferenţială fundamentală a filtrării prin mediu de filtrare incompresibil, cu formare de strat de precipitat incompresibil:

$$\frac{dV}{A \cdot dt} = \frac{\Delta p}{\left(\alpha \cdot y \cdot \frac{V}{A} + \beta\right) \cdot \eta} \quad (3)$$

Analysis of the filtration process through incompressible filter media with incompressible solid particles cake formation is done for two particular cases commonly found in liquid suspension filtration practice, namely: if the filtering process takes place under a constant pressure difference (Δp = ct) and if the filtering process takes place with constant filtration rate (w_f = ct), namely, the flow rate separation of the filtrate is constant ($\dot{V}$ = ct).

If the filtering process takes place with constant filtration rate, respectively constant filtered flow (w_f = ct, respectively $\dot{V}$ = ct) the pressure difference under which the process takes place should increase throughout its duration. In this case the relation 3 can be linearized as:

Analiza procesului de filtrare prin mediu de filtrare incompresibil, cu formare de strat de precipitat incompresibil se face pentru două cazuri particulare elementare, frecvent întâlnite în practica filtrării suspensiilor lichide şi anume: cazul în care procesul de filtrare are loc sub o diferenţă constantă de presiune (Δp = ct) şi cazul în care procesul de filtrare are loc cu viteză de filtrare constantă (w_f = ct), adică debitul de separare al filtratului este constant ($\dot{V}$ = ct).

În cazul în care procesul de filtrare are loc cu viteză de filtrare constantă, respectiv cu debit de filtrat separat constant (w_f = ct, respectiv $\dot{V}$ = ct) diferenţa de presiune sub care se desfăşoară procesul va trebui să crească pe toată durata sa. În acest caz relaţia 3 poate fi liniarizată sub forma:

$$\Delta p = \frac{\eta \cdot y \cdot \dot{V} \cdot \alpha}{A^2} \cdot V + \frac{\eta \cdot \dot{V} \cdot \beta}{A} \quad (4)$$

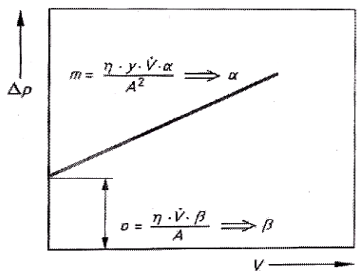

Fig. 1 – Filtration at constant filtrate flow rate

If the function Δp = f(V) is plotted, it will result a straight line (Figure 1) characterized by the slope and ordinate interval at the origin. Determining the values of the slope and ordinate interval of the line drawn on

Dacă se reprezintă grafic funcţia Δp = f(V) rezultă o dreaptă (Figura 1) [5] caracterizată de panta sa şi de ordonata la origine. Determinându-se valorile pantei şi ordonatei la origine ale dreptei construite pe baze experimentale, se pot determina valorile rezistenţelor α şi

experimental basis, we can determine α and β resistance values opposed by precipitate layer formed on the surface during filtration process, respectively filtrate medium, which are constant values and are the main indices of the filtration process under constant filtration rate, respectively constant filtered flow to a certain suspension and a filter medium.

If the filtering process takes place under a constant pressure difference (Δp = ct), filtration rate wf (filtrate volume) decreases as the process takes place.

In this case the relation 3 can be linearized as:

β pe care le opun stratul de precipitat format pe suprafaţa de filtrare în timpul procesului, respectiv mediul filtrant la trecerea filtratului, care sunt valori constante şi se constituie în indicii principali ai procesului de filtrare la viteză de filtrare, respectiv debit de separare a filtratului constante pentru o anumită suspensie şi un anumit mediu de filtrare.

În cazul în care procesul de filtrare are loc sub o diferenţă constantă de presiune (Δp = ct), viteza de filtrare w_f (adică debitul $\dot{V}$ de filtrat separat) scade pe măsură ce procesul se desfăşoară. În acest caz relaţia 3 poate fi liniarizată sub forma:

$$\frac{1}{\dot{V}} = \frac{\eta \cdot \alpha \cdot y}{2 \cdot A^2 \cdot \Delta p} \cdot V + \frac{\eta \cdot \beta}{A \cdot \Delta p} \quad (5)$$

Algorithm and calculation program

For processing the experimental data obtained in laboratory experiments, we used an algorithm whose structural scheme is shown in Figure 2.

Algoritmul şi programul de calcul

Pentru procesarea datelor experimentale obţinute în experimentul de laborator, s-a utilizat un algoritm de calcul a cărui schemă structurală este prezentată în Figura 2.

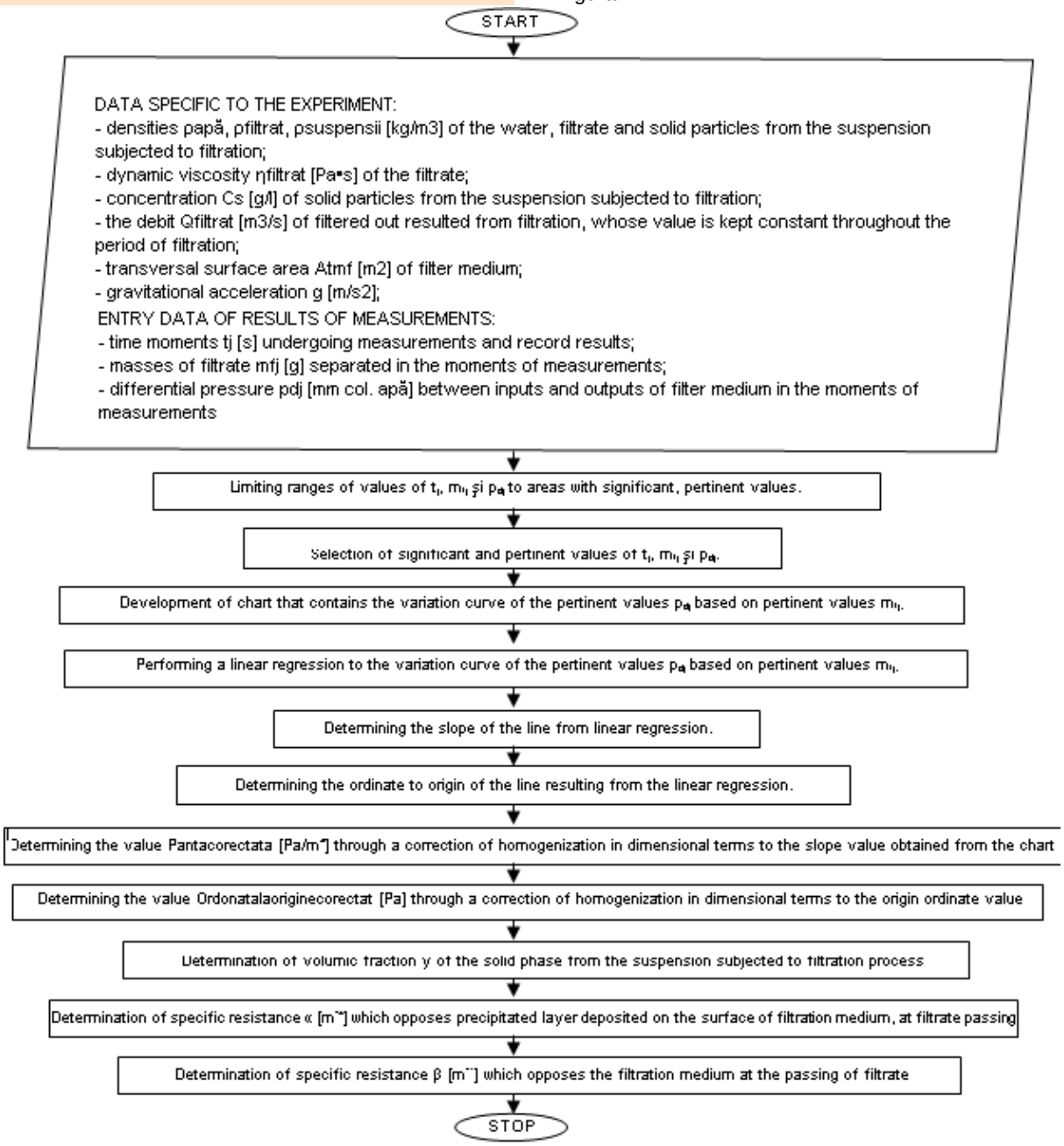

Fig.2 - Structural scheme of the algorithm for determination of characteristic indices of the filtration process

RESULTS

Based on previously presented algorithm, was developed a calculation program in MathCad programming software which is shown in Figure 3.

REZULTATE

Pe baza algoritmului prezentat anterior a fost conceput un program de calcul în mediul de programare MathCad care este prezentat în figura 3.

CALCULUS PROGRAM OF THE FILTRATION PROCESS PARAMETERS OF A AQUEOUS SUSPENSION THROUGH AN INCOMPRESSIBLE MEDIUM WITHINCOMPRESSIBLE SOLID PARTICLES CAKE FORMATION
PROGRAM DE CALCUL AL PARAMETRILOR PROCESULUI DE FILTRARE A UNEI SUSPENSII APOASE PRIN MEDIU INCOMPRESIBIL CU FORMARE DE STRAT DE PRECIPITAT INCOMPRESIBIL

The density ρapa [kg/mc] of the water at the environmental temperature during the experiment.
Densitatea ρapa [kg/mc] apei la temperatura mediului ambiant din timpul experimentului.

$\rho apa := 998$

The density ρfiltrat [kg/mc] of the filtrate resulted from the aqueous suspension filtration at the environmental temperature.
Densitatea ρfiltrat [kg/mc] filtratului rezultat din filtrarea emulsiei apoase la temperatura mediului ambiant.

$\rho filtrat := 998$

The density ρparticule [kg/mc] of the aqueous suspension solid particles (calcium acid carbonate).
Densitatea ρparticule [kg/mc] particulelor solide din suspensia apoasă (carbonat acid de calciu).

$\rho particule := 2710$

The dynamic viscosity ηfiltrat [Pa.s] of the filtrate at the environmental temperature during the experiment.
Vascozitatea ηfiltrat [Pa.s] dinamică a filtratului la temperatura mediului ambiant din timpul experimentului.

$\eta filtrat := 1.002 \cdot 10^{-3}$

The concentration Cs [g/l] of solid particles from the aqueous suspension subjected to the filtration process.
Concentratia Cs [g/l] de particule solide din suspensia apoasă supusă procesului de filtrare.

$Cs := 59$

The volumetric flow Qfiltrat [mc/s] of filtrate, kept constant during the experiment.
Debitul volumic Qfiltrat [mc/s] de filtrat, păstrat constant în timpul experimentului.

$Qfiltrat := 1.67 \cdot 10^{-6}$

The area Atmf [mp] of the transversal surface of the filtration medium.
Aria Atmf [mp] suprafetei transversale a mediului de filtrare

$Atmf := 1.11 \cdot 10^{-3}$

The gravity aceeleration g [m/sp].
Acceleratia g [m/sp] gravitationala.

$g := 9.81$

The elaboration of the input data matrix DI concerning the measurments, with 3 rows and 25 columns, whereat:
- on the row 0, there are written the moments (of time) tj [h] when the measurments are effectuated and registered their results, noted as DI 0,j;
- on the row 1, there are written the filtrate mass mfj [g] separated in the measurment moments, noted as DI 1,j;
- on the row 2, there are written the differential pressures pdj [mm water col.,] between the entrance and the exit of the filtration medium, in the measurment moments noted as DI 2,.

Se întocmeste matricea DI a datelor de intrare privitoare la măsurări, cu 3 linii si 25 coloane, la care:
- pe linia 0 sunt trecute momentele de timp tj [s] la care se efectuează măsurările si se înregistrează rezultatele acestora, notate cu DI 0,j;
- pe linia 1 sunt trecute valorile masei mfj [g] filtratului separat în momentele măsurărilor, notate cu DI 1,j;
- pe linia 2 sunt trecute valorile presiunii pdj [mm col. apă] diferentiale dintre intrarea si iesirea mediului de filtrare, în momentelemăsurărilor, notate cu DI 2,j;

$$DI := \begin{pmatrix} 30 & 60 & 90 & 120 & 150 & 180 & 210 & 240 & 270 & 300 & 330 & 360 & 390 & 420 & 450 & 480 & 510 & 540 & 570 & 600 & 630 & 660 & 690 & 720 & 750 \\ 39 & 82 & 125 & 165 & 208 & 250 & 294 & 337 & 380 & 420 & 470 & 512 & 560 & 606 & 650 & 691 & 738 & 775 & 825 & 870 & 916 & 960 & 1005 & 1048 & 1089 \\ 140 & 155 & 160 & 168 & 179 & 185 & 191 & 191 & 197 & 199 & 209 & 220 & 217 & 215 & 225 & 222 & 232 & 236 & 243 & 250 & 245 & 275 & 300 & 307 & 300 \end{pmatrix}$$

wherein, with j is noted the number of measurments effectuated durring the experiment, which corresponds to the number of columns of the matrix DI.
în care cu j se notează numărul de măsurări care se efectuează în timpul experimentului, care corespunde numărului de coloane ale matricei DI;

The limitation of the range of the moments of time tj to the zone with significant values (when can be measured relevant values of the filtrate mass mfj and differential pressure pdj).
Se limitează intervalul de momente de timp tj la zona de momente semnificative (când se pot măsura si înregistra valori pertinente ale masei de filtrat mfj si presiunii diferentiale pdj).

$j := 0..24$

The elaboration of the vector t of moments of time, significant regarding the measurments and of the vectors mf and pd of relevant values of the separated filtrate mass, and respectively, of the differential pressure between the entrance and the exit of the filtration medium .
Se întocmesc vectorul t de momente de timp semnificative din punct de vedere al măsurărilor si vectorii mf si pd de valori pertinente ale masei de filtrat separate, respectiv ale presiunii diferentiale dintre intrarea si iesirea mediului de filtrare;

$t_j := DI_{0,j}$

$mf_j := DI_{1,j}$

$pd_j := DI_{2,j}$

$$t = \begin{pmatrix} 30 \\ 60 \\ 90 \\ 120 \\ 150 \\ 180 \\ 210 \\ 240 \\ 270 \\ 300 \\ 330 \\ 360 \\ 390 \\ 420 \\ 450 \\ 480 \\ 510 \\ 540 \\ 570 \\ 600 \\ 630 \\ 660 \\ 690 \\ 720 \\ 750 \end{pmatrix} \quad mf = \begin{pmatrix} 39 \\ 82 \\ 125 \\ 165 \\ 208 \\ 250 \\ 294 \\ 337 \\ 380 \\ 420 \\ 470 \\ 512 \\ 560 \\ 606 \\ 650 \\ 691 \\ 738 \\ 775 \\ 825 \\ 870 \\ 916 \\ 960 \\ 1.005 \times 10^{3} \\ 1.048 \times 10^{3} \\ 1.089 \times 10^{3} \end{pmatrix} \quad pd = \begin{pmatrix} 140 \\ 155 \\ 160 \\ 168 \\ 179 \\ 185 \\ 191 \\ 191 \\ 197 \\ 199 \\ 209 \\ 220 \\ 217 \\ 215 \\ 225 \\ 222 \\ 232 \\ 236 \\ 243 \\ 250 \\ 245 \\ 275 \\ 300 \\ 307 \\ 300 \end{pmatrix}$$

The graphical representation of the variation curve of pdj values depending on the correspondant mfj values.
Se reprezintă grafic curba de variatie a valorilor pdj în functie de valorile mfj corespunzătoare.

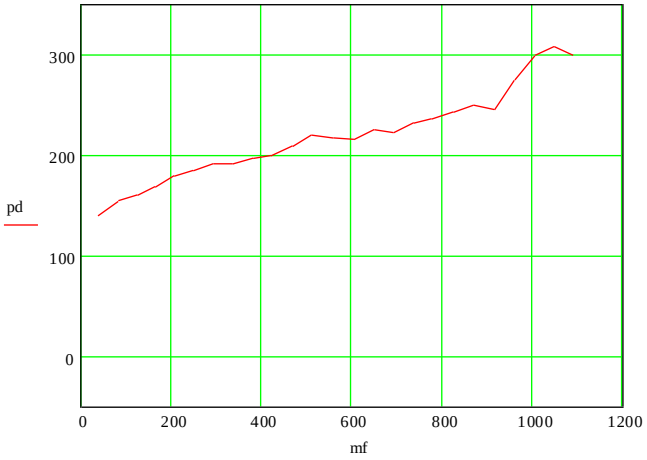

The application of o linear regression to the variation curve pdj values depending on the mfj values, in order to determinate the slope Panta [mm col.apă/g](noted as m in the explicative graph) and the ordinate interval Ordonatalaorigine [mm col.apă](noted as o in the explicative graph)of the regresion line.
Se efectuează o regresie liniară a curbei de variatie a valorilor pdj în functie de mfj, în scopul determinării pantei Panta [mm col.apă/g] (notată cu m în graficul explicativ) si ordonatei la origine Ordonatalaorigine [mm col.apă](notată cu o în graficul explicativ) ale dreptei de regresie

$Panta := slope(mf, pd)$ $Panta = 0.135$

$Ordonatalaorigine := intercept(mf, pd)$ $Ordonatalaorigine = 142.948$

The correlation index square R of the linear regression has the following value:
Indicele de corelatie R pătrat al regresiei liniare are următoarea valoare:

$Rpatrat := corr(mf, pd)^2$ $Rpatrat = 0.944$

The effectuation of a dimensional homogenizating correction of the regresion line slope, noted as Pantacorectata [Pa/mc].
Se efectuează o corectie de omogenizare din punct de vedere dimensional a pantei dreptei de regresie, notată cu Pantacorectata [Pa/mc].

$Pantacorectata := Panta \cdot g \cdot \rho apa \cdot \rho filtrat$ $Pantacorectata = 1.316 \times 10^{6}$

The effectuation of a dimensional homogenizating correction of the regresion line ordinate interval, noted as Ordonatalaoriginecorectata [Pa].
Se efectuează o corectie de omogenizare din punct de vedere dimensional a ordonatei la origine a dreptei de regresie, notată cu Ordonatalaoriginecorectata [Pa].

$Ordonatalaoriginecorectata := 10^{-3} Ordonatalaorigine \cdot g \cdot \rho apa$ $Ordonatalaoriginecorectata = 1.4 \times 10^{3}$

The determination of the volumic fraction y of the solid phase of the the aqueous suspension submitted to the filtration process, in order to calculate the specific resistance α.
Se determină fractia volumică y a fazei solide din suspensia apoasă supusă procesului de filtrare, în scopul calculării rezistentei specifice α.

$$y := \frac{Cs}{\rho particule} \qquad y = 0.022$$

The determination of the specific resistance α [1/mp] opposed by the cake formed on the surface of the filtration medium at the filtrate passage.
Se determină rezistenta specifică α [1/mp] pe care o opune stratul de precipitat depus pe suprafata mediului de filtrare la trecerea filtratului

$$\alpha := \frac{Pantacorectata \cdot Atmf^{2}}{\eta filtrat \cdot y \cdot Qfiltrat} \qquad \alpha = 4.45 \times 10^{10}$$

The determination of the specific resistance β [1/m] opposed by the filtration medium at the filtrate passage.
Se determină rezistenta specifică β [1/m] pe care o opune mediul de filtrare la trecerea filtratului

$$\beta := \frac{Ordonatalaoriginecorectata \cdot Atmf}{\eta filtrat \cdot Qfiltrat} \qquad \beta = 9.284 \times 10^{8}$$

Fig. 3 – Program for calculating characteristic indices of the filtration process

CONCLUSIONS

The algorithm was developed in order to quickly perform the computations related to processing of results obtained in laboratory experiments for determining the characteristic parameters of filtering process in granular material incompressible layer .

CONCLUZII

Algoritmul a fost realizat în scopul efectuarii rapide şi comode a calculelor aferente prelucrării rezultatelor obţinute în urma experimentelor de laborator pentru determinarea indicilor caracteristici ai procesului de filtrare prin strat incompresibil de material granular.

The algorithm allows obtaining the values of characteristic parameters of filtering process, α (the specific resistivity of the layer deposited on the filter surface opposite to the passage of filtrate), respectively β (the resistivity of filter media opposite the filtrate passing) in a very short time. This wouldn't have been possible if the calculations required were carried out graphically – analytically with hand tools (calculator, graph paper).

It is to be noted that this algorithm is original, designed by the authors in the Department of Biotechnical Systems, in order to improve educational technology used in the laboratory sessions.

Acknowlegement

The work has been funded by the Sectoral Operational Programme of Human Resources Development 2007-2013 of the Romanian Ministry of Labour, Family and Social Protection through the Financial Agreement POSDRU/107/1.5/S/76903.

REFERENCES

[1]. Gösele W., Alt C., (2000) – *Filtration*, Ullmann's Encyclopedia of Industrial Chemistry;
[2]. Safta V.V., Toma M.L., Ungureanu N., (2012) - *Experiments in water treatment domain* - PRINTECH Publishing;
[3]. Soare S., (1979) – *Hydrodynamic processes,* Didactic and Pedagogic Publishing House, Bucharest;
[4]. Rushton A., Ward A.S., Holdich R.G., (1996) – *Solid – liquid filtration and separation technology,* VCH Publishers, Inc., New York, NY (USA);
[5]. *** (2004) – *CE 116 Filtrability index unit –experiment instructions* – G.U.N.T Geratebau GmbH, Germany.

Algoritmul permite obţinerea indicilor caracteristici ai procesului de filtrare, α (rezistenţa specifică a stratului de precipitat depus pe suprafaţa de filtrare opusă la trecerea filtratului), respectiv β (rezistenţa mediului de filtrare opusă la trecerea filtratului) într-un interval de timp foarte scurt, ceea ce nu ar fi fost posibil dacă calculele necesare ar fi fost efectuate grafo – analitic cu mijloace manuale (calculator, hârtie milimetrică).

De menţionat faptul că acest algoritm de calcul este original, conceput de către autori în cadrul Departamentului Sisteme Biotehnice, în scopul perfecţionării tehnologiei didactice utilizate în orele de laborator.

Menţiune

Rezultatele prezentate în acest articol au fost obţinute şi cu sprijinul Ministerului Muncii, Familiei şi Protecţiei Sociale prin Programul Operational Sectorial Dezvoltarea Resurselor Umane 2007-2013, Contract nr. POSDRU/107/1.5/S/76903.

BIBLIOGRAFIE

[1]. Gösele W., Alt C., (2000) – *Filtrare*, Ullmann's Encyclopedia of Industrial Chemistry;
[2]. Safta V.V., Toma M.L., Ungureanu N., (2012) - *Experimente în domeniul tratării apelor* - Editura PRINTECH;
[3]. Soare S., (1979) – *Procese hidrodinamice,* Editura Didactică şi Pedagogică, Bucureşti;
[4]. Rushton A., Ward A.S., Holdich R.G., (1996) – *Filtrarea solid – lichid şi tehnologii de separare,* VCH Publishers, Inc., New York, NY (USA);
[5]. *** (2004) – *CE 116 Indice de unitate al filtrabilităţii – instrucţiuni experimentale* – G.U.N.T Geratebau GmbH, Germania.

TESTING IN SIMULATED AND ACCELERATED REGIME OF RESISTANCE STRUCTURES / *TESTAREA IN REGIM SIMULAT SI ACCELERAT A STRUCTURILOR DE REZISTENTA*

Eng. Matache M.[1)], Eng. Persu I.[1)], Prof. Ph.D. Eng. Voicu Gh.[2)], Ph.D.Eng. Manea I.[3)], Assoc. Prof. PhD. Eng. Biriş S.Şt.[2)]
[1)]INMA Bucharest / Romania; [2)]P.U. Bucharest / Romania; [3)]SC Softronic SRL Craiova / Romania
Tel: 0727-957693; E-mail: matache@inma.ro

Abstract: *In the paper there are presented experimental researches regarding testing in simulated and accelerated regime of bogie frame type resistance structures. Starting from the loads at which the structure is exposed in daily exploitation , there was developed a testing programme in simulated and accelerated regime in order to verify its structural integrity and estimate its span of.*

Keywords: *testing, simulated and accelerated regime, resistance structure.*

INTRODUCTION

Testing in accelerated regime is the testing process of a product by subjecting it to working conditions (stress, specific strain, temperatures etc.) exceeding the normal operating parameters for discovering the failures and ways of failure in a short period of time. The purpose of the accelerated testing is to provide information on the reliability of the equipment over an as short as possible period of time [1]. By analyzing the product response to such tests, the engineers can predict the active span of life and its maintenance intervals.

Testing in simulated and accelerated regime of the resistance structure of bogie frame type equipping the passenger wagons is imposed mainly by the product final destination. The bogie frame is a critical resistance structure of the component of passenger wagons that support the wagon bodywork and taking over the most of the stresses that occur in operation. Thus, this structure must be subjected to a validation program, consisting of the following stages:

- designing;
- structural analysis with finite element;
- simulated and accelerated regime testing in the laboratory;
- testing on the railway.

As shown, the testing stage follows after the stage of structural analysis. Within the stage of structural analysis it simulates on the computer the stresses that may arise in operation and which will generate some internal stress states within the structure of the bogie. Thus, it identifies the simulated loading configurations of the bogie frame and the points likely to be subjected to maximum stresses during service duration. Within the testing phase is verified the structural integrity of the bogie frame and its resistance to fatigue. Thus the testing stage is composed of two types of tests: tests carried out in static regime and test carried out in dynamic regime that follows on the first ones.

The tests carried out in static regime simulate the stress that occurs in service. The static tests are divided into tests in which the loadings are made with exceptional strains, loads that rarely occur during exploitation of the bogie frame and testings in which the loadings are done with service chargings, strains that occur routinely during its exploitation. The tests with exceptional loads have the role to check the condition

Rezumat: *In lucrare sunt prezentate cercetările experimentale privind testarea in regim simulat si accelerat a structurilor de rezistenta de tip rama de boghiu. Plecând de la sarcinile la care este supusa structura in exploatare zilnic, s-a dezvoltat un program de testare in regim simulat si accelerat cu scopul de a verifica integritatea structurala a acesteia si de a-i estima durata activa de viata.*

Cuvinte cheie: *testare, regim simulat si accelerat, structura de rezistenta.*

INTRODUCERE

Testarea in regim accelerat reprezinta procesul de testare a unui produs prin supunerea la conditii de lucru (tensiune, deformatie specifica, temperaturi etc) care depasesc parametrii normali de exploatare in scopul descoperirii defectelor si a modalitatilor de esuare intr-o perioada scurta de timp. Scopul incercarilor accelerate este acela de a furniza informatii privind fiabilitatea echipamentelor intr-o perioada cat mai scurta de timp [1]. Prin analizarea raspunsului produsului la asemenea teste, inginerii pot previziona durata activa de viata si intervalele de mentenanta ale acestuia.

Testarea in regim simulat si accelerat a structurii de rezistenta de tip rama de boghiu care echipeaza vagoanele de calatori este impusa in principal de destinatia finala a produsului, acesta intrand in componenta unui tren de calatori. Rama de boghiu este o structura de rezistenta critica din componenta vagoanelor de calatori pe care se sprijina caroseria vagonului si care preia majoritatea sarcinilor care apar in exploatare. Astfel aceasta structura trebuie supusa unui program de validare, compus din urmatoarele etape:

- proiectare;
- analiza structurala cu element finit;
- testare in regim simulat si accelerat in laborator;
- testare pe cale ferată.

Dupa cum se observa, etapa de testare urmeaza etapei de analiza structurala. In cadrul etapei de analiza structurala se simuleaza pe calculator sarcinile care pot aparea in exploatare si care vor genera anumite stari de tensiuni interne in cadrul structurii de boghiu. Astfel se identifica configuratiile de incarcare simulata ale ramei de boghiu si punctele susceptibile a fi supuse unor tensiuni maxime in timpul duratei de exploatare. In cadrul etapei de testare se verifica integritatea structurala a ramei de boghiu si rezistenta acesteia la oboseala. Astfel etapa de testare este compusa din doua tipuri de teste: teste efectuate in regim static si teste efectuate in regim dinamic care le succeda pe primele.

Testele efectuate in regim static simuleaza sarcinile care apar in exploatare. Testele statice sunt impartite in teste in care incarcarile se fac cu sarcini exceptionale, sarcini care apar foarte rar in timpul exploatarii ramei de boghiu si teste in care incarcarile se fac cu sarcini de serviciu, sarcini care apar in mod curent in timpul exploatarii. Testele cu sarcini exceptionale au rolul de a verifica conditia ca in lucru sa nu se depaseasa limita de

that during work the yield strength of the material in which the bogie frame it is built,should not be surpassed, namely not to enter the field of plastic deformations. The tests with exploitation loadings represent tests that are performed in static regime, using for loading the extreme values that occur in the testing phase in dynamical regime. Using the results of these tests it checks the framing within the Goodmann-Smith diagram of the recorded stresses, thus estimating an "infinite" lifetime.

The tests carried out in dynamic regime actually verify the active length of life of the resistance structure of bogie frame type, this being subjected to a combination of loadings that simulate the state of stresses at which it is subjected in real working regime. The testing is accelerated because the loads are applied with a higher frequency than the actual working frequency, ratio between the two frequencies being the acceleration factor.

The test program presented is based on the European norm EN 13749:2011 which stipulates the methods for specifying the requirements regarding the resistance of the bogie frame structures.

MATERIALS AND METHODS

Researches regarding testing in simulated and accelerated regime of resistance structures of bogie frame type were carried out on a Hidropuls type testing installation, following a fatigue testing accelerated programm for one bogie frame. This paper presents the program of accelerated fatigue testing regime of a prototype bogie frame.

In operation, the bogie frame is subjected to the following load cases:

- vehicle weight including the payload,
- variations in the payload,
- irregularities of the rolling track,
- travel in curves,
- accelerations and brakings,
- minor derailments,
- impact (collision).

In reality, the loads are combining in a complex manner difficult to achieve in laboratory testing conditions. Therefore, in the current practice, are normalized load cases that are considered to be coverings for the real situations encountered on the duration of exploitation.

Fatigue tests are intended to confirm that the bogie frame is able to withstand the stresses caused by operating loads on its whole lifetime. The main acting loads are those responsible for inducing mechanical stresses in the whole structure of the bogie frame, namely: vertical forces, transversal forces and the forces due to twisting strains.

Fatigue testing program consists of repeating of cycles based on vertical and transversal forces combined with the shear demands (twisting)

The vertical forces applied on both longerons comprise:

- one statical part (1))
- one quasi-statical part: (2)
- one dynamical part: (3)

(defined in Annex G2 of SR EN 13749:2011).

curgere a materialului din care este construita rama de boghiu, adica de a nu intra in domeniul deformatiilor plastice. Testele cu sarcini de exploatare reprezinta teste care se fac in regim static, folosind pentru incarcare valorile extreme care apar in cadrul etapei de testare in regim dinamic. Folosind rezultatele acestor teste se verifica incadrarea in interiorul diagramei Goodmann-Smith a tensiunilor inregistrate, estimandu-se astfel o durata de viata ”infinita”.

Testele efectuate in regim dinamic verifica efectiv durata activa de viata a structurii de rezistenta de tip rama de boghiu, aceasta fiind supusa la o combinatie de sarcini care simuleaza starea de tensiuni la care aceasta este supusa in regim real de lucru. Testarea este accelerata deoarece sarcinile sunt aplicate cu o frecventa superioara frecventei reale de lucru, raportul dintre cele doua frecvente fiind factorul de accelerare.

Programul de testare prezentat are la baza norma europeana EN 13749:2011 care stipuleaza metodele pentru specificarea cerintelor referitoare la rezistenta structurilor cadrelor de boghiuri.

MATERIALE ŞI METODE

Cercetările privind testarea in regim simulat si accelerat a structurilor de rezistenta de tip rama de boghiu s-au realizat pe o instalaţie de incercari de tip Hidropuls, urmărind un program de testare in regim accelerat la oboseala pentru un prototip de rama de boghiu.

In exploatare, rama de boghiu este supusa la urmatoarele cazuri de incarcare:

- greutatea vehicolului, incluzând sarcina utila,
- variaţii in sarcina utila,
- neregularitaţi ale caii de rulare,
- mers in curbe,
- acceleraţii şi frânari,
- deraieri minore,
- impact (tamponare).

In realitate sarcinile se combina intr-o maniera complexa, greu de realizat in condiţiile incercarilor de laborator. In consecinţa, in practica curenta, sunt normate cazuri de incarcare, care se considera a fi acoperitoare pentru situaţiile reale intâlnite pe durata de exploatare.

Incercarile la oboseala sunt destinate sa confirme ca rama boghiului este capabila sa reziste solicitarilor datorate sarcinilor de exploatare pe toata durata de viaţa a acestuia. Sarcinile principale care actioneaza sunt cele responsabile de inducerea solicitarilor mecanice in intreaga structura a ramei de boghiu, anume: forţele verticale, forţele transversale şi forţele datorate solicitarilor de răsucire.

Programul incercarilor la oboseala consta in repetarea ciclurilor bazate pe forţele verticale şi transversale combinate cu solicitarile de forfecare (răsucire).

Forţele verticale, aplicate pe ambele lonjeroane cuprind:

- o parte statica (1)
- o parte cvasi-statica: (2)
- o parte dinamica: (3)

(definite conform anexei G2 din SR EN 13749:2011).

$$Fz1 = Fz2 = \frac{Fz}{2} = \frac{\left(Mv + 1.2P2 - 2m^{+}\right)g}{4} \quad (1)$$

$$Fzqs1 = Fzqs2 = \frac{\pm 0.1Fz}{2} \quad (2)$$

$$Fzd1 = Fzd2 = \frac{\pm 0.2Fz}{2} \quad (3)$$

The transversal forces applied on each axis, comprise:
- the quasi-static component (4);
- the dinamical component (5).

(defined in Annex G2 of SR EN 13749:2011).

Forţele transversale, aplicate pe fiecare axa, cuprind:
- componenta cvasi-statica (4);
- componenta dinamica (5).

(definite conform anexei G2 din SR EN 13749:2011).

$$Fyqs1 = Fyqs2 = \pm 0.063\left(Fz + m^{+}g\right) \quad (4)$$

$$Fyd1 = Fyd2 = \pm 0.063\left(Fz + m^{+}g\right) \quad (5)$$

where "g" has the approximate value of 9.81 m/s^2 and represents the gravitational acceleration and m + represents the mass of the wagon loaded.

The variations of these forces in relation to the time are indicated in Figure 1.

unde „g" are valoarea aproximativa 9.81 m/s2 şi reprezinta acceleraţia gravitaţionala si m^+ reprezinta masa vagonului incarcat.

Variaţiile acestor forţe in raport cu timpul sunt indicate in figura 1.

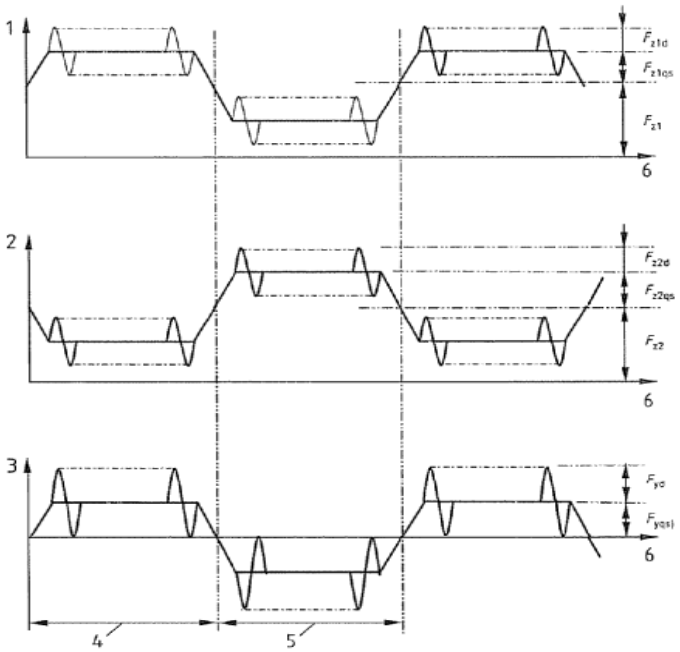

Fig.1 – The form of strains at the dynamic test to fatigue of bogies [5]

where:
1 – Fz1 – the vertical force applied on the longeron 1;
2 – Fz2 – the vertical force applied on the longeron 2;
3 – Fy – transversal force;
4 – n cycles in the curve on the right side;
5 – n cycles in the curve on the left side;
6 – number of cycles;
Fz1d – dynamic force applied on the longeron 1;
Fz2d – dynamic force applied on the longeron 2;
Fz1qs – quasi-statical force on the longeron 1;
Fz2qs – quasi-statical force on the longeron 2;
Fyqs – quasi-statical transversal force;
Fyd – dynamic transversal force.

The quasi-static stress cycles are normally reversed every 10 ... 20 dynamic cycles and the number of these cycles will be proportionally lower comparing to the number of dynamic cycles.

The torsional stress cycles (of twisting) consist of loads (or equivalent displacements) applied to primary suspension to generate a torsion in vertical plane of angle $+\theta_y$ followed by a torsion of angle $-\theta_y$ of the bogie frame longerons, which are synchronous with the

unde:
1 – Fz1 – forta verticala aplicata pe lonjeronul 1;
2 – Fz2 – forta verticala aplicata pe lonjeronul 2;
3 – Fy – forta transversala;
4 – n cicluri in curba pe partea dreapta;
5 – n cicluri in curba pe partea stanga;
6 – numarul de cicluri;
Fz1d – forta dinamica aplicata pe lonjeronul 1;
Fz2d – forta dinamica aplicata pe lonjeronul 2;
Fz1qs – forta cvasistatica pe pe lonjeronul 1;
Fz2qs – forta cvasistatica pe lonjeronul 2;
Fyqs – forta transversala cvasistatica;
Fyd – forta transversala dinamica.

Ciclurile de solicitare cvasi-statica sunt inversate in mod normal la fiecare 10 ... 20 cicluri dinamice, iar numarul acestor cicluri va fi proporţional mai mic comparativ cu numarul ciclurilor dinamice.

Ciclurile de solicitare de torsiune (de răsucire) constau in sarcini (sau deplasari echivalente) aplicate suspensiei primare pentru a genera o torsiune in plan vertical de unghi $+\theta_y$ urmata de o torsiune de unghi $-\theta_y$, a lonjeroanelor cadrului boghiului, acestea fiind sincrone cu

sequence of quasi-static loads. The twisting force applied to the bogie frame corresponds to an angular misalignment of the longerons in vertical plane of 0.5%.

The dynamic components of vertical and transversal forces are applied in phase, at the same frequency, so that to allow a simulation of loadings acting on the bogie frame. The same thing applies to the quasi-static components at an appropriate frequency of changing the curves direction. The sense of curves is alternately changed at every 10 dynamic cycles.

Dynamic stress fatigue loads are applied to a total of $10x10^6$ cycles as follows:

- 6×10^6 cycles with the loads calculated according to 5.2.2 and Annexes C, F and G of SR EN 13749:2011;
- 2×10^6 cycles with the loads calculated above, increased by 20%;
- 2×10^6 cycles with the loads calculated at the first point, increased by 40%.

The assessment method of resistance to fatigue chosen was the method of fatigue limit achieving, which according to [2] is the most commonly used method. For this purpose, during the application of loads are recorded the mechanical stresses and the forces applied to the bogie frame. It analyzes mechanical stresses and it is evaluated the return to "zero" after removal of loadings. For each measurement point is determined the maximum values, σ_{max}, and minimum values, σ_{min}, from which are calculated the mean values and the mechanical stress amplitudes (σ_m - the abscissa and σ_a – the ordinate in the Goodman-Smith diagram) using the relations (6):

secvenţa sarcinilor cvasi-statice. Forţa de răsucire aplicată ramei boghiului corespunde unei dezalinieri unghiulare a lonjeroanelor in plan vertical de 0.5%.

Componentele dinamice ale forţelor verticale şi transversale sunt aplicate in faza, la aceeaşi frecvenţa, astfel incât sa permita o simulare a sarcinilor care acţioneaza asupra ramei boghiului. Acelaşi lucru se aplica la componentele cvasi-statice, la o frecvenţa corespunzatoare schimbarii sensului curbelor. Sensul curbelor este schimbat alternativ, la fiecare 10 cicluri dinamice.

Sarcinile de solicitare dinamica la oboseala sunt aplicate pe un numar total de $10x10^6$ cicluri, dupa cum urmeaza:

- 6×10^6 cicluri cu sarcinile calculate conform 5.2.2 şi anexelor C, F si G din SR EN 13749:2011;
- 2×10^6 cicluri cu sarcinile calculate mai sus crescute cu 20%;
- 2×10^6 cicluri cu sarcinile calculate la primul punct crescute cu 40%.

Metoda de evaluare a rezistentei la oboseala aleasa a fost metoda atingerii limitei de oboseala, care dupa [2] este cea mai des utilizata metoda. In acest scop, pe durata aplicarii sarcinilor se inregistreaza tensiunile mecanice si fortele aplicate ramei de boghiu. Se analizeaza tensiunile mecanice şi se evalueaza revenirea la „zero” dupa indepartarea sarcinilor. Pentru fiecare punct de masura se determina valorile maxime, σ_{max}, si minime, σ_{min}, din care se calculeaza valorile medii si amplitudinile tensiunilor mecanice (σ_m - abscisa si σ_a – ordonata in diagrama Goodman-Smith) utilizand relatiile (6):

$$\sigma_m = \frac{\sigma_{max} + \sigma_{min}}{2}$$
$$\sigma_a = \frac{\sigma_{max} - \sigma_{min}}{2} \quad (6)$$

Table 1 shows the calculated values of the loadings that have been applied within the bogie frame fatigue testings performed in simulated and accelerated regime for the first 6×106 dynamic stress cycles to fatigue.

Figure 2 shows a schematic diagram of loadings used for the application of loadings at static and fatigue tests of the trailer bogie frame.

In tabelul 1 se prezinta valorile calculate ale sarcinilor care au fost aplicate ramei de boghiu purtator in cadrul testarilor de oboseala efectuate in regim simulat si accelerat, pentru primele 6×10^6 cicluri de solicitare dinamica la oboseala.

In figura 2 este prezentata schema de principiu folosita pentru aplicarea sarcinilor la incercarile statice si oboseala ale ramei de boghiu purtator.

Table 1

Values of the loadings

Type of strain	Component type	Strain value	
		[kN]	[mm]
F_y (Transversal)	quasi-static	19.85	-
	dynamic	19.85	-
F_z (Vertical)	static	128	-
	quasi-static	12.8	-
	dynamic	25.6	-
Twisting (Torsion)	quasi-static	-	1,6

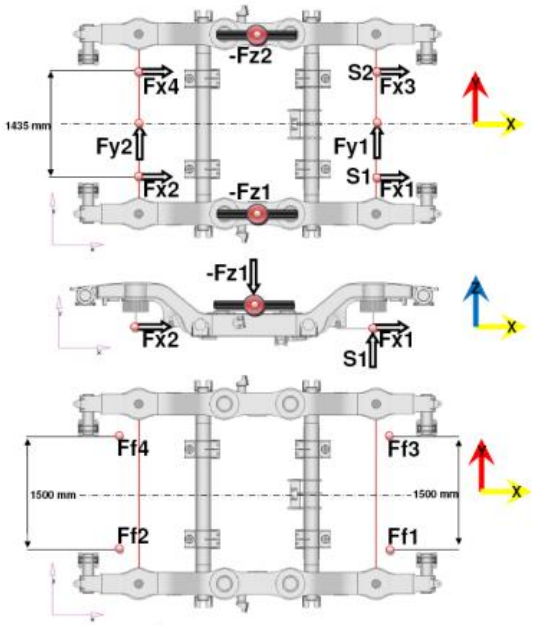

Fig. 2 – Application scheme of static and fatigue loads for the bogie frame

The frequency for the dynamic application of loadings was chosen at 3.5 Hz, after modal identification tests previously undertaken [3]. Thus it has complied to a good practice rule, the test frequency not exceeding the value of 1/3 of the first fundamental frequency of the bogie frame, which has been identified around the value of 18Hz.

For monitoring the evolution of fatigue tests, were performed stresses measurements recorded in the critical points of the bogie frame, previously identified through finite element analysis.

Were applied a total of 44 strain gauges LY11-6/350 manufactured by Hottinger having the base of 6mm and the electrical resistance of 350 Ohm, the factor k=2.09 ±0.7%, transversal sensitivity -0.9%.

Also were acquired and the data relating at the amplitude and frequency of the applied loads to the bogie frame.

Frecventa de aplicare dinamica a sarcinilor a fost aleasa la 3.5 Hz, in urma testelor de identificare modala intreprinse anterior [3]. Astfel s-a respectat o regula de buna practica, frecventa de incercare nedepasind valoarea de 1/3 din prima frecventa fundamentala a ramei de boghiu, care a fost identificata in jurul valorii de 18 Hz.

In scopul urmaririi evolutiei testelor de oboseala, s-au efectuat masuratori ale tensiunilor inregistrate in punctele critice ale ramei de boghiu, identificate anterior prin analiza cu element finit.

Au fost aplicate un numar de 44 de marci tensometrice LY11-6/350, produse de firma Hottinger avand baza de 6mm si rezistenta de 350Ohm, factorul k=2,09 ±0,7%, sensibilitate transversala -0,9%.

De asemenea au fost achizitionate si datele referitoare la amplitudinea si frecventa sarcinilor aplicate ramei de boghiu.

Fig.3 – Detail of strain gauge application

RESULTS

Product for which the dynamic test was performed was the trailer bogie frame for electrical frames which is shown in Figure 4.

The trailer bogie frame is made of welded steel type S355J2G3-STD01W03 (ERRI B12/RP60) of varying thicknesses (8,10,12mm), with the mechanical breaking effort of 510 MPa and the proportionality elastic limit of 350 MPa for unwelded material, respectively 325 MPa, for welded material.

REZULTATE

Produsul pentru care s-au efectuat incercarile dinamice a fost rama de boghiu purtator pentru rame electrice prezentata in figura 4.

Rama de boghiu purtator este o constructie sudata confectionata din otel tip S355J2G3-STD01W03 (ERRI B12/RP60) de diferite grosimi (8,10,12mm), cu efortul mecanic la rupere de 510 MPa si limita de proportionalitate elastica de 350 MPa pentru material nesudat, respectiv 325 MPa, pentru material sudat.

Fig. 4 – Bogie frame

Accelerated fatigue tests were performed on a specialized stand (fig.5) that simulates the real operating conditions. Installation used for the application of loadings in dynamic regime was the installation of Hydropulse type from the endowment of Testing Department within INMA Bucharest. For the application of vertical loads were used two hydraulic cylinders of 250 kN, one for each longeron. The application of transversal loads was made through two 100 kN hydraulic cylinders, one for each axle. The twisting strains were applied through two hydraulic cylinders of 250 kN.

To succeed in the application of a test frequency of 3.5 Hz, the primary suspension of the bogie frame was artificially stiffened by pre-stressing with a force of 90 kN, the twisting strain being recalculated for this reason.

Incercarile accelerate de oboseala s-au efectuat pe un stand specializat (figura 5) care simuleaza conditiile reale de exploatare. Instalatia folosita pentru aplicarea sarcinilor in regim dinamic a fost instalatia de tip Hidropuls din dotarea Departamentului de Incercari din cadrul INMA Bucuresti. Pentru aplicarea sarcinilor verticale s-au folosit doi cilindri hidraulici de 250 kN, cate unul pentru fiecare lonjeron. Aplicarea sarcinilor transversale s-a facut prin intermediul a doi cilindrii hidraulici de 100 kN, cate unul pentru fiecare osie. Solicitarile de răsucire au fost aplicate prin intermediul a doi cilindrii hidraulici de 250 kN.

Pentru a se reusi aplicarea unei frecvente de incercare de 3.5 Hz suspensia primara a ramei de boghiu a fost rigidizata artificial prin precomprimare cu o forta de 90 kN, solicitarea de răsucire fiind recalculata din acest motiv.

Fig. 5 – Mounting made on the Hydropulse type installation for carrying out the dynamic fatigue tests

Figure 6 shows the diagram of forces applied to the bogie frame in dynamic regime for the first 6 million dynamic load cycles. Looking at the chart we can identify the static, quasi-static and dynamic characteristic of each applied force or displacement. Also it should be noticed the correlation between the reference signal (fig.2) and the real signal acquired (fig.6).

Diagrams are associated with color displays placed in the bottom of each graphics. In the displays, the represented parameters mean values are transmitted at selected time points in the second race of red and blue. The corresponding values of the first red cursor are transmitted among superior and inferior displays or are transmitted among corresponding values of the second blue cursor.

For all types of strains are available the following rules for reading and interpretation:

In figura 6 se prezinta diagrama fortelor aplicate ramei de boghiu in regim dinamic, pentru primele 6 milioane cicluri de incarcare dinamica. Analizand diagrama se pot identifica componentele statica, cvasi-statica si dinamica caracteristice fiecarei forte sau deplasari aplicate. De asemenea se observa corelarea intre semnalul de referinta (fig.2) si semnalul real achizitionat (fig.6).

Diagramele sunt asociate prin culoare cu display-uri plasate in partea inferioara a fiecarei reprezentari grafice. In display-uri sunt transmise valorile parametrilor reprezentati, la momente de timp selectate prin cele doua cursoare de culoare rosu si albastru. Valorile corespunzatoare primului cursor, rosu, sunt transmise in randul superior de display-uri, iar in randul inferior sunt transmise valorile corespunzatoare celui de al doilea cursor, cel albastru.

Pentru toate tipurile de solicitari sunt valabile urmatoarele reguli de citire si de interpretare:

Forces applied vertically FZ1 and FZ2 are reported in right ordinate. Forces applied horizontally FY1 and FY2 are ordered relative to the left. Twisting sites S1 (DTw1) and S2 (DTw2) are relative to the middle ordinate.

In the diagram in Figure 7 is observed a part of the strains measured in the critical points of the bogie frame during the 10 million cycles of dynamic load. Mechanical stresses were obtained by multiplying the measured specific deformation modulus E = 206000 MPa which is specific for the steel from which the bogie frame is built. It can be seen that the shape of the mechanical stresses complies with the profile of the strains applied to bogie frame.

Fortele aplicate pe directia verticala, Fz1 si Fz2, sunt raportate la ordonata din dreapta. Fortele aplicate pe directia orizontala, Fy1 si Fy2, sunt raportate la ordonata din partea stanga. Răsucire-urile S1 (DTw1) si S2 (DTw2) sunt raportate la ordonata din mijloc.

In diagrama din figura 7 se observa o parte din tensiunile masurate in punctele critice ale ramei de boghiu pe durata celor 10 milioane de cicluri de incarcare dinamica. Tensiunile mecanice au fost obtinute prin inmultirea valorii deformatiei specifice masurate cu modulul de elasticitate E=206000 MPa specific otelului din care a fost construita rama de boghiu. Se poate observa ca forma tensiunilor mecanice respecta profilul solicitarilor aplicate ramei de boghiu.

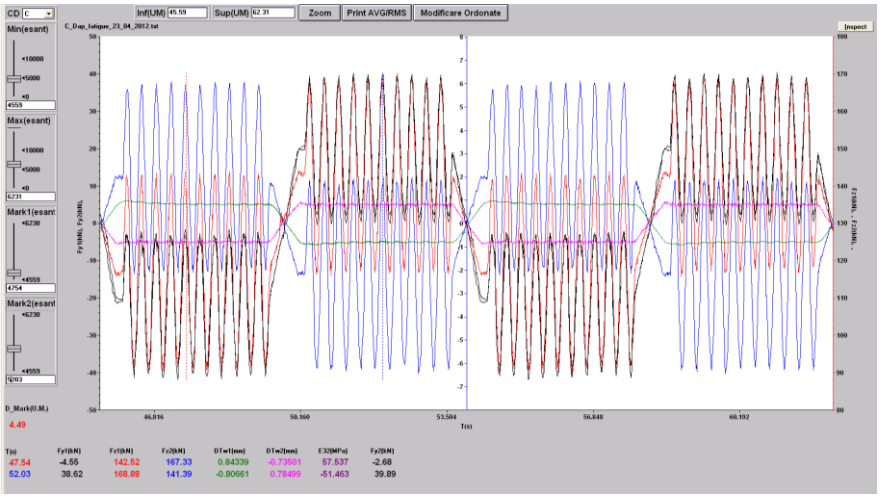

Fig. 6 – Applied forces diagram / *Diagrama forte aplicate*

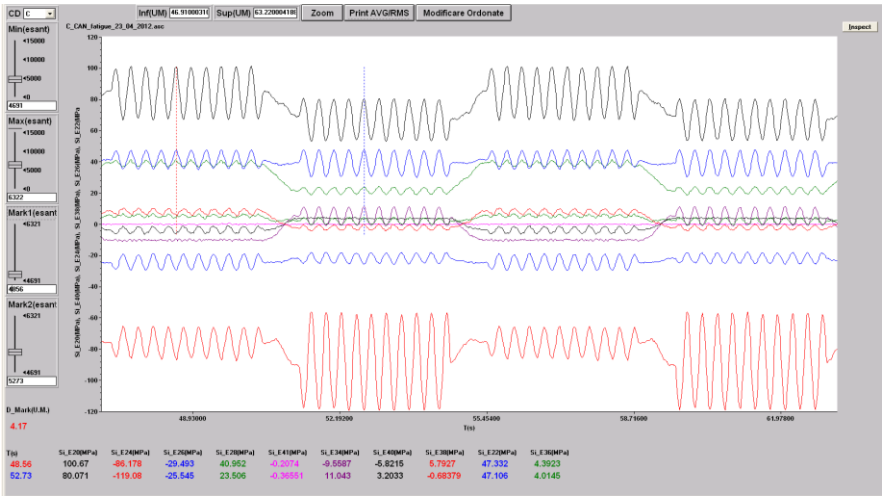

Fig.7 – Mechanical tensions diagram

Figure 8 shows the framing into the Goodman-Smith stress diagram σ_m and σ_a calculated for each specific deformation measured in the critical points of the bogie frame. It can be seen that all the points of coordinates (σ_m, σ_a) are within the chart except one, which is on the border. Framing points within the chart predicts a value of strains below the limit of fatigue. The point from the boundary suggests possible fatigue limit reaching in the critical area which it represents. This area was observed until the end of tests, and have not presented the appearance of cracks or fractures caused by fatigue.

In figura 8 se prezinta incadrarea in diagrama Goodman-Smith a tensiunilor σ_m si σ_a calculate pentru fiecare deformatie specifica masurata in puntele critice ale ramei de boghiu. Se poate observa ca toate punctele de coordonate (σ_m, σ_a) se afla in interiorul diagramei cu exceptia unuia singur, care se afla pe frontiera. Incadrarea punctelor in interiorul diagramei previzioneaza o valoare a tensiunilor sub limita de oboseala. Punctul de pe frontiera sugera o eventuala atingere a limitei de oboseala in zona critica pe care o reprezinta. Aceasta zona a fost tinuta sub observatie pana la finalul testelor si nu a prezentat aparitia unor fisuri sau rupturi datorate oboselii.

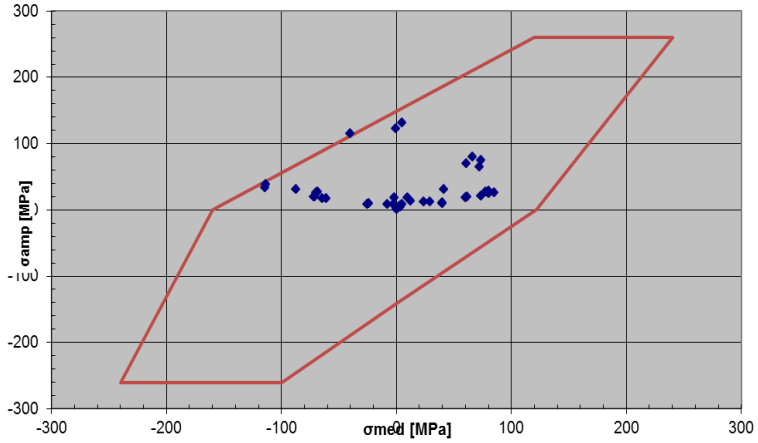

Fig. 8 – Goodman-Smith diagram and framing of the blue marked points representing the calculated tensions σ_m and σ_a

CONCLUSIONS

Testing in simulated and accelerated regime of the bogie frames is done in order to verify the structure from the perspective of the resistance to fatigue.

Within the dynamic tests to fatigue the assessment of fatigue strength using the fatigue diagrams GOODMAN - SMITH only allows assessing of a compliance with the limits imposed by diagrams [4]. It can assess the fatigue resistance using the approach of accumulation of flaws, based on summation of effects of stresses due to all load cases and including them into the Wohler curve for the material in which is constructed the structure. Then, using a hypothesis for damages accumulation due to the fatigue (Palmer-Miner for example) can be estimated the total degree of fatigue that will be accumulated during the active period of life of the structure [2]. However, this method requires complex calculations and definition of the complete spectrum of stresses to which may be subjected the structure.

The groups of stresses to which was subjected the structure are based on waveforms experimentally established on the railways and accelerated from the perspective of increasing the testing frequency and the amplitudes of the strains in order to obtain results as correlated with reality in good time.

Acknowlegement

The paper is realized within contract PN II-PCCA, no. 192/2012.

REFERENCES

[1]. Escobar L.A., Meeker W.Q., (2006) - *A Review of Accelerated Test Models*, Statistical Science, Vol. 21, No. 4, 552–577;

[2]. Mancini G., Cera Al., (2006) – *Design of railway bogies in compliance with new EN 13749 European Standard,* http://www.uic.org/cdrom/2006/wcrr2006/pdf/609.pdf;

[3]. Manea I., Gîrnită I., Matache M. et al, (2012) - *Research for modal analysis utilization as a tool for fatigue and structural change assessment of mechanical structures*, International Symposium ISBINMATEH 2012;

[4]. Tănăsoiu A., Copaci I., (2011) – *On the span life of the carrying structures of railway vehicles*, AIR Bulletin no.3, July-September;

[5]. ***- EN13749:2011 - *Railway Applications- Wheelsets and bogies- Method of specifying the structural requirements of bogie frames*.

CONCLUZII

Testarea in regim simulat si accelerat a ramelor de boghiu se face in scopul verificarii structurii din punctul de vedere al rezistentei la oboseala.

În cadrul încercărilor dinamice la oboseala aprecierea rezistenţei la oboseală folosind diagramele de oboseală GOODMAN – SMITH permite doar evaluarea unei încadrări în limitele impuse de diagrame [4]. Se poate evalua rezistenta la obosela folosind abordarea cumulului de defecte, prin insumarea efectelor tensiunilor datorate tuturor cazurilor de incarcare si incadrarea acestora in curba lui Wohler pentru materialul din care este construita structura. Apoi folosind o ipoteza pentru acumularea stricaciunilor datorita oboselii (Palmer-Miner de exemplu) se poate estima gradul total de oboseala care va fi acumulat pe parcursul duratei active de viata a structurii [2]. Totusi aceasta metoda presupune calcule complexe si definirea spectrului complet de sarcini la care poate fi supusa structura.

Colectivele de solicitare la care a fost supusa structura au la baza forme de unda stabilite experimental pe calea ferata si accelerate din punctul de vedere al cresterii frecventei de testare si a amplitudinilor solicitarilor in scopul obtinerii unor rezultate cat mai corelate cu realitatea în timp util.

Recunoaştere

Lucrarea este realizata in cadrul contractului PN II-PCCA, nr. 192/2012.

BIBLIOGRAFIE

[1]. Escobar L.A., Meeker W.Q., (2006) – *Un review asupra modelelor de testare accelerata*, Statistical Science, Vol. 21, No. 4, 552–577;

[2]. Mancini G., Cera Al., (2006) – *Proiectarea boghiurilor de cale ferata in conformitate cu noul standard european EN 13749,* http://www.uic.org/cdrom/2006/wcrr2006/pdf/609.pdf;

[3]. Manea I., Gîrnită I., Matache M. ş.a., (2012) - *Cercetări privind utilizarea analizei modale ca instrument pentru evaluarea stării de oboseală si a modificărilor structurale ale structurilor mecanice*, Simpozion International ISBINMATEH 2012;

[4]. Tănăsoiu A., Copaci I., (2011) – *Asupra duratei de viaţă a structurilor portante ale vehiculelor feroviare*, Buletinul AIR nr.3, iulie-septembrie;

[5]. ***- EN13749:2011 - *Aplicatii Feroviare, Osii montate si boghiuri, Metode pentru specificarea cerintelor referitoare la rezistenta structurilor cadrelor de boghiuri.*

REDUCTION OF A BENT PLATE, WITH CONCURRENT EDGES
/
REDUCEREA UNEI PLĂCI OMOGENE ÎNDOITE, CU MUCHIILE CONCURENTE

Lecturer PhD. Eng. Orăşanu N., Assoc. Professor PhD. Eng. Craifaleanu A.
„Politehnica" University of Bucharest, Department of Mechanics / Romania
Tel: 021-4029503; E-mail: norasanu62@yahoo.com

Abstract: *The paper presents a method to determine the inertial characteristics (coordinates of the mass center, moments and products of inertia) of a plate with concurrent bending edges, each face representing a homogeneous triangle. By generalising a method previously published by the first author, the plate is assimilated, from the inertial point of view, with a discrete system of material points, applied in the corners and in the mass centres of the faces. The results are particularised for several cases frequently found in practice: homogeneous bent plate, plane plate with the shape of an arbitrary polygon, of a quadrilateral and of a right-angled trapezoid, respectively. Two applications are also presented.*

Keywords: *bent plate, mass center, moment of inertia, product of inertia.*

INTRODUCTION

In references [2] and [3] a calculation method is presented for the inertial characteristics of simple bodies, based on their assimilation with finite systems of material points. It is shown that, in the case of a homogeneous triangular plate of mass *m*, the equivalent system is composed of three points of mass $\frac{m}{12}$ applied in the corners and one of mass $\frac{3m}{4}$ applied in the mass center.

Let $OA_1A_2 \ldots A_iA_{i+1}\ldots A_{n-1}A_n$ be a plate of mass *m*, with bending edges concurrent in point *O* (Fig. 1a).

Rezumat: *Lucrarea prezintă o metodă de calcul al caracteristicilor inerţiale (coordonatele centrului de masă şi momente de inerţie mecanice) ale unei plăci cu muchii de îndoire concurente, fiecare dintre feţele acesteia reprezentând un triunghi omogen. Generalizând o metodă publicată anterior de către primul autor, placa este echivalată, din punct de vedere inerţial, cu un sistem discret de puncte materiale, aplicate în colţuri şi în centrele de masă ale feţelor. Rezultatele sunt particularizate pentru mai multe cazuri frecvent întâlnite în practică: placă îndoită omogenă, placă plană având forma unui poligon oarecare, respectiv al unui patrulater şi al unui trapez dreptunghic. Sunt prezentate, de asemenea, două aplicaţii.*

Cuvinte cheie: *centru de masă, momente de inerţie, placă îndoită.*

INTRODUCERE

În lucrările [2] şi [3] este prezentată o metodă de calcul al caracteristicilor inerţiale ale unor corpuri simple pe baza echivalării acestora cu anumite sisteme finite de puncte materiale. Se arată că în cazul unei plăci omogene triunghiulare de masă *m*, sistemul echivalent se compune din trei puncte de masă $\frac{m}{12}$ aplicate în colţuri şi unul de masă $\frac{3m}{4}$ aplicat în centrul de masă.

Fie placa $OA_1A_2 \ldots A_iA_{i+1}\ldots A_{n-1}A_n$ de masă *m*, cu muchiile de îndoire concurente în punctul *O* (fig. 1a).

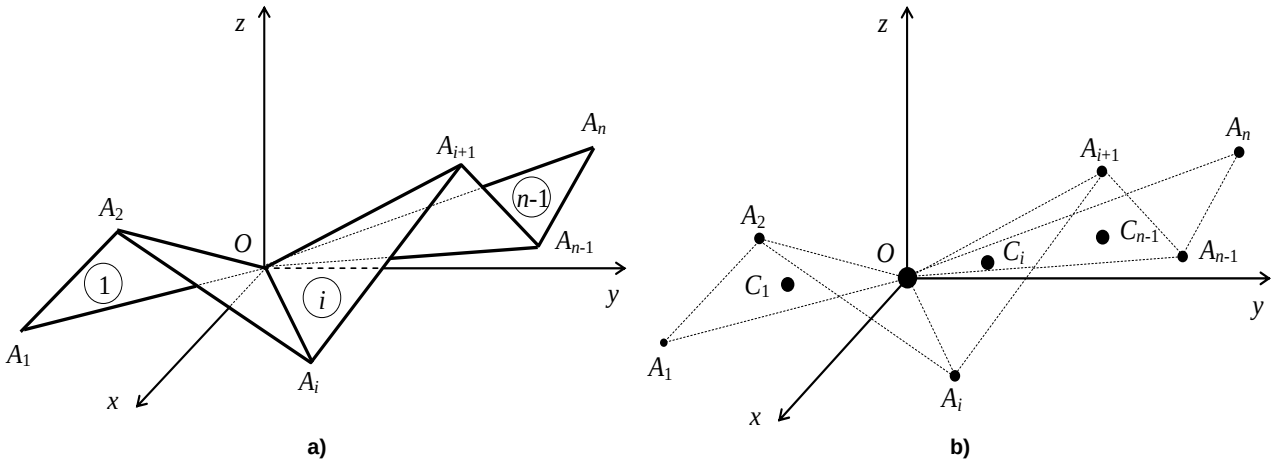

Fig. 1 - Bent plate, with concurrent edges

MATERIALS AND METHODS

The orthogonal reference system *Oxyz* is considered, with the origin in point *O*. External edges OA_1 and OA_n are supposed to pass also through the corner *O*, which is the concurrence point of all visible edges of the plate. On the figure, the bending edges are drawn with solid line: OA_2, OA_3,..., OA_{n-1}.

MATERIALE ŞI METODE

Se consideră sistemul de referinţă ortogonal *Oxyz*, cu originea în punctul *O*. Se presupune că muchiile de tăiere exterioare, OA_1 şi OA_n trec, de asemenea, prin vârful *O*, care este punctul de concurenţă al tuturor muchiilor vizibile ale plăcii. Pe figură, muchiile de îndoire sunt

The coordinates of all corners are also considered known: $O(0, 0, 0)$, $A_1(x_1, y_1, z_1)$, $A_2(x_2, y_2, z_2)$,..., $A_n(x_n, y_n, z_n)$.
It is also supposed that all triangles OA_1A_2, OA_2A_3,..., OA_iA_{i+1},..., $OA_{n-1}A_n$, which define the faces of the body, are homogeneous plates. The coordinates of the mass center of an arbitrary triangle, OA_iA_{i+1}, can be easily calculated:

desenate cu linie continuă: OA_2, OA_3,..., OA_{n-1}.

Se consideră cunoscute coordonatele vârfurilor plăcii: $O(0, 0, 0)$, $A_1(x_1, y_1, z_1)$, $A_2(x_2, y_2, z_2)$,..., $A_n(x_n, y_n, z_n)$.
Se presupune că toate triunghiurile OA_1A_2, OA_2A_3,..., OA_iA_{i+1},..., $OA_{n-1}A_n$, care constituie feţele corpului, sunt plăci omogene. Coordonatele centrului de masă al unui triunghi oarecare, OA_iA_{i+1}, pot fi uşor calculate:

$$C_i\left(\frac{x_i+x_{i+1}}{3},\frac{y_i+y_{i+1}}{3},\frac{z_i+z_{i+1}}{3}\right)\quad (i=1,2,...,n-1) \tag{1}$$

Taking into account the above mentioned equivalence theorem, it results that the plate can be reduced to a system of material points with the following masses (fig. **1**b): $O\left(\frac{m}{12}\right)$, $A_1\left(\frac{m_1}{12}\right)$, $A_2\left(\frac{m_1+m_2}{12}\right)$,..., $A_i\left(\frac{m_{i-1}+m_i}{12}\right)$,..., $A_{n-1}\left(\frac{m_{n-2}+m_{n-1}}{12}\right)$, $A_n\left(\frac{m_{n-1}}{12}\right)$, $C_1\left(\frac{3m_1}{4}\right)$, $C_2\left(\frac{3m_2}{4}\right)$,..., $C_i\left(\frac{3m_i}{4}\right)$,..., $C_{n-1}\left(\frac{3m_{n-1}}{4}\right)$.

Având în vedere teorema de echivalenţă menţionată mai sus, rezultă că orice placa poate fi redusă la un sistem de puncte materiale cu următoarele mase (fig. **1** b): $O\left(\frac{m}{12}\right)$, $A_1\left(\frac{m_1}{12}\right)$, $A_2\left(\frac{m_1+m_2}{12}\right)$,..., $A_i\left(\frac{m_{i-1}+m_i}{12}\right)$,..., $A_{n-1}\left(\frac{m_{n-2}+m_{n-1}}{12}\right)$, $A_n\left(\frac{m_{n-1}}{12}\right)$, $C_1\left(\frac{3m_1}{4}\right)$, $C_2\left(\frac{3m_2}{4}\right)$,..., $C_i\left(\frac{3m_i}{4}\right)$,..., $C_{n-1}\left(\frac{3m_{n-1}}{4}\right)$.

RESULTS

Calculation of the inertial characteristics of an arbitrary bent plate

The abscissa of the mass center is:

REZULTATE

Calculul mărimilor inerţiale în cazul unei plăcii îndoite oarecare

Abscisa centrului de masă este:

$$x_C=\frac{\sum_{i=1}^{n-1}\frac{m_i}{12}(x_i+x_{i+1})+\sum_{i=1}^{n-1}\frac{3m_i}{4}\frac{x_i+x_{i+1}}{3}}{12m} \tag{2}$$

By arranging this expression and by proceeding in the same manner for the other coordinates, it follows:

Prelucrând această expresie şi procedând asemănător pentru celelalte coordonate, rezultă:

$$x_C=\frac{1}{3m}\sum_{i=1}^{n-1}m_i(x_i+x_{i+1}),\quad y_C=\frac{1}{3m}\sum_{i=1}^{n-1}m_i(y_i+y_{i+1}),\quad z_C=\frac{1}{3m}\sum_{i=1}^{n-1}m_i(z_i+z_{i+1}) \tag{3}$$

The calculation relations of the moments and products of inertia are based on the definition formulae of these quantities, for discrete systems of material points [1]. Thus,

Relaţiile de calcul ale momentele de inerţie axiale şi centrifugale se bazează pe formulele de definiţie ale acestor mărimi, în cazul sistemelor discrete de puncte materiale [1]. Astfel,

$$J_x=\sum_{i=1}^{n-1}\frac{m_i}{12}\left[\left(y_i^2+z_i^2\right)+\left(y_{i+1}^2+z_{i+1}^2\right)\right]+\sum_{i=1}^{n-1}\frac{3m_i}{4}\left[\left(\frac{y_i+y_{i+1}}{3}\right)^2+\left(\frac{z_i+z_{i+1}}{3}\right)^2\right] \tag{4}$$

$$J_{xy}=\sum_{i=1}^{n-1}\frac{m_i}{12}(x_iy_i+x_{i+1}y_{i+1})+\sum_{i=1}^{n-1}\frac{3m_i}{4}\frac{x_i+x_{i+1}}{3}\frac{y_i+y_{i+1}}{3} \tag{5}$$

By arranging these expressions and by proceeding in the same manner for the other moments and products of inertia, it follows:

Prelucrând aceste expresii şi procedând asemănător pentru celelalte momente de inerţie, rezultă:

$$\begin{cases} J_x=\frac{1}{6}\sum_{i=1}^{n-1}m_i\left(y_i^2+y_iy_{i+1}+y_{i+1}^2+z_i^2+z_iz_{i+1}+z_{i+1}^2\right)\\ J_y=\frac{1}{6}\sum_{i=1}^{n-1}m_i\left(z_i^2+z_iz_{i+1}+z_{i+1}^2+x_i^2+x_ix_{i+1}+x_{i+1}^2\right)\\ J_z=\frac{1}{6}\sum_{i=1}^{n-1}m_i\left(x_i^2+x_ix_{i+1}+x_{i+1}^2+y_i^2+y_iy_{i+1}+y_{i+1}^2\right), \end{cases} \tag{6}$$

$$\begin{cases} J_{xy} = \frac{1}{12}\sum_{i=1}^{n-1} m_i\left(2x_iy_i + 2x_{i+1}y_{i+1} + x_iy_{i+1} + x_{i+1}y_i\right) \\ J_{yz} = \frac{1}{12}\sum_{i=1}^{n-1} m_i\left(2y_iz_i + 2y_{i+1}z_{i+1} + y_iz_{i+1} + y_{i+1}z_i\right) \\ J_{zx} = \frac{1}{12}\sum_{i=1}^{n-1} m_i\left(2z_ix_i + 2z_{i+1}x_{i+1} + z_ix_{i+1} + z_{i+1}x_i\right). \end{cases} \quad (7)$$

Calculation of the inertial characteristics of a homogeneous plate

If the bent plate is homogeneous, its superficial density, ρ_s, is constant and has the expression:

Calculul mărimilor inerţiale în cazul unei plăcii îndoite omogene

Dacă placa îndoită este omogenă, densitatea superficială a acesteia, ρ_s, este constantă şi are expresia:

$$\rho_s = \frac{m}{S} \quad (8)$$

The total area, *S*, can be obtained by adding the areas of the composing triangles:

Aria totală, *S*, se poate obţine însumând ariile triunghiurilor în care a fost împărţită placa:

$$S = S_1 + S_2 + ...S_i + ...S_{n-1} = \sum_{i=1}^{n-1} S_i \quad (9)$$

As it is known, the modulus of the vector product of two position vectors equals twice the area of the triangle determined by the vectors:

Aşa cum se cunoaşte, modulul produsului vectorial a doi vectori de poziţie este dublul ariei triunghiului determinat de vectorii respectivi:

$$S_i = \frac{1}{2}\left|\overrightarrow{OA_i} \times \overrightarrow{OA_{i+1}}\right| = \frac{1}{2}\sqrt{(y_iz_{i+1} - y_{i+1}z_i)^2 + (z_ix_{i+1} - z_{i+1}x_i)^2 + (x_iy_{i+1} - x_{i+1}y_i)^2} \quad (10)$$

where:

unde:

$$\overrightarrow{OA_i} \times \overrightarrow{OA_{i+1}} = \begin{vmatrix} \vec{i} & \vec{j} & \vec{k} \\ x_i & y_i & z_i \\ x_{i+1} & y_{i+1} & z_{i+1} \end{vmatrix} \quad (11)$$

The masses of the triangular plates have the expressions:

Masele plăcilor triunghiulare au expresiile:

$$m_1 = \rho_s \cdot S_1 = m\frac{S_1}{S}, \quad m_2 = \rho_s \cdot S_2 = m\frac{S_2}{S},..., \quad m_i = \rho_s \cdot S_i = m\frac{S_i}{S},..., \quad m_{n-1} = \rho_s \cdot S_{n-1} = m\frac{S_{n-1}}{S} \quad (12)$$

It follows that, in the case of a homogeneous plate, formulae (4)-(7) can be brought to simpler forms:

Rezultă de aici că, în cazul unei plăci omogene, formulele (4)-(7) pot fi aduse la forme mai simple:

$$x_C = \frac{1}{3S}\sum_{i=1}^{n-1} S_i\left(x_i + x_{i+1}\right), \quad y_C = \frac{1}{3S}\sum_{i=1}^{n-1} S_i\left(y_i + y_{i+1}\right), \quad z_C = \frac{1}{3S}\sum_{i=1}^{n-1} S_i\left(z_i + z_{i+1}\right) \quad (13)$$

$$\begin{cases} J_x = \frac{m}{6S}\sum_{i=1}^{n-1} S_i\left(y_i^2 + y_iy_{i+1} + y_{i+1}^2 + z_i^2 + z_iz_{i+1} + z_{i+1}^2\right) \\ J_y = \frac{m}{6S}\sum_{i=1}^{n-1} S_i\left(z_i^2 + z_iz_{i+1} + z_{i+1}^2 + x_i^2 + x_ix_{i+1} + x_{i+1}^2\right) \\ J_z = \frac{m}{6S}\sum_{i=1}^{n-1} S_i\left(x_i^2 + x_ix_{i+1} + x_{i+1}^2 + y_i^2 + y_iy_{i+1} + y_{i+1}^2\right), \end{cases} \quad (14)$$

$$\begin{cases} J_{xy} = \frac{m}{12S}\sum_{i=1}^{n-1} S_i\left(2x_iy_i + 2x_{i+1}y_{i+1} + x_iy_{i+1} + x_{i+1}y_i\right) \\ J_{yz} = \frac{m}{12S}\sum_{i=1}^{n-1} S_i\left(2y_iz_i + 2y_{i+1}z_{i+1} + y_iz_{i+1} + y_{i+1}z_i\right) \\ J_{zx} = \frac{m}{12S}\sum_{i=1}^{n-1} S_i\left(2z_ix_i + 2z_{i+1}x_{i+1} + z_ix_{i+1} + z_{i+1}x_i\right). \end{cases} \quad (15)$$

Case of a homogeneous plane polygon
The general relations determined above can be used for any homogeneous plane polygon, if the following geometrical condition is fulfilled: point *O* can be chosen in any corner or in any point placed inside the polygon, so that no segment OA_i (i=1,2,…,n) intersects any edge of the polygon:

Cazul poligonului plan omogen
Relaţiile generale determinate mai sus îşi găsesc o utilizare imediată pentru orice poligon plan omogen, dacă se respectă următoarea condiţie geometrică: punctul *O* poate fi ales în orice vârf sau în orice punct situat în interiorul unui poligonului, astfel încât nici un segment OA_i (i = 1,2,…,n) să nu intersecteze vreo muchie a poligonului:

$$OA_i \cap A_j A_{j+1} = \Phi \ (i = 1,2,..., n;\ j = 1,2,..., n-1) \tag{16}$$

where the corners are consecutively counted.
In the case of plane polygons, all *z*-coordinates are null: z_i=0 (i=1,2,…,n). If such bodies present symmetries, calculations are simplified by choosing point *O* on the symmetry element (point, axis or plane). The same reasoning is valid for the choice of axis *Ox*.
The triangle areas are:

unde vârfurile sunt numerotate consecutiv.
În cazul corpurilor plane, toate cotele sunt nule: z_i=0 (i=1,2,…,n). Dacă aceste corpuri prezintă simetrii, calculele se simplifică alegând punctul *O* pe elementul de simetrie (punct, axă sau plan). Acelaşi raţionament este valabil şi pentru alegerea axei *Ox*.
Ariile triunghiurilor sunt:

$$S_i = \frac{\left| x_i y_{i+1} - x_{i+1} y_i \right|}{2} \tag{17}$$

The coordinates of the mass center have the following general expressions:

Coordonatele centrului de masă au următoarele expresii generale:

$$x_C = \frac{1}{3S}\sum_{i=1}^{n-1} S_i \left(x_i + x_{i+1}\right), \quad y_C = \frac{1}{3S}\sum_{i=1}^{n-1} S_i \left(y_i + y_{i+1}\right), \quad z_C = 0 \tag{18}$$

The moments and products of de inertia become:

Momentele de inerţie devin:

$$\begin{cases} J_x = \dfrac{m}{6S}\displaystyle\sum_{i=1}^{n-1} S_i \left(y_i^2 + y_i y_{i+1} + y_{i+1}^2\right) \\ J_y = \dfrac{m}{6S}\displaystyle\sum_{i=1}^{n-1} S_i \left(x_i^2 + x_i x_{i+1} + x_{i+1}^2\right) \\ J_z = \dfrac{m}{6S}\displaystyle\sum_{i=1}^{n-1} S_i \left(x_i^2 + x_i x_{i+1} + x_{i+1}^2 + y_i^2 + y_i y_{i+1} + y_{i+1}^2\right), \end{cases} \tag{19}$$

$$\begin{cases} J_{xy} = \dfrac{m}{12S}\displaystyle\sum_{i=1}^{n-1} S_i \left(2x_i y_i + 2x_{i+1} y_{i+1} + x_i y_{i+1} + x_{i+1} y_i\right) \\ J_{yz} = 0 \\ J_{zx} = 0. \end{cases} \tag{20}$$

Application 1
Half of the cross-section of a symmetrical part of a mechanical device has the polygonal shape in Figure 2.

Aplicaţia 1
Jumătate din secţiunea transversală a unei piese simetrice din componenţa unui dispozitiv mecanic are forma poligonală din figura 2.

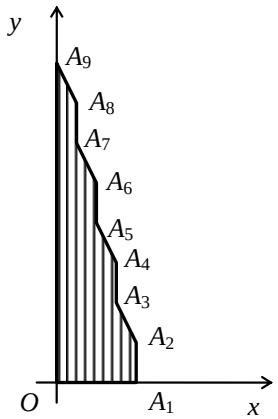

Fig. 2 - Example of a homogeneous plane plate

The coordinates of corners A_i are defined in Table 1.

Coordonatele vârfurilor A_i sunt definite în tabelul 1.

Table Error! Reference source not found.

Geometrical characteristics of the plate

Punct	A_1	A_2	A_3	A_4	A_5	A_6	A_7	A_8	A_9
x_i	4*a*	4*a*	3*a*	3*a*	2*a*	2*a*	*a*	*a*	0
y_i	0	2*a*	4*a*	6*a*	8*a*	10*a*	12*a*	14*a*	16*a*

Assuming that the plate is homogeneous, its inertia properties can be determined.
By applying relation (17), the areas result of the eight triangles composing the polygon:

Presupunând că placa este omogenă, se pot determina proprietăţile de inerţie ale acesteia.
Aplicând relaţia de calcul (17), rezultă ariile celor opt triunghiuri în care poate fi împărţit poligonul:

$$S_1 = 4a^2,\quad S_2 = 5a^2,\quad S_3 = 3a^2,\quad S_4 = 6a^2,\quad S_5 = 2a^2,\quad S_6 = 7a^2,\quad S_7 = a^2,\quad S_8 = 8a^2$$

The area of the whole polygonal section is:

Aria întregii secţiuni poligonale este:

$$S = \sum S_i = 36a^2 .$$

After some elementary operations, the coordinates of the center of mass are obtained:

După câteva calcule elementare rezultă coordonatele centrului de masă:

$$C(x_C = 1.426a, y_C = 6.556a)$$

The elements of the matrix of inertia can be also easily calculated:

Elementele matricei de inerţie pot fi şi ele uşor calculate:

$$J_x = 44.39ma^4,\quad J_y = 3.037ma^4,\quad J_z = 47.333ma^4,$$

$$J_{xy} = 6{,}093ma^4,\quad J_{yz} = J_{zx} = 0 .$$

Application 2
Let $OA_1A_2A_3A_4A_5A_6$ be a homogeneous plate of mass *m*, part of the header of a corn-picker-husker, with the shape of a pyramid surface (fig. **3**).

Aplicaţia 2
Fie placa omogenă de masă *m*, din componenţa unui heder al unei combine de recoltat porumb, care are forma unei suprafeţe piramidale $OA_1A_2A_3A_4A_5A_6$ (fig. **3**).

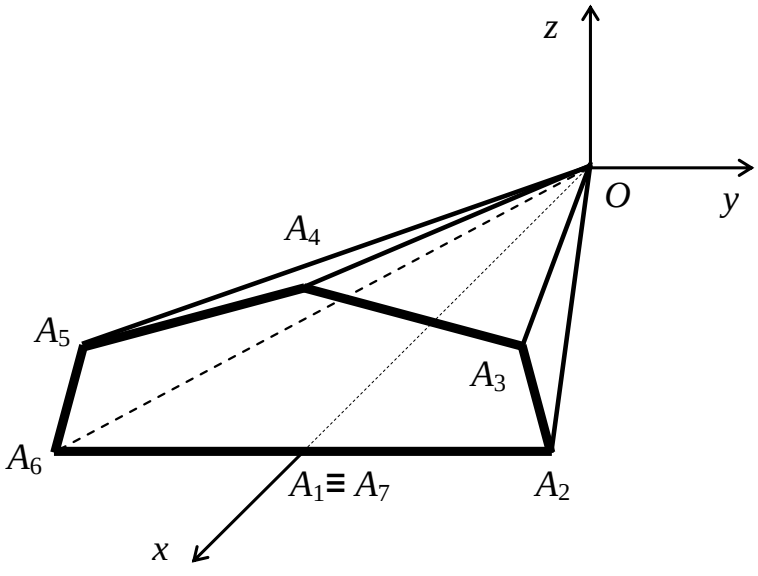

Fig. 3 - Header of a corn-picker-husker

The orthogonal reference system with plane *Oxy* situated in the plane of the plate OA_1A_2 is used, with axis *Ox* in the symmetry plane of the body, perpendicular on the side A_2A_6.
The plate is divided into six triangles: OA_1A_2, OA_2A_3,…, OA_6A_7.
The coordinates of the corners of the surface are: *O*(0, 0, 0), A_1(*l,* 0, 0), A_2(*l*, *a*, 0), A_3(*l*, *a-b*, *c*), A_4(*l*, 0, *d*), A_5(*l, b-a, c*), A_6(*l, -a,* 0) and $A_7 \equiv A_1$(*l,* 0, 0).

Se utilizează sistemul de referinţă ortogonal, cu planul *Oxy* situat în planul plăcii OA_1A_2, alegându-se axa *Ox* în planul de simetrie al corpului, perpendiculară pe latura A_2A_6.
Placa se împarte în şase triunghiuri: OA_1A_2, OA_2A_3,…, OA_6A_7.
Coordonatele vârfurilor suprafeţei sunt: *O*(0, 0, 0), A_1(*l,* 0, 0), A_2(*l*, *a*, 0), A_3(*l*, *a-b*, *c*), A_4(*l*, 0, *d*), A_5(*l, b-a, c*), A_6(*l, -a,* 0) şi $A_7 \equiv A_1$(*l,* 0, 0).

According to formula (10), the areas of the triangles composing the body are

Conform formulei (10), ariile triunghiurilor care compun corpul sunt:

$$S_1 = S_6 = \frac{la}{2}, \quad S_2 = S_5 = \frac{\sqrt{a^2c^2 + l^2(b^2 + c^2)}}{2}, \quad S_3 = S_4 = \frac{\sqrt{(a-b)^2(d^2 + l^2) + l^2(c^2 - d^2)}}{2}$$

By replacing the particular values of the studied body into relation (13), the following coordinates of the mass center are obtained:

Înlocuind valorile particulare ale corpului studiat în relaţiile (13), se obţin următoarele coordonate ale centrului de masă:

$$x_C = \frac{2l}{3}, \quad y_C = 0, \quad z_C = \frac{2}{3} \cdot \frac{cS_2 + (c+d)S_3}{\sum_{i=1}^{6} S_i}$$

Case of an arbitrary homogeneous quadrilateral

The homogeneous plate described by quadrilateral $OA_1A_2A_3$, situated in plane Oxy, is considered (Fig.4a). The plate is divided into triangles OA_1A_2 and OA_2A_3.

The coordinates of the corners are known: $O(0, 0, 0)$, $A_1(x_1, 0, 0)$, $A_2(x_2, y_2, 0)$, $A_3(x_3, y_3, 0)$.

Cazul patrulaterului omogen oarecare

Se consideră placa omogenă plană descrisă de patrulaterul $OA_1A_2A_3$, situată în planul Oxy (fig.4a). Placa se împarte în triunghiurile OA_1A_2 şi OA_2A_3.

Sunt cunoscute coordonatele punctelor plăcii: $O(0, 0, 0)$, $A_1(x_1, 0, 0)$, $A_2(x_2, y_2, 0)$, $A_3(x_3, y_3, 0)$.

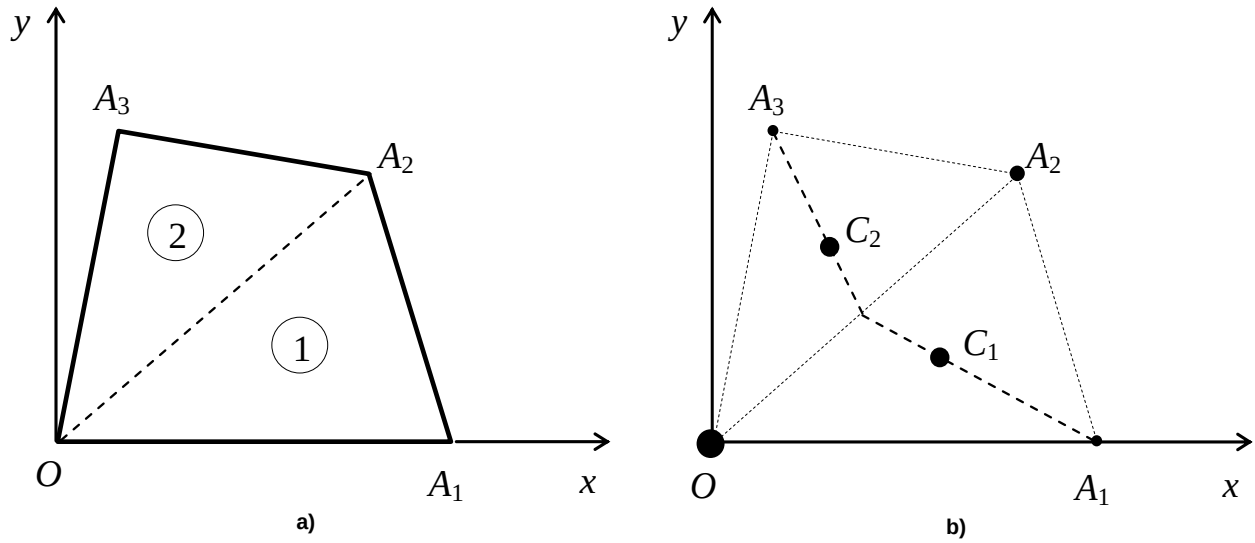

Fig. 4 - Homogeneous plate with the shape of an arbitrary quadrilateral

The areas have the expressions

Ariile au expresiile

$$S_1 = x_1 y_2, \quad S_2 = |x_2 y_3 - x_3 y_2|, \quad S = x_1 y_2 + |x_2 y_3 - x_3 y_2| \tag{21}$$

The superficial density is

Densitatea superficială este

$$\rho_s = \frac{m}{S} \tag{22}$$

The masses of the two triangular plates are:

Masele celor două plăci triunghiulare sunt:

$$m_1 = \rho_s S_1 = \frac{m x_1 y_2}{x_1 y_2 + |x_2 y_3 - x_3 y_2|}, \quad m_2 = \rho_s S_2 = \frac{m|x_2 y_3 - x_3 y_2|}{x_1 y_2 + |x_2 y_3 - x_3 y_2|} \tag{23}$$

The coordinates of the mass centers of the two triangles can be easily calculated:

Coordonatele centrelor de masă ale celor două triunghiuri pot fi uşor calculate:

$$C_1\left(\frac{x_1 + x_2}{3}, \frac{y_2}{3}\right), \quad C_2\left(\frac{x_2 + x_3}{3}, \frac{y_2 + y_3}{3}\right) \tag{24}$$

By taking into account the presented results, it can be concluded that an arbitrary quadrilateral may be reduced to a system of six material points, with the following masses (fig. **4**b): $O\left(\frac{m}{12}\right)$, $A_1\left(\frac{m_1}{12}\right)$, $A_2\left(\frac{m}{12}\right)$, $A_3\left(\frac{m_2}{12}\right)$, $C_1\left(\frac{3m_1}{4}\right)$, $C_2\left(\frac{3m_2}{4}\right)$.

Luând în considerare rezultatele prezentate, se desprinde concluzia că un patrulater oarecare poate fi redus la un sistem de şase puncte materiale, cu următoarele mase (fig. **4**b): $O\left(\frac{m}{12}\right)$, $A_1\left(\frac{m_1}{12}\right)$, $A_2\left(\frac{m}{12}\right)$, $A_3\left(\frac{m_2}{12}\right)$, $C_1\left(\frac{3m_1}{4}\right)$, $C_2\left(\frac{3m_2}{4}\right)$.

The coordinates of the mass center of the quadrilateral are:

Coordonatele centrului de masă ale patrulaterului sunt:

$$x_C = \frac{\sum m_i x_i}{m} = \frac{1}{3}\left(x_2 + \frac{m_1 x_1 + m_2 x_3}{m}\right), \quad y_C = \frac{\sum m_i y_i}{m} = \frac{1}{3}\left(y_2 + \frac{m_2 y_3}{m}\right). \tag{25}$$

The moments and products of inertia with respect to the chosen reference system take, respectively, the forms:

Momentele de inerţie în raport cu sistemul de referinţă ales iau, respectiv, formele:

$$\begin{cases} J_x = \sum m_i y_i^2 = \frac{1}{6}\left[m y_2^2 + m_2 y_3 (y_2 + y_3)\right] \\ J_y = \sum m_i x_i^2 = \frac{1}{6}\left[m x_2^2 + m_1 x_1 (x_1 + x_2) + m_2 x_3 (x_2 + x_3)\right] \\ J_z = J_x + J_y, \end{cases} \tag{26}$$

$$\begin{cases} J_{xy} = \sum m_i x_i y_i = \frac{1}{12}\left[2m x_2 y_2 + m_1 x_1 y_2 + m_2 (x_2 y_3 + x_3 y_2 + 2 x_3 y_3)\right] \\ J_{yz} = 0 \\ J_{zx} = 0. \end{cases} \tag{27}$$

Case of a right-angled trapezoid

A right-angled trapezoid is represented in Figure 5, corresponding to a homogeneous plate of mass *m*, with the following geometrical characteristics: the large base *B*, the small base *b* and the height *h*.

Cazul trapezului dreptunghic

În figura 5 este reprezentat trapezul dreptunghic corespunzător unei plăci omogene de masă *m*, cu următoarele caracteristici geometrice: baza mare *B*, baza mică *b* şi înălţimea *h*.

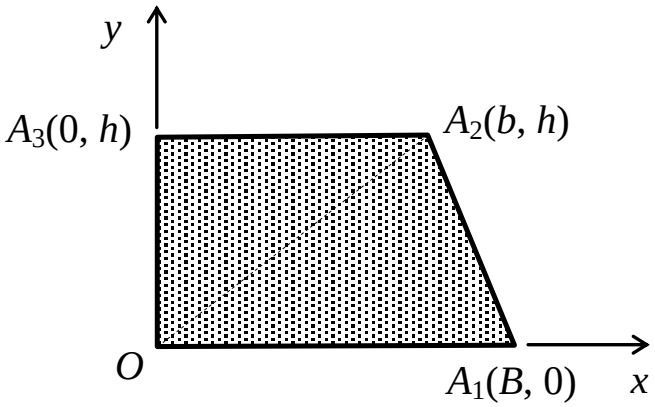

Fig. 5 - Homogeneous plate with the shape of a right-angled trapezoid

According to relations (10) and (12), the masses of the two composing triangles are:

În conformitate cu relaţiile (10) şi (12), masele celor două triunghiuri componente sunt:

$$m_1 = \frac{mB}{B+b}, \quad m_2 = \frac{mb}{B+b} \tag{28}$$

By applying relations (3), the coordinates of the mass center can be calculated:

Aplicând relaţiile (3), se calculează coordonatele centrului de masă:

$$x_C = \frac{B^2 + Bb + b^2}{3(B+b)}, \quad y_C = \frac{h(B+2b)}{3(B+b)}. \tag{29}$$

The moments and products of inertia, determined by relations (6)- (7), have the following expressions:

Momentele de inerţie, determinate cu ajutorul relaţiilor (6)- (7), au următoarele expresii:

$$J_x = \frac{mh^2(B+3b)}{6(B+b)}, \quad J_y = \frac{m(B^2+b^2)}{6}, \quad J_z = \frac{m}{6}\left[\frac{h^2(B+3b)}{B+b} + B^2 + b^2\right] \tag{30}$$

$$J_{xy} = \frac{mh(3b^2 + B^2 + 2bB)}{12(B+b)}, \quad J_{yz} = 0, \quad J_{zx} = 0 \tag{31}$$

CONCLUSIONS

The presented method allows a fast calculation of the inertia characteristics of a plate with concurrent bending edges, as well as of a plane plate with polygonal shape and, in particular, of a quadrilateral one.
The method, which can be easily implemented in a computer code, represents a useful tool in machine and mechanical device design activity.
The two chosen applications certify for its benefits.

REFERENCES

[1]. Craifaleanu A., (2001) – *Dynamics for engineers* (in Romanian), PRINTECH Publishing House, Bucharest;
[2]. Orăşanu N., (2009) – *The reduction of continuous bodies to a system of the material points. Applications on regular polygons*, National Conference on Mechanics of Solids - CNMS-XXXIII, Bucharest.
[3]. Orăşanu N., (2010) – *Reduction of the elementary bodies to systems of material points with the same inertial proprieties*, University "Politehnica" of Bucharest Scientific Bulletin, Series D: Mechanical Engineering, Vol.72, Issue 3.

CONCLUZII

Metoda prezentată permite calculul rapid al caracteristicilor inerţiale ale unei plăci cu muchii de îndoire concurente, precum şi al unor plăci plane de forme poligonale şi, în particular, de formă patrulateră.
Metoda, care poate fi uşor implementată în programe de calcul automat, reprezintă un instrument valoros în activitatea de proiectare a maşinilor şi utilajelor mecanice. Cele două aplicaţii alese atestă avantajele sale.

BIBLIOGRAFIE

[1]. Craifaleanu A., (2001) – *Dinamica pentru ingineri*, Ed. PRINTECH, Bucureşti.
[2]. Orăşanu N., (2009) – *Reducerea corpurilor continue la un sistem de puncte materiale. Aplicaţii la poligoane regulate* (în limba engleză), Conferinţa Naţională de Mecanica Solidului - CNMS-XXXIII, Bucureşti.
[3]. Orăşanu N., (2010) – *Reducerea corpurilor elementare la sisteme de puncte materiale cu aceleaşi proprietăţi inerţiale* (în limba engleză), Buletinul ştiinţific al Universităţii "Politehnica" din Bucureşti, Seria D: Inginerie Mecanică, Vol.72, nr.3.

STUDY ON THE DEVELOPMENTAL EFFICIENCY EVALUATION OF RURAL INFORMATIZATION IN CHINA AND ITS INFLUENCE FACTOR ANALYSIS
/
中国农村信息化发展效率测度及影响因素分析

Prof. Ph.D. Tao Tian[1)], Prof. Xiaochun Xu[1)*], Prof. Ph.D. Pengling Liu[1)], Sn. Engr. Chung-chia Lee [2)]
[1)] College of Economics and Management, Anhui Agricultural University, Hefei / China;
[2)] Hong Kong Polytechnic University, Kowloon / Hong Kong
Tel: +86-0551-65786359; E-mail: xxc@ahau.edu.cn

Abstract: *Rural informatization is an inevitable requirement of agricultural development. In the paper a two-phase model with DEA-Tobit was adopted to analyze the developmental efficiency and the influencing factors of rural informatization in China during 2007-2010. The results showed that, on the whole, the overall developmental efficiency of rural informatization in the Middle and Northwest China was lower than that in other regions of China. In addition, the decisive influencing factors on developmental efficiency of rural informatization were resulted from the nation's macro policy and the global construction of rural informatization projects. The level difference in regional economic development was the main reason for the variation in developmental efficiency. Moreover, the structure and level of consumption by rural residents was an important source that had affected the developmental efficiency. Furthermore, the age of rural population and the education level had a significant influence on the developmental efficiency of rural informatization.*

Keywords: *Rural Informatization; Developmental Efficiency; DEA; Tobit Model*

INTRODUCTION

With the development of information technology and the advance of agricultural globalization, governments all over the world have attached great importance to the development of rural informatization. Since the 21st century, rural informatization has been a continual concern by Chinese central government in its No. 1 Document. Rural informatization has been comprehensively organized, promoted and implemented by the central government and institutional sectors at all levels, therefore great progress has been made in rural informatization. However, constrained by various factors such as lack of technical equipment, funding and human resources, the rural informatization in China is still less developed compared with other countries in the world (see Table 1). What is the status quo of rural informatization? What factors influence the development of rural informatization? Study and answer of these two questions will contribute to a reasonable resource allocation, the structural optimization of construction and improvements to management strategy when further studying the development of rural informatization.

摘要：*农村信息化是现代农业发展的必然要求。本文运用DEA-Tobit两阶段法对2007-2010年间中国农村信息化发展效率及影响因素进行了研究分析，研究发现，整体上来看，中部和东北地区的农村信息化整体发展效率低于全国其他区域；农村信息化发展效率的决定性影响因素源于国家全局性农村信息化宏观政策及全局性农村信息化项目的建设；地区经济发展水平差异是造成发展效率差异的原因；农村居民消费结构和消费水平是影响发展效率的重要原因；农村人口年龄和文化程度结构同样显著影响农村信息化发展效率。*

关键词：*农村信息化; 发展效率; DEA; Tobit模型*

引言

随着信息技术的发展和农业全球化浪潮的推进，各国对农村信息化的重视正与日俱增。进入新世纪以来，中国政府一号文件持续关注农村信息化，政府及各机构部门组织、推动、实施的农村信息化建设全面展开，农村信息化取得了巨大的进步。然而由于存在技术设备、资金和人力资源等方面的制约，相对于世界其他国家，中国农村信息化发展仍然滞后（见表 1）。农村信息化目前的发展现状如何？哪些因素影响着农村信息化的发展？研究并回答这两个问题，有助于在农村信息化后续发展中合理配置资源、优化建设结构、完善管理策略，具有积极的现实意义。

Table 1

Characteristic and current status of rural informatization in 5 countries all over the world (2013)

Country	Infrastructure of informatization	Environment of informatization	Stage
United States	Powerful information infrastructure Internet access : 67 percent of the farms Computers per 100 farmers: 68	Adequate funds Perfect legislation Advanced modern information technology	Developed
France	Complete and sound infrastructure Internet access : 50 percent of the farmers	Multi-level pattern of rural information service Diversification of service provider Well-established policy environment	Developed
Japan	Complete rural information infrastructure Computers per 100 farmers: 34 Internet access : 12 percent of the farmers	Government-led investment Focus on the construction of information systems services	Developed

Country	Infrastructure of informatization	Environment of informatization	Stage
India	Imperfect Infrastructure Low popularizing rate of telephone and computer Telephones per 100 farmers:39.29 Wireless users: 345.85 million farmers	Developing the application of agricultural information service Public-private partnerships Priority to the development strategy of Rural informatization Extra subsidy	Developing
China	Inadequate infrastructure Rapidly increasing Fixed telephones per 100 farmers:42.2 Computers per 100 farmers: 21.4	Government-led investment Mobilizing all positive senses of farmers Focus on the development of network system and database construction Extra subsidy	Developing

Sources: U.S. Department of Agriculture [11]; European Commission[1]; Ministry of Agriculture, Forestry and Fisheries of Japan [7]; Ministry of Agriculture of India[8]; National Bureau of Statistics of China[10].
Note: According to present research achievements [4-5], the indexes system for the measurement of rural informatization level consists of six categories of the resources, infrastructure, technology application, industry, human resource and external environment of rural informatization. In Table 1, this paper chooses three indicators of infrastructure, technology application and external environment to analyze and compare characteristic and current status of rural informatization in 5 countries all over the world.

To date, studies on rural informatization of China can be grouped into the following aspects: 1) theoretical studies of strategies and suggestions for rural informatization development, which includes the improvement of the policy system for rural informatization development (Yang Cheng, 2009)[13] and the market development strategies for rural informatization products (Ma Mingyuan et al., 2009)[9]; 2) comparative studies of rural informatization in China and abroad about domestic and overseas experiences and lessons in rural informatization development, and the advantages in Chinese rural informatization process (He Hongming et al., 2011)[2]; 3) detailed technical frameworks and schemes, in which the platform construction of rural informatization is discussed (Zhou Wei, 2011)[14]. This part emphasizes on technology although literature for reference is lacking; and 4) evaluative studies on rural informatization construction. As rural informatization construction has further deepened, literature in this area has also increased; however, most studies are restricted to the evaluation index system of rural informatization and comparison among different levels of informatization in different regions on the basis of the evaluation index system(Zhou yuefeng, et al., 2011)[15]. It is noteworthy that only a small number of studies analyzed influencing factors in rural informatization. The specific methods employed in these studies include regression analysis (Liu Chunnian et al., 2006)[6], grey relational analysis (Wang Shuangying, 2008)[12], and factor analysis (Zhao Hui et al., 2010)[16]. Other studies in this area have characterized rural informatization as a social economic phenomenon and discussed the relationship between rural informatization and other social phenomena, e.g., the relationship between rural informatization and rural income (Zeng Shuoxun et al., 2010)[17], the relationship between rural informatization and economic development (Huang Zhiwen)[3], and the effects of rural informatization on improving farmers livelihoods (Zhang Li et al., 2011) [18] etc.

The paper belongs to the fourth aspect above. Through analysis of the existing literature, it can be found that the method of subjective model analysis is applied to most current studies and the selection of model indexes and the determination of index weights differ largely from each other. Therefore the result of previous studies lacks reliability and is less convincing. In this study, the widely used two-phase analysis method is adopted in related studies. In Phase I, the output-oriented CCR Model from DEA (Data Envelopment Analysis) method is used in order to measure the overall efficiency of rural informatization; in Phase II, Tobit regression model is used in order to empirically test the influencing factors of developmental efficiency of rural informatization and to carry out a systematic analysis.

目前中国农村信息化研究大致可分为以下几个方面：一是关于农村信息化发展对策建议的理论研究。这方面研究的内容涉及农村信息化发展政策体系的完善（杨诚，2009）[13]，农村信息化产品市场发展政策（马明远等，2009）[9]等；二是关于中国与国外农村信息化的比较研究，讨论国外农村信息化建设的经验与教训，探讨在中国农村信息化建设过程中的可资借鉴之处（贺洪明等，2011）[2]；三是关于农村信息化发展的具体技术框架及方案，讨论农村信息化平台建设（周卫，2011）[14]等等，这部分研究技术色彩较重，文献数量不多；四是对农村信息化建设状况进行评估研究。随着农村信息化建设的深入，此方面的研究文献在最近几年开始增加，其中大多数研究限于讨论农村信息化评价指标体系并在此基础上进行不同地区信息化发展水平的比较（周跃锋等，2010）[15]，只有少数研究同时进行了影响信息化发展因素的分析，具体分析方法包括回归分析法（刘春年等，2006）[6]，灰关联分析法（王爽英，2008）[12]，因子分析法（赵晖等，2010）[16]等。其他关于农村信息化的研究是把农村信息化作为社会经济现象，讨论它与其他社会经济现象之间的关联关系，如农村信息化与农户收入的关系（曾硕勋等，2010）[17]，农村信息化与经济发展的关系（黄志文，2010）[3]，农村信息化对农民生计改善的影响（张莉等，2011）[18]等等。

本文的研究可归为上述第四个方面，分析现有文献发现，现有研究大多采用的是主观模型分析方法，模型指标的选择和指标权重的确定都存在较大差异，研究结论存在可信度和说服力的欠缺。本文拟采用成熟的 DEA-Tobit 两阶段分析方法进行相关研究，第一阶段首先利用 DEA（Data Envelopment Analysis，数据包络分析）方法中产出导向的 CCR 模型测算农村信息化发展整体效率，第二阶段应用 Tobit 回归模型，实证检验影响农村信息化发展效率的因素并进行系统的分析。

METHODS AND MATERIALS

Research methods and index data

The DEA method is a nonparametric evaluating method that uses a mathematical programming model to measure the relative efficiency of DMUs (Decision Making Units) in multi-input and multi-output situations. By observing numerous and practical production data, we construct a relatively effective frontier efficiency surface, and then calculate efficiency level of the preset DMU relative to the efficiency level on the efficiency surface, i.e., the preset DMU's relative efficiency value. As a nonparametric method, the DEA method neither needs specific production function specifying its input and output, nor considering the efficiency of parameter estimation and reasonable inspection. This method has an advantage when evaluating the efficiency of DEA in complicated productive relations. Moreover, in the DEA model, the input and output variables' weights are produced by mathematical programming precisely according to practical data, the result of which cannot be affected by human factors. Therefore, the DEA method is often applied to studies of developmental efficiency of rural informatization, and furthermore it has advantages over most current methods.

By analyzing slack variables of input and output, the DEA method could determine the degree of the effect of the input and output factors on its efficiency and improvement approaches. However, with regard to factors that are not appropriate as input and output indexes, but that have objectively affected DMU efficiency, the DEA method could not directly analyze the effects of these factors on efficiency. Therefore, on the basis of the DEA method, a two-phase method is developed. In Phase I, the relative efficiency value of DMU is calculated by the DEA model. In Phase II a regression model is constructed to analyze data with the efficiency value obtained in Phase I as an explained variable and influencing factor on external environment as an explanatory variable. Due to the fact that the efficiency value calculated by the usual DEA method is between 0 and 1 (maximum 1), the explained variable of the regression equation in Phase II is restricted to this interval. Since it has a censored feature, Tobit regression model is usually selected.

The DEA-Tobit two-phase method is a mature approach when analyzing efficiency and influencing factors. But it is not applied in studies of Chinese rural informatization. So in this paper, the method is employed to study Chinese rural informatization development so as to improve current methods and compensate for present deficiencies.

According to the DEA-Tobit two-phase requirement, corresponding indexes are selected for different phases. Rural informatization could be regarded as a productive system, in which the investment in certain production resources should lead to corresponding economic and social output. Therefore, in the analysis phase of DEA, output and input indexes are usually selected. With present research achievements and informatization development index of the International Telecommunication Union as references, DEA indexes for this study are selected. See Table 2.

研究方法与材料

研究方法与指标数据

DEA 方法是一种利用数学规划模型在多投入多产出情况下测算 DMU（Decision Making Units，决策单元）相对效率的非参数评估方法，通过观测到的大量生产实践数据，构建出相对有效的前沿效率面，然后计算出某个给定 DMU 相对于那些处于效率面的 DMU 的效率水平，即该给定 DMU 的相对效率值。作为一种非参数方法，DEA 方法不需要指定投入产出的具体生产函数形态，也不需要考虑参数估计的有效性和合理性检验方面的问题，在评价具有非常复杂生产关系的决策单元的效率时具有优势，DEA 模型中投入、产出变量的权重由数学规划严格根据实际数据产生，不存在人为因素的影响。可见，DEA 方法不仅适用于研究农村信息化发展效率，而且相对目前大多数研究采用的方法具有优势。

DEA 方法可以进一步通过投入产出数据的差额变量分析，确定投入产出因素对效率的影响程度及改进途径，但对于某些不适合作为投入产出指标却客观影响 DMU 效率的因素，DEA 方法不能直接分析这些因素对效率的影响，因此在 DEA 方法的基础上发展出现了“两阶段法”，该方法第一阶段先通过 DEA 模型测算出 DMU 的相对效率值，第二阶段以第一阶段得到的效率值作为被解释变量，以外部环境影响因素等作为解释变量建立回归模型进行分析。由于常见的 DEA 方法测算出来的效率值都处于 0 和 1 之间，最大值为 1，第二阶段回归方程的被解释变量就被限制在这个区间，具有截断（censored）特征，因此通常选择 Tobit 回归模型。

DEA-Tobit 两阶段法分析效率及其影响因素是成熟的分析方法，但在涉及中国农村信息化的研究中尚未得到应用。本文拟将该方法引入中国农村信息化发展研究，以改善研究方法，弥补现有研究中存在的不足。

根据 DEA-Tobit 两阶段研究需要，本文按照不同阶段的要求选择相应的指标项。农村信息化可以视为一个生产系统，投入一定的生产性资源要素带来相应的经济和社会产出，因此在 DEA 分析阶段，选择的是具有投入产出性质的指标，在参考借鉴了现有研究成果以及国际电信联盟信息化发展指数基础上，研究选择的 DEA 指标见表 2。

Table 2

The input and output indexes of DEA analysis

Index Category	Index Name
`Input Index	Consumption levels of rural residents in different regions
	Average living consumption of a rural family (transportation, communication, cultural and educational entertainment products and services) in different regions
	Employment numbers in telecommunication industry and other service industries of information transmission
	Expenditure on education, culture, media and finance in different regions

Index Category	Index Name
Output Index	Total investment in fixed assets of information transmission, computer services and software industry in different regions
	Average number of televisions by every 100 rural households in different regions
	Average number of home computers by every 100 rural households in different regions
	Average number of telephone s by every 100 rural households in different regions

In Tobit analysis, economic and social factors that affect developmental efficiency of rural informatization are of great concern. The World Bank has reported that the development of Chinese rural informatization mainly depends on the construction of informatization projects conducted and participated in by government and telecommunication enterprises. Thus, the paper put forward the following assumptions. The first is the assumption that various overall construction projects are important influencing factors in determining developmental efficiency of rural informatization. As there are no fundamental differences between these construction projects in different regions, they can be grouped as a comprehensive influencing factor, which is represented by a constant term in Tobit Model. The second is the assumption that the difference in developmental efficiency in different regions is mainly affected by rural informatization consumption and regional levels in economic development. Specific indexes and descriptions of corresponding theoretical assumption are shown in Table 3.

在 Tobit 分析阶段，研究关注的是哪些经济社会因素影响着农村信息化的发展效率。根据世界银行的研究报告，中国农村信息化的发展，主要是依靠一系列中央政府和基础电信企业主导和参与的信息化项目的建设。据此本文提出以下假设：假设各种全局性项目建设是决定农村信息化发展效率的重要影响因素，由于这些项目建设不存在地区之间的根本性差异，因此归纳为一个综合性影响因素，通过 Tobit 模型中的常数项表示；假设地区之间的发展效率差异，主要受农村信息化消费和地区经济发展水平影响，具体指标和相应的理论假设描述见表 3。

Table 3

Explanatory variable indexes of Tobit regression analysis

Index	Assumption
Total dependency proportion of rural population	Rural population age structure is related to developmental efficiency of rural informatization
Proportion of education level (junior high schools and below) of labor force in rural households	Education level is related to developmental efficiency of rural informatization
Final consumption expenditure of rural residents	Consumption ability of informatization is related to developmental efficiency of rural informatization
Proportion of the primary industry's employment in all employments	Economic development level is related to developmental efficiency of rural informatization
Proportion of primary industry's total output value in regional total output value	

According to the assumptions above, an empirical Tobit regression model is established as follows:

根据以上假设确定实证 Tobit 回归模型如下：

$$Y_{it} = \beta_0 + \beta_1 DR_{it} + \beta_2 EDU_{it} + \beta_3 Ln(CE_{it}) + \beta_4 EP_{it} + \beta_5 VA_{it} + \varepsilon_{it} \quad (1)$$

In this model, *t* represents Year; *i* represents DMU; Y_{it}, the overall relative efficiency value of different regions and years in Phase I; DR_{it}, the total dependency proportion of rural population; EDU_{it}, the Proportion of education level; CE_{it}, final consumption expenditure; EP_{it}, proportion of primary industry employment in all employment; VA_{it}, proportion of primary industry's employment in all employments; β_1 to β_5 are regression coefficients of corresponding explanatory variables; β_0, a constant term; ε_{it}, a residual term. A logarithmic transformation of rural residents' final consumption expenditure index data is conducted to facilitate the explanation of model measurement results and to ensure a good fit.

其中，*t* 表示年份，*i* 表示 DMU，Y_{it} 为第一阶段得到的各地区各年整体相对效率值，DR_{it} 为农村人口总抚养比，EDU_{it} 为文化程度比重，CE_{it} 为最终消费支出，EP_{it} 为第一产业人员占就业人员比重，VA_{it} 为第一产业增加值占地区生产总值比重，β_1 至 β_5 为相应解释变量的回归系数，β_0 为常数项，ε_{it} 为残差项。为方便解释模型计量结果及保证拟合优度，对农村居民最终消费支出指标数据进行了对数转换。

研究基于公开数据进行，所有数据收集自《中国统计年

The study is based on public data, all of which have been collected from *China Statistical Yearbook, China Rural Statistical Yearbook, China City Statistical Yearbook, China Population and Employment Statistical Yearbook* and *China Information Yearbook*. Part of the data is from province and city statistical yearbooks and the survey report of rural internet development from China Internet Network Information Center.

RESULTS, ANALYSIS AND DISCUSSIONS

Empirical analysis

1) DEA analysis: study of the overall efficiency of rural informatization development

In this paper, the provincial administrative region is taken as the DMU of DEA analysis. Due to the restriction of data availability and integrity, Tibet, Taiwan, Hong Kong and Macao are not included.

Different DEA models can measure and decompose different relative efficiencies. However, this paper only involves the overall relative efficiency of rural informatization development, which can be obtained by CCR model. For now, the development strategy of urban-rural integration has been determined, but there are still big differences between rural and urban informatization both now and in the future. So the key to studies of rural informatization development is to improve output ability as much as possible under the constraints of fixed resources or in the situation of maintaining the present input level and environment; thus an output-oriented model is adopted.

鉴》、《中国农村统计年鉴》、《中国城市统计年鉴》、《中国人口和就业统计年鉴》和《中国信息年鉴》，部分数据来自各省市统计年鉴和中国互联网络信息中心农村互联网发展状况调查报告。

结果分析与讨论

实证分析

1)DEA 分析：农村信息化发展整体效率研究

本文将省级行政区作为 DEA 分析的 DMU，受数据可得性和完整性限制，研究不包括西藏、台湾、香港和澳门地区。

不同的 DEA 模型能够测算分解出不同的相对效率，而本文研究只涉及农村信息化发展的整体相对效率，通过 CCR 模型就可以直接得到。同时，在城乡一体化发展战略已经确定，而城乡信息化差距仍然较大的现实状况下，现阶段乃至今后相当长的一段时期，研究农村信息化发展首要是关注在既定的资源约束条件下，或在维持现有水平的投入和环境的情况下，尽可能提高产出水平，因而模型采用产出导向形式。

Table 4

The overall developmental efficiencies of China rural informatization in different regions during 2007-2010

DMU		2007	2008	2009	2010	DMU		2007	2008	2009	2010
East	Beijing	1	1	1	1	West	Inner Mongolia	0.6541	0.6515	0.6290	0.6344
	Tianjin	1	1	0.9610	0.9676		Guangxi	1	0.9805	1	1
	Hebei	0.8270	0.8852	1	1		Chongqing	1	0.9128	0.8835	0.9482
	Shanghai	1	1	1	1		Sichuan	1	1	0.9133	0.8689
	Jiangsu	0.9436	0.6522	0.6062	0.5976		Guizhou	1	1	1	0.9875
	Zhejiang	0.8850	0.9631	1	0.9752		Yunnan	0.8047	0.8772	0.8162	0.8211
	Fujian	1	1	1	1		Shaanxi	1	1	1	0.9801
	Shandong	0.7364	0.7435	0.7905	0.9198		Gansu	1	1	1	1
	Guangdong	1	1	1	1		Qinghai	1	1	1	1
	Hainan	1	0.9375	0.9272	0.9502		Ningxia	1	1	1	1
Average value		0.9392	0.9181	0.9285	0.9410		Xinjiang	0.8835	0.8614	0.8641	0.8301
Standard deviation		0.0936	0.1239	0.1311	0.1237	Average value		0.9402	0.9349	0.9187	0.9155
Middle	Shanxi	0.8888	0.8797	0.8943	0.8424	Standard deviation		0.1149	0.1082	0.1176	0.1168
	Anhui	0.9373	0.9235	0.8396	0.8818	Northwest	Liaoning	0.7823	0.7427	0.6883	0.7131
	Jiangxi	0.9089	0.8321	0.9136	0.8934		Jilin	0.8895	0.8453	0.7861	0.7835
	Henan	0.9205	0.8938	0.8903	0.8905		Heilongjiang	0.9040	0.8409	0.8520	0.9169
	Hubei	0.8692	0.8569	0.9142	0.9544	Average value		0.8586	0.8096	0.7755	0.8045
	Hunan	0.7051	0.7062	0.7221	0.7363	Standard deviation		0.0665	0.0580	0.0824	0.1035
Average value		0.8716	0.8487	0.8624	0.8665						
Deviation		0.0850	0.0765	0.0739	0.0732						

It can be seen in DEA analysis that developmental efficiencies of rural informatization in the middle and northeast regions are lower than that of the east and west regions. Observation of standard deviations of the developmental efficiency in different provinces and cities also finds that rural informatization of provinces and cities

DEA 分析发现，中部和东北地区的农村信息化发展效率低于东部和西部地区。观察各区域内不同省区市之间发展效率的标准差，又可以发现中部和东北地区各省区市农村

in the middle regions is close to that of the northeast regions, and its difference is lower than that of provinces and cities in the east and west regions.

The Kruskal-Wallis Regional Difference Test is conducted to learn China's developmental efficiency of rural informatization in different regions. However, the data need to be regrouped to avoid a distortion of results due to insufficient sample sizes of a group. China has successively developed and strengthened its macro development strategies in different regions, e.g., East Open, West Development, Northeast Promote and Rising of Central China. The strategies and corresponding preferential policies, project construction as well as domestic and foreign investment promotion are the main reasons for social and economic development in different regions. Since 2005, divisions of Chinese economic regions in national statistics have been consistent with the divisions determined by the above strategies. In view of the actual influence of regional development strategies and the economic development levels in other provinces and cities, this paper incorporates the northeast region into the middle; and then conducts a difference test according to trichotomy of dividing the country to the east, the middle and the west.

信息化发展效率较为接近，差异程度小于东部和西部地区各省区市的差异程度。

进一步对中国不同区域农村信息化发展效率进行 Kruskal-Wallis 区域差异性检验。为避免分组样本容量不足导致检验结果失真，需要进行重新分组处理。中国先后确立实施了东部开放、西部开发、振兴东北和中部崛起的宏观区域发展战略，实践中这些战略及其相应的优惠政策、项目建设以及所带动国内外投资是决定区域社会经济发展的主要原因，自 2005 年起，国家统计资料中对中国经济区域的划分开始与以上战略所确定的区域划分保持一致。从区域发展战略实际影响的角度考虑，同时参考各省市经济发展水平，本文将东北地区并入中部地区，按照东部、中部和西部三分法划分全国区域进行差异性检验。

Table 5

An investigation of regional differences in Chinese developmental efficiency of rural informatization

Regional comparison	2007	2008	2009	2010
East-Middle	3.962(0.0465)**	4.947(0.0261)**	6.190(0.0128)**	7.844(0.0051)***
East-West	0.113(0.7372)	0.023(0.8791)	0.097(0.7549)	0.436(0.5093)
Middle-West	4.659(0.0309)**	6.653(0.0099)***	3.558(0.0592)*	2.944(0.0862)*
East-Middle-West	6.100(0.0474)**	7.920(0.0191)**	6.667(0.0357)**	7.373(0.0251)**

Notes: *, ** and *** represent 10%, 5%, and 1% significance levels of statistics respectively; the number in brackets is the p value.

At the national level, the investigation shows that differences are significant at the 5% level regarding the three regions' developmental efficiency of rural informatization. Further studies of differences show that there are significant differences between the west and the middle, the east and the middle regarding their developmental efficiencies. It can't be denied that there is no significant difference between the developmental efficiency of the east and west regions. In light of the relative average efficiency value of different regional development (Table 5), it is clear that the phenomenon of "central China subsidence" still exists in rural informatization development in 2007-2010.

在全国意义上，检验证明三个区域农村信息化发展效率的差异性在 5%水平上是显著的。继续进行两两差异性检验，结果发现，西部和中部，东部和中部发展效率都存在显著差异，东部和西部之间的发展效率，都不能拒绝二者无显著差异的假设。联系表 5 中不同区域发展相对效率均值的大小，可以发现，2007-2010 年期间，“中部塌陷”现象在农村信息化发展中也同样有所表现。

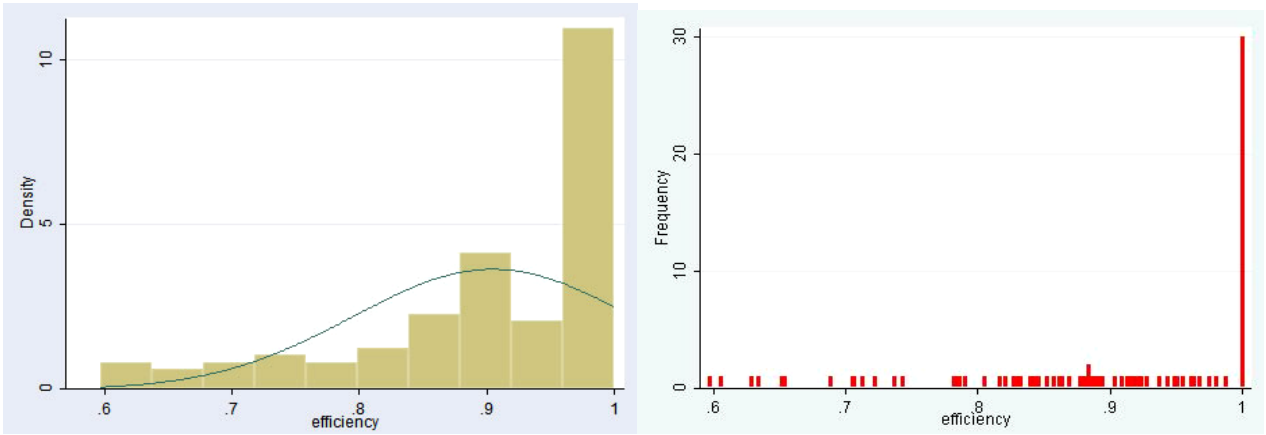

Fig.1 - Distribution and discrete option of developmental efficiency

2) Tobit regression analysis: the influencing factor analysis of developmental efficiency of rural informatization

This paper uses stata12.0 to carry out regression analysis and estimation.

Figure 1 depicts the distribution and discrete option of developmental efficiency of rural informatization. We can see the censoring in the data, because the efficiency values are bounded to the interval [0, 1]. In the right of discrete option, the spike is the frequencies for cases where efficiency=1. The relationship between developmental efficiency with explanatory variables is shown in Figure 2. The total dependency proportion of rural population seems to present a positive correlation with efficiency and other variables present a negative correlation.

Two indexes, i.e., the proportion of primary industry's employment in all employments and proportion of primary industry's total output value in regional total output value are similar indexes that reflect development level of economy. Although they can be used as explanatory variables for now, these two indexes cannot pass a multi-co-linearity examination. Therefore a different model is used for analysis. Regression results are shown in Models 1 and 2, Table 6. Model 3 is the regression results of the effects of rural informatization consumption factors on its developmental efficiency.

2) Tobit 回归分析：农村信息化发展效率影响因素分析

本研究运用 stata12.0 软件对模型及其统计数据进行回归分析和估计。

图 1 描述了农村信息化发展效率的分布和离散项，由于效率值被界定在 0 和 1 之间，可以看出数据截断的情况。在离散项最右边的那条竖线，是效率值等于 1 时的频数。图 2 反映的是发展效率与其他解释变量之间的关系。农村人口总抚养比与发展效率似乎呈正相关关系，其他变量则呈负相关关系。

第一产业就业人员占就业人员比重和第一产业生产总值占地区生产总值比重这两个指标，是反映经济发展水平的同类指标，这两个指标同时作为解释变量时不能通过多重共线性检验，因此使用不同模型进行分析，回归结果见表 6 中的模型 1 和模型 2。模型 3 是仅考察农村信息化消费因素对农村信息化发展效率影响的回归结果。

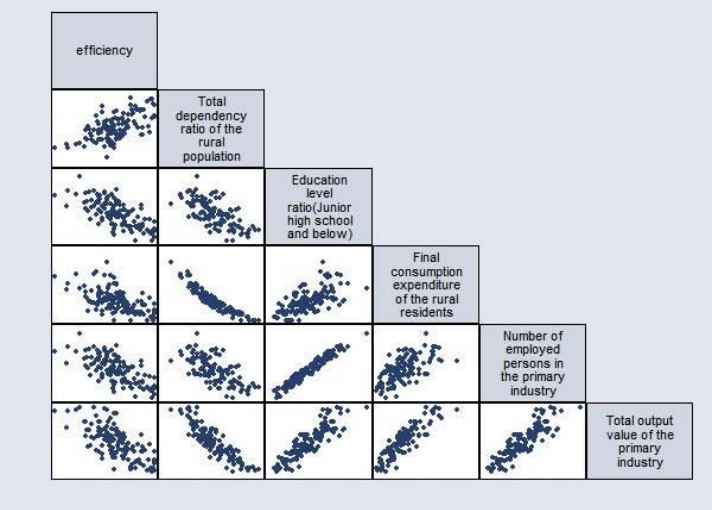

Fig.2 - The relationship between pairs of the six variables

Table 6

Tobit regression results of influencing factors on developmental efficiency of rural informatization

Explaining variable	Model 1	Model 2	Model 3
Total dependency proportion of rural population	1.358***	1.252***	1.002***
	(0.263)	(0.243)	(0.235)
Proportion of education level (Junior high school and below)	-0.950***	-0.638**	-1.152***
	(0.281)	(0.313)	(0.278)
Final consumption expenditure of the rural residents	-0.0873***	-0.0860***	-0.0840***
	(0.0170)	(0.0166)	(0.0168)
Proportion of the employed in primary industry		-0.432***	
		(0.145)	
Total output value of the primary industry	-0.884***		
	(0.296)		
Constant term	1.927***	1.759***	2.095***
	(0.261)	(0.270)	(0.257)
Sigma	0.129***	0.127***	0.133***

Explaining variable	Model 1	Model 2	Model 3
	(0.0113)	(0.0112)	(0.0117)
VIF average value	1.68	1.96	1.46
Log likelihood	18.63	18.47	14.14
LR chi2	52.52	52.19	43.53
Prob > chi2	1.08e-10	1.26e-10	1.90e-09
Pseudo R-squared	3.444	3.423	2.855

Notes: *, ** and *** represent 10%, 5% and 1% significance levels of statistics respectively; the number in brackets is the standard deviation.

In this paper, the proposed theoretical assumptions that the rural population age structure, education level of rural households, consumption ability and development level of economy are related to developmental efficiency of rural informatization are strongly supported by regression results and mainly stay at the 1% level which is statistically significant. The total dependency proportion of rural population and constant term present a positive correlation with developmental efficiency of rural informatization, whereas proportion of education level (Junior high school and below), final consumption expenditure of rural residents and proportion of the employed in the primary industry present a negative correlation with the total output value of the primary industry.

When comparing Models 1 and 2, it is found that as two indexes to measure regional economic development level, the proportion of the employed in the primary industry leads to less loss that affects developmental efficiency of rural informatization than that of the total output value of the primary industry. Moreover, the overall variation degree is much smaller whilst its reliability as an explanatory factor is bigger.

本文所作的农村人口年龄结构、农村居民家庭劳动力文化程度、消费能力、经济发展水平与农村信息化发展效率相关的理论假设，都得到了模型回归结果的稳健支持，并且基本上都在 1%水平上统计显著。其中，农村人口总抚养比和常数项与农村信息化发展效率呈现正相关关系，文化程度比重（初中及以下）、农村居民最终消费支出、第一产业就业人员比重和第一产业生产总值比重则呈现负相关关系。

比较模型 1 和模型 2 发现，作为衡量地区经济发展水平的两个指标，第一产业就业人员比重相对于第一产业生产总值比重，前者对导致农村信息化发展效率损失的影响程度要小于后者，并且总体上变异程度更小，解释可靠性更大。

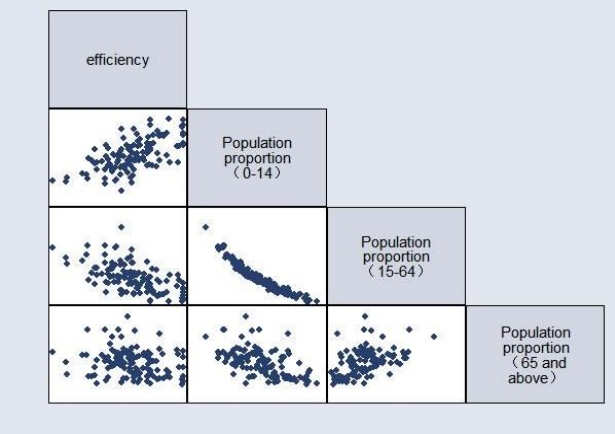

Fig.3 - The relationship between pairs of the efficiency and the structure of population age

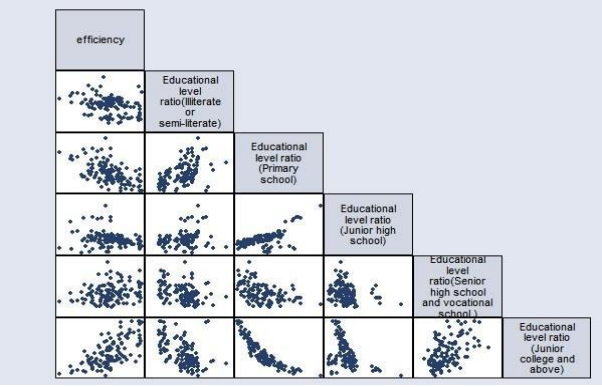

Fig.4 - The relationship between pairs of the efficiency and the structure of education level

From Figure 3 and 4, we can see the different structure of population age seems to have influence on developmental efficiency, the same as the structure of education level. Thus, based on the regression analysis in Table 6, and in order to further study the effects of consumption on developmental efficiency of rural informatization, a further regression analysis is carried out which decomposes the total dependency proportion of rural population and education level indexes. The results are shown in Tables 7 and 8 respectively.

通过图 3 和 4，我们发现不同的年龄结构和教育程度对于发展效率均会产生一定的影响。因此，为更深入研究消费因素对农村信息化发展效率的影响，在表 6 回归分析的基础上，进一步分解了农村人口总抚养比和文化程度比重指标进行回归分析，结果分别见表 7 和表 8。

Table 7

Tobit regression results of the effects of rural population's age structure on developmental efficiency of rural informatization

Explaining variable	Model 1	Model 2	Model 3	Model 4	Model 5	Model 6
Proportion of education level (Junior high school and below)	-1.305***	-1.091***	-0.637**	-0.726**	-0.650**	-0.443
	(0.278)	(0.267)	(0.283)	(0.299)	(0.314)	(0.344)
Final consumption expenditure of rural resident	-0.0687***	-0.0864***	-0.0827***	-0.0668***	-0.0882***	-0.0801***
	(0.0164)	(0.0168)	(0.0202)	(0.0160)	(0.0168)	(0.0203)
Proportion of the employed in primary industry				-0.521***	-0.338**	-0.155
				(0.145)	(0.140)	(0.160)
Population proportion from 0-14 years old	1.773***			2.326***		
	(0.367)			(0.388)		
Population proportion of 15-64 years old		-1.677***			-1.877***	
		(0.354)			(0.358)	
Population proportion of 65 years old and above			0.278			-0.0153
			(0.864)			(0.910)
Constant term	2.158***	3.637***	1.996***	1.766***	3.558***	1.905***
	(0.247)	(0.445)	(0.292)	(0.251)	(0.436)	(0.305)
Sigma	0.130***	0.131***	0.146***	0.122***	0.128***	0.145***
	(0.0114)	(0.0115)	(0.0129)	(0.0106)	(0.0111)	(0.0129)
VIF average value	1.63	1.39	1.32	2.14	1.82	1.78
Log likelihood	16.59	16.25	5.339	22.97	19.14	5.803
LR chi2	48.42	47.75	25.93	61.19	53.54	26.85
Prob > chi2	1.73e-10	2.40e-10	9.88e-06	0	6.58e-11	2.13e-05
Pseudo R-squared	3.175	3.132	1.700	4.013	3.511	1.761

Notes: *, ** and *** represent 10%, 5% and 1% significance levels of statistics respectively; the number in brackets is the standard deviation.

In Table 7, the results in Models 4, 5, 6 and those in Models 1, 2, 3 can verify each other, and the six models have verified the regression results of the proportion of education level (Junior high school and below), final consumption expenditure of rural residents, proportion of the employed in primary industry and the constant term in Table 6. Further analysis of the consumption population's age structure finds that the population proportion from 0-14 years old presents a positive correlation with developmental efficiency of rural informatization, whereas the population proportion from 15-64 years old presents a negative correlation. Both indexes are statistically significant at the 1% level; however statistic verification of population proportion of 65 years old and above is not statistically significant in Model 3 and 6. Moreover the goodness of fit in Models 3 and 6 is obviously lower than that of other models.

表 7 中的模型，模型 4、5、6 与模型 1、2、3 的结果可以互相验证，同时这 6 个模型又验证了表 6 中模型对文化程度比重（初中及以下）、农村居民最终消费支出、第一产业就业人员比重和常数项的回归结果。对消费人口年龄结构的更深入分析发现，0-14 岁人口比重与农村信息化发展效率呈现正相关，15-64 岁人口比重与农村信息化发展效率呈现负相关，这两个指标都在 1%水平上统计显著，而 65 岁及以上人口比重指标的统计检验在模型 3、6 中均不显著，并且模型 3、6 的拟合优度明显低于其他模型。

Table 8

Tobit regression results of the effects by education level on developmental efficiency of rural informatization

Explaining variable	Model 1	Model 2	Model 3	Model 4	Model 5
Proportion of population independency	0.267	0.826***	0.285	0.891***	1.036***
	(0.268)	(0.247)	(0.243)	(0.230)	(0.248)
Final consumption expenditure of rural residents	-0.0705***	-0.0855***	-0.0684***	-0.0858***	-0.0759***
	(0.0188)	(0.0175)	(0.0186)	(0.0169)	(0.0172)
Proportion of education level (Illiterate or semi-literate)	0.621				
	(0.439)				
Proportion of education level (Primary school)		-0.562**			
		(0.215)			
Proportion of education level (Junior high school)			-0.437*		
			(0.231)		
Proportion of education level (Senior high school and vocational school)				1.351***	
				(0.346)	
Proportion of education level (Junior college and above)					3.563***
					(1.097)
Constant term	1.277***	1.349***	1.522***	0.992***	0.993***
	(0.137)	(0.136)	(0.191)	(0.143)	(0.142)
sigma	0.144***	0.139***	0.144***	0.135***	0.136***
	(0.0128)	(0.0123)	(0.0128)	(0.0119)	(0.0119)
VIF average value	1.49	1.43	1.32	1.41	1.42
Log likelihood	5.307	7.626	6.099	12.09	13.37
LR chi2	25.86	30.50	27.45	39.43	41.98
Prob > chi2	1.02e-05	1.08e-06	4.75e-06	1.41e-08	4.05e-09
Pseudo R-squared	1.696	2.000	1.800	2.586	2.753

Notes: *, ** and *** represent 10%, 5% and 1% significance levels of statistics respectively; the number in brackets is the standard deviation.

Likewise, the regression results in Table 8 and those in Table 6 and 7 can verify each other. The results of the final consumption expenditure of rural residents and the constant term are highly consistent with each other. The regression results of different education levels show that, apart from the statistic non-significance at the illiterate and semi-literate education levels, education levels at 5% and 10% significance levels in primary schools and junior high schools retain a negative correlation with developmental efficiency of rural informatization. Senior high school, vocational school, junior college and above at the 1% significance level retains a positive correlation.

In the analysis of Tobit regression results, it can be seen that in all models the constant term passed the statistically significant verification at the 1% significance level. Further comparison of regression coefficients in various models shows that the constant term has the greatest influence on developmental efficiency of rural informatization. According to the theoretical assumptions above, the regression results show that with the macro policies aimed at strengthening agriculture and benefiting farmers during 2007-2010, various overall rural informatization development projects focused in infrastructure construction have been the main influencing factors in improving the overall developmental efficiency of rural informatization. About the development modes of China's rural informatization, the World Bank research report (2009) holds that the mode dominated by the Chinese central government has obvious and

表 8 中的模型回归结果同样能够与表 6 和表 7 中各模型结果互相验证，特别是对农村居民最终消费支出和常数项的结果高度一致。对不同文化程度分别回归的结果显示，除不识字或识字很少文化程度的统计不显著以外，小学、中学文化程度在 5%和 10%显著水平上与农村信息化发展效率呈现负相关，而高中和中专、大专及以上文化程度在 1%水平上与农村信息化发展效率呈现正相关。

分析以上 Tobit 回归结果，首先注意到在所有模型中，常数项均以 1%的水平通过统计显著性检验，进一步比较各模型中的回归系数，常数项对农村信息化发展效率值的影响也是最大的。按照前述理论假设，回归结果表明：2007-2010 年间，在中国惠农强农的宏观政策环境下，各种全局性的、主要集中在基础设施建设方面的农村信息化建设发展项目，是推动农村信息化整体发展效率提升的主要影响因素。世界银行研究报告（2009 年）在对中国农村信息化发展模式的分析研究中，认为中央政府主导模式具

practical advantages and a promotional value in future. The result can be verified by the result of this paper in this part.

Urbanization and industrialization would lead to inevitable loss of social and economic resources in rural areas. Although the present policies and measures set by non-market systems compensate for resource loss, the overall efficiency loss of resource allocation is inevitable. Research shows that the level of regional economic development presents a significantly negative correlation with the overall developmental efficiency of rural informatization. Since Chinese urbanization is generally lagging behind industrialization, the extent of influence that regional urbanization and industrialization have on the overall developmental efficiency of rural informatization also differs. The regression results show that relatively hysteretic urbanization avoids the rapid decline in rural population, thus stabilizing the number of consumption population of rural informatization. Under the condition of a vigorous national construction of infrastructure projects related to rural informatization, a quantitative balance between consumption and production could alleviate to a certain extent the negative effects by rural social and economic resource loss.

The rural residents' final consumption expenditure has a significantly negative correlation with developmental efficiency of rural informatization. During 2007-2010, the rural per capita net income and per capita annual living expenditure have increased by 12.69% and 10.79% respectively. About the expenditure constitution, consumption is inclined to be more material-oriented than spirit-oriented. Material consumption, represented by housing and household facilities, keeps increasing in absolute amount and in the proportion of all consumption. However, spiritual consumption, represented by cultural, educational and entertainment products and services, accounts for a smaller proportion of expenditure, and this trend continues to decrease. This indicates that the consumption structure of a Chinese rural resident is still at a low stage and is characterized by meeting basic needs, with food and shelter accounting for the most shares. In addition the infrastructure construction for rural informatization is still weak with insufficient basic services. Rural residents lack knowledge and skills of how to apply informatization. Inappropriate ideas and understanding, the unchanged traditional consumption structure, consumption custom and consumption mode all lead to insufficient informatization consumption.

The rural population structure correlates with the overall efficiency of informatization development. From the perspective of the population age structure, a large rural population outflow for work in urban areas aggravates the issues of the left-behind children and population aging. However, the demand of migrant workers contacting their hometown increases the demand of rural informatization consumption, which is a reasonable explanation for the regression results. From the perspective of the education level, the higher the education level is, the more it contributes to the developmental efficiency of rural informatization. The proportions of education levels at senior high school, vocational school and above are important factors of improving efficiency. Based on the common understanding that education level not only affects income but also influences consumption expenditure and structure, this paper assumes that a higher education level contributes to improving informatization consumption level and optimizing consumption structure appropriately, thus can improve the overall developmental efficiency of rural informatization.

有明显实践优势和未来推广价值，与本文此处的研究结论可以相互验证。

城市化和工业化必然带来农村社会经济资源的流失，虽然现有的各种非市场制度安排的政策措施对资源流失起到了补偿作用，但整体上出现资源配置效率损失是难免的，研究表明区域经济发展水平与农村信息化整体发展效率之间呈现显著负相关性。由于中国城市化普遍滞后于工业化，区域城市化和工业化水平对农村信息化整体发展效率的影响程度应存在差异，分析回归结果发现：城市化相对滞后，从另一角度看是避免了农村人口数量的快速下降，从而稳定了农村信息化的消费人口数量，在国家大力建设农村信息化基础设施的情形下，保持消费与生产之间数量上的相对平衡，在一定程度上缓解了农村社会经济资源流失产生的负面效应。

农村居民最终消费支出与农村信息化发展效率之间具有显著负相关性。2007-2010 年，农村居民人均纯收入和人均生活消费支出年均增速分别达到了 12.69%和 10.79%，从消费支出构成看，消费偏重于物质性消费，精神性消费少，以住房和家庭设备用品为代表的物质消费，在绝对量和所占消费支出的比重都呈增长趋势，文教娱乐用品及服务支出为代表的精神性消费不仅比重小，而且呈下降趋势，说明总体上中国农民的消费结构基本上仍然处于低级阶段，特征是满足基本生存需求，吃和住占主要份额。此外，农村信息化基础建设仍然比较薄弱，基础服务匮乏，农村居民信息化应用知识和技能欠缺，观念和认知偏差，变化不大的传统消费结构、消费习惯和消费模式等也造成信息化消费不足。

农村人口结构与信息化发展整体效率之间存在相关性。从人口年龄结构来看，农村劳动年龄人口的大量外出务工流出，加重了农村留守儿童和老龄化问题，外出务工人员与家乡之间的联系需要增加了农村信息化消费需求，这应该是对回归结果的一个合理解释；从文化程度结构来看，文化程度越高则对农村信息化发展效率的贡献程度就越大，其中高中和中专及以上文化程度比重是发展效率改善提高的显著因素，本文认为，基于文化程度不仅影响收入水平，而且影响消费支出和消费结构的普遍认知，较高的文化程度有助于提高信息化消费水平、合理优化消费结构，从而改善农村信息化整体发展效率。

CONCLUSIONS

Evaluation on the developmental efficiency of rural informatization is of great importance for improving the overall informatization level and optimizing the informatization input structure. In this paper, a CCR model of DEA is used to measure the developmental efficiency of Chinese rural informatization during 2007-2010. The results show that the developmental efficiencies in the middle and northeast regions are lower than those in the east and west regions. The Kruskal-Wallis difference investigation also indicates that there are significant differences of developmental efficiency between the east and west regions, and between the east and middle regions. The phenomenon of "central China subsidence" is clearly manifested in rural informatization. A Tobit analysis shows that the construction projects of rural informatization are the main influencing factor improving the overall developmental efficiency. Both the developmental level of regional economy and the final expenditure output of rural residents have negative correlation with the developmental efficiency of rural informatization. The structure of population age, the structure of education level and the overall developmental efficiency of informatization are all correlated with one another.

With regard to the strategies that could improve the developmental efficiency of rural informatization, one is to increase the overall construction of rural informatization infrastructure; the other is to supplement local projects according to different development levels in various regions. The construction of rural informatization conducted by the central government is the main reason for the great achievements in a short period. However, rural informatization is a complicated and comprehensive social project, and construction of infrastructure like information facilities and information services, is just one part of it. Therefore, a long-term development should be based on a sound market for rural informatization. Thus, to guarantee a healthy development of rural informatization, we should encourage a shift away from policy support to development of market consumption, enhance the level of rural informatization consumption and optimize the structure of consumption.

The methods used in this paper have great significance and implications for future studies of developmental efficiency of rural informatization in similar areas; however there is still room for further improvements and discussion on the study. For example, there are certain controversies over the selection of model variable indexes in the DEA analysis phases, and controversies over whether the index of education level and the variable index of information industry macro contribution should be included in evaluating informatization levels. Moreover, in the Tobit analysis phase, in light of the consumption environment and external macro development environment, certain representative influencing factors are selected in this paper, and the effects of the overall and regional factors on rural informatization are decomposed in the Tobit analysis. However, comprehensive external influencing factors can also be further divided in other manners, e.g., division of system factors and non-system factors, division of market factors and non-market factors. Other external influencing factors like differences in regional development strategy are also noteworthy. All of these factors are not considered in this paper, so they can be used for future in-depth researches.

结论

农村信息化发展效率评价对于提高农村信息化整体水平、优化农村信息化投入结构具有重要作用。本文运用 DEA 的 CCR 模型对 2007-2010 年间中国农村信息化发展效率进行了测度，研究发现，中部和东北地区的农村信息化发展效率低于东部和西部地区，Kruskal-Wallis 差异性检验显示，西部和中部，东部和中部发展效率都存在显著差异，“中部塌陷”现象在农村信息化发展表现明显；Tobit 分析表明，农村信息化建设发展项目是推动农村信息化整体发展效率提升的主要影响因素，区域经济发展水平、农村居民最终消费支出与农村信息化整体发展效率之间均呈现显著负相关性，人口年龄结构、文化程度结构与信息化整体发展效率之间存在相关性。

改善提高农村信息化发展效率的对策措施，首先仍然是继续加大全局性农村信息化基础设施建设，不同地区根据经济发展水平不同应实施地方性项目加以补充；中央政府主导的政策性农村信息化建设是在短期内取得巨大成就的主要原因，但农村信息化是一个复杂的社会化综合性工程，信息设施、信息服务等基础建设只是其中一部分内容，长期发展应建立在健全的农村信息化市场的基础上，因此要保证未来农村信息化的健康发展，应逐步从强调政策性供给转向同时重视发展市场消费需求、扩大农村信息化消费水平、优化消费结构。

本文的研究思路和方法对于深入进行农村信息化发展效率的相关研究具有一定的启示和借鉴意义。当然，本研究仍存在需要改进和讨论之处：DEA 分析阶段主要涉及模型变量指标的选取，在评价信息化水平中是否应该包括教育变量指标，信息产业宏观贡献变量指标等，有一定的争论；Tobit 分析阶段本文从消费环境和外部宏观发展环境角度选择了具代表性的影响因素指标，在模型分析中初步分解出全局性和地区性因素对农村信息化发展效率的影响，可以进一步考虑以其他方式细分外部综合性影响因素，如分为制度和非制度、市场和非市场因素，还可以考虑其他一些外部影响因素，如区域发展战略差异等，这些在本文中没有涉及，有继续深入研究的价值。

ACKNOWLEDGEMENT

The work is partially supported by the MOE (Ministry of Education in China) Project of Humanities and Social Sciences (Grant No.10YJC790174), Humanities and Social Sciences Key Program of Anhui Province: " Informatization of Farmers' Cooperatives: Institutional Arrangements, Organizational Behavior and Organizational Performance", Humanities and Social Sciences Program of Anhui Province, China (Grant No.SK2012B567) and the Soft Science Research Program of Anhui Province, China (Grant No.14020 52027).

REFERENCES

[1]. European Commission's Directorate-General for Agriculture and Rural Development., (2013) – *Rural Development in the European Union Statistical and Economic Information*. Available from: http://ec.europa.eu/agriculture/statistics/rural-development/2013/index_en.htm, Accessed on 20th June, 2014;
[2]. He H M., Xiao Y G., (2011) – *China and the United States: the Characteristics of Rural Informatization Comparative Study*. Library and Information, no.1, pp.82-85. (In Chinese)
[3]. Huang Z W., (2010) – *Empirical research of relationship between rural informatization and rural economic development*. Modern Agricultural Science and Technology, no.12, pp.332-334. (In Chinese)
[4]. Liu S H., (2007) – *Study on the Indicator System for Measuring the Rural Area Informatization Level in China*. Library and Information Service, vol.51, no.9, pp.33-36. (In Chinese)
[5]. Liu C., (2011) – *The myth of informatization in rural areas: The case of China's Sichuan province*. Government Information Quarterly, vol.29, no.1, pp.85-97.
[6]. Liu C N., Wang L., (2006) – *Measures and correlated factor analysis of China rural informatization level*. Science & Technology Progress and Policy, vol.23, no.12, pp.131-132. (In Chinese)
[7]. Ministry of Agriculture, Forestry and Fisheries of Japan, (2013) – *Annual Report on Food, Agriculture and Rural Areas in Japan*. Available from: http://www.maff.go.jp/j/wpaper/w_maff/h24/pdf/e_all.pdf , Accessed on 20th June, 2014;
[8]. Ministry of Agriculture Government of India, (2013) – *ANNUAL REPORT 2012-2013*. Available from: http://agricoop.nic.in/documentreport.html , Accessed on 20th June, 2014;
[9]. Ma Y M., Qin X Y., (2009) – *Economic analysis of rural informatization product market*. Chinese Agricultural Science Bulletin, vol. 25, no.7, pp. 268-271. (In Chinese)
[10]. National Bureau of Statistics of China., (2013) – *Annual Data 2013*. Available from: http://data.stats.gov.cn/workspace/index?m=hgnd, Accessed on 20th June, 2014;
[11]. U.S. Department of Agriculture., (2013) – *Farm Computer Usage and Ownership*. Available from: http://usda01.library.cornell.edu/usda/current/FarmComp/FarmComp-08-20-2013.pdf, Accessed on 20th June, 2014;
[12]. Wang S Y., (2008) – *Calculation and research of China rural informatization level*. Journal of Information, vol. 27, no.3, pp.8-10. (In Chinese)
[13]. Yang C., (2009)– *Evolution and improvement of China rural informatization strategies*. Modern Information, vol.29, no.3, pp.42-46. (In Chinese)
[14]. Zhou W., (2011) – *The construction of rural informatization comprehensive service platform*. Agriculture Network Information, no.2, pp.102-104.

致谢

本文的写作得到中国教育部人文社科项目（编号：10YJC790174），中国安徽省高校人文社科重点项目：农民专业合作社信息化建设发展研究：制度安排、组织行为与组织绩效，中国安徽省人文社科项目（编号：SK2012B567)和中国安徽省软科学研究计划（编号：1402052027）项目支持。

参考文献

[1]. 欧盟农业农村发展总局. (2013) – *欧盟农村经济信息与发展统计*. 来源: http://ec.europa.eu/agriculture/statistics/rural-development/2013/index_en.htm, 20/6/2014;
[2]. 贺洪明,肖友国. (2011) – *中美农村信息化建设的特点比较研究*. 图书与情报, 第 1 期, 82-85;
[3]. 黄志文. (2010) – *农村信息化与农村经济发展相关关系的实证研究*. 现代农业科技, 第 12 期, 332-334;
[4]. 刘世洪. (2007) – *中国农村信息化测度指标体系研究*. 图书情报工作, 第 51 卷, 第 9 期, 33-36;
[5]. 刘春.(2011) – *农村信息化的神话: 来自中国四川省的案例*. 政府信息季刊, 第 29 卷, 第 1 期, 85-97;
[6]. 刘春年,王兰. (2006) – *我国农业信息化水平的测度及关联因素分析*. 科技进步与对策, 第 23 卷, 第 12 期, 131-132;
[7]. 日本农林省. (2013) – *日本粮食、农业和农村地区年度报告*. 来源: http://www.maff.go.jp/j/wpaper/w_maff/h24/pdf/e_all.pdf, 20/6/2014;
[8]. 印度农业部. (2013) – *2012-2013 年度报告*. 来源: http://agricoop.nic.in/documentreport.html, 20/6/2014;
[9]. 马明远,秦向阳. (2009) – *农村信息化产品市场的经济学分析*. 中国农学通报, 第 25 卷, 第 7 期, 268-271;
[10]. 中国统计局. (2013) – *2013 年统计数据*. 来源: http://data.stats.gov.cn/workspace/index?m=hgnd, 20/6/2014;
[11]. 美国农业部. (2013) – *计算机在农场使用和普及情况*. 来源:http://usda01.library.cornell.edu/usda/current/FarmComp/FarmComp-08-20-2013.pdf, 20/6/2014;
[12]. 王爽英. (2008) – *我国农业信息化水平的测算研究*. 情报杂志, 第 27 卷, 第 3 期, 8-10;
[13]. 杨诚. (2009) – *我国农村信息化政策的演进与完善*. 现代情报, 第 29 卷, 第 3 期, 42-46;
[14]. 周卫. (2011) – *农村信息化综合服务平台的构建*. 农业网络信息, 第 2 期, 102-104;

[15]. Zhou Y F., Ding W W., Qi X., et al., (2010) – *Index system research of rural informatization base on fuzzy comprehensive evaluation method*. Rural Economy and Science Technology, vol. 21, no.8, pp.20-22. (In Chinese)
[16]. Zhao H., Wen X F., Hao X H., et al., (2010) – *Analysis of rural informatization development in Ningxia Autonomous Region based on factor analysis.* Anhui Agricultural Sciences, vol.38, no.13, pp.6995-6996. (In Chinese)
[17]. Zeng S X., Shi S T., (2010) – *Factor analysis of effects of rural informatization on rural income.* Hunan Agricultural Sciences, no.1, pp.132-13. (In Chinese)
[18]. Zhang L., Zhang Y., Liu F J., et al., (2011) – *Analysis of the cts of rural informatization on rural living standard improvement*. Journal of Agrotechnical Economics, no.5, pp.13-19. (In Chinese)

[15]. 周跃锋,丁旺旺,齐鑫,等. (2010) – *基于模糊综合评价法的农村信息化指标体系研究*. 农村经济与科技, 第 21 卷, 第 8 期, 20-22;
[16]. 赵晖,温学飞,赫晓辉, 等. – *基于因子分析法分析宁夏农村信息化的发展*. 安徽农业科学, 第 38 卷, 第 13 期, 6995-6996;
[17]. 曾硕勋,施绍亭. (2010) – *农村信息化对农户收入影响的因子分析*. 湖南农业科学, 第 1 期, 132-134;
[18]. 张莉,张艳,刘福江,等. (2011) – *农村信息化对农民生计改善的影响分析*. 农业技术经济, 第 5 期, 13-19.

WRITING NORMS / *NORME DE REDACTARE*

Article Types

Three types of manuscripts may be submitted:

1. Regular articles: These should describe new and carefully confirmed findings, and experimental procedures should be given in sufficient detail for others to verify the work. The length of a full paper should be the minimum required to describe and interpret the work clearly (max. 8 pages);

2. Short Communications: A Short Communication is suitable for recording the results of complete small investigations or giving details of new models or hypotheses, innovative methods, techniques or apparatus. The style of main sections has not necessarily to be in accordance with that of full-length papers (max. 6 pages);

3. Reviews: Submissions of reviews and perspectives covering topics of current interest are welcome and encouraged (max. 8 pages).

Review Process

All manuscripts are reviewed by the 2 members of the Scientifically Review. Decisions will be made as rapidly as possible, and the journal strives to return reviewers' comments to authors in approx. 3 weeks. The editorial board will re-review manuscripts that are accepted pending revision.

NOTE: Submission of a manuscript implies: that the work described has not been published before (excepting as an abstract or as part of a published lecture, or thesis) that it is not under consideration for publication elsewhere.

1. REGULAR ARTICLES

- All portions of the manuscript must be typed *single-spaced, A4***,** top and bottom: 2 cm; left: 2 cm; right: 2 cm, font: **Arial,** size 9 pt, except the title which will be 11 pt. and explicit figures, which will be 8 pt.
- Text paper will be written in two equal columns of 8.3 cm, 0.4 cm space between them, except the title, authors and their affiliations, tables, figures, graphs and equations to be entered once.
- Text will be written in English in the left column, respectively in native language in the right column.
- The chapter titles are written Uppercase (eg: INTRODUCTION, MATERIAL AND METHODS), between chapters is left a space for 9 pt. At the beginning of each paragraph to leave a tab of 0.5 cm.
- The paper will be written in Word, "Justify" alignment;
- The paper should be transmitted by E-mail.
- There are allowed 2 papers by each first author.

The **Title** should be a brief phrase describing the contents of the paper. PAPER'S TITLE will be uppercase, Bold (the title in English language) and *Bold italic (the title in native language),* center, 11 pt. Under the paper's title, after an space (enter) 9 pt., write *authors' names* (eg: Vasilescu G.). (font: 9 pt., bold) and *affiliations*, the *name of the corresponding author* (next row), (9 pt., regular). Also be passed: the phone, fax and E-mail information, for the first author of paper's (font: 8 pt., italic).
Title should be short, specific and informative. Avoid long titles; a running title of no more than 100 characters is encouraged (without spaces).

The ***Abstract*** should be informative and completely self-explanatory, briefly present the topic, state the scope of the experiments, indicate significant data, and point out major findings and conclusions. The Abstract should be 100 to 300 words in length. Complete sentences, active

Tipuri de Articole

Trei tipuri de manuscris pot fi trimise:

1. Articole obişnuite (normale): acestea trebuie să descrie cercetări noi şi confirmate, iar procedurile experimentale să fie descrise pentru a putea fi verificate in detaliu, fără a leza dreptul de proprietate intelectuală. Mărimea unei lucrări trebuie să cuprindă minimul necesar pentru a descrie şi interpreta în mod clar conţinutul (ma.8 pagini);

2. Comunicări scurte: o comunicare scurtă este folosită pentru înregistrarea rezultatelor din investigaţii complete de dimensiuni reduse sau pentru a oferi detalii despre modele noi de ipoteze, metode inovative, tehnici sau infrastructuri. Tipul secţiunilor (capitolelor) principale nu trebuie să fie neapărat în concordanţă cu articolele normale (max. 6 pagini);

3. Sintezele: Prezentarea unor comentarii şi perspective acoperind subiecte de interes actual sunt binevenite şi încurajate (maxim 8 pagini).

Procesul de evaluare (recenzie)

Toate manuscrisele sunt evaluate de către 2 membri ai Comitetului Ştiinţific. Deciziile vor fi luate cât mai rapid posibil şi revista va returna comentariile evaluărilor înapoi la autori în aproximativ 3 săptămâni. Conducerea editorială va reevalua manuscrisele care sunt acceptate în vederea publicării în revistă.

Notă: Sunt acceptate numai lucrările care nu au mai fost publicate anterior. În cazul în care autorii trimit spre publicare lucrări ce conţin date, informaţii, capitole, etc., din alte lucrări publicate anterior şi nu se fac referiri la acestea în text, răspunderea aparţine acestora.

1. ARTICOLE OBIŞNUITE

- Toate capitolele manuscrisului trebuie să fie scrise *single-spaced, A4***,** sus şi jos: 2 cm; stânga: 2 cm; dreapta: 2 cm, font: **Arial,** mărime 9 pt, cu excepţia titlului care se scrie cu 11 pt. şi figurile explicite, care se scriu cu 8 pt.
- Textul lucrării va fi scris în două coloane egale de 8,3 cm, 0,4 cm spaţiul dintre ele, exceptând titlul, autorii şi afilierea acestora; tabelele, figurile şi ecuaţiile care nu se scriu pe coloane ci pe toată pagina (vezi modelul ataşat);
- Textul se va scrie în limba engleză în coloana din stânga, respectiv în limba maternă - coloana din dreapta.
- Titlurile capitolelor sunt scrise cu majuscule (ex: INTRODUCERE, MATERIAL ŞI METODE), între capitole se lasă un spaţiu de 9 pt. La începutul fiecărui paragraf se lasă un "tab" de 0.5 cm;
- Lucrarea va fi scrisă în Word, aliniere "Justify".
- Lucrarea trebuie trimisă prin e-mail.
- Sunt permise max. 2 lucrări ca prim autor.

Titlul trebuie să fie o frază scurtă care să descrie conţinutul lucrării. Acesta *va fi scris cu majuscule, centrat*, mărime: 11 pt., bolduit, (titlul in engleză) şi *bolduit italic (titlul în limba maternă)*. Sub titlul lucrării după un spaţiu de 9 pt., se scriu numele autorilor (ex: Vasilescu G.) (9 pt., bold), imediat sub numele autorilor se scrie: afilierea autorilor (9 pt., normal) iar pe următorul rând: telefonul, faxul, e-mailul corespunzător celui care a trimis lucrarea - primului autor (8 pt., italic).
Titlul trebuie să fie scurt, specific şi informativ. Evitaţi titlurile lungi, un titlu de sub 100 caractere este recomandat (fără spaţii).

Rezumatul trebuie să fie informativ şi uşor de înţeles; prezentaţi pe scurt topica, stadiul experimentelor, date semnificative, şi evidenţiaţi descoperirile majore şi concluziile. Rezumatul trebuie să cuprindă între 100 şi 300 cuvinte. Propoziţiile complete, verbele active, şi persoana

verbs, and the third person should be used, and the abstract should be written in the past tense. Standard nomenclature should be used and abbreviations should be avoided. No literature should be cited (font: 9 pt., the title - *bold italic*; the text of abstract: *italic*).

Following the abstract, about 3 to 10 ***Keywords*** that will provide indexing references should be listed (font: 9, bold italic - the title and 9 pt., *italic* - the text).

A list of non-standard **Abbreviations** should be added. In general, non-standard abbreviations should be used only when the full term is very long and used often. Each abbreviation should be spelled out and introduced in parentheses the first time it is used in the text. Only recommended SI units should be used. Authors should use the Solidus presentation (mg/ml). Standard abbreviations (such as ATP and DNA) need not to be defined.

INTRODUCTION should provide a clear statement of the problem, the relevant literature on the subject, and the proposed approach or solution. It should be understandable to colleagues from a broad range of scientific subjects.

MATERIALS AND METHODS should be complete enough to allow experiments to be reproduced. However, only truly new procedures should be described in detail; previously published procedures should be cited, and important modifications of published procedures should be mentioned briefly. Capitalize trade names and include the manufacturer's name and address. Subheadings should be used. Methods in general use need not be described in detail.

RESULTS should be presented with clarity and precision. The results should be written in the past tense when describing findings in the authors' experiments. Results should be explained, but largely without referring to the literature. Discussion, speculation and detailed interpretation of data should not be included in the Results but should be put into the Conclusions section. Subheadings should be used.

The **CONCLUSIONS** should interpret the findings in terms of the results obtained in this and in past studies on this topic. State the conclusions in a few sentences at the end of the paper. The Results and Discussion sections can include subheadings, and when appropriate, both sections can be combined.

The **Acknowledgments** of people, grants, funds, etc should be brief (if necessarily).

Tables should be kept to a minimum and be designed to be as simple as possible. Tables are to be typed single-spaced throughout, including headings and footnotes. Each table must be written on the entire width of the page, into the text where reference is made, the columns are broken - one column (see attached sample). Tables should be self-explanatory without reference to the text. The details of the methods used in the experiments should preferably be described in the legend instead of in the text. The same data should not be presented in both table and graph form or repeated in the text. Table's title will be centered bold (in English) and bold italic native language then separated by a slash. In the table, each row will be written in English (Arial, regular, size: 9 pt.) / *native language* (Arial, italic, 9 pt.). The table and its number is written right justified, bold - in English and bold italic - native language, separated by a slash (/).

a III-a trebuiesc folosite (rezumatul să fie scris la timpul trecut). Se va utiliza nomenclatura standard iar abrevierile trebuiesc evitate. Nu se vor utiliza citări de lucrări în "rezumat" (font: 9 pt., titlu - *bold italic*; textul rezumatului - *italic*).

Cuvinte cheie: ca urmare a rezumatului, între 3 şi 10 cuvinte cheie trebuiesc listate, aceste oferind referinţe de indexare (font: 9 pt., **bold italic** – titlul şi 9 pt., *italic* - textul).

Trebuie adăugată o listă de abrevieri specifice. În general, aceste abrevieri se folosesc atunci când termenul folosit este foarte lung şi des întâlnit în lucrare. Fiecare abreviere ar trebui introdusă în paranteză pentru prima dată când este folosită în text. Doar unităţi din SI trebuiesc folosite. Autorii trebuie să folosească prezentarea Solidus (mg/ml). Abrevierile standard (ca ATP sau ADN) nu trebuiesc definite.

INTRODUCEREA trebuie să ofere o expunere clară a problemei, esenţa relevantă a subiectului şi abordarea propusă sau soluţia. Aceasta trebuie să poată fi înţeleasă de către colegi din diferite domenii ştiinţifice.

MATERIALE ŞI METODE: trebuie să fie suficient de complete pentru a permite experimentelor să fie reproduse. Totuşi, numai metodele cu adevărat noi trebuie descrise în detaliu; metodele publicate anterior trebuie citate; modificările importante ale metodelor publicate trebuie menţionate pe scurt. Scrieţi cu majuscule denumirile comerciale şi includeţi numele şi adresa producătorilor. Subcapitolele trebuie utilizate. Metodele utilizate în general, nu trebuie descrise în detaliu.

REZULTATELE trebuie prezentate cu claritate şi precizie. Acestea trebuie scrise la timpul trecut, atunci când descriu constatările în experimentele autorilor. Rezultatele trebuie să fie explicite, dar în mare măsură, fără a se face referire la literatura de specialitate. Discuţiile, speculaţiile şi interpretarea detaliată a datelor nu trebuie să fie incluse în rezultate, ci trebuie incluse în capitolul Concluzii. Subcapitolele trebuie utilizate.

CONCLUZIILE trebuie să interpreteze constatările în ceea ce priveşte rezultatele obţinute în această lucrare şi în studiile anterioare pe această temă. Concluziile generale vor fi prezentate în câteva fraze la sfârşitul lucrării. Rezultatele şi discuţiile pot include subpoziţii, şi atunci când este cazul, ambele secţiuni pot fi combinate.

Mulţumirile către oameni, cei care au acordat burse, fonduri, etc., trebuie să fie scurte (dacă este necesar).

Tabelele trebuie menţinute la un nivel minim şi să fie proiectate pentru a fi cât mai simple posibil. Tabelele vor fi scrise la un rând, inclusiv titlurile şi notele de subsol. Fiecare tabel trebuie scris pe întreaga lăţime a paginii, între textul în care se face trimitere; coloanele sunt eliminate - o singură coloană (vezi ataşat modelul). Tabelele trebuie să fie auto-explicative, fără referire la text. Detaliile cu privire la metodele utilizate în experimente trebuie să fie, de preferinţă, descrise în legendă şi nu în text. Aceleaşi date nu trebuie prezentate atât în tabel cât şi sub formă grafică (decât dacă este absolut necesar) sau repetate în text. Titlul tabelului va fi scris centrat, bold (în engleză) şi bold italic (în limba maternă), separate de un slash (/). În tabel, fiecare rând va fi scris în limba engleză (9 pt., normal) / limba maternă (9 pt., italic). Tabelul şi numărul acestuia se scrie aliniat la dreapta, bold - în limba engleză şi bold italic în limba maternă, despărţite de un slash (/).

Figure legends should be typed in numerical order. Graphics should be prepared using applications capable of generating high resolution JPEG before to introducing in the Microsoft Word manuscript file (Insert - From File - ...jpeg). Use Arabic numerals to designate figures and upper case letters for their parts (Figure 1). Begin each legend with a title and include sufficient description so that the figure is understandable without reading the text of the manuscript. Information given in legends should not be repeated in the text. Each figure must be inserted on the entire width of the page, into the text where reference is made, single columns (see attached sample). Leave a space between the figure and the text of figure, size: 3 pt., figure number is written in **Arial bold**, size: 8 pt., followed by what represent the figure or graph, written with Arial, regular, 8 pt. Left to write in English (regular), followed by a separating slash (/) and text in native language (*Arial italic*). Eg:

Fig 1 - Test stand / *Stand de testare* (size: 8 pt.)

The figures should be "*In line with text*" - Center, not "*Square*"; "*Tight*"; "*Behind text*" or "*In front of text*" (from "*Format picture*" - right mouse button on picture and then "*Layout*".

Figurile trebuie scrise în ordine numerică. Grafica trebuie realizată utilizând aplicaţii capabile să genereze JPEG de înaltă rezoluţie, înainte de a introduce în dosarul manuscris Microsoft Word (Insert - From File - ... JPEG). Folosiţi cifre arabe, pentru a desemna cifre şi litere majuscule pentru părţile lor (Figura 1). Începeţi fiecare legendă cu un titlu care să includă o descriere suficientă, astfel încât figura să poată fi înţeleasă, fără citirea textului din manuscris. Informaţiile furnizate în legende, nu trebuie repetate în text. Fiecare figură trebuie introdusă pe întreaga lăţime a paginii, în text, acolo unde se face referire, o singură coloană (vezi ataşat eşantion), centrat. Lăsaţi un spaţiu între figură şi textul figurii, mărimea: 3 pt.; numărul figurii va fi scris cu bold, 8 pct., centrat, urmat de ceea ce reprezintă figura sau graficul, scris cu 8 pt., normal. Prima dată se scrie textul în limba engleză (normal), urmat de un slash (/) apoi textul în limba maternă (italic). Exemplu:

Fig. 1 - Test stand / *Stand de testare* (mărimea: 8 pt.)

Figurile introduse trebuie să fie "*In line with text*" - Center, nu "*Square*"; "*Tight*"; "*Behind text*" or "*In front of text*" (din "*Format picture*" - butonul dreapta mouse pe figură şi apoi "*Layout*").

Mathematics

Authors must provide instructions on how symbols and equations should be set. Equations should be numbered sequentially in the right-hand side and in parenthesis. They should be referred to in the text as Equation (4) or Eg. (4). Each equation must be written on the entire width of the page, into the text where reference is made, the columns are broken (see attached sample).

Formulele matematice, ecuaţiile: autorii trebuie să furnizeze instrucţiuni privind modul de simbolizare şi de ecuaţii stabilite şi utilizate. Ecuaţiile trebuie numerotate secvenţial, în partea dreaptă şi în paranteze. Ele trebuie menţionate în text ca ecuaţia (4) sau Ex. (4). Fiecare ecuaţie trebuie scrisă pe întreaga lăţime a paginii, în text, acolo unde se face referire, o singură coloană (vezi ataşat model).

REFERENCES: are made in the text; a reference identified by [1], [2], ... [n] is written in the order that was placed at the end of the work - alphabetically.

Example:

[1], [2], [3], ..., [n]

References should be listed at the end of the paper in alphabetical order. Articles in preparation or articles submitted for publication, unpublished observations, personal communications, etc. should not be included in the reference list but should only be mentioned in the article text (e.g., A. Danciu, University of Bucharest, Romania, personal communication). Authors are fully responsible for the accuracy of the references.

REFERINŢELE: se fac în text; o referinţă identificată prin intermediul [1], [2], ...[n], se scrie în ordinea în care a fost trecută la sfârşitul lucrării - ordine alfabetică.

Exemplu:

[1], [2], [3], ..., [n]

Referinţele trebuie prezentate la sfârşitul lucrării în ordine alfabetică. Articole în curs de pregătire sau articole trimise spre publicare, observaţiile nepublicate, comunicările cu caracter personal, etc, nu trebuie incluse în lista de referinţă, dar pot fi menţionate în textul lucrării (exemplu, A. Danciu, Universitatea din Bucureşti, România, comunicare personală). Autorii sunt pe deplin responsabil pentru exactitatea referinţelor.

Examples:

Journal / Magazine:

[1]. Nicolescu M.A. (2007) - *Relevant characteristics of alternative liquid fuels aimed at Diesel engines exploitation in polycarburation duty*. INMATEH - Agricultural Engineering, vol. 27, no. 1/2009, ISSN 1583-1019, pg. 50-55.

[2]. Pirna I, Nicolescu M., Marin M., Voicea I (2009) - *Alternative supply of agricultural tractors with raw oils*. INMATEH - Agricultural Engineering, vol. 29, no. 3/2009, ISSN 1583-1019, pg. 89-92.

Conference or Symposium:

[1]. Bungescu S, Stahli W, Biriş S, Vlăduţ V, Imbrea F, Petroman C (2009) - *Cosmos programm used for the strength calculus of the nozzles from the sprayers,* Proceedings of the 35 International Symposium on Agricultural Engineering *"Actual Tasks on Agricultural Engineering",* Opatija - Croaţia, ISSN 1333-2651, pg. 177÷184.

Book:

[1]. Vlăduţ V (2009) - *Studiul procesului de treier în aparatul cu flux axial*, Editura "Terra Nostra", ISBN 973-1888-26-8, Iasi - Romania.

Exemple:

Jurnal / Revistă

[1]. Nicolescu M.A. (2007) - *Proprietăţile relevante ale combustibililor lichizi alternativi vizaţi pentru exploatarea motoarelor Diesel în regim policarburat*, INMATEH - Inginerie Agricolă, vol. 27, nr. 1 / 2009, ISSN 1583-1019, pg. 50-55;

[2]. Pirna I, Nicolescu M., Marin M., Voicea I (2009) - *Alimentarea alternativă a tractoarelor agricole cu uleiuri vegetale crude,* INMATEH - Inginerie Agricolă, vol. 29, nr. 3 / 2009, ISSN 1583-1019, pg. 89-92.

Conferinţă / Simpozion

[1]. Bungescu S, Stahli W, Biriş S, Vlăduţ V, Imbrea F, Petroman C (2009) - *Cosmos programm used for the strength calculus of the nozzles from the sprayers,* Proceedings of the 35 International Symposium on Agricultural Engineering *"Actual Tasks on Agricultural Engineering",* Opatija - Croaţia, ISSN 1333-2651, pag. 177÷184.

Carte

[1]. Vlăduţ V (2009) - *Studiul procesului de treier în aparatul cu flux axial*, Editura "Terra Nostra", ISBN 973-1888-26-8, Iaşi - România.

Book Chapter:
[1]. Vlăduţ V (2009) - Consideraţii şi ipoteze privind modelarea unui proces de treier şi separare. In: *Studiul procesului de treier în aparatul cu flux axial*, Editura "Terra Nostra", ISBN 973-1888-26-8, pg. 61-69, Iasi - Romania.

Dissertation / Thesis:
[1]. Constantinescu A (2010) - *Optimizarea agregatelor formate din tractoare de putere mare cu maşini agricole pentru pregătirea terenului în vederea însămânţării*. PhD dissertation, University of Transylvania Braşov, Braşov, Romania.

Units, Abbreviations, Acronyms

- Units should be metric, generally SI, and expressed in standard abbreviated form.
- Acronyms may be acceptable, but must be defined at first usage.

2. SHORT COMMUNICATIONS

Short Communications are limited to a maximum of two figures and one table. They should present a complete study that is more limited in scope than is found in full-length papers. The items of manuscript preparation listed above apply to Short Communications with the following differences: (1) Abstracts are limited to 100 words; (2) instead of a separate Materials and Methods section, experimental procedures may be incorporated into Figure Legends and Table footnotes; (3) Results and Conclusions should be combined into a single section.

3. REVIEWS

Summaries, reviews and perspectives covering topics of current interest in the field, are encouraged and accepted for publication. Reviews should be concise (max. 8 pages). All the other conditions are similar with regular articles.

Capitol din carte
[1]. Vlăduţ V (2009) - Consideraţii şi ipoteze privind modelarea unui proces de treier şi separare. În: *Studiul procesului de treier în aparatul cu flux axial*, Editura "Terra Nostra", ISBN 973-1888-26-8, pg. 61-69, Iaşi - România.

Disertaţii / Teze de doctorat
[1]. Constantinescu A (2010) - *Optimizarea agregatelor formate din tractoare de putere mare cu maşini agricole pentru pregătirea terenului în vederea însămânţării*. Teză de doctorat, Universitatea Transilvania Braşov, Braşov, România.

Unităţi, Abrevieri, Acronime

- unităţile metrice trebuie să fie, în general, SI, şi exprimate în formă prescurtată standard;
- acronimele pot fi acceptate, dar trebuie să fie definite la prima utilizare.

2. COMUNICĂRILE SCURTE

Comunicările scurte sunt limitate la maxim 2 figuri şi un tabel. Acestea trebuie să prezinte un studiu complet, care este mai limitat decât în cazul articolelor normale (de dimensiuni mai mari). Elementele de pregătire a articolelor normale (manuscriselor) enumerate mai sus se aplică şi la comunicările scurte, cu următoarele diferenţe: (1) Rezumatul este limitat la 100 cuvinte; (2) capitolele Materiale şi Metode, Procedurile experimentale pot fi scrise împreună, încorporând figurile şi tabelele; (3) Rezultatele şi Concluziile pot fi combinate într-o singură secţiune.

3. SINTEZELE

Sintezele, comentariile şi perspectivele acoperind subiecte de interes din domeniu sunt încurajate şi acceptate spre publicare. Sintezele trebuie să fie concise şi nu mai mari 8 pagini. Toate celelalte condiţii sunt similare cu cele de la articolele normale (obişnuite), enumerate mai sus.

Edited by INMA Bucharest
6 Ion Ionescu de la Brad Blvd., sect. 1, Bucharest, ROMANIA
Tel: +4021.269.32.60; Fax: +4021.269.32.73
http://www.inma.ro/inmateh-agricultural%20engineering
http://www.inmateh.eu